Secondary channel of the RNA polymerase, a target for transcriptional regulation in bacteria

Llorenç Fernández Coll

Departament de Microbiologia
Facultat de Biologia
Universitat de Barcelona

Secondary channel of the RNA polymerase, a target for transcriptional regulation in bacteria

Memòria presentada per Llorenç Fernàndez Coll per optar al títol de Doctor per la Universitat de Barcelona

Programa de Doctorat: Microbiologia Ambiental i Biotecnologia

VºBº del director i tutor de la Tesi,

Dr. Carlos Balsalobre Parra

Memòria presentada per

Llorenç Fernàndez Coll

I don’t see the logic of rejecting data just because they seem incredible

Sir Fred Hoyle (1915-2001) English astronomer

Ha arribat el moment de fer un petit balanç del que ha sigut aquesta tesi, i és el moment en que et poses a pensar en tota la gent que has conegut durant aquest procés. Mires les llibretes velles i te n'adones que realment són més velles del que creies, la qual cosa implica / suggereix que el temps ha passat volant. Vaig començar col·laborant com estudiant de llicenciatura (si, jo no sóc de Grau, y con mucha honra) al Departament de Microbiologia al Setembre de 2005 (si la memòria no em falla i la llibreta no m'enganya). Des de llavors he conegut a molta gent, amb alguns ens hem portat més bé, d'altres més malament i d'altres ens hem portat a matar (per què negar-ho?). El fet d'haver vist passar tanta gent pel Departament fa encara més estrany entrar un dia per la porta i veure que no coneixes ni la meitat dels que hi ha ara. D'això se'n diu relleu generacional. O fins i tot entristeix quan veus que no hi ha ni la meitat del volum de gent que hi solia haver. Però això són figues d'un altre paner.

Com comprendreu, no puc posar-vos a tots i per això abans de començar a parlar de forma més individual, vull donar-vos les gràcies per tot, sense vosaltres no hagués sigut el mateix (moment llagrimeta).

Primer de tot li vull agrair al Carlos tot el que ha fet per mi i tot el temps que hi ha dedicat. Sempre ha tingut un moment o un segon per una pregunta o un consell, i això és d'agrair. Sé que no ha sigut fàcil, sé que ha tingut una enoooorme paciència, però d'una manera o altre ens n'hem sortit. He aprés moltes coses i no totes eren de ciència. Ha estat un plaer.

Si el Carlos és el "papi" del laboratori, sense cap mena de dubte la "mami" és la Cristina, sobretot quan entra a fer neteja... Motes gràcies per tots els bons consells.

M'agradaria agrair a l'Antonio l'oportunitat que em va donar al principi de tot de la tesi. Quan cap ministeri ni conselleria donava un duro per mi (literalment) ell em va oferir una plaça de professor associat. Moltes gràcies.

Vull agrair a tots els meus companys de laboratori, tant si estan al lab 4, al lab 3 o a l'IBEC. Alguns encara hi són, d'altres han marxat i d'altres tenen un peu dins i l'altre fora. A la Marta, també coneguda com a Santa Marta de los Becarios FPU, la meva companya directe de poiata i de laboratori 3, la que ha

hagut d'aguantar-me durant... jo que sé quant de temps. Ella era la guia de referència dels pesos moleculars de qualsevol element, no se'n sabia cap, però com que és química sempre li havia de preguntar. Al Mario, l'altre boig del laboratori 3 amb el seu genial sentit de l'humor. A la Carla, amb la que hem rigut i hem passat molt bones estones (bé, sempre i quant no ens tiréssim els plats pel cap). Quins dos ens hem anat a ajuntar... la gana amb les ganes de menjar... A la Tania, també coneguda com a Pelucas, Srta. Rottenmeier (només quan porta monyo), Mamita rica.... etc. Com vas dir un cop, nosaltres som germans per part de "papi". Ara anem a per les Sonies. A la Sonia A. (altrament coneguda com a Sonieta), no sé que hauria fet sense tu. La meva companya de sopars de Departament (be, durant la època que hi anàvem). A la Sonia P. (La Paytu) sempre disposada a ajudar i a fumar un cigarro. Apa que no hem parlat cops de les patades que dono a judo... Al Youseff, Yussi para los amigos, amb qui sempre pots compartir un cacaolat. Et passo el càrrec de responsable de laboratori, cuida-me'l bé, eh? També hi ha noves incorporacions d'estudiants de Grau, com la Cintia, o de màster com la Lídia (Campygirl) que, tot i que no hem coincidit molt, també hem rigut una estona, o si més no, ho hem intentat. I aquests són els que encara estan en "actiu" al laboratori. També vull agrair el seu suport i amistat a tots els que ja no hi són, com la Rosa, l'Aitziber, la Mar, la Laura, la Nahia, el Nacho, el Jorge, el Juanda, etc.

Però el Departament no només és laboratori 4. Per això vull agrair a tota la gent del Departament les bones estones que hem passat, tant de la fase I com de la fase II. Moltes gràcies per les bones estones, les bromes, les birres compartides a biofestes, sopars de tesis i altres.

A els secretaris i tècnics del Departament, Macu, Manolo, Rosario, Bea i Susana. Moltes gràcies per estar sempre disposats a resoldre qualsevol dubte i donar un cop de ma quan ha sigut necessari.

I would like to thank to Kasia for giving me the opportunity to collaborate with her at Gdansk, as well as for all what she did when I was there. Thank you very much for all the advices, supervision and help that you give me. Thank you for the Tea / Coffee time. It was a pleasure. Dziękuję!

També m'agradaria agrair a tots els meus amics que han aguantat durant aquest anys les histories sobre la Tesi, i altres coses. Al Kux, la Patty, la Gemma, la Curis i l'Ali, moltes gràcies per els mojitos compartits i el Jagger. Per els nostres xous a restaurants, viatges o ficant gent a taxis. Sort en tenim de la Jefa que posa ordre, menys quan esta al cangrejo i sona la Rafaela Carrà, que es descontrola. Al Dani, a la Sílvia i a la Lorena, el grupet 5 pisos... a part d'escandalitzar restaurants, hem rigut força amb les nostres històries.

A tu Mac, moltes gràcies pel teu suport en tot, la tesi i el que no era la tesi. Tot i estar a uns 1500 Km de distància sempre hi has estat quan t'he necessitat. Moltes gràcies. ;)

Finalment vull agrair a la meva família tot el suport que m'han donat durant tot aquest temps. Vull donar les gràcies als meus pares, a les iaies i a la tieta per preocupar-vos per mi i per preguntar (tot i patir el risc de ser fulminats amb la mirada) "i com va la Tesi?". A la Txell, la senyoreta dinosaure, que tot i no tenir-ne necessitat, és capaç empassar-se uns rotllos interminables sense queixar-se. I en especial al monstre de la casa, la Laia. Un petó molt gran a tots.

Moltes gràcies a tots per fer que el temps passés volant. I com diuen a judo: Hajime! (Que comenci el combat).

Table of contents

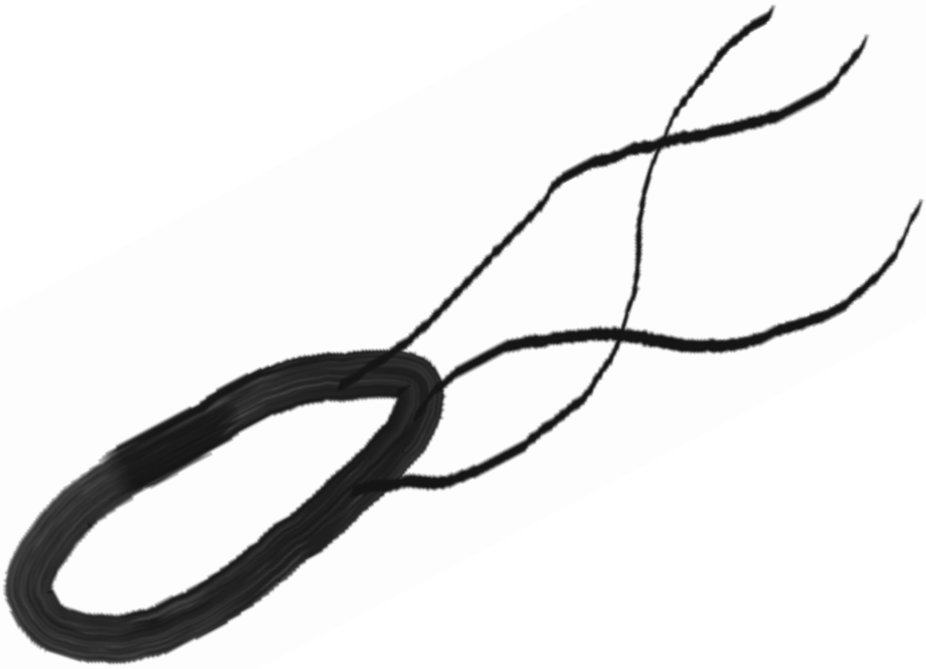

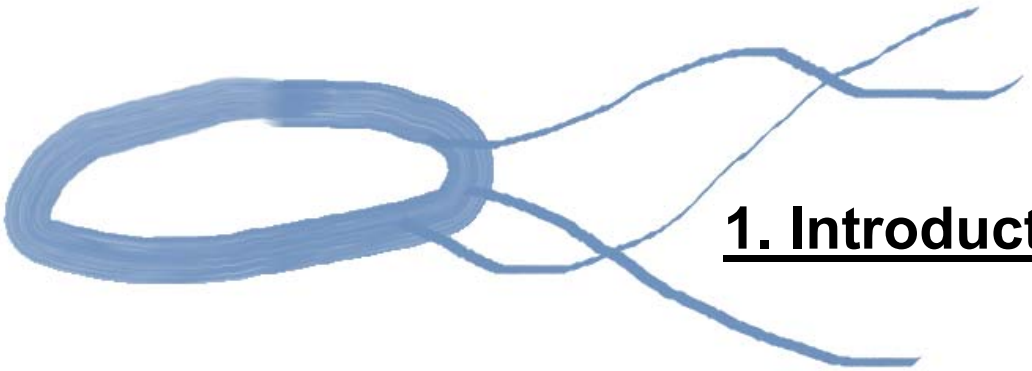

1. Introduction

The biological concept of species had changed from the one defined by Gordon and Mihm, (1962): “a collection of strains that all share the same major properties but differ in one or more significant properties from other collection of strains”; to the one used nowadays: “the phylogenetic definition of a species generally would include strains with approximately 70% or greater DNA-DNA relatedness and with 5ºC or less ΔT_m” (Wayne *et al.*, 1987; Stackebrandt *et al.*, 2002). Genomic studies showed that a great genetic variation among bacterial species exists. Comparing genomes of several strains of the same species, geneticist created new terms to be able to rationalize all this diversity (**fig. 1**):

- Core-genome includes the common genes among different strains of a species.
- Pan-genome includes all the genes associated to a species, comprising both core-genome and variable genes, being the last ones genes which are in some but not all the strains.

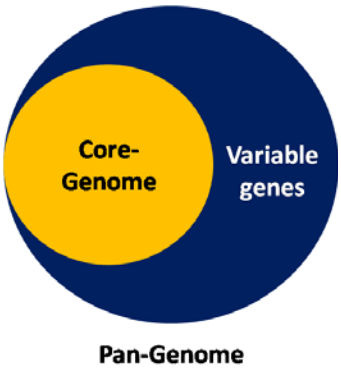

Figure 1: Scheme of a Pan-genome.

Most of the variable genes are clustered likewise on islands distributed among the genome (Mira *et al.*, 2010). While the core-genome contains genes essential to define a species, variable islands are considered to contain genes required for the adaptation of the different strains to specific habitat. This accessory or variable pool includes genes coding, among others, for antibiotic and heavy-metal resistances, bacteriocins, cell-wall components, nitrogen fixation, virulence, and many metabolic properties (Gogarten *et al.*, 2002). It has been suggested that environmental pressures are able to induce changes in the genome size (**fig. 2**). In general, it is considered that bacteria with largest

genomes can easily cope with a higher diversity of changing environments as they may have a larger metabolic and stress tolerance potential. On the other hand, bacteria adapted to live in a very specific and stable environment, such as obligatory intracellular bacteria, may suffer massive genome reductions (Ranea *et al.*, 2004; Dini-Andreote *et al.*, 2012).

It has been suggested (Mira *et al.*, 2010) that the main mechanisms responsible of this genomic plasticity are i) DNA duplication and subsequent sequence divergence (Pushker *et al.*, 2004) and ii) horizontal transfer of DNA sequences between different bacterial strains or species (Ochman *et al.*, 2000). Horizontal gene transfer (HGT) processes includes plasmid transmission by conjugation or natural transformation, and natural transduction of bacterial DNA packaged into bacteriophage capsids. Regarding evolution of bacterial patho-genes, transduction is considered the major HGT mechanism involved among transfer of virulence factors in bacteria (Boyd and Brüssow, 2002; Daubin and Ochman, 2004; Penadés *et al.*, 2014).

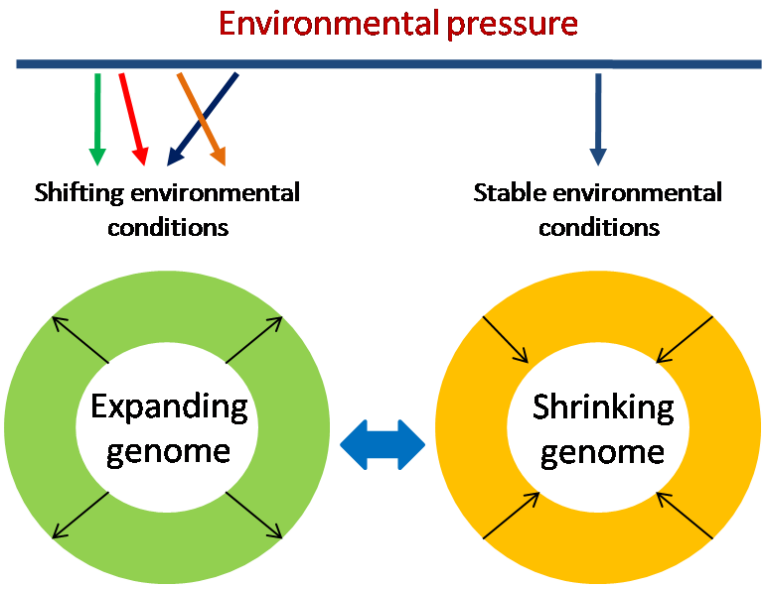

Figure 2: Effect of environmental pressure on genome size. Adapted from Dini-Andreote *et al.*, (2012).

The contribution of horizontally transferred genes to the non-core, variable genome fraction is vast, as indicated by the high proportion of mobile elements, phage-related genes, and pathogenicity islands present in the pan-genome of many studied bacteria (Mira *et al.*, 2010).

1.1. "Of environment and genes": effect of environmental alterations on gene expression in bacteria.

Environmental pressure might produce some effect on genome size (**fig. 2**), but this is a slow process that requires a long time and many bacterial generations. However, bacteria have the ability to detect environmental variations and modify its genetic expression pattern in order to rapidly adapt to the changing conditions. This ability is crucial for survival of the bacteria during drastic changes in environmental conditions. This rapid adaptability is crucial among pathogenic bacteria since an infection can be understood as a process where bacteria need to adapt to continuous environmental alterations during its transit through the host organism. The different genes needed to successfully establishing an infection must be expressed co-ordinately, simultaneously and/or sequentially.

1.1.1. Gene transcription, the key of the adaptative response

In the genes or cistrons, functional genetic units, independently of coding for proteins or non coding RNAs, the transcribed sequences are delineated by a region called promoter – where RNApol binds to initiate transcription – and a downstream sequence called a transcription terminator – where transcription ends (Krebs *et al.*, 2011). The sequence between the promoter and the terminator is transcribed to RNA, and in the case that codes for proteins, the sequence that specify the amino acids of the protein is denoted "Open Reading Frame" (ORF). All coding sequences are preceded by a Shine-Dalgarno sequence that is recognized by the ribosomes to start the translation of the RNA to protein. In bacteria, the basic expression unit is the operon (Jacob *et al.*, 1960), composed by a set of adjacent genes transcribed from a single promoter and subject to the same regulatory regime (Brown, 2010). Operons are termed monocistronic when contains a single cistron, bicistronic when encodes two cistrons and polycistronic operon when more than two cistrons are under the same promoter.

Gene expression is initiated with the transcription process, when the information coded in the DNA is transcribed to RNA by an enzymatic complex known as

RNA polymerase (RNApol). Different types of RNA products are produced by the RNApol during transcription:

- Messenger RNA (mRNA), molecules that contains the information to synthesize proteins.
- Ribosomal RNA (rRNA), molecules that act as structural components of the ribosomes.
- Transfer RNA (tRNA), carriers of specific amino acids to the ribosome during protein synthesis.
- Small non-coding RNA (snRNA), molecules that are involved in gene expression regulation.

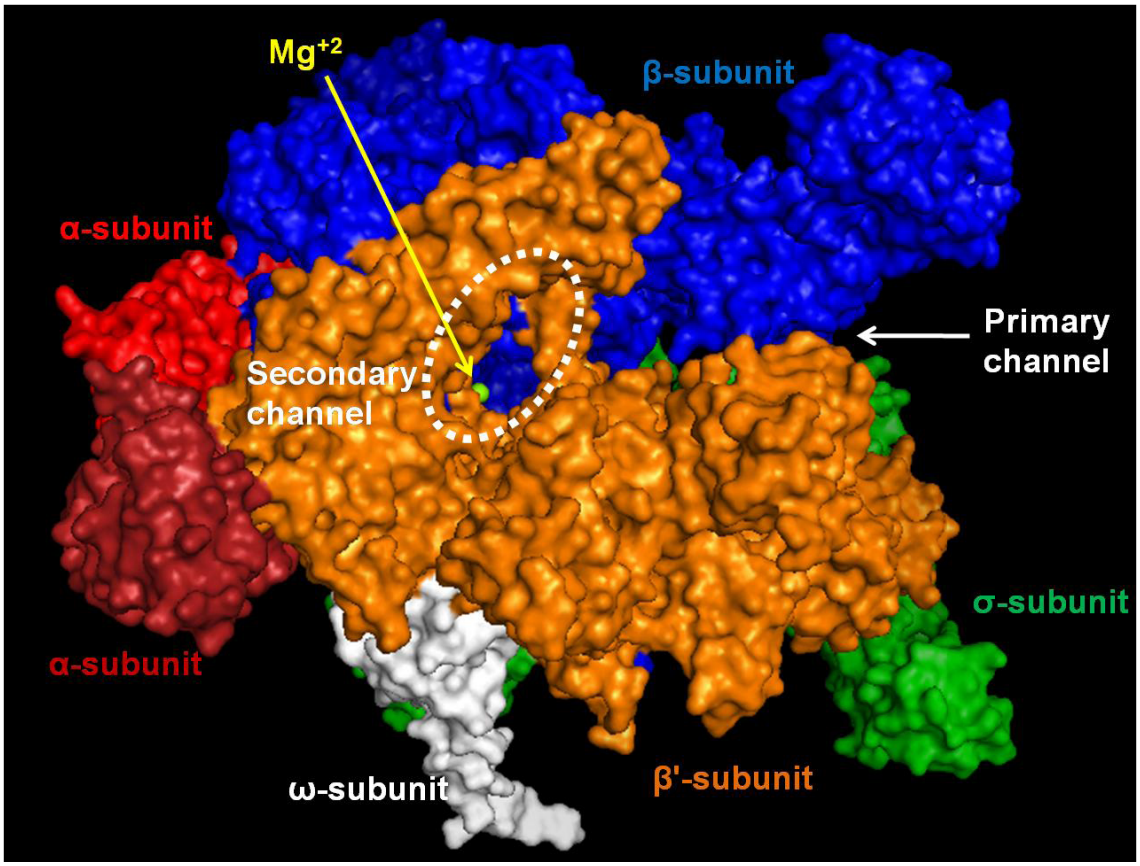

Figure 3: Three-dimensional structure of holoenzyme RNApol with its several subunits and Mg^{+2} ions that correspond to the catalytic centre. The Primary and Secondary channels of the RNApol are indicated.

The basic unit (core) of RNApol is formed by 5 protein subunits (**fig. 3**): 2 α, 1 β, 1 β' and 1 ω subunit, often indicated as $\alpha_2\beta\beta'\omega$. Subunit α contains two domains: the N-terminal domain (αNTD) provides the dimerization interface as well as the scaffold for core-enzyme assembly, whereas the C-terminal domain

(αCTD) binds to DNA. The β and β' subunit are the catalytic subunits. Two Mg^{+2} ions, known as cMG1 and cMG2, are responsible of RNA synthesis (Korzheva *et al.*, 2000) coordinating amino acids from both subunits (Artsimovitch *et al.*, 2004). The NTP substrate is bound to the two catalytic Mg^{+2} ions forming a perfect base pair with the template strand nucleotide and being incorporated to the nascent RNA. It has been described that the active site, contains 2 more Mg^{+2} ions where ppGpp binds (pMG1 and pMG2, discussed more in detail below) (Artsimovitch *et al.*, 2004). The ω subunit, although not being directly involved in transcription, is essential for the proper binding between β' and α subunit. The three-dimensional structure of the RNApol (**fig. 3**) defines two spaces that play a relevant role during transcription and defined as primary and secondary channel. The holoenzyme needs the binding of a σ subunit to be able to recognise promoter sequences and initiate the transcription process (Haugen *et al.*, 2008). The σ subunit interacts with the subunits β and β', located within the primary channel. *E. coli* contains seven different σ factors divided in two families, i) σ^{70}-like family and ii) σ^{54}-like family (Ishihama, 2000; Österberg *et al.*, 2011).

The members of the σ^{70}-like family are:

- σ^{70} (σ^{D}), involved in expression of most housekeeping genes.
- σ^{38} (σ^{S}), controls the expression of stationary phase genes and stress response genes.
- σ^{32} (σ^{H}), involved in expression of genes coding for heat shock proteins.
- σ^{24} (σ^{E}), involved in expression of genes whose product deal with misfolded proteins in the periplasm.
- σ^{28} (σ^{F}), controls the expression of flagella and chemotaxis genes.
- σ^{19} (σ^{FecI}) controls the expression of *fec* operon (ferric-citrate transport).

While, in *E. coli,* the σ^{54}-like family only contains a single σ subunit: σ^{54} (σ^{N}), that controls the expression of genes involved in nitrogen scavenging.

The different σ subunits recognise different promoters, therefore, variations in the σ subunit binding the holoenzyme, would produce variations in the genes

expression pattern. The promoter sequence may vary in complexity, since different functional boxes might be present (**fig. 4**).

Promoters recognized by the σ^{70}-like family contains two hexameric sequences, separated by a spacer, placed at 10 and 35 bp upstream of the transcription start point (+1), known as -10 and -35 boxes which are recognized by the σ subunit. The sequence of the spacer is not important, but the length is crucial to define the appropriate recognition of the promoter by different domains of the sigma subunit (Campbell *et al.*, 2002; Murakami *et al.*, 2002). Some promoters contain an extended -10 element, which is a motif of 3-4 bp immediately upstream of the -10 element that has been suggested to be important for those promoters that lack -35 or with a poor consensus -10 element (Mitchell *et al.*, 2003; Hook-Barnard *et al.*, 2006). Another functional element that can be present in some promoters is the Up element, a DNA sequence of about 20bp, located upstream of the -35 box. UP elements are widely distributed in bacterial promoter and are the site for interacting with the αCTD of the RNApol, promoting efficient transcription (as revised in Haugen *et al.*, 2008). The presence of the Up element promotes binding of the α subunit of the RNApol to the DNA and greatly stimulating transcription. Another element is the discriminator that refers to the region between the positions -10 and +1 of one promoter. The bp composition of this region might be important for specific regulation of the promoter (see section 1.2.2.3) (Gummesson *et al.*, 2013; Aseev *et al.*, 2014).

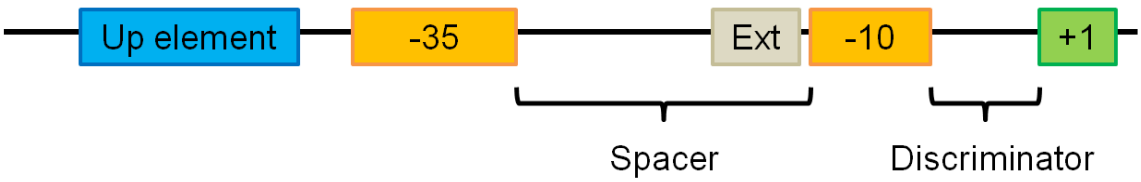

Figure 4: Scheme of the promoter elements recognized by the σ^{70}-like family.

Promoters recognized by the σ^{54}-like family have a different structure and they are composed by two motifs (recognized by the σ subunit) placed at 12 and 24 bp upstream of the transcription start point (+1) (Österberg *et al.*, 2011). Considering that this family of σ subunits were not further studied in this thesis,

little more would be mentioned about them. From now on, we would refer to the σ^{70}-like family and the promoter sequences recognised for them.

Transcription is a cycle that could be divided into three major steps i) promoter binding and initiation, ii) elongation and iii) termination.

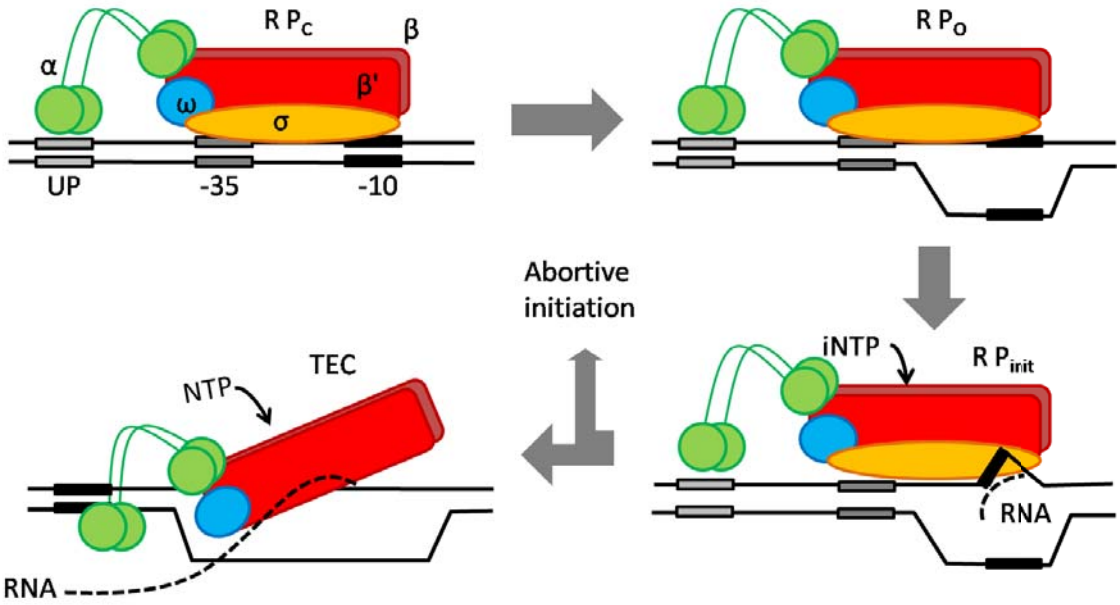

Figure 5: Transcription initiation process step by step (Browning and Busby, 2004; Haugen *et al.*, 2008).

During transcription initiation (**fig. 5**), RNApol binds the promoter forming the closed complex (**fig. 5 RP$_C$**). In this complex, the DNA is still double stranded and the RNApol covers the DNA approximately from −55 to +1, relative to the transcription start site. Next, the open complex (**fig. 5 RP$_O$**) is formed when the DNA strand are separated from −11 to +3, approximately, and the DNA enter into the primary channel (Haugen *et al.*, 2008). In the case of holoenzymes binding the σ^{54} subunit are not able to form open complexes spontaneously and need the presence of assistant proteins (Österberg *et al.*, 2011). Once the formation of the open complex occurs, NTP incorporation drives the transcription reaction forward. However, at most promoters, RNApol synthesizes short abortive products before transitioning to the elongation complex. During the cycles of abortive initiation, the leading edge of the nascent RNA molecule together with the active site of the enzyme move forward, but the contacts between the RNApol and the −35 hexamer remain intact. Both DNA strands in the vicinity of the −10 hexamer are extruded from the primary

channel onto the surface of the holoenzyme during this transition in a process that is called scrunching (**fig. 5 RP_{init}**). It has been proposed that the energy stored in this scrunched intermediate is used to break the interactions between RNApol and the promoter, thereby allowing RNApol to begin the transition to the transcription elongation complex (**fig. 5 TEC**) (Haugen *et al.*, 2008).

Formation of the elongation complex involves the disruption of the contacts between the σ subunit and the core of the RNApol. However, complete detachment of the σ subunit is not obligatory for escaping from the promoter and occurs during the early stages of the elongation process. The detachment is a consequence of a decrease in the affinity of the σ subunit for RNApol (Mooney *et al.*, 2005; Reppas *et al.*, 2006; Pupov *et al.*, 2014). A partially attached σ subunit can cause elongation stalling by binding sequences that mimic -10-elements within DNA that is being transcribed (Murakami *et al.*, 2002; Nickels *et al.*, 2005; Pupov *et al.*, 2014).

The elongation complex (TEC) is much stable and processive as compared to the initiation complex, having a constant elongation rate (Guajardo and Sousa, 1997; Nudler *et al.*, 1997). During elongation, the RNApol-DNA complex can change between an active and inactive state, also called paused state. Not all the transcribing RNApol molecules are stop when a paused signal is encountered, a fraction of the RNApol may be to bypass it. How efficient is the paused signal may depend on several factors: the nucleotide sequence, the specific composition of the RNApol, etc (Landick, 2006). The overall elongation rate of the RNApol is determined by the intrinsic elongation rate and pauses occurring during this process (Bar-Nahum *et al.*, 2005).

During pausing, transcription is only temporarily stalled, and the polymerase will eventually resume elongation. Single-molecules studies of transcription at high temporal resolution revealed that, even at saturating NTP concentrations, bacterial RNApol pauses frequently (once every 100–200 bp) for durations of 1–6 s on average (Adelman *et al.*, 2002; Neuman *et al.*, 2003). Pauses can be induced by certain DNA sequences, DNA lesions and mismatched nascent base pair resulting from a misincorporation event. There are two distinct classes of pausing signals depending on DNA sequences: hairpin-dependent (e.g. *his*

leader pause) and hairpin-independent pauses (e.g. *ops* pause) (Artsimovitch and Landick, 2000). These pauses if became longer-lived may cause rearrangements of RNApol that further slow the rate of pause escape, such as backtracking (Landick, 2006). In fact, it was observed than *ops* pauses are prone to produce backtracking, but not *his* pauses (Artsimovitch and Landick, 2000).

Backtracked RNApol would move backwards along DNA and RNA, producing a detachment of the RNA 3′-end from the active site and extruding it through the secondary channel. Backtracked RNA traps RNApol in an inactive conformation and prevents forward translocation and NTP binding (Martinez-Rucobo and Cramer, 2013). When these pausing occurs the elongation complex does not disassociate from the DNA. Therefore, stalled RNApol might promote conflicts between transcription and replication machinery due to physical collisions that has as a consequence events of DNA instability (Tehranchi *et al.*, 2010).

Pause and backtracking situations could be solved by several factors, such as NusG (Artsimovitch and Landick, 2000) or the Gre factors (GreA and GreB) (Sergei Borukhov *et al.*, 1993) or by the translation process (Dutta *et al.*, 2011). Interestingly, GreA is able to solve only *ops* pauses and backtracked RNApol (Artsimovitch and Landick, 2000).

Elongation continues until the RNApol encounters a termination signal. There are two different classes of terminators, i) the Rho-independent, also known as intrinsic terminator, and ii) the Rho-dependent (Henkin, 2000). The intrinsic terminator is composed of a G+C dyad symmetry element followed by an oligo(T) sequence, so that in RNA it appears as a stable RNA hairpin followed by a run of seven to nine U residues (Nudler, 1999). After TEC reaches the end of the T stretch, it pauses and become irreversibly inactivated due the stable RNA hairpin and finally it falls apart (Gusarov and Nudler, 1999). The Rho-dependent termination requires the binding of the Rho-factor to a *rut* site (Rho utilization) in the nascent mRNA that are 80nt (approximately) C-rich sequences without secondary structures (or weak) (reviewed by Peters *et al.*, (2011)). The binding of Rho to the mRNA is followed by the interaction with the RNApol, but

recent studies showed that Rho may need the presence of accessory proteins, such as NusG, to produce termination (Shashni *et al.*, 2014).

Similarly to the initiation process, elongation and termination are dynamic processes controlled at different levels. As discussed below, genetic regulation during transcription initiation has been highly studied, and several mechanisms of regulation described exist. However, the aim of this project mostly focused is to study some aspects of the regulation during transcription elongation and the effect of pausing over gene expression.

1.1.2. Transcriptional regulation

Bacteria use different strategies to adapt to varying environmental conditions, allowing them to live in a wide range of niches. Unfavourable environmental conditions induce a stress response consisting of a characteristic change in the pattern of gene expression. This stress response helps to protect vital processes, to restore cellular homeostasis and increases the cellular resistance against subsequent stress challenges (Aertsen and Michiels, 2008). But sometimes it is better to run. To ensure survival to stress conditions, bacteria may move by “swimming” using their flagellum, to more favourable location (Mitchell and Kogure, 2006).

Changes in the environmental signals may be sensed by very diverse mechanisms. The cell can sense the presence of determined molecules such as carbohydrates or ions, in the medium by specific receptors (Forst and Roberts, 1994; Deutscher, 2008; Zhao *et al.*, 2008; Richet *et al.*, 2012); can also detect absence of pivotal components, such as amino acids (Magnusson *et al.*, 2005); or can detect the consequence of an alteration in the environment as the detection of denatured proteins in the periplasm due to either high temperatures or hyperosmotic stress (Bianchi and Baneyx, 1999; Ruiz and Silhavy, 2005). Those are some examples of mechanisms related with sensing environment and the response that may induce in the cell is also very diverse. The levels of either small non proteinaceous molecules (Kalia *et al.*, 2013) or proteins may be altered; or some proteins might be modified as a consequence of the detection of changes in the environment (Mascher *et al.*, 2006).

The response to environmental signals in transcription might be mediated by a vast number of regulatory factors which can be classified into two groups attending if they bind or not to the DNA.

- Factors directly interacting with the DNA.

▪ 1.1.2.1. Regulatory proteins: Regulatory proteins could act as repressors or activators. These regulatory proteins restrict their effects to specific promoters by binding to specific DNA sequences that are near to or overlapping the promoter. Usually, activators bind near RNApol, affecting the transcription efficiency. Often after binding of the activator to the DNA, it establish contact with the α subunit facilitating a change in the structure of the double stranded DNA of the promoter (Haugen *et al.*, 2008). Other class of activators might contact with the σ subunit promoting the recruitment of the RNApol to the promoter. Repressors usually prevent binding of RNApol either by occulting the promoter after binding to the vicinity of the −10 and −35 region or by competing for the binding to the UP element (Quinones *et al.*, 2006). Moreover, some repressors act as anti-activators, preventing the function of specific activators. Many promoters are controlled by two or more transcription factors, responding each factor to environmental signals; and producing a coordinated response (Browning and Busby, 2004; Haugen *et al.*, 2008).

▪ 1.1.2.2. Changes in σ subunits: As mentioned in section 1.1.1, *E. coli* contains several σ subunits. The σ^{70} is responsible for expression from most of the housekeeping genes, expressed during exponential-phase growth. Other σ factors are required for the expression of groups of genes required for coordinated response to specific stresses or for the expression of genes functionally related. The different σ subunits compete for binding a limited supply of core RNApol. The output will depend on the concentration of the different σ subunits and its affinity for the core enzyme. This mechanism of regulation has been named as σ subunits competition. Although it has been postulated that the concentration of core enzyme remain constant, the concentration of each σ subunit is subject to variation depending on the cell growth conditions. The intracellular concentration of the σ^{70} subunit is higher in both exponential and stationary phases, as well as under various stress

conditions. In exponential-phase cells, two of the alternative σ subunits, σ^N and σ^F, are present in significant concentrations, but, the level of σ^S only becomes detectable in stationary phase of growth. Among the seven σ subunits from *E. coli*, σ^{70} has the highest affinity to the core enzyme. *In vitro* experiments has shown that the affinities of the other six σ subunits ranged downwards from σ^{70} to σ^S, which has the weakest binding activity (Ishihama, 2000). However, it has been shown *in vivo* that ppGpp is required for the subunits σ^S, σ^{32}, σ^{54} to bind to the core RNApol (Jishage *et al.*, 2002; Laurie *et al.*, 2003). There are other factors that might interfere in the competition of the different σ subunits with the RNApol. The affinity might be altered by the presence of certain molecules such as alarmones and the concentration of functional σ subunits might be importantly affected by the presence of anti-sigma and anti-anti-sigma factors (Alba and Gross, 2004; Magnusson *et al.*, 2005; Barembruch and Hengge, 2007).

- 1.1.2.3. DNA topology: The bacterial chromosome is a circular DNA, which is in a supercoiled conformation. In fact the supercoiling, as well as the interaction with several proteins, is necessary for the compaction of the bacterial genome to form the nucleoid. It has been suggested that the gene expression might depend on the topological state of the promoter prior to the RNApol binding and consequently affecting transcription initiation. Moreover, DNA topology could influence transcription elongation and termination. Topoisomerases and gyrases would reduce or increase the supercoiling of the DNA, but also the binding of different nucleoid-associated proteins could affect DNA topology. It has been observed that several factors could vary the amount of topoisomerases or gyrases, producing changes on the DNA topology and as a consequence to the gene expression (reviewed in Travers and Muskhelishvili, 2005).

E. coli contains several nucleoid-associated proteins such as Fis, IHF, H-NS, StpA or Dps. Although most of these proteins bind to DNA non-specifically, some bind with weak specificity occupying sites distributed throughout the chromosome. The binding of these proteins to the DNA, and the resulting folding of the bacterial chromosome, affects the distribution of RNApol between

promoters, influencing transcription, causing activation or repression, depending on the context of their binding sites (Browning and Busby, 2004).

- Regulators that not bind to DNA.

▪ 1.1.2.4. sRNA: The major role for sRNA is to regulate gene expression at post-transcriptional level, affecting mRNA translation or stability. However, 6S RNA inhibits transcription by binding directly to the active site of RNApol, blocking the access to promoter DNA and being used as a template for transcription. This sRNA regulates some σ^{70}-dependent genes (Wassarman, 2007).

▪ 1.1.2.5. Anti-sigma factors: An anti-σ factor has the ability to form complex with a determined σ subunit and thereby inhibiting its function (Ishihama, 2000). Several anti-sigma factors had been described for the different σ subunits in *E. coli* (**fig. 6**). Two classes of anti-sigma factors were defined: i) the cytoplasmatic anti-sigma factors and ii) the inner-membrane-bound anti-sigma factors (Treviño-Quintanilla *et al.*, 2013).

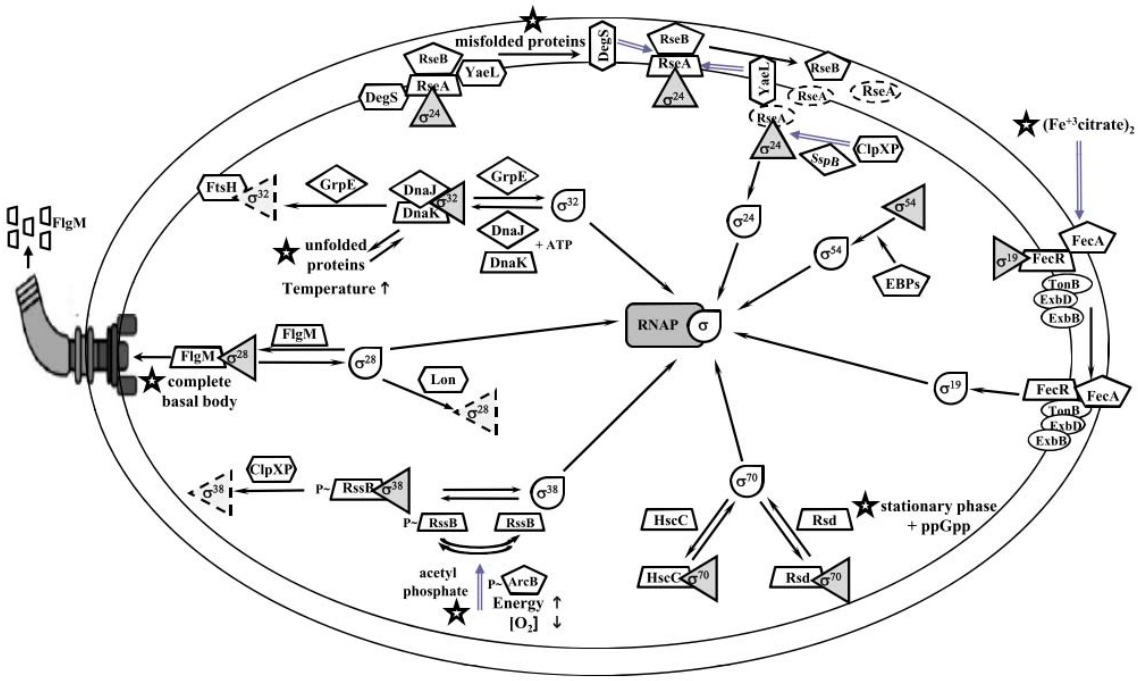

Figure 6: Regulation of σ factors by anti- σ factors in *E. coli*. The forms in figure represent: tear (σ factor active form), solid triangle (σ factor inactive form), dashed triangle (σ factor degraded form), star (environmental signal that releases the σ factor), trapezoid (anti- σ factor), pentagon (anti-sigma factor sensor or modulator), solid ellipse (transducer signal complex), hexagon

(protease), rhombus (chaperone), dashed ellipse (any protein in degraded form), and rounded rectangle (RNApol core). Adapted from Treviño-Quintanilla *et al.*, (2013).

In *E. coli* anti-sigma subunits have been discussed for all the σ^{70}-like subunits. Next, I will briefly discus the mechanisms of action for the different anti-sigmas.

The subunit σ^{70} has two anti-sigma factors, Rsd and HscC, acting during stationary phase and heat shock, respectively (Treviño-Quintanilla *et al.*, 2013). It has been described that Rsd binds to σ^{70}, avoiding its association with the RNApol (Jishage and Ishihama, 1998; Ishihama, 2000). The amount of Rsd increases at stationary phase respect exponential phase, as well as its ability to bind to σ^{70} (Piper *et al.*, 2009). HscC forms a complex with σ^{70} and it has been shown that overexpression of HscC produces a decrease of σ^{70}-dependent activity. *In silico* studies suggested that *hscC* is under control of two promoters, a σ^{70} and a σ^{32}-dependent promoter, suggesting that its expression would increase during heat shock (reviewed in Treviño-Quintanilla *et al.*, (2013)).

RssB is an anti-sigma factor that plays a critical role in the control of cellular to σ^{S} levels in *E. coli* (**fig. 6**). When RssB is phosphorylated, it is able to bind to σ^{S} and promote its degradation by the protease ClpXP. It has been suggested that the two-component system ArcB/ArcA, monitoring both the oxygen and energy supplies, are the responsible of the phosphoylation of RssB. Once the cell enters in stationary phase, σ^{S} concentration increases above that of non-phosphorylated RssB, allowing σ^{S} to bind to the RNApol core (reviewed in Treviño-Quintanilla *et al.*, (2013)).

During optimal growth conditions, the chaperones DnaJ, DnaK and GrpE form a complex with σ^{32}, preventing its binding to the RNApol core, and promoting its degradation by the protease FtsH (**fig. 6**). But under heat shock conditions, the chaperones DnaJ, DnaK and GrpE would bind unfolded proteins, releasing σ^{32} and allowing its binding to the RNApol core (reviewed in Treviño-Quintanilla *et al.*, (2013)).

The alternative σ^{E}, essential in *E. coli* (Connolly *et al.*, 1997), is responsible for the response to envelope or extracytoplasmic stress after detection of unfolded proteins in the periplasm (Alba and Gross, 2004). Under no-stress conditions, the inner-membrane-bound anti-sigma factors RseA binds to σ^{E}, avoiding its

binding to the RNApol (**fig.6**). Unfolded proteins –accumulated during heat shock (Rouvière *et al.*, 1995), hyperosmotic stress (Bianchi and Baneyx, 1999) or other stresses – interact with the membrane protein DegS, activating its protease activity and causing degradation of RseA. The σ^E subunit will be liberated and able to interact with the RNApol and induce gene expression changes (Alba and Gross, 2004).

The anti-sigma factor FlgM binds to FliA (σ^F) and prevents its association with the RNApol inhibiting transcription of several flagella genes (**fig. 6**). However, when the basal body and motor structure is formed, FlgM is secreted through the basal body of the flagella and σ^F get free to bind the RNApol and induce transcription of several flagella genes, such as *fliC*, coding for the main subunit of flagella (Chevance and Hughes, 2008).

The expression of *fecABCDE* (under the control of the subunit σ^{19}) is activated during iron starvation with the presence of ferric citrate. The anti-sigma factor FecR, anchored in the cytoplasmic membrane, bind σ^{19} during normal conditions. The presence of ferric citrate is sensed by FecA that contact FecR, producing the liberation of σ^{19}.

The subunit σ^{54} does not have an anti-sigma factor, but it requires the presence of assistant proteins to form the open complexes, as previously mentioned.

- 1.1.2.6. Alarmones: Alarmones, or secondary messengers, are low molecular weight non-proteinaceous molecules that control and modify gene expression, affecting a vast range of genes. Environmental signals would produce changes on the amount of these secondary messengers by acting over the proteins responsible of its synthesis or degradation (Pesavento and Hengge, 2009; Kalia *et al.*, 2013).

In *E. coli* it has been described several alarmones, but the most important ones are cAMP, c-di-GMP and ppGpp. The levels of cAMP increases in absence of glucose, binding to CRP, and producing changes on the gene expression pattern (Deutscher, 2008). Several environmental factors stimulate the production of c-di-GMP that would affect the expression of several genes involved in motility and biofilm formation (Kalia *et al.*, 2013). The alarmone

ppGpp is produced during amino acid starvation and is able to produce its effect, mainly binding into the catalytic centre of the RNApol (Cashel *et al.*, 1996; Magnusson *et al.*, 2005). This alarmone will be more extensively described below.

- 1.1.2.7. Regulation through the secondary channel of the RNApol: The structural study of the RNApol determined a space between the subunits β and β' – known as secondary channel (**fig. 3**) – that connects the cytoplasm with the catalytic centre, suggested initially as the entrance for nucleotides (Landick, 2005; Stepanova *et al.*, 2010). It has been described that the alamone ppGpp, as well as several proteins, such as GreA, GreB or DksA, enter inside the secondary channel and interact directly with the catalytic centre of the RNApol (Browning and Busby, 2004; Haugen *et al.*, 2008; Lamour *et al.*, 2008; Blankschien *et al.*, 2009). The swap between the different factors that bind to the secondary channel of the RNApol could produce changes in the expression pattern. This regulation would be more extensively studied during this thesis.

1.2. Factors that bind into the secondary channel

In *E. coli,* several factors, the alarmone ppGpp and several proteins, have the ability to interact into the secondary channel of the RNApol and consequently affecting its activity (**fig. 7**) (Browning and Busby, 2004; Haugen *et al.*, 2008; Lamour *et al.*, 2008; Blankschien *et al.*, 2009; Stepanova *et al.*, 2010). The proteins that bind into the secondary channel of the RNApol include homologous and unrelated low-molecular-weight proteins with similar spatial organization. The three-dimensional structure of those proteins is adapted to bind into the secondary channel of the RNApol. They have a domain that enters inside the channel and interact with the active site of the RNApol, and a second domain that remains outside the secondary channel. These proteins are GreA, GreB (Sergei Borukhov *et al.*, 1993), DksA (Perederina *et al.*, 2004) and Rnk (Lamour *et al.*, 2008), in *E. coli*. These proteins are also detected in other Enterobacteria such as *Salmonella.*

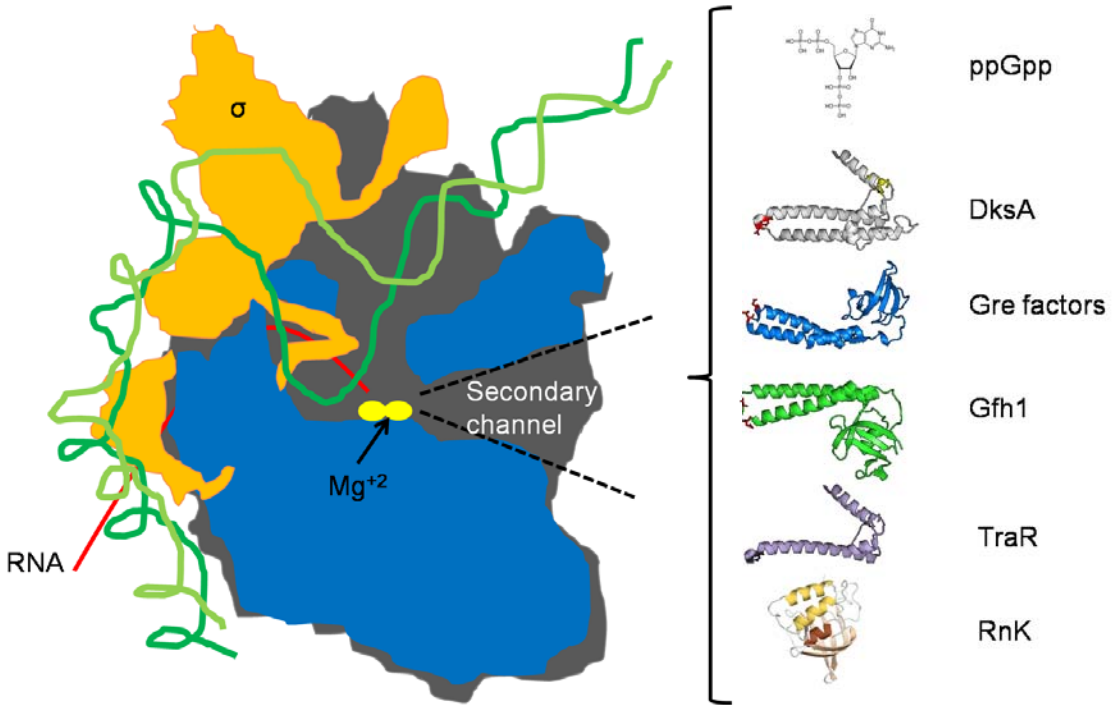

Figure 7: Factors that bind into the secondary channel of RNA polymerase. Adapted from (Haugen *et al.*, 2008; Lamour *et al.*, 2008; Blankschien *et al.*, 2009)

Moreover, it has been described the presence of proteins that bind to the secondary channel in some conjugative plasmids, such as F plasmid in *E. coli* or pSLT in *Salmonella*, the protein TraR (Blankschien *et al.*, 2009), as well as

the presence of similar proteins in other bacteria, such as Gfh1 of *Thermus thermophilus*. A section of this thesis is denoted to discuss the existing diversity of those proteins from a phylogenetic perspective.

The fact that several proteins can bind to the same target producing different effects suggest that there should be a competence between the different factors for binding the secondary channel of RNApol with consequences in the functionality of the holoenzyme. In the following sections, different factors interacting with the secondary channel of the RNApol are introduced.

1.2.1. GreA, a transcription elongation factor

In *E. coli*, two proteins, GreA and GreB (**fig. 8**), interact with the secondary channel of RNApol suppressing arrest situation or pause during transcription that could cause premature termination (Laptenko *et al.*, 2003). GreA was described as a suppressor of the negative effect in the growth at high temperature produced by the RNApol mutation S522F at the β subunit in *E. coli* (Sparkowski and Das, 1991). Therefore, from the beginning its possible interaction with the RNApol was detected.

Moreover it has been described that a mutant lacking both proteins, GreA and GreB, is not able to grow at high temperature (42ºC) (Trautinger and Lloyd, 2002), suggesting that these factors are essential for the transcription process under this conditions, due to its anti-pause effect.

GreA and GreB show a high structural homology among them, and also with DksA. GreA is a low-molecular-weight protein, 17.5 kDa (158 amino acids), with 2 domains: a N-terminal coiled-coil (CC) domain, that is formed by two antiparalel α-helix linked by a turn; and a C-terminal globular domain that contains a β-barrel structure with an α-helix (**fig. 8**). Both domains are linked by an interdomain flexible linker (Sparkowski and Das, 1990; Stebbins *et al.*, 1995). It has been determined that the coiled-coil domain enters inside the secondary channel of the RNApol, being responsible of the RNA cleavage and antipause activity, while the globular domain remains outside, being responsible of the binding of GreA to the RNApol (Koulich *et al.*, 1998). The coiled-coil domain contains two residues, D41 and E44 (**fig. 8**), that interact directly with

the Mg^{+2} ion of the catalytic centre (cMG1) and has been described as responsible of the antipause activity of GreA (Opalka *et al.*, 2003; Laptenko *et al.*, 2003).

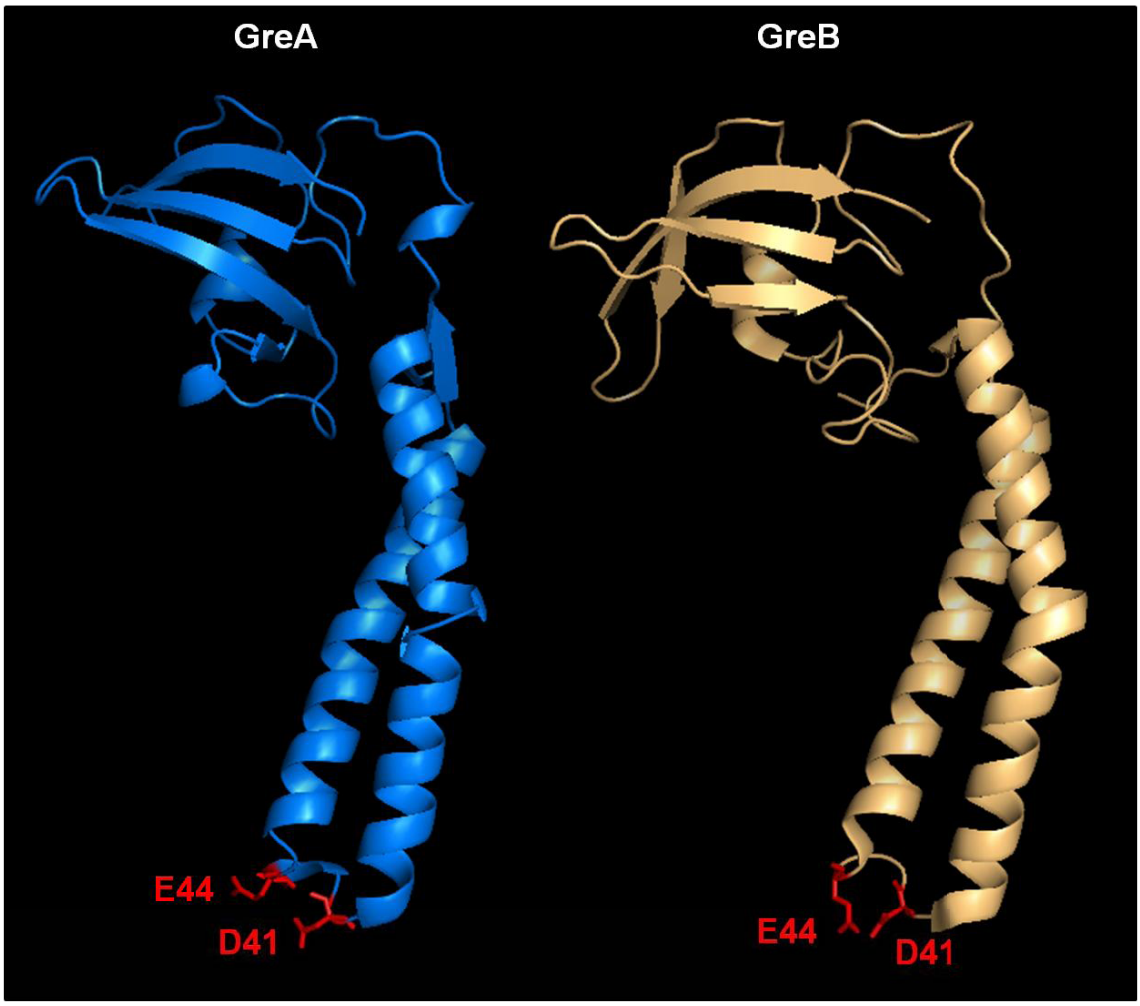

Figure 8: Structure of the Gre factors. GreA is indicated in blue and GreB in pale orange. The residues D41 and E44 are indicated in red.

Studying the charge distribution around the surface of GreA and GreB, a remarkably asymmetry was observed in both proteins. One face of the GreA protein is strongly acidic, whereas the opposite face is neutral. This asymmetry in the charge distribution is more dramatic in GreB: while one face of GreB is acidic, the opposite face is strongly basic (Koulich *et al.*, 1997). This basic area on GreB, not present in GreA, is hypothetically responsible for GreB affinity to the RNApol, as well as its activity (Kulish *et al.*, 2000).

The binding of GreA to the secondary channel restores backtracked RNApol, as described in section 1.1.1, by inducing the intrinsic endopyrophospholytic

activity of the RNApol to cause the hydrolytic removal of the 3'-proximal segment of the nascent RNA (Orlova *et al.*, 1995). It has been observed that GreA is able to solve hairpin-independent pauses (e.g. *ops* pause), but not those dependent of hairpin (e.g. *his* pause) (Artsimovitch and Landick, 2000). Although both Gre factors (GreA and GreB) had similar activity, and it has been observed that the absence of one factor could be substituted by the other, the cleavage produced by GreA and GreB is different. GreA-induced cleavage yields di- and trinucleotide products, whereas GreB stimulates the accumulation of excised products in a much wider size range (2–18 nucleotide long RNAs; (Sergei Borukhov *et al.*, 1993; Kulish *et al.*, 2000)). Moreover, Gre factors remove misincorporated nucleotides and thus may contribute to transcription proofreading and fidelity, by a cleavage reaction (Shaevitz *et al.*, 2003; Zenkin *et al.*, 2006).

In order to determine the effect of Gre factors on the physiology cell, several analysis have been performed showing that while cells lacking GreB are virtually indistinguishable from WT cells, *greA* mutants exhibit several growth defects, including sensitivity to salt and divalent metal ions (Susa *et al.*, 2006). Moreover, transcriptomic studies of double mutant *greA greB* compared with simple mutant *greB* and under conditions of overexpression of GreA, showed that GreA is required for the expression of several genes like ribosomal proteins or genes associated to cellular respiration and energy metabolism, suggesting that transcript cleavage by GreA contributes to optimal expression levels of those genes *in vivo* (Stepanova *et al.*, 2007). Moreover there are several genes related with metabolism and stress response that are down-regulated by GreA, most of them only under overexpression conditions. However GreA does not inhibit transcription from the corresponding promoters *in vitro*, suggesting that the observed inhibitory effect of GreA is indirect and may depend on additional factors (Stepanova *et al.*, 2007).

Apart of its role in RNA cleavage, it has been described that GreA has activity as chaperone. It has been shown that GreA is able to suppress the heat-induced aggregation of proteins and promotes reactivation of denatured proteins in *E coli*. Moreover, overexpression of GreA promotes survival during heat shock and oxidative stress (Li *et al.*, 2012). These data suggests that GreA

not only has a role on genetic expression controlling transcription elongation, but also at post-transcriptional processes, affecting protein stability.

1.2.2. The alarmone ppGpp

Guanosine tetra- and penta-phosphate – known as (p)ppGpp – is a modified nucleotide that acts as alarmone in bacteria (**fig. 9A**). Although being discovered in *E. coli*, it is not restricted to Gram negative bacteria. It can be found in Gram positive, and even in the chloroplasts of plant cells (Braeken *et al.*, 2006; Atkinson *et al.*, 2011). RelA and SpoT are the enzymes involved in the turnover of ppGpp in *E. coli* (**fig. 9B**). The amount of ppGpp will fluctuate in response to several environmental signals. As discussed below in more detail, the RelA-mediated ppGpp synthesis is an ATP:GDP/(GTP) pyrophosphoryl group transfer of the β,γ-phospates from the ATP donor to the ribose 3' hydroxyl group of the acceptor nucleotides (GDP or GTP). This reaction only uses dATP as a donor among the eight common ribo- and deoxyribonucleosides triphosphates, and as acceptor GTP/GDP or even ITP but not pyrimidine nucleotides, deoxypurine nucleotides, or ATP. According to the cellular pool of GTP / GDP and having in consideration that RelA had the same affinity for both nuclotides, pppGpp is the most likely product *in vivo* (Cashel *et al.*, 1996).

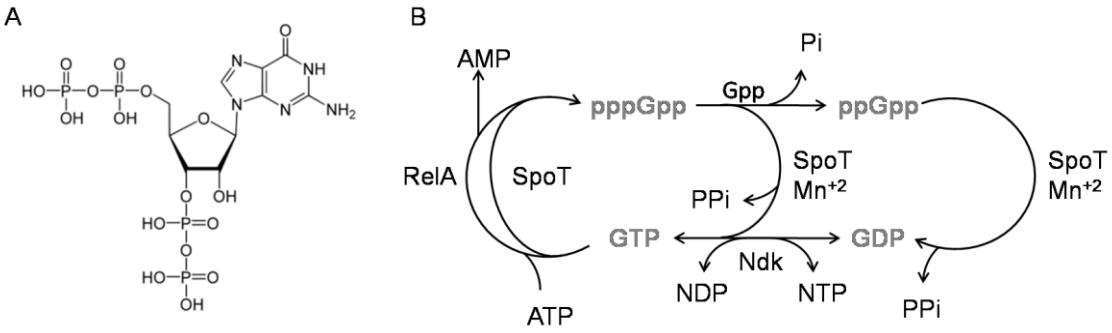

Figure 9: Structure, synthesis and degradation of ppGpp. A) Molecular structure of ppGpp. B) Synthesis and degradation of ppGpp. Adapted from Cashel *et al.*, (1996)

SpoT is a bifunctional enzyme (**fig.9 B**) possessing both (p)ppGpp 3'-pyrophosphohydrolase activity (degradation) as well as 3'-pyrophosphotransferase (synthesis) with GTP as acceptor, but it has higher activity as hydrolase than transferase. Its hydrolase activity requires Mn^{+2} and is further stimulated by Mg^{+2}. It has been described that *relA* and *spot,* present in

γ- and β- proteobacteria, evolved via gene duplication of a bifunctional ancestral gene known as *rel* and found in many bacterial groups. These data suggest that *relA* had lost the hydrolase activity (Cashel *et al.*, 1996; Atkinson *et al.*, 2011). In *E. coli*, the double mutant Δ*relAspoT* is denominated ppGpp^0; indicating that it is not able to produce ppGpp under any condition.

There are other genes involved in the turnover of (p)ppGpp (**fig. 9 B**) such as *gpp* and *ndk*. Gpp is a pppGpp γ-phosphohydrolase, responsible of the degradation of pppGpp to ppGpp. Modifications on the activity of this enzyme would produce variations in the relative amount of pppGpp and ppGpp and it has been described that they could produce different effects in the cell, being more active ppGpp than pppGpp (Travers and Muskhelishvili, 2005; Mechold *et al.*, 2013). Ndk is a nucleoside diphosphate kinase that produces conversion of GDP to GTP and vice versa in order to regenerate the principal substrates for pppGpp synthesis (Cashel *et al.*, 1996).

It has been described that (p)ppGpp levels increases dramatically at stationary phase (**fig. 10**) and after that there is a decrease, reaching a steady-state plateau (Cashel, 1969). The peak of ppGpp coincides with the interphase between exponential and stationary phase. Experiments under amino acid starvation showed a simultaneous reduction of the amount of stable RNA (tRNA and rRNA).

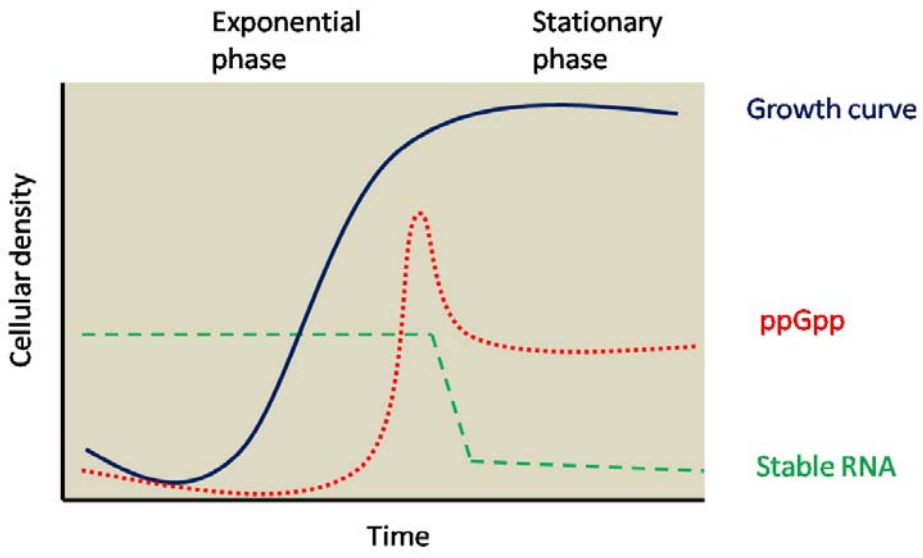

Figure 10: Effect of growth phase on the amount of (p)ppGpp (in red) and stable RNA (in green). Adapted from (Cashel, 1969; Ryals *et al.*, 1982)

This regulatory relationship between amino acid availability and stable RNA accumulation was termed stringent control. The amount of stable RNA could be restored in mutants termed “relaxed” (Neidhardt, 1964). Studies determining the amount of nucleotides during amino acid starvation showed a significant increase in the levels of ppGpp (Cashel, 1969) and that this increase of ppGpp was not observed in “relaxed” mutants. The relaxed mutants, were mutants in the *relA* gene, the synthetase of ppGpp under amino acid starvation. Moreover, ppGpp is produced not only in response to amino acid limitation but also in response to many different kinds of nutrient limitations and circumstances that cause growth arrest, such as stationary phase (Cashel *et al.*, 1996).

During amino acid starvation, uncharged tRNA placed in the ribosomal A-site produces a pause of translation with stalled ribosomes, stimulating RelA binding (Cashel *et al.*, 1996) (**fig. 11**).

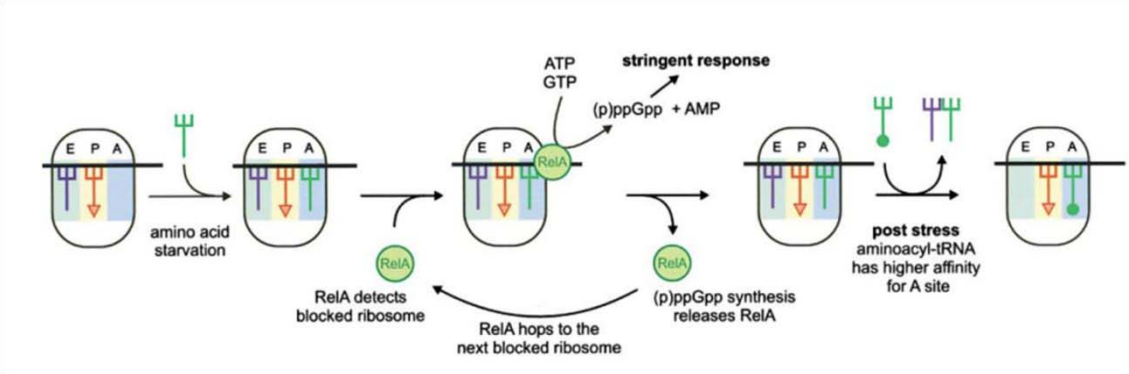

Figure 11: Mechanism of RelA-mediated (p)ppGpp synthesis. Adapted from Wendrich *et al.*, (2002).

RelA interacts with the ribosomal protein L11 (coded for the gene *relC*) of the 70S subunit and this interaction induces (p)ppGpp synthesis simultaneously with its release from the ribosome. RelA “hops” to the next stalled ribosome, and the induction of (p)ppGpp synthesis is repeated. The intracellular high levels of (p)ppGpp will promote an intense change in the gene expression pattern, known as the stringent response (Wendrich *et al.*, 2002). Charged / uncharged tRNA ratios can be continuously sensed by the demands of the active population of mRNA codons for translation, and modification of this ratio would produce changes in the ppGpp levels. Recently it has been shown that the cell respond differently depending on the intracellular concentration of

ppGpp. Amino acid starvation produces an initial increase of ppGpp levels that would induce an early response to solve it by activating the Lrp regulon. If this early response is not able to solve the amino acid starvation, the amount of ppGpp would further increase and produce the stringent response (Traxler *et al.*, 2011).

The mechanism behind SpoT-dependent production of ppGpp and how SpoT senses starvation conditions is not well defined. The protein SpoT is able to bind CgtA that bind to 50S of ribosomes suggesting that SpoT, similarly to RelA, is able to interact with ribosomes (Jiang *et al.*, 2007). Moreover, CgtA affects the ratio ppGpp / pppGpp in response to amino acid deprivation (Persky *et al.*, 2009). It has been suggested that uncharged tRNA inhibits ppGpp hydrolysis (Richter, 1980). Nevertheless, it appears that SpoT-mediated synthesis of ppGpp respond mostly to stresses others than amino acid starvation (Cashel *et al.*, 1996; Magnusson *et al.*, 2005).

The protein SpoT is able to sense fatty acid starvation and consequently activate the ppGpp production (Battesti and Bouveret, 2006; Potrykus and Cashel, 2008). In absence of fatty acids, the acyl carrier protein (ACP) binds to SpoT, activating the synthesis of ppGpp.

The alarmone ppGpp interact with the RNApol by binding within its active site, located into the secondary channel, between the β and β' subunits (**fig. 3**). As discussed above, the active site contains 4 Mg^{+2} ions, two catalytic ions, (cMG1 and cMG2), and two ions that bind ppGpp (pMG1 and pMG2). In the interaction with the RNApol, three different zones of the ppGpp molecule can be differentiated: i) proximal diphosphate, respect to the distance of the catalytic centre, binding β and β' residues as well as pMG1, ii) the distal diphosphate that bind to β' residues and the pMG2 and iii) the guanosine base, enters into a cavity on the RNApol surface but this contact do not produce an specific recognition of the guanosine base or restrict its orientation, allowing that ppGpp could change its orientation (Artsimovitch *et al.*, 2004). It has been described that the binding of ppGpp to the RNApol produces conformational changes varying the stability of the open complex (**fig.5 RP_O**) (Magnusson *et al.*, 2005; Potrykus and Cashel, 2008).

1.2.2.1. The stringent response

The increase of ppGpp produces relevant changes in the gene expression pattern promoting the rearrangement of the expression profile to pass from actively growing cells (exponential phase) to cells that need to adapt and survive different environmental stress (stationary phase), known as stringent response (**fig. 12**). The alarmone ppGpp has a pleiotropic effect over transcription expression.

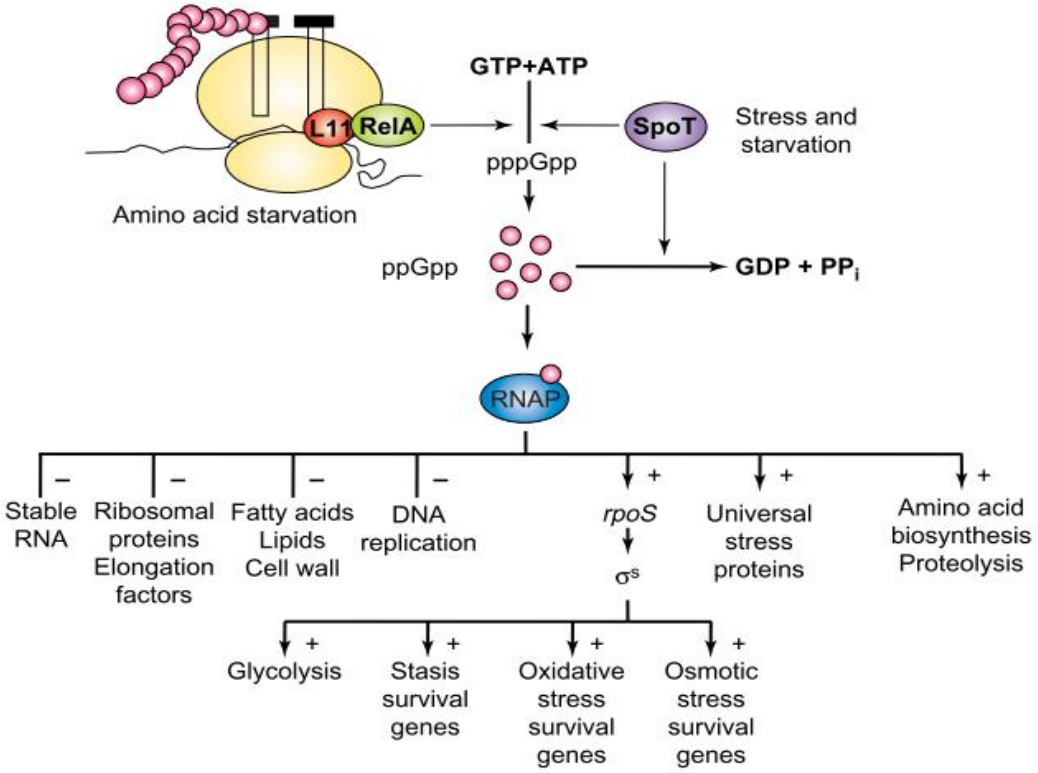

Figure 12:Scheme of the stringent response adapted from Magnusson *et al.*, (2005)

During stringent response, there is a decrease of cellular functions related to bacterial growth while it stimulates genes related with survival to different stress situations. Apart from the stable RNA, ppGpp represses the synthesis of ribosomal proteins, elongation factors, fatty acids and lipids, cell wall production and DNA replication. Direct negative effects of ppGpp on promoters have been detected *in vitro* and several mechanisms for direct negative regulation by ppGpp have been suggested, such as the destabilization of the RNAP–promoter open complex. The rRNA promoters form intrinsically unstable open complexes with RNAP and are therefore thought to be specifically sensitive to

further destabilization mediated by ppGpp. However, an unstable open complex is not an absolute requirement for negative regulation by ppGpp because direct negative effects have also been detected on promoters that form apparently very stable open complexes (Magnusson *et al.*, 2005).

It has also been suggested that ppGpp could compete with the NTPs to bind to the active centre, inhibiting hence gene transcription (Jöres and Wagner, 2003). Moreover, *in vitro* experiments had suggested that ppGpp could have a negative effect over gene expression due delays during promoter escape process. Different possible mechanisms for negative regulation by ppGpp are not exclusive and might be working in concert to exert negative regulation.

The alarmone ppGpp may also act as positive regulator. The expression of a very huge set of genes related with amino acid biosynthesis, proteolysis, and resistance of different types of stress, is induced in a ppGpp-dependent manner upon growth arrest (**fig. 12**). It has been shown that ppGpp regulates the differential binding abilities of sigma factors to the core RNApol (Magnusson *et al.*, 2005; Costanzo *et al.*, 2008; Lemke *et al.*, 2009; Gopalkrishnan *et al.*, 2014). Apart of affecting the activity of the alternative sigma factors or its affinity for RNApol, it has been shown that ppGpp might affect the stability of some σ subunits. During cell proliferation, σ^S is synthesized but rapidly degraded by ClpXP protease, but σ^S become stabilized upon entry into stationary phase, probably when binds to RNApol (as described in section 1.1.2.5.). However, ClpXP does not directly recognize the protein; due it requires the binding of RssB. The alarmone ppGpp promotes σ^S protein stability by inducing expression of the anti-adaptor proteins IraP and IraD, which bind RssB (Bougdour and Gottesman, 2007; Merrikh *et al.*, 2009). Although less is known about the mechanism for direct positive regulation by ppGpp than about the mechanism for negative regulation, it has been proposed that the destabilization of the open complex actually helps promoter-escape and transcription initiation from very stable promoters, such as the promoters present in several ppGpp-stimulated genes (Magnusson *et al.*, 2005).

In addition to the proposed direct mechanisms for ppGpp action, other models suggest that ppGpp acts indirectly, perhaps through changes in the availability

of RNApol. During exponential phase, a major part of the RNApol transcribes operons that code for stable RNA (tRNA and rRNA). In optimal growth conditions, up to an 80% of the RNApol might be transcribing those genes (Neidhardt and Curtis, 1996). But at stationary phase, the levels of ppGpp would increase producing an inhibition of the expression of the stable RNA operons, liberating a huge amount of RNApol, that would transcribe other genes such as genes involved in amino acid biosynthesis (Magnusson *et al.*, 2005).

1.2.2.2.Phenotype of the ppGpp-deficient mutants

As described before, RelA-mediated stringent response is induced by an increase in the level of uncharged tRNAs during amino acid starvation, and as a consequence ppGpp produces stimulates the expression of amino acid biosynthesis genes. Therefore, $ppGpp^0$ mutants are not able to grow on minimal media due to its incapacity to synthesize amino acids, becoming auxotrophic at minimal media (H Xiao *et al.*, 1991; Vinella *et al.*, 2012). Interestingly, suppressor mutants have been isolated, meaning $ppGpp^0$ mutants able to grow in minimal media, and the mutations mapped in the β and β' subunit (Xu *et al.*, 2002; Murphy and Cashel, 2003; Harinarayanan *et al.*, 2008), in the vicinity of the secondary channel, suggesting that the binding of ppGpp to the RNApol produces conformational changes, as previously mentioned.

The effect of ppGpp over alternative σ subunits competition would produce different sensibility to several stress conditions due the lack of stimulation of several stress response genes, like *rpoE* regulon (Costanzo *et al.*, 2008; Gopalkrishnan *et al.*, 2014). Moreover it has been described that ppGpp is required for UV survival (McGlynn and Lloyd, 2000; Trautinger *et al.*, 2005).

Deficiency of ppGpp also produces an enlargement of bacterial cells, producing filamentation (Traxler *et al.*, 2008; Aberg *et al.*, 2009), possibly because of the involvement of ppGpp to cellular division affecting FtsZ (Navarro *et al.*, 1998; Magnusson *et al.*, 2005).

Due to its pleiotropic effect, the ppGpp deficiency of causes several phenotypes affecting different cellular functions (Cashel *et al.*, 1996; Magnusson *et al.*, 2005). It has been observed using transcriptomic studies that over 265 genes of

E. coli, distributed among a broad range of cellular functions, are significantly affected in a ppGpp deficient strain in cultures grown in rich medium (LB) (Aberg *et al.*, 2009). However, transcriptomic studies performed during isoleucine starvation, showed that ppGpp regulates significantly (up to 2-fold) over 1400 genes (Traxler *et al.*, 2008). Several studies has been performed in other enterobacteria, such as *Salmonella enterica*, using RNAseq (Ramachandran *et al.*, 2014) showing a vast effect of ppGpp over gene transcription (Pizarro-Cerdá and Tedin, 2004; Song *et al.*, 2004; Thompson *et al.*, 2006). Among the different cellular functions affected by ppGpp it has been shown that ppGpp, as an stress-related secondary messenger, deeply affects expression of virulence related genes. In fact, it has been described that ppGpp is essential for transcription of virulence factors in several pathogens (Dalebroux *et al.*, 2010): *Mycobacterium tuberculosis* (Primm *et al.*, 2000)*, Listeria monocytogenes* (Taylor *et al.*, 2002)*, Legionella pneumophila* (Hammer and Swanson, 1999; Zusman *et al.*, 2002)*, Vibrio cholera* (Haralalka *et al.*, 2003; Oh *et al.*, 2014)*, Pseudomonas aeruginosa* (Erickson *et al.*, 2004)*, Campylobacter jejuni* (Malde *et al.*, 2014)*, Escherichia coli* (Aberg *et al.*, 2006; Aberg *et al.*, 2008) or *Salmonella enterica* (Pizarro-Cerdá and Tedin, 2004).

1.2.2.3. Influence of the promoter discriminator in ppGpp-mediated regulation

It has been observed that the discriminator sequence of the promoters (sequence from -10 to +1, **fig. 4**) could be important for direct regulation by ppGpp (Gummesson *et al.*, 2013). It has been postulated that many genes which are repressed by ppGpp have a GC rich discriminator whereas many ppGpp-stimulated operons have an AT rich discriminator. The GC rich motif on the discriminator of P2-*rrnB* promoter is essential for ppGpp inhibition of rRNA promoter during amino acid starvation or stationary phase (Zacharias *et al.*, 1989). Similar results has been observed with the promoter of the operon *rpsB-tfs* (Aseev *et al.*, 2014). However, the AT rich motif on the discriminator of *his* promoter is required for ppGpp stimulation during amino acid starvation (Da Costa and Artz, 1997). Moreover, the promoters of the *usp* genes, encoding the universal stress proteins UspA, -C, -D, -E, -F, and -G, are strongly stimulated by ppGpp during stringent response. It has been found that the 5-bp AT-rich discriminator region immediately downstream from the P*uspA*−10 element is

required for positive control by ppGpp. Swapping the AT-rich P*uspA* discriminator for a GC-rich, produces a switch on the regulation by ppGpp, repressing P*uspA* (Gummesson *et al.*, 2013). These data suggest that direct negative and positive regulation produced by ppGpp depends on the discriminator sequence of the promoter.

The discriminator element defines the stability of the open complex. As mentioned in section 1.2.2.1., a proposed direct mechanism of ppGpp repressing transcription is by inducing collapse of instable open complexes. Therefore genes with a G-C discriminator are potential targets for ppGpp mediated repression. On the other hand, the presence of A-T rich discriminators makes the open complex extremely stable. In this case the presence of ppGpp might promote expression from this promoter by destabilizing the complex and inducing promoter escape.

1.2.2.4 ppGpp mediated mechanism of regulation not-related with the RNApol

Apart from binding to the RNApol, it has been suggested that ppGpp could affect other regulators by binding or interacting with them (Dalebroux and Swanson, 2012). Several examples of this kind of regulation has been described: Inhibition of DNA replication in *S. aureus* by DnaG (Rymer *et al.*, 2012; Maciąg-Dorszyńska *et al.*, 2013), acid tolerance in *E. coli* by LdcI or virulence regulation in *S. enterica* Typhimurium by SlyA (Dalebroux and Swanson, 2012).

DNA replication is carried out by a dynamic, multi-protein complex known as the replisome. The protein DnaG is responsible for catalyzing primer synthesis during DNA replication. In *S. aureus* the replication is inhibited by ppGpp due to its binding to DnaG and blocking its primase activity (Rymer *et al.*, 2012). Similar results were obtained in *E. coli* (Maciąg-Dorszyńska *et al.*, 2013).

Cytoplasmic LdcI (lysine decarboxylase, also known as CadA) of *E. coli* is induced in response to acid stress and is crucial for survival in low-pH environments. LdcI increases the cytoplasmic pH by decarboxylation of L-lysine to cadaverine. It has been described that ppGpp bind to LdcI, being important for enzyme activity. At mildly acidic conditions meaning an extracellular pH of

4–5, or a cytoplasmic pH of 6–7, ppGpp acts as an allosteric inhibitor of LdcI. In extremely acidic conditions, LdcI continues converting lysine to cadaverine despite the binding of ppGpp to ensure cell survival. (Kanjee *et al.*, 2011).

After phagocytosis, *S. enterica* serovar Typhimurium activates the two-component virulence regulatory system PhoPQ that would induce *slyA.* Moreover, SlyA is required to control the transcription of genes essential for virulence in *S. enterica* serovar Typhimurium (Fass and Groisman, 2009). SlyA requires ppGpp to dimerize and bind to the DNA (**fig. 13**) (Zhao *et al.*, 2008).

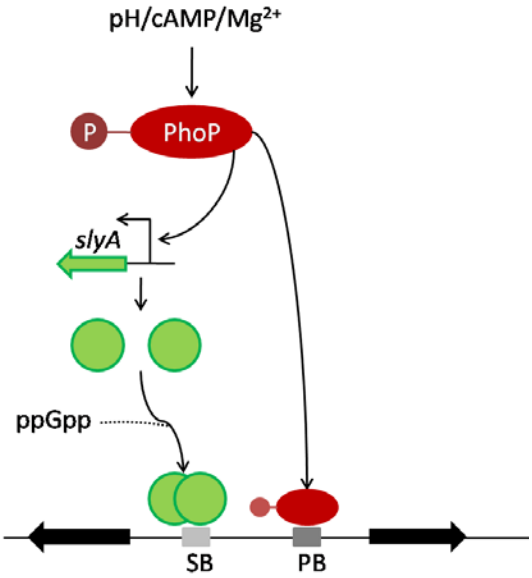

Figure 13: Scheme of the effect of ppGpp on the regulation of genes regulated by SlyA and PhoPQ system. Adapted from Zhao *et al.*, (2008)

1.2.3. Protein DksA as a ppGpp co-regulator

In *E. coli,* as well as in *Salmonella,* DksA is a 17 kDa protein (151 amino acids) formed by several α-helix structures. It can be divided in two domains: a globular domain (G) that is composed by the N- and C-terminal region and contains a canonical C4 Zinc-finger; and a coiled coil domain (CC) that consist of two long α helices connected by a linker formed by an α-helical turn (**fig. 14A**).

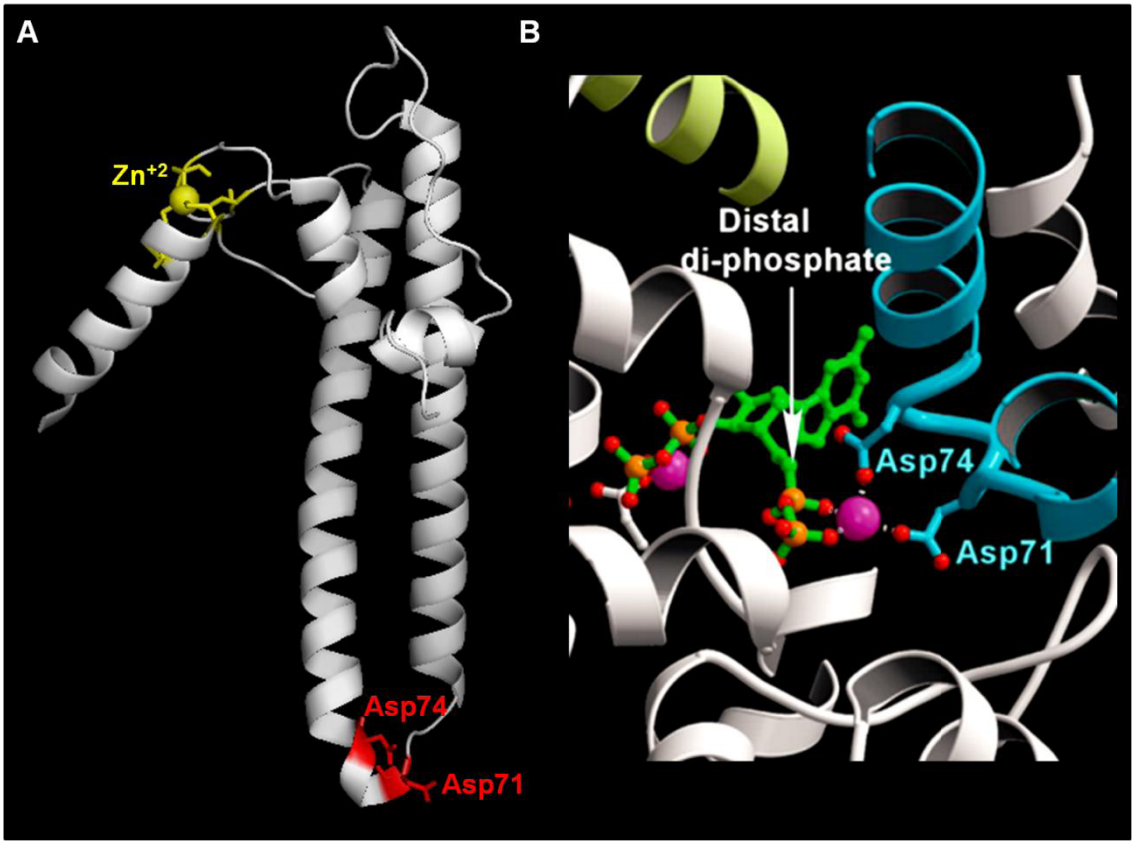

Figure 14: A) Structure of the protein DksA (in white) where the zinc-finger is shown in yellow, and the Asp 71 and 74 residues are shown in red. B) Close-up view of the complex in vicinity of the ppGpp binding site and catalytic centre. The RNApol is shown in white, DksA in cyan, ppGpp in green and Mg^{+2} in magenta spheres. The putative coordination bonds of Asp71 and Asp74 of DksA with the Mg^{+2} ion bound to the ppGpp distal phosphates are shown by white dashed lines (adapted from Perederina *et al.*, (2004)).

Structural studies, showed that DksA binds to the secondary channel of the RNApol (Perederina *et al.*, 2004). The globular domain stays outside the RNApol, interacting with the external surface of the secondary channel, presumably with the N-terminal coiled coil domain of the β' subunit of the RNApol (Perederina *et al.*, 2004). The described interaction, anchor DksA to the RNApol and provide the proper orientation of the CC domain into the secondary channel. The CC domain enters inside the secondary channel. It contains two residues, Asp71 and Asp 74 (**fig. 14 B**), that directly bind to the Mg^{+2} ion interacting with ppGpp (pMG2). These acidic residues are also conserved among GreA and GreB factors, corresponding to the D41 and E44, but they had a different orientation in DksA compared with GreA and GreB. Considering that DksA and GreA bind different Mg^{+2} ions, DksA binds pMG2 whereas GreA and

GreB binds cMG1, it seems reasonable that DksA and the Gre factors, although interacting in the same place, had different activities (Perederina *et al.*, 2004; Vassylyeva *et al.*, 2007).

The binding of DksA into the secondary channel produces conformational changes in the RNApol, lowering the free energy required to pass intermediate or transition states during the open complex formation (RPo). Similarly to the strain ppGpp^0, the *dksA* mutants are auxotrophic and unable to grow in minimal media. This phenotype allowed selection of spontaneous suppressor mutants (with recovered prototrophy). Interestingly most of the mutants that have been characterized, localize in the β and β' subunits of the RNApol, next to the secondary channel (Rutherford *et al.*, 2009). Although it has been shown that the absence of DksA severely impaired growth in minimal media plates, after 3 days of incubation, a *dksA* deficient strain was able to grow in minimal media. Therefore the *dksA* mutant now is considered bradytroph (grow slowly) instead of auxotroph (Vinella *et al.*, 2012).

DksA was originally identified in *E. coli* as a multicopy suppressor of the temperature sensitivity of *dnaKJ* mutants (Kang and Craig, 1990). It has been shown that DksA represses rRNA expression by decreasing promoter gen complex lifetime. DksA amplify the effect of ppGpp *in vitro*. Moreover, it has been observed that rRNA promoter activity does not respond to changes in growth phase or to amino acid starvation in a *dksA* deficient strain (Paul *et al.*, 2004). Taking in account that DksA, as well as ppGpp, interact with pMG2, it is suggested that DksA is required for the correct binding of ppGpp with pMG2, and vice versa (Perederina *et al.*, 2004). Moreover, it has been suggested that Val73 of DksA could interact with ppGpp (Perederina *et al.*, 2004). These data suggest that DksA might require the presence of the alarmone ppGpp to bind to the secondary channel. It has been suggested that DksA acts as a cofactor of ppGpp. Deletion of *dksA* also has a pleiotropic effect on gene expression, resulting in defects in cell division, σ^S expression, amino acid biosynthesis, quorum sensing, and virulence; highlighting its effect as a cofactor of ppGpp (Brown *et al.*, 2002; Paul *et al.*, 2004; Haugen *et al.*, 2008). This role would suggest that either absence of ppGpp or DksA would have a similar effect for

the cell. Thereby it was suggested that *dksA* mutants and ppGpp^0 strains should be phenotypically identical.

Recent data obtained by chromatin immunoprecipitation (CHIP) experiments showed that DksA was enriched not only at the promoter region but across the entire transcription unit (Zhang *et al.*, 2014), suggesting a possible role of DksA during elongation process. Moreover, it was suggested that DksA prevents collisions with replication fork possibly by destabilising elongation complexes (Trautinger *et al.*, 2005; Tehranchi *et al.*, 2010) or by inhibiting RNAP backward movement (Zhang *et al.*, 2014). However, one report suggested that, at least in vitro, DksA does not bind to backtracked or active elongation complexes (Furman, Tsodikov, *et al.*, 2013). Another study showed that DksA do not affect gene transcription during elongation and suggested that DksA, with ppGpp, increases the fidelity of RNA synthesis, and thus possibly prevents formation of misincorporated nucleotides during elongation complexes that could interfere with replication (Roghanian *et al.*, 2015).

1.2.4. Other proteins that bind into the secondary channel of the RNApol

It has been also described other proteins that could bind into the secondary channel of the RNApol that are similar to GreA, such as Gfh1 in *Thermus aquaticus* or RnK in *E. coli* (Lamour *et al.*, 2008), or similar to DksA, such as TraR of the conjugative F plasmid or DksA2 in *Pseudomonas aeruginosa*.

Gfh1 from *Thermus aquaticus* has a highly structural homology to GreA. It has been described that it suffers conformational changes that modify its affinity for the secondary channel of the RNApol (**fig. 15**). The interdomain linker is quite flexible and could vary its orientation producing two conformations (one active and other inactive) responding to different pH (Lamour *et al.*, 2006; Laptenko *et al.*, 2006).

Despite having similar secondary structure with GreA, Rnk is a globular protein (**fig. 15**) that is able to bind to the secondary channel, blocking it and it has been suggested that acts as anti-Gre factor (Lamour *et al.*, 2008).

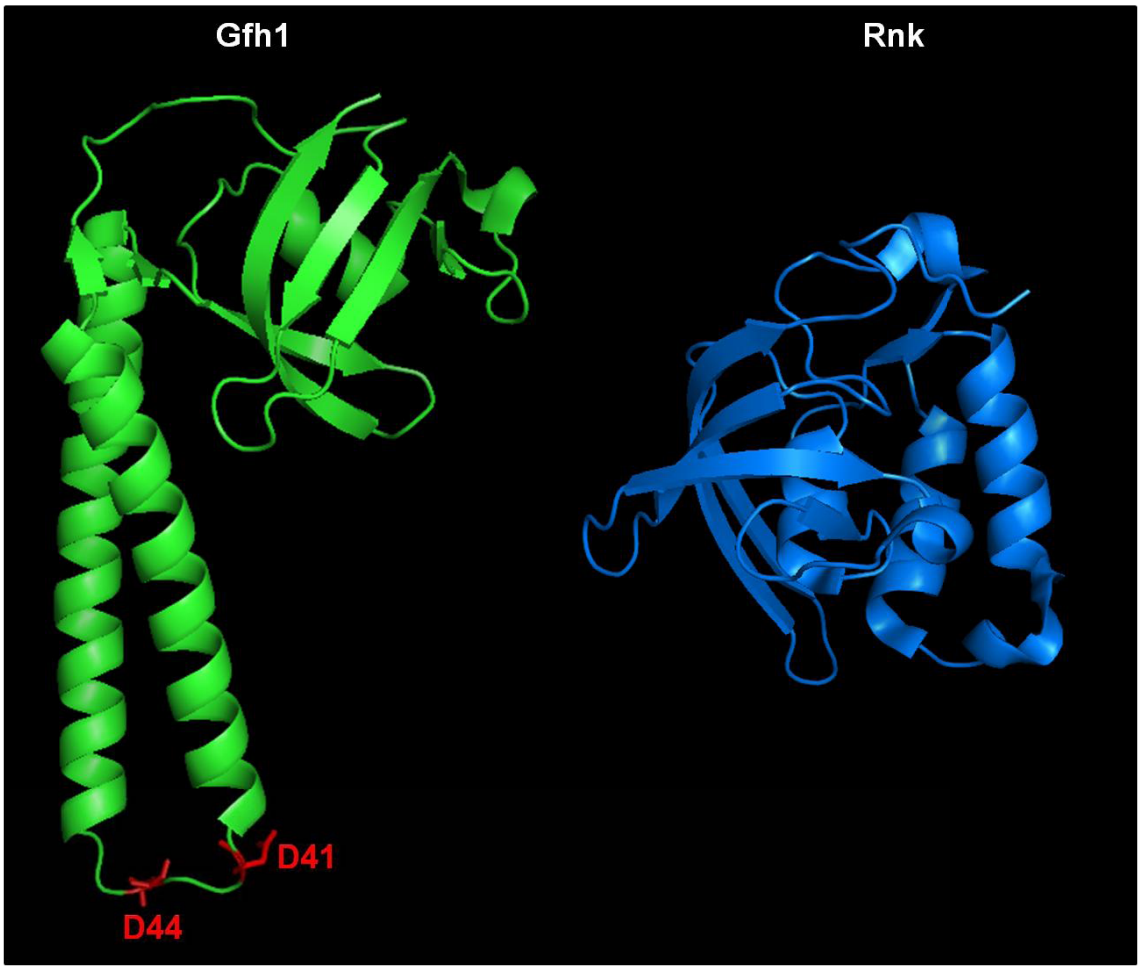

Figure 15: Structure of the Gfh1 of *Thermus aquaticus,* in green, and Rnk of *E. coli* in blue. The residues D41 and D44 are indicated in red.

It has been found proteins similar to DksA in several conjugative plasmids and bacteriophages (Blankschien *et al.*, 2009; Stepanova *et al.*, 2010). These proteins are smaller that DksA, but contains the zinc-finger and part of the CC domain with the Aspartic residues that interact with the Mg^{+2} ion pMG2. These findings suggest that these mobile elements had acquired mechanisms to regulate transcription through interaction of those proteins with the secondary channel of the RNApol. Moreover it has been described in *Pseudomonas*, as well as in other bacteria, the presence of DksA-like proteins without zinc-finger, known as DksA2. This protein is related with Zn^{+2} metabolism and Zn^{+2} caption (Blaby-Haas *et al.*, 2011; Furman, Biswas, *et al.*, 2013). Despite not having the ability to bind Zn^{+2}, due to the loss of 2 cysteines, DksA2 conserve the 2 acidic residues that interact with Mg^{+2} of the RNApol (Furman, Biswas, *et al.*, 2013).

1.2.5. Competition between the different factors that bind to the secondary channel of the RNApol

The presence of different proteins that can bind to the same target, the secondary channel of RNApol, suggests that there must be a competition between the different factors for the binding with the secondary channel of the RNApol.

The relative amount of the principal proteins that bind to the secondary channel of the RNApol of *E. coli* and its affinity was determined. It has been shown that DksA is the more abundant secondary channel interacting protein in the cell, followed by GreA (2-3-fold less than DksA), and GreB (10-fold less than DksA). The amount of Rnk is approximately equimolar with GreB (Rutherford *et al.*, 2007; Lamour *et al.*, 2008). The determination of the amount of the different proteins was performed in rich MOPS medium at different $OD_{600nm,}$ showing that the amount of DksA keeps constant at early-stationary phase, compared with exponential phase, but it suffers a decrease at late-stationary phase. The amount of GreA decreases at early-stationary phase, compared with exponential phase. Moreover, GreB and Rnk keep constant levels through the growth.

It has also been shown that DksA, GreB and Rnk had similar affinity, that is approximately 100-fold higher than GreA (Koulich *et al.*, 1997; Rutherford *et al.*, 2007; Lamour *et al.*, 2008). Rutherford *et al.* concludes that DksA is basically binding the RNApol and GreA is not able to compete for entering into the secondary channel.

Interesting results obtained in our research group suggested that competition at the level of the secondary channel might have a relevant impact in gene expression. Mutants lacking either DksA or ppGpp had different effect on the expression of different genes (Magnusson *et al.*, 2007; Aberg *et al.*, 2008; Aberg *et al.*, 2009). Some of these genes are *fimB* that codes for type 1 fimbriae, and *fliC*, coding for the main subunit of the flagella. It has been observed that in absence of ppGpp there is a decrease in the expression of these genes, whereas in absence of DksA it increases dramatically. Remarkably the increase in the expression of these genes observed in a *dksA*

mutant, vanished in a *greA* mutant. We hypothesized that in absence of DksA, GreA could interact more efficiently with the secondary channel and increase the expression of these genes (Aberg *et al.*, 2008; Aberg *et al.*, 2009). This artificial switch between of DksA and GreA suggest that there could be a competition between the different proteins that bind the secondary channel under certain circumstances.

As previously mentioned (section 1.2.3.), it has been described that $ppGpp^0$ mutants are auxotrophic in minimal media (Hua Xiao *et al.*, 1991), but a *dksA* mutant is bradytroph (slow-growing). Interestingly, a double mutant *dksA greA* is not able to growth in minimal media, suggesting that GreA is essential for growth under amino acid starvation in absence of DksA. In fact the prototrophy of the double mutant *dksA greA* could be restored overexpressing GreA. In addition, the overexpression of GreA do not restores prototrophy in a $ppGpp^0$ strain, but in absence of DksA ($ppGpp^0$ *dksA*), overexpression of GreA could restore it. This fact suggests that in presence of DksA, in the $ppGpp^0$ strain, GreA is not able to bind to the secondary channel and restore prototrophy, but when DksA is not present, GreA is able to bind to the secondary channel and restore prototrophy (Vinella *et al.*, 2012).

Moreover it has been observed that there is a crosstalk between factors that bind to the secondary channel of the RNApol. It has been shown that GreA stimulates expression of *dksA*, and DksA stimulates expression *greB* (Vinella *et al.*, 2012). This crosstalk suggests that the binding of these factors to the secondary channels, would produce changes in the amount of the other factors, and therefore in the competence for the secondary channel of the RNApol.

It was recently described, using ChIP experiments, that DksA binds the RNApol during the whole process of transcription. In several genes, the ChIP-signal for DksA is the same that for RNApol, suggesting that all the RNApol is binding to DksA during all the transcription process for those genes. But in other genes – like the flagella genes – the ChIP signal of DksA is lower than RNApol (Zhang *et al.*, 2014). These data might suggest that for some of the genes, DksA might be important binding the RNApol, but there are other genes that the RNApol would be binding other proteins.

It has been recently shown (Henard *et al.*, 2014) that, in *Salmonella*, the C4 Zinc-finger domain of DksA is able to sense oxidative and nitrosative stress. They have shown that during oxidative stress the cysteines of the Zinc-finger are oxidised, releasing the Zn^{+2} ion and producing changes on the secondary structure of DksA. These conformational changes on DksA produce its dimerization and avoid its binding to the secondary channel of RNApol (Henard *et al.*, 2014). This finding strongly suggests that during these conditions, DksA does not bind to the secondary channel and it is replaced presumably by other factors. Taking in account these data and the fact that Gfh1 changes its conformation as a response to changes of pH (Lamour *et al.*, 2008), it has been suggested that different environmental conditions could produce conformational changes on the factors that bind to the secondary channel of RNApol, producing changes on its affinity, and as a result, changes on its competition.

1.3. The players

The bacteria used in this thesis, *Escherichia coli* and *Salmonella enterica* subsp. *enterica* serovar Typhimurium, are members of the family Enterobacteriaceae, which comprises Gram-negative, non-spore forming, oxidise-negative, rod-shaped bacterium that are often motile with peritrichous flagella.

1.3.1. *Escherichia coli* inhabit the large intestine of all humans and warm-blooded animals. The comensal stains of *E. coli* comprise nearly a 1% of the total bacterial microbiota biomass in humans (Balows *et al.*, 1992). *E. coli* has been extensively used as indicator strain of faecal contamination in water and food. *E. coli* strains are classified by surface antigens in serogroups, based on 3 classes of antigens: O (LPS), K (surface polysaccharides) and H (flagella). The *E. coli* strains of the serotype K12 are comensal strains and they has been used as model organism in research on genetics and molecular biology because it grows very quickly on common used media under aerobic and anaerobic conditions and because are generally recognized as safe (GRAS)(Balows *et al.*, 1992).

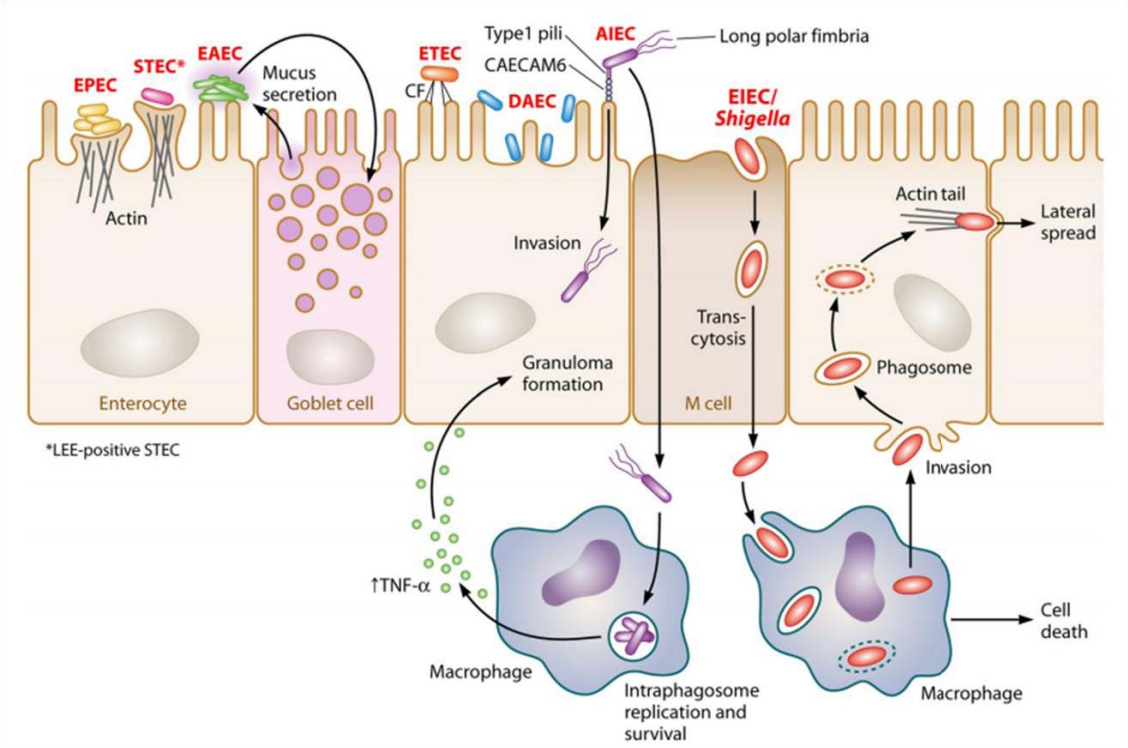

Figure 16: Adherence patterns of enteric *E. coli* pathotypes and its infection process. Adapted from Croxen *et al.*, (2013)

On the other hand, some *E. coli* strains are also important pathogens in humans and animals, producing mainly diarrheal diseases, but also extraintestinal infections, such as urinary tract infections or infections of the central nervous system (associated with neonatal meningitis). Diarrheagenic *E. coli* are classified in seven major pathotypes (EPEC, STEC, EIEC, EAEC, ETEC, DAEC and AIEC) which are characterized by the pathogenesis that causes (Croxen *et al.*, 2013) (**fig. 16**).

It has been proposed that different HGT events are the origin of the generation of the different *E. coli* pathotypes (**fig. 17**). Those events cause acquisition of several set of genes that confer different abilities and highlight the plasticity of its genome. A clear example of this plasticity is the recent outbreak in Germany at 2011 that sickened 4075 healthy individuals from 16 countries, with 50 deaths (World Health Organization, 2011). The *E. coli* strain responsible of the outbreak was an hybrid strain of EAEC and STEC (O104:H4), derived from a EAEC that has acquired the Shiga-like toxin encoded in a lambda-like bacteriophage, as well as several antibiotic resistance genes encoded in a plasmid and other virulence factors obtained from several *E. coli* strains and other Enterobacteria (Bloch *et al.*, 2012; Croxen *et al.*, 2013).

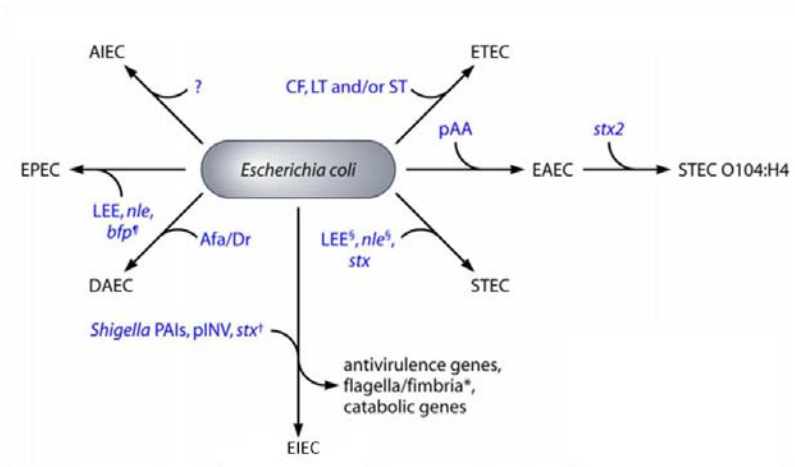

Figure 17: General overview of pathogenic genes acquisition and loss for different pathotypes. Adapted from Croxen *et al.*, (2013)

Some of these HGT events showed on **figure 17** have happened long time ago, but other events – like the responsible of the O104:H4 generation – are quite recent, highlighting the importance of HGT events on pathogenicity evolution.

MG1655 is a K12 *E. coli* strain that do not contain the F plasmid. At difference of other laboratory *E. coli*, MG1655 is a *recA*$^{+}$ strain and it does not accumulate many mutations (Guyer *et al.*, 1981). Although MG1655 is not pathogenic, it is a comensal strain which, therefore, is proficient to efficiently colonize animal host.

1.3.2. *Salmonella enterica* subsp. *enterica* serovar Typhimurium is an enteric food-borne pathogen that infects both humans and animals. It produces gastroenteritis in humans and typhoid-like disease in mouse. For this reason it has been extensively used as a model to study host-pathogen interaction at the molecular level (Hansen-Wester and Hensel, 2001).

Salmonella's infection begins with the ingestion of organisms in contaminated food or water. *Salmonella* Typhimurium has an acid tolerance response (ATR) that provides an inducible pH-homeostatic function to maintain the intracellular pH within a physiological range and to promote survival to acid during the stomach transit. After entering the small intestine, *Salmonella* crosses the intestinal mucous layer and reaches the epithelium. It has been shown that *Salmonella* adhere preferentially to the M cells of the Peyer's patches, although invasion of normally non-phagocytic enterocytes can also occur. After adherence to apical surface (**fig. 18 A**), *Salmonella* induces a rearrangement of host's cytoskeleton, producing the engulfment of adhered bacteria in vesicles called *Salmonella*-containing vacuoles (SCVs). *Salmonella* avoids SCVs fusion with the lysosomes and produces a migration of those SCVs to a perinuclear position, to facilitate nutrients uptake and bacterial replication (**fig. 18 B**). A fraction of SCVs crosses the basolateral membrane and could re-infect epithelial cells or macrophages (**fig. 18 A**). When *Salmonella* enters into macrophages by phagocytosis, it is able to avoid the fusion of SCV with lysosomes, as well as it does in epithelial cells, and avoids its degradation. *Salmonella* could spread among the body by macrophages invasion, but *Salmonella* Typhimurim does not produce typhoid fever and body dissemination in humans (Haraga *et al.*, 2008; Fàbrega and Vila, 2013).

There are different virulence factors that are required for this pathogenic process. These virulence factors consist on effectors proteins that interact with host cells proteins (**fig. 18**), adhesins, flagella and components of biofilm

formation. Many of the genes coding for virulence factors are located in highly conserved *Salmonella* pathogenicity islands (SPIs), bacteriophages and the plasmid pSLT (Fàbrega and Vila, 2013).

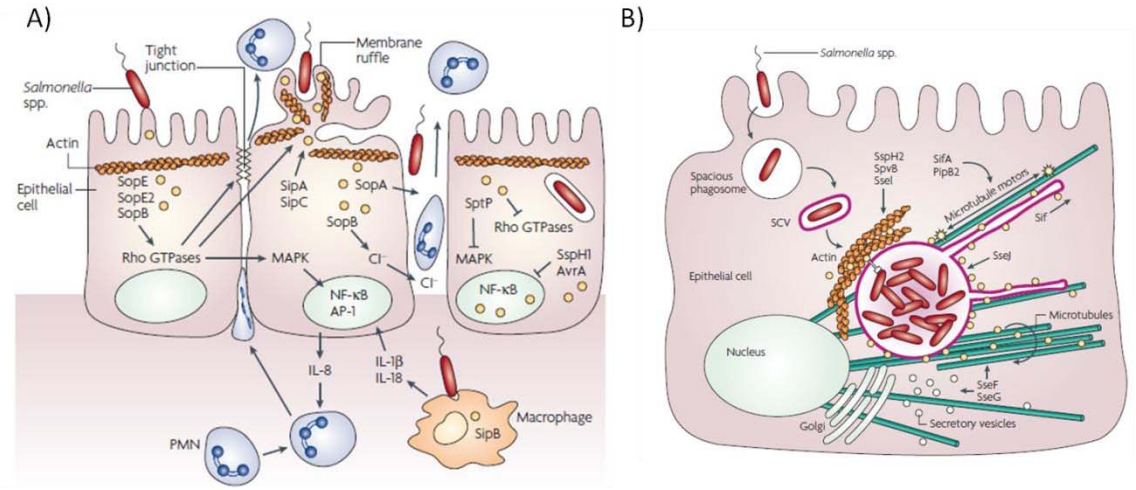

Figure 18: Biology of *Salmonella* infection pathway. A) SPI1 T3SS-induced changes on host cells producing bacterial endocytosis. B) SCV formation and induction of the SPI2 T3SS within host cells. Adapted from Haraga *et al.*, (2008)

S. enterica serovar Typhimurium contains 5 SPIs, as described in **Table 1**. The SPI1 and SPI2 code for proteins required for invasion of epithelial cells and survival within macrophages, respectively. Remarkably, each island, SPI1 and SPI2, codes for a type 3 secretion system (TTSS) which will be important in the translocation of different effector proteins from the cytoplasm of *Salmonella* directly to the host cell cytoplasm. Many, but not all, the effector proteins injected by those TSS are encoded in SPI-1 and SPI-2.

Pathogenicity island	Type secretion system encoded	Functions
SPI-1	Type III secretion system (T3SS)	Invasion of intestinal epithelium; development of SCV; encodes effector proteins important for: actin cytoskeleton rearrangements; membrane ruffling; induces IL-8 and pathogen-elicited epithelial chemo-attractant secretion. **Fig. 18A**
SPI-2	Type III secretion system (T3SS)	Survival within phagocytic cells by inhibiting fusion between lysosomes and SCVs; endocytic trafficking inhibition, avoidance of NADPH oxidase-depenant killing by macrophages; encodes effector proteins,

		chaperone proteins and translocon proteins. **Fig. 18B**
SPI-3		Intramacrophage survival, encodes macrophage survival protein MgtC; encodes Mg^{+2} transporter MgtB.
SPI-4	Type I secretion system (T1SS)	Mediates adhesion to epithelial cells; encodes genes of non-fimbrial adhesion protein
SPI-5		Encodes protein effectors – secreted by T3SS of SPI-1 or SPI-2.

Table 1: Features and functions of SPIs of *Salmonella enterica* serovar Typhimurium. Adapted from Hurley *et al.*, (2014)

Some of the effector proteins secreted by T3SS, either from SPI1 or SPI2 are encoded on plasmids (SpvB) or bacteriophages (SopE (**fig. 18 A**)) (Fàbrega and Vila, 2013). There are other virulence factors located in HGT elements such as Pef fimbriae, encoded on pSLT (Fàbrega and Vila, 2013), or SodC (superoxide [Cu,Zn]-dismutase, essential for intramacrophage survival and encoded in the bacteriophage *Gifsy-2* (Figueroa-Bossi *et al.*, 2001)). It has also been described that flagella, in addition to be under phase variation of two different flagellins (FliC and FljB), contains a variable zones susceptible of HGT events in order to provide *Salmonella* with a higher antigenic variability (Selander *et al.*, 1996).

The different virulence factors are required at different infection steps. In order to ensure the proper expression of in the appropriate moment, there is an intricate crosstalk between regulatory pathways (**fig. 19**). There are several global regulatory proteins involved in this crosstalk, as well as, specific regulatory proteins encoded in each virulence determinant (Fàbrega and Vila, 2013).

The strain SV5015 is a derivate from SL1344. This strain is auxotrophic for histidine, while the SV5015 is a *his*$^{+}$ derivative, recovering the prototrophy.

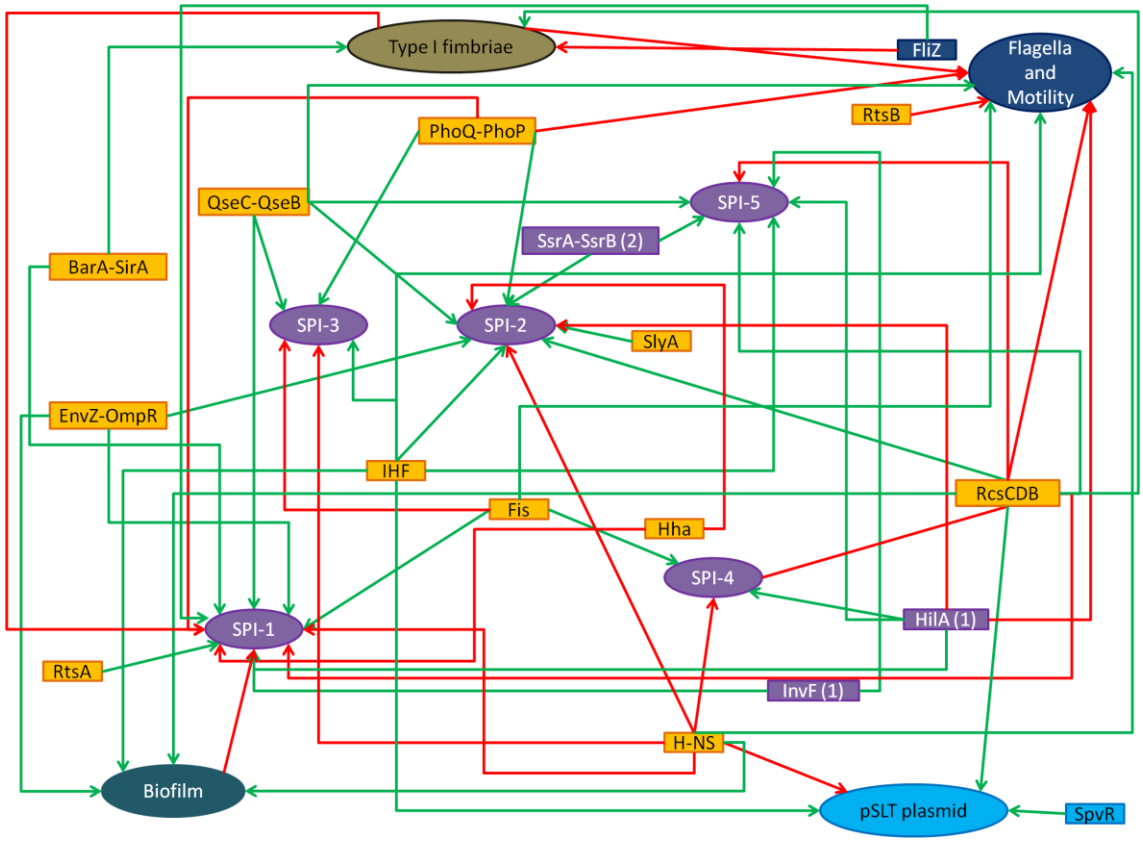

Figure 19: Cross-talk between the different virulence elements. Green arrows represent activators, while red ones are repressors. Squares are regulator proteins and ellipses are virulence factors. The squares coloured as the same colour than virulence elements, are encoded on those elements. In ( ) is indicated the SPI were the regulatory proteins are encoded. Adapted from Fàbrega and Vila, (2013)

Escherichia coli and *Salmonella enterica* evolved from the same ancestor long time ago and both of them had acquired a huge arsenal of virulence elements by HGT processes (**fig. 17**), showing a huge plasticity of its genomes. Moreover, this foreign DNA had acquired complicated regulatory networks (**fig. 19**), in order to ensure its own survival and of the bacteria.

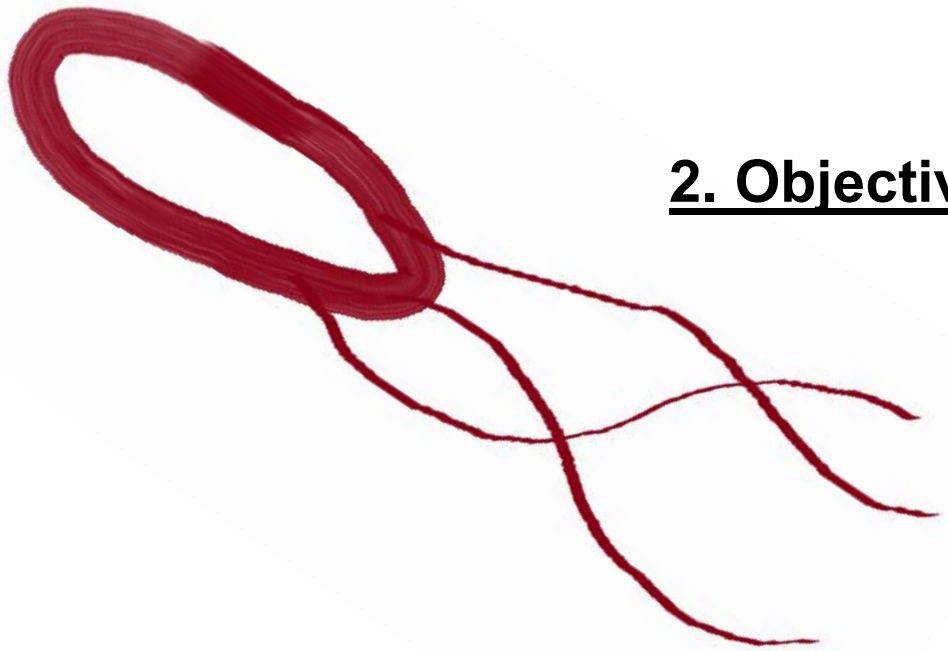

2. Objectives

Previous studies in our research group suggest that, in *Escherichia coli*, ppGpp and DksA may have different effects in the expression regulation of some genes (Aberg *et al.*, 2009). These results let us to hypothesize that the observed differences between mutants deficient for DksA and ppGpp were due to changes in the proteins that bind to the secondary channel of the RNApol. Therefore, we suggest that a possible competence between those factors, DksA, GreA and GreB, exist. Simultaneously, it was postulated that the amount of DksA and its affinity for the RNApol was higher than the affinity and amount of GreA and GreB, being suggest by the authors that these competition was not possible (Rutherford *et al.*, 2007; Rutherford *et al.*, 2009). In this work we further explore the possible existence of a competition between factors interacting into the secondary channel of the RNApol and its impact in gene expression regulation. The two main objective of this thesis are specified below.

1. Study the possible competition between different factors that bind to the secondary channel of the RNApol. In order to fulfil this objective, the following specific objectives were proposed:
    A. To monitor *greA* expression under different conditions, to determine if changes in the amount of GreA could affect the possible competition between the different proteins that bind to the secondary channel of the RNApol.
    B. To study the possible crosstalk between the factors that bind into the secondary channel of the RNApol.
    C. To study the mechanisms of action of GreA in the modulation of expression of a target gene, *fliC*.
    D. To determine the effect of overexpressing GreA on bacterial growth in several genetic backgrounds, in order to study the hierarchy between the different factors that bind to the RNApol.
    E. To study the structure of the protein GreA, by determining which residues are important for the functionality of GreA and the interaction with the secondary channel of RNApol.
    F. To determine how the different factors that bind to the secondary channel of the RNApol evolved from its ancestor. This phylogenetic

study would let us determine the evolutive pressure that produced the variability of factors that bind the secondary channel of the RNApol.

2. Determine the effect of these factors on mobile elements and HGT elements. The effect of ppGpp and DksA over the transcriptional profile of *Salmonella enterica* serovar Typhimurium, have been determined.

3. Materials and methods

3.1. Strains and plasmids:

The strains and plasmids used on this study are listed below:

Strains

Name	Observations	Origen
	Escherichia coli	
MG1655	F-, *ilvG*, *rph*1	(Guyer *et al.*, 1981)
TE8114	MG1655 *dksA::*Tc^R	(Brown *et al.*, 2002)
CF11657	MG1655 *greA::Cm*	(Aberg *et al.*, 2009)
AAG101	MG1655 *dksA::Tc greA::Cm*	(Aberg *et al.*, 2009)
AAG93	MG1655 Δ*relA* Δ*spoT* (ppGpp^0)	(Aberg *et al.*, 2006)
CF11663	MG1655 *greB::Km*	(Aberg *et al.*, 2009)
AAG1	MG1655 Δ*lacZ*	(Aberg *et al.*, 2008)
JFV14	AAG1 Δ*relA* Δ*spoT dksA::*Tc^R	(Aberg *et al.*, 2009)
LFC1	AAG1 attBgreA1	This study
LFC2	CLT254 attBgreA1	This study
LFC3	AAG1 attBgreA2	This study
LFC4	CLT254 attBgreA2	This study
LFC28	AAG1 greA+685	This study
LFC29	AAG1 greA+193	This study
LFC5	AAG1 attBgreA3	This study
LFC6	CLT254 attBgreA3	This study
LFC7	AAG1 Δ*greA* ΔGraL attBgreA2	This study
LFC8	AAG1 *dksA*::Tc attBgreA2	This study
LFC9	AAG1 Δ*relA* Δ*spoT* attBgreA2	This study
LFC10	AAG1 greA+685 *rpoS*::Tc	This study
LFC11	AAG1 greA+685 *hns*::Tc	This study
LFC12	AAG1 greA+685 *lrp*::Tc	This study
LFC13	AAG1 greA+685 Δ*hfq*	This study
LFC14	AAG1 attBgreA2 Δ*narL*	This study
LFC15	AAG1 attBgreA2 Δ*ompR*	This study
LFC16	AAG1 attBgreA2 Δ*metR*	This study
LFC17	AAG1 attBgreA2 Δ*argP*	This study
LFC18	AAG1 attBgreA2 Δ*cytR*	This study
LFC19	AAG1 attBgreA2 Δ*rcsA*	This study
LFC20	AAG1 attBgreA2 Δ*pdhR*	This study
LFC21	AAG1 attBgreA2 Δ*argR*	This study
LFC22	AAG1 attBgreA2 Δ*gadX*	This study
LFC23	AAG1 attBgreA2 Δ*dgsA*	This study
LFC24	AAG1 attBgreA2 Δ*fadR*	This study
LFC25	AAG1 attBgreA2 Δ*fis*	This study
LFC26	AAG1 attBgreA2 Δ*crp*	This study
LFC27	AAG1 attBgreA1 Δ*crp*	This study
LFC30	AAG1 greA+3	This study
LFC31	AAG1 greA+5	This study

LFC32	AAG1 greA+101	This study
PRG13	AAG1 *fliC::lacZ* (+70)	(Aberg *et al.*, 2009)
PRG14	AAG1 *fliC::lacZ* (+70) *dksA*::Tc^R	(Aberg *et al.*, 2009)
PRG15	AAG1 *fliC::lacZ* (+70) *dksA*::Tc^R *greA*::Cm^R	(Aberg *et al.*, 2009)
PRG16	AAG1 *fliC::lacZ* (+1210)	(Aberg *et al.*, 2009)
PRG17	AAG1 *fliC::lacZ* (+1210) *dksA*::Tc^R	(Aberg *et al.*, 2009)
PRG18	AAG1 *fliC::lacZ* (+1210) *dksA*::Tc^R *greA*::Cm^R	(Aberg *et al.*, 2009)
LFC33	PRG13 *flgAM*::Cm	This study
LFC34	PRG13 *fliA*::Cm	This study
LFC35	PRG14 *flgAM*::Cm	This study
LFC36	PRG14 *fliA*::Cm	This study
LFC37	PRG16 *flgAM*::Cm	This study
LFC38	PRG16 *fliA*::Cm	This study
LFC39	PRG17*flgAM*::Cm	This study
LFC40	PRG17 *fliA*::Cm	This study
N4849	MG1655 *rpoB35*	(Trautinger *et al.*, 2005)
LFC41	N4849 Δ*lacZ fliC::lacZ* (+70)	This study
LFC42	N4849 Δ*lacZ fliC::lacZ* (+70) *greA::*Cm	This study
LFC43	N4849 Δ*lacZ fliC::lacZ* (+1210)	This study
LFC44	N4849 Δ*lacZ fliC::lacZ* (+1210) *greA::*Cm	This study
LFC45	MG1655 *rpoB*111 Δ*lacZ fliC::lacZ* (+70)	This study
LFC46	MG1655 rpoB111 Δ*lacZ fliC::lacZ* (+70) *greA::*Cm	This study
LFC47	MG1655 rpoB111 Δ*lacZ fliC::lacZ* (+1210)	This study
LFC48	MG1655 rpoB111 Δ*lacZ fliC::lacZ* (+1210) *greA::*Cm	This study
LFC49	N4849 *dksA*::Tc	This study
LFC50	N4849 *greA*::Cm	This study
LFC51	N4849 *dksA*::Tc *greA*::Cm	This study
LFC52	N4849 Δ*lacZ fliC::lacZ* (+1210) *dksA*::Tc	This study
LFC53	N4849 Δ*lacZ fliC::lacZ* (+1210) *dksA*::Tc greA::Cm	This study
LFC54	AAG1 attBgreB	This study
LFC55	AAG1 attBgreB *greA*::Cm	This study
LFC56	AAG1 attBgreB Δ*greB*	This study
LFC57	AAG1 attBgreB *dksA*::Tc	This study
LFC58	AAG1 attBdksA	This study
LFC59	AAG1 attBdksA *greA*::Cm	This study
LFC60	AAG1 attBdksA *dksA*::Tc	This study
LFC61	AAG1 *fliC::lacZ* (+70) *greA*::Cm^R	This study
LFC62	AAG1 *fliC::lacZ* (+1210) *greA*::Cm^R	This study
CBP34	MG1655 *crp*::Tc^R	C. Balsalobre
CMM2	MG1655 *cyaA*::Km^R	(Müller *et al.*, 2009)
TP1196	MG1655 *greA* D41N	(Poteete, 2011)
TP1204	MG1655 *greA* D41A	(Poteete, 2011)
TP1216	MG1655 *greA* E44K	(Poteete, 2011)
TP1260	MG1655 *dksA* D71N D74N	(Poteete, 2011)
	Salmonella enterica	
SV5015	*Salmonella enteric* serovar Typhimurium SL1344 *his*$^+$	J. Casadesus

SV5015 ppGpp	SV5015 Δ*relA* Δ*spoT*	This study
SV5015 *dksA*	SV5015 Δ*dksA*	This study
SV4522	Δ*finO spvA*::Km^R	(Camacho and Casadesús, 2002)
LFC63	SV5015 Δ*relA* Δ*spoT finO*::Km	This study
LFC64	SV5015 Δ*dksA finO*::Km	This study
WG49	*Salmonella enterica* serovar Typhimurium WG49, F$^+$	M. Muniesa
MA6247	SL1344 Gifsy-1$^-$ Gifsy-2$^-$	(Figueroa-Bossi and Bossi, 1999)
SV5015 pdu	SV5015 *pduAH*::lacZ	S. Paytubi
LFC65	SV5015 ppGpp^0 *pduAH*::lacZ	This study
LFC66	SV5015 dksA *pduAH*::lacZ	This study
TT1704	A *his* -9533	(Torreblanca and Casadesús, 1996)

Plasmids

Name	Observations	Origen
pTrc99a	Cb/Ap^R, lacI^q, P*trc* expression vector	(Amann *et al.*, 1988)
pDNL278	lacI^q, *greA* under control of P*trc* on pTrc99a	(Feng *et al.*, 1994)
pGF296	*greB* under control of P*trc* on pTrc99a	(Feng *et al.*, 1994)
pZA4	Spec^R, lacI^q, pACYC derivative plasmids with p15A origin	Bernd Bukau
pKD3	*bla* FRT *cat* FRT PS1 PS2 oriR6K	(Datsenko and Wanner, 2000)
pKD4	*bla* FRT *cat* FRT PS1 PS2 oriR6K	(Datsenko and Wanner, 2000)
PKD46	*bla* P_{BAD} *gam bet exo* pSC101 oriTS	(Datsenko and Wanner, 2000)
pCP20	*bla cat cI857* λP_R*flp* pSC101 oriTS	(Datsenko and Wanner, 2000)
PKG136	*ahp* FRT *lacZY*$^+$ t_{his} oriR6K	(Ellermeier *et al.*, 2002)
pKG137	*ahp* FRT *lacZY*$^+$ t_{his} oriR6K	(Ellermeier *et al.*, 2002)
pRS551	*bla-kan-Tl$_4$*-EcoRI-SmaI-BamHI-*lacZ**	(Simons *et al.*, 1987)
pBR322	*ori$_P$*MB1 Ap^R Tc^R	(Bolivar *et al.*, 1977)
pBR-GreA	*greA* with its promoter cloned on pBR322	This study
pBR-GreA D41A	*greA* D41A with its promoter cloned on pBR322	This study
pBR-GreA E44K	*greA* E44K with its promoter cloned on pBR322	This study
pBR-GraL	*greA* promoter cloned on pBR322	This study
pLC245	*rpoE* under control of P*trc* on pTrc99a	(Rhodius *et al.*, 2006)
pBA166	Chimerical *ompC*-YYF under control of P*trc* on pTrc99a	(Walsh *et al.*, 2003)
pLG339	RK2 based low copy number plasmids	(Stoker *et al.*, 1982)
pLG-*crp*	pLG339 carrying crp under the crp promoter	(Bell *et al.*, 1990)
pLG-*crp* H159L	pLG339 carrying crp H159L under the crp promoter	(Bell *et al.*, 1990)
pLG-*crp* H159L/K52N	pLG339 carrying crp H159L/K52N under the crp promoter	(Bell *et al.*, 1990)
pLG-*crp* K21L	pLG339 carrying crp K21L under the crp promoter	(Bell *et al.*, 1990)
pHM1883	pGB2 origin, Ptrc expression vector, Spec^R	(Vinella *et al.*, 2012)
pHM1873	pGB2 origin, greA under control of Ptrc, Spec^R	(Vinella *et al.*, 2012
pHM1854	pGB2 origin, greA D41A E44Y under control of Ptrc, Spec^R	(Vinella *et al.*, 2012

3.2. Media and antibiotics

During this work, several media were used. Its composition and preparation is described below:

- LB-Lennox (Atlas and Parks, 1993): liquid rich medium used for bacterial growth. Composition: 10 g/L tryptone, 5 g/L yeast extract and 5 g/L NaCl (other concentrations of NaCl were used when indicated).
- LB agar: solid rich medium used for bacterial growth. Composition: LB with 15 g/L of bacteriological agar.
- LB top agar: semisolid rich medium used to obtain bacteriophages lysates or bacteriophage titration (section 3.7.2). Composition: LB with 6 g/L of bacteriological agar.
- Minimal medium M9 agar (as described in Vinella *et al.*, (2012)): solid minimal medium used to determine the amino acid auxotrophy of different strains. Composition: 1x M9 salts, 1 mM $MgSO_4$, 0.1 mM $CaCl_2$, 2 µM $FeSO_4$, 10 µg/ml thiamine (vitamin B1), 0.2% (w/v) glucose and 15 g/L bacteriological agar.
- Salts M9 10x: salts solution used to prepare the minimal medium M9 agar. Composition: 90 g/L Na_2HPO_4 heptahydrate, 30 g/L KH_2PO_4, 5 g/L NaCl and 10 g/L NH_4Cl.
- SOB (Hanahan *et al.*, 1991): liquid medium used for SOC medium preparation and for gene inactivation protocol (section 3.8.1). Composition: 20 g/L tryptone, 5g/L yeast extract, 0.58 g/L NaCl, 0.18 g/L KCl and 20 mM of Mg^{+2} solution (1M $MgCl_2$ and 1M $MgSO_4$).
- SOC (Hanahan *et al.*, 1991): liquid medium used to recover cell after transformation of genetic material by electroporation (section 3.7.1.2). Composition: SOB with 20mM of glucose.
- EBU agar: solid medium used to identify pseudolysogens after P22 transduction (section 3.7.3). Composition: LB agar with 2.5 g/L glucose, 2.5 g/L KH_2PO_4, 0.0125 g/L, Evans Blue and 0.025 g/L fluorescein.
- Motility agar (Aberg *et al.*, 2009): solid medium to observe bacterial swimming (section 3.9.3). Composition: 10 g/L tryptone, 5g/L NaCl (other concentrations of NaCl were used when indicated) and 2.5 g/L bacteriologic agar (Difco).

- McConkey base agar: solid medium used to determine carbon source usage. Composition: 17 g/L peptone, 3 g/L protease peptone, 1.5 g/L bile salts Nº 3, 5 g/L NaCl, 0.03 g/L neutral red, 0.0001 g/L, crystal violet and 15 g/L agar.
- Minimal medium E: liquid medium used for pSLT conjugation (section 3.7.4). Composition: 1x E salts, 0.2% glucose.
- Salts E 50x: salts solution used to prepare the minimal medium E. Composition: 40 mM $MgSO_4$, 0.47 M citric acid, 2.85 M K_2HPO_4, 0.85 M $Na(NH_4)HPO_4$.
- CFA: liquid medium used to determine biofilm formation (section 3.9.4). Composition: 10 g/L casaaminoacids, 1.5 g/L yeast extract, 50 mg/L $MgSO_4$ and 5 mg/L MnCl.
- CR agar: solid medium used to determine biofilm formation (section 3.9.4). Composition: 10 g/L tryptone, 5 g/L yeast extract, 40 µg/ml Congo Red, 20 µg/ml Coomassie brilliant blue G, and 15 g/L bacteriologic agar.

When it was required, the indicated antibiotics were added at the appropriate concentration, as follows: 50 µg/ml ampicilin (Ap), 12.5 µg/ml tetraciclin (Tc), 15 µg/ml cloramphenicol (Cm), 25 µg/ml kanamycin (Km) and 25 µg/ml spectinomycin (Spec).

3.3. Oligonucleotides

The different oligonucleotids used on this work are listed below.

Oligonucleotids

Name	Sequence (from 5' → 3')
Error-Prone PCR	
G11	CACTGCAGCAACATCTTGAGTATTGGG
G6	CAGAATTCATGCAAGCTATTCCGATGAC
One-step inactivation of chromosomal genes using PCR products	
G8	CAAGCTATTCCGATGACCTTACGCGGCGCTGAAAAATTACGCGT GTAGGCTGGAGCTGCTTC
G9	GGCGAAGTAGAATTTGAAGTAATTAAGGTGGAATACCTGTAAGT GTAGGCTGGAGCTGCTTC
G12	CATTTGCTGTGTAAAACGAGGGGTTTTCCGCAGGCAGGAGAGC ATATGAATATCCTCCTTAGT
G10	TTACAGGTATTCCACCTTAATTACTTCAATTCTACTTCGCCCATA TGAATATCCTCCTTAGT
G3	AGTAAACGATGACCCTTCGGGAACTTCAGGTAAAATGCTATCGT GTAGGCTGGAGCTGCTTC
G4	GACCCTTCGGGAACTTCAGGGTAAAATGACTATCAAAATGTGAA TTGTGTAGGCTGGAGCCTGCTTC
G5	CTGGTCCCGGTAAGGAGTTATGCCGGGCAGGCCGAACAGCCG GGTGTAGGCTGGAGCTGCTTC
Real Time qPCR	
zwf-RV	CCAAGATAGTGGTCGATACG
zwf-FW2	CACGCGTAGTCATGGAGAAA
fliC-RT8	GCTATCGCATCTGTAGACAA
fliC-RT9	GTAGTGGTGTTGTTCAGGTT
General PCR / sequencing	
greApl1	CGTGTCGCTCAAGGCGCAC
greApl2	CGCGCTACTGCCGCCAGGC
G1	GAGAATTCGCGATCATGTTGTCCGAC
G2	CAGAATTCCATCAACTTTGCGGCCTG
G7	CAGGATCCCGTAAGGTCATCGGAATAGC
attB	GAGGTACCAGCGCGGTTTGATC
attP	TTTAATATATTGATATTTATATCATTTTACGTTTCTCGTTC
λ-int	ACTCGTCGCGAACCGCTTTC
greAcr1	GGCAGGCAGCGCCATCTG
greAcr2	GGAAGCTATCGTGCGCG
B1	CAGAATCCCACCAGAATCTTGTAGTTC
B2	CAGGATCCCGCCAGAGATAATTAAGCTC
D1	CAGAATTCGGGTAGAAATTCTGGCTTAC
D2	CAGGATCCGAGAATACTCAGGGACGATG

3.4. DNA manipulation

3.4.1. Plasmidic DNA isolation

Plasmidic DNA was isolated using the commercial Kit QIAprep® Spin Miniprep Kip from QIAGEN. This kit is based on alkaline lysis method and a posterior recuperation of plasmidic DNA by affinity chromatography.

3.4.2. DNA fragments amplification by Polymerase Chain Reaction (PCR)

Two different commercial products were used to amplify DNA fragments by PCR. In both cases the manufacturer instructions were followed for the DNA amplification.

1. Accuzyme from Bioline, it is a thermostable DNA polymerase with proofreading activity. It was used to amplify DNA fragments for cloning or gene disruption.

2. Dream Taq Master Mix from Fermentas (Thermo Fisher) consist in a Taq polymerase – without proofreading activity – mixed with dNTP and an appropriate buffer, provided in a 2x solution. It was used to amplify DNA as a routine genotyping of bacterial strains.

For genotyping samples for PCR amplification from bacterial colonies were obtained by resuspending a colony in 100µl of sterile ddH_2O and heated to 100ºC 5 minutes in order to break bacterial cells. For cloning purpose purified DNA was used as template.

The PCR reactions were performed using a basic program: denaturing at 94ºC during 5 minutes, followed by 30 cycles of denaturing at 94ºC during 30 seconds, annealing *at 55ºC* during 30 seconds and extension at 72ºC during *30 seconds*. A final extension step at 72ºC during 10 minutes was performed. The *Annealing temperature* and *Extension time* of the PCR cycle were modified in function of the primers and the expected size of the amplified fragment.

3.4.3. Error-prone PCR

This method to randomly mutagenize is based on the fact that Taq polymerase has not proofreading activity (Bossi and Figueroa-Bossi, 2007). Target genes were amplified using a PCR reaction with Taq polymerase from New England Biolabs, standard Taq Buffer (10mM Tris-HCl pH 9.0, 50mM KCl, 1.5mM $MgCl_2$), 0.1% Triton X-100 and 0.2mg/ml BSA. The PCR amplification program is depicted in **figure 20**. During the first 10 cycles, the PCR reaction program (annealing temperature 64ºC or 58ºC) was characterized by a slow decrease from denaturing to annealing temperature (0.1ºC/second). The following 15 cycles were characterized by having the regular quick temperature decrease between the denaturing and the annealing cycle.

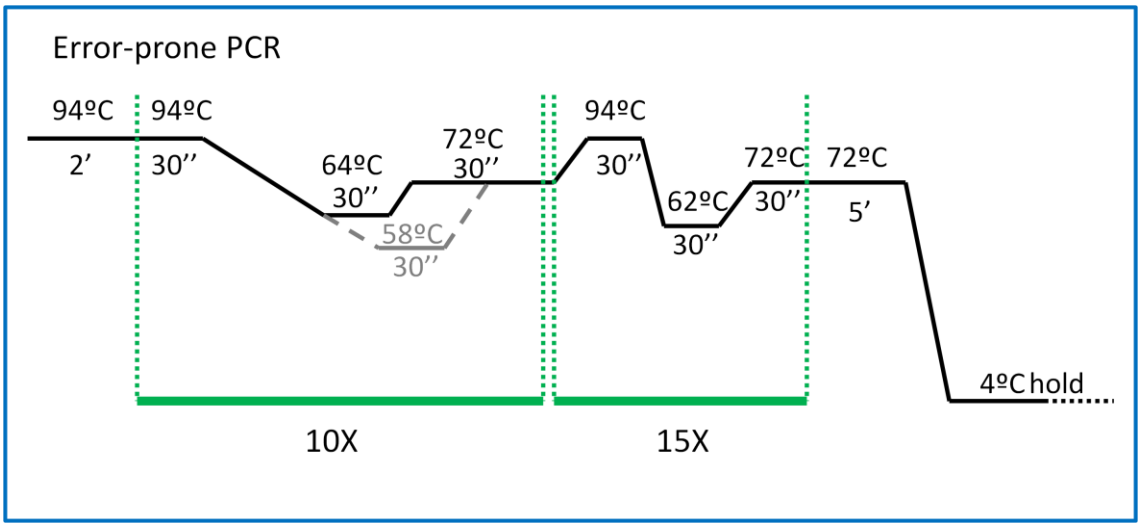

Figure 20: Scheme of the error prone PCR reaction programme.

3.4.4. DNA fragments sequencing

DNA fragments were sequenced by Sanger method, based on synthesis and termination of DNA fragment using fluorescent labelled dideoxinucleotides. It has been used the BigDye® Terminator v3.1 Cycle Sequencing Kit from Applied Biosystems, using the instructions of the manufacturer. Samples were analyzed in an ABI Prism 3700 Genetic analyzer from Applied Biosystems, at the CCiTUB, Centres Cientifics i Tecnologics de la Universitat de Barcelona.

3.4.5. DNA electrophoresis in agarose gels

DNA samples were analyzed by electrophoresis in horizontal agarose gels. The agarose gels were prepared with TBE 0.5 x buffer (45 mM Tris, 45 mM Boric acid, 1 mM EDTA pH 8.3). Agarose concentration depends on the expected length of the DNA fragment. For fragments shorter than 1 Kb were used 2% agarose gels, while for longer fragments were used 0.8% agarose gels.

Loading buffer 5x (0.25% bromophenol blue, 0.25% xylene cyanol, 60% glycerol, Tris 10mM, EDTA 1mM) was added to all samples.

Different DNA ladders were used:

- λDNA-HindIII (Fermentas) from 125 bp to 23.1 Kb .
- GeneRuler^{TM} 1Kb DNA Ladder (Fermentas) from 250 bp to 10 Kb.
- GeneRuler^{TM} 50pb DNA Ladder (Fermentas) from 50 bp to 1 Kb.

DNA electrophoresis gels were run in Mupid® EXu/One equipment at 100–135 volts00 in TBE 0.5 x and then stained with ethidium bromide in order to visualize the DNA using Gel Doc^{TM} XR system with Image Lab^{TM} software.

3.4.6. Gel band extraction

To extract and purify DNA from standard agarose gels in TBE buffer, the DNA bands were excised from the agarose gel and purified using QIAquick® gel extraction kit from QIAGEN.

3.5. RNA manipulation

3.5.1. RNA isolation

Samples (1ml) of bacterial culture were taken and centrifuged in order to eliminate supernatant. Pellets were processed immediately or stored at -80ºC. RNA of the samples was isolated with the kit SV total RNA isolation system from Promega following the manufacturer instructions. This kit produces the bacterial lysis with lysozyme and a posterior recuperation of the RNA with a membrane-based purification system. The RNA was stored at -80ºC.

In order to eliminate any possible contamination with genomic DNA, an extra treatment with DNAsa Turbo from Ambion was performed: to the previously isolated RNA, 11 µl of 10 x Turbo DNAsa buffer and 2 µl of Turbo DNAsa were added and incubated at 37ºC during 30 minutes. The DNAsa inactivation reagent (10 µl) contains beads that would bind to the DNAsa and would inactivate the DNAsa. It was added and was incubated at room temperature for 5 minutes with occasional agitation. In order to eliminate the inactivation beads the solution was centrifuged at 10000 g and pellet was discarded (this step could be performed twice in order to ensure that all the inactivation beads are discarded). The supernatant was stored at -80ºC.

Samples were analyzed with Bioanalyzer 2.100 from Agilent in order to verify that RNA is not degraded or contaminated with genomic DNA and quantified with NanoDrop Spectrophotometer ND-1000.

3.5.2. cDNA transcription

To obtain cDNA from the RNA, the kit transcription one-step RT-PCR from Roche was used. This kit is based on a retrotranscription step amplifying with random primers. Each reaction contains 2 µl of the retrotranscriptase Buffer, 0.8 µl dNTP, 2 µl random primers, 1µl retrotranscriptase, 4.2 µl water and 10 µl RNA (0.1 µg/µl). As a negative control, to rule out genomic DNA contamination, the same reaction without retrotranscriptase was used. The program used was: 10 minutes at 25ºC, 120 minutes at 37ºC, 5 minutes at 85ºC and stored at -20ºC.

3.5.3. Real-Time qPCR

In order to design optimal primers for Real-time qPCR, the following rules were taken in account (Applied Biosystems by life technologies, 2011):

1. Amplicons (short segments of the target gene amplified) should be between 50 to 150 bp
2. The optimal primer length is 20 bases
3. GC content must be between 20-80% range
4. There must be fewer than four consecutive G residues

5. Keep the Tm between 58-60ºC
6. The five nucleotides at the 3' end contain no more than two G and/or C bases.

In order to evaluate the efficiency of the used primers, qPCR reactions were performed with 5 serial dilutions of cDNA (1/10) and 3 technical replicates (Schmittgen and Livak, 2008). Each reaction contains: 10 µl SYBR Green PCR Master Mix, 1 µl of each primer (at 10 µM) and 8 µl of cDNA. SYBR Green is able to bind to double-stranded DNA producing fluorescent signal reflecting the amount of PCR product. The reactions were run in a Step One Real-Time PCR system by Applied Biosystems. The PCR program used was: initial denaturing at 95ºC during 10 minutes, followed by 40 cycles of denaturing at 95ºC during 15 seconds and extension at 60ºC during 1 minute (Applied Biosystems by life technologies, 2011). To detect nonspecific amplifications the melting curve was determined. It consist in a temperature increment of 0.3ºC/second from 60ºC to 95ºC and the signal corresponding to the presence of double-stranded DNA was plotted. The presence of a single peak (corresponding of the melting point of the double-stranded DNA) suggests specific amplification of the amplicon, but additional peaks would reflect nonspecific amplification.

Data was collected and analyzed with Step One Software version 2.2.2 from life technologies, plotting the fluorescent signal detected at each cycle (**fig. 21A**).

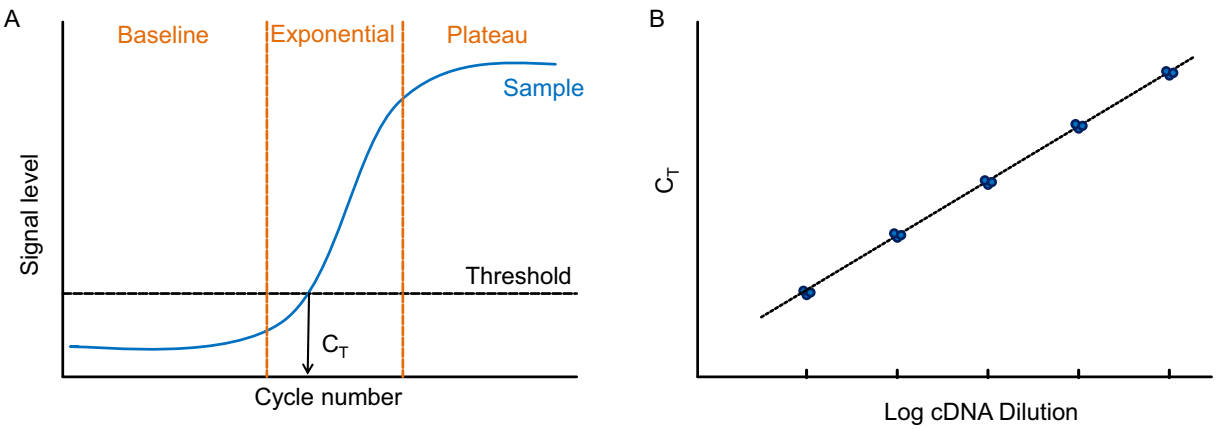

Figure 21: Schematic results of a qPCR experiment. A) Representative amplification plot showing the signal threshold and C_T. B) Representative efficiency plot with 3 technical replicates for each of the 5 dilutions of the cDNA.

The fluorescent signal (also known as R_n) increases at each cycle as well as the PCR product. As shown in **figure 21A** during the first cycles no increase of fluorescence is detected due the low amount of PCR product, phase known as baseline. After that the fluorescent signal increases exponentially since reaching a plateau, where the levels of fluorescent signal are saturated (**fig. 21A**). The detection threshold is automatically determined (or manually set) within the exponential region above the baseline. The cycle when the fluorescent signal of the samples crossed the threshold is denominated C_T (**fig. 21A**) and it is related with the initial amount of cDNA. To calculate the efficiency of the primers used, the C_T obtained for each sample was plotted against the log of the cDNA dilutions (**fig. 21B**). The slope of the line was determined and used to calculate the efficiency using the following equation: $E= (10^{-1/a}-1)100$ where E is efficiency expressed in % and a is the slope of the line. It is acceptable an efficiency of 100% ± 10%.

To determine gene expression, the Real-Time qPCR data is presented relative to another gene, known as endogenous control (Schmittgen and Livak, 2008), that in our case was *zwf,* gene coding for glucose 6-P dehydrogenise. The primers used to amplify the target gene and the endogenous control must have similar efficiency. Data was analyzed with Step One Software version 2.2.2 from life technologies and relative expression between two conditions (A and B) was calculated as follows:

$$\text{fold change} = 2^{-[(C_T\text{Target A} - C_T\text{Endogenous A}) - (C_T\text{Target B} - C_T\text{Endogenous B})]}$$

3.5.4. Transcriptomic study

Tree independent cultures for each strain were grown in LB at 37ºC up to an OD_{600nm} of 2.0 and 1 ml aliquots were collected by duplicate to isolate RNA as described in section 3.5.1. Samples were analyzed by Bioanalyzer 2.100 from Agilent in order to verify that RNA is not degraded or contaminated with genomic DNA. Transcriptomic analysis was performed using a costume high-density DNA microarray (4x72K) prepared with Maskless Array Sinthesizer technology form NimbleGen. Our array covers 4735 ORF represented with seven selected probes for each ORF by duplicate, using the genome sequence

of *Salmonella enterica* serovar Typhimurium SL1344 provided by the Wellcome Trust Sanger Institute. The transcriptomic experiment was performed as recommended by NimbleGen standard protocol (Roche, 2010). Briefly, the total RNA was retrotranscribed to cDNA using the Invitrogen SuperScript double-stranded cDNA synthesis kit, labelled with Cy3 using NimbleGen one-colour DNA labelling kit and hybridized to probes of the array using the NimbleGen hybridization system. Scanning and data analysis was performed as indicated by Nimblegen standard protocol (Roche, 2010). The raw data was subjected to RMA (Robust Multi-array Analysis), quantile normalization and background correction as implemented in the NimbleScan software package.

RMA algorithm (Irizarry *et al.*, 2003) was used as quality control to prepare data for the analysis. The log2 expression shows no different average expression within groups either before or after normalization. The Principal Components Analysis showed no biases and no outlying chips. For the pairwise comparisons the moderated t-test statistics (Smyth, 2004) were computed, as implemented in the Bioconductor library *limma*. The annotation of probesets was done with the information provided for the Nimblegen custom array.

The transcriptomic experiment was carried out in the IRB (Institut de Recerca Biomedica) and the statistical analysis of the microarray data was performed by the Bioinformatics Units at CCiTUB (Centres Cientifics i Tecnologics de la Universitat de Barcelona).

Classification of the ORF of *Salmonella enterica* serovar Typhimurium SL1344 was performed according the functional classification of the ORF of *Salmonella enterica* serovar Typhimurium LT2 in the JCVI classification (Torrieri *et al.*, 2012). The relation between the genes of the strain SL1344 and the genes of the strain LT2 was performed according its annotation. In the cases that the relation was not clear, it was compared by blast between both species.

3.6. Protein manipulation

3.6.1. Protein electrophoresis in SDS polyacrilamide gels (SDS-PAGE)

These gels have 2 sections, the stacking part (upper part), that compact the sample proteins before entering to the resolving phase (lower part) where proteins are separated attending to its molecular weight.

The stacking phase contains a 5% of polyacrilamide (Acrilamide/Bis 30.8% T 2.6% C), staking buffer (0.375 M Tris and SDS 0.1% at pH 8.8), and to produce the polymerization of polyacrilamide, APS 10% (0.07% final concentration) and TEMED (0.2% final concentration) was added. The percentage of polyacrilamide of the resolving phase is variable (10%, 12.5% or 13.5%), depending on the size of the protein to study. The resolving phase also contains the resolving buffer (0.125 M Tris and SDS 0.1% at pH 6.8) and to produce the polymerization of polyacrilamide again APS 10% (0.05% final concentration) and TEMED (0.083% final concentration) was added.

Gels were run on Miniprotean II™ equipment from Bio-Rad, the running buffer contains 25 mM Tris, 192 mM glycine and SDS 0.1%.

Coomassie brilliant Blue staining: Gels were incubated during 30 minutes with staining dye (0.5‰ Coomassie Brilliant Blue R-250, 10% Acetic Acid, 25% Isopropanol) at room temperature. To eliminate the dye excess, the gels were cleaned with 10% Acetic Acid.

3.6.2. Protein immunodetection

For protein immunodetection, proteins were transferred from SDS-PAGE to a PVDF membrane using EBU-4000 equipment from CBS scientific. Before transferring, membranes were activated with methanol and equilibrated in transfer buffer (48 mM Tris, 39 mM glycine, 20% of methanol, 1.3 mM SDS). Polyacrilamide gels were equilibrated in transfer buffer for at least 10 minutes and placed on top of a PVDF membrane. Transfer was performed between 8 Whatman 3mm papers – 4 on top and 4 on bottom – wet with transfer buffer.

Proteins were transferred into the PVDF membrane applying 55 mA during 1 hour.

After the transfer, PVDF membranes were blocked on PBS-Tween (20 mM Tris, 136 mM NaCl, 0.1% Tween-20) with 5% skimmed milk as blocking agent at room temperature for 1 hour or overnight at 4ºC. It was incubated with primary antibody diluted in PBS-Tween for 1 h at room temperature. Next, the membrane was incubated with secondary antibody conjugated with peroxydase diluted in PBS for 1 h at room temperature. The signal was detected with a chemiluminescent reaction, using ECL™ Western Blotting from GE Healthcare, and detected by Molecular Imager ChemiDoc XRS System from BioRad.

The antibodies used were:

Antibody	Origen	Dilution	Reference / Source
Primary antibody			
α-GreA	mouse	1/5000	Neoclone
α-RpoD	mouse	1/5000	Neoclone
α-FliA	mouse	1/5000	Neoclone
α-FliC	rabbit	1/2000	(Majander *et al.*, 2005)
Secondary antibody			
α-mouse	Goat	1/5000	Promega
α-rabbit	Donkey	1/20000	GE Healthcare Life biosciences

3.7. Genetic transfer methods

3.7.1. Bacterial transformation

Different methods were used to transform bacteria:

3.7.1.1. Transformation by $CaCl_2$ treated competent cells: First chemically induced competent cells were obtained. A bacterial culture was grown in LB medium to early exponential phase (OD_{600nm} 0.2-0.3) and 10 ml were centrifuged at 3000 rpm during 10 minutes at 4ºC and the pellet was resuspended in cold $CaCl_2$ (50 mM). Again, cell suspension was centrifuged and pellet was resuspended in cold $CaCl_2$. Several cleaning cycles were done, reducing at each cycle the amount of $CaCl_2$ in order to concentrate the cells

reducing up to a final volume of 0.5 ml. This suspension was kept on ice for more than 30 minutes.

To transform, 100µl of competent cells and 1-10µl of DNA were mixed and kept on ice 30 minutes. Then, a heat shock was produced to introduce the DNA into the cells by incubating the mixture at 42ºC during 45 seconds and then 2 minutes on ice. After that, 1 ml of LB were added and incubated at 37ºC during 1 hour and then plated on LB plates with the suitable antibiotic.

3.7.1.2. Transformation by electroporation: A bacterial culture was grown in LB medium to exponential phase (OD_{600nm} of 0.6) and 10 ml were centrifuged at 3000 rpm during 10 minutes at 4ºC and the pellet was resuspended in cold 10% glycerol solution. Several cleaning cycles with cold 10% glycerol solution were done, reducing at each cycle the amount of glycerol solution in order to concentrate the cells reducing up to a final volume of 0.5 ml. This suspension was kept on ice for more than 30 minutes.

To transform, 50 µl of electrocompetent cells and 2-5 µl of DNA were mixed. The mixture was placed in a 1 mm cubette pre-chilled on ice. The DNA was introduced into the cell by permeabilization of the membrane by an electric pulse using an Electroporator 2510 from Eppendorf®. After that, 1 ml of SOC was added immediately and samples were incubated at 37ºC during 1 hour. Transformants were selected on LB plates with the suitable antibiotic.

3.7.1.3. TSS transformation: This rapid protocol to transform was useful with the *E. coli* but not with *Salmonella*. The competent cells were obtained from a bacterial culture grown in LB medium up to an OD_{600nm} of 0.3 - 0.8, chilled on ice for at least 10 minutes. An equal volume of 2x TSS buffer (8 g/L tryptone, 5 g/L yeast extract, 5 g/L NaCl, 0.2 g/L PEG 8000, 0.1 M $MgSO_4$, 100 ml/L DMSO) ice cold was added. The samples were thoroughly mixed by vortex avoiding warm up the cells. The competent cells were kept on ice for 10 minutes to several hours.

To transform, 1 ml cells and 1 µl of DNA were mixed, and let it stand on ice for another 30 minutes to several hours. If the selection was made by ampicilin, samples were spread on ampicilin containing plates immediately. When other

antibiotic was used, samples were incubated at 37ºC for 1 hour and a half, before inoculating on LB plates with the suitable antibiotic.

3.7.2. Transduction with bacteriophage P1*vir* in *E. coli*

Bacteriophage P1*vir* is a virulent derivate of the lysogenic phage P1. Transduction with this phage was used to introduce, by homologous recombination, mutations associated with an antibiotic resistance.

To obtain a P1*vir* lysate of the donor strain containing the mutation to transduce, a bacterial culture was grown in LB medium up to an OD_{600nm} of 0.5. A 0.5 ml of the culture were mixed with existent P1*vir* phage stock and added to 3 ml of top agar supplemented with Cl_2Ca 5 mM. To promote an efficient infection, several dilutions of the P1*vir* phage stock were tested. The bacterial-phage-top agar mix was spread on a LB plate and incubated at 37ºC overnight. To recover the P1*vir* lysate, the top agar was recovered using 2 ml of fresh LB and mixed in a tube with 0.5 ml of chloroform. The tube was shaken vigorously to separate P1*vir* from top agar and then the mixture was centrifuged at 3500 rpm during 10 minutes. The supernatant – containing P1*vir* – was recovered in a new tube with 0.5 ml of chloroform and stored at 4ºC.

The P1*vir* lysate were ultimately titrated. For this purpose, a culture of the indicator strain (AAG1) was grown in LB medium up to an OD_{600nm} of 0.8, centrifuged and resuspended with half-volume of absorption buffer (10 mM $MgSO_4$, 5 mM Cl_2Ca). Serial dilutions of the phage lysate on NaCl 0.15% were made, and 100 µl of each dilution were mixed with 100 µl of the indicator strain suspension. The mix was incubated at 37ºC during 20 minutes, to promote phage absorption. Top agar (2 ml) was added and the mixture was spread on LB agar plates. After incubating the plates at 37ºC the phage was titrated by counting the lytic plaques.

For transduction with P1*vir*, a culture of the recipient strain was grown in LB medium up to an OD_{600nm} of 0.4. A 10 ml aliquot of the culture was centrifuged at 3500 rpm during 10 minutes and the pellet was resuspended with 1 ml of LB. A 0.5 ml aliquot of this cellular suspension was mixed with 0.5 ml of different dilutions of the P1*vir* obtained and 0.5 ml of transduction buffer (15 mM Cl_2Ca

and 30 mM $MgSO_4$) and incubated at 37ºC during 20 minutes. After that, samples were centrifuged and pellet resuspended in NaCl 0.15%. The mixtures were spread on LB plates with the suitable antibiotic and incubated at 37ºC for transductants selection.

3.7.3. Transduction with bacteriophage P22 in *Salmonella*

Bacteriophage P22 HT *int4* (Schmieger, 1972) was used to introduce mutations by homologous recombination in *Salmonella.* This bacteriophage contains two mutations – HT and *int* – in order to increase transduction rate.

To obtain P22 lysates of the donor strain containing the mutation to transduce, a bacterial culture was grown in LB medium up to an OD_{600nm} of 1.5. A 10 ml aliquot of the culture was mixed with 100 or 200 µl of existent P22 stock obtained in TT1704 strain and grown at 37ºC for 4 hours. After 4 hours, the culture should be less turbid due the production lysis of infected cells. Aliquots of 10 ml were collected and 0.5 ml of chloroform was added. The tube was shaken vigorously to break the bacterial cells and centrifuged at 4000 rpm during 20 minutes to eliminate the cellular debris. Supernatant was collected in a new tube and stored at 4ºC with 0.5 ml of chloroform.

The P22 lysate was titrated. Overnight cultures of TT1704 (200 µl) was mixed with 100 µl of serial dilutions of the obtained lysate in $MgSO_4$ 10mM. The mixtures were incubated at 37ºC during 20 minutes. Top agar (3 ml) was added and the mixture was spread on LB plates and incubated overnight at 37ºC.

For transduction with P22, an overnight culture of recipient strain (100 µl) was mixed with 100 µl of phage dilutions in $MgSO_4$ (10 mM) and incubated at 37ºC during 1.5 hours. As negative control, 100 µl of culture or phage were mixed with 100 µl of LB. After incubation, the samples were centrifuged and pellets resuspended with LB, in order to eliminate bacteriophages. The mixture was spread on LB plates with the appropriate antibiotic. During this process, transductant cells could be re-infected by P22, pseudolysogens, integrated into the chromosome and becoming resistant to other P22 infection – it is not possible to transduce again. Transducants were plated on EBU in order to identify pseudolysogens. In colonies containing pseudolysogens, many cells are

lysated decreasing the pH of the medium and producing a colour change on the pH indicators, resulting in dark blue colonies. The “phage-free” cells will form light-coloured colonies while the pseudolysogens will remain blue.

3.7.4. pSLT conjugation

For pSLT conjugation, cultures of the donor and recipient strain were grown in 20 ml of Minimal media E + Casaaminoacids 0.3%. Medium was inoculated 1/50 using overnight cultures. The strains were grown at 37ºC up to an OD_{600nm} of 0.7. Aliquots (5 ml) of each strain were collected, centrifuged at 6000 rpm for 5 minutes, supernatant was discarded and the pellet resuspended in 5 ml of $MgSO_4$ (10 mM). To conjugate, 500 µl of donor and 500 µl of recipient cells suspensions were mixed. As negative controls mixtures of either 500 µl of donor cells or 500 µl of recipient cells with 500 µl of $MgSO_4$ solution (10 mM) were performed.

The mixtures were centrifuged 30 seconds at 13000 rpm in order to eliminate the supernatant and resuspended softly with 50 µl of $MgSO_4$ and placed on a 0.45 nm pore-diameter cellulose filter on top of a LB agar plate at 37ºC during 4 hours. Cellulose filters were collected and reused with 2 ml of $MgSO_4$ solution. Dilutions of the suspension were made and spread on LB agar plates with the appropriate antibiotic for transconjugants selection. Proper dilutions were also spread on LB agar plates containing the antibiotic required for the donor selection. Plates were incubated at 37ºC and the number of transconjugants and donor cells was calculated after cfu determination. The conjugation rate (transconjugants / donor cells) was determined.

3.7.5. Transcriptional-fusion’s insertion at the *attB* locus of the *E. coli* chromosome

To insert transcriptional *lacZ* fusions at the *attB* locus of the chromosome of *E. coli,* was used a method described by Simons *et al* (1987). First step is to clone the promoter region of interest in the plasmid pRS551, containing a reporter promoter-less *lacZ* gene. The promoter region was amplified by PCR adding an *Eco*RI and *Bam*HI restriction sites at each edge of the PCR-amplified fragment. The PCR products were cloned in pGEM-T Easy (Promega) vector. After

selecting an appropriate plasmid the containing promoter fragment was obtained after restriction with *Eco*R1 and *Bam*H1 and cloned in same restriction sites of pRS551.

The transcriptional fusions were transferred to the bacteriophage λRS45 by homologous recombination *in vivo*. A culture of the strain containing the transcriptional fusion on pRS551 was grown in LB medium supplemented with maltose 0.2% at 37ºC overnight. Infection with λRS45 was performed by mixing 200 µl of the bacterial culture with 100 µl of λRS45 phage and then incubated at 37ºC during 20 minutes. Top agar (3 ml) was added to the mix, spread on a LB plate and incubated at 37ºC during 7-8 hours. Since pRS551 contains sequences highly homologous to the λRS45 phages, during infection would be expected that homologous recombination occurs resulting in the incorporation of pRS551 based plasmid in the λRS45 phage. After infection, phage particles were recovered by adding 3 ml of TM buffer (50 mM Tris pH 7.5, 10 mM $MgSO_4$) on the plates and then incubated at 4ºC during 2 hours. Top agar and TM buffer were recovered and mixed together in a tube with 0.5 ml of chloroform. The tube was shaken vigorously to separate the phage from top agar and then centrifuged at 3500 rpm during 10 minutes. The supernatant was recovered in a new tube with 0.5 ml of chloroform and stored at 4ºC

To obtain lysogenic cells carrying a λRS45 derivative containing the pRS551 based vector as a prophage in the *attB* locus of the chromosome, a culture of the recipient strain was grown in LB supplemented with maltose 0.2% until stationary phase. A 200 µl aliquot of the culture was mixed with 100 µl of the phage previously obtained. After incubation at 37ºC during 20 minutes to promote the absorption of the phage, the free phages were cleaned after centrifugation and discarding the supernatant. The cells were plated on LB plates with kanamycin and incubated at 37ºC overnight. The lysogenic cells were genotyped by PCR – using the primers attB, attP and λ-int – to check that λRS45-derived phage was inserted into the *attB* locus just once.

3.8. Bacterial mutagenesis methods

3.8.1. One-step inactivation of chromosomal genes using PCR products

This method causes disruption of chromosomal genes based in λRed based recombination. The first step is to amplify an antibiotic resistance gene flanked by FRT sites (Datsenko and Wanner, 2000) adding to each edge of the fragment an approximately 40 bp region which is fully homologous to the place in the chromosome were insertion is wanted. These homologous sequences promote recombination with the target locus in the chromosome by the Red recombinase. The antibiotic resistance gene could be removed afterwards by FLP recombinase acting on the flanking FRT sites (**fig. 22**).

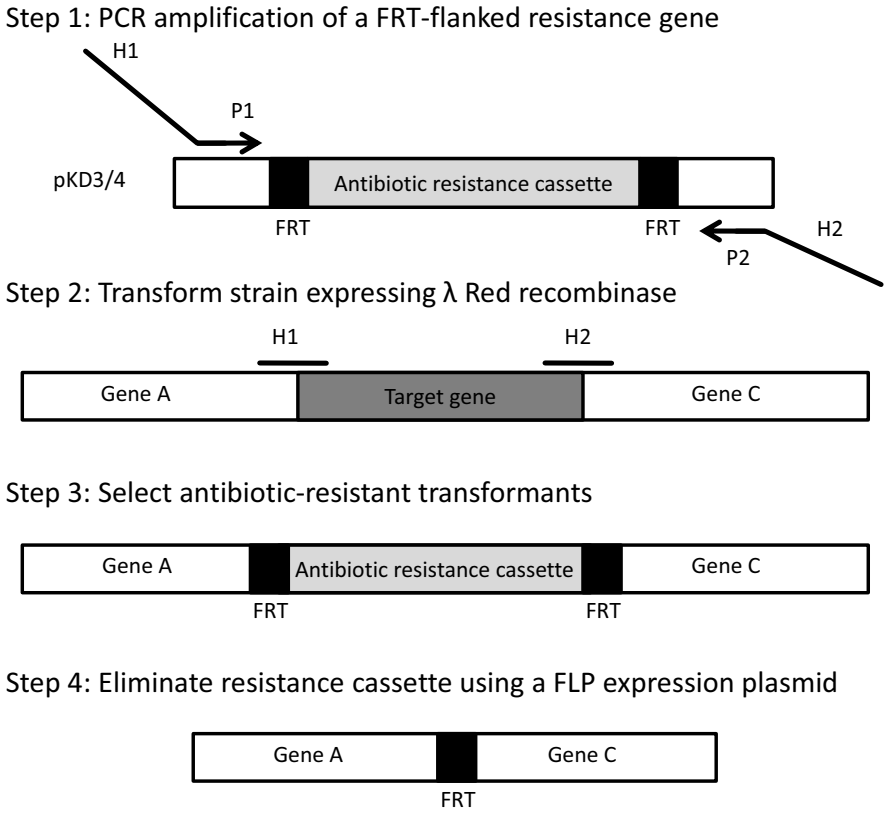

Figure 22: Schematic steps of the methodology to inactivate chromosomal genes using PCR products. H1, H2 represent the homologous part of the primer to the target locus of the chromosome and P1 and P2 correspond at the homologous part of the primer to the plasmid pKD3 and pKD4 (described in the text).

As mentioned above, the first step is the PCR amplification of the FRT-flanked resistance gene. Two different genes might be used, chloramphenicol and kanamycin resistance genes located in the plasmid pKD3 and pKD4

respectively. The primers used to do this amplification must have a 3'-end complementary to the plasmid, what is indicated P1 and P2 for the forward and reverse primers (**fig. 22**) and a 5'-end homolog to the target gene with an approximate length of 40nt, H1 and H2. The PCR fragment obtained will contain the antibiotic resistance cassette flanked by FRT sequences and the homologous zones to the target gene. Once obtained, the PCR mixture was digested with DpnI (1unit per 50µl of PCR mixture) to promote degradation of the template plasmid pKD3 and pKD4 that could be present in the PCR reaction. This step is required in order to avoid false positive during transformation (see below).

Next, the PCR fragment is transformed to the recipient strain expressing λ Red recombinase. To do that, plasmid pKD46 is introduced to the recipient strain of interest. The plasmid pKD46 is a thermosensible plasmid coding for λ Red recombinase, whose expression is under a L-arabinose inducible promoter. Red recombinase promotes recombination and inhibits exonuclease V, allowing lineal DNA fragments enters into the cell.

To transform the PCR amplified fragment, the target strain containing pKD46 was grown at 30ºC in SOB medium supplemented with 10 mM L-arabinose and ampicillin 100 µg/ml up to an OD_{600nm} of 0.6. Those cells were electroporated with 1 – 10 µg of the PCR-amplified fragment. After the electric pulse, cells were resuspended immediately with 1ml SOC medium and were incubated at 37ºC during 1.5 – 3 hours. Half of the reaction was then spread on LB agar plates with the appropriate antibiotic (either Cm or Km depending if either pKD3 or pKD4 were used) at 37ºC overnight.

The other half of the reaction was kept on the bench overnight and plated the next day. At 37ºC Red recombinase produces the recombination of the homologue fragment with the target gene producing a gene disruption (**fig. 22**). Moreover the plasmid pKD46 get cured due to its thermo-sensibility. Colonies resistant to the antibiotic were checked by PCR.

If required the resistance cassette could be eliminated by using a FLP expressing plasmid. To do that, the mutant strain was transformed with plasmid

pCP20. This plasmid is thermosensible, resistant to ampicillin and codes a FLP recombinase. The FLP is expressed at 42ºC. Transformants of pCP20 were selected on LB agar plates supplemented with ampicillin at 30ºC overnight. After selection, the transformants were incubated in LB at 42ºC during several hours and then plated on LB agar plates and incubated at 42ºC in order to induce express FLP recombinase. The enzyme will promote site specific recombination in the FRT sites causing elimination of the resistance cassette flanked by FRT and simultaneously curing the pCP20 plasmid (**fig. 22**). To check the lost of the antibiotic resistance cassette, the colonies were streak on LB agar plates, LB agar ampicillin and LB agar chloramphenicol / kanamycin, depending on the cassette introduced. Those colonies that were not able to grow in the presence of antibiotic were PCR genotyped to demonstrate that has lost the antibiotic resistance cassette.

3.8.2. *lacZ* genetic fusions constructed by FLP recombination

The previously described method to obtain chromosomal mutants might also used to create *lacZ* fusions within the site where insertion was made (Ellermeier *et al.*, 2002).

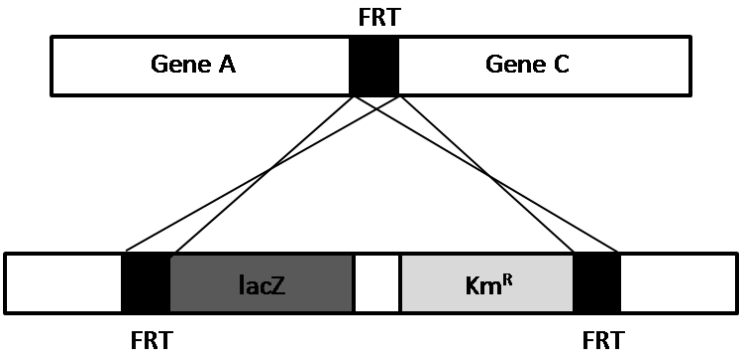

Figure 23: Scheme of the methodology used to introduce a promoter-less *lacZ* gene in the FRT by site specific recombination.

Once antibiotic free mutants were obtained, the process causes a genomic scarp, the presence of a FRT sequence in the site of initial insertion of the PCR-amplified fragment. To generate a *lacZ* fusion, those mutants with a FRT site were transformed with pCP20 and either pKG136 or pKG137. Those plasmids contain a promoter-less *lacZ* gene next to a kanamycin resistance cassette,

flanked with FRT sites. To use pKD136 or pKG137 depends in the orientation of the FRT site relative to the direction of transcription. These plasmids require *λpir* protein to replicate, therefore, after transformation the clones resistant to kanamycin had the plasmid integrated in the FRT site (**fig. 23**).

3.9. Bacterial physiology studies

3.9.1. Bacterial growth monitoring

Bacterial cultures were grown in Erlenmeyer culture flasks in a volume of medium (200 rpm), never higher to 1/5 of total volume of the flask, in constant agitation to produce a homogeneous aeration. Growth was monitored measuring the OD_{600nm} at different times with a Genesys 10S UV-Vis Spectrophotometer from Thermo scientific. Optical Density at 600 nm is proportional with the amount of bacteria in the culture and it is considered that an OD_{600nm} of 0.5 units corresponds to mid-log phase.

3.9.2. β-galactosidase activity determination

When β-galactosidase was determined, 1 ml aliquots of the culture were collected and kept on ice until its analysis (always a period inferior to 24 hours). A 100 µl aliquot of each sample was mixed with 900 µl of Buffer Z (60 mM Na_2HPO_4, 40 mM NaH_2PO_4, 10 mM KCl, 1 mM $MgSO_4$ and 50 mM β-mercaptoethanol). Cells were lysated by adding 15 µl of toluene and vigorous shaking during 15 seconds. Toluene was eliminated by incubation at 37ºC during 45 minutes. To detect β-galactosidase activity, 200 µl of ONPG (ortho-nitrophenyl-β-galactoside) in Buffer Z at a concentration of 4 mg/ml were added and mixtures incubated at 28ºC. β-galactosidase mediated hydrolysis of ONPG produces a yellow product, detectable with OD_{420nm}. Reaction was stopped with 0.5 ml Na_2CO_3 (1 M) when the reaction had an OD_{420nm} between 0.3-0.9. The OD_{420nm} and OD_{550} were measured for each reaction. To calculate β-galactosidase activity, the following formula was used:

$$\beta - \text{Galactosidase activity (MU)} = \frac{1000 \times (\text{OD}_{420} - 1.75 \times \text{OD}_{550})}{\text{t} \times \text{v} \times \text{OD}_{600}}$$

Where:

MU: Miller Units
OD_{420nm}: proportional to the ONPG hidrolysis.
OD_{550}: measures cell debris.
OD_{600}: measures culture biomass.
t: time between adding ONPG and the moment to stop the reaction (minutes).
v: volume of the culture used for the reaction (ml).

3.9.3. Motility assay

Motility assay was performed as described in Aberg *et al.*, (2009). The motility agar – with 2 mM of a chemo-attractants or repellents – was plated on the bench (25 ml each plate) less than 18 hours before the experiment, in order to prevent excessive drying of the agar plates. When solidified, 5 µl of bacterial suspension were spotted on top of the agar surface, and incubated at the temperature and time indicated. After incubation time, the swimming movement of the colony was measured by monitoring the diameter of the colony size. Images were taken with Gel Doc™ XR System with Image Lab™ Software. To ensure statistical significance, four replicates were made.

3.9.4. Biofilm formation

The biofilm formation was measured with the ability to form macrocolonies with RDAR morphotype, and the ability to produce biofilm on a plastic surface.

The ability to form macrocolonies was determined using CR agar plates. The cells were grown in LB at 37ºC up to an OD_{600nm} of 2.0. An aliquot (5 µl) of the bacterial suspension was spotted on CR agar plates and incubated at 28ºC during 7 days. After that, the RDAR morphotype (red, dry and rough colonies) was determined.

The production of biofilm on plastic surface was performed as described by Aberg *et al.*, (2006). Briefly, 10 µl of bacterial culture, grown in LB at 37ºC up to an OD_{600nm} of 2.0, was inoculated into 190 µl of LB without NaCl. Cultures in wells of non-tissue culture treated U-bottom 96-wells plastic plate were incubated statically at 25ºC for 48 hours. Thereafter the medium was discarded and the wells were washed with phosphate-buffered saline (PBS). The quantification of the attached bacteria was performed as follows: cells were fixed with 200 µl of methanol during 15 minutes. After being emptied and dried,

the wells were stained with 200 µl of crystal violet 2% during 5 minutes and the excess of staining was eliminated by placing the plate under running tap water. The dye adhered to the cells was resolubilised with 160 µl of acetic acid 33% and the OD_{570nm} was determined (Stepanovic *et al.*, 2000).

3.9.5. Haemolytic activity

The haemolytic activity was determined as described by Field *et al.*, (2008). Briefly, the strains were grown in LB at 37ºC up to an OD_{600nm} of 2.0 and an aliquot of 5 ml was centrifuged 15 minutes at 6000 rpm. The supernatant was collected, filtered through a 0.22 µm pore-diameter filter and kept on ice. An aliquot (50 µl) of different dilutions of the filtered supernatant were mixed with 50 µl of defribrinated sheep blood in a 96-wells plate. Before use, the defribrinated sheep blood must be centrifuged at 3000 rpm during 5 minutes at 4ºC and the blood cells resuspended with cold PBS in order to eliminate the broken ones. This process must be repeated as many times as required. The mixtures were incubated statically at 37ºC during 2.5 hours. After that, 150 µl of PBS were added and the plates were centrifuged 10 minutes at 2000 rpm. The haemoglobin of the supernatant was quantified measuring the optical density at 550nm.

3.10. Microscopy techniques

3.10.1. Optical microscopy

For cell observation by optical microscopy, a small part of a colony was resuspended in water, fixed on a microscope slide and stained with crystal violet for 6 minutes. After eliminating the excess of dye with water, samples were visualized with a Nikon ECLIPSE E600 optical microscope with 100x (immersion) objective and the images were taken with an OLYMPUS DP72 camera.

3.10.2. Transmission electron microscopy (TEM)

The bacterial samples for TEM visualization were used in a saline (R 1/4) suspension. An aliquot (1 ml) of bacterial culture grown until desired OD_{600nm}

was centrifuged 10 minutes at 6000rpm at room temperature. The cellular pellet was resuspended with filtered Ringer ¼, in order to avoid impurities. Samples were fixed on MESH 200 Carbon/Copper grids. Carbon/Copper grids must be activated with UV light in order to fix the sample to the Carbon surface. Samples were negatively stained with Uranyl acetate 2%, and visualized on a JEM1010 (JEOL Ltd, Tokio, Japan) Transmission Electron Microscope and the images were acquired by AnalySIS (Soft Imaging System GmbH, Münster, Germany).

3.11. Bioinformatics methods

Gene sequences used for the phylogenetic study were aligned with ClustalX (Thompson *et al.*, 1997). The phylogenetic trees of Maximum Likelihood (ML) (Felsenstein, 1981) were constructed by RAxML 7.0.3 (Stamatakis, 2014) – "Randomized Axelerated Maximum Likelihood", a program for sequential and parallel ML based inference– using a GTR (General Time Reversible) model of nucleotide substitution with a Gamma distribution of 4 discrete categories to rate heterogeneity (Yang, 1996). To test phylogeny tree, a boostrapt test was performed using 500 replications. The finale tree with the boostrapt was assembled with FigTree 1.3.1 (Rambaut, 2006).

Estimation of average codon-based evolutionary divergence over sequence pairs of target gene within groups was performed using the modified Nei-Gojobori (assumed transition/transversion bias = 2) model (Zhang *et al.*, 1998). The analysis involved 42 nucleotide sequences. All positions containing gaps and missing data were eliminated. There were a total of 70 positions in the final dataset. Evolutionary analyses were conducted in MEGA5 (Tamura *et al.*, 2011).

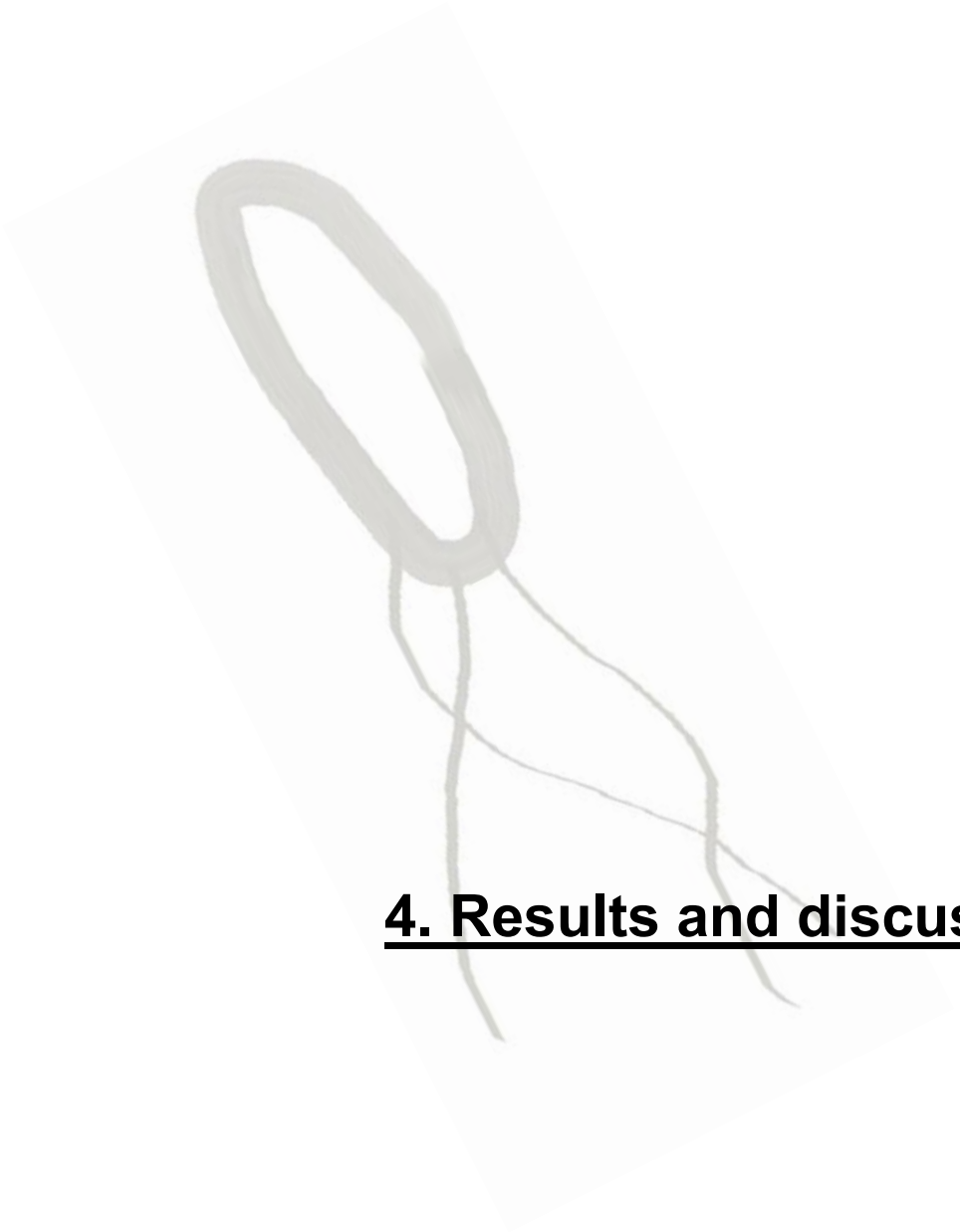

4. Results and discussion

4.1. Study of *greA* expression

GreA is encoded in a monocistronic operon located in the chromosome of *E. coli*. The gene *greA* is flanked by other monocistronic genes, upstream by the gene *dacB* and downstream by the gene *yhbY*. Both, *dacB* and *yhbY* are orientated in the opposite direction as compared to *greA* (**fig. 24**). Interestingly, YhbY and CgtA, encoded in the gene upstream of *dacB*, are proteins that bind to the 50S subunit of the ribosome (Jiang *et al.*, 2006). The protein CgtA, as described in section 1.2.2., is responsible of the interaction of SpoT with the ribosome (Jiang *et al.*, 2007). SpoT, as early mentioned, is involved in the ppGpp turnover. DacB is a penicillin binding protein involved in the synthesis and maintenance of the cell wall (Kishida *et al.*, 2006). The gene organization around *greA* is common for all Enterobacteria.

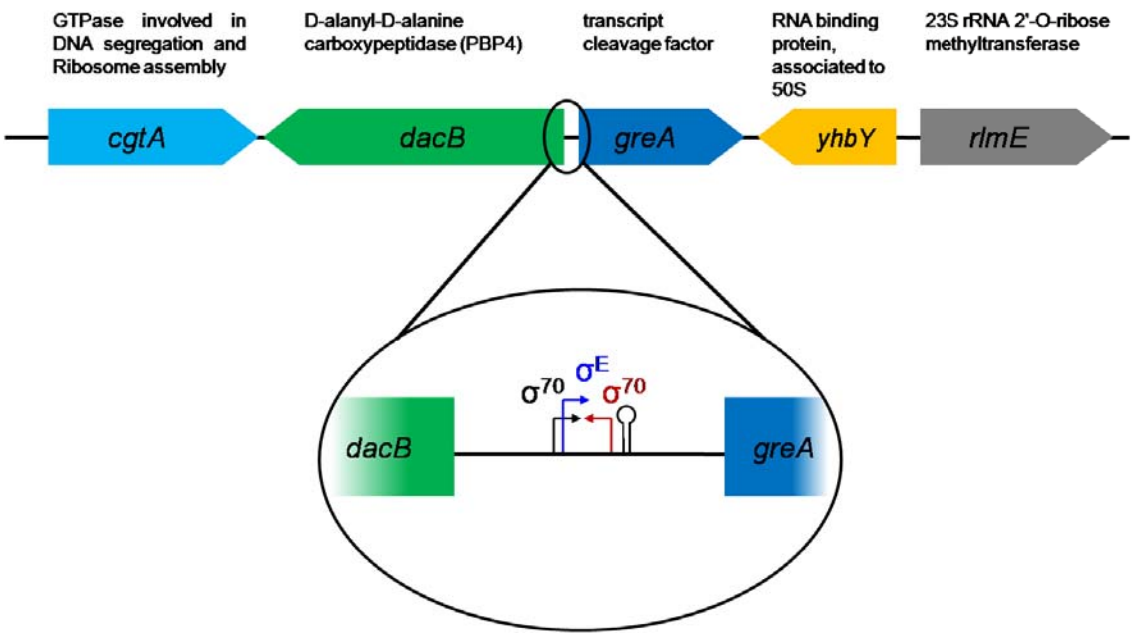

Figure 24: Genomic context of the *greA* gene in *E. coli*. In the amplification (ellipse), the intergenic region between *greA* and *dacB* is shown. Black and blue arrows show the σ^{70}-dependent and σ^{E}-dependent promoters of *greA*, respectively. The red arrow shows a putative σ^{70}-dependent promoter of gene *dacB*, as predicted by Virtual Footprint (Münch *et al.*, 2005).

Two predicted *greA* promoter sequences are found in the intergenic region between *dacB* and *greA,* one σ^{70}-dependent promoter and one σ^{E}-dependent promoter. The possible effect of σ^{E} on *greA* expression was shown by overexpressing σ^{E} and transcriptomic studies and the σ^{E} promoter location was confirmed by 5' RACE (Rhodius *et al.*, 2006).

Figure 25: Partial sequence of the *E. coli* genome, including the *greA* gene. In capital letters are indicated the coding sequences of *dacB* (in red), *greA* (in black) and *yhbY* (in green). The dotted line represents 721nt of *dacB*. The boxes -10 and -35 of the σ^{70} (in orange) and σ^{E} (in blue) *greA* promoters are indicated. The transcription initiation +1 for each promoter is indicated in capital letters in black. The early imprecise terminator is indicated in bold and underlined. The transcription terminator of the gene *greA,* predicted by RNAold (Naville *et al.*, 2014), is shown in dark blue in bold and underlined. The predicted -10 box of the putative promoter of *dacB* is indicated in purple. The sequences of the primers used either to produce different lacZ fusions

or to clone greA sequences into different vectors are indicated in grey and underlined by brackets. The name of the primer and the orientation is indicated.

Moreover, using primer extension and *in vitro* transcription assays (Potrykus *et al.*, 2010), it was experimentally demonstrated that *greA* expression is under control of two distinct promoters separated by 11nt: the σ^{70}-dependent and the σ^{E}-dependent promoters (**fig. 24 and 25**).

Between the *greA* promoters and the translation start, there is an imprecise transcription terminator, located 18 and 7 nucleotides downstream of +1σ^{70} and +1σ^{E}, respectively (**fig. 25**), that produces an array of short transcripts – known as GraL. Transcriptomic studies suggest that overexpression of GraL might alter the expression of some genes in *E. coli* (Potrykus *et al.*, 2010).

Very little is known about the regulation of *greA* expression. In order to gain knowledge in the *greA* expression regulation, different transcriptional and translational fusions of the *greA* promoter region with the *lacZ* reporter gene were constructed. These fusions are listed in **Table 5**, divided into two categories, I and II, depending on the methodology used to construct them.

	Name	Upstream sequence	Position of *lac* insertion	Primers	Pσ^{70}	Pσ^{E}	GraL	ORF	Type
I	greA +3	∞	+3	G3-G9	+	-	-	-	T
	greA +101	∞	+101	G5-G9	+	+	+	-	T
	greA +193	∞	+193	G8-G9	+	+	+	-	T
	greA +685	∞	+685	G10-G12	+	+	+	+	T
II	attBgreA1	-171	+175	G2-G7	+	+	+	-	T
	attBgreA2	-1030	+175	G1-G7	+	+	+	-	T
	attBgreA3	-1030	+175	G1-G7	+	+	+	-	t

Table 5: List of *greA-lacZ* fusions constructed. It is shown the position of the different fusions, as well as the elements that contain. The position of *lac* insertion is determined from the +1 of σ^{70}. The type of fusion could be transcriptional (T) or translational (t), as indicated. The primers used to construct the *lacZ* fusions, are shown. The two subgroups of *lacZ* fusions, I and II, are defined as discussed in the text.

The *lacZ* fusions of the category I were constructed by insertion of a *lacZ* promoter-less gene into the desired chromosome location following allele replacement (Datsenko and Wanner, 2000; Ellermeier *et al.*, 2002). As described in section 3.8, for gene replacement purposes by homologous

recombination, a DNA fragment containing an antibiotic resistance gene, flanked by sequences homologous to *greA,* was PCR-amplified. The primers used containing the homologous zones to *greA,* are shown in **figure 25** and **table 5**.

The *lacZ* fusions of the category II, were constructed by cloning the promoter sequences within vectors, generating transcriptional and translational fusions with a *lacZ* promoter-less gene. Next, the plasmid was transferred into the *attB* locus of the *E. coli* chromosome (Simons *et al.*, 1987), as described in section 3.7.5. The primers used are shown in **figure 25** and **table 5**.

The different *greA-lacZ* fusions generated have specific characteristics as described in **table 5**.

4.1.1. Autoregulation: Effect of GreA over its own expression

Many regulators are autoregulated, meaning that are able to control its own transcriptional expression (Thieffry *et al.*, 1998). While the positive autoregulation amplify the response to a signal, the negative autoregulation reduce background noise and produces a quicker response to environmental factors (Becskei and Serrano, 2000; Rosenfeld *et al.*, 2002). The possible autoregulation of GreA was explored (**fig. 26**).

To perform transcriptional studies of *greA* expression, the fusions attBgreA1 and attBgreA2 were transduced to a *lacZ* derivative of MG1655, the strain AAG1 (referred as WT) and to its *greA* counterpart CLT254 strain, (referred as *greA*). The *greA* expression in the different genetic background was monitored in cultures grown in LB at 37ºC up to early-stationary phase (OD_{600nm} of 1.5). When using the attBgreA1 fusion (**fig. 26A**), containing a short promoter sequence (-171), a clear increase (2-fold) in the transcriptional expression was detected in the *greA* mutant strain indicating that *greA* expression is negatively autoregulated, since GreA seems to repress its own expression.

Considering that promoters might contain regulatory elements in extended upstream regions of the -35 and -10 sequences, same experiments were performed using the fusion attBgreA2 that contains a larger promoter region than attBgreA1 (-1030). As expected, similar results were obtained (**fig. 26B**),

the *greA* expression increases in the *greA* mutant strain, as compared to WT. With the extended promoter region fusion, the increase detected was higher (up to 2.5-fold) than with the shorter promoter fusion. Transcriptional *greA* expression in a *greA*$^+$ and *greA*$^-$ background was also tested using *lacZ* fusions in the native genomic context of *greA* by using the greA+685 and greA+193 constructs (**table 5**). As could be observed in **figure 26C**, the expression from greA+193 fusion (*greA*$^-$ background) is up to 3-fold higher than from greA+685 (*greA*$^+$ background), showing similar results as the obtained with the attBgreA1 and attBgreA2 fusions (**fig. 26A and 26B**). Moreover, a translational fusion was also used (**fig. 26D**), obtaining similar results.

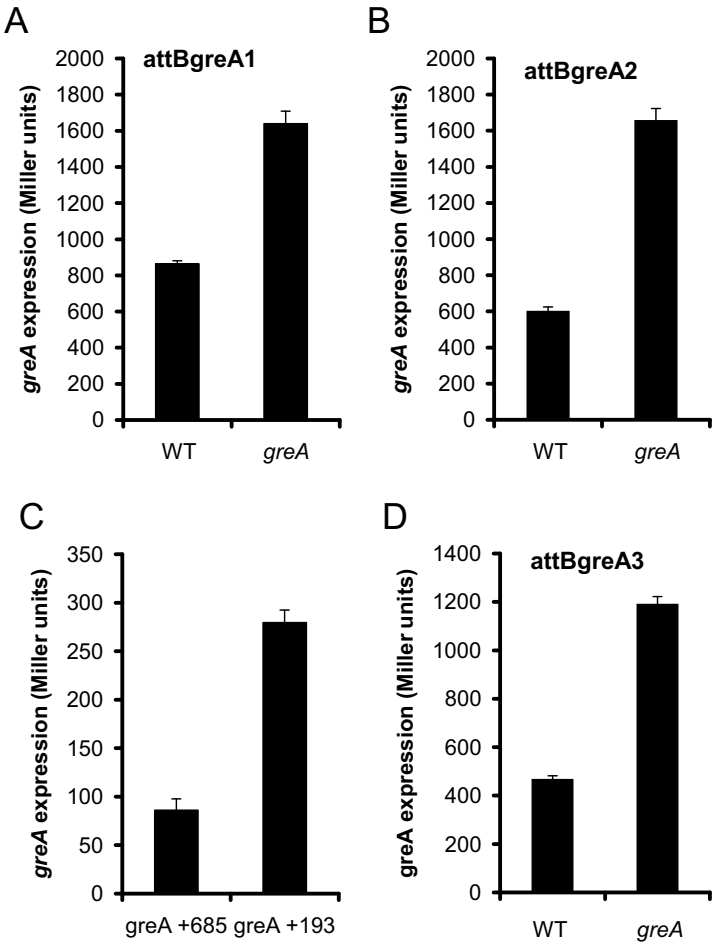

Figure 26: Expression of *greA* in AAG1 (WT) and CLT254 (*greA*) in cultures grown in LB at 37ºC up to an OD_{600nm} of 1.5. Different *lacZ* fusions were assessed: attBgreA1 (A), attBgreA2 (B), greA +685/+193 (C) and attBgreA3 (D). Average and standard deviation of β-galactosidase activity determined from three independent cultures are shown.

Altogether, these data clearly indicate that *greA* expression is autoregulated. GreA represses its own expression presumably to guarantee that GreA levels in

the cell do not increase over a specific threshold. As previously mentioned, GreA might compete with other proteins, maintaining a narrow equilibrium, for interacting with the secondary channel of the RNApol. In such scenario, such negative autoregulatory loop might play a very significant role since a very strong increase of GreA could cause that it would be occupying the secondary channel of most of the holoenzyme complexes in the cell, somehow causing alterations in the equilibrium with all the other proteins that could also interact with the secondary channel of the RNApol. In fact, it would be shown in chapter 4.4. that very high levels of GreA in the cell have a deleterious effect for the cell growth, clearly indicating that maintaining a proper expression of *greA* is pivotal for the physiology of the cell.

The autoregulation of GreA was published by Potrykus *et al.*, in 2010, they performed transcriptional studies of *greA* expression similar to those shown in **figure 26**. They determined the expression of *greA* with a *lacZ* fusion similar to attBgreA1 in presence and absence of GreA. They also observe an increase of *greA* expression in absence of GreA (3-fold higher), suggesting that *greA* expression is subject to autorepression.

To further characterize the autoregulatory loop, the *greA* gene was cloned in pBR322 to determine if it complements the *greA* mutation regarding the autoregulation. The *greA* D41A allele was also used. The amino acid D41 is essential for GreA antipause activity and, consequently, the *greA* D41A allele is defective in rescuing paused complexes of the RNApol (Opalka *et al.*, 2003; Laptenko *et al.*, 2003). To clone the alleles, the *greA* genes with its own promoters were amplified by PCR using the primers G1 and G11 from MG1655 and TP1204 (*greA* D41A), respectively. The resulting plasmids pBR-GreA and pBR-GreA D41A, as well as pBR322 as a control, were transformed into the strain LFC4 (CLT254 attBgreA2). The expression of *greA* was determined in cultures grown in LB at 37ºC up to early-stationary phase ($OD_{600nm}$of 1.5) of the strains LFC3 (AAG1 attBgreA2) pBR322 and LFC4 carrying either pBR322, pBR-GreA or pBR-GreA D41A (**fig. 27**). As previously shown (**fig. 26**), the absence of GreA (LFC4/pBR322) increases the expression of *greA* as compared to WT strain. When plasmid pBR-GreA was introduced, a significant decrease in the expression of *greA* to the levels of the WT strain was observed,

indicating that pBR-GreA complement the chromosomal deficiency of *greA*. Interestingly, when the plasmid pBR-GreA D41A was introduced, it was observed that this allele is not able to complement GreA deficiency, showing a high expression of *greA* (**fig. 27**). These data indicates that antipause activity is required for autoregulation of GreA. Somehow, it means that the ability to solve paused transcription elongation complexes (TEC) would reduce the expression of *greA*. While it is easily understandable that solving paused TEC may increase gene expression, it is difficult to explain how antipause activity can decrease gene expression. To explain it, we hypothesized that GreA may affect *greA* expression indirectly by activating an unknown factor that would repress *greA* expression. This hypothesis is in agreement with previous results from Potrykus *et al.*, (2010), where they were unable to detect GreA autoregulation when performing *in vitro* transcription experiments, indicating that additional factors were necessary to observe the autoregulation phenomenon *in vitro*.

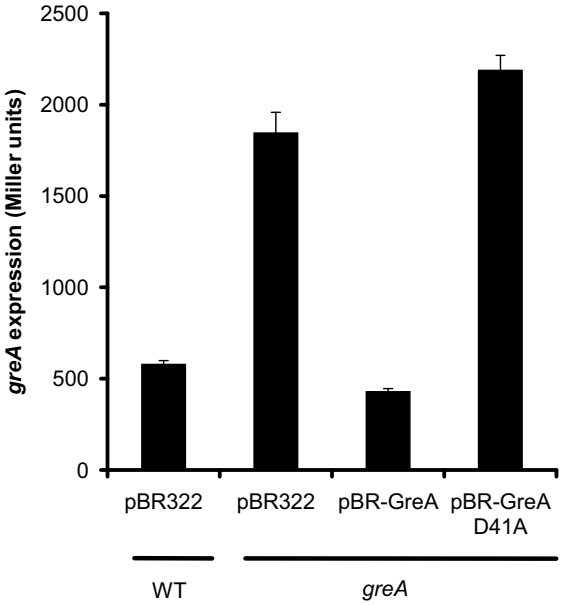

Figure 27: Complementation of Δ*greA* mutation *in trans*. LFC3 pBR322 and LFC4 carrying pBR322, pBR-GreA or pBR-GreA D41A were grown in LB at 37ºC up to an OD_{600nm} of 1.5 and β-galactosidase activity was determined. Average and standard deviation of β-galactosidase activity determination from three independent cultures are shown.

The *greA* gene encodes at least two regulatory elements, the protein GreA and a set of small RNAs, known as GraL that might play a role in gene expression regulation (Potrykus *et al.*, 2010). To elucidate the effect of GraL on *greA* autoregulation, we obtained a GraL GreA deficient strain (Δ*greAgraL*) by gene

replacement, using the primers G4 and G9 and we transduced the fusion attBgreA2 into this strain to generate LFC7 (AAG1 Δ*greAgraL* attBgreA2). A partial sequence of the *greA* gene with its own promoter was cloned in pBR322, allowing production of GraL but not the protein GreA. The *greA* cloned fragment was amplified from MG1655 with primers G1 and G7, and cloned into pBR322. The plasmids pBR322, pBR-GreA and pBR-GraL were transformed into LFC3 and LFC7. The resulting strains were grown in LB at 37ºC up to an OD_{600nm} of 1.5 and β-galactosidase activity was determined (**fig.28A**). The plasmid pBR-GraL did not produce any effect over *greA* expression in a WT strain. Remarkably, the presence of pBR-GreA produces a decrease (2-fold) on *greA* expression in the WT strain, indicating that increasing the levels of GreA within the cell has consequences in the gene expression profile. In the mutant strain for GreA and GraL, *greA* expression is 5-fold higher than in WT suggesting that GraL represses *greA* expression as well as GreA. Both factors affect negatively the expression of *greA* in an additive effect. The plasmid pBR-GraL produces a decrease of *greA* expression in the mutant Δ*greAgraL*, but *greA* expression is still 3-fold higher than in WT (**fig. 28A**). However, in the mutant Δ*greAgraL,* pBR-GreA (that produces both GreA and GraL) reduces the expression of *greA* almost to the WT expression levels.

These data shows that GraL and GreA produce an additive effect over *greA* expression. Among different possible regulatory models that may explain the observed results, the data may suggest that both, GreA and GraL, might stimulate the expression of an unknown factor that would repress the expression *greA* expression. It should be mentioned that the strain Δ*greAgraL* is not completely deficient in GraL since the *lacZ* fusion attBgreA2 is presumably proficient in GraL production. Transcriptomic studies performed during GraL overexpression (Potrykus *et al.*, 2010) showed that GraL has an effect over gene expression, but no effect over *greA* was detected. They predict that GraL could interact with the mRNA of *yhiY*, gene located downstream of *greA* (**fig. 24**).

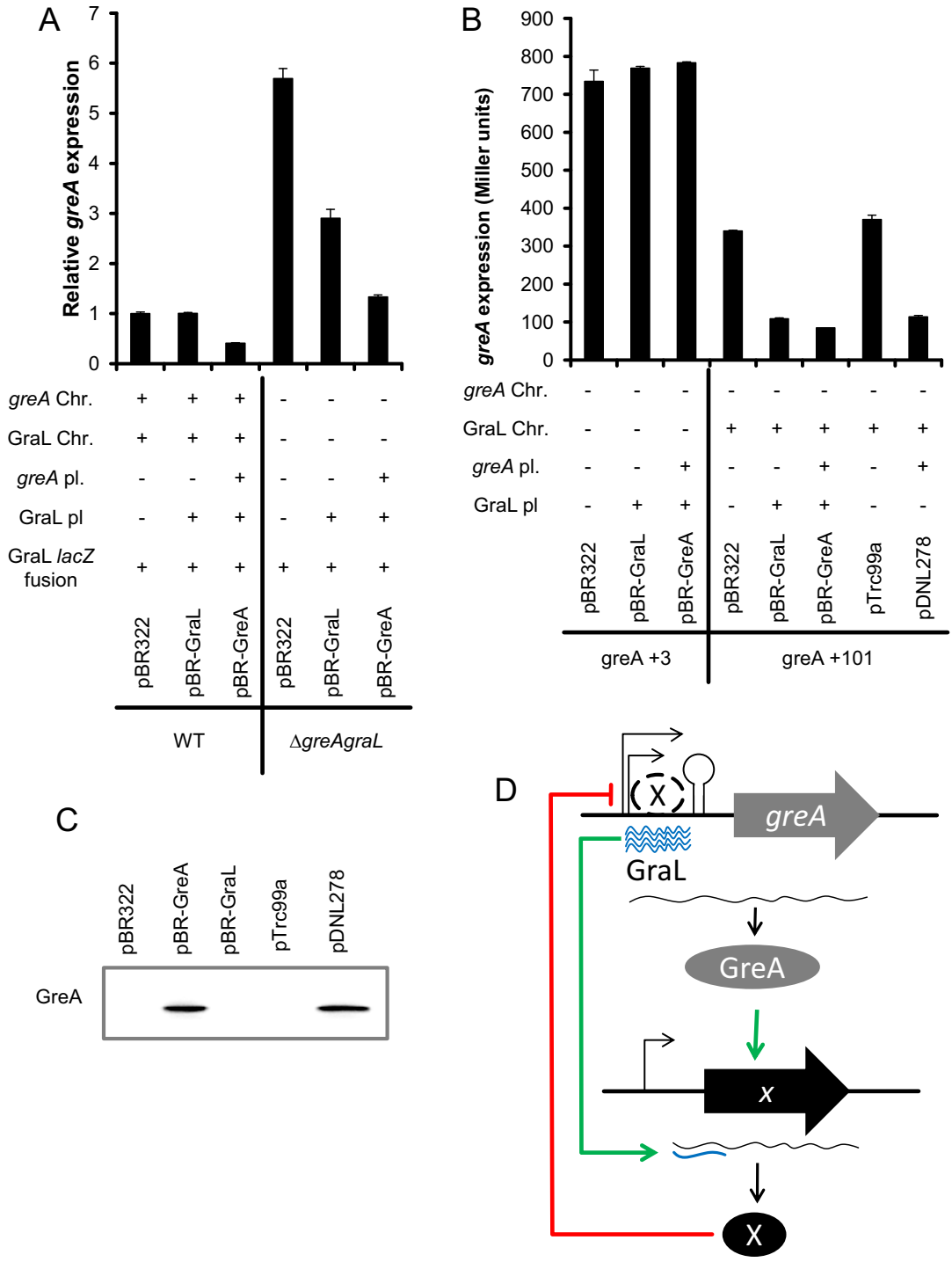

Figure 28: Effect of GreA and GraL over *greA* expression.. A) Effect of pBR322, pBR-GreA and pBR-GraL into LFC3 and LFC7. B) Effect of pBR322, pBR-GreA and pBR-GraL into LFC30 (greA+3) and the effect of pBR322, pBR-GreA, pBR-GraL, pTrc99a and pDNL278 into LFC32 (greA+101). C) The presence of GreA was determined in the strain LFC32 carrying the plasmids pBR322, pBR-GreA, pBR-GraL, pTrc99a and pDNL278 by Western blot using antibodies against GreA. In A, B and C, cultures were grown in LB at 37ºC up to an OD_{600nm} of 1.5 D) Hypothetical model of the autoregulation of *greA* and the effect of GraL on it. Average and standard deviation of β-galactosidase activity determination from three independent cultures are shown.

To further dissect the effect of GreA and GraL in the autoregulation of *greA*, we constructed several *lacZ* fusions by gene disruption: greA+3 and greA+101 carrying different genetic elements found in the promoter region. As defined on **table 5**, greA+3 is fused at the transcription start of the σ^{70} promoter and greA+101 is fused downstream the terminator located within the *greA* 5' UTR, as observed in **figure 25**.

The strains LFC30 (greA+3) and LFC32 (greA+101) were transformed with the plasmids pBR322, pBR-GreA and pBR-GraL, and the β-galactosidase activity was measured in cultures grown in LB at 37ºC up to an OD_{600nm} of 1.5 (**fig. 28B**). Comparing the expression of greA+3 with greA +101 (with pBR322), we could observe that the expression from greA+3 was much higher than for greA+101. These results are consistent with a role in the autorepression of *greA* by the GraL transcripts, since greA+3 lacks GraL whereas greA+101 produce the GraL. Interestingly, the presence of pBR-GraL and pBR-GreA causes further induction on *greA* expression with the fusion carrying the GraL sequences (+101) whereas the fusion +3 was fully insensitive to either the presence of GraL and GreA. These results suggest that the autoregulation does not occur at the level of transcription initiation. The fusion responding to antirepression by GraL and GreA (+101) is GraL proficient and therefore it contains the partial terminator present within the *greA* promoter. Our results suggest that autoregulation occurs independently of the σ^{70}-dependent promoter and it requires the sequence between +1 of σ^{70} and the end of the partial terminator. In a work by Potrykus *et al.* (2010), they determined using *lacZ* fusions that contain either the σ^{70}-dependent promoter or both σ^{70} and σ^{E} promoters, but lacking GraL, that the expression was higher than when using a *lacZ* fusion carrying all the regulatory elements, σ^{70}, σ^{E} and GraL. These results suggest that the presence and expression of the GraL sequences had a negative impact on *greA* expression. Similarly to what we observe with our greA+3 fusion, in Potrykus *et al.* (2010) the *lacZ* fusions containing the *greA* promoters, but not GraL, did not respond to the presence of GreA

Our data suggest that the presence of the sequence between +3 and +101 was required for GraL, as well as GreA, to produce its effect on the expression of *greA*.

Using the +101 fusion similar effect on *greA* expression was observed when carrying either pBR-GraL or pBR-GreA. Having in consideration that pBR-GreA code for both GraL and GreA, we design experiments to determine whether GreA is autoregulating *greA* expression or it is only GraL the crucial regulatory factor. The plasmid pDNL278, a pTrc99a derivative carrying the *greA* coding sequence under the control of a P_{tac} promoter that expresses GreA but not GraL, was transformed into the strain LFC32 (greA+101) and the *greA* transcriptional expression was monitored after growing in LB at 37ºC up to an OD_{600nm} of 1.5 (**fig.28B**). As a control, strain carrying the cloning vector pTrc99a was also used. The presence of plasmid pDNL278, as well as pBR-GraL and pBR-GreA, causes a drop in the expression of *greA* using the fusion greA+101. These data suggest that GreA is carrying repression of the *greA* transcriptional expression and it might be requiring the presence of the sequence present in the regulatory region between +3 and +101 to produce its autoregulatory effect. As a control, the expression of the GreA protein in the different strains was monitored by Western blot (**Fig. 28C**). As expected, GreA is produced in the strains with pBR-GreA and pDNL278.

This autoregulation might be required to keep GreA and GraL levels controlled and maintaining the steady-state level of these regulation and the appropriate expression pattern in the different conditions. As mentioned before, the overexpression of GreA and GraL causes several effects in the gene expression profile (Stepanova *et al.*, 2007; Potrykus *et al.*, 2010). Therefore, systems to tightly regulate those factors may be pivotal to do not cause negative effects on the fitness of the bacterial cell. Changes in the amount of GreA would produce alterations in the competition for the secondary channel of the RNApol, while an increase on GraL would produce the binding of this sRNA to complementary mRNA and as a consequence, changes on the gene expression pattern affecting transcription elongation and post-transcriptional processes respectively.

While the mechanism is already not well understood, we have determined that the antipause activity of GreA is required (**fig. 27**). Considering that it is difficult to understand how antipause activity may be responsible of direct gene repression, and that *in vitro* experiments suggest that GreA negative effect on

its own gene expression requires additional factors (Potrykus *et al.*, 2010). An indirect model was hypothesized (**fig. 28D**). GreA would stimulate the expression of an unknown factor (X), requiring GreA antipause activity. Moreover GraL might be required to stabilize the mRNA of the unknown factor, increasing its protein levels. The X factor could bind into the promoter of *greA*, between the sequences +3 and +101, repressing the expression of *greA* or could act at the post-transcriptional step by interacting with the mRNA of *greA*. This model is a reductionist view of the possible mechanism that may cause the observed autoregulation.

4.1.2. Expression of *greA* through the growth curve

Under laboratory conditions and using discontinuous cultures, a typical bacterial growth curve allows definition of distinctive growth phases: lag, exponential, stationary and death phases. The transition between the different growth phases produces extensive changes on the gene expression pattern of the bacterial cells. Special attention has been done in the adaptation of actively growing cells (exponential phase cultures) when they encounter harsh conditions causing slow down the growth and entering in an adaptative mode for survival (stationary phase). In the interphase between exponential and stationary phase, important rearrangements in the gene expression pattern occurs promoted, at least in part, by the binding of ppGpp to the RNApol. The expression levels of several regulators changes during the transition of exponential to stationary phase.

Expression of *greA* was monitored during growth of the LFC3 (attBgreA2 fusion) strain in LB at 37ºC after inoculation from plate at an initial OD_{600nm} of 0.001 (**fig. 29A**). The expression of *greA* was determined after the first 3 hours. A characteristic *greA* expression profile was detected. The expression of *greA* decreases (nearly 2 fold) in the transition between exponential and stationary phase, showing that *greA* expression depends on the growth phase.

Transcriptional *greA* expression at exponential (OD_{600nm} of 0.5) and early-stationary phase (OD_{600nm} of 1.5) was also tested using *lacZ* fusion in the genomic context of *greA* by using the fusions greA+685 and greA+193 (**fig. 29B**).

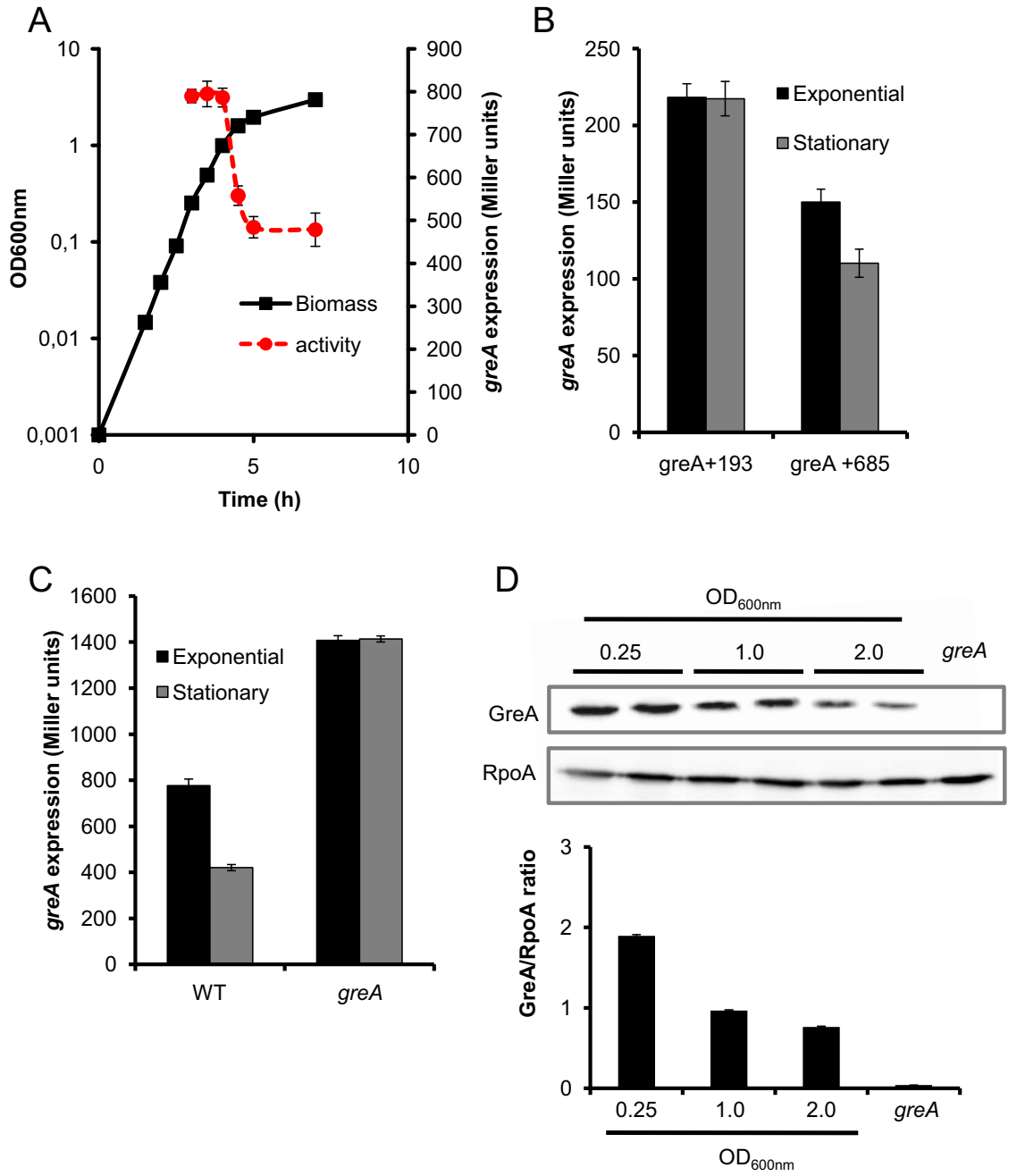

Figure 29: Effect of growth phase on *greA* expression. A) Transcriptional expression of *greA* at different time points of the growth curve in cultures of the strain LFC3 (AAG1 attBgreA2) grown in LB at 37ºC. B) Expression of *greA* in cultures of the strains LFC29 (greA+193) and LFC28 (greA+685) grown in LB at 37ºC up to an OD_{600nm} of 0.5 (exponential phase) and 1.5 (early stationary phase). C) Expression of *greA* in cultures grown of the strains LFC3 (AAG1 attBgreA2) and LFC4 (CLT254 attBgreA2) in LB at 37ºC up to an OD_{600nm} of 0.5 (exponential phase) and 1.5 (early stationary phase). D) Western Blot using antibodies against GreA and RpoA (RNApol α subunit) in cultures grown of the strain MG1655 and CF11657 (*greA*) in LB at 37ºC at different points of growth phase (OD_{600nm} of 0.25, 1.0 and 2.0). The ratio GreA/RpoA was determined. Average and standard deviation of β-galactosidase activity determination from three independent cultures are shown.

A drop in *greA* expression was observed in stationary phase when using fusion +685 (*greA*$^+$ background). Interestingly, when using the fusion greA+193 (*greA*$^-$ background) a drop in *greA* expression in stationary phase was not detected, suggesting that the GreA autoregulatory loop is required for the growth phase dependent control. To corroborate this, the *greA* expression using the attBgreA2 fusion in presence and absence of GreA was determined. With this purpose, LFC3 and LFC4 strains were grown in LB at 37ºC up to an OD_{600nm} of either 0.5 (exponential phase) or 1.5 (early-stationary phase). Similar results as the obtained with fusions greA+685 and greA+193 were observed (**fig. 29C**): a 2-fold decrease on *greA* expression in presence of GreA, but not in its absence. Somehow, the presence of GreA is required to repress the expression of *greA* at stationary phase. These results also suggest that the stationary phase induced down-regulation of *greA* does not requires GraL.

To corroborate the transcriptional studies, the amount of GreA present in the cell was detected at different points of the bacterial growth phase (OD_{600nm} of 0.25, 1.0 and 2.0) by Western blot, using specific antibodies against GreA (**fig. 29D**). As a loading control the α subunit of the RNApol (RpoA) was used, since expression is constant during the growth curve. Consistent with transcriptional data, the amount of GreA decreases 2 fold at stationary phase (OD_{600nm} of 1.0 and OD_{600nm} of 2.0) as compared with exponential phase (OD_{600nm} of 0.25).

A decrease in the amount of GreA during stationary phase might indicate that the binding of GreA to the secondary channel of the RNApol is not required in stationary phase cells. A decrease in the amount of GreA may facilitate the binding of other factors to the secondary channel. DksA, protein that also interact with the secondary channel of the RNApol acting as a cofactor of ppGpp (as discussed previously in 1.2.3.), is crucial for the adaptation of the bacteria to the stationary phase. Conversely a decrease in the amount of GreA, might facilitate the required interaction of DksA with the RNApol for the proper adaptation of the bacteria to the new conditions.

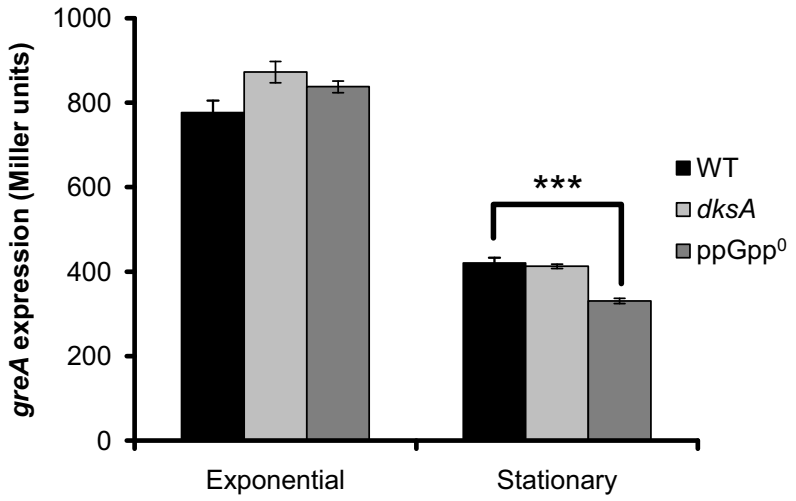

Figure 30: Effect of ppGpp and DksA on *greA* transcriptional expression at exponential and stationary phase of growth. Expression of *greA* in cultures strains LFC3 (WT), LFC9 (ppGpp) and LFC8 (dksA) grown in LB at 37ºC up to an OD_{600nm} of 0.5 (exponential phase) and OD_{600nm} of 1.5 (early stationary phase). *** means p-Value < 0.001. Average and standard deviation of β-galactosidase activity determination from three independent cultures are shown.

The effect on the expression of *greA* of ppGpp and DksA, main responsible of the gene expression changes produced during entry into stationary phase, was determined. Transcriptional studies, using *lacZ* fusions, were performed (**fig. 30**). The strains LFC3 (WT) and its derivatives LFC9 (ΔrelA ΔspoT, referred as $ppGpp^0$) and LFC8 (*dksA*), all carrying the attBgreA2 fusion, were grown in LB at 37ºC. The *greA* transcriptional expression was monitored in samples at OD_{600nm} of 0.5 (exponential phase) and 1.5 (early-stationary phase).

The data (**fig. 30**) indicate that DksA and ppGpp do not have any relevant effect on the growth phase dependent regulation of *greA* expression. A modest decrease in the expression of *greA* in absence of ppGpp was observed at stationary phase. With the results obtained we might hypothesized that the drop of *greA* expression in stationary phase is GreA-dependent and might be indirect by the same unknown factor responsible of the autoregulation of *greA* expression (as discussed in **fig. 28D**). Somehow, this factor might increase its expression in stationary phase, causing a concomitant reduction in the expression of *greA*.

4.1.3. Effect of changes in diverse environmental parameters in the *greA* expression

Bacteria are used to adapt to changing conditions in the living environment to survive. Bacteria have mechanisms to vary gene expression as a response of several environmental changes sensed by the cell, (described in section 1.1) (Aertsen and Michiels, 2008). Transcriptional studies were performed using *lacZ* fusions, testing the effect of several environmental conditions such as oxygen and magnesium availability, pH, osmolarity and temperature on *greA* expression.

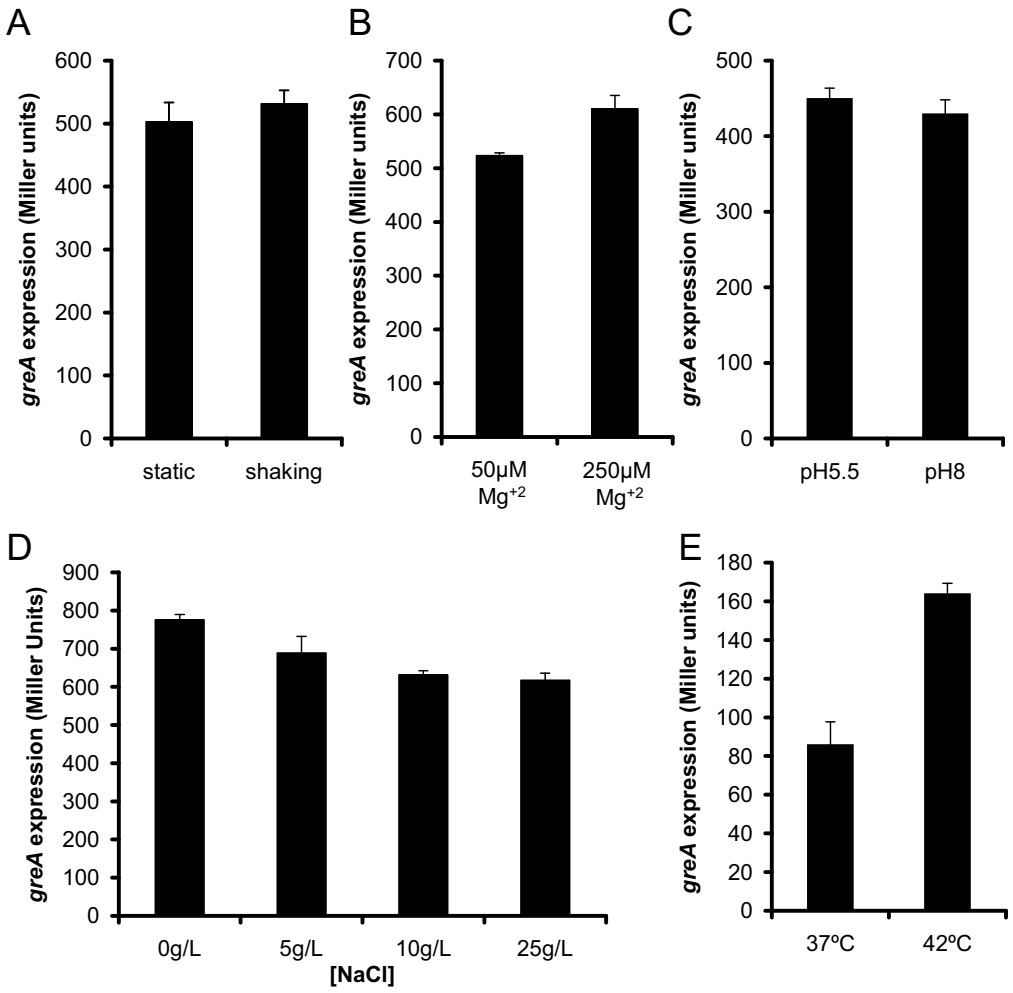

Figure 31: Effect of environmental factors on *greA* transcriptional expression. A) Expression of *greA* in cultures of the strain LFC3 (attBgreA2) grown at 37ºC overnight in LB with different aeration conditions. B) Expression of *greA* in cultures of the strain LFC3 grown in LB with different concentrations on $MgSO_4$ / $MgCl_2$ up to an OD_{600nm} of 1.5. C) Expression in cultures of *greA* of the strain LFC3 grown in LB buffered at either pH5.5 or pH8 at 37ºC up to an OD_{600nm} of 1.5. D) Expression of *greA* in cultures of the strain LFC3 grown in LB with different concentrations of NaCl at 37ºC up to an OD_{600nm} of 1.5. E) Expression of *greA* in cultures of

the strain LFC28 (greA+685) grown in LB at either 37ºC or 42ºC up to an OD_{600nm} of 1.5. Average and standard deviation of β-galactosidase activity determination from three independent cultures are shown.

- **Oxygen availability:** *E. coli* is a facultative anaerobic organism, being able to grow in either presence or absence of O_2. Variations in the level of O_2 produce relevant changes in the gene expression pattern of *E. coli*. To determine the effect of O_2 over *greA* expression, the strain LFC3 (attBgreA2 fusion) was grown at 37ºC under conditions of high and low concentration of O_2. The conditions of high concentration of O_2 was achieved by culturing bacteria in 100ml culture flasks with 20ml of LB in constant shaking (200 rpm), producing a proper aeration of the culture.

  By contrast, conditions of low O_2 concentration were achieved by growing the bacteria in 12ml sealed tubes with 10ml of LB on static. Under those conditions a decreasing gradient of oxygen within the tube will be generated by the bacterial growth, being very low O_2 concentration in the bottom of the tube (**fig. 31A**). As could be observed in **figure 31A,** there is no effect of aeration in *greA* expression in LB at 37ºC, suggesting that the amount of GreA do not depend on the availability of O_2.

- **Magnesium availability**: Low magnesium and mildly acidic pH are sensed in the periplasm by the two-component system PhoQ-PhoP (Park and Groisman, 2014). In order to determine the effect of this system on *greA* expression, the effect of presence of Mg^{+2} in the media was determined after growing the stain LFC3 (attBgreA2 fusion) in LB with either 50 μM or 250 μM of Mg^{+2} salts (Montero *et al.*, 2009) (**fig. 31B**). No differences were observed on *greA* expression as a response to Mg^{+2} concentrations under these conditions tested.

- **pH**: It has been described that overexpression of GreA stimulates the expression of *gadE* and *gadA* genes (Vinella *et al.*, 2012), that are involved in the glutamate-dependent acid response (*gad* system). The *gadE* gene product is the transcriptional regulator of the *gadABC* operon induced by acid and salt shock. To determine the effect of pH on *greA* expression, the strain LFC3 was grown in LB buffered at either pH 5.5 with MES 100mM or pH 8 with MOPS 100mM at 37ºC up to an OD_{600nm} of 1.5 and β-galactosidase activity was

monitored (**figure 31C**). No effect on *greA* expression was observed at the different pH tested.

- **Osmolarity**: It has been described that GreA is involved in salt stress response in *Sinorhizobium meliloti* and *Rhizobium tropic* (Nogales *et al.*, 2002; Wei *et al.*, 2004). For this reason, the effect of media osmolarity on *greA* expression was determined by growing the strain LFC3 at 37ºC in LB with 0, 5, 10 and 25 g/l of NaCl up to an OD_{600nm} 1.5, and β-galactosidase activity was measured (**fig. 31D**). The osmolarity of the media does not affect *greA* expression.

- **Temperature**: The environmental temperature affects gene expression. Both, high and low temperatures would produce rearrangements in the gene expression pattern to adapt to this situations (Inouye and Phadtare, 2004; Guisbert *et al.*, 2008). The expression of *greA* at high temperature (42ºC) was determined in the strain LFC28 (greA+685) was grown in LB at 37ºC and 42ºC up to an OD_{600nm} of 1.5 (**fig. 31E**). The expression of *greA* increases at high temperature, suggesting that the GreA protein might be required at higher concentrations during the heat shock response. To corroborate this hypothesis, it was monitored the growth of MG1655 strain and its derivative strains deficient in *dksA, greA* and *greAgreB* on LB plates at 30ºC and 42ºC after 18 hours incubation (**fig. 32**).

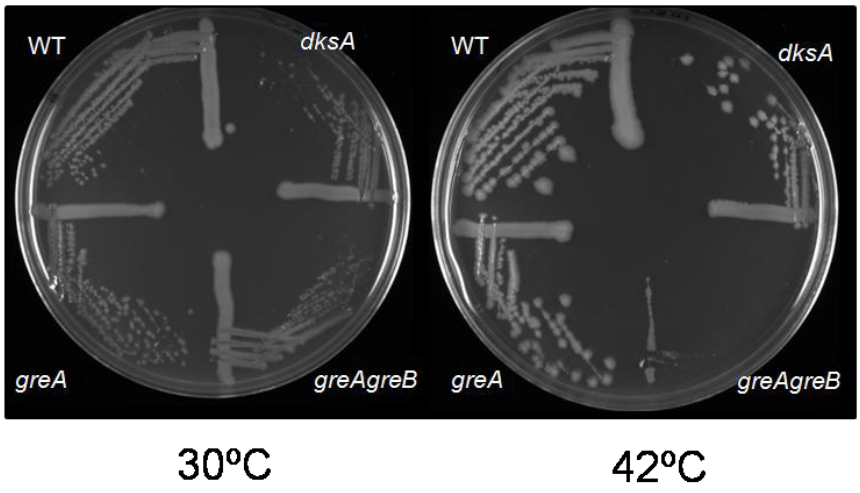

Figure 32: Effect of high temperature in bacterial growth of MG1655 strain and its derivative mutant strains *dksA, greA* and *greAgreB*, grown on LB agar plates at the indicated temperatures.

As shown in **figure 32,** in absence of GreA and GreB, bacteria are not able to grow at 42ºC, showing the essentiality of these factors for the adaptation of the bacteria to high temperatures. This effect was suggested by Baharoglu *et al.*, (2010), where they show how mutations in the RNApol that prevent pausing are able to survive at 42ºC in absence of GreA and GreB, suggesting that paused TEC might be lethal in this condition. The alternative σ^E subunit is activated by unfolded proteins in the periplasm affected by different stress conditions, such as heat shock (Alba and Gross, 2004). Taking in consideration the presence of a σ^E-dependent promoter in the *greA* gene and that *greA* expression increases at 42ºC, we decided to study more in detail the effect of σ^E on *greA* expression.

4.1.3.1. Effect of the σ^E subunit of the RNApol on *greA* expression

The alternative σ^E, as previously described in section 1.1.2.2, is responsible of the extracytoplasmic stress response. Unfolded proteins –mainly outer membrane proteins (OMP) (Walsh *et al.*, 2003) – interact with the membrane protein DegS (**fig.32**), activating its protease activity and producing degradation, among others, of RseA – the anti-sigma factor that binds to σ^E – releasing σ^E (Alba and Gross, 2004).

In studies performed by Walsh *et al.* (2003), was shown that the C-terminal of unfolded OMP, such as OmpC, activate DegS. They generate chimerical proteins fusing the C-terminal (50 amino acids) of OmpC to the N-terminal *pelB* leader sequence and modifying the last 3 amino acids of OmpC in order to generate the so called OmpC-YYF. The gene *pelB* codes for a pectate lyase (Lei *et al.*, 1987) that contains a leader sequence that has been extensively used to target chimerical peptide fragment to the periplasm and allow proteolytic removal of the signal sequence (Singh *et al.*, 2013). Walsh *et al.* (2003) demonstrate that overexpressing OmpC-YYF causes an efficient activation of the σ^E pathway.

To determine the effect of σ^E on *greA* expression, we decided to induce extracytoplasmic stress response by overexpression of OmpC-YYF with the IPTG-inducible plasmid pBA166 (Walsh *et al.*, 2003). The plasmid pBA166 (referred as pOmpC-YYF) and pTrc99a (referred as pControl) were transformed

into LFC3 and the resulting strains were grown in LB at 30ºC up to an OD_{600nm} of 0.1. Overexpression of OmpC-YFF was induced by addition of IPTG (1 mM).

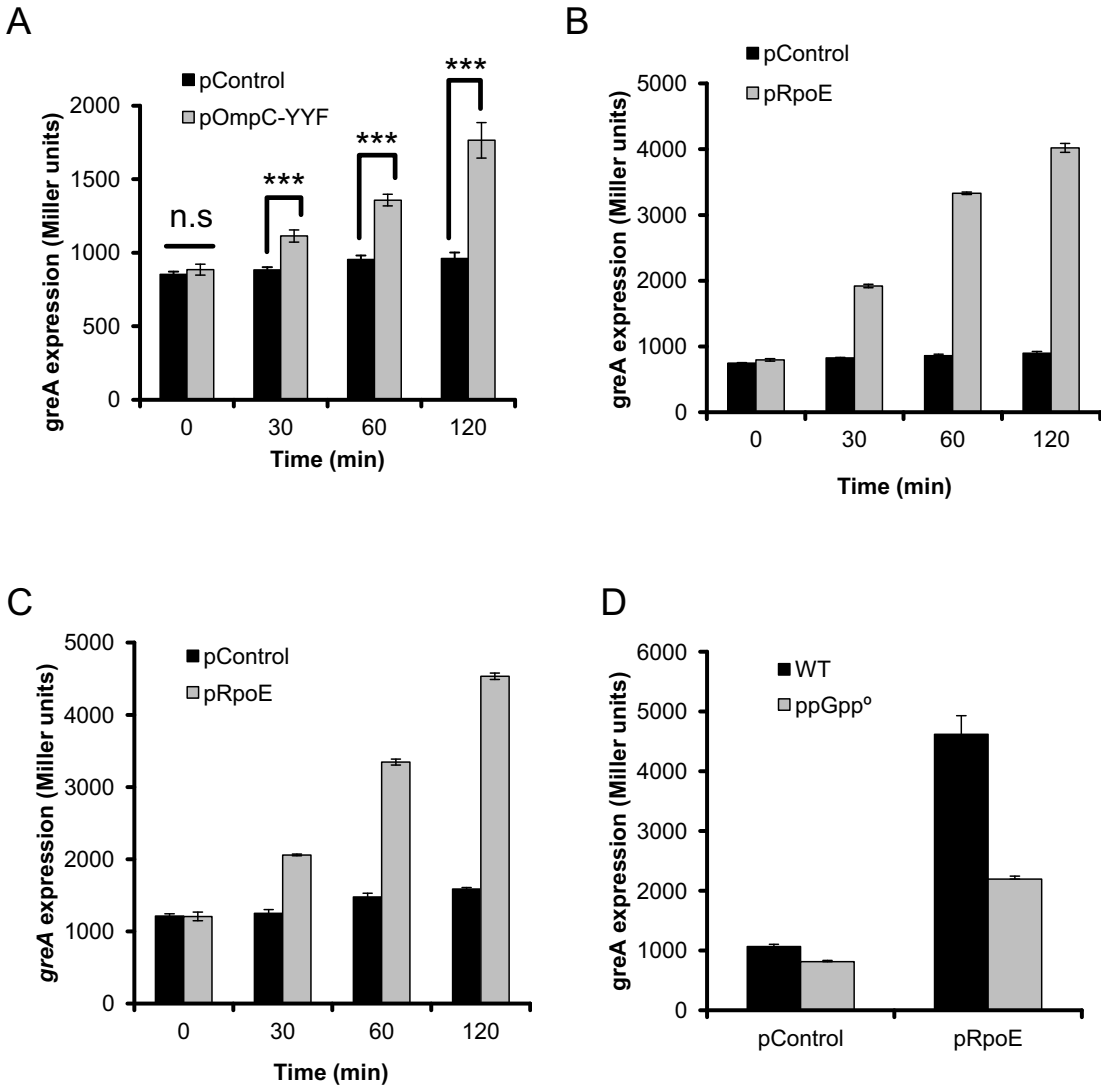

Figure 33: Effect of σ^E on *greA* transcriptional expression. A) Expression of *greA* in cultures of the strain LFC3 (AAG1 attBgreA2) grown in LB at 30ºC up to an OD_{600nm} of 0.1. At this point, *ompC*-YYF was induced with 1 mM of IPTG and samples were analyzed at different time points as indicated in the X axis. *** means p-value < 0.001 B) Expression of *greA* in cultures of the strain LFC3 carrying either pTcr99a or pLC249 grown in LB at 30ºC up to an OD_{600nm} of 0.1. At this point, *rpoE* was induced with 1 mM of IPTG and samples were analyzed at different time points as indicated in the X axis. C) Expression of *greA* in cultures of the strain LFC4 (CLT245 attBgreA2) grown in LB at 30ºC up to an OD_{600nm} of 0.1. At this point, *rpoE* was induced with 1mM of IPTG and samples were analyzed at different time points as indicated in the X axis. D) Expression of *greA* in cultures of the strain LFC3 and LFC9 grown in LB at 30ºC up to an OD_{600nm} of 0.1. At this point, *rpoE* was induced with 1 mM of IPTG and samples were analyzed at different time points as indicated in the X axis. Average and standard deviation of β-galactosidase activity determination from three independent cultures are shown.

Samples were taken at 30, 60 and 120 minutes after induction to monitor *greA* expression by measuring β-galactosidase activity (**figure 33A**). The induction of

extracytoplasmic stress, by accumulation of unfolded chimerical OmpC-YFF, produces a significant (p-value < 0.001) induction of *greA* expression. After 30min of induction, a clear increase of *greA* expression was observed, and after 120min of the induction, a 2-fold increase in the expression of *greA* was detected.

To further corroborate that *greA* expression is responsive to changes in the levels of functional σ^E subunit, the effect of overexpression of σ^E on *greA* expression was determined. To do that, LFC3 strain was transformed with the plasmid pLC245 (pRpoE) and pTrc99a (pControl). The resulting strains were grown in LB at 30ºC up to an OD_{600nm} of 0.1 and the overexpression the σ^E subunit was induced with IPTG (1 mM). Samples were taken at 30, 60 and 120 minutes after induction to monitor *greA* expression (**fig. 33B**).

A dramatic induction of *greA* was detected (**fig. 33B**). After 30min a 2-fold increase in *greA* expression was detected, and after 120min the expression of *greA* was up to 4 times higher that the non-induced culture. Our data shows that *greA* is induced by the extracytoplasmic stress, due the presence of a σ^E-dependent promoter, and this mechanism might be the responsible of the increase of *greA* expression observed at high temperature (**fig. 31E**). When *E. coli* suffer a heat shock, unfolded proteins are generated in the periplasm that would promote the degradation of the anti-sigma factor RseA, releasing σ^E and allowing it to form complex with the RNApol. Finally the holoenzyme would activate the σ^E-dependent promoters, among them *greA*.

Considering that GreA represses the expression of *greA* being responsible of the decrease of its own expression in stationary phase, whether GreA is required for the activation of *greA* by σ^E was established (**fig. 33C**). The plasmids pLC245 (pRpoE) and pTrc99a (pControl) were transformed into the *greA* deficient strain LFC4 (*greA* attBgreA2). The resulting strains were grown in LB at 30ºC up to an OD_{600nm} of 0.1 and the overexpression of the σ^E subunit was induced by addition of IPTG (1 mM). Samples were taken at 30, 60 and 120 minutes after induction to monitor *greA* transcriptional expression. Similar results as previously observed in the WT strain were detected (compare **fig.33C** and **fig. 33B**), the expression of *greA* increases up to 2 fold after 30 minutes of

induction, and a 3.5-fold increase after 120 minutes, suggesting that GreA is not required for the activation of *greA* by σ^E.

It has been suggested that ppGpp (as described in 1.2.2.1) acts in the sigma factors competition (Magnusson *et al.*, 2005), and, as previously described, ppGpp is necessary for σ^E activity (Costanzo *et al.*, 2008). For this reason, the effect of ppGpp over the induction of *greA* by σ^E was monitored (**fig. 33D**). The plasmids pLC245 (pRpoE) and pTrc99a (pControl) were transformed into the ppGpp deficient strain LFC9 (attBgreA2 fusion). The resulting strains and the proficient ppGpp strain LFC3 carrying the same plasmids, were grown in LB at 30ºC up to an OD_{600nm} of 0.1 and the overexpression of the σ^E subunit was induced by the addition of IPTG (1 mM). Samples were taken at 60 minutes after induction to measure β-galactosidase activity. As previously described, the overexpression of σ^E increases the expression of *greA*. However, in absence of ppGpp (strain LFC9), the induction of *greA* by σ^E overexpression was 2-fold lower than in the presence of ppGpp (LFC3), showing that ppGpp affects *greA* expression by affecting σ^E activity. It is remarkable that only a partial reduction was observed in a $ppGpp^0$ strain. Costanzo *et al.* (2008) observed a complete lost of σ^E-dependent activation of the *rpoH* promoter in absence of ppGpp.

These data show that GreA is required during extracytoplasmic stress and adaptation of bacteria to high temperature, probably its ability to restore paused transcription elongation complexes (TEC) would be necessary for the response to this stress, as it has been suggested previously (**fig. 32** (Baharoglu *et al.*, 2010)). Another possible explanation to the σ^E dependency of *greA* expression is the recent finding that GreA seems to act as a chaperone (Li *et al.*, 2012). Considering that main part of the target genes of σ^E are chaperones, it might suggest that GreA could be required as a response to extracytoplasmic stress, acting as a chaperone.

4.1.4. *In silico* analysis of the promoter region of *greA* gene

With the aim to determine which factors could control the expression of *greA*, *in silico* analysis searching for putative binding sites in the promoter sequence of global regulators were performed (**fig. 34**). This prediction was developed with the online software Virtual Footprint (Münch *et al.*, 2005) that identify putative

binding sites depending on the consensus sequence and described patterns. The whole sequence used to produce the fusion attBgreA2 (**table 5** and **fig. 25**) was used to search for putative binding sites for global regulators upstream and downstream of *greA* promoter.

Figure 34: Partial sequence of the *E. coli* genome, including the *greA* gene. In capital letters are indicated the coding sequences of *dacB* (in grey) and *greA* (in black). The boxes -10 and -35 of the σ^{70} (in orange) and σ^{E} (in blue) *greA* promoters are indicated. The transcription initiation +1 for each promoter is indicated in capital letters in black. The early imprecise terminator is indicated in bold and underlined. The putative binding sites are indicated in different colours or underlined.

Several putative binding sites for global regulators were detected (**fig. 34**). Some of them are located upstream of the defined promoter, overlapping the *dacB* coding sequence, while others are detected between the promoter and the *greA* coding sequence. One of them, a binding site for GadX was detected overlapping the -10 box of the σ^{70}-dependent promoter of *greA*. The expression of *greA* was determined in mutants defective for the different proteins with a predicted binding site in the *greA* promoter. Moreover, the effect of mutants for other global regulators with a relevant role in the control of gene expression in *E. coli* was also monitored.

The *greA* expression in the different mutant strains was monitored using the *lacZ* fusion in the *greA* gene attBgreA2 and greA+685. The resulting strains were grown in LB at 37ºC up to an OD_{600nm} of 1.5 and the *greA* transcriptional expression was measured (**fig. 35**).

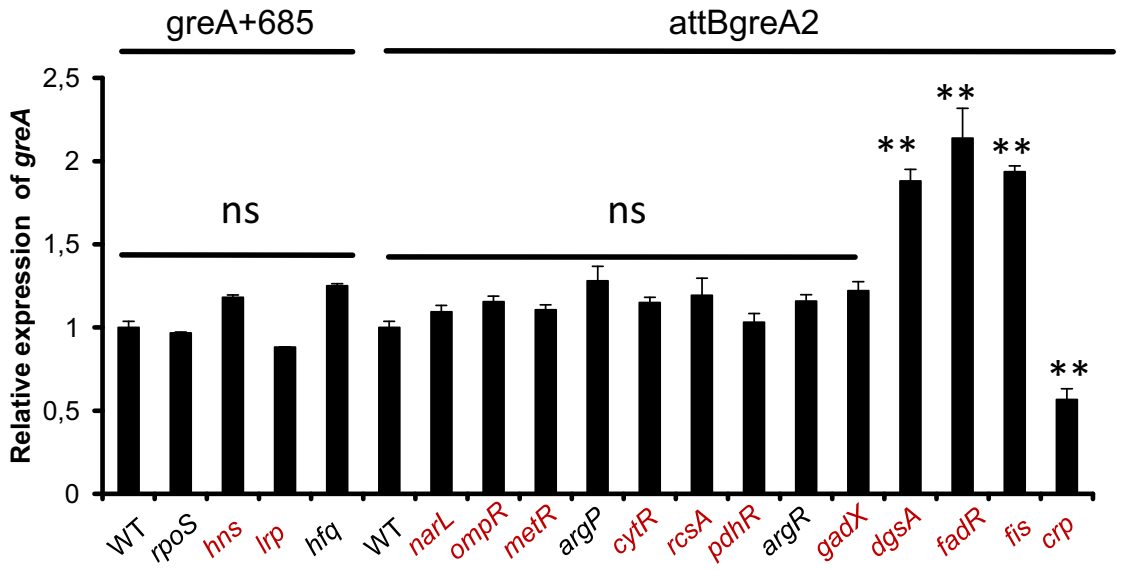

Figure 35: Effect of different global regulators on *greA* expression. The strains LFC28, LFC10, LFC11, LFC12, LFC13, LFC3, LFC14, LFC15, LFC16, LFC17, LFC18, LFC19, LFC20, LFC21, LFC22, LFC23, LFC24, LFC25 and LFC26 (in the same order than in the figure) were grown in LB at 37ºC up to an OD_{600nm} of 1.5, and the β-galactosidase activity was measured. ns means no significant. ** means p-value < 0.01. The global regulators predicted to bind to *greA* promoter are labelled in red. Average and standard deviation of β-galactosidase activity determination from three independent cultures are shown.

Our results indicate that under the experimental conditions tested, most of the regulators do not affect the expression of *greA*. In absence of DgsA, FadR and Fis, the expression of *greA* increases, suggesting that the expression of *greA* is directly or indirectly repressed by this factors. Moreover, in absence of CRP,

there is a decrease in the expression of *greA*, suggesting that CRP somehow activates the expression of *greA*.

Fis is a structural protein involved in the organization of the nucleoid, involved in DNA topology and DNA compaction (as previously mentioned in section 1.1.2.3). Moreover, Fis affects the expression of several genes in *E. coli*. The regulation mechanism widely accepted is that Fis influences transcription by modulating the level of DNA supercoiling in the cell, hiding the promoter region and avoiding that the RNApol could bind it (Cho *et al.*, 2008). Considering the putative binding site of Fis (**fig. 34**) it might be this mechanism how Fis affect *greA* expression.

DgsA (also known as Mlc) and CRP are involved in the regulation of glucose metabolism, and FadR is involved in fatty acid metabolism. We would study more in detail the effect of these proteins on *greA* expression.

4.1.4.1. Effect of FadR on *greA* expression

The FadR protein has a dual role in fatty acid metabolism. It acts as a repressor of the β-oxidation pathway (*fad* operon) and as activator of the unsaturated fatty acid biosynthetic genes (*fab* operon). FadR bind to the DNA repressing or stimulating genes, depending on the position of its DNA binding site respect the -35 and -10 boxes. The FadR regulator binds long chain fatty acids, producing the release from the DNA and changing the gene expression pattern (Feng and Cronan, 2009; My *et al.*, 2013).

It has been observed that in genes stimulated by FadR, its binding site localized few nucleotides upstream of, or partially overlapping, the -35 box of the promoter (My *et al.*, 2013). In the promoters repressed by FadR, it is observed that its binding site overlaps with -10 box or the transcription start site (Feng and Cronan, 2012). Some genes, such as *fadD* or *fadL*, contain 2 FadR-binding sites. In the case of *fadD*, one binding site is located at the position -120 and the other overlapping -10 box (Feng and Cronan, 2012). In the case of *greA*, the putative FadR-binding site is located 130 nucleotides upstream of the transcription start site of the σ^{70}-dependent promoter.

In absence of FadR, an increase in the *greA* expression was detected. If the *greA* expression would be physiologically related with the fatty acid metabolism, one would expect that in absence of fatty acids, FadR might bind the promoter of *greA* and repress its expression. On the other hand, in presence of fatty acids (oleic acid) we would expect a derepression of *greA* expression similar to the observed in absence of FadR, as observed in the gene *fadD* (Feng and Cronan, 2012).

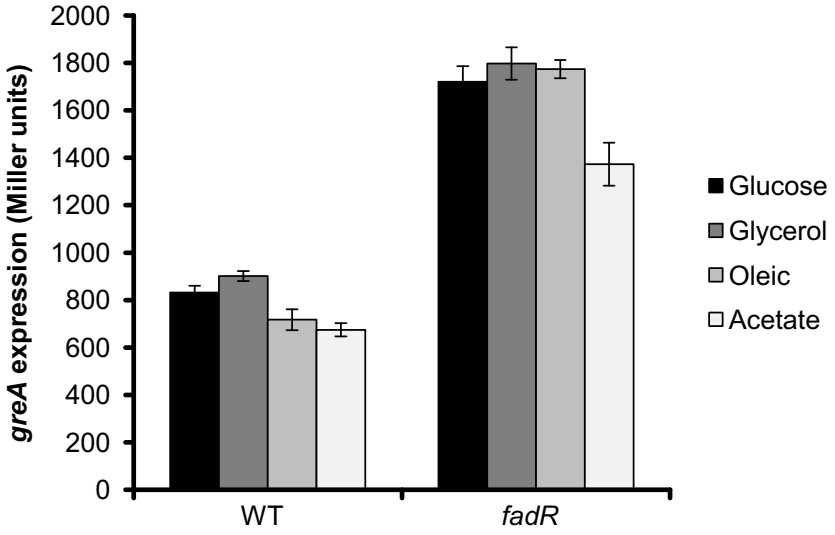

Figure 36: Effect of FadR in *greA* transcriptional expression. The strains LFC3 and LFC24 were grown in cultures in LB with 0.2% of the different compounds as indicated at 37ºC up to an OD_{600nm} of 1.5. Average and standard deviation of β-galactosidase activity determination from three independent cultures are shown.

The strain LFC3 and LFC24 were grown in minimal media M9 supplemented with 0.2% casaaminoacids (vitamin-free) and 0.2% of glucose, glycerol, oleic acid or acetate (as described by My et al. (2013)). Cultures were grown at 37ºC up to an OD_{600nm} of 1.5 and the *greA* transcriptional expression was determined (**fig. 36**). Unexpectedly, any effect was observed by the presence of oleic acid in the expression of *greA*. All the genes that has been described to be regulated by FadR, are regulated by long chain fatty acids such as oleic acid (Feng and Cronan, 2009; Feng and Cronan, 2012; My *et al.*, 2013), suggesting that the effect of FadR in *greA* could be an artefact.

4.1.4.2. Effect of CRP and DgsA on *greA* expression

Carbon catabolite repression allows bacteria, when they are exposed to more than one carbohydrate, to discriminate which carbon source should be assimilated preferentially. This phenomenon was initially described as diauxic growth (Monod, 1949). CRP is the transcriptional regulator responsible together with other factors of this phenomenon. CRP is a homodimer that requires the alarmone cAMP to bind to DNA and modulates gene expression (Popovych *et al.*, 2009). In *E. coli* the presence or absence of glucose could vary the amount of cAMP in the cell; in absence of glucose, the adenylate cyclase (CyaA) is activated by the phosphorylated EIIB of the PTS system (Deutscher, 2008) and produces an increase in the intracellular cAMP levels. In contrast, when glucose is present, the transported glucose is phosphorylated to glucose-6P from EIIB, causing that the levels of phosphorylated EIIB are very low and consequently no activation of the adenylate cyclase occurs. The protein DgsA, also known as Mlc, represses gene expression by binding the promoter region of the target genes in absence of glucose. When glucose is present in the media, DgsA release its DNA binding site and binds to the dephosphorylated EIIB. Then, CRP and DgsA (Mlc) act as activator and repressor, respectively, in absence of glucose.

The crosstalk between DgsA and CRP might be important for the tight regulation of *greA* expression, as discussed more in detail below.

We decided to study more in detail the effect of the presence or absence of glucose on the expression of *greA*. The expression of *greA* was determined from the strain LFC3 grown in LB with either 0.2% of glucose or 0.4% of glycerol at 37ºC up to an OD_{600nm} of 1.5 (**fig. 37A**).

No significant effect on *greA* expression was observed by the presence of glucose in LB (**fig. 37A**). However, performing the same experiment in M9 with glucose or glycerol (**fig. 37B**) it was shown a significantly increase of the *greA* expression in presence of glycerol as compared with medium with glucose. Although, it is difficult to predict the effect of the glucose on *greA* expression, attending that both, an activator (CRP) and a repressor (DgsA), responsive to glucose, were found to be involved in *greA* expression regulation. The increase observed in presence of glycerol it is consistent with a CRP mediated regulation

of *greA* expression. The expression of *greA* would be stimulated and repressed at the same time by the complex cAMP-CRP and DgsA, suggesting that DgsA would modulate the CRP-dependent activation of *greA.* There are several examples of genes regulated by CRP and DgsA, such as *malX* or *malT* (Decker *et al.*, 1998; Plumbridge, 1998).

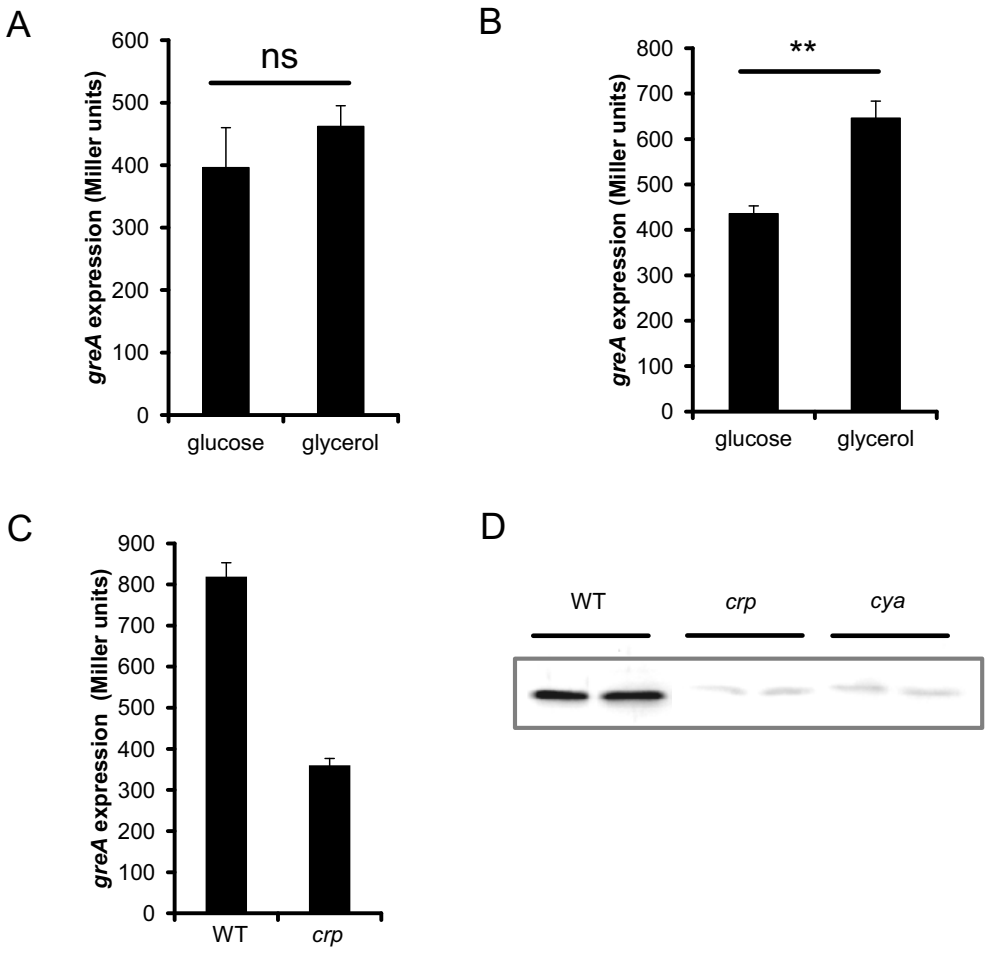

Figure 37: Effect of CRP on *greA* expression. A) Expression of *greA* in LFC3 cultures grown in LB supplemented with either 0.2% of glucose or 0.4% glycerol at 37ºC up to an OD_{600nm} of 1.5. B) Expression of *greA* in LFC3 cultures grown in minimal media M9 supplemented with either 0.2% of glucose or 0.4% glycerol at 37ºC up to an OD_{600nm} of 1.5. C) Expression of *greA* in LFC1 and LFC27 cultures grown in LB at 37ºC up to an OD_{600nm} of 1.5. D) Western blot against GreA in whole cell extracts of cultures of the strains MG1655 and its mutants *crp* and *cya* grown in LB at 37ºC up to an OD_{600nm} of 1.5. ns means no significant. ** means p-value < 0.01. Average and standard deviation of β-galactosidase activity determination from three independent cultures are shown.

The *in silico* studies (**fig. 34**) showed 2 possible CRP binding sites, one far upstream of the transcription start site (CRP1, position -464), and another between the transcription start site and the coding sequence (CRP2, position

+119). The *lacZ* fusion used to determine the effect of *crp* (**fig. 35**) contains both CRP sites. Considering the different *lacZ* fusions in *greA* that we constructed (**table 5** and **figure 28**) we observed that the fusion attBgreA1 only contains CRP2. It was determined the expression of *greA* in the strain LFC1 (WT, attBgreA1 fusion) and LFC27 (*crp,* attBgreA1 fusion) in cultures grown in LB at 37ºC up to an OD_{600nm} of 1.5 (**fig. 37C**). Using the attBgreA1 *greA-lacZ* fusion a decrease in the *greA* expression was detected in absence of CRP, suggesting that the binding site CRP2 is promoting the binding of CRP.

The effect of cAMP-CRP on the levels of GreA protein was determined by immunodetection using specific antibodies against GreA. The strain MG1655 and its mutants *crp* and *cya* were grown in LB at 37ºC up to an OD_{600nm} of 1.5 and the levels of GreA were determined in whole cell extracts (**fig. 37D**). In absence of either CRP or cAMP, the amount of GreA decreases dramatically. According to our model, in absence of CRP the expression of *greA* decreases.

It has been described that CRP might bind to specific DNA sites and contact with the α subunit of the RNApol. CRP-dependent promoters can be grouped on three classes depending on the interaction of CRP with the RNApol. Class I requires only one CRP-cAMP complex and has a single DNA binding site, located upstream of the UP element that recognise the RNApol. Class II requires only a CRP-cAMP complex and has a single DNA binding site, overlapping the UP element. Class III could require more than one CRP-cAMP complex that could bind such as class I and/or II, as well as it requires other global regulators (Busby and Ebright, 1999).

In order to further characterize the role of CRP in the control of *greA* expression, we perform complementation experiments with different *crp* alleles to elucidate what kind of CRP binding site is required for *greA* regulation. Plasmids derived from pLG339 carrying different CRP alleles: WT CRP, CRP H159L (this allele is not able to contact the α subunit of the RNApol), CRP H159L/K52N (is not able to bind class I promoters) and CRP K21L (is not able to bind class II promoters) (Bell *et al.*, 1990; Williams *et al.*, 1991; Busby and Ebright, 1999) were used. These plasmids were transformed into MG1655 *crp* and the resulting strains were grown in LB at 37ºC up to an OD_{600nm} of 1.5 to

determine the amount of GreA by Western blot using specific antibodies against GreA (**fig. 38**).

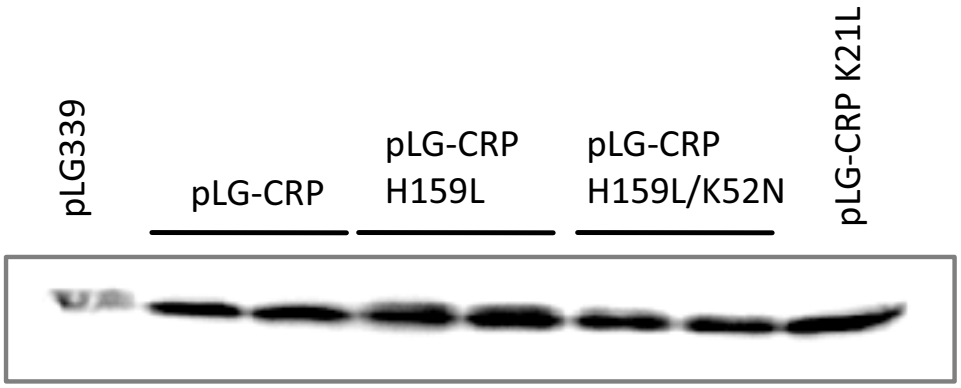

Figure 38: Complementation of *crp* mutation with different alleles of CRP by Western blot. MG1655 *crp* with the plasmids pLG339, pLG339/CRP, pLG339/CRP H159L, pLG339/CRP H159339L/K52N or pLG339/CRP K21L were grown in LB at 37ºC up to an OD_{600nm} of 1.5 and the amount of GreA was determined by Western blot with the antibodies against GreA.

As it can be seen, all alleles tested were able to complement *crp* mutation as well as WT CRP. This would mean that the effect of CRP over *greA* expression is not dependent of binding with the α subunit of RNApol. These results suggest that the regulation mediated by CRP is through a mechanism independent of contact with the RNApol, suggesting it requires a class III CRP-dependent promoter. Whether the binding site is functional or the effect of CRP is indirect needs to be elucidated.

4.1.4.3. Effect of GadX on *greA* expression

As mentioned earlier, a putative binding site for GadX was found overlapping the -10 and -35 of the σ^{70} promoter. The protein GadX activates the expression of *gadE* at low pH, and it is involved on the glutamate-dependent acid response (*gad* system). It has been previously described that GreA regulates the expression of *gadE* and *gadA* (Vinella *et al.*, 2012). Although it was not observed any effect on the expression of *greA* by *gadX* mutation, further studies have been performed.

The effect of GadX in the expression of *greA* in LB supplemented with glucose at different pH as described by Sayed *et al.*, (2007) was determined. The strains

LFC3 (WT, attBgreA2 fusion) and LFC22 (*gadX,* attBgreA2) were grown in LB and LBG (LB with 0.4% of glucose) buffered at either pH 5.5 with MES 100mM or pH 8 with MOPS 100mM at 37ºC up to an OD_{600nm} of either 0.5 (exponential phase) or 1.5 (early stationary phase) and *greA* transcriptional expression was monitored (**fig. 39**)

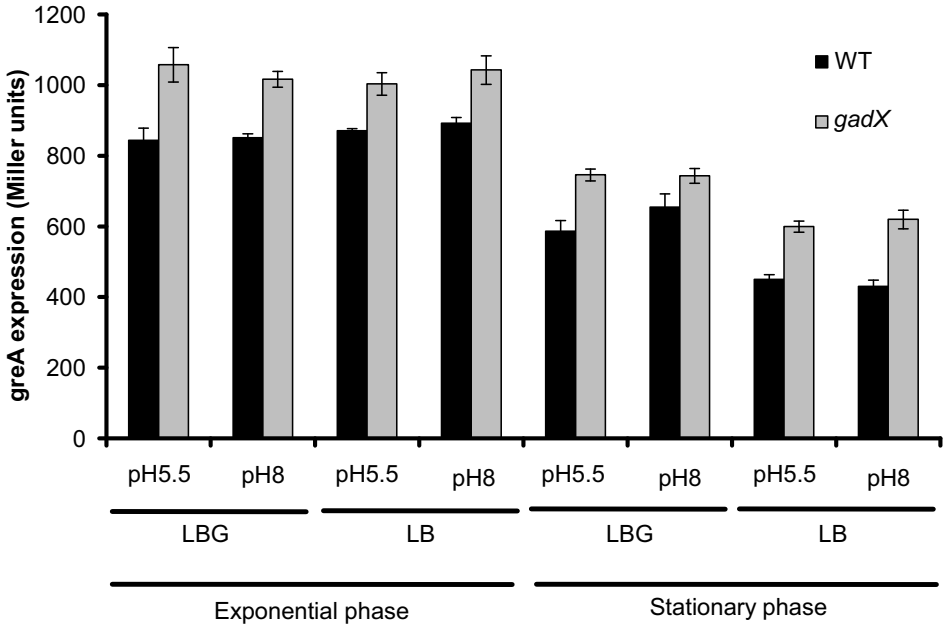

Figure 39: Effect of GadX on the expression of *greA.* The strains LFC3 (WT) and LFC22 (*gadX*) were grown in LB and LBG at pH5.5 and pH8 up to an OD_{600nm} of 0.5 and 1.5. Average and standard deviation of β-galactosidase activity determination from three independent cultures are shown.

It was observed a slight increase of *greA* expression in absence of GadX in all conditions tested, but the substantial increase that it would be expected attending to the presence of a functional binding site of GadX in the promoter region of *greA* (overlapping the -10 box of the σ^{70}-dependent promoter) was not observed (**fig. 39**).

4.2. Crosstalk between the factors that bind to the secondary channel of the RNApol

When complex regulatory networks have been studied, it has been noticed that often a crosstalk among regulators that are involved in the same regulatory pathway exists. There are several examples of crosstalk within pathways that control expression of virulence/colonisation factors (Babu *et al.*, 2011; Mouslim and Hughes, 2014). Considering that a possible competence between different factors (GreA, GreB and DksA) for binding to the secondary channel of the RNApol, studies have been performed to establish whether a crosstalk between those factors exists. In the section 4.1.2, it was described that DksA and ppGpp do not affect the expression of *greA*. However, the GreA effect in the expression of *greB* and *dksA*, and the possible cross-regulation between the different factors remained unknown. Parallel to our study, two more groups performed similar experiments in order to determine this possible crosstalk and to study the expression of the different factors that bind to the secondary channel (Chandrangsu *et al.*, 2011; Vinella *et al.*, 2012). Therefore, in this section I am describing our data and comparing it with the published data.

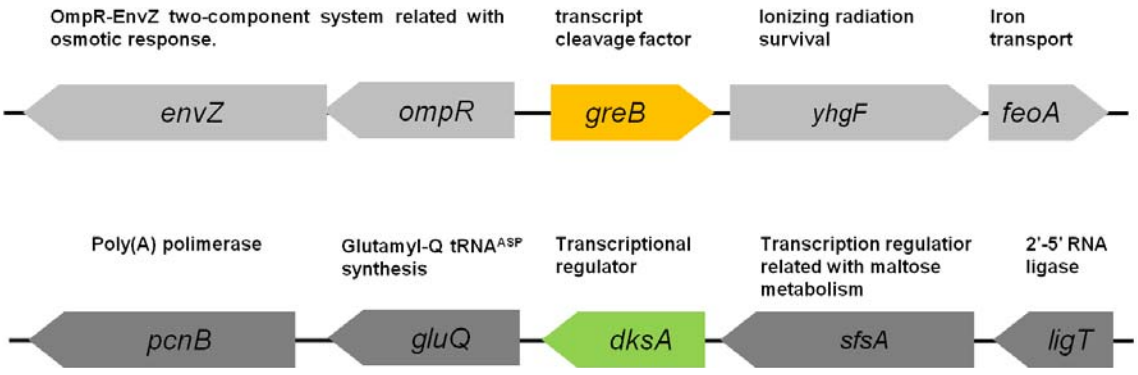

Figure 40: Genomic context of the *greB* and *dksA* genes in *E. coli*.

The genomic location of *greA* was shown in **figure** 24. The genes *greB* and *dksA* are monocistronic operons located in the chromosome of *E. coli* (**fig. 40**). The *greB* gene is flanked upstream by the bicistronic operon *ompR-envZ* that codes for a two-component system responsible of the osmotic response (Mizuno and Mizushima, 1990), and downstream by the gene *yhgF* that is related with survival to ionizing radiation (Byrne *et al.*, 2014). The gene *dksA* is flanked upstream by the gene *sfsA* that codes for a transcription regulator

related with maltose metabolism (Takeda *et al.*, 2001), and downstream by the gene *gluQ* that codes for the glutamyl-Q tRNA^{ASP} synthetase (Campanacci *et al.*, 2004).

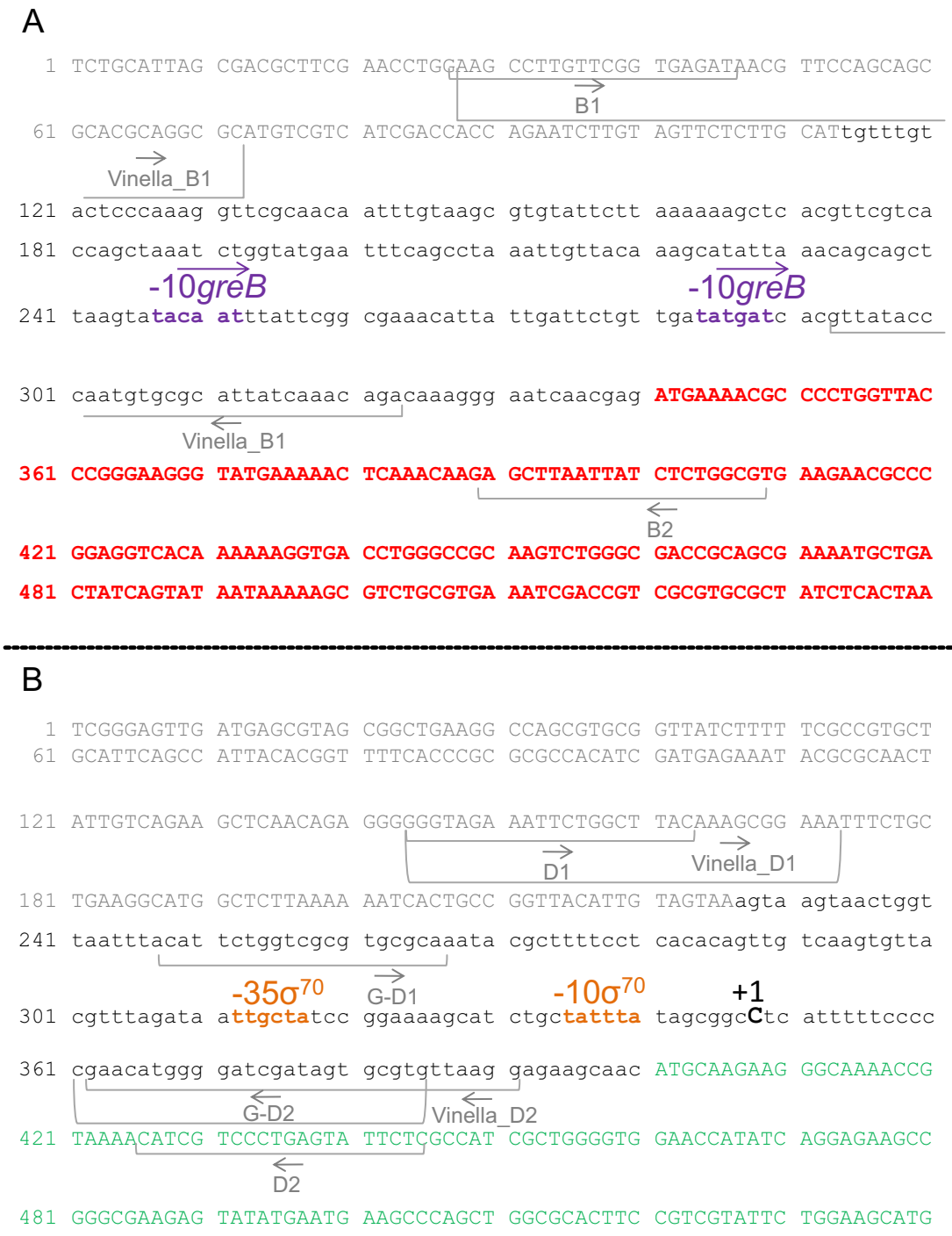

Figure 41: Partial sequences of the *E. coli* genome, including the *greB* (A) and *dksA* (B) genes. In capital letters are indicated the coding sequences of the different genes: *ompR* and *sfsA* (in grey, A and B respectively), *greB* (in red, A) and *dksA* (in green, B). The predicted -10 boxes of the putative promoters of *greB* are indicated in purple (Münch *et al.*, 2005). The boxes -10 and -35 of the σ^{70} (in orange) of *dksA* promoter are indicated and its transcription initiation +1 is

indicated in capital letters in black. The sequence of the primers used to produce the different *lacZ* fusions used in this study are indicated in grey and underlining by brackets, as well as those primers used by Vinella et al. (2012) and Chandrangsu *et al.* (2011). The name of the primer and the orientation is indicated.

While the promoter of *greB* has not been experimentally identified, the promoter of *dksA* was located in the intergenic region between *dksA* and *sfsA* (**fig. 41B**) by primer extension (Chandrangsu *et al.*, 2011). Moreover, overlapping the *sfsA* coding sequence, weak promoters were also located that seem to control *dksA* expression to some extent, since its absence causes a reduction of a 23% of the gene expression (Chandrangsu *et al.*, 2012).

In the previous section, the expression of *greA* using several *lacZ* fusions was determined. Therefore transcriptional fusions of the *greB* and *dksA* 5' intergenic regions with the *lacZ* reporter gene were constructed using the primers shown in **figure 41**. The intergenic region of *greB* (323bp) was PCR-amplified with the primers B1 and B2 (**fig. 41A**), while the intergenic region of *dksA* (303bp) was amplified with the primers D1 and D2 (**fig. 41B**). These sequences were cloned within vector pRS551 generating transcriptional fusions. Finally, generated fusions, attBgreB (from -255 to +68 respect the translation start site) and attBdksA (from -205 to +98 respect the transcriptional start site), were subsequently transfer to the *attB* locus of the *E. coli* chromosome as indicated in section 3.7.5 (Simons *et al.*, 1987). To determine the expression of *greA*, the fusion attBgreA2 (**fig. 25**) was used.

The expression of *greB* was determined in WT and *greA*, *dksA* and *greB* derivative mutants in cultures grown in LB at 37ºC up to an OD_{600nm} of 0.5 (exponential phase) and 2.0 (early-stationary phase) (**fig. 42A**). The expression of *greB* increases (1.5-fold) at stationary phase respect to exponential phase. While no effect was observed by GreA and GreB, in absence of DksA the induction of *greB* at stationary phase do not occur, suggesting that the induction of *greB* expression at stationary phase depends on DksA and presumably on its cofactor ppGpp (**fig. 42A**). Similar experiments were performed by Vinella *et al.* (2012), amplifying the *greB-ompR* intergenic region with the primers Vinella_B1 and Vinella_B2 (**fig. 41A**) and cloning this DNA fragment into pRS415*,* a pRS551derivative plasmid that not contains the kanamycin resistance cassette located upstream of the *lacZ* gene (Simons *et al.*, 1987). The results obtained

when they look at *greB* transcriptional expression in cultures grown in LB at 37ºC up to an OD_{600nm} of 0.4 (exponential phase) and 2.0 (early-stationary phase), were similar to ours since also stationary phase induction was detected (**fig. 42A**), but, instead a 1.5-fold induction at stationary phase, they observe a much higher induction, about 10 fold. The observed differences could be caused by the sequences fused to the *lacZ* gene; in our case it contained a larger sequence than in Vinella *et al.* (2012).

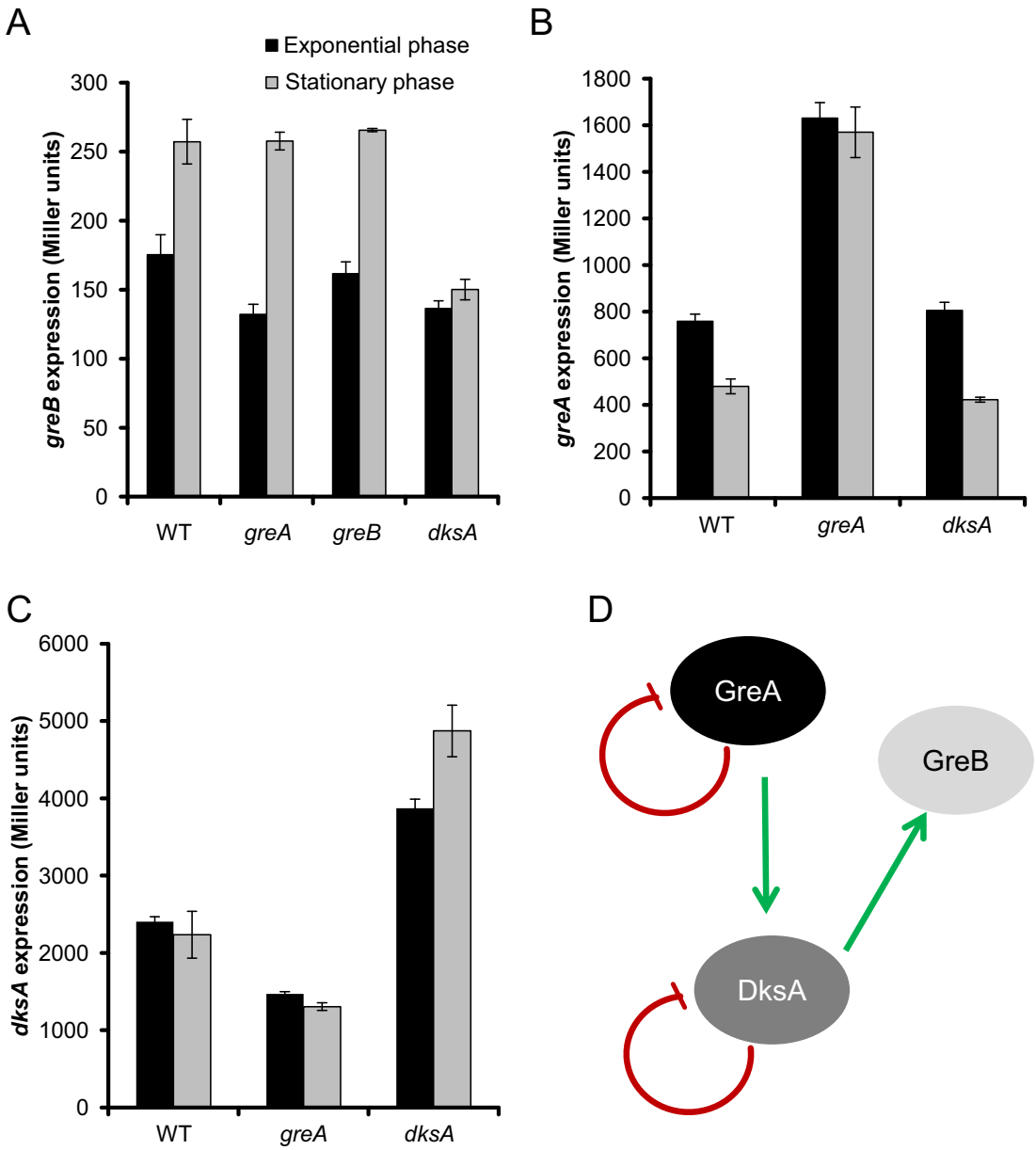

Figure 42: Crosstalk between the different proteins that bind to the secondary channel. A) Expression of *greB* determined using the *lacZ* fusion attBgreB in the strains LFC54 (WT), LFC55 (*greA*), LFC56 (*greB*) and LFC57 (*dksA*) grown in LB at 37ºC up to an OD_{600nm} of 0.5 and 2.0. B) Expression of *greA* determined using the *lacZ* fusion attBgreA2 in the strains LFC3

(WT), LFC4 (*greA*) and LFC8 (*dksA*) grown in LB at 37ºC up to an OD_{600nm} of 0.5 and 2.0. C) Expression of *dksA* determined using the *lacZ* fusion attBdksA in the strains LFC58 (WT), LFC59 (*greA*) and LFC60 (*dksA*) grown in LB at 37ºC up to an OD_{600nm} of 0.5 and 2.0. D) Model of the crosstalk hypothesized. Average and standard deviation of β-galactosidase activity determination from three independent cultures are shown.

Moreover they observe that this induction requires DksA (as observed in the **figure 42A**) and ppGpp. These data suggest that in stationary phase ppGpp and DksA induce *greB* expression, modifying the interplay between the proteins that bind to the secondary channel.

The expression of *greA* was determined with the strain LFC3 (attBgreA2, referred as WT) and its derivative mutants in *greA* and *dksA* in cultures grown in LB at 37ºC up to an OD_{600nm} of 0.5 and 2.0 (**fig. 42B**). As described in the previous section, the expression of *greA* decreases in stationary phase, but it is not dependent of DksA. Moreover the expression of *greA* increases in absence of GreA (**fig. 42B**). Surprisingly, while we observe an increase of *greA* expression in absence of GreA in both growth phases (exponential and stationary phase), the results obtained by Vinella *et al.* (2012) shows autoregulation of *greA* only in stationary phase. Moreover they do not observe differences in *greA* expression between exponential and stationary phase, whereas we did (**fig. 42B** and section 4.1.2). As well as observed by *greB*, these divergences could be due the different *lacZ* fusions used, in our case we have used attBgreA2 that fuses a larger sequence (from -1030 to +175) than in Vinella *et al.* (2012) that they fused a sequence from -91 to +135 respect the transcription start site. Our data (**fig. 29**) showing that the levels of GreA protein was downregulated in stationary phase, strongly corroborate the transcriptional data obtained with the attBgreA2 fusion.

It is interesting that while the expression of *greA* decreases in stationary phase, the expression of GreB increases (**fig. 42A** and **B**). These data may suggest an exchange between GreA and GreB to bind into the secondary channel of the RNApol. In exponential phase, where the cells are dividing in a maximal rate, GreA might be the encharged protein to release RNApol pauses by binding to the secondary channel, but in stationary phase the amount of GreA decreases and it might be substituted by GreB. Although both factors (GreA and GreB) are able to solve paused RNApol, the RNA cleavage produced is different (S

Borukhov *et al.*, 1993). This exchange of factors might suggest that the genes expressed during exponential and stationary phase might require different mechanisms of solving pauses, or it is simply an evolutive response to the decrease of GreA in stationary phase, in order to keep a mechanism to solve paused RNApol.

The expression of *dksA* was determined with the fusion attBdksA in WT and *greA* and *dksA* derivative mutants in cultures grown in LB at 37ºC up to an OD_{600nm} of 0.5 and 2.0 (**fig. 42C**). No differences of expression were observed at different growth phases (exponential *vs.* early-stationary phase). The expression of *dksA* decreases in absence of GreA (1.5 fold), suggesting that GreA is required for the proper expression of *dksA*. In absence of DksA, the expression of *dksA* increases (1.5 fold), suggesting that *dksA* autoregulates its own expression, as well as GreA does. This autoregulation was described by Chandrangsu *et al.* (2011), performing similar experiments by amplifying the *dksA-sfsA* intergenic region with the primers G_D1 and G_D2 (**fig. 41B**) and cloning this DNA fragment into pRS551 (Simons *et al.*, 1987). The transcriptional studies of the expression of *dksA* in cultures grown in LB at 37ºC up to an OD_{600nm} of 0.5 (exponential phase) in either presence or absence of DksA, showed that the expression of *dksA* increases up to 2-fold (Chandrangsu *et al.*, 2011).

Although Chandrangsu *et al.* (2011) showed that the expression of *dksA* decreases up to 5 times in late-stationary phase (OD_{600nm} of 5.0). However, we do not observe any significant difference in the expression of *dksA* between exponential (OD_{600nm} of 0.5) and stationary phase (OD_{600nm} of 2.0). It was described by western blot, that the amount of DksA decreases (2 fold) at late-stationary phase (OD_{600nm} of 5.6) but not at early-stationary phase (OD_{600nm} of 2.1) (Rutherford *et al.*, 2007). These results at protein level are consistent with the transcriptional studies, while at early-stationary phase none effect was observed (**fig. 42C**), at late-stationary phase it decreases (Chandrangsu *et al.*, 2011).

A similar experiment was also performed by Vinella *et al.* (2012), using a lacZ fusion obtained by PCR-amplification of the *dksA-sfsA* intergenic region with the

primers Vinella_D1 and Vinella_D2 (**fig. 41B**) and posterior cloning of this DNA fragment into pRS415 (Simons *et al.*, 1987). They obtained similar results as observed in **figure 42C** and the ones described by Chandrangsu *et al.* (2011), showing that GreA stimulates the *dksA* expression, as well as the autoregulation of *dksA*. Surprisingly, when monitoring the expression of *dksA* in cultures grown in LB at 37ºC up to an OD_{600nm} of 0.4 (exponential phase) and 2.0 (early-stationary phase), they observed a 2-fold increase of the expression of *dksA* in early-stationary phase respect to exponential phase. These results are in discrepancy on the results observed in **figure 42C** or the results previously published by Chandrangsu *et al.* (2011), as well as the data shown by Rutherford *et al.* (2007). These discrepancies may be consequence for the different *dksA-lacZ* fusions used for these experiments.

Although further studies would be required, all these data show a cross-regulation between the different factors that bind to the secondary channel of the RNApol (**fig. 42D**). GreA and DksA are able to repress its own gene expression in order to modulate the amount of these proteins. GreA stimulates the expression of *dksA*, and DksA stimulates the expression of *greB* during stationary phase. This cross-regulation would keep the equilibrium between these factors. Small changes of one of these proteins (GreA, GreB or DksA) could produce changes on the amount of the other proteins in order to keep the equilibrium or to change it completely. Changes in this equilibrium would change the gene expression pattern. Attending to the discrepancies in the data obtained by several research groups regarding the transcriptional expression of those factors using *lacZ* fusions, methodologies based in mRNA quantification (qPCR) and protein immunodetection would be required for proper dissection of the existing crosstalk.

4.3. Effect of the interplay between factors that bind to the RNApol on flagella genes expression in *E. coli*

In our research group we performed, some years ago, transcriptomic studies to determine the effect of ppGpp and DksA in *E. coli* (Aberg *et al.*, 2009). It was found that similar amount of genes were significantly affected (fold-change of ±2) by ppGpp (265 genes) and DksA (311 genes). Up to 30% (95 genes) of these genes were significantly affected by both factors. Surprisingly, 36 of the 95 genes were differentially regulated: 4 genes were up-regulated in absence of ppGpp and down-regulated in absence of DksA, and 32 genes in the other way around (Aberg *et al.*, 2009). The opposite gene regulation by ppGpp and DksA was previously described for the *fim* operon, coding for the type-1 fimbriae. It was shown that *fimB* expression was upregulated in a *dksA* mutant and downregulated in a $ppGpp^0$ mutant. The increase of *fimB* expression in absence of DksA depends on GreA and GreB (Aberg *et al.*, 2008). These data suggested that in absence of DksA, the secondary channel of the RNApol is free to accept GreA and GreB, allowing them to interact more efficiently and causing alterations in the gene transcription profile. A major part of the genes differently regulated by ppGpp and DksA in *E. coli* codes for proteins involved in motility, flagella genes and chemotaxis (Aberg *et al.*, 2009).

Flagella biosynthesis and chemotaxis genes are distributed in 18 operons transcribed following a strict hierarchy. These genes are classified, depending on its temporally expression, into three promoter classes: early, middle and late operons (Chevance and Hughes, 2008). The early operon *flhDC* is expressed first and is under control of a σ^{70}-dependent promoter. FlhD and FlhC produces an hexameric complex (FlhD4C2) that is essential for the expression of middle genes (Wang *et al.*, 2006). Middle genes contain structural genes of the basal body and motor structure, complex known as HBB, and the genes *fliA* and *flgM,* that code for the alternative subunit σ^F (essential for late operons transcription) and its anti-sigma factor, respectively. As described previously in section 1.1.2.5, the anti-sigma factor FlgM bind to FliA, preventing its association with the RNApol and inhibiting the late genes transcription (Treviño-Quintanilla *et al.*, 2013). When HBB structure is formed, FlgM is secreted through the basal body

and σ^F is free to bind to the RNApol and induce transcription of the late genes, such as *fliC*, that encodes the main subunit of the flagella filament (Chevance and Hughes, 2008).

The transcriptomic study referred above (Aberg *et al.*, 2009) showed that in absence of DksA the expression of *fliC* increases 37 fold, while it decreases 2 fold in absence of ppGpp. In order to determine whether the divergences between the effect of ppGpp and DksA depends of GreA, as described by *fimB* (Aberg *et al.*, 2008), transcriptional studies, using *lacZ* fusions to *fliC,* were performed. Using a distal *lacZ* fusion with *fliC,* located at +1210 of the transcriptional start site, the expression of *fliC* increases up to 4 times in absence of DksA (**fig. 43A**). However, in a strain deficient for DksA and GreA, similar expression levels as in WT strain were observed, suggesting that the increase of *fliC* in absence of DksA strictly depends on the presence of GreA, as previously described by *fimB* (Aberg *et al.*, 2008). Remarkably when using a proximal *lacZ* fusion with *fliC* (located at +70 of the transcription start site) surprising results were obtained (**fig. 43A**): the increase of *fliC* expression in absence of DksA was not observed.

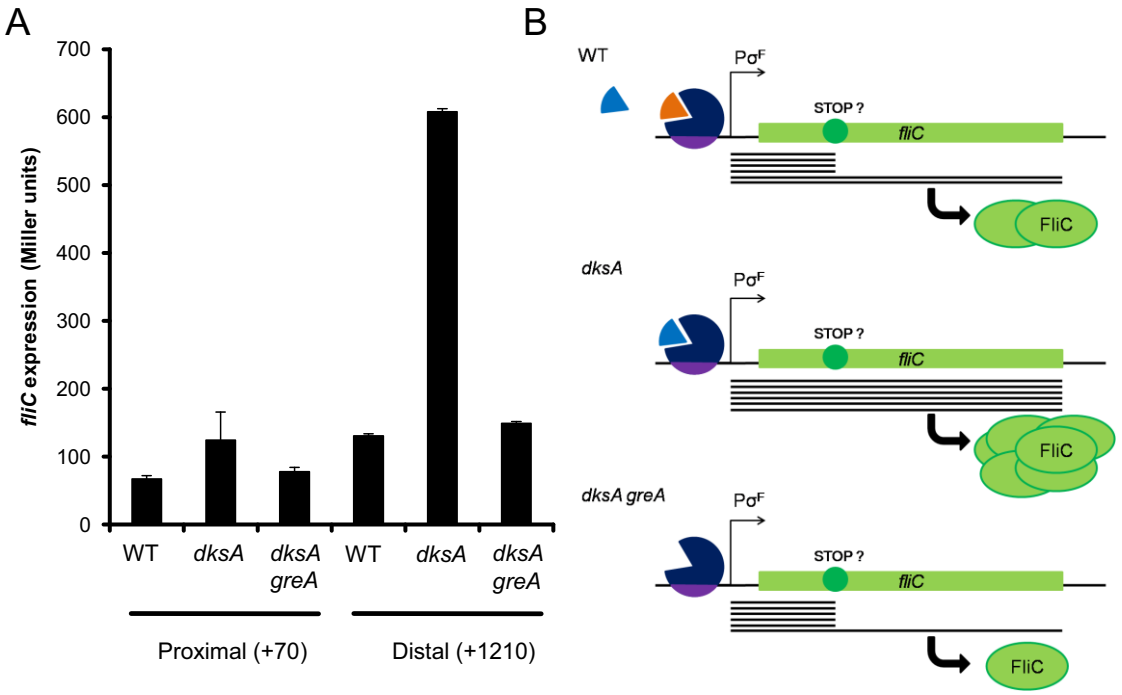

Figure 43: Effect of DksA on expression of *fliC.* A) Expression of *fliC* using the proximal (+70) and distal (+1210) *lacZ* fusions. The strains PRG13 (AAG1 $fliC_{+70}$::*lacZ*) and PRG16 (AAG1 $fliC_{+1210}$::*lacZ*) and its derivative mutant strains for *dksA* (PRG14 and PRG17, respectively) and for *dksA greA* (PRG15 and PRG18, respectively), were grown in LB at 37ºC up to an OD_{600nm} of

1.5 and β-galactosidase activity was determined. Average and standard deviation of β-galactosidase activity determination from three independent cultures are shown. B) Hypothetical model to explain the effect of GreA and DksA over *fliC* expression. Orange triangle represents DksA while blue triangle represents GreA.

To explain the differences observed between the proximal and distal fusion, we hypothesized (**fig. 43 B**) that within the *fliC* gene a transcriptional pause zone might exist, between the position +70 and +1210. To alleviate the transcriptional pause, GreA will interact with the RNApol. Our model suggests that this pause zone is not efficiently solved by the RNApol in normal conditions. However, in absence of DksA, GreA is able to bind to the secondary channel of the RNApol, solving the pause situation and, as a consequence, increasing the expression of *fliC*. Consistent with a requirement of GreA for the expression of *fliC,* in absence of both factors, RNApol is not able to solve the pause efficiently and produces low amount of *fliC.*

4.3.1. Effect of the factors that bind into the secondary channel of the RNApol on *fliC* expression

To further corroborate the effect of DksA on *fliC* expression, Real Time qPCR experiments were performed to corroborate it. The strains MG1655 (as WT) and its mutant *dksA* and *dksA greA* were grown in LB at 37ºC up to an OD_{600nm} of 1.5 and the total RNA was isolated as indicated in section 3.5.1. The expression of *fliC* was determined by qPCR with SYBR Green using the primers fliC-RT8 and fliC-RT9. The primers zwf-FW2 and zwf-RV were used to detect the expression of the *zwf* gene, coding for glucose 6-P deshydrogenase, as endogenous control. Data was collected and its normalization was performed as described in section 3.5.3. The fold-change value after normalization, relative to the WT strain, is represented in **figure 44**.

As previously observed in **figure 43A**, the expression of *fliC* (**fig. 44**) increases dramatically in absence of DksA (up to 80-fold), but in absence of both factors (DksA and GreA) the induction of *fliC* expression by the *dksA* mutation is importantly abolished, since it decrease more than 5 fold. However, the expression of *fliC* in a *dksA greA* mutant is 14 times higher than in a WT strain. This increase on the expression of *fliC* in the *dksA greA* mutant could be explained as a possible effect of DksA during transcription initiation, affecting

the expression of either *fliA* or *flhDC*, but it is not observed with the *lacZ* fusions. It is important to highlight that qPCR is a more sensitive technique than transcriptional fusions.

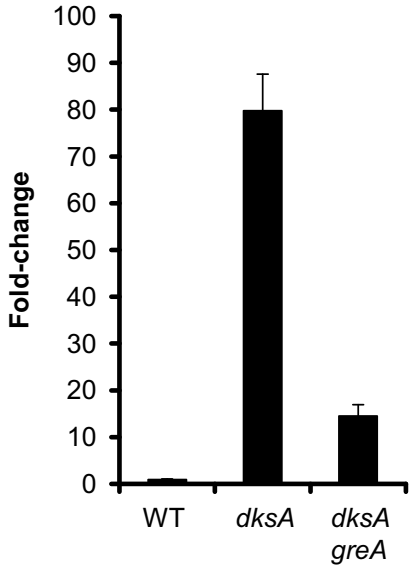

Figure 44: Effect of *dksA* and *dksAgreA* mutation on expression of *fliC* by qPCR. The strains MG1655 (WT), TE8114 (*dksA*) and AAG101 (*dksA greA*) were grown in LB at 37ºC up to an OD_{600nm} of 1.5 and total RNA was isolated. The expression of *fliC* was determined by qPCR with SYBR Green using the primers fliC-RT8/fliC-RT9. Amplification of the gene *zwf* mRNA with the primers zwf-FW2/zwf-RV was used as endogenous control.

Since *fliC* codes for the main subunit of the flagellum, variations on the expression of *fliC* might be associated with variations on motility. In fact, it was shown by Aberg *et al.*, (2009) that the DksA and ppGpp affects motility. Therefore, we decided to determine the effect of the different factors that bind to RNApol on bacterial motility. The motility was determined (**fig. 45**) as described in section 3.9.3, using motility agar plates with a 0.25% of agar allowing swimming of bacteria (Aberg *et al.*, 2009) to promote detection of motility, 2mM of maltose as chemo-attractant was added. Plates were incubated at 30ºC during 12 hours. The strain MG1655, TE8114 (referred as *dksA*), AAG93 (referred as $ppGpp^0$), AAG101 (referred as *dksA greA*), CF11657 (referred as *greA*) and CF11663 (referred as *greB*) were assessed.

When comparing with the phenotype of the WT strain (**fig. 45**) we might conclude that the mutant $ppGpp^0$ is no-motile and the mutant deficient in *dksA*

is hypermotile, as it would be expected considering the expression of *fliC* in these mutants (Aberg *et al.*, 2009).

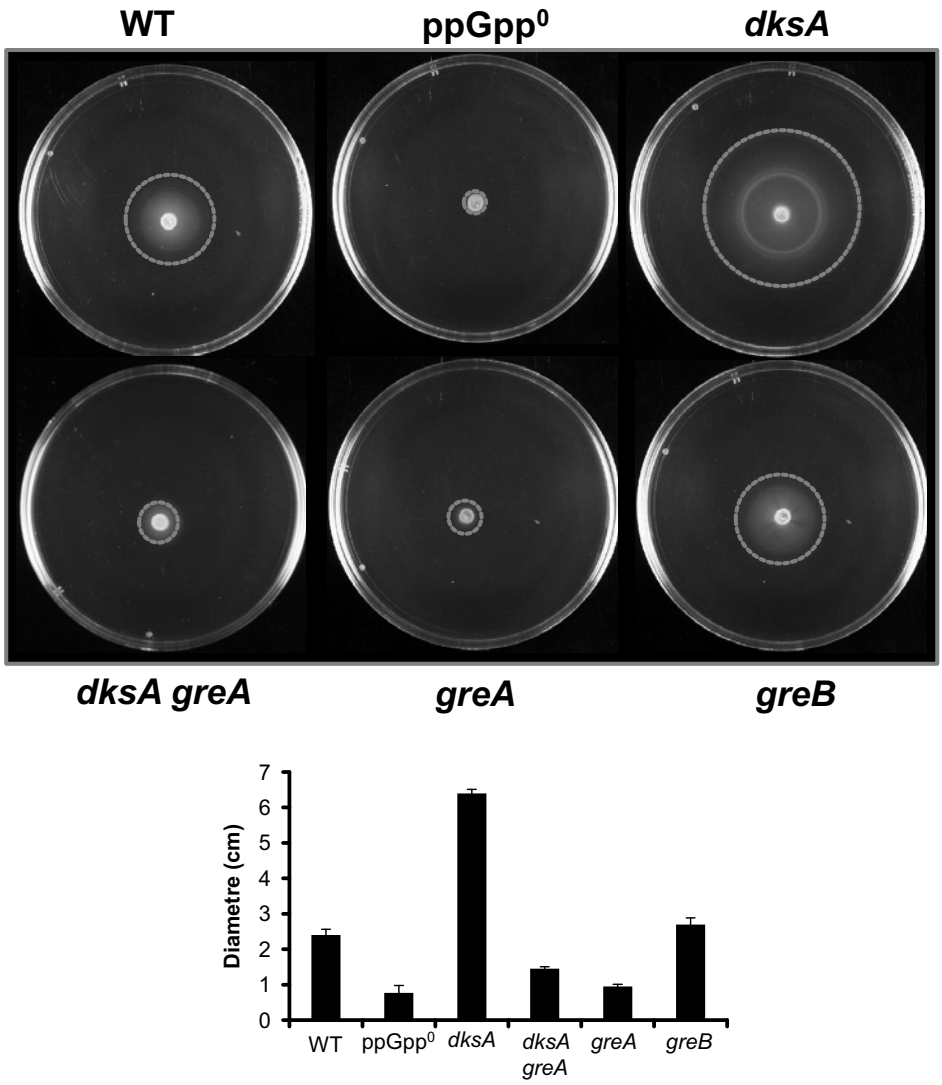

Figure 45: Effect of the different factors that bind to RNApol in *E. coli* motility. The different strains were inoculated on motility agar plates supplemented with maltose 2mM as chemo-attractant and incubated at 30ºC during 12 hours. The strains used are MG1655 (referred as WT), TE8114 (referred as dksA), AAG93 (referred as ppGpp^0), AAG101 (referred as *dksA greA*), CF11657 (referred as *greA*) and CF11663 (referred as *greB*).

Moreover, in the strain *dksA greA* the motility decreases dramatically, being even less motile than the WT strain. The motility results are in agreement with the transcription data shown in **figure 43**, but in disagreement with the qPCR data (**fig. 44**). The discrepancies between β-galactosidase activity and qPCR were explained due the higher sensitivity of qPCR, but it does not explain the discrepancies with motility assay.

The effect of GreA and GreB on motility was also determined. The mutant *greA* was nearly no-motile, whereas the mutant *greB* has the same motility than WT. These data indicate that GreA is required for motility in *E. coli* even in presence of DksA whereas GreB does not seem to have any effect. It has been postulated, according to its protein amount and affinity to the secondary channel of the RNApol, that GreA is not able to compete with DksA to bind the RNApol (Rutherford *et al.*, 2007). However, it has been shown, at least in vitro, that DksA does not bind to backtracked elongation complexes (Furman, Tsodikov, *et al.*, 2013), suggesting that in this conditions, the possible conformational changes produced on the RNApol during backtracking, would promote at least practically the substitution between GreA and DksA.

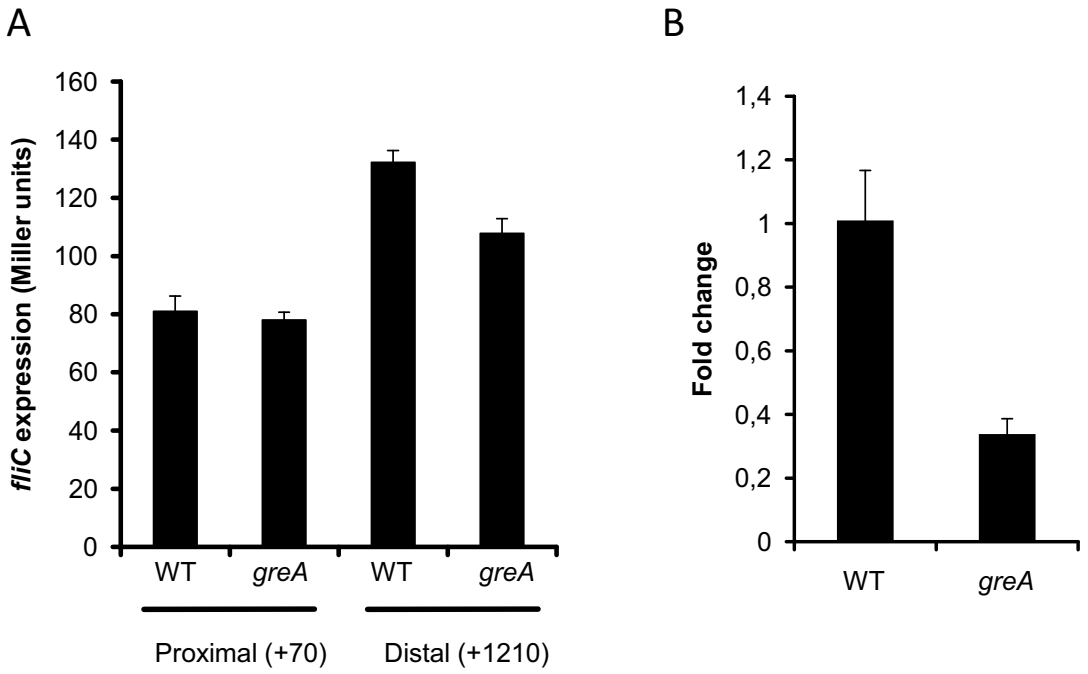

Figure 46: Effect of GreA on the expression of *fliC*. A) The strains PRG13 (AAG1 *fliC*::*lacZ* (+70)) and PRG16 (AAG1 *fliC*::*lacZ* (+1210)) and its derivative mutant strains for *greA* (LFC61 and LFC62, respectively), were grown in LB at 37ºC up to an OD_{600nm} of 1.5 and β-galactosidase activity was measured. Average and standard deviation of β-galactosidase activity determination from three independent cultures are shown. B) The strains MG1655 (WT) and CF11657 (*greA*) were grown in LB at 37ºC up to an OD_{600nm} of 1.5 and total RNA was isolated. The expression of *fliC* was determined by qPCR with SYBR Green using the primers fliC-RT8/fliC-RT9. Amplification of the gene *zwf* mRNA with the primers zwf-FW2/zwf-RV was used as endogenous control.

Since the motility assay indicates that GreA is required for motility (**fig. 45**), the effect of GreA on the transcriptional expression of *fliC* was determined. The

strain PRG13 and PRG16 carrying the proximal (+70) and distal (+1210) *fliC*::*lacZ* fusions and the corresponding *greA* mutant derivative strain were grown in LB at 37ºC up to an OD_{600nm} of 1.5 (**fig. 46A**) and *fliC* expression was monitored.

It was not possible to detect any effect of GreA on the *fliC* transcriptional expression under the experimental conditions used (**fig. 46A**), neither using the proximal *lacZ* fusion nor the distal fusion. A slight decrease in absence of GreA with the distal fusion was observed. For this reason we decided to determine the effect of GreA by qPCR. The strain MG1655 (referred as WT) and CF11657 (referred as greA) were grown in LB at 37ºC up to an OD_{600nm} of 1.5 and the total RNA was isolated as indicated in section 3.5.1. The expression of *fliC* was determined by qPCR with SYBR Green using the primers fliC-RT8 and fliC-RT9 the primers zwf-FW2 and zwf-RV were used to detect the expression of the *zwf* gene as endogenous control. The fold-change value after normalization, relative to the WT strain, is represented in **figure 46B**.

The expression of *fliC* (**fig. 46B**) suffers a 3-fold decrease in absence of GreA, suggesting that the expression of *fliC* is activated by GreA, even in presence of DksA. According to our model (**fig. 43B**), GreA might be required for efficient transcription of *fliC*. As previously mentioned, paused RNApol might change its affinity from DksA to GreA, for this reason in absence of GreA the RNApol is not able to solve the pause and, therefore, the expression of *fliC* decreases.

The differences observed between the β-galactosidase study (**fig. 46A**) and the qPCR (**fig. 46B**) could be due the basal background of the *lacZ* fusion. If we do not observe a decrease on the β-galactosidase activity in absence of GreA, would be because it is the minimal activity that we can detect with this fusion. However, the results obtained with qPCR, *lacZ* fusions and the phenotypic studies (motility plates) are not in full agreement. We should have in consideration whether the culture conditions used are the more appropriated for those studies. Evidently the strength of the results regarding the effect of *greA* on motility is the phenotypic assay, GreA is required for motility in both, presence and absence of DksA. This clear result is not fully explained with the data obtained by both, qPCR and *lacZ* fusions. The discrepancies might be

result of the differences in culture, on solid media for phenotypic studies and liquid for transcriptional studies. Our data (**fig. 47**) indicates that when MG1655 strain grew in liquid media the degree of flagellation is very low. Therefore, if growth in LB is not permissive conditions for flagella expression that can explain that we cannot efficiently detect the effect of *greA* in the *fliC* expression from liquid cultures (*lacZ* fusions assays). Nonetheless, the *lacZ* fusion has been very useful to study the interplay of DksA and GreA on *fliC* expression.

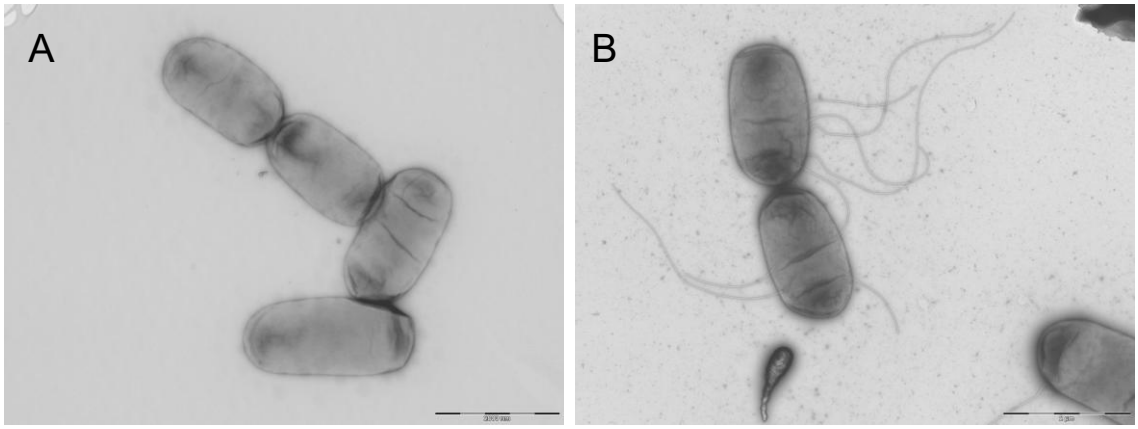

Figure 47: Observation of flagella in cultures grown in liquid and solid media. A) The strain MG1655 in cultures grown in LB at 37ºC up to an OD_{600nm} of 2.0 was observed at TEM. B) The strain MG1655 was grown on motility agar plates supplemented with maltose 2mM incubated at 30ºC during 12 hours. Bacterial growth was removed from the agar surface and gently mixed with 3 ml of filtered Ringer ¼ and observed at TEM. Scale bar: 2 µm.

4.3.2. Effect of GreA, DksA and ppGpp on the regulatory pathway of flagella

In the previous section, it has been discussed that GreA, DksA and ppGpp affects *fliC* expression. However, considering the complexity of the regulatory cascade that control expression of flagella genes, we decided to determine if those regulatory factors are affecting the expression of the flagella at different levels. It has been described that in absence of DksA, the expression of *flhDC*, master regulator of the flagella biosynthesis, and *fliA*, alternative σ factor required for flagella genes transcription, increases in rich MOPS media (Lemke *et al.*, 2009). Moreover, in absence of DksA, increases the secretion on FlgM, the anti-sigma factor (Guo *et al.*, 2014), suggesting that the absence of DksA might, by these effects, increases the expression of the flagella operons.

It was determined the role of FliA or FlgM in the regulation of *fliC* expression mediated by DksA using the proximal and distal *lacZ* fusion (+1210) (**fig. 48**). The strains PRG16 (WT) and PRG17 (*dksA*) with its derivative mutant strains for *flgM* (LFC37 and LFC39) and *fliA* (LFC38 and LFC40), were grown in LB at 37ºC up to an OD_{600nm} of 1.5 and the transcriptional expression of *fliC* was determined.

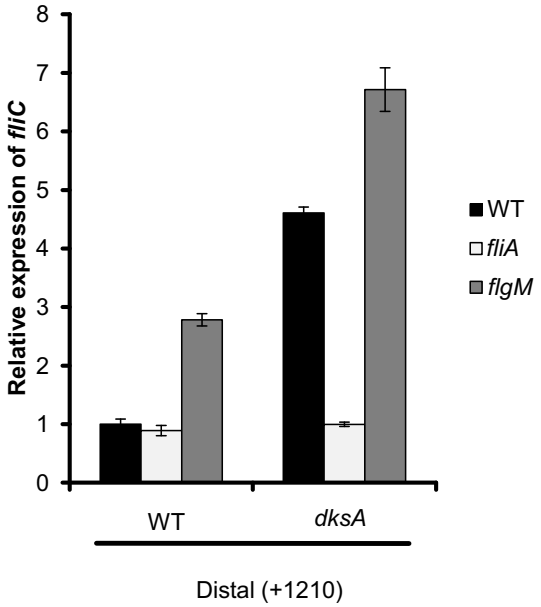

Figure 48: Expression of *fliC* in the strains PRG16 (WT) and PRG17 (*dksA*) with its derivative mutant strains for *flgM* (LFC37 and LFC39) and for *fliA* (LFC38 and LFC40), were grown in LB at 37ºC up to an OD_{600nm} of 1.5. The *fliC* expression of the different strains was expressed in relative values, being 1.0 the value in Miller units for the strain PRG16 (WT). Average and standard deviation of β-galactosidase activity determination from three independent cultures are shown.

As previously described, *dksA* mutation causes a *fliC* induction. However, the absence of FliA suppresses the *fliC* expression in all strains (**fig. 48**). This result is the expected attending that the expression of *fliC* is strongly dependent of σ^F. Interestingly, the expression of the WT strain is similar than the expression in absence of *fliA*, suggesting that under this culture conditions, the expression levels of *fliC* is very low, as previously discussed.

As expected by the role of FlgM as anti-sigma factor for FliA, the absence of FlgM (**fig. 48**) causes an increase in the *fliC* expression in the DksA proficient strain (2.8 fold). Similar behaviour has been observed by Ding *et al.*, (2009) in

Yersinia pseudotuberculosis. Interestingly, in absence of DksA, the effect of *flgM* mutation is less pronounced, a 2.1-fold increase was observed.

Transcriptomic studies showed an increase in the expression of the flagella operons (Aberg *et al.*, 2009) in the *dksA* mutant strain. Among them, those that codes for FlgM and the basal body which might promote secretion of FlgM in the medium (Guo *et al.*, 2014). As a consequence, there is more FliA available that could interact with the RNApol and increase the expression of *fliC* at transcription initiation level. Additionally, the absence of DksA would produce the interaction of GreA into the secondary channel of the RNApol and increasing the expression of *fliC* at transcription elongation level. Our data suggest that *fliC* is affected by the *dksA* mutation at two different levels, a first level during transcription initiation by its regulatory cascade and during transcription elongation.

The effect of DksA, ppGpp and GreA in the amount of FliA and FliC was determined by immunodetection (**fig. 49**).The amount of FliA on MG1655 and in its derivative mutant *greA, dksA, dksA greA, relAspoT* ($ppGpp^0$) and *fliA* (as a negative control) was determined in cultures grown in LB at 37ºC up to an OD_{600nm} of 1.5 (**fig. 49A**). In absence of ppGpp, FliA is no detectable, whereas in absence of DksA, the amount of FliA increases over 2-fold. Those results are consistent with a previous report (Aberg *et al.*, 2009). Remarkably *greA* mutation does not have a significant effect on the expression of *fliA* since the amount of FliA does not decrease by the absence of GreA neither in a $dksA^+$ nor in a $dksA^-$ strain.

Regarding the levels of FliC (**fig. 49B**), in absence of ppGpp no expression of FliC was observed, as well as in the control strains *fliC* and *fliA*. However, in absence of DksA, as observed in transcriptional studies, a very huge increase in the amount of FliC was detected (57-fold). This increase depends on the presence of GreA since in a *dksA greA* strain the amount of FliC was only 2-fold compared to the WT strain. The levels of FliC in absence of GreA, are really low, nearly inexistent (**fig. 49B**).

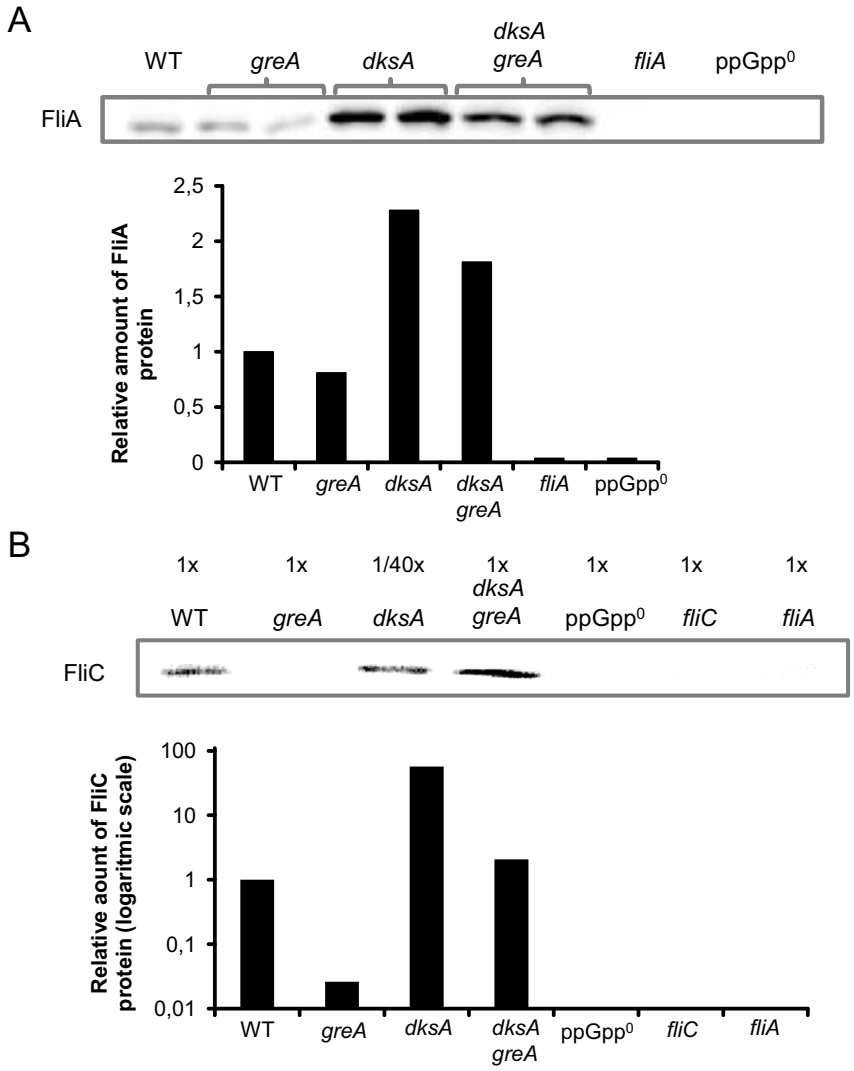

Figure 49: Effect of the factors that bind the secondary channel on the cellular levels of FliA and FliC. A) Western blot using monoclonal antibodies against FliA. The strains MG1655 (WT), CF11657 (*greA*), TE8114 (dksA), AAG101 (*dksA greA*), AAG93 (ppGpp^0) and XX (*fliA*) were grown in LB at 37ºC up to an OD_{600nm} of 1.5. Whole cell extracts were analyzed in a 12.5% SDS-PAGE, transferred onto PVDF membrane and immunodetection performed as described (section 3.6.2). The chemiluminiscence signal was visualized using a Chemidoc XRS System from BioRad. B) Western blot using polyclonal antibodies against FliC. The strains MG1655 (WT), CF11657 (*greA*), TE8114 (dksA), AAG101 (*dksA greA*), AAG93 (ppGpp^0), XY (*fliC*) and XX (*fliA*) were analyzed as in A.

The fact that the amount of FliA in a *dksA* strain is nearly the same than in a *dksA greA* strain but the FliC levels are really different, suggests that as proposed above, *dksA* mutation affect *fliC* expression at two different levels, by its role affecting *fliA* expression and directly affecting *fliC* expression. These results together with the fact that the effect of the *dksA* mutation is only observed in distal *lacZ* fusions suggest that the effect is not at the level of

transcription initiation, which seems to be strictly dependent on FliA. Our results are in agreement with a possible role of GreA in the transcription elongation of *fliC*. That might explain how a 60-fold increase on FliC (**fig. 49B**) was observed in absence of DksA, having only a 2-fold increase of the FliA levels (**fig. 49A**). Moreover, this 60-fold increase is dependent on the presence of GreA, since the FliC level decreases 30 fold in the *dksAgreA* strain as compared to the *dksA* strain. We also had observed that in absence of ppGpp there is no expression of *fliC*, suggesting that ppGpp is required also for the expression of FliC, as previously described (Aberg *et al.*, 2009). We hypothesized a regulatory network that controls flagella expression from the secondary channel of RNApol which is depicted in **figure 50**.

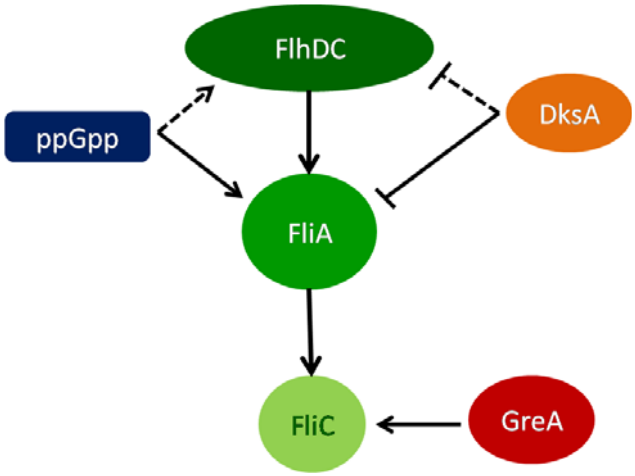

Figure 50: Scheme of the effect of ppGpp, DksA and GreA over flagella pathway.

The expression of the flagella genes is sequential and highly regulated (Chevance and Hughes, 2008). According to our data DksA represses the expression of the alternative sigma factor, FliA, as could be observed on **figure 49A**, while ppGpp is required for its expression (**fig. 49A**). How this differential regulation occurs, being independent of GreA is unknown. This effect over *fliA* could be direct on its expression, or indirect by affecting *flhD* and *flhC* expression, coding for the major regulator of the flagella expression (Lemke *et al.*, 2009). In fact, the transcriptomic studies performed in Aberg *et al.* (2009) showed that ppGpp and DksA affects the expression of *flhD* and *flhC*. Moreover GreA plays a critical role in the control of *fliC* expression which seems to be independent of σ^F levels supporting a possible role of GreA in the control of *fliC* transcription elongation.

4.3.3. Effect of possible pausing sequences on the expression of *fliC*

The main activity described for GreA is to solve pauses during transcription elongation by producing a cleavage of the nascent RNA (Laptenko *et al.*, 2003). Considering that GreA is essential for motility (**fig. 46**), we decided to determine how GreA mediated antipause activity affects *fliC* expression. First, we decided to test if the amino acids responsible of antipause activity (D41 and E44) are required for the motility (**fig. 51**). The motility of the strain MG1655 (WT) and TP1216 (*greA* E44K) with the plasmids pTrc99a, as a control, and pDNL278 (encodes *greA*) was determined (**fig. 51A**).

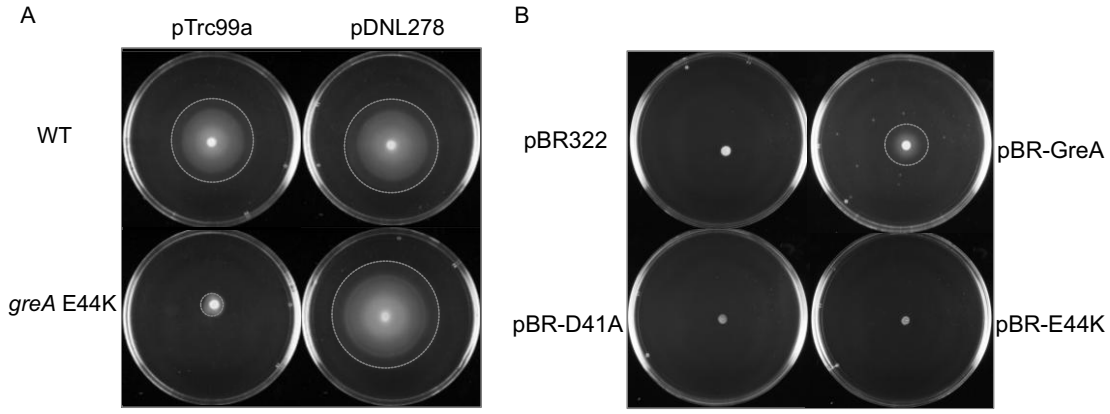

Figure 51: Effect of GreA antipause activity on motility. A) The strain MG1655 (WT) and TP1216 (*greA* E44K) carrying the plasmids pTrc99a (control) and pDNL278 ($GreA^{WT}$) were grown on motility agar plates supplemented with maltose 2m M as chemo-attractant at 30ºC during 12 hours. B) The strain CF11657 (*greA*) carrying the plasmids pBR322 (control), pBR-GreA, pBR-D41A (encodes *greA* D41A) and pBR-E44K (encodes *greA* E44K) were grown on motility agar plates supplemented with maltose 2 mM as chemo-attractant at 30ºC during 12 hours.

The strain containing the E44K *greA* allele in the chromosome is no motile (**fig. 51A**). Moreover, this mutation could be complemented *in trans* by $GreA^{WT}$ since it become motile when using the plasmid pDNL278. These results clearly suggest that the antipause activity of GreA during transcription elongation is required for motility.

Moreover, experiments were performed to determine the effect of mutations in the catalytic amino acid D41 and E44 in motility. The motility of the strain CF11657 (*greA*) carrying pBR322 (as a control), pBR-GreA, pBR-GreA D41A or pBR-GreA E44K (**fig. 51B**) was monitored. In absence of GreA, strain carrying plasmid pBR322, no movement was observed, but the introduction of WT *greA*

(pBR-GreA) *in trans*, restores the cellular motility. However, the introduction of *greA* D41A or *greA* E44K alleles did not restores motility, corroborating that the antipause activity of GreA is required for the motility in *E. coli*. Our data highlight the idea that *fliC* contains a sequence located between the proximal (+70) and distal (+1210) *lacZ* fusion that produces a pause of transcription elongation and GreA is required to solve it.

To further establish that regulation at the transcriptional elongation of *fliC* exists, experiments with *rpoB* alleles were performed. It has been described that several mutations in the *rpoB* gene, coding for β subunit of the RNApol, that affect the sensibility of the RNApol to pause during transcription causing increase or reduction in the pausing rate (I. Artsimovitch and Landick, 2000; Trautinger *et al.*, 2005; Tehranchi *et al.*, 2010). The effect of two *rpoB* alleles that reduce transcriptional pauses on *fliC* expression was monitored. Both, the rpoB35 (*rpoB* H1244Q) and the rpoB111 (*rpoB* P564L) alleles decrease the rate of pausing during transcription elongation as described by Trautinger *et al.*, (2005) and Tehranchi *et al.*, (2010), respectively.

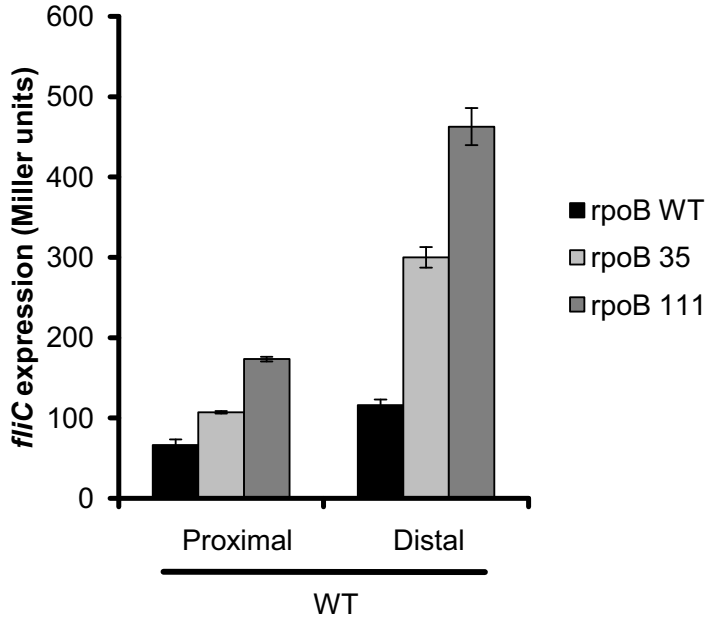

Figure 52: Effect of *rpoB* 35 and *rpoB* 111 alleles on *fliC* expression using the proximal (+70) and distal (+1210) *lacZ* fusion. The $rpoB^{WT}$ strains PRG13 and PRG16, proximal and distal fusion respectively, together with their derivative mutants *rpoB*35 (LFC41, LFC42, LFC43 and LFC44) and *rpoB*111 (LFC45, LFC46, LFC47 and LFC48) were grown in LB at 37ºC up to an OD_{600nm} of 1.5. Average and standard deviation of β-galactosidase activity determination from three independent cultures are shown.

The expression of *fliC,* using the proximal and distal *lacZ* fusion, in the rpoB35 and rpoB111 mutants, was determined (**fig. 52**).

Both alleles, rpoB35 and rpoB111, causes an increase in *fliC* expression (**fig. 52**), which is much more evident when using the distal *fliC* fusion, 2.5 and 4 fold respect $rpoB^{WT}$ respectively, as compared with the proximal fusion, 1.5 and 2.5 fold respect $rpoB^{WT}$ respectively. This results indicates that *fliC* expression is sensitive to the ratio of pausing.

We decided to determine how the *rpoB*35 allele affects the regulation of *fliC* by the different factors that bind to the secondary channel. The motility of strains containing either *rpoB* WT or *rpoB*35 alleles and their derivatives *greA*, *dksA* and *dksA greA* mutants was determined (**fig. 53**).

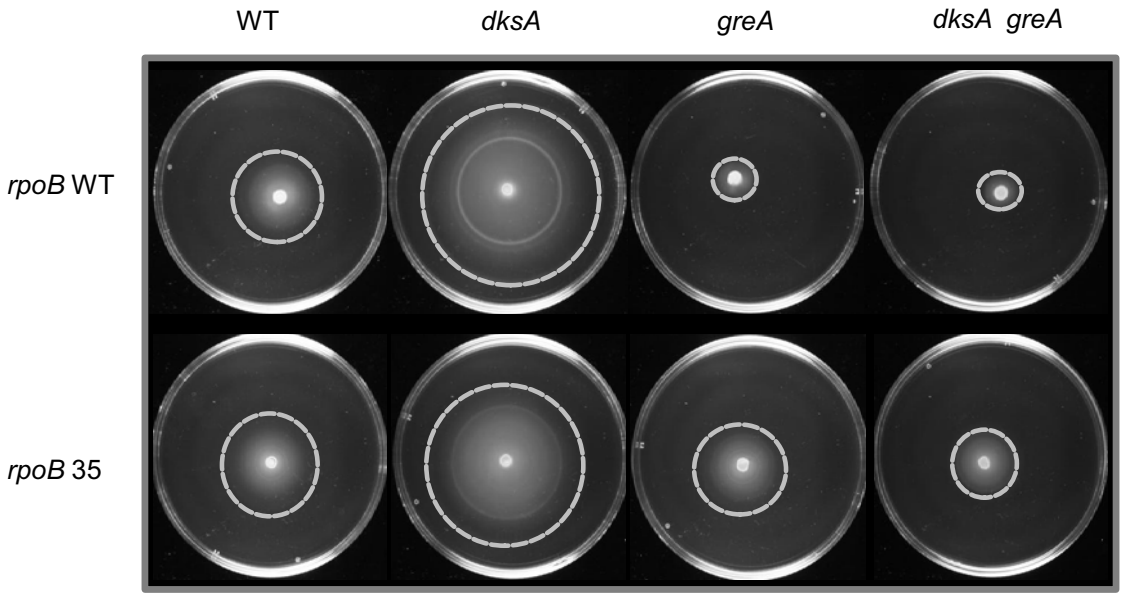

Figure 53: A) The strains MG1655 (WT), CF11657 (*greA*), TE8114 (dksA), AAG101 (*dksA greA*) and its derivative *rpoB*35 mutants (N4849 and LFC49, LFC50 and LFC51, respectively) were grown on motility agar plates supplemented with maltose 2 mM as chemo-attractant at 30ºC during 12 hours.

The *rpoB*35 had no effect in the motility of MG1655 or in the *dksA* mutant. However, in absence of GreA (in the *greA* and *dksA greA* strain), the motility in the rpoB35 was recovered to levels similar to WT. These data is consistent with the hypothesis that GreA is required for *fliC* expression, and consequently for motility, by promoting efficient transcription elongation of *fliC*. In absence of GreA, with the WT *rpoB* allele, the RNApol would not be able to pass through them, decreasing *fliC* expression (**fig. 46B**) and motility (**fig. 53**).

4.3.4. Effect of changes in environmental parameters in the expression of *fliC*

Cellular motility and chemotaxis may play an important role on survival of bacteria in the environment promoting movement towards favourable conditions or avoiding detrimental environments (Soutourina and Bertin, 2003). It has been described that flagella synthesis is inhibited by high temperature, osmolarity or extreme pH as well as by other environmental factors (Li *et al.*, 1993; Soutourina and Bertin, 2003). It has also been observed that flagella genes vary its expression through the growth phase, being inhibited at exponential phase, and reaching its maximum expression at early-stationary phase (Dudin *et al.*, 2014).

The effect of mutations in the factors that bind to the secondary channel of RNApol on motility through the growth curve or osmolarity variations has been studied.

4.3.4.1. Expression of *fliC* through the growth phase

To determine the effect of the factors that bind to the secondary channel on *fliC* expression at different points of the growth phase, *fliC* transcription was monitored at different time points of the growth phase: exponential phase (log), early-stationary phase (Early-Stat) and stationary phase (Stat). First, the expression of *fliC* was determined using the proximal (+70) and distal (+1210) *lacZ* fusions at the different time points in presence and absence of DksA in cultures grown in LB at 37ºC (**fig. 54A**).

The expression of *fliC* increases at stationary phase (**fig. 54A**). Interestingly the induction rate differs among the *lacZ* fusions used. With the proximal fusion, a 3.8-fold induction was detected, when comparing between log and stat cultures. However, this induction ratio for the distal fusion was 6-fold. These results suggest that *fliC* expression is stimulated at stat phase in a manner independent of transcription elongation (proximal fusion data) and also suggest that regulation at the level of transcription elongation might be involved in the growth phase regulation of flagella biosynthesis.

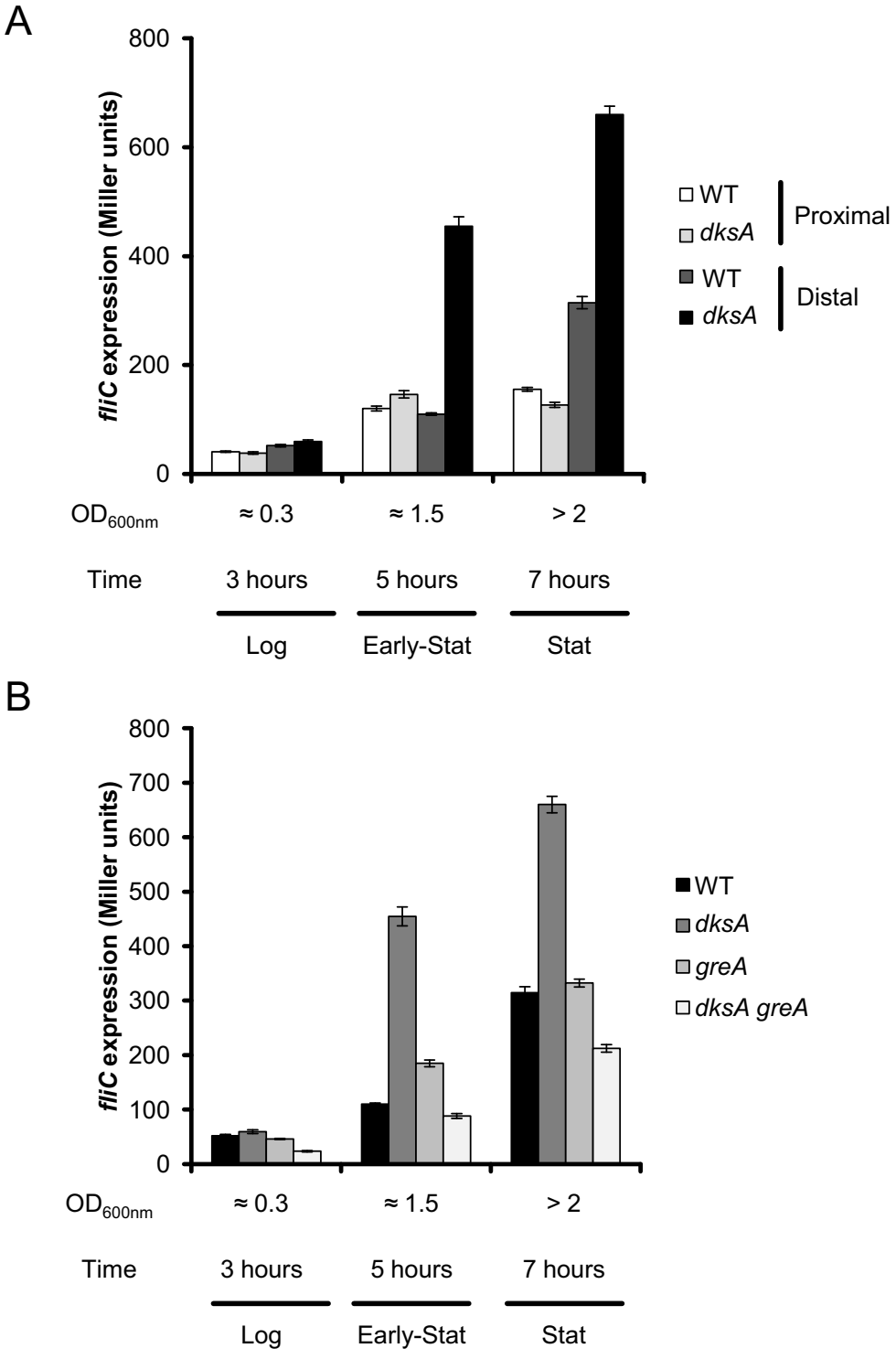

Figure 54: Expression of *fliC* at different points of the growth phase. A) Strains with either the proximal (+70) or the distal (+1210) fusion were grown in LB at 37ºC and samples were taken at different points of the growth curve (Log, Early-Stat, and Stat) to measure the β-galactosidase activity. The *dksA*$^{+}$ derivates (PRG13 and PRG16) and *dksA*$^{-}$ derivatives (PRG14 and PRG17) were used. B) The *fliC* expression using the distal fusion was monitored in strains PRG16 (WT), PRG17 (*dksA*), LFC62 (*greA*) and PRG18 (*dksA greA*) grown in LB at 37ºC and samples were taken at different points of the growth curve (Log, Early-Stat, and Stat) to measure the β-galactosidase activity. In both A and B, cultures were inoculated from plate an initial OD_{600nm} of

0.001. Average and standard deviation of β-galactosidase activity determination from three independent cultures are shown.

In the *dksA* mutant strain, no differences as compared to WT was observed with the proximal fusion. However, with the distal fusion the induction of *fliC* at stat phase is higher in the *dksA* strain (11-fold) as compared to WT (6-fold). In fact, it could be observed that in exponential phase, *dksA* mutation has nearly no effect on the expression of *fliC*, but on early stationary phase the expression of *fliC* in a *dksA* mutant increases dramatically. Our data shows that the expression of *fliC* increases on stationary phase, which is higher in a *dksA* mutant, and the induction more pronounced when the distal *lacZ* fusion was used, indicating that pausing might be involved in the fine-tuning of *fliC* expression.

The effect of *greA* and *dksA* mutations on *fliC* expression, using the distal fusion, through the growth curve was also determined. For this reason the strain PRG16 and its mutant derivatives *dksA, greA, and dksA greA* were grown in LB at 37ºC (**fig. 54B**). At early stationary phase, the expression of *fliC* increases dramatically in the *dksA* strain whereas such increase is not observed in the *dksA greA* strain. Interestingly, at late-stationary phase a significant induction of *fliC* expression was detected even in absence of GreA. Considering that the expression of *greA* decreases at stationary phase (as described in section 4.1.2), but the expression of *greB* increases (as described in section 4.2), someone could suggest that the increase of *fliC* observed with the distal fusion at stationary phase could be produced by interaction of GreB into the secondary channel of the RNApol instead of GreA, but, as shown in **figure 45**, GreB has no effect on bacterial motility in *E. coli*. These data might suggest that, even the amount of GreA is lower in exponential phase than in stationary phase, it would be enough to compete for the secondary channel of the RNApol on these conditions.

4.3.4.2. Effect of osmolarity on the expression of *fliC*

The effect of increasing concentrations of NaCl in the culture media on *fliC* expression was determined by using the strain PRG16 (distal fusion) and its derivative mutants *dksA* and *dksA greA* (**fig. 55A**).

It could be observed in **figure 55A** that the effect of *dksA* mutation over *fliC* expression is completely dependent on the osmolarity of the media. At 5 g/L NaCl the expression of *fliC* in absence of DksA is nearly 4-fold higher the expression of WT and at 0 g/L the expression of *fliC* in absence of DksA is even higher (nearly 6-fold respect WT). Surprisingly, at 10 g/L there is no effect of DksA on *fliC* expression. Moreover, in absence of both factors (DksA and GreA), the expression of *fliC* is restored to WT levels at the different osmolarities. Altogether, these results suggest that in absence of DksA, GreA bind to the RNApol, increasing the expression of *fliC* and this effect is dependent on osmolarity.

We also determined the effect of osmolarity over motility WT and DksA deficient strain (**fig. 55B**). At high osmolarity (10 and 25 g/L NaCl), there is a clear reduction in the motility of both strains (WT and *dksA*). Taking in account that GreA is essential for motility, even in presence of DksA (**fig. 46**), and that its activity could be dependent on osmolarity (**fig. 55A and C**), it is not surprising that osmolarity – via GreA – could affect motility, even in presence of DksA

Having in consideration our results, one could hypothesize that the effect of osmolarity on motility may be due changes on GreA amount at different osmolarities. The amount of GreA was determined by Western blot of the strain MG1655 and its derivative *dksA* mutant grown in LB with different concentrations of NaCl. The results indicate that the amount of GreA is constant at these conditions (**fig. 55B**). This fact make us hypothesize that it could be due changes on GreA activity.

The strain PRG18 (*dksA greA*) was transformed with plasmid pDNL278 (encodes *greA* under a P_{tac} promoter) and pTrc99a as a control, and the resulting strains were grown in LB with different NaCl concentrations (0, 5 and 10 g/L) at 37ºC up to an OD_{600nm} of 1.5 and samples for measuring β-galactosidase activity were taken (**fig. 55D**). The complementation *in trans* of the deficiency in GreA increases the expression of *fliC* at 0 and 5 g/L NaCl. However, at 10g/L we observe only a slightly increase on the expression of *fliC*. The amount of GreA produced was also determined by western blot (**fig. 55E**) at the same conditions tested.

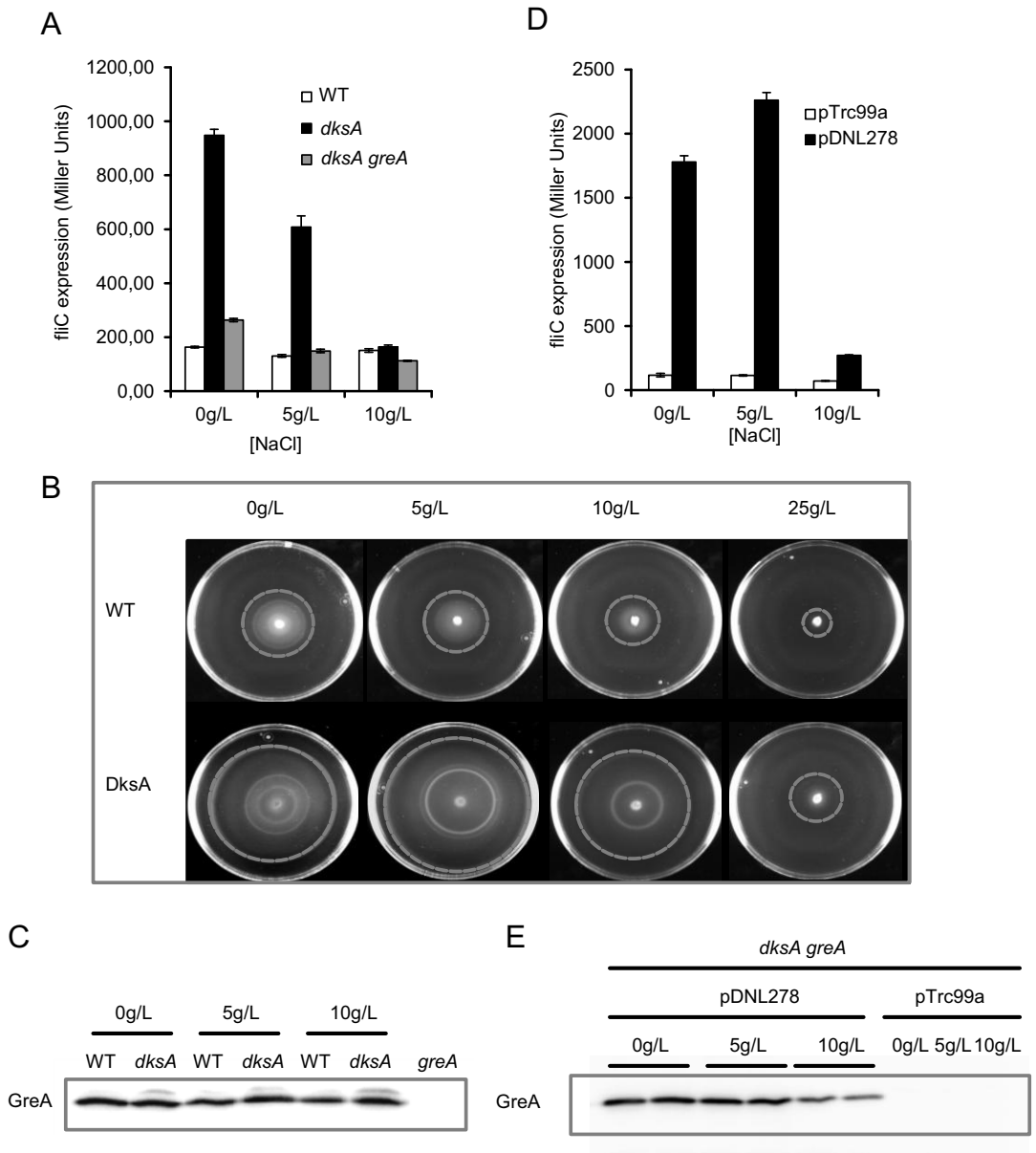

Figure 55: Effect of osmolarity over *fliC* expression and motility. A) The strain PRG16 (WT), PRG17 (*dksA*) and PRG18 (*dksA greA*) were grown in LB with different concentrations of NaCl (0, 5 and 10 g/L) at 37ºC up to an OD_{600nm} of 1.5, *fliC* expression was monitored by β-galactosidase activity determination. B) The strains MG1655 (WT), and TE8114 (*dksA*) were grown on motility agar plates with different concentrations of NaCl (0, 5, 10 and 25 g/L) supplemented with maltose 2 mM as chemo-attractant at 30ºC during 12 hours. C) Western blot using monoclonal antibodies against GreA. The strains MG1655 (WT), TE8114 (*dksA*) and CF11657 (*greA*) were grown in LB with different concentrations of NaCl (0, 5 and 10 g/L) at 37ºC up to an OD_{600nm} of 1.5. Whole cell extracts were analyzed in a 13.5% SDS-PAGE, transferred onto PVDF membrane and immunodetection performed as described (section 3.6.2). The chemiluminiscence signal was visualized using a Chemidoc XRS System from BioRad. D) PRG18 (*dksA greA*) carrying the plasmids pTrc99a (control) and pDNL278 (encodes *greA*) were grown in LB with different concentrations of NaCl (0, 5 and 10 g/L) at 37ºC up to an OD_{600nm} of 1.5. *fliC* expression was monitored by β-galactosidase activity determination. E) Western blot using monoclonal antibodies against GreA. The strain AAG101 (*dksA greA*) carrying the plasmid pDNL278 (encodes *greA*) and pTrc99a were grown in LB with different concentrations of NaCl (0, 5 and 10 g/L) at 37ºC up to an OD_{600nm} of 1.5 were analyzed as in C.

Average and standard deviation of β-galactosidase activity determination from three independent cultures are shown.

It was observed that at 10g/L there is a decrease on the basal expression of pDNL278, suggesting that Ptac promoter is dependent of media osmolarity, but this decrease does not seem to be the main responsible of the decrease of *fliC* expression since level are higher than in not overexpressing strain. We could propose that either the binding affinity of GreA to the secondary channel of the RNApol, the vacancy of the secondary channel of the RNApol in a *dksA* mutant or GreA activity, depends on the external osmolarity of the media It has been described that Gfh1 from *Thermus thermophilus* suffer conformational changes at different pH (Laptenko *et al.*, 2006). It is feasible that GreA could suffer also conformational changes at different osmolarities attending its ability to alter gene expression output.

Another possible explanation would be that at high osmolarity (10 g/L) there is some repressor of *fliC* expression that can abolish the superproduction caused by *dksA* mutation.

4.4. Effect of GreA overexpression on bacterial growth

It has been described (as previously discussed in section 1.2.5) that DksA is more abundant than GreA and GreB in *E. coli*. It has been estimated that DksA amount is up to 2 and 10 times higher than GreA and GreB, respectively. DksA and GreB have nearly the same affinity for the RNApol whereas GreA has lower affinity than the other factors (Rutherford *et al.*, 2007). Interestingly, as we have observed in section 4.1, *greA* expression could vary at different conditions such as during extracytoplasmic stress or stationary phase, suggesting that GreA levels variations could produce changes in the proteins that bind the secondary channel of the RNApol. Moreover, our results also suggest that external environmental parameters, such as the osmolarity, could alter the affinity of GreA for the RNApol. Finally, the autoregulation of *greA* and the crosstalk between DksA, GreB and GreA, highlights the possible competition between the different factors to bind the secondary channel of the RNApol.

In order to determine the hierarchy of the different factors that bind to the secondary channel of the RNApol and to observe the displacement of one factor by another, we decided to overexpress GreA and GreB on different genetic backgrounds, and observe its effect on the cell physiology. It has been described that overexpressing GreA causes a deleterious effect in the growth of *E. coli* in LB (Potrykus *et al.*, 2006). Therefore, we would like to determine the effect of overexpressing of GreA and GreB in presence or absence of DksA and ppGpp.

To overexpress GreA and GreB, we used plasmids derivates of pTrc99a, where the *greA* and *greB* genes were cloned under the IPTG inducible promoter Ptac resulting pDNL278 (GreA) and pGF296 (GreB) (Fengs *et al.*, 1994).

First, the plasmid pDNL278 and pTrc99a were transformed to MG1655 (WT), AAG93 ($ppGpp^0$), TE8114 (dksA) and JFV14 ($ppGpp^0$ dksA) strain and the resultant strains were grown in LB at 30ºC for 12 (**fig. 56A**) and 24 (**fig. 56B**) hours with increasing concentrations of IPTG, from 0 to 0.4 mM. The OD_{600nm} of the cultures after incubation was measured.

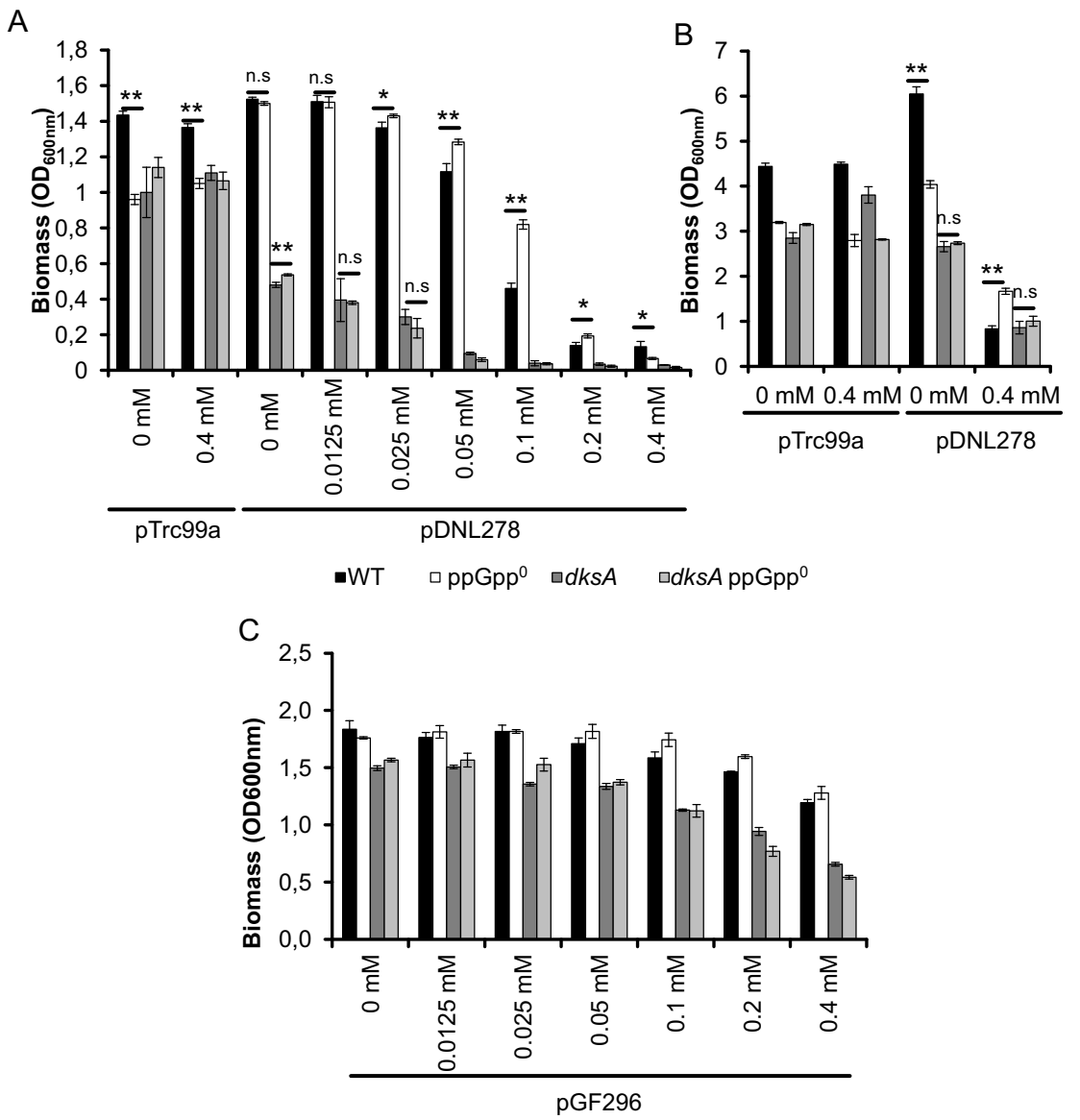

Figure 56: Effect of overexpression of the Gre factors using increasing concentrations of IPTG in different bacterial backgrounds. A and B) The strains MG1655 (WT), AAG93 (ppGpp^0), TE8114 (*dksA*) and JFV14 (ppGpp^0 *dksA*) transformed with pTrc99A (control) and pDNL278 (*greA*) were grown in LB at 30ºC and the OD_{600nm} was measured after 12 (A) and 24 (B) hours of growing, respectively. Cultures were inoculated from plate to an initial OD_{600nm} of 0.001. Significant changes had been shown (**n.s.**: no significant, *: pValue < 0.05, **: pValue < 0.01). C) The strains MG1655 (WT), AAG93 (ppGpp^0), TE8114 (*dksA*) and JFV14 (ppGpp^0 *dksA*) transformed with pGF296 (contains *greB*) were grown in LB at 30ºC and the OD_{600nm} was measured after 12 hours. Cultures were inoculated from plate with to an initial OD_{600nm} of 0.001.

The overexpression of GreA causes a negative effect on growth in *E. coli* as shown by the decrease when increasing the amount of IPTG in the OD_{600nm} after 12 (**fig. 56A**) and 24 (**fig. 56B**) hours. After 12 hours of growth (**fig. 56A**) the WT strain with pDNL278 strain suffers a reduction in the final OD_{600nm} at 0.05 mM of IPTG and higher concentrations. An 11-fold reduction in the final

OD_{600nm} was observed between cultures with 0 mM and 0.4 mM of IPTG in WT strain with pDNL278, while no effect was observed in cultures of WT strain carrying the control vector pTrc99a (**fig. 56A**). Considering that the WT strain is proficient in the expression of DksA, these results suggest that GreA when overexpresses might be able to move DksA from the secondary channel of the RNApol, forcing to increase the concentration of the complex RNApol-GreA up to levels that cause a deleterious effect to the cell physiology. Interestingly, the effect of the presence of pDNL278 is much more drastic when the cell is deficient in DksA (*dksA* mutant strain). The negative effect of overexpressing GreA is observed at a concentration of 0.025 mM of IPTG in the *dksA* strain with pDNL278, with a 17-fold decrease of its growth comparing the OD_{600nm} between 0 mM and 0.4 mM. Moreover, the highest OD_{600nm} reached by *dksA* strain with pDNL278 in absence of IPTG is significantly lower than the same strain with pTrc99a (2 fold), indicating that the basal expression of *greA* from the multicopy plasmid pDNL278 has a negative effect on growth when the bacteria lack DksA. Comparing the maximum OD_{600nm} that reach the *dksA* strain with pTrc99a and pDNL278 at 0.4 mM of IPTG (**fig. 56A**) a 37-fold decrease of bacterial growth was observed (compared to the 11-fold decrease of WT strain). These results may indicate that in absence of DksA the interaction between RNApol and GreA is promoted and consequently the deleterious effect due to GreA overexpression is enhanced.

It is remarkable that when growth was monitored in a ppGpp deficient strain, the effect observed is lighter than for WT strain. At 0.1 mM, for example, bacterial growth of the $ppGpp^0$ strain is nearly 2-fold higher than in a WT strain (**fig. 56A**). This effect could be also observed after 24 hours of growth (**fig. 56B**) where the WT strain suffers a 7-fold decrease comparing 0 and 0.4 mM of IPTG, while $ppGpp^0$ suffers only a 2.5-fold decrease. The lack of DksA seems to be epistatic over ppGpp (Brown *et al.*, 2002). These results suggest that ppGpp may be required for efficient interaction of GreA with the secondary channel of the RNApol, and that the presence of the modified nucleotide might interfere in the proposed competence between the Gre factors and DksA.

The OD_{600nm} of the WT strain compared with the $ppGpp^0$ strain carrying the control plasmid is higher (**fig. 56A**). Surprisingly, the same strains carrying

pDNL278, in absence of IPTG, reach the same OD_{600nm} after 12 hours of growth (**fig. 56A**). After 24 hours (**fig. 56B**) we observe that $ppGpp^0$ strain had lower OD_{600nm} than WT with pTrc99a and pDNL278 at 0 mM of IPTG, but had higher OD_{600nm} than WT at 0.4 mM of IPTG the $ppGpp^0$. These data might suggest that the absence of ppGpp is a disadvantage for the cell. However, tolerable extra copies of *greA*, basal expression of pDNL278, would recover, somehow, the ability to grow to WT ratios.

The effect of overexpression of GreB was determined using pGF296 (*greB* cloned under the IPTG inducible promoter Ptac) in WT, $ppGpp^0$, *dksA* and $ppGpp^0$ *dksA* strain, similarly as described for GreA overexpressing assay (**fig. 56C**). When overexpressing GreB, a similar behaviour was observed as when overexpressing GreA. However, the deleterious effect in growth is weaker than for GreA. The overexpression of GreB is less toxic than the overexpression of GreA. At the highest concentration of IPTG, the WT strain, carrying pGF296, suffers a 1.5-fold reduction of final OD_{600nm} compared with the cultures without IPTG. In absence of DksA, the effect of the overexpression of GreB is higher, a 2.3-fold decrease in the final OD_{600nm} was observed, suggesting that GreB had to compete for binding to the secondary channel with DksA as well as with GreA. No significant effect by ppGpp deficiency was observed either in $dksA^+$ or $dksA^-$ strains.

To study more in detail the competence between GreA and DksA, and its effect on bacterial growth, it has been determined the effect of overexpression of GreA on the growth curve using the WT and *dksA* strains. For this purpose, the MG1655 (WT) and TE8114 (*dksA*) strains carrying the plasmid pDNL278 (overexpression of GreA) were grown in LB in the absence or presence of IPTG (0.2 mM) at 37ºC and the OD_{600nm} of the cultures was measured every 45 minutes. The cultures were inoculated from plate to an initial OD_{600nm} of 0.001.

Both strains, WT and *dksA*, suffers a negative effect when overexpressing GreA (**fig. 57A**), and this effect was higher in a *dksA* strain that in WT, as has been previously shown (**fig. 56A**). Bacterial growth is reduced in WT strain, when IPTG was added, growing slower than without IPTG. This effect is also

observed in a *dksA* strain, but much more dramatic. In fact, the *dksA* strain showed very slow growth during the first 6-10 hours.

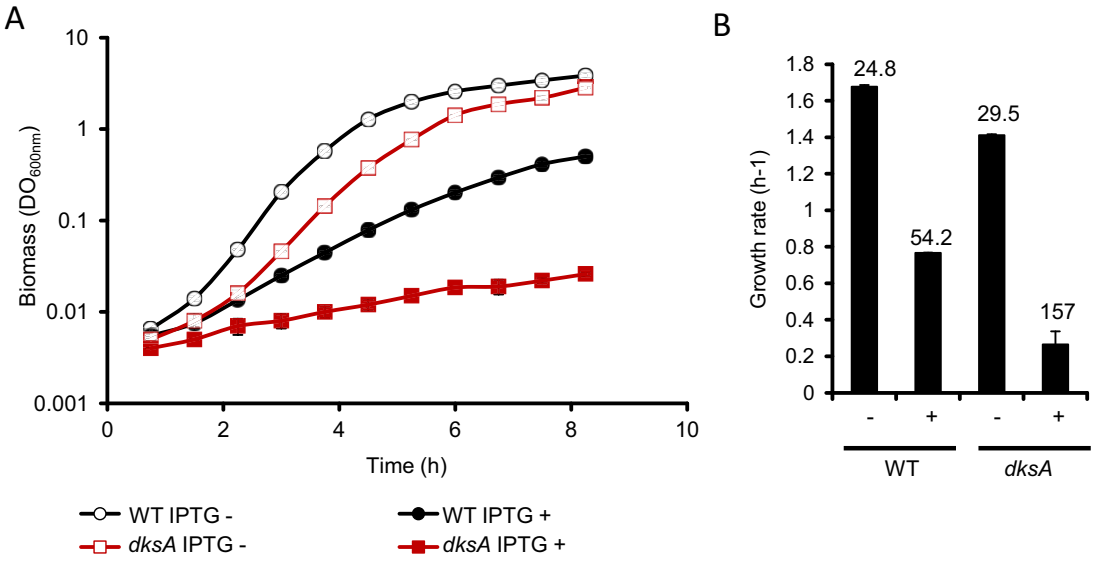

Figure 57: Effect of overexpressing GreA in bacterial growth. A) The strains MG1655 (WT) and TE8114 (*dksA*) transformed with pDNL278 were grown in LB with either 0.2 mM of IPTG (referred as +) or without IPTG (referred as -) at 37ºC. The OD_{600nm} was measured every 45 minutes. Cultures were inoculated from plate to an initial OD_{600nm} of 0.001. The growth rate and generation time of the different strains were calculated (B). The generation time is indicated in minutes over the bars.

The overexpression of GreA (**fig. 57 B**) produces a decrease in the growth rate of 2- and 7-fold in WT and *dksA* strain, respectively. As a consequence, the generation time of the *dksA* mutant was 157 minutes (2.6 hours) with IPTG, while in absence of IPTG was 29.5 minutes.

The negative effect of the overexpression of *greA* is not only observed in liquid media, it also could be observed on LB plates. There is an evident inhibitory effect on colonies formation during overexpression conditions (**fig. 58A**). The addition of IPTG (0.2 mM) in LB plates inhibits the formation of colonies in WT and *dksA* strain. The inhibitory effect was determined more in detail with LB cultures of the strain TE8114 (*dksA*) and JFV14 ($ppGpp^0$ *dksA*) which were serially diluted (1/10 dilutions) and dropped (2 µl of each dilution) on LB agar plates with IPTG 0.2 mM and without (**fig. 58B**). Plates were incubated for 12 hours at 37ºC. No differences were observed in absence of IPTG, since all the cultures had similar amount of bacteria. However, in presence of IPTG the survival of *dksA* and $ppGpp^0$ *dksA* deficient strain carrying pDNL278 decreases

drastically. Tiny translucent heterogeneous colonies were observed in the highest concentration (d) in the *dksA* pDNL278 strain with IPTG. The presence of heterogeneous colonies, translucent small and pale big colonies, suggests the apparition of suppressor mutations tha counteract the negative effect of overexpressing *greA*.

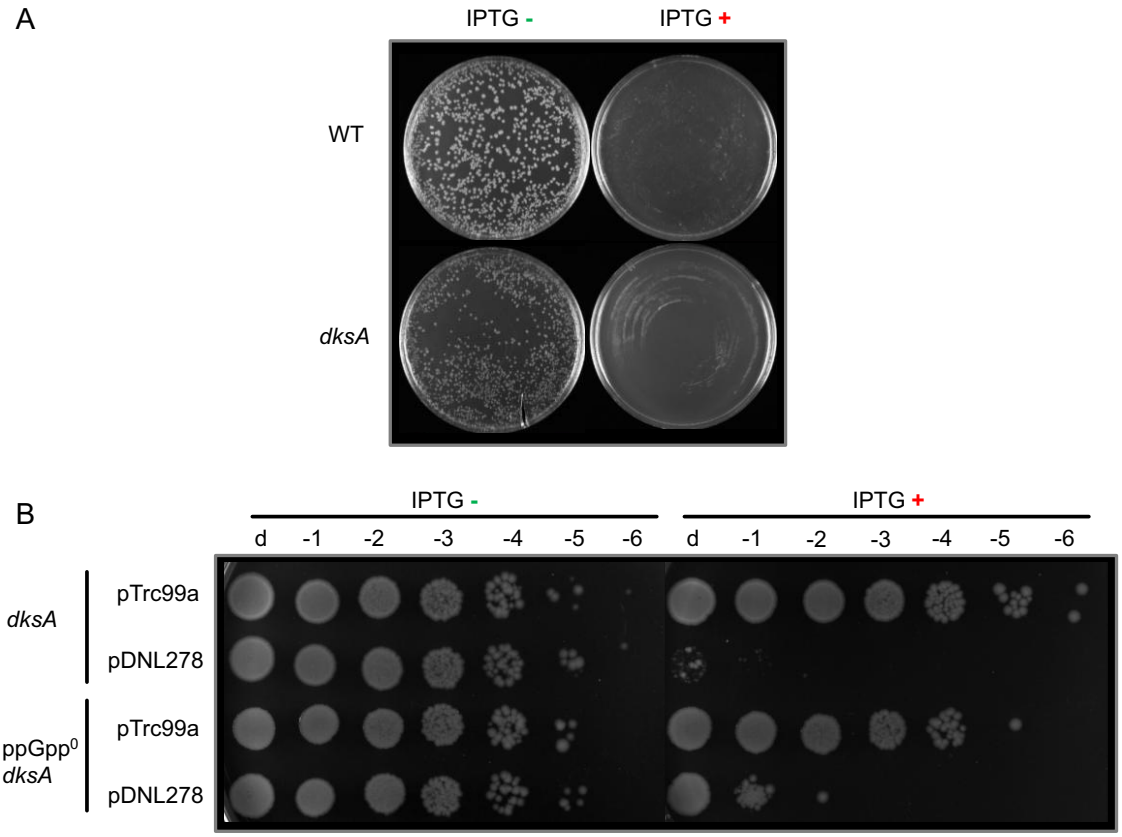

Figure 58: Effect of overexpressing GreA over colonies formation. A) The strain MG1655 (WT) and TE8114 (*dksA*) carrying either pTrc99a or pDNL278 plasmid on LB agar plates with IPTG 0.2 mM and without. B) The strain TE8114 (*dksA*) and JFV14 (ppGpp^0 *dksA*), were grown in LB several hours, serially diluted (1/10 dilutions) and dropped (2 µl of each dilution) on LB agar plates with IPTG 0.2 mM and without IPTG. The following dilutions were dropped: direct (d) and serial dilutions 1/10 from the culture up to a dilution 1/10^6 (from -1 to -6).

In the strain ppGpp^0 *dksA* (**fig. 58B**), colonies were observed in dilution -1 (1 colony in -2), suggesting that the absence of ppGpp makes bacteria less sensitive to overexpression of *greA*, as previously suggested. Moreover, colony heterogeneity was not observed, suggesting that in those conditions is more difficult to produce suppressor mutations.

We observed a negative effect of overexpressing GreA on bacterial growth in liquid as well as on solid media, for this reason we decided to observe the effect

of overexpression of GreA at the cellular level (**fig. 59**). WT and *dksA* strain with the pTrc99a and pDNL278 were grown on LB plates at 37ºC with different concentrations of IPTG (0, 0.05 and 0.1 mM), stained with crystal violet and observed by optical microscopy.

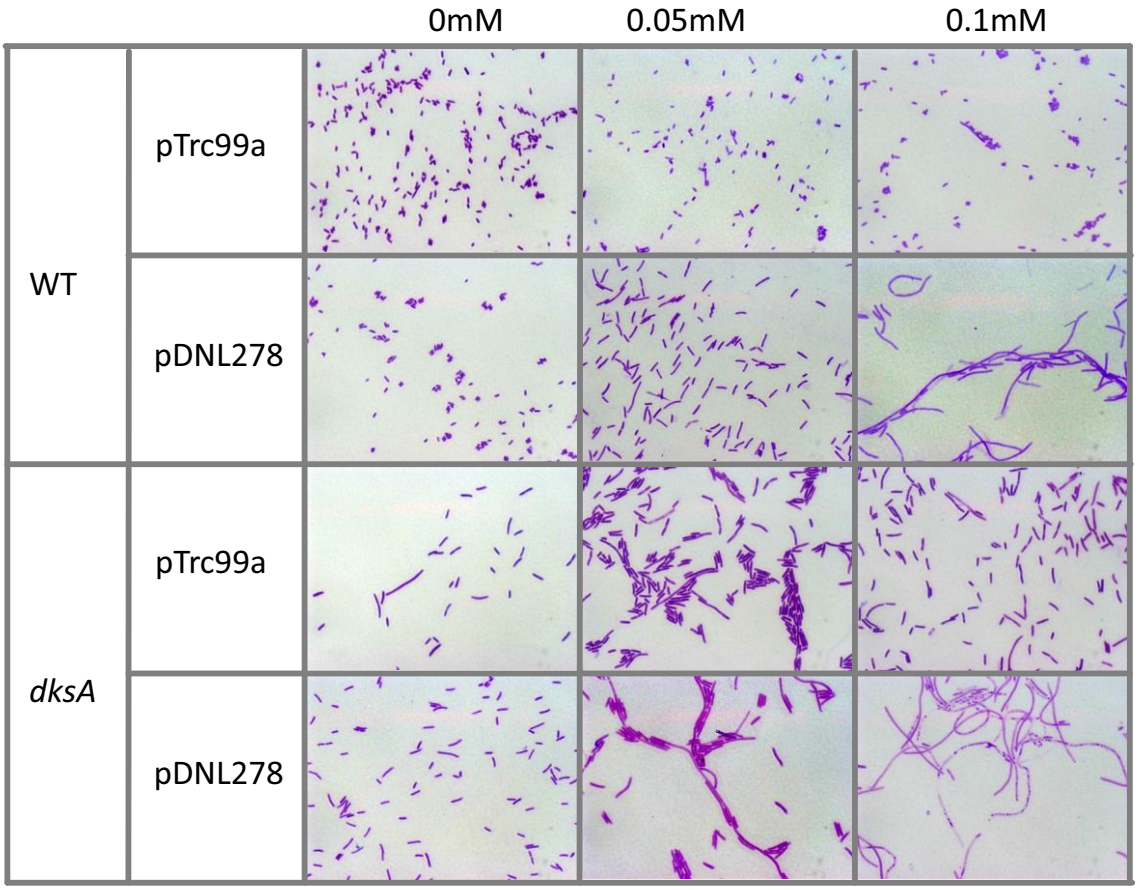

Figure 59: Effect of GreA overexpression over cell shape. The strain MG1655 (WT) and TE8114 (*dksA*) carrying either pTrc99a (control plasmid) or pDNL278 (contains *greA*) were grown on LB plates with 0, 0.05 and 0.1 mM of IPTG at 37ºC during 16-18 hours. Several colonies were resuspended in water, fixed on a microscope slide and stained with crystal violet. The samples were observed with 100x objective.

The overexpression of GreA in a WT strain produces an enlargement of the cell producing cellular filaments which is clearly detected at 0.1 mM. The absence of DksA (at 0 mM of IPTG) produces an enlargement of cells as compared to WT similar to the observed by $ppGpp^0$ (Magnusson *et al.*, 2005; Aberg *et al.*, 2009). This filamentation induced by *dksA* mutation has been previously described by Magnusson *et al.*, (2007). During overexpression conditions in the *dksA* strain, an important enlargement of the cells was observed at lower concentrations of inductor than in the WT strain. This enlargement could be produced by a deficit

on cellular division. Interestingly, transcriptomic studies (Stepanova *et al.*, 2007) indicate that overexpressing *greA* causes repression on *ftsN* expression. FtsN is a crucial factor during cellular division. The depletion of *ftsN* produces cell filamentation and eventual death, but the lack of FtsN did not affect DNA synthesis and nucleoid segregation (Dai *et al.*, 1993).

Overexpression of GreA may cause an increase on the amount of RNApol-GreA complex in the cell, causing an enlargement of the cell, perhaps by a decrease of FtsN – protein essential for the localization of the Z-ring during cellular division process (Busiek and Margolin, 2014). As mentioned above, the lack of *ftsN* produces cell filamentation and eventual death (Dai *et al.*, 1993), that is a similar effect that we observe under GreA overexpression conditions. This cellular effect produces a negative effect on the bacterial growth on liquid media and an effect on colonial size on plate. Moreover, this effect is higher in absence of DksA – or appears earlier – suggesting that GreA is able to compete directly with DksA for the secondary channel. In absence of DksA, GreA is able to interact more easily with the secondary channel and produces cell filamentation that could be observed by optical microscopy.

4.5. Structural study of the protein GreA

The protein Gfh1, as mentioned in section 1.2.4, is a protein from *Thermus aquaticus* that has a highly structural homology to GreA. It has been described that it is susceptible to suffers conformational changes which are pH-induced that modify its affinity for the secondary channel of the RNApol (Lamour *et al.*, 2006; Laptenko *et al.*, 2006). Studies performed with the crystallized complex RNApol-Gfh1 from *Thermus thermophilus* showed that the coiled-coil domain enters inside the secondary channel of the RNApol, while hydrophobic residues of the globular domain interact with the external edge of the secondary channel, binding to the surface of the RNApol. Moreover it is shown that the entrance of the secondary channel is expanded by the binding of Gfh1, due to conformational changes in the RNApol, suggesting that this expansion of the secondary channel is required to allow the entrance of Gfh1 (Tagami *et al.*, 2010). GreB contains hydrophobic residues in an equivalent position than Gfh1, but GreA no. Although, it is suggested that those amino acids could be involved in the binding of GreA to the RNApol, there is no clear knowledge on the residues involved in the functional interaction of GreA with the RNApol. In order to determine structural aspects that may be relevant for the interaction of GreA with the secondary channel of the RNApol, we decided to perform a random mutagenesis to select mutants that had lost the functionality of GreA or its ability to bind the secondary channel of the RNApol.

Considering that *greA* overexpression produces a negative effect on bacterial growth, as indicated by a significant reduction of the colonies size, we decided to use this phenotype to isolate GreA mutants with altered functionality or affinity to the RNApol. We rationalize that if overexpressing $GreA^{WT}$ causes a negative effect on bacterial growth in a dose dependent manner and no colonies would form under high concentrations of the inductor (IPTG), when overexpressing no-functional GreA alleles or with a reduced affinity to the RNApol, those clones would have mild effects on cell physiology and colonies will be formed.

The experimental strategy used is depicted in **figure 60**. First, a library of mutants in *greA* by Error-prone PCR was obtained. As described in section

3.4.3, this method is based in using PCR amplification conditions that promote nucleotide misincorporations, leading to protein changes, by the Taq polymerase that lack proof-reading activity. The gene *greA* was amplified by Error-Prone PCR using different temperatures of annealing in order to ensure missense mutations (64ºC and 58ºC) with primers G6 and G11 (**fig.25**, section 4.1). As a control, *greA* was amplified with a normal PCR protocol. Then, the library of random mutants was cloned into pTrc99a, under an IPTG-inducible promoter, and transformed into MG1655 and TE8114 (*dksA*) in absence of IPTG. In order to select those mutants that were able to grow under *greA* overexpressing conditions, the resulting clones were striked on LB plates with either IPTG 0.2mM or without IPTG. Finally, the mutants (growth^{+}) were genotyped by PCR and sequenced.

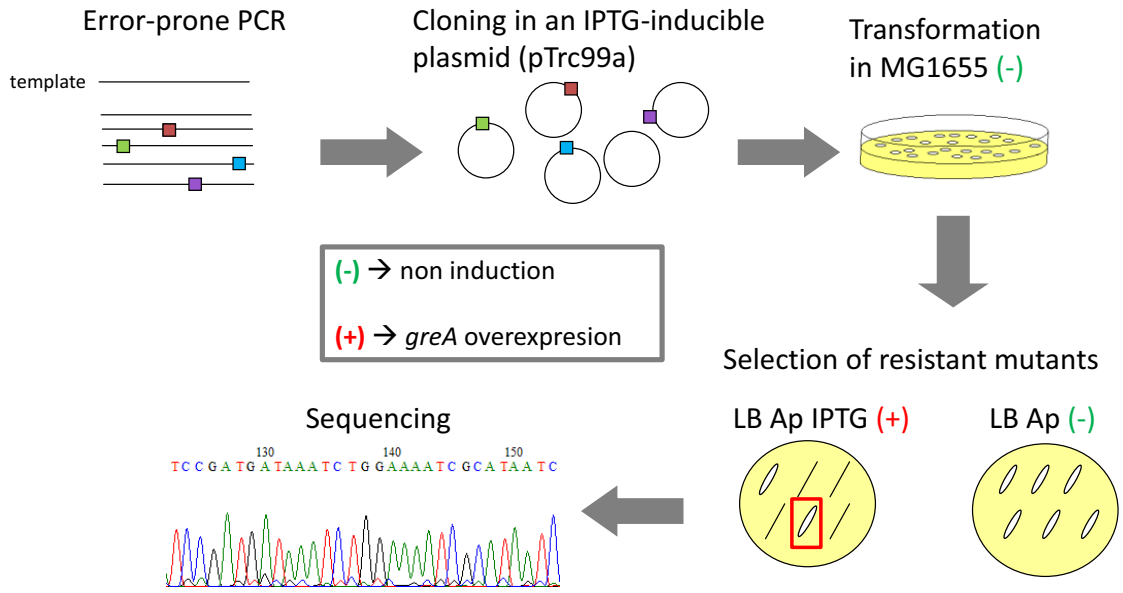

Figure 60: Scheme of the random mutagenesis experiment by error-prone PCR. The coloured squares represent nucleotide mutations. It is indicated the conditions of no-induction **(-)** and induction of *greA* overexpression **(+)** conditions.

The PCR genotyping of the mutants let us to distinguish between mutations deletions, insertion and missense mutations by using the primers greApl1 and greApl2, located flanking the MCS of the plasmid pTrc99a. The MCS of the plasmids of the growth^{+} mutants, as well as from pDNL278 (positive control, C+) and pTrc99a (negative control, C-), was PCR-amplified and visualized in a 2% agarose gel as indicated in section 3.4.5. The plasmid pDNL278 (GreA^{WT}) produces a band of 760 bp, while the plasmid pTrc99a produces a band of 350

bp. Significant insertions or deletions would be detected by changes in the size of the electrophoresis band. In the **figure 61**, it is shown an example of the genotyping of some of the selected mutants. Those mutants that present important deletions are labelled with a #.

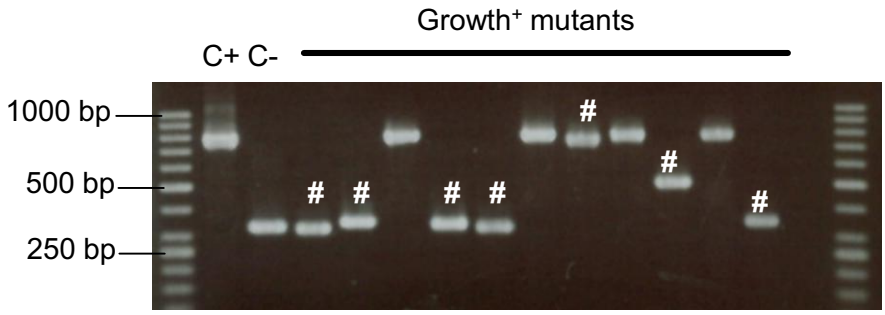

Figure 61: Genotyping of some selected mutants. The MCS was amplified by PCR using the primers greApl1 and greApl2, and the fragments were analyzed in a 2% agarose gel. Fragments labelled of # contain deletions.

Up to 484 clones obtained after transformation of pTrc99a-*greA* library. From those two kinds of growth^{+} mutants were selected: resistant and intermediate-resistant mutants. From the 484 clones obtained, 84 were resistant mutants (17% of the clones) and 15 intermediate-resistant mutants (3% of the clones). All the mutants were characterized and classified according to the type of mutation (**table 6**).

		WT			***dksA***		
		Normal	58ºC	64ºC	58ºC	64ºC	
Resistants	Deletions	8	24	21	4	2	84
	Insertion	4	3	1	0	0	
	Missense	0	10	6	1	0	
Intermediate	Deletions	0	1	0	0	0	15
	Insertion	0	1	0	0	0	
	Missense	2	6	2	0	0	
	No changes	0	1	1	0	0	
	Promoter	0	0	1	0	0	
	% of missense mutants						**27.5%**

Table 6: Numbers of resistant and intermediate mutants are distributed by the characteristics of its mutations. It is indicated the number of mutants that carries deletions, insertions, missense mutations, mutations in the promoter or that not contains any mutation either in the *greA* coding sequence or in its promoter (No changes). The 58ºC and 64ºC are the annealing temperature used. Normal refers that it has been used a normal PCR protocol.

We have selected resistant mutants in both WT and *dksA* strains but the selection of missense mutations was more efficient in presence of DksA than in its absence. Perhaps when looking at WT (with *dksA*) mutations that affect affinity to interact with the RNApol, will easily be selected, since the presence of DksA with a $GreA^{Mut}$ with low affinity will provide $growth^{+}$ mutants.

From the 99 resistant and intermediate-resistant clones, 27 contain missense mutations that produce changes in the amino acidic sequence, changing 20 different amino acids of the protein GreA (a 12.6% of its sequence). From the 27 clones, 7 carry repeated mutations and were not considered for the forthcoming study.

It is important to highlight that the mutants that contain deletions and insertions were not produced by the Error prone PCR experiment; they must be produced during natural selection of mutants due a strong selective pressure produced by the overexpression of GreA. This outcome of this selective pressure was also observed by the appearance of resistant mutants using plasmids carrying fragments obtained by normal PCR (referred as Normal in **table 6**).

None of the resistant mutants obtained in the normal PCR, contains missense mutations (except 2 intermediate-resistant mutants), instead they contain deletions and insertions. We also obtained some mutations that affected the IPTG inducible promoter, while others did not present mutations either in the *greA* gene or in its promoter (referred as no changes). While no changes are observed in *greA*, these clones would have chromosomal mutations conferring ability to survive *greA* overexpression. Those mutants are of great interest since may provide interesting information regarding how *greA* overexpression causes a deleterious effect in bacterial growth. Further studies will be required.

Before further characterization of the 20 selected mutants, it was corroborated that overproduction of the mutant protein take place (**fig. 62**). Cultures carrying the plasmid pTrc99a (control plasmid), pDNL278 ($GreA^{WT}$) and the pTrc-$greA^{Mut}$ plasmids were induced, or not, with IPTG, in order to determine that the mutations produced did not affect the production of GreA (**fig. 62**). None of the mutations produce important effects in the amount of GreA produced,

suggesting that the mutations alter its functionality or affinity for the RNApol, but not its production.

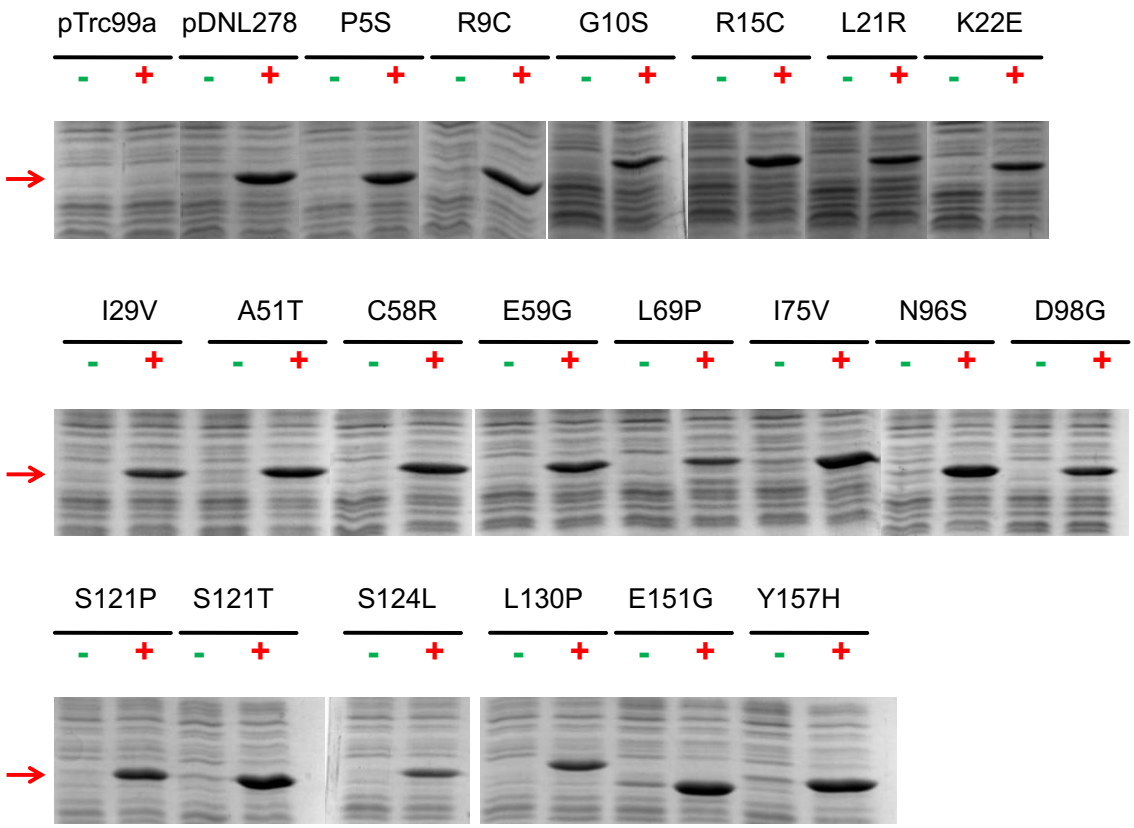

Figure 62: GreA production of the plasmids pTrc-greA^{mut}. The strain MG1655 carrying the plasmids pTrc99a (control), pDNL278 (GreA^{WT}) and the different pTrc-greA^{mut} were grown in LB at 37ºC up to an OD_{600nm} of 0.1 and the production of GreA was induced with 0.2mM of IPTG (+) or not induced (-) during 3 hours. Whole cell extracts were analyzed in a 12.5% SDS-PAGE stained with coomassie brilliant blue. Red arrow indicates the position of GreA.

The different mutants obtained were localized in both domains (**fig. 63**), the coiled-coil domain that would enter inside the secondary channel of the RNApol, and also in the globular domain, that would remain outside. It is also interesting to highlight that none of the mutants obtained are located in the described catalytic centre of GreA (D41 and E44). Somehow it seems that these two amino acids maybe are not responsible of the negative effect on the bacterial growth produced by overexpressing *greA.* Moreover, the fact that several mutations were localized in the globular domain, might suggest that it would be more important than previous thought for the functionality of GreA or it affinity for the RNApol.

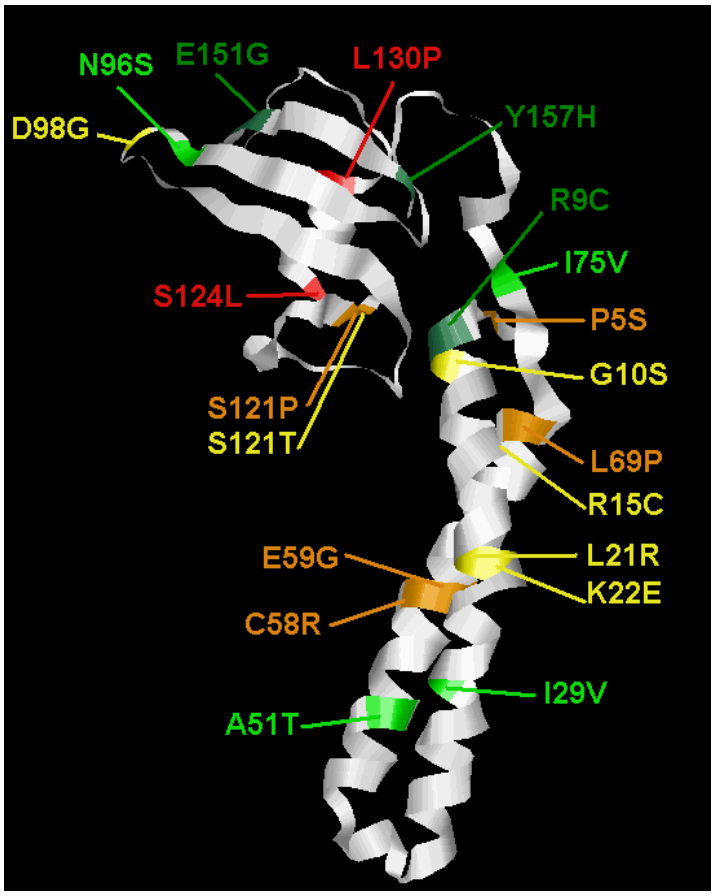

Figure 63: Distribution of the different mutations in GreA 3D structure.

To determine the effect of the different mutation in the function of *greA* the software (SIFT), a program that predicts whether amino acid substitutions affect the protein function, was used (Ng and Henikoff, 2003). As it is shown on the **table 7,** nearly all the mutations are predicted to be non-acceptable (NO), except for 3 mutations that are predicted as tolerable (AC).

		pTrc99a	pDNL278	Nonsense	P5S	R9C	G10S	R15C	L21R	K22E	I29V	A51T	C58R	E59G	L69P	I75V	N96S	D98G	S121P	S121T	S124L	L130P	E151G	Y157H
	SIFT				NO	NO	NO	NO	AC	NO	AC	NO	NO	NO	NO	NO	NO	NO	NO	NO	NO	NO	NO	NO	AC
growth	**WT**	+	-	+	+ / -	+ / -	+	+ / -	+ / -	+	+	+ / -	+	+ / -	+	+	+	+	+	+	+	+	+	+ / -	+ / -
	dksA	+	-	+	+ / -	-	+	-	-	-	+ / -	-	+ / -	+ / -	+	+ / -	-	+ / -	+	-	+	+	-	-

Table 7: Prediction of the tolerance of the different mutations by SIFT software and the effect of overexpression of the different *greA* alleles on MG1655 (WT) and TE8114 (*dksA*) strains on LB plates supplemented with 0.2 mM IPTG (described in the text).

We hypothesize that these mutants are able to growth under overexpressing conditions because the mutations have effect on:

- The functionality of the GreA protein
- The ability to bind to the secondary channel of RNApol, either because affect:
    - Affinity to the secondary channel.
    - Ability to compete with other proteins that bind to the secondary channel of the RNApol.

In order to know if the ability of these mutants to compete with DksA for the secondary channel is affected, the different plasmids pTrc-greA^{mut} were transformed into MG1655 (WT) and TE8114 *dksA* (*dksA*) and plated on LB and LB IPTG 0.2 mM. The results shown in **table 7**, indicate the ability to grow, scored as follows:

- Positive (**+**), when in presence of IPTG there are colonies and its size was similar than in absence of IPTG.
- Negative (**-**), when in presence of IPTG no colonies were detected.
- Intermediate (+ / -), when in presence of IPTG there were colonies but its growth was affected, producing smaller colonies than without IPTG.

Those mutants that are positive in presence and absence of DksA, such as G10S, L69P, S121P, S124L and L130P, are mutants that either GreA is not active or it does not bind to the RNApol. By contra, those mutants that produce a negative effect on bacterial growth in absence of DksA but not to the same extent in the WT strain, such as R9C, R15C, L21R, K22E, A51T, N96S, S121T, E151G and Y157H would have a lower affinity to the RNApol or lower ability to compete with DksA.

To further elucidate the effect of the different mutations, two phenotypes associated to GreA were monitored: i) Antipause effect on *fliC* transcriptional expression and ii) Prototrophy recovery in *dksA* / ppGpp^0 strains.

These phenotypes would help us to predict the effect of the different mutations in the GreA protein and perhaps to identify relevant amino acids for the functionality and affinity of GreA.

4.5.1. Antipause effect on *fliC*

As previously described in section 4.3.1, GreA stimulates the expression of *fliC* during transcription elongation and its effect is higher in absence of DksA. To evaluate the effect of the different mutation on the functionality of GreA and its antipause activity we decided to use this phenotype.

In absence of DksA the expression of *fliC* increases (4-fold) compared with the WT strain, but in a *dksA greA* deficient strain the expression of *fliC* decreases, to the WT expression levels (Aberg *et al.*, 2009). To determine the activity of the different mutants, the strain deficient in *dksA* and *greA* with the *fliC* distal fusion (PRG18) was transformed with pTrc99a (Control), pDNL278 ($GreA^{WT}$) and the 20 missense mutants (pTrc-$GreA^{Mut}$). Moreover, the nonsense mutant was used as a control. The resulting strains were grown in LB at 37ºC up to an OD_{600nm} of 1.5 and the β-galactosidase activity was measured (**fig. 64A**). It was observed that GreA overexpression was not required to induce *fliC* expression. Therefore, the effect on *fliC* of the basal expression from these plasmids was tested in cultures not induced.

In absence of both factors (DksA and GreA) with the pTrc99a plasmid *fliC* expression is low (as previously shown in section 4.3). When GreA was introduced *in trans* (pDNL278) *fliC* expression increases (15-fold) compared with pTrc99a (**fig. 64A**). The effect of the different mutants was also determined.

The $GreA^{Mut}$ produce different effects on *fliC* expression levels indicating variations in their activity. If $GreA^{Mut}$ has similar antipause activity than $GreA^{WT}$, we would expect high expression levels of *fliC*, but if the $GreA^{Mut}$ had lost the antipause activity we would expect low levels of *fliC* (as with pTrc99a). The nonsense mutant had the same activity than the strain with pTrc99a, suggesting that the presence of not functional proteins (or truncated in this case) would not affect the expression of *fliC*, validating our experimental model. The antipause activity could be expressed as a percentage, considering the *fliC* expression detected for the strain carrying the pDNL278 ($GreA^{WT}$) as 100% antipause activity and calculating the corresponding percentage shown by the strains carrying the different $GreA^{Mut}$.

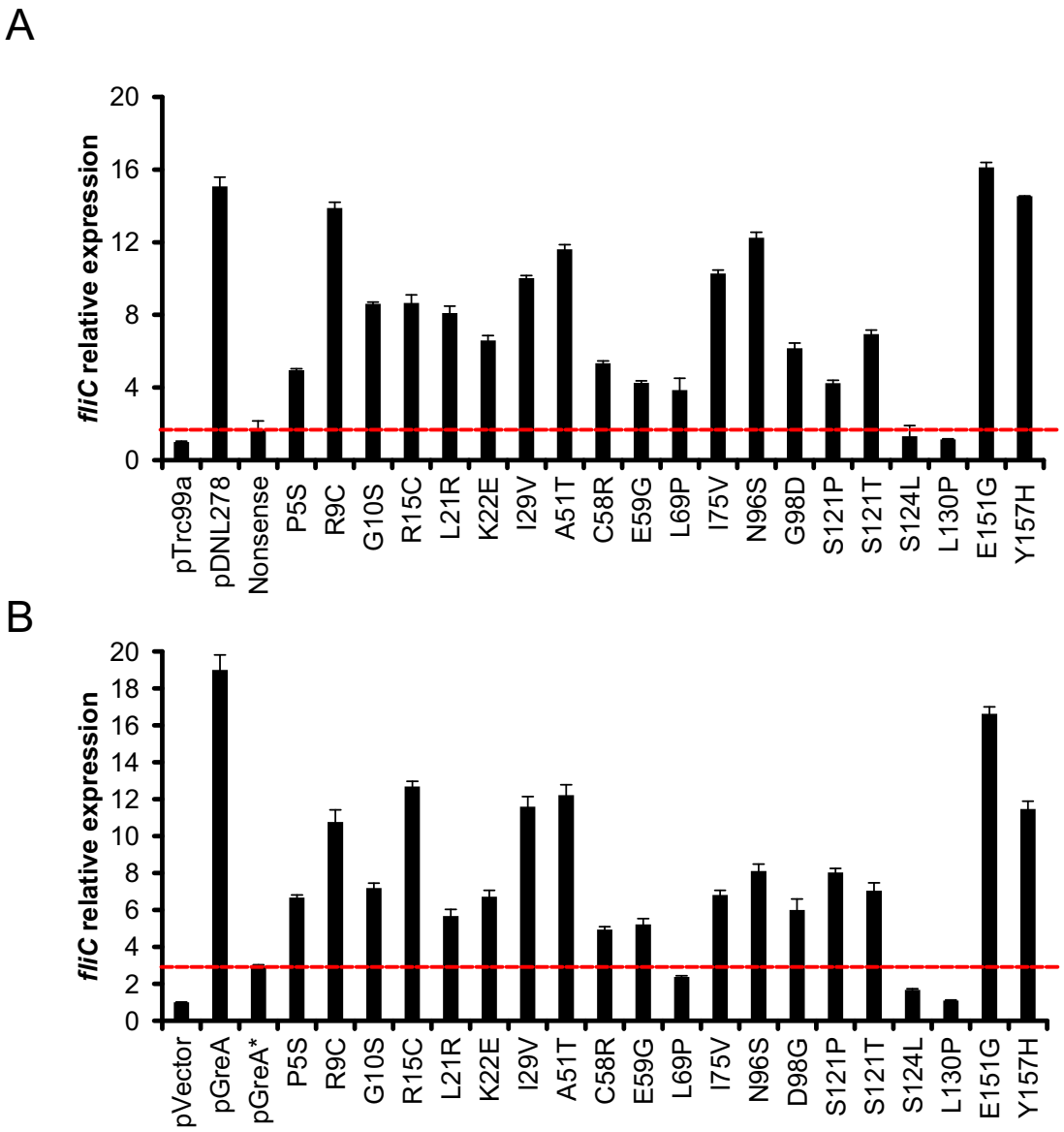

Figure 64: Effect of the different GreA^{Mut} on the expression of *fliC*. A) Expression of *fliC* in cultures of the strain PRG18 (*dksA greA fliC*::*lacZ* distal) carrying the plasmids pTrc99a (Control), pDNL278 (GreA^{WT}) and the 20 different pTrc-GreA^{Mut}. Cultures were grown in LB at 37ºC up to an OD_{600nm} of 1.5. B) Expression of *fliC* in cultures of PRG18 carrying the plasmids pHM1883 (pVector), pHM1873 (pGreA), pHM1854 (pGreA*) and the 20 different pHM-GreA^{Mut}. Cultures were grown in LB at 37ºC up to an OD_{600nm} of 1.5. At OD_{600nm} of 0.1 the cultures were induced with 0.1 mM of IPTG. The *fliC* expression of the different strains was expressed in relative values, being 1.0 the value in Miller units for pTrc99a (A) or pVector (B). Average and standard deviation of β-galactosidase activity determination from three independent cultures are shown. The red line indicates the threshold where it is considered that the mutants had lost the antipause activity.

While several mutants had intermediate antipause activities (**fig. 64A**), the mutants S124L and L130P, localized in the α-helix of the globular domain (**fig. 63**), produced the same levels of *fliC* expression than pTrc99a, with an antipause activity of the 2.22% and 1.01% respectively. These data suggest

that the α-helix of the globular domain is essential for the antipause activity of GreA. Surprisingly, the mutants R9C, E151G and Y157H produce similar *fliC* expression levels as $GreA^{WT}$ (pDNL278), and therefore they have barely normal antipause activities (91.61%, 107.52% and 96.16% respectively). Although the mutants R9C and E151G were predicted not acceptable by SIFT, they have normal antipause activities, suggesting that while the software could give a prediction, it may not be accurate.

In Vinella *et al.*, (2012), the gene *greA,* as well as the allele *greA* D41A E44Y, was cloned in a low-copy number plasmid (pHM1883) under a P_{tac} promoter in order to overexpress *greA*, but without producing the negative effect on the bacterial growth observed. Therefore we decided to use the same system to observe the effect of the overexpression of our mutants on the expression of *fliC* (**fig. 64B**). The different *greA* alleles were cloned into pHM1883 (referred as pVector) and the resulting plasmids were transformed into the strain pRG18 (*dksA greA fliC*::*lacZ* distal) as well as the plasmid pHM1883 (pVector), pHM1873 (containing *greA,* referred as pGreA) and pHM1854 (containing *greA* D41A E44Y, referred as pGreA*). The resulting strains were grown in LB at 37ºC up to an OD_{600nm} of 0.1 and were induced with 0.1 mM of IPTG, continued growing up to an OD_{600nm} of 1.5 and the β-galactosidase activity was measured (**fig. 64B**).

As observed with the pTrc99a system (**fig. 64A**), the expression of *fliC* in presence of pVector is low, while in presence of pGreA it suffers a 19-fold increase (**fig. 64B**). The allele GreA D41A E44Y (pGreA*), described to have no antipause activity, shows a similar effect on *fliC* expression as observed by pVector, highlighting that the antipause effect is required for the expression of *fliC,* as suggested in the section 4.3.3.

In order to determine that the effect of pGreA* on *fliC* expression is due to the antipause activity, and it is not a problem with the overexpression system, the amount of GreA D41A E44Y was monitored. The strain AAG101 (*dksA greA*) with the plasmids pVector, pGreA and pGreA* were grown in LB at 37ºC up to an OD_{600nm} of 0.1 and *greA* expression was induced with 0.1 mM of IPTG, and

growth was followed up to an OD_{600nm} of 1.5. Whole cell extracts were analyzed by Western blot using monoclonal antibodies against GreA (**fig. 65**).

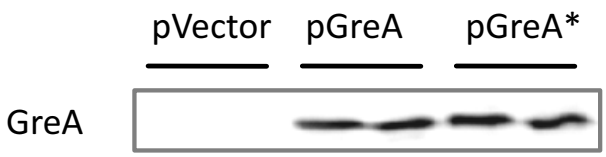

Figure 65: The strain AAG101 (*dksA greA*) carrying either pHM1883 (pVector), pHM1873 (pGreA) or pHM1854 (pGreA*) plasmid were grown in LB at 37ºC up to an OD_{600nm} of 0.1, overexpression was induced with 0.1 mM of IPTG, and growth was followed up to an OD_{600nm} of 1.5. Whole cell extracts were analyzed in a 13.5% SDS-PAGE, transferred onto PVDF membrane, and immunodetection performed as described in section X with monoclonal antibodies against GreA. The chemiluminiscence signal was visualized using a Chemidoc from Bio-Rad.

In a *dksAgreA* strain with the pVector plasmid, no GreA was detected as expected. In the whole cell extract from the strain carrying the plasmids pGreA and pGreA*, the same amount of GreA was detected, suggesting that the differences observed on *fliC* expression were due GreA activity and not to its quantity (**fig. 65**).

When the *fliC* expression of the different $GreA^{Mut}$, using both overexpression systems (**fig. 64A** and **B**) was compared, similar results were observed. However, the mutant R15C increases the *fliC* expression with the pHM system (**fig. 64B**) showing that it requires its overexpression to increase the expression of *fliC,* suggesting that its affinity for the secondary channel of the RNApol could be affected. However it has been observed that the overexpression of GreA* produces a negative effect on bacterial growth (even with the low-copy number plasmid), suggesting that the antipause activity is not required for the negative effect.

Some of the mutants able to grow in either presence or absence of DksA, **+**/**+** in **table 7**, such as L69P, S124L and L130P show lowest antipause activities, with a *fliC* expression below the threshold (**fig. 64B**) indicating that the lack of GreA activity allow bacterial growth. G10S and S121P also are able to grow in presence and absence of DksA, but their antipause activity is higher than the others. Considering that the results were obtained under overexpressing conditions, increasing the relative amount of the complex RNApol-GreA, it might

suggest that these mutants, G10S and S121P, had its affinity for the RNApol affected. If that would be the case, GreAG10S and GreAS121P could not efficiently interact with the RNApol, even in absence of DksA, not causing a deleterious effect on growth. However, as indicated with pTrc99a derivative plasmids (**fig. 64A**), the mutants with an intermediate resistance in presence of DksA but sensitive in absence of DksA (+/-/- in **table 7**) had the highest antipause activity, suggesting that perhaps its ability to compete with DksA might be affected.

We performed an experimental approach to determine the ability of binding of some of the mutants. Our approach is based in the fact that in a *dksA* mutant, the expression of *fliC* increases due the binding of GreA into the secondary channel of the RNApol. If the $GreA^{Mut}$ are able to bind to the RNApol but are not functional, under overexpression conditions, it would compete with the chromosomal GreA for binding the RNApol, and as a consequence would produce a decrease in *fliC* expression. However, if the $GreA^{Mut}$ is not able to bind to the secondary channel, under overexpression conditions it could not compete with the chromosomal GreA and the expression of *fliC* would not vary.

As we used the pTrc99a derivative plasmids, the overexpression of some of the mutants would produce a negative effect on the bacterial growth. Only the mutants C58R, S121P, S124L and L130P were tested. As a control the mutants D41A, D41N and E44K were also tested as a control of a protein without antipause activity but able to bind to the secondary channel of the RNApol (Opalka *et al.*, 2003; Laptenko *et al.*, 2003). To do that, the strain PRG17 (*dksA*, distal fusion) carrying the plasmid pTrc99a and the mentioned pTrc-$GreA^{Mut}$ were grown in LB supplemented with either 0 or 0.0125 mM of IPTG. For the mutant S124L an additional concentration of IPTG was used, 0.05 mM. Cultures were grown at 37ºC up to an OD_{600nm} of 1.5 and *fliC* expression was monitored (**fig. 66**). As a control, *fliC* expression was also monitored form the strain PRG17 (*dksA*) and PRG18 (*dksA greA*).

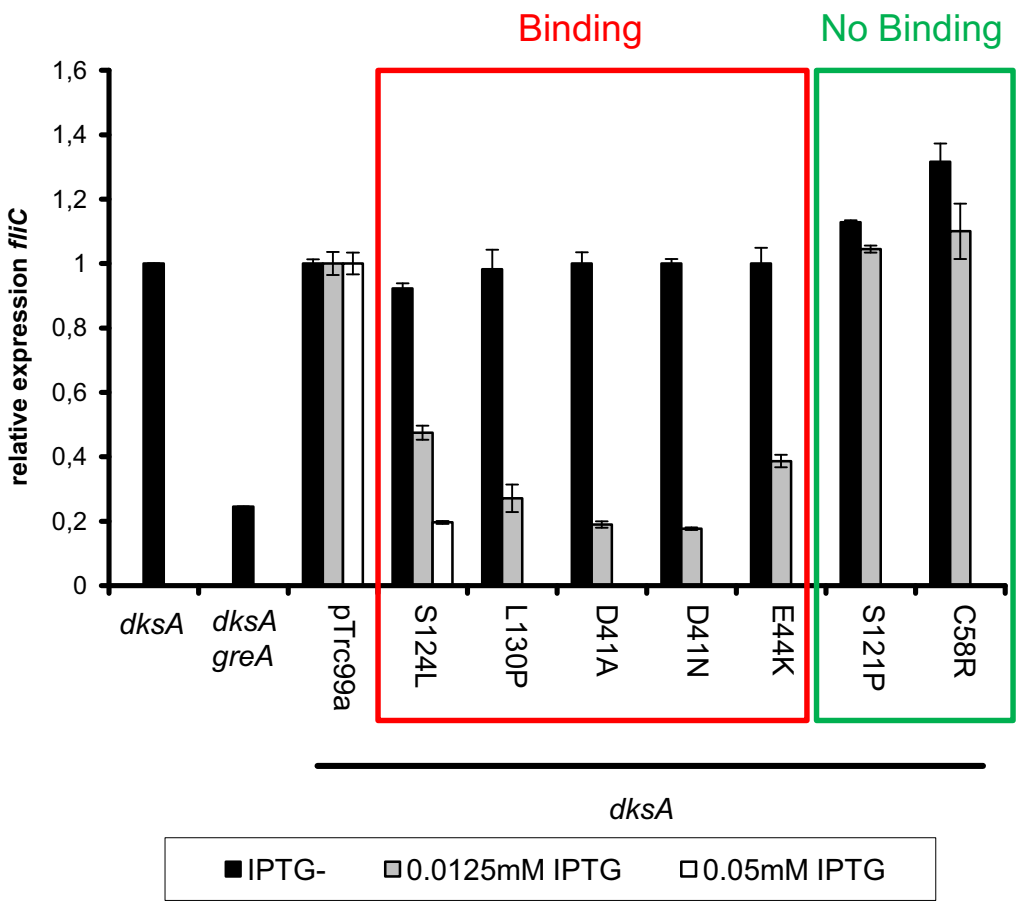

Figure 66: The strain PRG17 (*dksA*, distal fusion) carrying the plasmid pTrc99a and pTrc-GreA^{Mut}, with the indicated alleles were grown in LB supplemented with either 0, 0.0125 or 0.05 mM of IPTG as indicated. Cultures were grown at 37ºC up to an OD_{600nm} of 1.5 and the expression of *fliC* was monitored by β-galactosidase determination. The *fliC* expression of the different strains was expressed in relative values, being 1.0 the value in Miller units for the strain PRG17 (*dksA*). Average and standard deviation of β-galactosidase activity determination from three independent cultures are shown.

The overexpression of D41A, D41N and E44K *greA* alleles in a *dksA* mutant strain (**fig. 66**), proteins without antipause activity that bind to the RNApol, produces a decrease of the expression of *fliC* similar to the observed in a *dksAgreA* mutant which presumably corroborate that the experimental approach might be useful to characterize the different GreA alleles. The overexpression of the mutant S124L and L130P also produces a decrease on the expression of *fliC*, suggesting that these mutants are able to bind to the RNApol but they are not functional. However, the overexpression of the mutant S121P and C58R, did not produce any effect on the expression of *fliC* suggesting that these mutants are not able to bind to the RNApol. This functional assay may be useful to determine possible alterations in the ability of GreA for the RNApol.

Unfortunately those experiments were not continued with the other mutants due to two main problems: i) some of the mutants had a deleterious effect in strains deficient in *dksA*, as the strain used for this study, and ii) the lack of a control, a protein able to bind into the secondary channel and being functional, that in this case it should be GreA and it is known that overexpressing *greA* produces a negative effect in bacterial growth.

4.5.2. Prototrophy recuperation in *dksA* / ppGpp^0 strains

The alarmone ppGpp is required for induction of genes coding for amino acid biosynthesis during stringent response (Cashel *et al.*, 1996; Magnusson *et al.*, 2005). Consequently ppGpp deficient strains (ppGpp^0) are not able to grow in minimal media (M9 glucose) in absence of amino acids clearly indicating that are auxotrophic (H Xiao *et al.*, 1991; Vinella *et al.*, 2012). The DksA protein, defined as a cofactor of ppGpp, stimulates also the amino acid biosynthesis operons expression (Haugen *et al.*, 2008). DksA is also required for proper bacterial growth in minimal media without amino acids (Brown *et al.*, 2002). However, in a report by Vinella *et al.* (2012), it was discussed that the strain deficient in DksA instead of being auxotrophic, as the ppGpp^0 strain, it is able to grow after 72 hours at 37ºC in minimal media and it was suggested to be slow-growing bradytroph. In this report it was also shown that the *greA* mutation completely abolished the growth of the *dksA* strain, being the double mutant *dksA greA* auxotrophic in minimal media M9.

Moreover, it has been shown that the overexpression of GreA, using the low-copy number pHM system, is able to restore the prototrophy of the *dksA greA* deficient strain, but also of the *dksA* ppGpp^0 and the *dksA greA* ppGpp^0 strains, suggesting that GreA may promote expression from the amino acid biosynthesis genes under certain conditions. It was also described (Vinella *et al.*, 2012) that the overexpression of GreA D41A E44Y (GreA*) is able to restore the prototrophy in a dksA ppGpp^0 deficient strain, suggesting that the antipause activity of GreA was not required for this phenotype. With these results the authors concluded that GreA is able to restore prototrophy by having somehow a role during transcription initiation (Vinella *et al.*, 2012). Therefore we decided

to use this phenotype to determine the activity at transcription initiation of the different GreA^{Mut} obtained.

First, the effect of overexpressing *greA* and *greA**, by using plasmid pHM1873 and pHM1854, was determined in the strains MG1655 (WT), TE8114 (*dksA*), CF11657 (*greA*) and AAG101 (*dksA greA*) on M9 glucose plates with and without IPTG (0.1 mM). The diameter was measured after 3-days incubation at 37ºC (**table 8**).

mm		WT	*dksA*	*greA*	*dksA greA*
pVector	-IPTG	2	0	2,05	0
	+IPTG	2	0	2,05	0
pGreA	-IPTG	2	1	2	0,5
	+IPTG	3,5	2,2	3	1,75
pGreA*	-IPTG	3,5	1,2	2,8	0
	+IPTG	0	0	0	0

Table 8: Effect of multicopy *greA* and *greA** on the colony size of bacterial growing on M9 plates. The strains MG1655 (WT), AAG93 (ppGpp^0), TE8114 (*dksA*), CF11657 (*greA*) and AAG101 (*dksA greA*) carrying the plasmid pHM1883 (pVector), pHM1873 (pGreA) and pHM1854 (pGreA*) were grown on LB plates supplemented with 25 µg/ml spectinomycin. Cell suspensions in 10 mM $MgSO_4$ were plated on M9 glucose plates with (+) of without (-) IPTG (0.1 mM). Colony diameter was measured after 3-day incubation at 37ºC on plates containing less than 100 colonies.

As described by Vinella *et al.* (2012), the overexpression of *greA* is able to restore the prototrophy in the mutant strain *dksA greA* (**table 8**). Surprisingly, it is observed that the *dksA* deficient strain was auxotrophic on M9 instead of bradytrophic as described by Vinella *et al.* (2012). However the overexpression of GreA is able to restore the prototrophy (**table 8**). Deficient strain in GreA did not show any growth alteration on M9 glucose plates. When GreA* was overexpressed an unexpected negative effect was observed. In presence and absence of GreA (WT and *greA* strain) no colonies were observed in presence of IPTG, suggesting that the overexpression of the GreA* would not allow the growth on M9 plates, or it is toxic. In absence of DksA, the presence of pGreA* (without IPTG) is able to restore the prototrophy, but the addition of IPTG, as observed in a WT and *greA* strains, inhibits the bacterial growth. Those results

might indicate that overexpression of GreA* is able to exchange from RNApol-GreA^{WT} to RNApol-GreA* and under these conditions, growth cannot be restored. Our results clearly indicate that antipausing activity is required for recovering prototrophy by the *dksA* strain. Consistent with this, in absence of *greA* and *dksA*, pGreA* is not able to recover the auxotrophy caused, as could be observed in **table 8**. Again, our results differs form those of Vinella *et al.* (2012). Our data clearly indicate that to restore auxotrophy in a *dksA* deficient strain, it is required the antipause activity since the *dksAgreA* strain can grow on M9 plates when pGreA is present but not with pGreA*. These discrepancies among the results observed between Vinella *et al.* (2012) and our data, is only possible to be explained by differences in the preparation of the M9 plates, since the pGreA* plasmid is the same and the apparently also the bacterial strain.

The ability of the different GreA^{Mut} to restore the prototrophy at different backgrounds was tested. The strain MG1655 (WT), TE8114 (*dksA*) and AAG101 (*dksA greA*) carrying pHM1883 (pVector), pHM1873 (pGreA), pHM1854 (pGreA*) and the different pHM-greA^{Mut} were grown on M9 glucose plates with and without IPTG (0.1 mM). The colony diameter was measured after 3-day incubations at 37ºC. The average and standard deviation of the diameter of 10 colonies of two independent cultures is shown in the **table 9**. Also the antipause activity, measured according the *fliC* expression (**fig. 64**), is indicated.

It is observed that the overexpression of the different GreA^{Mut} in the WT strain on M9 glucose plates did not produce any effect on the growth (**table 9**). Surprisingly, when the WT strain carrying pGreA* was plated on M9 with IPTG a decrease of the viability of the strain was observed. This result, in agreement with our results (**table 8**), indicate that GreA antipause activity is important for prototrophy. Moreover, is suggest that somehow the overexpression of our GreA^{Mut} is not as toxic as GreA* or they kept enough antipause activity to survive on M9 glucose media.

The mutants S124L and L130P, mutants with low antipause activity (2.22% and 1.01%), were not able to restore the prototrophy in both *dksA* and *dksA greA*

strains (**table 9**, in orange), suggesting that had lost the activity associated to GreA. The fact that the phenotype is observed in absence of *dksA*, but not in WT, might indicate that those mutants although able to bind to RNApol, the affinity might be affected or that overexpression does not reach similar levels of protein that with GreA*.

mm	WT		*dksA*		*dksA greA*		Antipause activity
	+	-	+	-	+	-	
pVector	2,00 ± 0,1	2,05 ± 0,1	0	0	0	0	nd
pGreA	2,00	2,00	2,00	1.00	1.75	0.5	nd
pGreA* P5S	0	2,00	0	1.00	0	0	nd
R9C	2,00	2,00	1,2 ± 0	0	1,48 ± 0,04	1,68 ± 0,17	91,61%
G10S	2,00	2,00	0,77 ± 0,13	0,1 ± 0	1,57 ± 0,11	1,45 ± 0,08	54,06%
R15C	2,00	2,00	1,45 ± 0,11	0	1,33 ± 0,08	1,43 ± 0,13	54,41%
L21R	2,00	2,00	0,5 ± 0	0	1,85 ± 0,18	0	50,48%
K22E	2,00	2,00	0,46 ± 0,16	0	1,93 ± 0,17	0,45 ± 0,13	39,68%
I29V	2,00	2,00	1,5 ± 0	0,2 ± 0	1,51 ± 0,03	1,5 ± 0,05	64,11%
A51T	2,00	2,00	0,45 ± 0,15	0	1,95 ± 0,07	0	75,45%
C58R	2,00	2,00	0,2 ± 0	0	1,99 ± 0,15	0	30,84%
E59G	2,00	2,00	0	0	1,87 ± 0,14	0	23,11%
L69P	2,00	2,00	0	0	0	0	20,35%
I75V	2,00	2,00	1 ± 0	0	1,5 ± 0,06	1,37 ± 0,09	65,90%
N96S	2,00	2,00	1,5 ± 0	0,2 ± 0	1,54 ± 0,12	0,48 ± 0,2	79,91%
D98G	2,00	2,00	0,85 ± 0,15	0,35 ± 0,15	1,51 ± 0,02	0	36,64%
S121P	2,00	2,00	0	0	1,81 ± 0,12	0	22,96%
S121T	2,00	2,00	0,36 ± 0,11	0	2,03 ± 0,09	0	42,17%
S124L	2,00	2,00	0	0	0	0	2,22%
L130P	2,00	2,00	0	0	0	0	1,01%
E151G	2,00	2,00	1,34 ± 0,06	0,19 ± 0,03	1 ± 0,07	1,55 ± 0,09	107,52%
Y157H	2,00	2,00	1,5 ± 0	0,1 ± 0	1,53 ± 0,07	0,59 ± 0,11	96,16%

Table 9: Effect in the colony size of the different pHM-greA^{Mut} on strains MG1655 (WT), TE8114 (*dksA*), AAG101 (*dksA greA*), on M9 plates. The strains were grown on LB plates supplemented with 25 µg/ml spectinomycin. Bacterial cell suspensions in 10 mM $MgSO_4$ were plated on M9 glucose plates with (+) of without (-) IPTG 0.1mM. Colony diameters were measured after 3-day incubations at 37ºC on plates containing less than 100 colonies. Average and standard deviation of the diameter of 10 colonies of two independent cultures is shown. The antipause activity (measured according the *fliC* expression) is indicated. The antipause activity, measured according the *fliC* expression (**fig. 64**), is indicated. Colours are defined in the text.

As shown in **figure 66** these mutants are seem to be able to bind to the RNApol, suggesting that its functionality is affected. Moreover, these mutants had lost any negative effect on the bacterial growth in presence or absence of DksA (**table 7**). Due both mutants were located in the α-helix of the globular domain (**fig. 68A**), we could suggest that this α-helix is essential for GreA functionality.

As previously observed in **figure 64A**, the antipause activity of the mutants R9C, E151G and Y157H was similar to $GreA^{WT}$ (a 91.61%, 107.52% and 96.16% respectively). Moreover, they were able to restore prototrophy of the *dksAgreA* strain as did $GreA^{WT}$, and in a DksA deficient strain when they were overexpressed (**table 9**, in green). Considering that these mutant had an intermediate resistance when were overexpressed in the WT strain, and a negative effect in the *dksA* strain (**table 7**), it might be suggested that these mutants could have affected the ability and to compete with DksA to interact with the secondary channel.

The mutants L21R, A51T, C58R, E59G, D98G, S121P and S121T were able to restore the prototrophy in a *dksA greA* mutant in presence of IPTG but not in its absence (**table 9**, in blue), suggesting that its affinity for the secondary channel of the RNApol could be importantly affected. Moreover in a *dksA* deficient strain the mutant E59G and S121P are not able to restore the prototrophy even under overexpression conditions, suggesting that these GreA alleles are not able to interact with the secondary channel when chromosomic *greA* is present. The mutants L21R, A51T, C58R and S121L had low ability to restore the prototrophy of the *dksA* deficient strain under overexpression conditions.

While the mutation I75V is a conservative mutation (isoleucina and valine are both hydrophobic amino acids with a similar structure), it had lost a 34.1% of its antipause activity (**fig. 64A**). It was able to recover the prototrophy of the *dksA greA* strain (in presence and absence of IPTG) but only it was able to recover the prototrophy of the *dksA* strain in presence of IPTG (**table 9**).

4.5.3. Possible effect of the different mutations on the structure of GreA

Based in the existing three-dimensional models and the structure described for the interaction of Gfh1 with the RNApol of *Thermus thermophilus,* we have performed a highly speculative model of the effect of the different mutations on the structure of GreA.

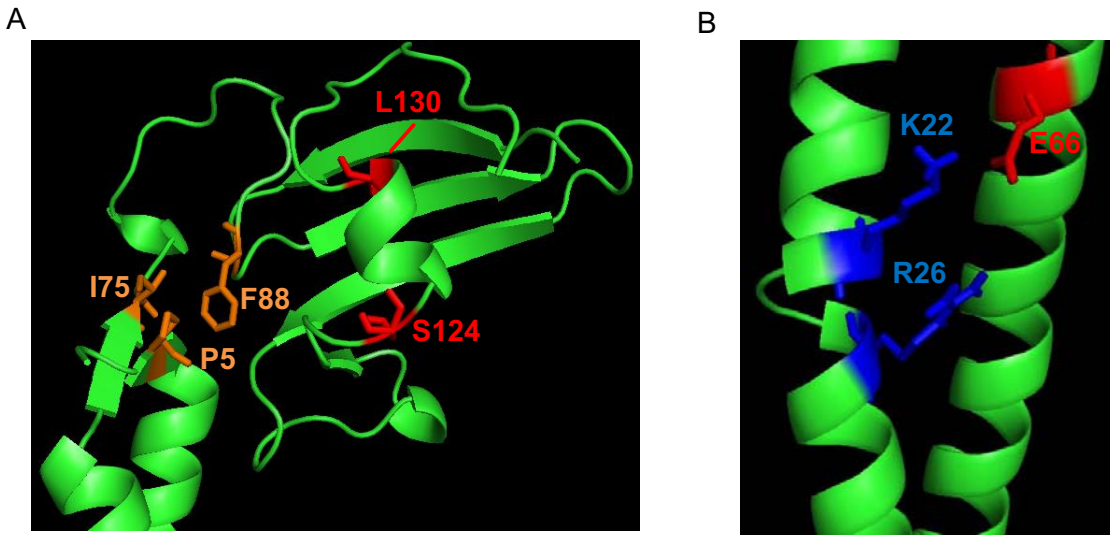

Figure 68: Distribution of some of the mutations identified in the 3D structure of GreA. A) Distribution of the hydrophobic amino acids I75, P5 and F88 (in orange) and the amino acid L130 and S124 (in red) in the structure of GreA. B) Distribution of amino acids K22, R26 and E66 in the coiled-coil domain of GreA.

There are several mutated amino acids (L21R, I29V, A51T, C58R, N96S and Y157H) with a predicted low solvent accessibility (Rost *et al.*, 2004), indicating that are buried into the structure and are considered the core of the protein. Changes on protein core amino acids could cause structural changes. Structural changes are also expected when mutations causing alterations of small amino acids, such as glycine (G10S, E59G, and E151G), are involved, since any other amino acid will not fit in a place of a glycine. Moreover, it is considered (Nilsson *et al.*, 1998) that introducing a proline (P) in a α-helix or β-barrel, disrupts the structure since proline is a cyclic amino acid that causes rigid structures. For this reason, L69P, S121P and L130P mutants are also presumably causing structural changes. The amino acid S124 forms part of an α-helix in the globular domain and changing it for a leucine (S124L) would not fit on this helix (**fig. 68A**). As mentioned above, the disruption of this α-helix in the

globular domain would produce important affectations in the functionality of GreA.

The amino acid P5, I75 and F88 forms a hydrophobic interaction, which presumably might affect the distance between the globular and coiled-coil domain (**fig. 68A**). The mutants P5S and I75V might affect this hydrophobic interaction and produce changes in the orientation of the globular domain. As previously described in 1.2.4, Gfh1 suffers conformational changes in a pH-dependent manner that produces a re-orientation of the globular domain allowing its interaction with the secondary channel (Laptenko *et al.*, 2006). As previously mentioned, the mutation I75V, being a conservative mutation, had lost a 34.1% of its antipause activity (**fig. 64A**) and it was able to recover the prototrophy of the *dksA greA* strain, in presence and absence of IPTG. However, it was able to recover the prototrophy of the *dksA* strain only in presence of IPTG (**table 9**), suggesting that changes in this amino acid, may change the orientation of the globular domain, decreasing its affinity for the RNApol.

The amino acid K22 (basic) interacts with E66 (acid). In the mutant K22E the basic amino acid has been exchanged by an acid, that may produce a repulsion of E66 and an interaction with R26 (another basic residue), producing a twist on the α-helix (**fig. 68B**). According to its antipause activity (39.68%) and ability to restore prototrophy in the mutant strain *dksA greA* but in the *dksA* strain only is able to restore it in presence of IPTG, suggesting that this mutation would produce a reduction of the affinity for the secondary channel of the RNApol.

All these data shows that GreA is a very flexible protein. Although many mutations are theoretically structural and would cause important alterations in the structure, the resulting proteins are still active. Moreover, some of these mutations has been predicted as non acceptable by SIFT software, highlighting the plasticity or flexibility of this protein. Somehow this flexibility might indicate the presence of possible conformational changes. Possible conformational changes in GreA is consistent with our results indicating that the effect of GreA on *fliC* expression is osmolarity dependent although osmolarity does not cause any alteration on *greA* transcription (**fig. 31D**) or GreA cellular content (**fig. 55**).

Our study on the distribution of synonymous and non synonymous mutations in the different domains of GreA indicates that conformation may play a very pivotal role in GreA functionality.

We have defined that some mutants had partially lost antipause activity, but it does not mean that these amino acids are required for the antipause activity *per se*. These mutations would produce changes on the orientation of the amino acids D41 and E44, defined as responsible of the antipause effect, avoiding its proper binding with the cMG1 of the active centre of the RNApol. Also, as previously suggested, the lost of antipause activity, would be also associated with a non efficient binding of GreA into the secondary channel of the RNApol.

Further studies must be performed to determine the exact effect of the different mutations on the functionality or affinity of GreA. However, this study gives a initial approach of important structures of the protein GreA that has not been noticed before, as the α-helix on the globular domain.

4.6. Phylogenetic analysis of the distribution of factors that bind to the secondary channel of the RNApol

Escherichia coli contains several proteins that bind into the secondary channel of the RNApol: GreA, GreB, DksA and Rnk (Sergei Borukhov *et al.*, 1993; Perederina *et al.*, 2004; Lamour *et al.*, 2008). In other species, other proteins could interact with the secondary channel of the RNApol such as Gfh1 in *Thermus aquaticus* (Lamour *et al.*, 2006) or DksA2 in *Pseudomonas aeruginosa*, similar to DksA but without C4 zinc-finger, (Furman, Biswas, *et al.*, 2013) have been described. Moreover, genetic elements such as plasmids and bacteriophages may carry also genes coding for secondary channel interacting proteins. It has been described that the conjugative F plasmid of *E. coli* and the pSLT plasmid of *Salmonella enterica,* code for TraR, protein able to bind into the secondary channel of the RNApol (Blankschien *et al.*, 2009). Several proteins homologous to TraR have been indentified in bacteriophages and prophages, such as YbiI in *E. coli*. These data suggest that several genetic elements had acquired genes coding for proteins that could interact with the secondary channel of the RNApol in order to modify the gene expression pattern of the recipient cells.

In order to analyse the variability between the proteins that bind into the secondary channel of the RNApol, we have performed a phylogenetic study of those factors, trying to determine the origins of this diversity as well as the distribution of these proteins in bacteria. Finally we decided to study the nucleotidic variability of GreA, in order to determine if the presence of other proteins that bind into the secondary channel of the RNApol could produce any evolutive pressure over GreA structure.

Among the factors described to bind to the secondary channel, two main families could be distinguished depending on its structure: those proteins similar to DksA and those similar to GreA. On one hand, the DksA family contains proteins formed by several α-helixes divided into a globular domain, containing the N and C-terminal regions and the coiled-coil domain. In the globular domain, DksA contains a C4 zinc-finger motif, where a Zn^{+2} binds 4 cysteins (Perederina *et al.*, 2004). Several proteins from bacteriophages, such as P2p38 of the P2

phage, or conjugative plasmids, such as TraR of pSLT or F plasmid, contain the C4 zinc-finger motif and a structure similar to DksA. Moreover it has been described another set of proteins that, although share a similar structure to DksA, they lack the C4 zinc-finger motif, such as PA5536 of *Pseudomonas aeruginosa*, also known as DksA2 (Blaby-Haas *et al.*, 2011).

On the other hand, the GreA family contains, apart from GreA, GreB, Gfh1 and Rnk. The proteins of this family had a highly similar structure among them, with a N-terminal coiled-coil domain similar to DksA and a C-terminal globular domain formed by a β-barrel and an α-helix structure. Moreover none of the members of the GreA family contains C4-zinc finger.

Both families had a similar spatial organization but their protein sequences share no homology, as could be observed in **table 10** where DksA share low identity and similarity with GreA.

	GreA	GreB	Gfh1	Rnk	DksA
GreA					
GreB	34.4% (56.9%)				
Gfh1	23.6% (47.2%)	25.9% (45.1%)			
Rnk	13.6% (25.4%)	11.9% (23.8%)	18.2% (29.4%)		
DksA	7.2% (24.5%)	8.4% (23.5%)	8.5% (20.6%)	8.4% (25.0%)	

Table 10: Identity and Similarity (indicated in parentheses) between the protein sequences of GreA, GreB, Rnk of *E. coli* and Gfh1 of *Thermus aquaticus*, using the software developed by Stothard, (2000).

4.6.1. Study of the GreA family

GreA and GreB are really similar proteins, not only in amino acidic sequence, sharing over 55% of similarity (**table 10**), but also in structure and function (Sergei Borukhov *et al.*, 1993; Stebbins *et al.*, 1995; Kulish *et al.*, 2000). Something similar has been observed for Gfh1 of *Thermus aquaticus* that has been described to be able to bind to the RNApol (Lamour *et al.*, 2006; Tagami *et al.*, 2010). The amino acid sequences of Gfh1 with GreA and GreB was also compared (**table 10**) and the percentages are quite similar to those for GreA and GreB. But comparing the protein Rnk with the other family members, low

similarity and identity values were observed between them (**table 10**). In fact, it has similar values as observed for DksA. However it has been described that Rnk has a similar structure to GreA and GreB, as well as ability to bind to the RNApol (Lamour *et al.*, 2008), it seems that Rnk had suffered a higher evolution or it is not phylogenetically related to GreA, forming its own family of factors.

To determine the relation between GreA, GreB and Gfh1, a ML phylogenetic tree with the sequences of *greA, greB* and *gfh1* was performed. The nucleotide sequences of *greA, greB* and *gfh1* of several species distributed in the different bacterial phyla, 27 sequences of *greA,* 7 of *greB*, and 3 of *gfh1* were used (**fig.69**). The Maximum Likelihood (ML) tree was constructed as described in section 3.11.

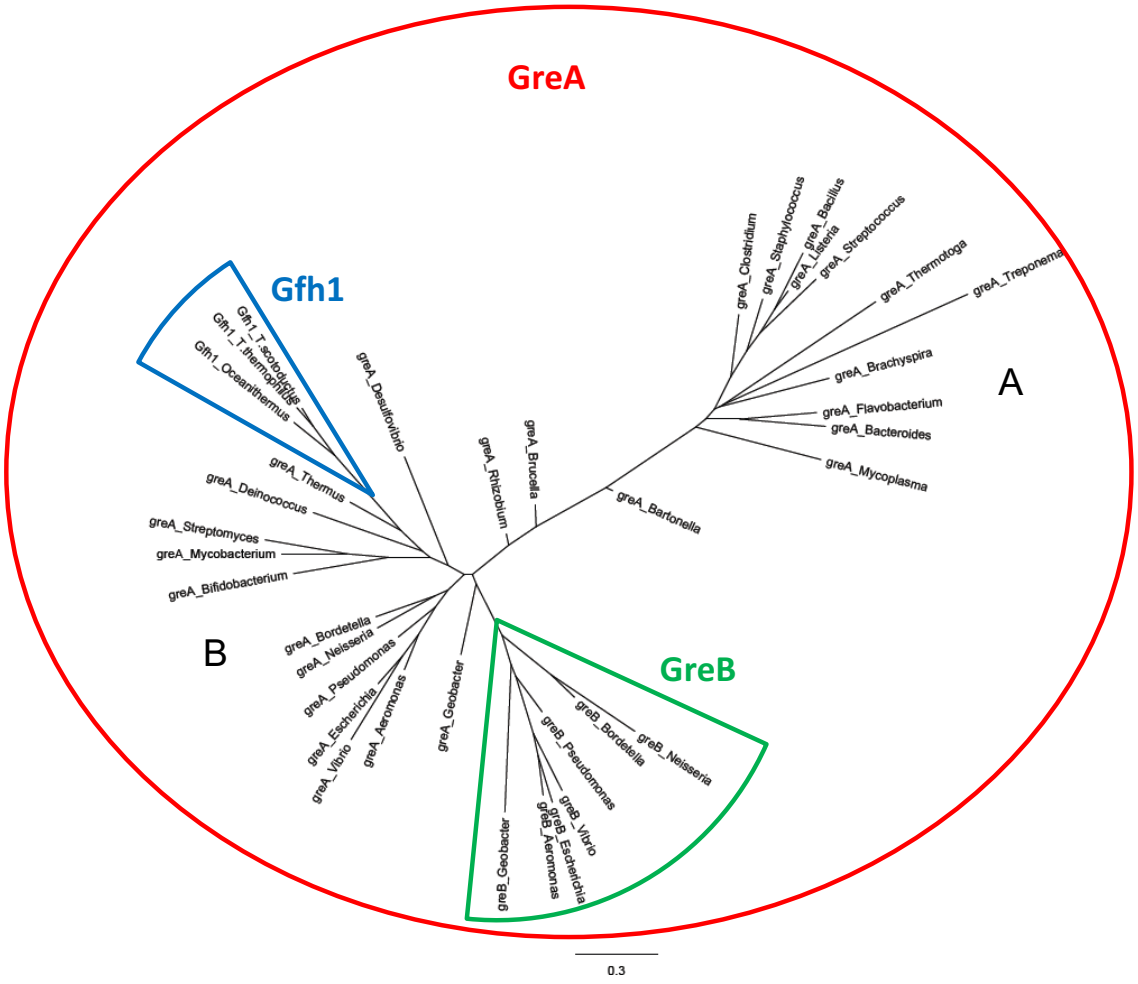

Figure 69: Radial unrooted phylogenetic tree of the gene *greA* (27 sequences of species that contains GreA), *greB* (7 sequences) and *gfh1* (3 sequences).

It is expected that if there is no relation between the different genes, *greA, greB* and *gfh1*, separated clades for long branches would be observed. But if they are related, the branches between the different proteins would be shorter. In the **figure 69** two main clades are observed: a first clade (A) with *greA* of *Firmicutes, Bacteriodetes*, and *Tenericutes*; and a second clade (B) with *greA* of *Proteobacteria, Deinococcus-Thermus* and *Actinobacteria*, as well as *greB* and *gfh1.* Interestingly, nearly all the *greA* sequences of species that only contains GreA (except *Actinobacteria*) are located in the clade A, while the *greA* sequences of the species that contains more proteins that bind into the secondary channel of the RNApol are located in the clade B. These data suggest that the presence of other proteins that could compete with GreA for binding into the secondary channel of the RNApol, such as GreB or Gfh1, might promote some evolutive pressure on *greA*, evolving in a different way that it would do without competition (discussed more in detail below).

The sequences of *greB* and *gfh1* form a defined clade, respectively, with a long branch and a sudden blooming. This clade structure is typical from duplication events as could be observed in different examples (Howarth and Donoghue, 2006; Warren *et al.*, 2008; Braasch and Salzburger, 2009; Atkinson *et al.*, 2011). Interestingly, the sequences of *greB* are related with the *greA gene* of *Geobacter bemidjiensis*; and the sequences of *gfh1* are related with the *greA gene* of *Thermus thermophilus*. These data suggest that both factors, GreB and Gfh1, appeared by gene duplication of *greA,* probably as a response to different cell necessities or environmental stress. Remarkably, the branches that separate *greB* and *gfh1* from *greA* are smaller than the branch that separates the A clade from the B, suggesting that these duplications are quite recent.

Focussing on GreB, it was observed that only *Proteobacteria* contains GreB, suggesting that it would appear after the division of this phyla from the others. However, not all the members of *Proteobacteria* contain GreB. GreB is not present in *Bartonella*, *Brucella* and *Desulfovibrio*. These data let us to propose two different hypotheses to explain this distribution of GreB among *Proteobacteria* (**fig. 70**).

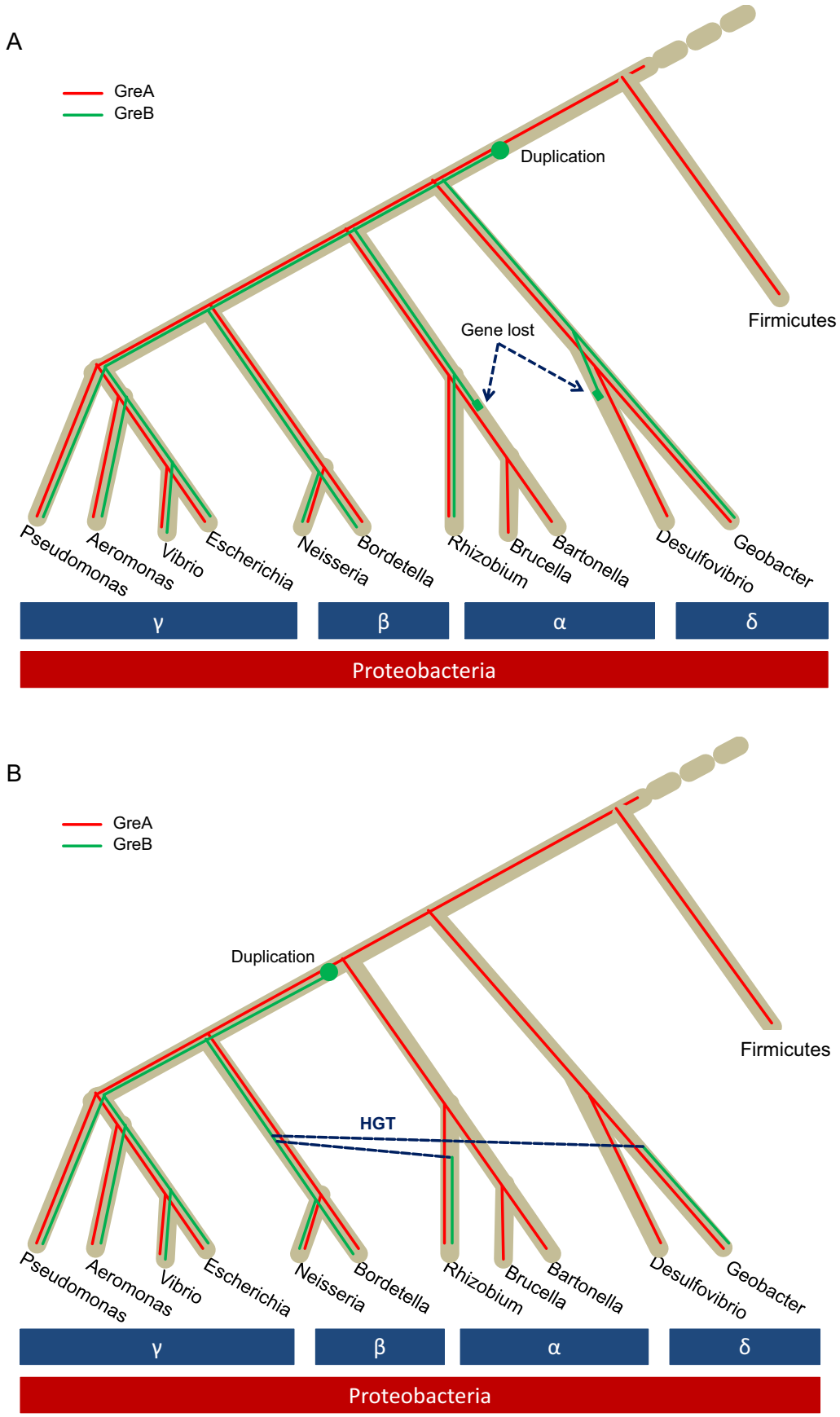

Figure 70: Two possible models of how GreB appeared among the *Proteobacteria* genome.

We may suggest that the duplication event that formed GreB took place after separation of Proteobacteria from other phyla, such as *Firmicutes*. After that, it took place a gene lost process in *Desulfovibrio* and in the common ancestor of *Bartonella* and *Brucella* (**fig. 70A**). Another possible explanation could be that the duplication event that formed GreB took place after separation of α and γβ ancestor. *Rhizobium* and *Geobacter*, acquired GreB by HGT events (**fig. 70B**).

Taking in account that HGT events are less common than gene lost (Mira *et al.*, 2001), and that there are not clear evidences of HGT events related to GreB, it seems more reasonable to accept the first hypothesis (**fig. 70A**). Moreover, as could be observed on **figure 69**, all GreB sequences analyzed are highly related with GreA of *Geobacter*, giving support to our hypothesis.

4.6.2. Study of the DksA family

As previously mentioned, the DksA family contains several proteins from bacteriophages, such as P2p38; or conjugative plasmids, such as TraR, as well as other proteins like YbiI or PtrB in pseudomonas that contain the C4 zinc-finger motif. Also this family contains a set of proteins without the C4 zinc-finger, such as DksA2 (PA5536).

When distributing the different members of the DksA family (**fig. 71**) in a ML phylogenetical tree, it could be observed that those sequences from genes coded in mobile elements, such as plasmids (TraR) or bacteriophages (P2p38), as well as *ptrB* and *ybiI*, forms a clade separated from the rest of sequences,(**fig. 71,** in green). The proteins coded for these genes are smaller than DksA, and are composed by α-helices and a C4 zinc-finger domain.

A second clade containing the genes that code for DksA and DksA2 genes was detected (**fig. 71**, in black and red, respectively). The genes that code for DksA2 forms a clade (**fig. 71**, in red) that emerges from the clade that contains both factors, suggesting that DksA2 evolved from DksA by substitution of two cysteins from the 4 needed to bind Zn^{+2}.

A third clade (**fig. 71**, in blue) was observed, containing a DksA-like protein of *Hydrogenobacter thermophilus, Thermocrinis albus* (both sequences from the phyla Aquificae) and *Borrelia garinii* (from the phyla *Spirochaetes*).

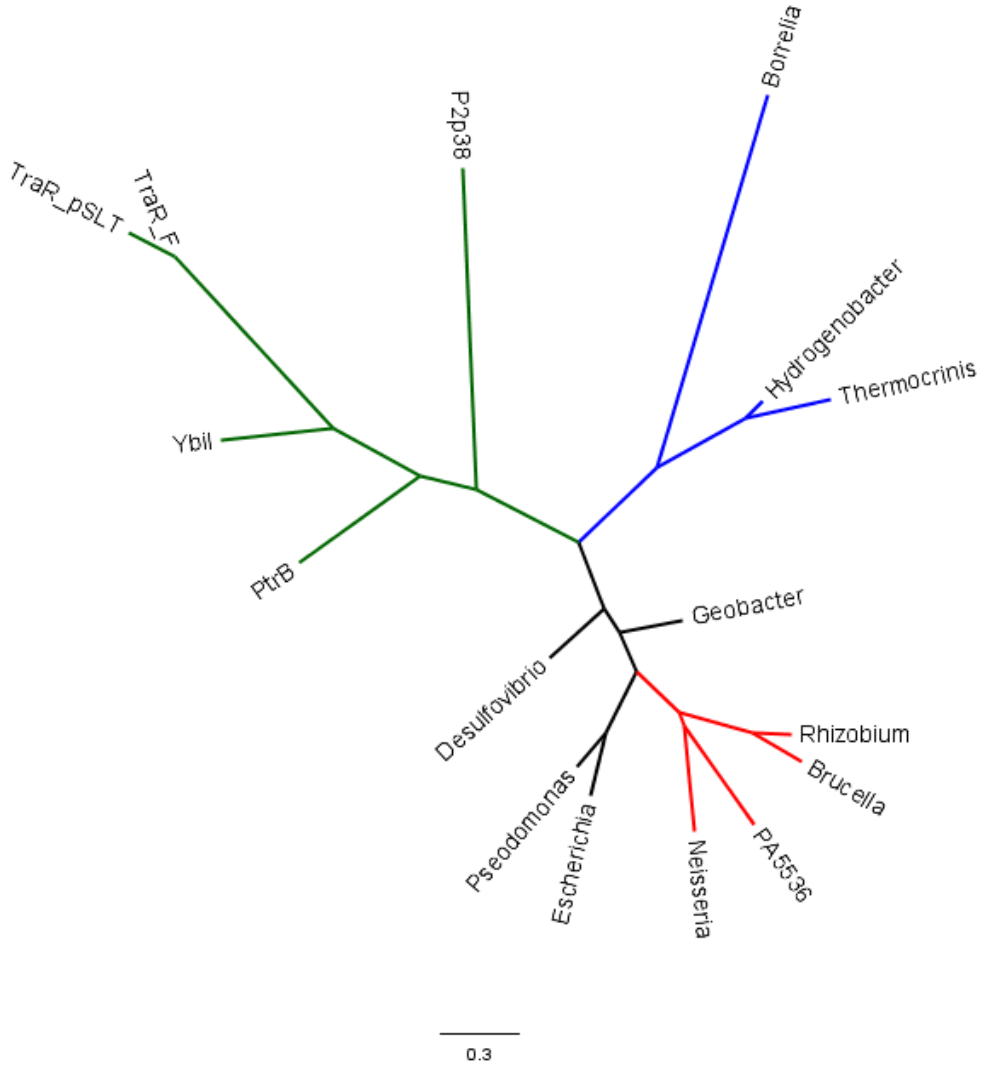

Figure 71: Phylogenetical ML tree of the different genes of the DksA family.

This DksA-like protein contains the C4 zinc-finger, but it is 30 amino acids smaller than the DksA of *E. coli*. The DksA-like of *H. thermophilus* has an identity of 27.64% and a similarity of 40.53% respect to the DksA of *E. coli* (the DksA-like protein of *H. thermophilus* and *T. albus* are highly homologous, with an identity of 76.86% and a similarity of 85.95%). Studying in detail the genomic contexts of this protein in *T. albus,* it was observed that the DksA-like protein is coded in a 32Kb-sequence flanked by two truncated genes, suggesting that could be encoded in a mobile element or a prophage. Comparing the DksA-like protein of *B. garinii* with DksA of *E. coli,* low identity and similarity was detected (18.54% and 34.44% respectively) These data suggest that the DksA-like protein detected in *B. garinii* as well as in *T. albus* and *H. thermophilus* is homolog to *E. coli* DksA but they cannot be considered as orthologs.

4.6.3. Distribution of the different factors that bind into the secondary channel of the RNApol in bacteria

It has been shown that there is a huge diversity of factors that bind the secondary channel of the RNApol among bacteria. Therefore, it was decided to determine its distribution in bacteria. For this purpose, the presence or absence of the members of either GreA or DksA family was determined by Blast of the protein sequence in the different phyla. The presence of these factors is shown over a phylogenetic tree of bacteria (**fig. 4**). The distribution of proteins presents on bacteriophages or plasmids (such as TraR) were not taken in consideration.

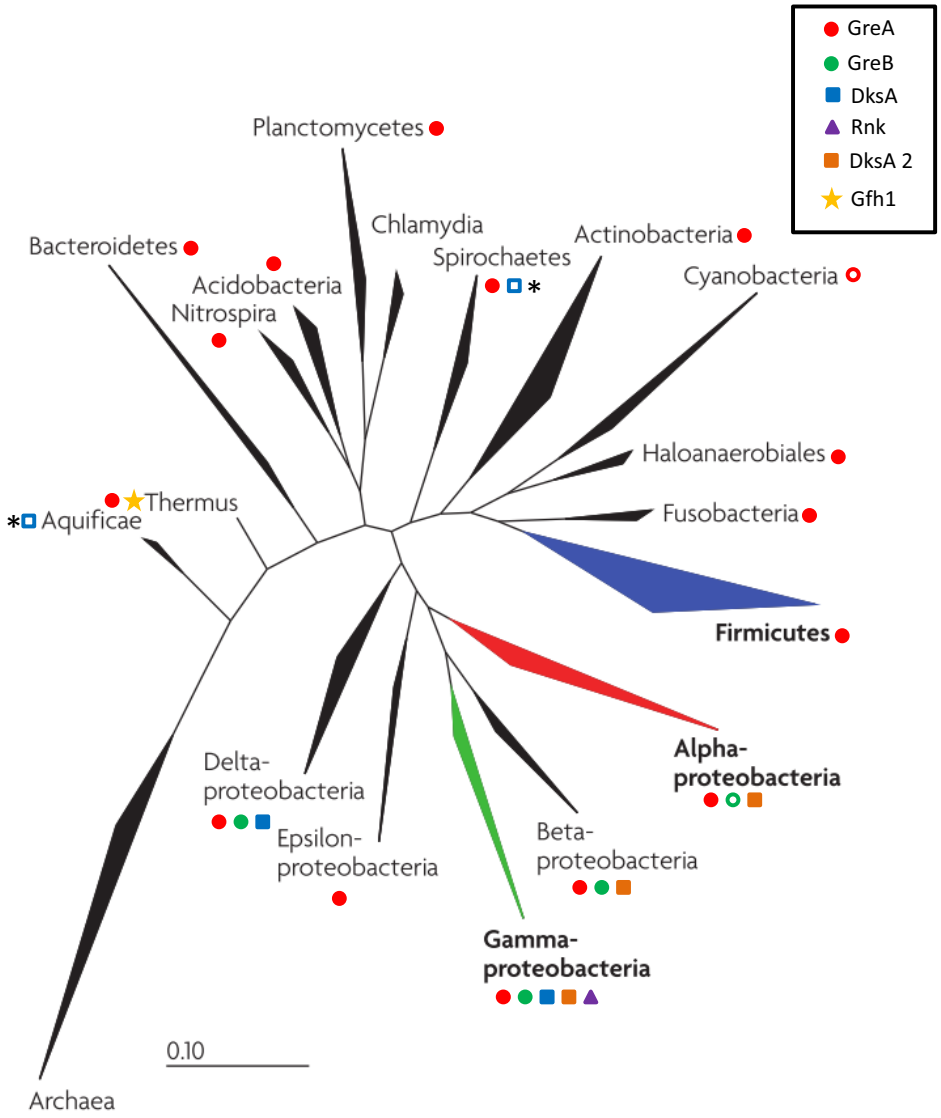

Figure 72: Distribution of the different factors that bind to the secondary channel of the RNApol over the phylogenetic tree of eubacteria adapted from Kearns, 2010. Open symbols mean than the factor is not present all the members of the phyla. The open square with an * correspond to DksA-like proteins.

When the presence or absence of the different proteins that bind to the secondary channel of the RNApol (**fig. 72**) was determined, it was shown that GreA is widely spread among bacteria – present in all phyla except *Aquificae*, *Chlamydia* and some *Cyanobacteria*. It has been observed the presence of GreA in some species of *Cyanobacteria*, such as *Mastigocoleus testarum* or *Scytonema millei,* but not in other species, such as *Nostoc punctiforme* or *Cyanothece sp.* We could theorize that GreA was present in all bacteria and then these phyla suffered a loss of GreA. Interestingly, GreA is nearly the only protein described to bind to the secondary channel of RNApol in most bacteria, except in proteobacteria, where a huge range of proteins that binds to the RNApol has been described. These data let us propose that GreA is an ancestral gene, and genes coding for other proteins interacting with the secondary channel appeared by duplication or convergent evolution as a response to several conditions or stresses. An example of this evolution is Gfh1 of the *Deinococcus-Thermus* phyla, a protein similar to GreA with capacity to suffer conformational changes by sensing differences in the pH of the medium (as previously discussed in 1.2.4). Gfh1 appears in this phyla, as well as GreB appears in proteobacteria, by gene duplication, as previously discussed.

4.6.4. Phylogenetic analysis of the structure of GreA

As discussed above, the competition of GreA with the different factors that bind into the secondary channel of the RNApol might promote some pressure on *greA* generating a diversity that would have not been seen in a situation with no competition. It has been determined that Gfh1 changes its affinity for the RNApol due to changes on the orientation of the globular domain as a response to differences of pH, and it has been proposed that something similar, induced conformational changes, may also occurs for GreA in order to bind into the secondary channel of the RNApol. The coiled-coil domain of GreA enters into the secondary channel of the RNApol. This domain is formed by two helix linked by a turn. It is in this turn where the catalytic residues D41 and E44 are located. Attending to the data derived from Gfh1, we hypothesize that changes on the flexibility of the linker that connected both, coiled-coil and globular domains would affect the possible conformational changes. If the linker domain plays an important role in these conformational switches and consequently for the

competition between factors, the linker would be positively selected or preserved in the species that contains several factors that bind into the secondary channel, compared with species that only contains GreA. The amount of synonymous and non-synonymous substitution has been determined within a group of bacteria that contains a huge variability of factors (Enterobacteriaceae) and a group where GreA has no competitors for its interaction with the RNApol (Bacillaceae). Synonymous substitutions do not produce changes in the protein sequence, while non-synonymous substitutions produce missense mutations. Therefore the sequence of the gene *greA* of 16 species of Bacillaceae and 26 species of Enterobacteriaceae was aligned with ClustalX and the rate of synonymous and non-synonymous was determined (**fig. 73**) for the different structural domains defined (helix1, turn, helix2, linker and globular) with MEGA5 software (Tamura *et al.*, 2011).

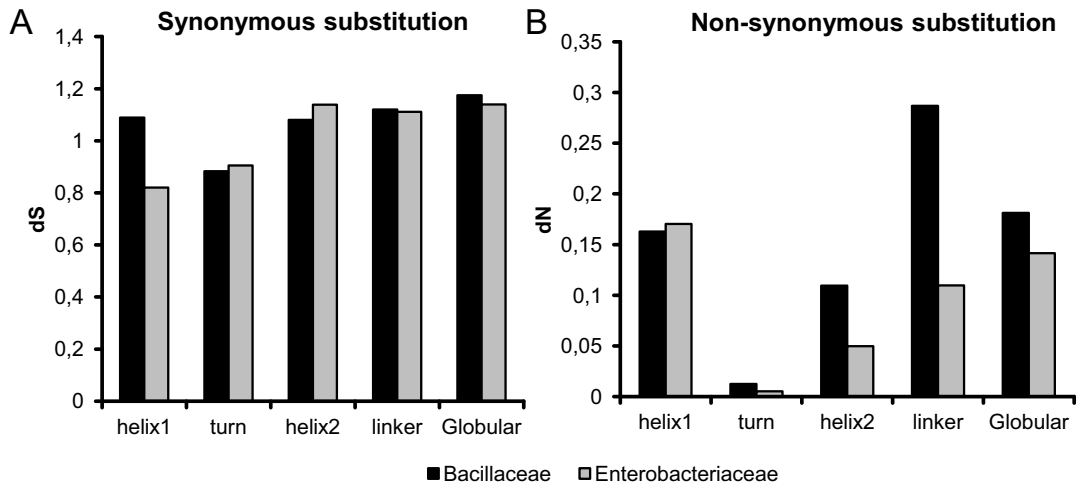

Figure 73: Estimation of average codon-based evolutionary divergence over sequence pairs of *greA* within the Bacillaceae and Enterobacteriaceae is shown. A) The number of synonymous substitutions per synonymous site (dS) from averaging over all sequence pairs within each group is shown. B) The number of non-synonymous substitutions per non-synonymous site (dN) from averaging over all sequence pairs of *greA* within groups is shown.

The rate of synonymous substitutions (dS, **fig. 73A**) is similar between both families in all the zones. Moreover, the dS is around 1, suggesting it occurs in nearly all the predicted sites that could suffer a synonymous substitution. Interestingly, determining the rate of non-synonymous substitutions (dN, **fig. 73B**), it is observed that the turn has a really small dN in both families, suggesting that this domain is highly conserved due the presence of the

residues D41 and E44, responsible of the GreA antipause activity. While in the helix1 and the globular domain both families had a similar dN, in the linker the dN of Bacillaceae is 2.5 fold higher than Enterobacteriaceae. In Enterobacteriaceae, where a higher amount of proteins that bind into the secondary channel is found, the linker domain is more conserved than in Bacillaceae, where only GreA is found. It was also observed that the helix2 suffer differences in the amount of non-synonymous substitutions when comparing between bacterial groups, suggesting that the evolution of helix2 it is also influenced by the pressure produced for the presence of other factors that bind into the secondary channel. This let us suggest that the presence of a competition between the different factors that bind into the secondary channel in the Enterobacteriaceae family, directed the evolution of the gene *greA* in order to conserve its ability to efficiently interact with the RNApol and consequently having ability to compete for the binding with the secondary channel. Moreover, the conservation of the linker that bind the coiled-coil and the globular domain of GreA, highlights the possibility that GreA could suffer conformational changes in order to compete for the secondary channel of the RNApol.

4.7. Effect of ppGpp and DksA in the gene expression profile of *Salmonella*

In our group, the finding that GreA may play a crucial role in the control of the expression of colonization factors in *E. coli* (strain MG1655), such as type 1 fimbriae and flagella, was found when studying the effect of ppGpp and DksA deficiencies in the gene expression profile. The finding of genes that were differentially expressed, being importantly upregulated in the *dksA* mutant strain, and downregulated in the $ppGpp^0$ strain, let us to predict that the upregulated genes in absence of DksA rather than be result of a role of DksA as a repressor, was consequence that in the absence of DksA, the no occupancy of the secondary channel of the RNApol might promote binding of another proteins which will be inducing the expression of those specific genes. Consistent with this model, the upregulation in a *dksA* mutant was abolished in the absence of GreA. Having in consideration that in *E. coli* the two genetic elements found to be sensitive to the interplay of proteins interacting with the secondary channel of the RNApol were colonization factors, we decided to perform studies to determine, using pathogenic bacteria, the impact in the global expression profile of the interplay among secondary channel interacting factors. The model organism chosen to perform those studies was *Salmonella enterica* serovar Typhimurium. Similarly to the studies performed in *E. coli*, the effect of ppGpp and DksA on the gene expression pattern of *Salmonella* was determined. Little is known about the effect of DksA on gene expression regulation in *Salmonella*. However, it has been described, using transcriptomic approaches, that ppGpp stimulates the expression of the virulence genes encoded in SPI1 and SPI2 (Thompson *et al.*, 2006), and by RNA-seq that ppGpp plays an important role modulating the stationary phase gene expression pattern (Ramachandran *et al.*, 2014). In the latest work it was shown that during late-stationary phase, the alarmone ppGpp represses (more than 4-fold) 511 transcriptions start sites (TSS) and stimulates 96 TSS (more than 4-fold).

In this work, transcriptomic studies have been used to determine the role of ppGpp and DksA in the expression pattern of *Salmonella enterica* serovar

Thypimurium SV5015 strain grown in LB at 37ºC up to early-stationary phase (OD_{600nm} of 2.0). The microarray used was a costume DNA microarray engineered by NimbleGen, containing probes for the chromosomal genes and for the genes from the different plasmids that carry the strain SV5015, pSLT, pCol1B and pSRF1010. It was considered that the genes significantly affected are those with a fold change between 3 and -3. Comparing mutant strains with WT strain, genes with a fold-change inferior to -3 are down-regulated in WT and consequently are genes that are directly or indirectly stimulated by the corresponding factor. On the other hand, genes with a fold-change higher than 3 are up-regulated and consequently are genes that are directly or indirectly repressed by the specific regulatory factor. The amount of genes down-regulated and up-regulated by ppGpp and DksA is indicated in the **table 11**.

	$ppGpp^0$	*dksA*	
Down-regulated (%)	286 (6)	258 (5.5)	SV5015 genes: 4735
Up-regulated (%)	109 (2.3)	252 (5.3)	
Total (%)	395 (8.3)	510 (10.8)	

Table 11: Distribution of genes affected by ppGpp and DksA. In parenthesis is indicated the percentage of genes affected.

As described on **Table 11**, similar amount of genes were affected by ppGpp (8.3%) and DksA (10.8%). In a ppGpp deficient strain, 72% of the genes affected are down-regulated, highlighting a general stimulating role of ppGpp. These results differed from the ones described by Ramachandran *et al.*, (2014), while they describes ppGpp as a repressor, we showed that it acts as stimulator. Both experiments were performed in LB, but at different growth curve phases: our experiment was performed at early-stationary phase, while their experiment was performed at late-stationary phase. It has been described that the response of bacteria to ppGpp in discontinuous cultures become more drastic through the time (Traxler *et al.*, 2011). The concentration of ppGpp increases gradually and the effect of the gene expression pattern become more and more drastic. Therefore, the difference between Ramachandran *et al.*, (2014) data and our data may be explained for the differences in the physiological stat of the cultures. When looking in a *dksA* deficient strain, the same amount of genes was up-regulated as well as down-regulated.

Comparing these results with the ones obtained in *E. coli* (Aberg *et al.*, 2009), the amount of genes affected by ppGpp in *Salmonella* and *E. coli* were 395 and 265, respectively, while in absence of DksA, in *Salmonella* and in *E. coli* were 510 and 311, respectively. The main difference was observed in the amount of genes that were stimulated by DksA (258 in *Salmonella vs.* 81 in *E. coli*), suggesting that the stimulatory effect of DksA would be more important in *Salmonella* than in *E. coli*.

In order to determine if the affected genes were distributed uniformly among the whole chromosome or in clusters, the M-value (log_2 fold change) of all the chromosomal genes were represented in a circular chromosomal diagram as shown in **figure 74**. We could observe that ppGpp and DksA affect genes spread throughout the chromosome, highlighting that these factors are global regulators of *Salmonella* as well as in *E. coli*. Nevertheless, discrete accumulation of genes affected either by ppGpp and DksA were detected (**fig. 74**), those clusters of genes that are stimulated by ppGpp and DksA (**fig. 74** in orange), are HGT genes, such as Pathogenesis islands, bacteriophages, and the operon *cob*/*pdu.*

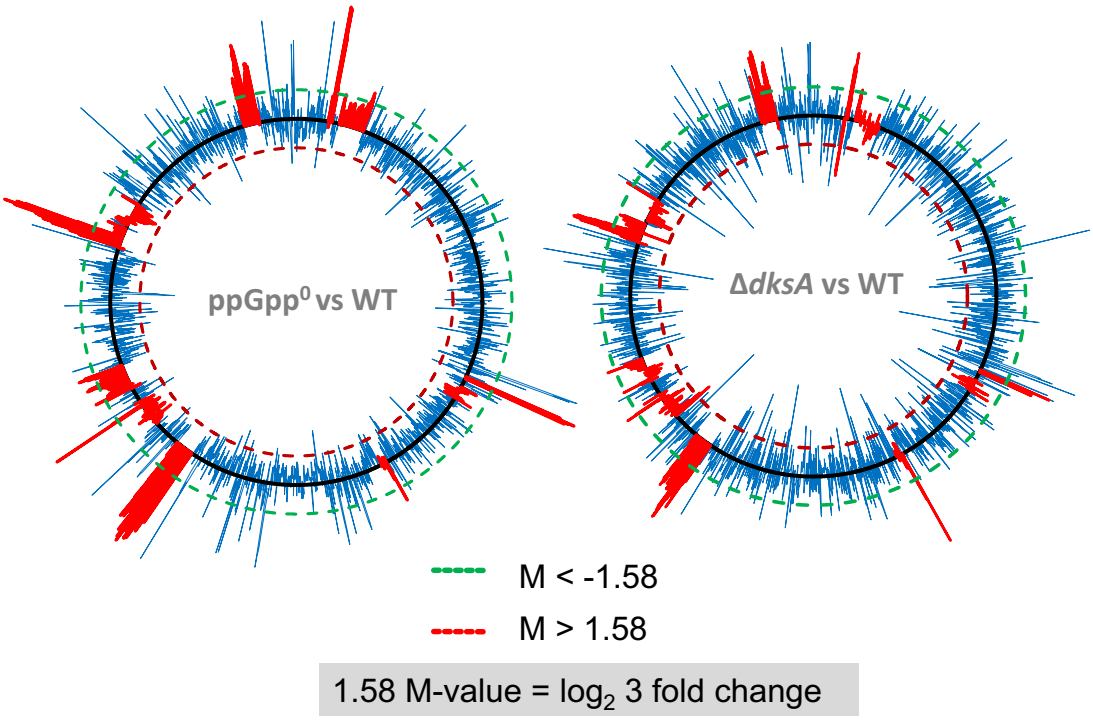

Figure 74 M-value (log_2 fold-change) of each gene from *Salmonella* genome. Dashed lines show the significance threshold. HGT genes are shown in red.

In this work, we considered HGT genes those genes present in plasmids, pathogenicity islands, bacteriophages and the operon *cob/pdu,* making a total of 603 genes. Consequently the amount of core genome genes is 4132. When the amount of genes affected by ppGpp and DksA were distributed according if they are HGT or core genome (**table 12**). The results indicate that the alarmone ppGpp and DksA affect both genes considered as HGT and core genome (**table 12**). When considering the genes of the core genome, ppGpp stimulates 4% of the genes and it represses a 2.6% indicating a more important role as stimulating gene expression than repressing.

		ppGpp	**dksA**	**Nº of genes**
Core genome	Down-regulated (%)	166 (4)	171 (4.1)	4132
	Up-regulated (%)	109 (2.6)	240 (5.8)	
	Total (%)	275 (6.6)	411 (9.9)	
HGT	Down-regulated (%)	120 (19.9)	87 (14.4)	603
	Up-regulated (%)	0	12 (2)	
	Total (%)	120 (19.9)	99 (16.4)	

Table 12: Amount of genes affected by ppGpp and DksA belonging to either the core genome or the HGT DNA. In parenthesis the percentage of the genes affected is shown.

Under the experimental conditions used, ppGpp stimulates the expression of up to 20% of HGT genes. All HGT genes affected by ppGpp are down-regulated, meaning that ppGpp is a regulatory molecule required for the expression of most HGT genes. These data let us suggest that ppGpp may act as a trigger factor for the expression of the expression of HGT genes in *Salmonella*. It was observed that DksA stimulates 4.1% of the core genome genes and it represses 5.8%. In contrast to what it was observed for ppGpp, DksA represses more genes that stimulates. DksA has also an important role in modulating the expression of HGT genes, since it affects a 16.4% of the HGT genes. Despite being mostly a stimulator factor like ppGpp, most probably acting simultaneously, it represses 12 of the 99 HGT genes affected by DksA (**table 12**).

4.7.1. Effect of ppGpp and DksA in core genome gene expression

The alarmone ppGpp and its cofactor DksA are master regulators in *Escherichia coli,* responsible of the stringent response – a very significant rearrangement of the gene expression profile during stress situations (Cashel *et al.*, 1996; Magnusson *et al.*, 2005). As described in section 1.2.2.1, during stringent response, ppGpp together with DksA represses stable RNA and ribosomal proteins, elongation factors, fatty acids and lipids synthesis, cell wall synthesis, and DNA replication. By contra, it stimulates universal stress proteins, amino acid biosynthesis, proteolysis and activation of the *rpoS* regulon, including glycolysis, stasis survival, oxidative and osmotic stress survival genes (Cashel *et al.*, 1996; Magnusson *et al.*, 2005). The effect on gene expression of ppGpp and DksA has been mostly studied when stringent response is elicited by amino acid starvation. Those growth conditions are different from the experimental conditions used in this report. We grew bacteria in a rich complex media, LB, containing a high concentration of peptides, up to the interphase between exponential and stationary phase.

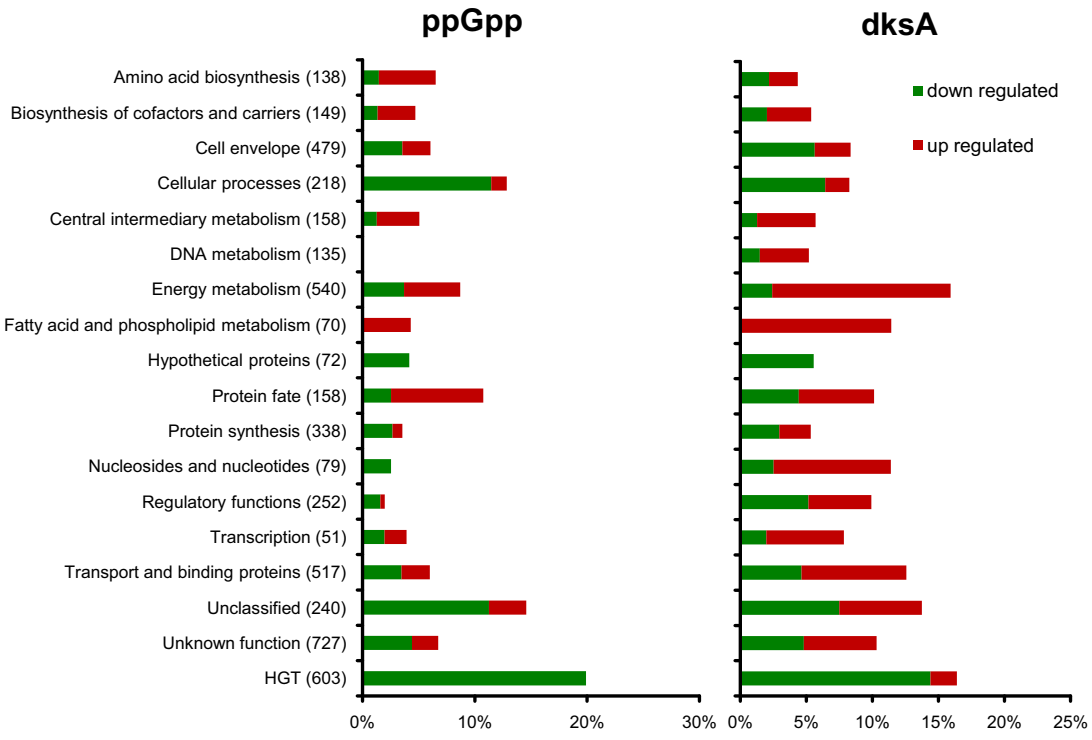

Figure 75: Distribution of the ORF affected by ppGpp and DksA in different functional categories according the JCVI distribution (Torrieri *et al.*, 2012). The down-regulated genes are shown in green and the up-regulated genes are shown in red.

In order to determine the effect of ppGpp and DksA in the expression of core genome genes, the ORFs with expression altered more than threefold were distributed into different functional groups (**supplementary table**) and presented as percentages of the total number of ORFs represented in the DNA microarray (**fig. 75**). Functional classification was performed according the functional classification of the ORF of *Salmonella enterica* serovar Typhimurium LT2 in the JCVI classification (Torrieri *et al.*, 2012).

The genes affected by ppGpp and DksA are distributed among the different functional groups. The functional groups with a higher amount of genes affected correspond to HGT category, being the genes mainly stimulated by both ppGpp and DksA.

Apart of the HGT genes, the functional classes with higher percentage of genes stimulated by ppGpp (**fig. 75**) are cellular processes (11%). Most genes affected are involved in motility and chemotaxis, biofilm formation and survival, among others (**supplementary table**). The group of unclassified genes contains a high number of genes stimulated (11%) that correspond to secreted proteins involved in virulence of *Salmonella,* among others.

By contra, the categories with higher percentage of genes repressed by ppGpp (**fig. 75**) are: i) protein fate (8%) that involve several chaperones such as *dnaK* or *ibpB* and proteases such as *lon* or *clpB,* indicating that protein turnover might be affected; ii) amino acid biosynthesis (5%) that will be further discussed below; and energy metabolism (5%), involving several cytochrome and the respiratory nitrate reductase chain (**supplementary table**). However, any gene of the category of genes related with DNA metabolism was affected by ppGpp neither repressing nor stimulating.

When observing at the categories with a higher percentage of genes affected by DksA (**fig. 75**). The categories that are stimulated by DksA in a higher percentage of genes are i) cell envelope (6%), stimulating different types of fimbriae such as type 1, curly or *saf* fimbriae; ii) cellular processes (6%), stimulating multidrug resistant proteins, and genes that are important for the response to oxidative stress; and iii) unclassified proteins (8%) (**supplementary table**). However, the categories repressed by DksA are energy metabolism

(14%), fatty acid and phospholipids metabolism (11%) and nucleotides biosynthesis (9%) such as the operon *pyrBI* or the gene *ndk*.

Comparing the effect of ppGpp and DksA (**fig. 75**), apparently similar behaviour was observed with both factors, as observed a similar pattern in amino acid biosynthesis, cellular intermediary metabolism and protein fate. However, there are other categories which are differently regulated by ppGpp and DksA, such as DNA metabolism that while none of the genes are affected by ppGpp, some operons such as *pyrBI* are repressed by DksA (**supplementary table**). Other functional categories with a differential regulation pattern for ppGpp and DksA comprise energy metabolism, where significantly more genes are repressed by DksA than by ppGpp; or regulatory functions, where few genes are stimulated by ppGpp (2%), whereas DksA affect in the expression of a higher number of genes of regulatory proteins (10%).

Comparing the functional categories affected by ppGpp and DksA in *E. coli* and *Salmonella* (Aberg *et al.*, 2009), some similarities were observed. In both species, the most stimulated categories by ppGpp are cellular processes and energy metabolism. However, an important divergence between *Salmonella* and *E. coli* in the effect of ppGpp and DksA in the category of cellular processes was observed. In *E. coli* the genes of this category, that were stimulated by ppGpp and repressed by DksA (Aberg *et al.*, 2009). Those were genes involved in motility and chemotaxis (Aberg *et al.*, 2009). However, in *Salmonella* the genes involved in motility and chemotaxis, as discussed more in detail below, are not differentially regulated by ppGpp and DksA as observed in *E. coli.*

Considering that the alarmone ppGpp is responsible of the stringent response during amino acid starvation, it would be expected an effect of ppGpp on amino acid biosynthetic genes. However, as the bacteria were grown in a rich media (LB) which contains high concentration of amino acids and peptides, no induction of amino acid biosynthesis would be expected. In *Salmonella*, our data indicate that ppGpp stimulates the *opp* and *dpp* operon, coding for oligo-dipeptid transporters (Pearce *et al.*, 1992; Wu and Mandrand-Berthelot, 1995), and the *sfbABC* operon coding for a methionine ABC-transporter (Pattery *et al.*, 1999), as can be seen in **supplementary table**. In general the expression of

metabolites transporters is increased, for peptides and amino acids, as the oligopeptid and amino acid transporters, previously mentioned, as well as sugar transporters such as maltose, melobiose or fructose. This increase on the amount of transporters was also observed in *E. coli* (Aberg *et al.*, 2009).

The biosynthetic pathways of Valine and Leucine (*ilvNB* operon) were up-regulated in absence of ppGpp in *Salmonella* (**fig. 75**). The expression of *ilvNB* is attenuated by a leader peptide (*ivbL*) that senses Valine or Leucine (Friden *et al.*, 1982). Taking in account that i) no effect was observed in the expression of the peptide leader by ppGpp and ii) ppGpp stimulates amino acids intaking from the medium, it is feasible that the ppGpp effect on the *ilvNB* operon is not direct. It might be the collateral effect due to the induced amino acids intake.

It has been described that both ppGpp and DksA represses stable RNA in *E. coli* (Cashel *et al.*, 1996; Paul *et al.*, 2004; Magnusson *et al.*, 2005). While we do not observe any effect on ribosomal proteins such as *rplQ* or *rplR*, as observed in *E. coli* by Traxler *et al.* (2008), a ppGpp-mediated repression on *rbfA*, essential for 16S processing (Bylund *et al.*, 1998) was observed in *Salmonella*. Moreover, a repression of several proteins involved on the modification of some nucleosides located in the D and T arms of tRNA, such as *trmH* and *truB*, was detected (protein synthesis in **fig. 75, supplementary table**). These modifications are necessary for the stability of tRNA, especially at high temperature, as well as the translation of certain codons (Urbonavicius *et al.*, 2002).

As shown in **figure 75** the metabolism of fatty acid is repressed by ppGpp, as well as by DksA. The genes responsible of fatty acid degradation *fadAB* (Yang *et al.*, 1990) are repressed by both factors. DksA also repress other genes related with the degradation of fatty acid, such as *fadH* and *caiA*. Our data suggest that ppGpp promotes the accumulation of fatty acid, while in *E. coli* (Magnusson *et al.,* 2005) it was shown that ppGpp represses fatty acid biosynthesis. Once again these discrepancies could be explained due that our results were obtained in rich media.

In *E. coli* it has been described that ppGpp stimulates the RpoS (σ^S) regulon (Traxler *et al.*, 2008). In fact it has been suggested that ppGpp is able to

modulate the competition between the alternative σ subunits to bind to the core of the RNApol (Magnusson *et al.*, 2005). The alternative σ^S subunit promotes expression of genes involved in survival and adaptation to several stress conditions. In *Salmonella*, no effect was detected on the *rpoS* expression (**supplementary table**) but in the expression of RpoS dependent genes. The alarmone ppGpp stimulates the expression of genes such as *katE* and *katN*, involved in oxidative stress (Mishra and Imlay, 2012), *qtxAB* coding for the cytochrome D ubiquinol oxidase (Borisov *et al.*, 2011) and several genes coding for unknown proteins such as *ymdF*, *yciG* or *ygaO*.

It has been described that ppGpp is required for dimerization of SlyA (as discussed in section 1.2.2.4). SlyA involved in the PhoP-PhoQ regulation and it has been shown that some of the genes regulated by ppGpp are *pag* genes, "PhoP/PhoQ activated genes". PhoP/PhoQ is a two components system which responds to different environmental signals including low-Mg^{+2}, acidic pH and cAMP (Zhao *et al.*, 2008). PhoP-PhoQ controls the expression of a large number of genes expressed during intracellular infection of macrophages and genes involved in apoptosis delay after *Salmonella* infection (Guiney and Fierer, 2011). SlyA, which expression is stimulated by PhoP-PhoQ, binds to the promoter of the target genes after forming a dimmer. No effect was observed in the expression of *slyA* by ppGpp or DksA (**supplementary table**), but when looking at the genes of the SlyA regulon it was determined that 16 of the 26 genes stimulated by SlyA (Zhao *et al.*, 2008) are stimulated by ppGpp while 2 of the 8 genes repressed by SlyA, are repressed by ppGpp. A similar effect was observed when looking at the effect of DksA. These data suggests that ppGpp and DksA are necessary for the stimulation of the SlyA regulon.

Several phenotypes presumably associated to genes whose expression is significantly altered in ppGpp or DksA have been further studied.

4.7.1.1. Response to low temperature

The expression of the *cspB* gene is down-regulated in absence of ppGpp but it is not affected by DksA (**supplementary table**). CspB is required for the response to low temperatures, also known as cold shock (Lee *et al.*, 1994; Ivancic *et al.*, 2013). The effect of ppGpp and *dksA* deficiency in the ability to

grow at low temperatures was used. The strain SV5015, and its derivative mutant *dksA* and ppGpp^0 were grown in LB at 37ºC and 20ºC and its growth rate and generation time was determined. While at 37ºC the three strains (WT, *dksA* and ppGpp^0) had the same generation time (23, 25 and 26 minutes, respectively), at 20ºC the generation time of the ppGpp^0 strain (108 min) is significantly higher than in WT or *dksA* (87 and 90 minutes respectively). These data are consistent with a role of ppGpp in the stimulation of *cpsB* expression.

4.7.1.2. Response to oxidative stress

The effect of ppGpp and DksA on the response to oxidative stress was determined (**fig. 76A**). The strains SV5015 (WT) and its derivative mutants ppGpp^0 and *dksA* were grown in LB at 37ºC up to an OD_{600nm} of 2.0 and treated with 0 and 0.5% of t-BOOH, an oxidizing agent (Yoon *et al.*, 2002), during 1 hour at 37ºC. After the oxidative stress induction, the viable count was determined (**fig. 76A**).

The treatment with 0.5% of t-BOOH causes a decrease in the cell viability (**fig. 76A**). The strains deficient in DksA and ppGpp were more sensitive to the oxidative stress than the WT strain. The ppGpp deficient strain suffers a dramatic reduction of survival to oxidative stress compared with both WT and *dksA* strains. Those results may be explained by the expression level of several genes involved in the oxidative stress.

Gene	ppGpp vs. WT	dksA vs. WT
katE	-3,08	1.48
katN	-2,93	-1,43
uspB	-2,10	-1,26
uspA	-2,11	1,26
ahpC	-2,04	-2,47
sodC1	-2,38	-1,21
sodC	-2,36	-1,18

Table 13: Effect of ppGpp and DksA on different genes related with oxidative stress response.

Genes, such as *katE*, *ahpC* (Mishra and Imlay, 2012), *sodC* (Rushing and Slauch, 2011) and the *usp* genes (Seifart Gomes *et al.*, 2011), involved in

oxidative stress response, are stimulated by ppGpp. While ppGpp stimulates all the genes listed in **table 13**, DksA stimulates *ahpC*.

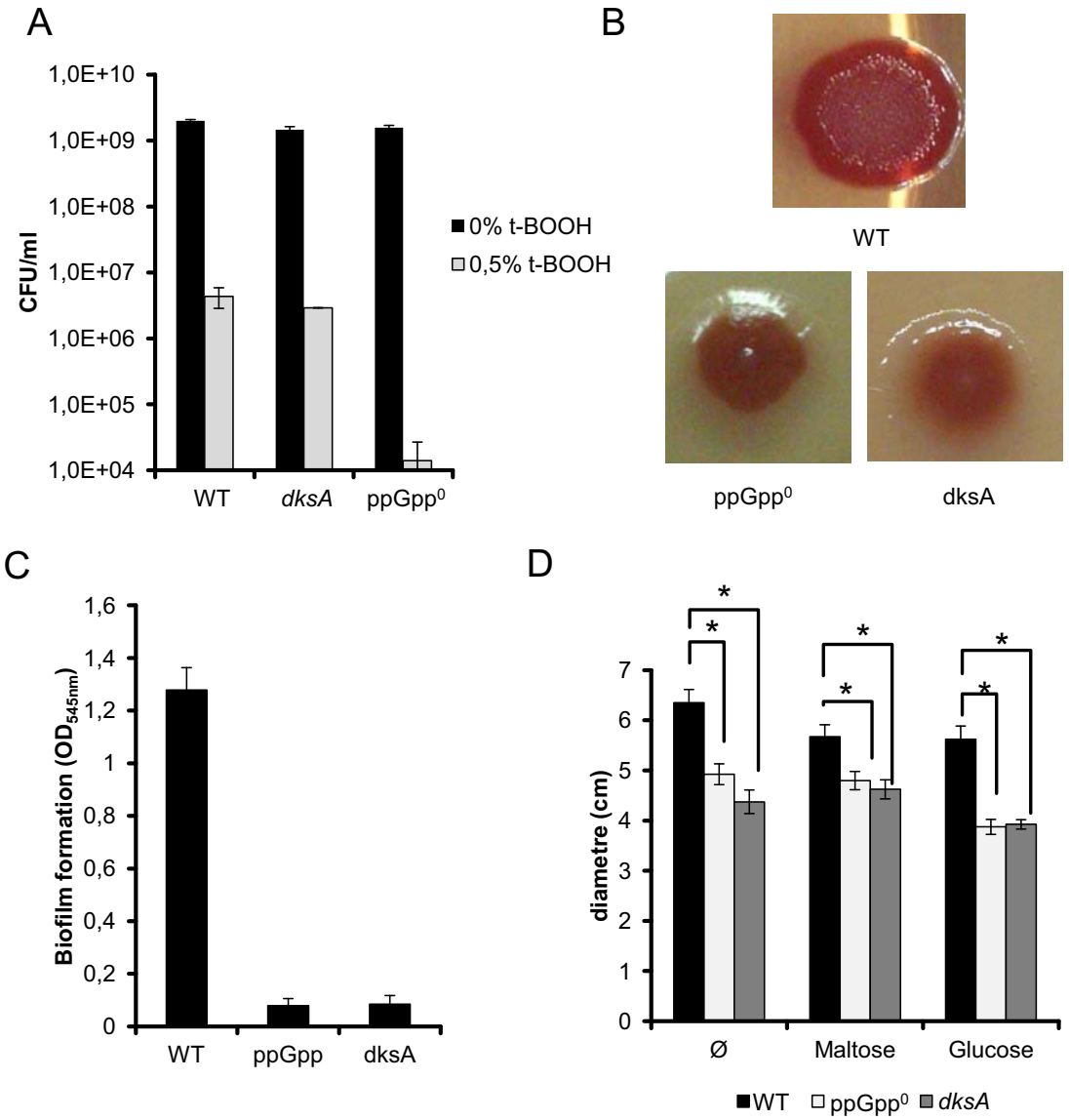

Figure 76: Effect of ppGpp and DksA on several phenotypes in *Salmonella enterica* serovar Typhimurium SV5015. A) Effect of ppGpp and DksA on the response to oxidative stress. The strain SV5015 and its derivatives ppGpp^0 and *dksA* were grown in LB at 37ºC up to an OD_{600nm} of 2.0 and treated during 60 minutes with t-BOOH at a final concentration of either 0 or 0.5%. After the treatment, the cfu/ml on LB plates was determined. B) The strain SV5015 and its derivative ppGpp^0 and *dksA* were grown on CFA-CR plates at 28ºC. After 7 days the R-DAR morphotype was observed. C) The strain SV5015 and its derivatives ppGpp^0 and *dksA* were grown in CFA at 25ºC during 48 hours, and the biofilm formation was determined as described in Aberg *et al.*, (2006). D) The strain SV5015 and its derivatives ppGpp^0 and *dksA* were grown on motility agar plates without chemo-attractants (ø) or supplemented with either maltose or glucose at a final concentration of 2mM as chemo-attractant. Plates were incubated at 37ºC during 5 hours. * means p-Value < 0.01.

These differences could be the reason to explain that the ppGpp^0 strain is more sensitive to oxidative stress than the *dksA* strain (**fig. 76A**). It is also important to highlight that while initially was considered the significance threshold at 3 / -3, perhaps it is excessive when looking a specific gene. As it is observed, 2-fold differences in the expression of some genes may have significant effect in the physiology of the cell (**table 13**).

4.7.1.3. Effect of biofilm and motility

In *Salmonella,* several core genome genes code for proteins that are involved in cellular functions that may be pivotal for the ability of *Salmonella* to cause infection. Genes involved in the synthesis of flagella and therefore in the bacterial motility and genes involved in biofilm formation may have a significant impact in the ability to colonize and cause clinical infections, respectively. The effect of ppGpp and DksA in the ability to form biofilm and the motility was determined.

One of the main structures involves in the biofilm formation in *Salmonella* are curlied fimbriae, also known as curli, and cellulose. Although other factors such as the flagella are involved (Serra *et al.*, 2013). As could be observed in **table 14** the expression of the different genes related with the curli synthesis are down-regulated in both ppGpp^0 and *dksA* strains. Interestingly, while some genes seem to be stimulated by both factors, such as *csgF*, other genes are only stimulated by one of the factors, such as *csgG* or *csgA*.

Gene	ppGpp vs. WT	dksA vs. WT
csgG	-1,23	-2,40
csgF	-2,42	-3,23
csgE	-2,05	-2,07
csgD	-2,40	-2,72
csgB	1,06	-1,03
csgA	-3,50	-1,69
csgC	-1,27	-1,24

Table 14: Effect of ppGpp and DksA on the different genes coding for curli.

To study the effect of ppGpp and DksA on biofilm formation, the RDAR phenotype of the strain SV5015 (WT) and the derivatives ppGpp^0 and *dksA* was

determined (**fig. 76B**). Colonies grown for several days on agar surfaces can adopt elaborate a three-dimension complex that have been termed as RDAR phenotype, since are red, dry and rough colonies in CFA-CR plates. The RDAR phenotype is indicative of production of curli and cellulose (Simm *et al.*, 2014). After 7 days at 28ºC, SV5015 is able to produce RDAR colonies (**fig. 76B**) showing that it is able to produce biofilm factors in these conditions. However, the strain deficient in ppGpp and DksA are not able to produce R-DAR colonies. Moreover the ability to form biofilm in plastic surfaces was determined (**fig. 76C**) as described in Aberg *et al.* (2006). The formation of biofilm after 48h in CFA at 25ºC decreases dramatically in absence of DksA and ppGpp, suggesting that both factors are essential for the formation of biofilm under these conditions. It is important to mention that the transcriptomic study was performed in LB at 37ºC while the biofilm assay were performed in CFA (medium with low amount of salt) at 25ºC/28ºC. This could be the reason why we do not detect such important effect of ppGpp and DksA on the transcription of the different genes related with biofilm formation, while we observe a clear effect in the phenotype at low temperature.

The flagella genes are divided in different operons with an important hierarchy. We had also shown (section 4.3) that ppGpp stimulates the expression of flagella genes in *E. coli.* In *Salmonella*, several flagella and chemotaxis genes are stimulated by ppGpp, such as the master regulator *flhDC*, as well as phase-2 flagellin (fljB) and chemotaxis genes (**supplementary table**). In *E. coli* the expression of flagella genes were increased in absence of DksA presumably due the binding of GreA into the secondary channel of the RNApol (Aberg *et al.*, 2009). In *Salmonella* this effect is observed in few genes, such as *fliE*, *flgA, trg* or *aer*. In absence of DksA a down-regulation of some genes involved in chemotaxis, such as *cheR* or genes involved on the basal body formation *fliPQR,* was observed. The motility of the strain SV5015 and the derivative mutant $ppGpp^0$ and *dksA* strain on motility plates without chemo-attractants or with either maltose or glucose (2 mM) was monitored at 37 (**fig. 76D**). The motility of the strain $ppGpp^0$ and *dksA* decreases compared with the WT strain. Therefore the control of flagella genes in *Salmonella* differ from *E. coli* regarding the effect of *dksA* mutation.

4.7.2. Is ppGpp a gene usher?

Focusing on the effect of ppGpp and DksA on HGT, we could observe that both factors act as activators of HGT. There are no genes repressed by ppGpp and only 12 of 99 HGT genes were repressed by DksA. Being a 12% of the *Salmonella* genome, HGT represent a 42% of the genes stimulated by ppGpp and 34% by DksA. HGT genes were classified, depending of its origin, in the following categories (**figure 77**): SPI (from 1 to 5), phages (Gifsy1 and 2, Fels-2, P4-like, remnant inactive prophage and SLP203), genomic islands (*cob, pdu*) and plasmids (pSLT, pCol1B and pSRF1010).

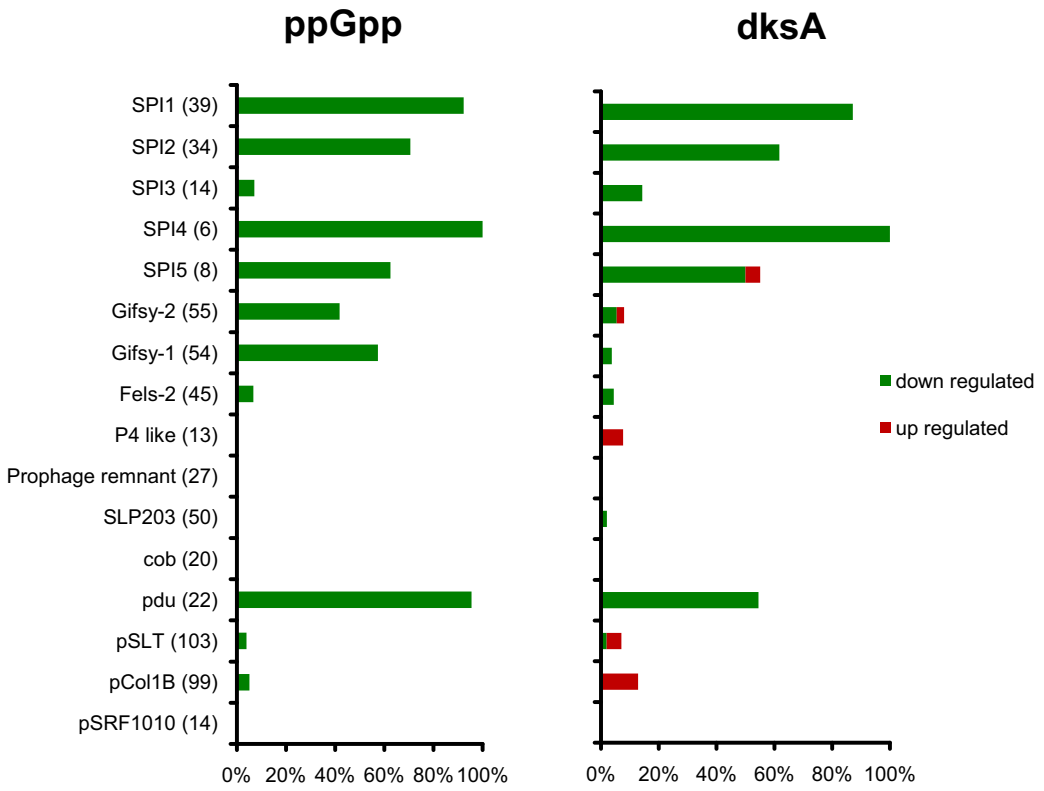

Figure 77: Distribution of the HGT genes affected by ppGpp and DksA in different categories, depending on its origin (SPIs, plasmids, phages or genomic islands).

As seen in **figure 77**, the factors ppGpp and DksA strongly stimulates the genes present in the pathogenicity islands, as well as the *pdu* operon (**fig. 77**). The alarmone ppGpp stimulates also genes from bacteriophages and plasmids, although to a much lower extent. It is remarkable that several genes are repressed by DksA, genes encoded in bacteriophages, plasmids and the SPI5.

These data strongly suggest that ppGpp stimulates genes acquired by horizontal gene transfer. We could consider an infection as a process where bacteria need to adapt to continuous environmental alterations during its transit through the host organism. Therefore the virulence genes could be understood as a response to these environmental changes that, as other stress response genes, are under the control of ppGpp and DksA.

It is astonishing that genes present in several genetic elements such as plasmids, SPIs or bacteriophages carry modules that allow regulation by chromosomal-encoded regulatory mechanisms to control its expression and ensure its proper expression at the correct moment. Those modules may have been organized during evolution to avoid that the mobile genes could cause a deleterious effect in the fitness of bacterial cells.

Further studies have been performed in the effect of ppGpp and DksA on HGT genes.

4.7.2.1. Effect of ppGpp and DksA on SPIs genes expression

It has been described that ppGpp is required for the stimulation of genes encoded in SPI1 and SPI2 (Thompson *et al.*, 2006). Our results showed that ppGpp is required for the expression of most genes encoded in the SPIs except SPI3 (**fig. 78A**). Moreover, a clear effect of DksA is also observed in the expression of most of the genes present in SPI1, 2, 4 and 5

Although ppGpp and DksA affects similarly the SPI's genes (**fig. 78A**), there is a higher effect on SPI1, 4 and 5 in absence of ppGpp than in absence of DksA. Both factors regulates same amount of genes but in absence of ppGpp the expression of these genes is down-regulated to a higher extent than in absence of DksA. Considering that these SPIs are related with epithelial invasion, we might suggest that ppGpp could have more effect on modulation of epithelial invasion than DksA. It was observed that both factors, ppGpp and DksA, regulates in a similar way the SPI2, involved in macrophages survival. On the other hand, DksA stimulates the gene *mgtC* (**fig. 78A**) that is encoded in the SPI3. The *mgtCB* is important for *Salmonella* pathogenesis, being required for the growth and replication within macrophages (Fàbrega and Vila, 2013).

Regarding SPI5 a differential effect of both factors was detected, DksA represses some genes whereas ppGpp does not and from some genes, ppGpp mediated stimulation was detected. Due the requirement of SPI encoded factors in different steps during infection by *Salmonella.* Our data indicates that ppGpp and DksA are pivotal regulators during different phases of the infection.

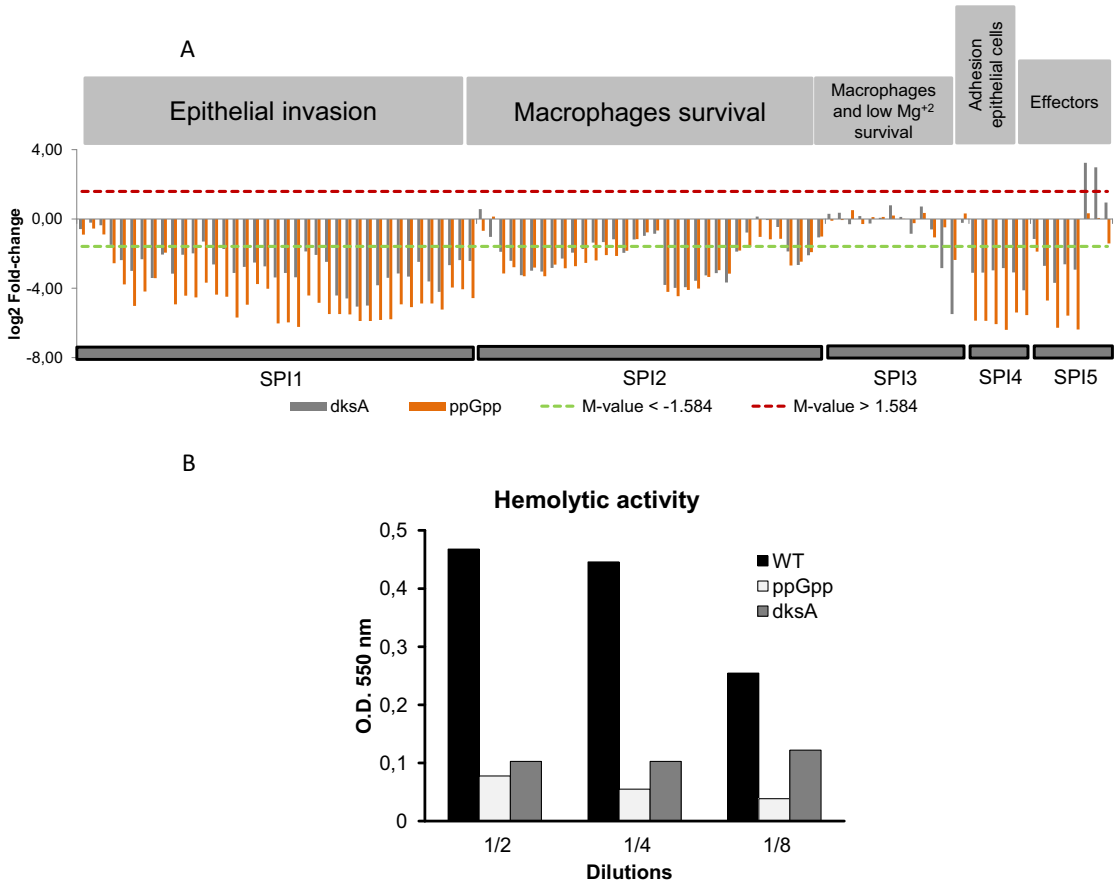

Figure 78: Effect of ppGpp and DksA on the expression of genes encoded in the SPIs. A) M-value in the expression level of the different genes in strains deficient for either of ppGpp or DksA as compared to WT. The 3 / -3 threshold is indicated with dashed lines. B) Haemolytic activity of the strains SV5015 and its derivative ppGpp^0 and *dksA* mutants, measured as described in section 3.9.5.

Our data suggest that ppGpp and DksA are required for expression of cellular invasion and intracellular survival genes. To corroborate that the haemolytic activity of cell-free supernatants from cultures of the SV5015 strain and its ppGpp^0 and *dksA* derivatives was determined. The haemolytic activity is related with the production of the translocator proteins SipB, SipC and SipD proteins, a pore-forming complex that is encoded in the SPI1 and corregulated with the majority of genes encoded in this pathogenicity island (Miki *et al.*, 2004; Field *et al.*, 2008). Different dilutions of cell-free supernatants obtained from cultures of

the different strain grown in LB at 37ºC up to an OD_{600nm} 2.0, were mixed with an aliquot of sheep erythrocytes suspension, and the haemolytic activity was determined measuring the OD_{550nm} after incubation at 37ºC for 2.5 hours (**fig. 78B**). In absence of ppGpp and DksA, the haemolytic activity associated to SipBCD, decreases dramatically, suggesting that these factors are essential for its expression and consequently for cellular invasion.

4.7.2.2. Effect of ppGpp and DksA on bacteriophages genes

It has been described that *Salmonella* contains 5 presumably active bacteriophages: Gifsy 1 and 2 (λ-phage like), SopEΦ (Fels2), P4-like phage and SLP203 (P22-like), and a remnant inactive prophage (Figueroa-Bossi *et al.*, 2001). Transcriptional data shows that ppGpp stimulates a 42% and 57% of the genes of Gifsy 2 and 1 (respectively) phages, as well as a 7% of the SopEΦ (**fig. 77**). However, DksA has a different role; it has a poor effect on these bacteriophages and a repressive effect on P4-like phage genes (**fig. 77**). Among the phage genes affected by ppGpp are some that are essential for the virulence of *Salmonella*, such as *sopE* or *sodC1*, and also genes required for the bacteriophage replication, as *recE* that codes for an exodeoxyribonuclease or genes that codes for proteins of the capside as the minor tail protein U.

For this reason we studied the ability of the strains deficient in *dksA* and ppGpp to produce bacteriophages during inducing and non-inducing conditions. The lytic cycle of bacteriophages is induced by mitomycin C addition to the culture, mitomycin C is a DNA damage agent that trigger the SOS response (Mirold *et al.*, 1999). The strains SV5015 and its derivative $ppGpp^0$ and *dksA* mutant were grown in LB at 37ºC up to an OD_{600nm} of 0.1. Then, cultures were split in two and one of them was induced with 50 µg/ml of mitomycin C, and continuing incubation for either 2 or 6 hours. Phage particles were detected by titration on top agar using two different indicator strains after 18 hours at 37ºC. The strain WG49, used to detect F^+-specific RNA coliphages in water samples (Rhodes and Kator, 1991), whereas the strain MA6247 is used to detect the bacteriophages Gifsy1 and Gifsy 2 (Figueroa-Bossi and Bossi, 1999). The results are shown in the **figure 79**. It is remarkable that SV5015 (WT) is able to produce bacteriophages during its growth in LB at 37ºC up to stationary phase

even in the absence of mitomycin. The amount of phages produced increases significantly by mitomycin C addition. In absence of ppGpp, there is a decrease in the bacteriophage production under induction and non-induction conditions, showing that ppGpp is necessary for appropriated bacteriophage production (**fig. 79**). While in absence of DksA there is no effect on the bacteriophage production, as compared to the WT strain.

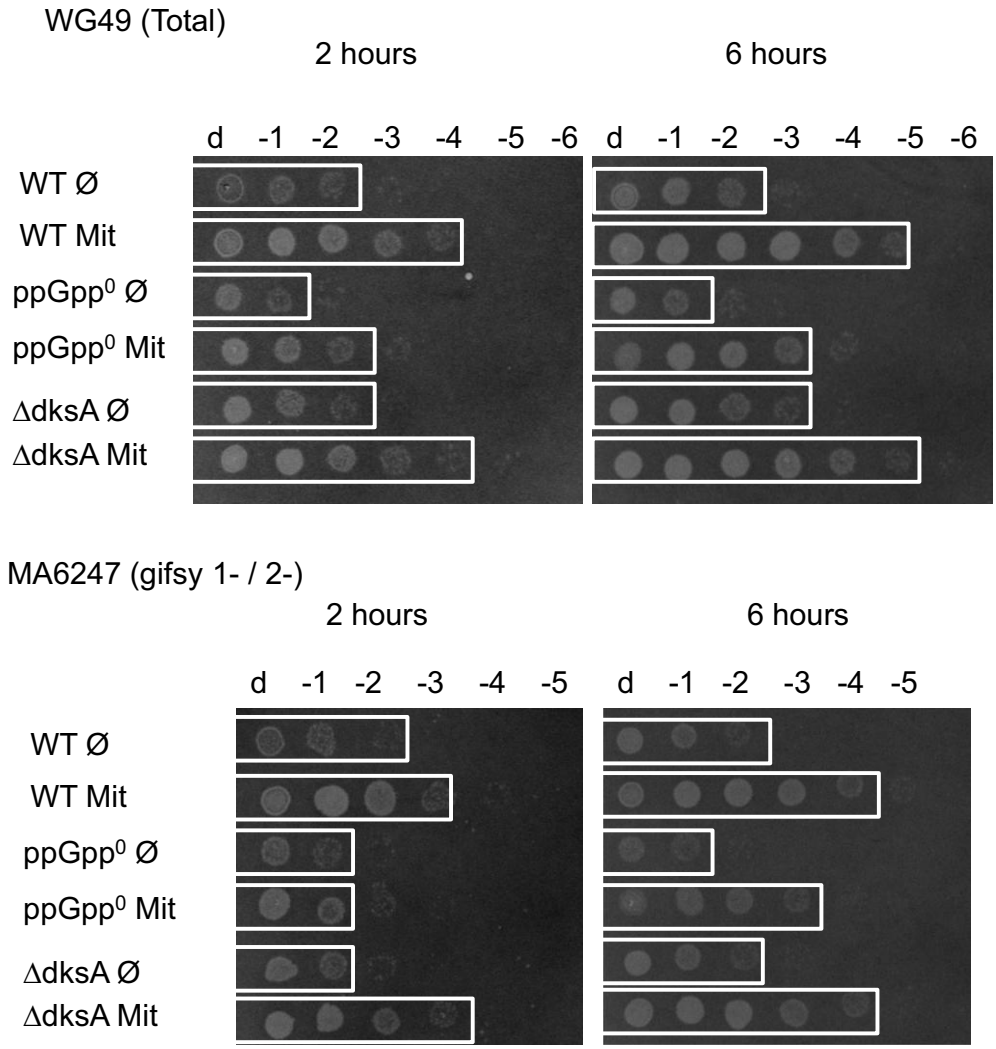

Figure 79: The strains SV5015 and the ppGpp^0 and *dksA* derivative mutants were grown in LB at 37ºC up to an OD_{600nm} of 0.1 and then induced with 50 µg/ml of mitomycin C (Mit) and incubated during 2 and 6 hours. As control, cultures with no addition of mitomycin C (ø) were used. Then, supernatant, containing the bacteriophages released, were diluted and dropped on top agar plates containing different indicator strains (WG49 and MA6247) at 37ºC during 18 hours.

These results (**fig. 79**) are consistent with the transcriptomic data showing that ppGpp affects expression of bacteriophages genes. Suggesting that ppGpp could be important for the movement of genes by natural transduction, where

the DNA is enclosed into capsids and transferred into a new host cell (Penadés *et al.*, 2014).

4.7.2.3. Effect of ppGpp and DksA on *Salmonella* plasmids

Salmonella strain SV5015 contains 3 plasmids: pSLT, pCol1B and pSRF100. While DksA and ppGpp produces non effect on the expression of genes present in pCol1B and pSRF100, ppGpp stimulates the expression of genes from pSLT plasmid (**fig. 80A** and **supplementary table**)

The genes stimulated by ppGpp in pSLT plasmid are the *spvABCD* operon. SpvB and SpvC are effectors proteins secreted by the TTSS from SPI2. SpvB contains an ADP-ribosyltransferase domain that prevents actin polymerization whereas SpvC has phosphothreonine lyase activity and has been shown to inhibit MAP kinase signalling. The exact mechanism of how these effectors enhance virulence is still unclear, but it has been shown that SpvB exhibits a cytotoxic effect on host cells and is required for late apoptosis of infected macrophages (Gotoh *et al.*, 2003; Guiney and Fierer, 2011).

The *spvABCD* is under the control of a σ^S promoter that is stimulated by SpvR. The alarmone ppGpp produced no effect on *spvR* indicating that the effect of ppGpp on *spvABCD* is independent of SpvR, either direct by affecting *spvABC* transcription initiation or indirect due to its effect on σ^S regulon(Gotoh *et al.*, 2003).

In absence of ppGpp and DksA the expression of the gene *traD* is down-regulated. TraD is an hexameric ATPase that forms the cytoplasmic face of the conjugative pore required for pSLT conjugation (Lu *et al.*, 2008), suggesting that both factors could affect the conjugation of pSLT plasmid in *Salmonella*. To determine the role of ppGpp and DksA on pSLT transfer, a conjugation experiment using a pSLT derepressed variant, a *finO* mutant, was used (Camacho and Casadesús, 2002). As a donor the strain SV4522 (WT) and its derivative $ppGpp^0$ and *dksA* mutants were used (**fig. 80B**).

In absence of ppGpp the conjugation rate decreases dramatically and no transconjugants were obtained, suggesting that ppGpp is crucial for pSLT

conjugation (**fig. 80B**). Surprisingly, in absence of DksA similar conjugation rate was observed as for the WT strain.

Our data shows that ppGpp is able to induce virulence factors encoded in the pSLT plasmid, and that it is required for its conjugation. Considering that ppGpp also stimulates bacteriophages production, it might be suggested that this alarmone is required for HGT mobilization or it is able to stimulate it.

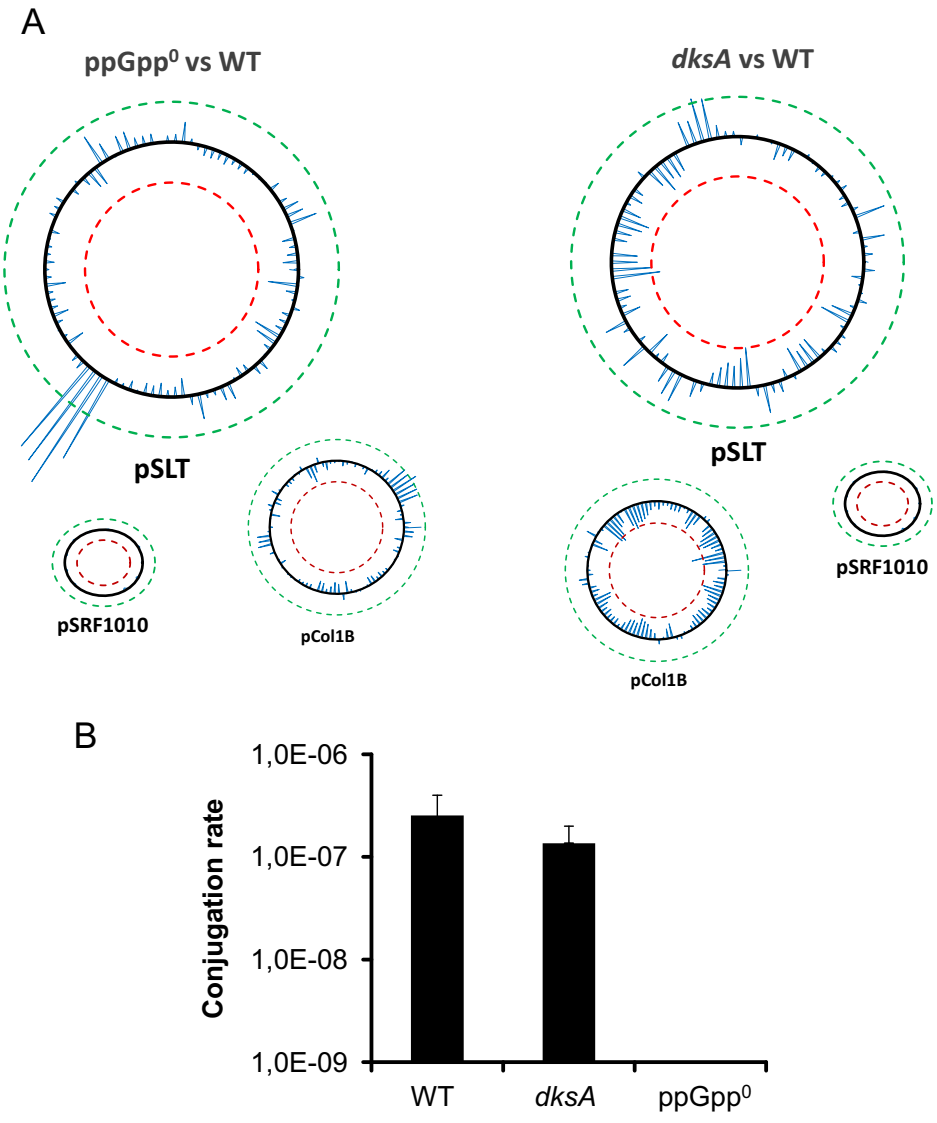

Figure 80: Effect of ppGpp and DksA on genes encoded in *Salmonella* plasmids. A) Representation of the M-value (log_2 fold-change) for each gene of the *Salmonella* plasmids. Dashed lines show the significance threshold (M-value < -1.58 in green and M-value > 1.58 in red). B) Conjugation rate of the strain the strain SV4522 (WT), LFC64 (*dksA*) and LFC63 ($ppGpp^0$). The conjugation assay was performed as described in section 3.7.4.

4.7.2.4. Effect of ppGpp and DksA on *cob/pdu* operon

The *cob* and *pdu* operons are two divergent operons considered HGT that codes for proteins responsible of cobalamin (vitamin B12) synthesis and propanediol degradation (Roth *et al.*, 1996). It has been shown that the pdu operon is important for the *Salmonella* survival into macrophages (Klumpp and Fuchs, 2007).

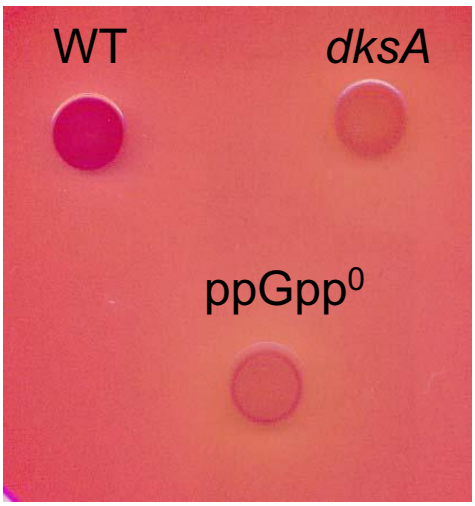

Figure 81: Effect of ppGpp and DksA on *pdu* operon in *Salmonella* Typhimurium. A) Degradation of 1,2-Propanediol by the strain SV5015 and its ppGpp and *dksA* derivative mutants in McConkey supplemented with 0.5% of 1,2-propanediol and 150 nM of vitamin B12 (Goudeau *et al.*, 2013).

As observed in **figure 77** and **supplementary table**, ppGpp and DksA stimulates a major part of the genes that forms the *pdu* operon. To further study the effect of ppGpp and DksA on the *pdu* operon expression, the ability of the SV5015 (WT) as well as the ppGpp^0 and *dksA* mutant strains to use 1,2-propanediol as a carbon source in presence of vitamin B12 was tested. The three strains were inoculated on McConkey plates supplemented with 0.5% of 1,2-propanediol and 150 nM of Vitamin B12 and incubated at 37ºC during 18 hours (**fig. 81**). The WT strain is able to use the propanediol as a carbon source and produces an acidification of the media, producing red colonies. But the strains deficient in ppGpp and DksA were not able to use the propanediol and, consequently, produce white colonies.

4.7.3. Global effect of ppGpp and DksA.

Despite of being described as cofactors, ppGpp and DksA in *E. coli*, it was described that both factors could have similar, independent and opposite effects in gene expression (Magnusson *et al.*, 2007; Aberg *et al.*, 2009). However, it was observed that the opposite effect of DksA and ppGpp on the expression of the flagella and fimbriae genes was dependent of the presence of GreA (Aberg *et al.*, 2008; Aberg *et al.*, 2009).

In this report, we considered significantly affected those genes with a fold-change between 3 and -3, but this would produce a bias. An example of that would be the gene *fruB*, in absence of ppGpp it has a fold-change of -11.58, but in absence of DksA, the fold-change is only of -2.71. With the 3 / -3 threshold, we would classify this gene as independently regulated by ppGpp, whereas it is being stimulated by both factors. For this reason we have considered genes with a fold-change between -1.5 and 1.5. Then, *fruB* is regulated similarly by ppGpp and DksA, but *fucP* (ppGpp^0 -3.82, *dksA* 1.27) it is only regulated by ppGpp. The results are shown in **figure 82**.

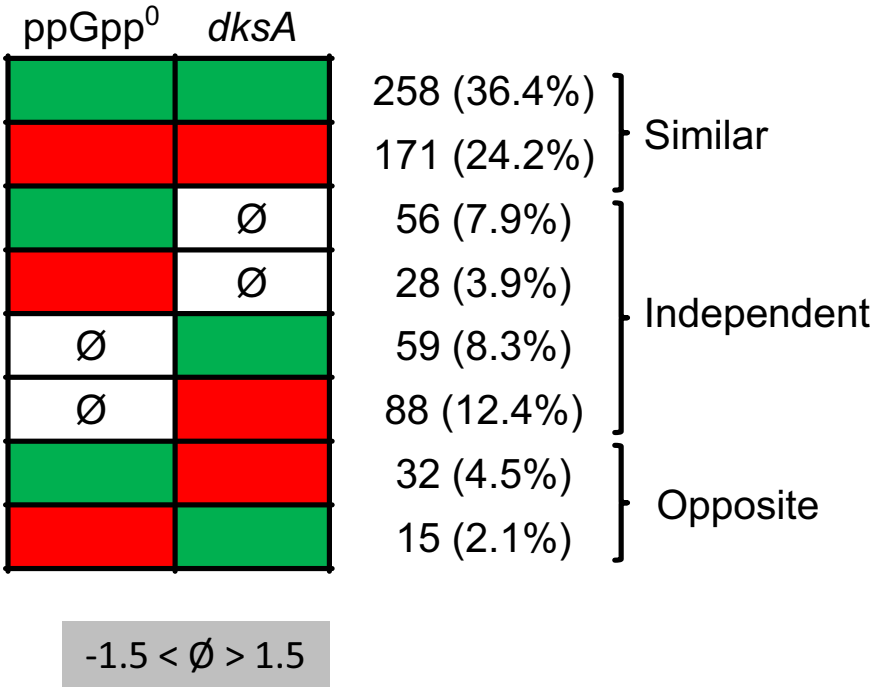

Figure 82: Amount of genes that are regulated in a similar, independent and opposite way between ppGpp and DksA.

From the genes affected by ppGpp and DksA (**fig. 82**), a 61% of the genes are regulated in a similar way by ppGpp and DksA (stimulated and repressed). However a 32% of the genes are affected by one of these factors and not affected by the other factor. Finally, only a 7% of the genes affected by ppGpp and DksA are affected in an opposite way in *Salmonella.* Some of the genes oppositely affected by ppGpp and DksA, are genes from the maltose degradation operon (*malM, E, F, K*), as well as other sugar transporters. But also include the gene that codes for the porine *ompF,* the H-NS-like protein StpA, or the small heat shock protein IbpB. Further studies will be required for determine whether in *Salmonella*, the differential role of ppGpp and DksA might also be a consequence of the vacancy of the secondary channel of the RNApol generated in a *dksA* mutant, and therefore results of promoted interaction by other proteins such as GreA, as it has been proposed in *E. coli*.

4.8. Epilogue: an overview of our contribution to the knowledge of the regulation through the secondary channel of the RNApol

A previous discovery in our research group, indicating that the phenotype of ppGpp and DksA deficiencies were not always identical (Aberg *et al.*, 2009), let us to show that the occupancy degree of the secondary channel of the RNApol may have significant impact in the expression pattern in *E. coli*. The data obtained clearly indicate that up-regulation of some specific genes that occurs in absence of DksA, was the result of the vacancy of the secondary channel generated in a *dksA* strain rather than being the result of DksA having a direct repressor effect. We suggested that in the absence of DksA, the interactions of other proteins, such as GreA, are promoted and responsible of the up-regulation observed. This phenomenon, GreA-dependent up-regulation detected in a *dksA* strain, was detected for type 1 fimbriae and flagella expression in *E. coli*, and indicates that a competence for the occupancy of the secondary channel of the RNApol might exist (Aberg et al., 2008 and 2009). Studies based in the amount of these proteins and its affinity for the RNApol, suggested that most of the RNApol molecules will be forming complex with DksA (Rutherford *et al.*, 2007), unless other factors with ability to interact in the same site of the RNApol, such as GreA and GreB, increases its expression and/or affinity under certain conditions.

In this work we try to obtain new insights in the possible interplay between the proteins that can interact with the secondary channel of the RNApol. Phylogenetic studies performed showed that GreA is the secondary channel interacting protein more broadly distributed among bacteria, clearly indicating the crucial role of this protein in transcription. Our data indicate that the ability of GreA to resume paused RNApol-DNA complexes is pivotal for proper gene expression and, consequently, for the physiology of the cell. GreA promotes expression of many different genes often associated with complexes cellular processes, such as fimbriation and motility in *E. coli*, and protein secretion and virulence in *Salmonella*. To trigger those processes, importantly stimulated by GreA, requires a significant part of the energetic and metabolic assets of the cell. Perhaps that is one of the reasons why overexpressing GreA and,

presumably, causing an artificial increase in the relative concentration of RNApol-GreA, causes a serious deleterious effect in bacterial fitness. Interestingly, this negative effect is importantly enhanced if the cell lacks the GreA-competitor DksA. However it cannot be ruled out that specific effect of GreA on *ftsN* expression may contribute to the deleterious effect in growth. An attractive model from an evolutionary point of view is that DksA appears in the bacterial evolution to act as an anti-GreA protein to allow a tight regulation of gene expression, especially of genes that requires ppGpp for its transcription. We have seen several examples of genes, coding for complex processes that are regulated by ppGpp at the level of transcription initiation and are also stimulated at the transcription elongation level by GreA. High expression of those genes in wrong conditions may compromise bacterial viability due to the important energetic burden. Therefore, having a protein that may counteract the stimulatory role of GreA may be a benefit for the bacterial cell.

Interestingly, it exist an interplay among secondary channel interacting factors. GreA levels seem to be inversely related with the ppGpp-DksA system. GreA contents drops in the interphase between logarithmic and stationary phase, exactly the physiological condition that trigger the production of ppGpp in the cell. The growth phase drop in GreA is concomitant with an increase in the GreB levels, promoted by DksA. The studies performed demonstrate that GreA amount in the cells is very tightly regulated and several mechanisms exist to control the amount of GreA in the cell, such as autoregulation (Potrykus *et al.*, 2010), presence of two promoters responding to different sigma subunits and a possible control by the metabolic sensor CRP/cAMP.

Recently it has been described that GreA may act as a chaperone by avoiding miss folding of proteins after high temperatures stress (Li *et al.*, 2012). Interestingly, the only condition found to importantly increase GreA is when the σ^E regulon is activated, which normally occurs as a response to unfolded proteins present in the periplasm due to some stress conditions, such as heat shock or hyperosmotic stress. Whether some of the GreA-induced protein under σ^E inducing conditions plays a role as a chaperone remains undercover.

In addition to changes in the amount of the protein, factors altering the affinity to the RNApol may play a crucial role in the competition for binding into the secondary channel of the RNApol. In this context, the data indicating that the conformation of the protein Gfh1 of *Thermus thermophilus* may vary in a pH dependent manner between two different states (active/inactive), it is the first example among those proteins that conformational switches may be relevant for its activity. GreA activity might also be dependent on conformational switches. The finding that the effect of GreA on *fliC* expression was dependent in external osmolarity but independent of a regulation of *greA* expression, as monitored by transcriptional studies and immunodetection, suggest that osmolarity could affect the activity of GreA, perhaps through conformational changes. Characterization of amino acids that are important for the functionality or affinity of GreA to the RNApol indicates that the α-helix of the globular domain is essential for the functionality of GreA. Mutations in S124 or L130 disrupt this helix and as a consequence eliminate the functionality of GreA. Moreover, changes that might affect the linker (such as I75V or P5S) could cause changes on the conformation of the protein GreA, and as a consequence, reducing its affinity. Moreover, phylogenetical studies had shown that the linker might be important for the competition between factors that bind into the secondary channel.

Considering that the competition between GreA and DksA was described during the study of *fliC* (Aberg *et al.*, 2009), the effect of the factors that bind into the secondary channel of the RNApol was determined. The *fliC* upregulation detected in a *dksA* mutant is strictly dependent on the presence of GreA. The data shown suggest that GreA may be regulating transcriptional elongation of *fliC* since: i) the antipause activity of GreA is required for the expression of *fliC,* ii) the effect of GreA mutations is more evident with a distal *fliC*::*lacZ* fusions (+1210) that with a proximal (+70). Most probably both, DksA and GreA, are required for *fliC* expression but act at different levels in the regulatory cascade of flagella expression regulation.

In fact it has been shown that GreA is required for the expression of *fliC* and motility, even in presence of DksA. These data suggest that under physiological conditions, GreA is able to substitute DksA in some cases. It has been

described that DksA does not bind to backtracked elongation complexes (Furman, Tsodikov, *et al.*, 2013). When the RNApol get paused, it changes its affinity for DksA, avoiding its binding, and allowing the interaction of GreA with the secondary channel of the RNApol. It has been observed that the presence of ppGpp seem to be required for the proper binding of GreA to the secondary channel, since ppGpp deficient strains suffer less toxic effect during overexpression conditions. Perhaps the increased affinity of GreA by the presence of ppGpp allows that the lower content of GreA in stationary phase has not a negative impact in transcription elongation of GreA regulated genes.

In order to determine the impact of the competition among the factors that bind to the secondary channel of the RNApol in the global expression profile of pathogenic bacteria, we performed a transcriptomic study of the effect of ppGpp and DksA in *Salmonella enterica* serovar Typhimurim. As observed in *E. coli*, both factors had global effect on the expression of gene expression. We observe that both factors, ppGpp and DksA, had an important regulatory role of gene expression of several virulence factors, but also controlling the mobilization of some genetic elements such as plasmids or bacteriophages. These data suggest that ppGpp and DksA, as well as other factors that could be comprised in these genetic elements, could promote the acquisition of HGT DNA in order to obtain an evolutive benefice.

.

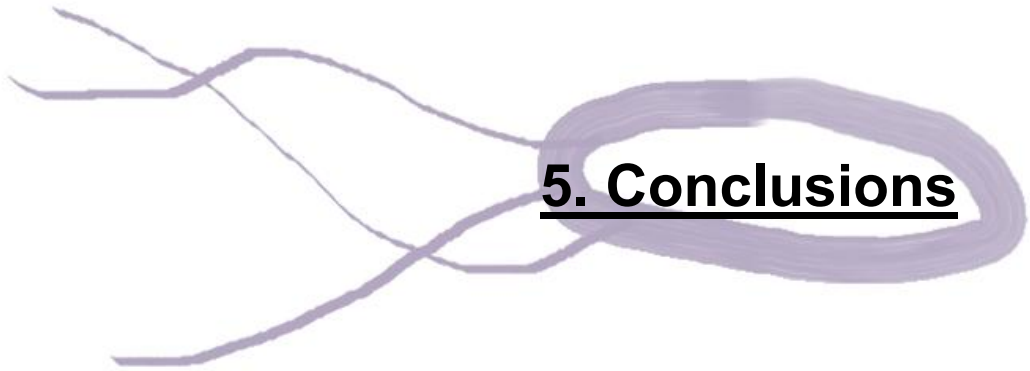

5. Conclusions

In this project different aspects of the interaction between the proteins that bind into the secondary channel of the RNApol were studied in order to determine a possible competence between them. To do that, the expression of *greA* at different conditions has been described. Changes in the amount of protein would affect the equilibrium between the different factors that bind to the secondary channel, and produce changes in the interplay between factors. Moreover, the cross regulation between the different proteins that bind into the secondary channel has been studied.

In our research group, it has been described that the interplay between factors could control the expression of several genes, such as those coding for type1 fimibriae (Aberg *et al.*, 2008) and flagella (Aberg *et al.*, 2009). In this project, we have determined the effect that the competition of these proteins for binding into the secondary channel would produce in a target gene (*fliC*).

Structural and phylogenetic studies of the protein GreA were used to further study the competition of the different factors that bind into the secondary channel, as well as the GreA domains relevant for this competition. Moreover, these studies let us to identify important amino acids for the functionality of GreA and its binding to the secondary channel.

Finally, transcriptomic studies in *Salmonella enterica* serovar Typhimurium were used to determine the effect of the different factors that bind into the secondary channel of the RNApol in the gene expression pattern.

The specific conclusions derived from this work are indicated as follows:

1. GreA autorepresses its own expression.
2. The autoregulation of *greA* requires the antipause activity of GreA, and the sequence localized between +3 and +101, respect to the transcriptional start site.
3. GraL, a short array of sRNA produced by an imprecise terminator localized between the *greA* promoter and the coding sequence, is involved in the autorepression of *greA*.

4. The expression of *greA* decreases at stationary phase. This effect requires the presence of GreA.

5. High temperature (42ºC) stimulates the expression of *greA*.

6. Overexpression of *rpoE* or production of an extracytoplasmic stress with unfolded proteins, increases the *greA* expression.

7. Variation in either oxygen or magnesium availability, pH or osmilarity, do not produce changes in the *greA* expression.

8. The regulatory complex cAMP-CRP regulates the expression of *greA*.

9. A crosstalk between GreA, GreB and DksA exist. GreA stimulates *dksA* expression, while DksA stimulates *greB* expression at stationary phase.

10. GreA and DksA affect the expression of *fliC* at transcription elongation and initiation level respectively.

11. The antipause activity of GreA is required for the expression of *fliC*.

12. Overexpressing GreA and presumably increasing the relative amount of the complex RNApol-GreA causes a deleterious effect to the cell physiology.

13. The alarmone ppGpp might be required for the interaction of GreA with the secondary channel of the RNApol.

14. The α-helix of the globular domain of GreA is essential for GreA functionality.

15. Mutations that would affect the linker that bind both domains of GreA, such as I75V and P5S, might produce hypothetical changes in the conformation of GreA.

16. The mutants L21R, A51T, C58G, D98G, S121P and S121L might have its affinity for the RNApol affected.

17. The mutants R9C, E151G and Y157H might not be able to compete with DksA for binding to the secondary channel.

18. The variability of factors that bind into the secondary channel appeared by gene duplication events.

19. All bacteria contain *greA*, except phyla *Aquificae*, *Chlamydia* and some members of *Cyanobacteria*.

20. A major diversity of factors is observed in proteobacteria than in the rest of Bacteria.

21. The presence of other factors that bind to the secondary channel of the RNApol, such as DksA or GreB, produced an evolutive pressure to conserve several structural features of GreA.

22. The alarmone ppGpp and DksA are global regulators of the gene expression in *Salmonella*.

23. The alarmone ppGpp and DksA stimulates the expression of several genes, ppGpp stimulates up to 4% of core genome genes and up to 19.9% of HGT. DksA stimulates up to 4% of core genome genes and 14.4% of the HGT.

24. The genes encoded in SPI 1, 2, 4 and 5 are stimulated by ppGpp and DksA.

25. The haemolytic activity, associated to effector proteins encoded in SPI1, is affected in mutants defective in ppGpp and *dksA*, suggesting that both factors might be important during cellular invasion.

26. The alarmone ppGpp and DksA stimulates gene expression of virulence factors encoded in bacteriophages and plasmids.

27. Mobilization of bacteriophages and conjugative plasmids is stimulated for ppGpp.

28. The alarmone ppGpp and DksA similarly regulate up to 61% of the affected genes.

29. Up to 7% of the affected genes for ppGpp and DksA, had an opposite behaviour between both factors.

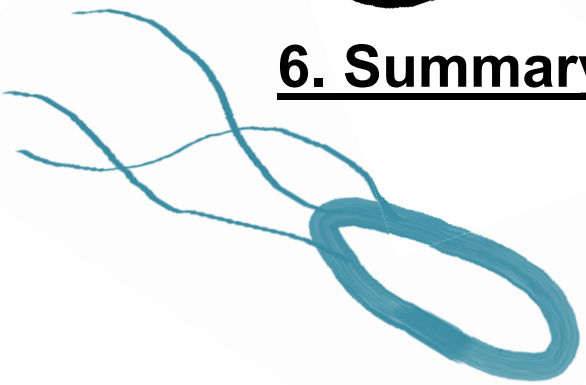

6. Summary in Catalan

Introducció

Les espècies bacterianes, tot i tenir un seguit de gens comuns entre les diferents soques, que les defineixen com a espècie (denominat "core-genome"), contenen una gran varietat de gens, específics de soca, i que els hi confereixen habilitats que permeten a cada soca adaptar-se a entorns específics (**fig. 1**). El conjunt de gens del "core-genome" i els gens variables, formen el que es coneix com a "Pan-genome" (Mira *et al.*, 2010). Els gens variables, que tendeixen a estar localitzats en illes gèniques, poden ser transferits per processos de transferència gènica horitzontal (HGT) a altres soques o espècies, mitjançant processos de conjugació, transformació natural o transducció. De fet s'ha observat que la transducció és considerada el principal mecanisme de transferència horitzontal de gens a bacteris (Boyd and Brüssow, 2002; Mira *et al.*, 2010; Penadés *et al.*, 2014).

S'ha vist que el medi ambient pot produir alguns canvis a la mida del genoma bacterià (**fig. 2**) però són mecanismes d'adaptació a llarg termini (Ranea *et al.*, 2004; Dini-Andreote *et al.*, 2012). Els bacteris tenen diferents mecanismes a curt termini d'adaptació al medi que permeten detectar els canvis ambientals i variar la seva expressió gènica, produint una resposta a les condicions del medi.

L'expressió gènica s'inicia amb el procés de transcripció durant el qual la informació continguda a l'ADN és transcrita a ARN. Aquest procés és dut a terme per un complex enzimàtic anomenat ARN polimerasa (ARNpol) on, en procariotes, la seva unitat bàsica (*core* o nucli) està formada per 5 subunitats proteiques: 2 subunitats α, una β, una β' i una ω ($\alpha_2\beta\beta'\omega$). S'ha determinat dos canals entre les diferents subunitats: el canal primari, per on entra l'ADN i es desenvolupa la transcripció, i el canal secundari, que comunica el medi exterior amb el centre catalític de l'ARNpol. Tot i així, aquest holoenzim necessita la unió d'una subunitat σ per ser capaç de reconèixer una seqüència promotora i iniciar la transcripció (Haugen *et al.*, 2008). *Escherichia coli* conté 7 subunitats σ alternatives que controlen l'expressió gènica de diferents gens en resposta a diferents estímuls. La competència de les diferents subunitats pel nucli de l'ARNpol determinarà l'expressió dels diferents gens que controlen. Per tant,

modificacions en aquesta competència produïda per altres factors, com alarmones o factors anti-sigma (**fig. 6**), provocarien variacions en l'expressió gènica.

La transcripció és un procés cíclic que es pot dividir en tres etapes: i) unió al promotor i iniciació, ii) elongació i iii) terminació.

Durant el primer pas, l'ARNpol s'uneix al promotor gràcies al reconeixement de la subunitat σ, s'obre la doble cadena d'ADN, l'introdueix dins el canal primari de l'ARNpol i comença la incorporació del nucleòtids (**fig. 5**). A molts promotors, l'ARNpol sintetitza fragments curts degut a cicles d'iniciació abortiva, on s'inicia i es finalitza prematurament la transcripció degut a que la subunitat σ no es desenganxa del promotor. Quan l'ARNpol aconsegueix desenganxar-se del promotor es produeix l'elongació de la transcripció (Browning and Busby, 2004; Haugen *et al.*, 2008).

Durant l'elongació de la transcripció, la subunitat σ es desenganxa del nucli de l'ARNpol. Durant aquesta etapa l'ARNpol pot variar entre un estat actiu i pausat. Les pauses durant l'elongació de la transcripció poden ser induïdes per determinades seqüències d'ADN, lesions o incorporació de bases errònies durant la transcripció. Si les pauses s'allarguen es poden produir alteracions de l'ARNpol, com ara el "backtracking", on l'ARNpol retrocedeix sobre de l'ADN i l'ARN es desenganxa del centre actiu, entrant dins del canal secundari de l'ARNpol (Artsimovitch and Landick, 2000; Landick, 2006). Els estats de pausa i el backtracking poden ser solucionats per diferents factors, com NusG o els factors Gre (GreA i GreB) o pel procés de traducció (Borukhov *et al.*, 1993; Artsimovitch and Landick, 2000; Dutta *et al.*, 2011). L'elongació de la transcripció continua fins que l'ARNpol detecta un senyal de terminació, que pot ser dependent o independent de la proteïna Rho (Henkin, 2000).

La transcripció gènica pot ser regulada tant a inici de la transcripció com durant l'elongació i la terminació. Diferents factors poden regular l'expressió gènica interactuant directament amb l'ADN o no. Alguns d'aquests factors són proteïnes reguladores que s'uniran a la regió promotora i contactaran directament amb l'ARNpol, activant-la o inhibint-la; diferents subunitats sigma

que competiran entre elles per unir-se al *core* de l'ARNpol, així com la presència de factors anti-sigma que alteraran aquesta competència; la topologia de l'ADN, que pot amagar la zona promotora, impedint així el reconeixement per part de l'ARNpol; alarmones, molècules petites d'origen no proteic que interaccionen amb proteïnes alterant la seva funcionalitat; o factors que interaccionen amb el canal secundari de l'ARNpol (Browning and Busby, 2004; Travers and Muskhelishvili, 2005; Haugen *et al.*, 2008; Kalia *et al.*, 2013; Treviño-Quintanilla *et al.*, 2013).

Factors que interaccionen amb el canal secundari de l'ARNpol

A *Escherichia coli*, diferents factors, l'alarmona ppGpp i diferents proteïnes, tenen l'habilitat d'interactuar amb el canal secundari de l'ARNpol afectant la seva activitat (**fig. 7**). Les proteïnes que interaccionen amb el canal secundari de l'ARNpol són proteïnes de baix pes molecular que comparteixen una organització espacial similar. Aquestes proteïnes tenen un domini que entra dins del canal secundari, interactuant amb el centre actiu, i un segon domini que es queda fora del canal secundari. A *E. coli*, així com en altres enterobacteris, aquestes proteïnes són GreA, GreB, DksA i Rnk (Borukhov *et al.*, 1993; Perederina *et al.*, 2004; Lamour *et al.*, 2008). A més, s'ha descrit altres proteïnes capaç d'unir-se al canal secundari de l'ARNpol en alguns plàsmids conjugatius, com el plàsmid F d'*E. coli* o pSLT a *Salmonella* (Blankschien *et al.*, 2009), o en altres especies com ara la proteïna Gfh1 de *Thermus thermophilus*.

El fet que diferents proteïnes s'uneixin a la mateixa diana produint diferents efectes suggereix que hi ha d'haver una competència entre els diferents factors que s'uneixen al canal secundari de l'ARNpol afectant la funcionalitat de l'holoenzim.

El factor transcripcional GreA

A *E. coli*, els factors Gre, GreA i GreB, interaccionen amb el canal secundari de l'ARNpol i suprimeixen les situacions de pausa o backtracking durant el procés de transcripció (Laptenko *et al.*, 2003). GreA va ser descrit com a supressor de l'efecte negatiu produït a alta temperatura en el mutant S522F de la subunitat β

de l'ARNpol a *E. coli.* És una proteïna de 158 aminoàcids (17.5 kDa) dividits a parts iguals en dos dominis (**fig. 8**): el domini N-terminal està format per un domini *coiled-coil* i el domini C-terminal, unit al N-terminal per un *loop*, és d'estructura globular (Sparkowski and Das, 1991; Stebbins *et al.*, 1995). S'ha determinat que és el domini *coiled-coil* el que entra dins del canal secundari de l'ARNpol on dos residus acídics (D41 i E44) són capaços d'interaccionar amb el centre catalític de l'ARNpol. La interacció d'aquests dos residus amb el centre catalític de l'ARNpol és necessari per a solucionar situacions de pausa. Així doncs, quan l'ARNpol s'atura, GreA indueix l'activitat ribonucleolítica intrínseca de l'ARNpol. Els residus D41 i E44 estan molt conservats en tots els factors Gre i en DksA, tot i que a DksA estan orientats de forma diferent als dels factors Gre (Perederina *et al.*, 2004; Vassylyeva *et al.*, 2007).

A part de la seva activitat antipausa, s'ha descrit que GreA té una certa activitat com a xaperona. S'ha vist que GreA és capaç de suprimir l'agregació de proteïnes induïda per calor i que promou la reactivació de proteïnes desnaturalitzades en *E. coli*. A més, la seva sobreexpressió confereix una major capacitat de supervivència a un xoc tèrmic o un estrés oxidatiu (Li *et al.*, 2012).

S'ha vist que GreB, amb una elevada homologia estructural i funcional amb GreA (**fig. 8**), conté una zona amb càrrega bàsica que es creu que li permet unir-se a la part externa del canal secundari de l'ARNpol, tot i així, no s'ha localitzat aquesta cavitat a GreA (Kulish *et al.*, 2000). A més, encara no es coneix com és exactament la unió entre GreA i l'ARNpol.

L'alarmona ppGpp

L'alarmona (p)ppGpp, tetra- o penta-fosfat de guanosina, és un nucleòtid modificat que actua com a alarmona o senyal d'estrès bacterià (Cashel *et al.*, 1996). Inicialment es va descriure que la seva síntesi s'induïa com a resposta a la manca d'aminoàcids produint una baixada en la quantitat de ARN estable (**fig. 10**) (Cashel, 1969). Posteriorment s'ha vist que ppGpp té un important efecte sobre l'expressió gènica, anomenada resposta estricta (Cashel *et al.*, 1996; Magnusson *et al.*, 2005). L'alarmona ppGpp, descoberta a *Escherichia*

coli, no està restringida a Gram-negatius, sinó que també es troba a Gram-positius i a cloroplasts de les cèl·lules vegetals (Braeken *et al.*, 2006; Atkinson *et al.*, 2011). La resposta estricta, en *E. coli*, consisteix en la inhibició de la síntesi de l'ARN estable (ARNt i ARNr) i de diferents gens relacionats amb el creixement bacterià, mentre que es produeix una inducció dels gens que codifiquen per les vies biosintètiques d'aminoàcids i de resposta a diferents situacions d'estrés. La síntesi de ppGpp està catalitzada per RelA i SpoT. RelA és la principal proteïna productora de ppGpp, responent a la manca d'aminoàcids, en canvi, SpoT es una proteïna bifuncional capaç de sintetitzar ppGpp com a resposta a altres condicions d'estrès i de degradar-lo (Cashel *et al.*, 1996).

S'ha descrit que ppGpp interacciona amb el centre catalític de l'ARNpol desestabilitzant el complex entre l'ARNpol i el promotor, produint així el seu efecte sobre l'expressió gènica. Tot i així, s'ha vist que ppGpp interfereix en la competència entre subunitats σ, o pot interaccionar amb altres proteïnes afectant la seva activitat, així com SlyA.

A *E. coli*, el doble mutant Δ*relAspoT* és considerat $ppGpp^0$, és a dir, incapaç de sintetitzar ppGpp sota cap condició. Aquestes soques han perdut la capacitat de créixer en medi mínim degut a la incapacitat de sintetitzar aminoàcids que tenen (Xiao *et al.*, 1991).

La proteïna DksA, un co-regulador de ppGpp

DksA és una proteïna de 151 aminoàcids (17 kDa) que conté un domini *coiled-coil*, dues α-hèlix antiparal·leles unides per un gir, i un domini en dits de zinc del tipus C4 (**fig. 14**). S'ha vist que DksA potencia tant l'efecte repressor de ppGpp sobre els promotors dels ARNr, com també l'efecte estimulador d'aquest sobre els promotors dels operons de biosíntesi d'alguns aminoàcids, suggerint que ppGpp i DksA són cofactors (Paul *et al.*, 2004). Degut al seu efecte sobre l'expressió del gens responsables de la biosíntesis d'aminoàcids, s'ha vist que l'absència de DksA afecta el creixement en plaques de medi mínim, tot i així, després de 3 dies d'incubació es va veure que certes soques deficients en *dksA* eren capaces de créixer en medi mínim M9. Per aquest motiu es

considera que els mutants *dksA* són bradítrofs, en comptes de auxòtrofs (Vinella *et al.*, 2012). S'ha determinat que DksA s'uneix al centre catalític de l'ARNpol, conjuntament amb ppGpp. Tot i així, DksA, per si sol, és incapaç d'unir-s'hi correctament (Perederina *et al.*, 2004).

Estudis realitzats al nostre grup han demostrat que els mutants $ppGpp^0$ i els Δ*dksA* tenen comportaments diferents, l'un respecte de l'altre, en l'expressió de diferents gens, relacionats amb la colonització i la virulència a *E. coli*. Es considera que de forma habitual DksA està unit a l'ARNpol impedint la unió d'altres proteïnes al canal secundari (Rutherford *et al.*, 2007), en canvi en absència de DksA, el canal secundari queda lliure perquè hi puguin accedir altres proteïnes, com ara GreA, i alterar l'expressió del gen estudiat. Aquest fet ens va permetre explicar algunes de les diferències observades entre els mutants ppGppº i *dksA* (Aberg *et al.*, 2009). A més s'ha descrit que DksA no s'uneix a l'ARNpol en situacions de pausa o backtracking, suggerint que sota aquestes condicions hi pot haver un canvi en les proteïnes que interaccionen amb el canal secundari.

Altres possibles factors que interaccionen amb l'ARNpol

Atenent a l'homologia estructural entre GreA i GreB, també s'han descrit en *E. coli* diferents proteïnes que potencialment interaccionen amb el canal secundari de l'ARNpol: DksA, Rnk, TraR, YbiI, etc (Perederina *et al.*, 2004; Lamour *et al.*, 2008; Blankschien *et al.*, 2009). Tenint en compte la quantitat relativa dels factors que interaccionen amb l'ARNpol i la seva afinitat per aquesta, com s'ha comentat abans, s'ha suggerit que en condicions normals la majoria de l'ARNpol es troba formant complex amb DksA i no amb els altres factors (Rutherford *et al.*, 2007). Tot i així, alguns estudis publicats indiquen que els factors Gre podrien patir canvis conformacionals atenent a diferents paràmetres ambientals i conseqüentment alterar l'afinitat relativa d'aquests factors pel canal secundari de l'ARNpol. S'ha vist que Gfh1, factor homoleg a GreA *Thermus thermophilus,* pateix un canvi conformacional com a resposta a canvis en el pH (de 6.5 a 7), sempre dins el rang fisiològic (Laptenko *et al.*, 2006).

Aquests descobriments suggereixen que el canal secundari de l'ARNpol podria actuar com a diana de múltiples interaccions proteiques que suposadament causarien alteracions en l'activitat de l'ARNpol. Dins d'aquest marc, s'ha determinat que l'expressió de GreA està regulada per la presència de σ^E, subunitat σ responsable de la resposta a l'estrès per xoc tèrmic. Això ens fa pensar que possiblement hi hagi una regulació a nivell del canal secundari de les respostes als canvis ambientals. El fet que proteïnes com TraR dels plàsmids conjugatius o algunes proteïnes fàgiques puguin interaccionar amb el canal secundari de l'ARNpol, ens planteja una qüestió evolutiva, on aquests elements mòbils haurien adquirit proteïnes amb capacitat de "segrestar" l'ARNpolimerasa pel seu propi ús. Per tant, l'estudi de la interacció de proteïnes reguladores que interaccionen en el canal secundari de l'ARNpol podria revelar l'existència d'un nivell de regulació de l'expressió gènica crucial i desconegut fins el moment.

Organismes model utilitzats

Les soques bacterianes utilitzades en aquesta tesi, *Escherichia coli* MG1655 i *Salmonella enterica* subsp. *enterica* serovar Typhimurium SV5015, són membres de la família de les Enterobacteriaceae, que comprenen bacils Gram-negatius, no esporulats, oxidasa positius, sovint mòtils amb flagels perítrics.

Escherichia coli viu a l'intestí d'humans i animals de sang calenta. Les soques K12, incloent-hi la soca MG1655, han estat extensivament utilitzades en investigació degut a que s'han reconegut com a segures (GRAS). Tot i així algunes soques d'*E. coli* són també importants patògens humans, podent produir diarrees, infeccions del tracte urinari o del sistema nerviós central. Es creu que diferents processos de transferència horitzontal gènica són l'origen de la generació de diferents soques patògenes d'*E. coli*. Aquests processos causen adquisició de diferents gens que els hi confereixen diferents habilitats (Balows *et al.*, 1992; Croxen *et al.*, 2013). Alguns d'aquests processos són força recents, com és el cas de la soca O104:H4, que va causar un brot de gastroenteritis a Alemanya al 2011 (World Health Organization, 2011; Bloch *et al.*, 2012), indicant la importància que té la transferència de gens en la patogènesi d'*Escherichia coli*.

***Salmonella enterica enterica* serovar Typhimurium** és un patogen de contagi fecal-oral, que produeix gastroenteritis en humans. *Salmonella* té una tolerància a l'àcid que li permet travessar l'estomac, arribar a l'intestí i creuar la mucosa intestinal. *Salmonella* s'uneix a la superfície apical de la cèl·lula hoste de l'epiteli intestinal, provocant una alteració del citoesquelet d'actina i promovent la seva entrada en vesícules (**fig. 18A**). Després, *Salmonella* evita que les vesícules es fusionin amb els lisosomes (**fig. 18B**). *Salmonella* pot creuar la membrana basolateral i infectar altres cèl·lules epitelials i macròfags. Diferents factors de virulència són necessaris per a la infecció de *Salmonella,* molts d'ells es troben localitzats en illes de patogenicitat, bacteriòfags i el plàsmid pSLT. Els diferents factors de virulència són requerits a diferents moments, per tant, hi ha una regulació creuada entre els diferents factors per assegurar la correcta expressió dels diferents factors en el moment correcte (Haraga *et al.*, 2008; Fàbrega and Vila, 2013).

Objectius

Estudis previs realitzats en el nostre grup de recerca mostren que ppGpp i DksA poden tenir diferents efectes a la regulació de l'expressió gènica a *Escherichia coli* (Aberg *et al.*, 2009). Aquests resultats ens van permetre hipotetitzar que les diferències observades entre mutants deficients per DksA i ppGpp eren degudes a canvis a les proteïnes que s'uneixen al canal secundari de l'ARNpol, suggerint una possible competència entre aquests factors: DksA, GreA o GreB. De forma simultània, altres grups sostenien que degut a la quantitat i afinitat de DksA respecte les altres proteïnes, tal competència no seria possible (Rutherford *et al.*, 2007; Rutherford *et al.*, 2009). En aquest estudi pretenem explorar la possible existència de la competència entre els factors que interaccionen amb el canal secundari de l'ARNpol i el seu impacte a la regulació de l'expressió gènica. Els dos objectius d'aquesta tesi són:

1. Estudi de la possible competència entre els diferents factors que s'uneixen al canal secundari de l'ARNpol. Per dur-ho a terme es vol monitoritzar l'expressió de *greA* a diferents condicions, així com determinar la possible regulació creuada entre els diferents factors que interaccionen amb l'ARNpol. També es pretén estudiar el mecanisme d'acció de GreA modulant l'expressió d'un gen diana, *fliC*. Per estudiar els aspectes estructurals de la competència entre els diferents factors, es pretén determinar l'efecte de la sobreexpressió de GreA sobre el creixement bacterià, així com fer mutagènesi a l'atzar que ens permeti determinar aminoàcids importants per a la interacció de GreA amb l'ARNpol i la funcionalitat de GreA. Finalment un estudi filogenètic ens permetrà avaluar l'evolució d'aquests factors, tal com la pressió evolutiva produïda per la variabilitat dels factors que s'uneixen al canal secundari de l'ARNpol, exercida sobre determinades estructures de la proteïna GreA.

2. Determinar l'efecte d'aquests factors d'elements mòbils i HGT. Per dur-ho a terme volem determinar l'efecte de ppGpp i DksA sobre el perfil transcripcional de *Salmonella enterica* serovar Typhimurium.

Resultats i discussió

Estudi de l'expressió de *greA*

S'han identificat 2 promotors que controlen l'expressió de *greA*: un σ^{70}-depenent i un σ^{E}-depenent (**fig. 25**). Entre aquests i l'inici de transcripció s'ha descrit l'existència d'un terminador parcial que produeix un seguit de petits transcrits amb capacitat reguladora anomenat GraL (Potrykus *et al.*, 2010). Per tal de monitoritzar l'expressió de *greA,* s'han obtingut diferents fusions entre els promotors de *greA* i el gen *lacZ* (**taula 5**).

Hem pogut determinar que GreA autoregula la seva pròpia expressió. En absència de GreA augmenta l'expressió de *greA* (**fig. 26**). Aquesta autorepressió de GreA requereix l'activitat antipausa de GreA, ja que al complementar un mutant deficient en *greA* amb la proteïna GreA D41A, mutant sense activitat antipausa (Opalka *et al.*, 2003), no es recuperen els nivells d'expressió de la soca WT, a diferencia del que passa al complementar amb la proteïna GreA WT (**fig. 27**).

Per una altra banda hem vist que GraL és capaç de produir també un efecte autoregulador sobre l'expressió de *greA* (**fig. 28A**). A més, mitjançant fusions fetes a l'inici de transcripció del promotor σ^{70}-depenent (+3), hem pogut observar que ni GreA ni GraL són capaç de reduir l'expressió de *greA* en una soca *greA*$^{-}$. Aquestes dades semblen indicar que l'autoregulació és independent de l'inici de transcripció del promotor depenent de σ^{70}-depenent. Per una altra banda, utilitzant una fusió que conté els dos promotors i el terminador (+101), i que per tant produeix GraL, recuperem l'autoregulació de *greA* (**fig. 28B**). Estudis similars duts a terme per Potrykus *et al.* (2010) mostren que l'autoregulació de *greA* no es duu a terme a nivell d'inici de transcripció, ja que no observen autoregulació mitjançant fusions transcripcionals amb l'inici de transcripció del promotor depenent de σ^{70} o σ^{E}. Aquestes dades suggereixen que la seqüència compresa entre +3 i +101 és requerida per l'autoregulació.

Considerant que difícilment l'activitat antipausa pugui reprimir l'expressió gènica, hem hipotetitzat que podria ser un efecte indirecte. GreA, mitjançant la seva activitat antipausa permet l'expressió d'un factor desconegut (X) que

reprimiria l'expressió de *greA*. A més, GraL podria ser requerit per l'estabilitat del seu ARN missatger, la qual cosa, també estaria augmentant la seva expressió i com a conseqüència, reprimint *greA* (**fig. 28D**). Aquesta factor X podria necessitar la presència de la seqüència compresa entre +3 i +101 per inhibir l'expressió de *greA.* Tot i així hi ha altres possibles models que podrien explicar aquests resultats, com ara que GreA i GraL estiguessin estimulant de forma paral·lela diferents factors que puguin reprimir l'expressió de *greA*.

Per una altra banda hem vist que l'expressió de *greA* disminueix a fase estacionària, respecte a fase exponencial. Aquest efecte a nivell de la corba de creixement requereix també de la presència de GreA (**fig. 29**). És a dir, GreA produeix una reducció de l'expressió de *greA* a fase estacionària, possiblement per evitar la seva acumulació o per afavorir la interacció d'altres factors amb el canal secundari de l'ARNpol.

També s'ha determinat l'efecte de diferents factors ambientals sobre l'expressió de *greA*, com ara la disponibilitat d'oxigen i de magnesi, pH, osmolaritat i temperatura (**fig. 31**). Hem pogut determinar que només la temperatura, més concretament l'alta temperatura, té un efecte sobre l'expressió de *greA*, produint un augment de l'expressió de *greA*. Considerant que *greA* conté un promotor depenent de σ^E que és responsable de la resposta a l'estrès extracitoplasmàtic, produït per proteïnes mal plegades al periplasma degut a altes temperatures o a un xoc hiperosmòtic, decidim comprovar quin efecte té l'activació d'aquesta via sobre l'expressió de *greA*. Veiem que tant la sobreexpressió de σ^E com la seva activació sobreexpressant proteïnes quimèriques incapaces de plegar-se correctament al periplasma, produeixen una forta inducció de *greA* (**fig. 33**). Aquestes dades suggereixen que GreA és requerit a la cèl·lula en aquestes condicions, tant sigui pel seu paper antipausa, com el possible paper com a xaperona (Li *et al.*, 2012).

Per una altra banda hem dut a terme un anàlisi *in silico* de possibles llocs d'unió de diferents reguladors globals a la regió promotora de *greA* (**fig. 34**). Veiem possibles llocs d'unió de reguladors globals, dels quals només Fis, FadR, DgsA i Crp, semblen tenir un efecte sobre l'expressió de *greA* (**fig. 35**).

Degut al seu paper en el manteniment del nucleoide, Fis pot interferir en l'expressió de *greA* degut a un superenrrotllament de la zona, que impedeixi la unió de l'ARNpol a la zona promotora.

FadR esta implicat en el metabolisme dels àcids grassos. S'ha vist que FadR reprimeix l'expressió de *greA* (**fig. 35**) igual que s'ha determinat per a l'operó *fad*, responsable de la degradació d'àcids grassos. S'ha observat que FadR reconeix la presència de diferents àcids grassos, com l'àcid oleic, i en aquestes condicions es desenganxa de l'ADN alliberant el promotor. Per aquest motiu en gens reprimits per FadR, després de l'addició d'àcid oleic, es produeix una desrepressió del gen. Un efecte similar esperaríem veure per el gen *greA,* però l'addició d'àcid oleic no produeix cap efecte sobre l'expressió de *greA* (**fig. 37**). El fet que no detectem una resposta a alteracions fisiològiques de la regulació depenent de FadR, suggereix que els resultats obtinguts en el mutant *fadR*, podrien ser deguts a un efecte pleiotròpic o indirecte sobre l'expressió de *greA*.

Per una altra banda hem vist que mentre CRP estimula l'expressió de *greA*, DgsA la reprimeix. Curiosament ambdós reguladors s'unirien l'ADN, produint el seu efecte en absència de Glucosa en el mateix temps, produint un efecte contradictori. Tot i això, aquesta distribució s'ha observat en altres gens com *malT* o *ptsG* (Plumbridge, 2002). Veiem que en absència de glucosa l'expressió de *greA* augmenta respecte en presència de glucosa (**fig 38B**), tot i això no és un efecte molt dràstic, suggerint una modulació per part de DgsA. A més, experiments de complementació d'una soca deficient per *crp*, mostren que proteïnes CRP incapaces de contactar amb l'ARNpol (CRP H159L) poden recuperar l'expressió de *greA* en absència de *crp* (**fig. 39**), indicant que no es produeix un contacte directe de l'ARNpol amb CRP, i que podria ser una regulació directa o indirecta sobre l'expressió de *greA* a través d'un promotor CRP depenent de tipus 3.

Regulació creuada entre factors

Fusions *lacZ* similars a les que es van fer per *greA*, es van fer també per *greB* i *dksA* (**fig. 41**). Aquestes fusions ens han permès determinar que tant *greA*, com *dksA* autoregulen la seva expressió. A més, hem vist que existeix una

regulació creuada entre aquests factors, on GreA estimula l'expressió de *dksA*. DksA estimula l'expressió de *greB* (**fig. 42**). Estudiant l'expressió dels diferents factors a diferents punts de la corba de creixement, hem pogut determinar que, com s'ha mencionat anteriorment, mentre que l'expressió de *greA* disminueix a fase estacionària (OD_{600nm} 2.0), l'expressió de *greB* augmenta, suggerint un intercanvi en les proteïnes que interaccionen en el canal secundari de l'ARNpol. Aquestes diferències d'expressió podrien variar l'equilibri entre les proteïnes que interaccionen amb el canal secundari de l'ARNpol. Aquest augment de l'expressió de *greB* és depenent de DksA.

Altres grups d'investigació (Chandrangsu *et al.*, 2011; Vinella *et al.*, 2012) han fet experiments similars, obtenint resultats similars en alguns aspectes, mentre que en altres obtenim resultats discrepants. Vinella *et al.* observa, igual que nosaltres, que GreA estimula l'expressió de *dksA*, així com que DksA estimula l'expressió de *greB* durant fase estacionària. Ells també observen l'autoregulació de *greA* i de *dksA*. De fet l'autoregulació de *dksA*, també és observada per Chandrangsu *et al.* (2011). En canvi, mentre nosaltres no veiem un efecte a diferents punts de la corba de creixement sobre l'expressió de *dksA,* a Chandrangsu *et al.* (2011) observen una disminució de l'expressió de *dksA* a fase estacionària tardana, respecte fase estacionària. Per una altra banda, Vinella *et al*. (2012) observen un augment de l'expressió de *dksA* a fase estacionària. Les diferències descrites poden ser degudes a les diferents fusions utilitzades als diversos estudis. Estudis fent servir tècniques de detecció de l'ARN missatger i de immunodetecció de proteïnes serien necessaris per caracteritzar apropiadament la regulació creuada entre els diferents gens.

<u>Efecte de la competència entre els factors que interaccionen amb l'ARNpol sobre l'expressió gènica del flagel a *E. coli*.</u>

En el nostre grup de recerca, mitjançant estudis transcriptòmics, hem determinat l'efecte de ppGpp i DksA en *E. coli* (Aberg *et al.*, 2009). Es va observar que ppGpp i DksA regulen de forma oposada diferents gens, alguns d'ells relacionats amb la motilitat, com ara *fliC* (Aberg *et al.*, 2009). En absència de ppGpp, l'expressió de *fliC* disminueix, mentre que en absència de DksA, augmenta. Aquest augment de l'expressió de *fliC* en absència de DksA depèn

de la presència de GreA, la qual cosa ens va fer hipotetitzar una possible competència entre DksA i GreA per la unió amb el canal secundari de l'ARNpol. En absència de DksA, GreA s'uneix a l'ARNpol i estimula l'expressió de *fliC*. Aquests resultats van ser corroborats mitjançant estudis transcripcionals utilitzant una fusió distal (+1210) del gen *fliC* amb *lacZ* (**fig. 43A**). De forma interessant, quan es va utilitzar una fusió proximal (+70) no s'observa cap augment en l'expressió de *fliC* en absència de DksA (**fig. 43A**). Per explicar aquestes diferències entre la fusió distal i proximal, es va hipotetitzar que el gen *fliC* contenia una zona de pausa transcripcional, entre la posició +70 i +1210. GreA seria requerida per poder alliberar l'ARNpol de la seqüència de pausa. Per tant, en absència de DksA la interacció entre l'ARNpol i GreA es veu clarament afavorida, augmentant així l'expressió de *fliC* (**fig. 43B**).

L'efecte produït per l'absència de DksA també s'observa en la motilitat d'*E. coli* (**fig. 45**). La soca deficient en *dksA* té una motilitat major que la soca WT, mentre que en la soca *dksA greA* és pràcticament no mòtil. A més, la soca deficient en *greA* és no mòtil, indicant que GreA és necessari per la motilitat d'*E. coli*.

Experiments de qPCR mostren que GreA estimula l'expressió de *fliC* (**fig. 46B**). Aquesta dada indica que GreA, fins i tot en presència de DksA, pot unir-se a l'ARNpol. Curiosament, aquest efecte no el veiem mitjançant les fusions *lacZ* (**fig. 46A**). Podem suposar que les diferències entre els experiments de qPCR i d'activitat β-galactosidasa són degudes a que l'activitat basal de la fusió *lacZ* és similar a l'expressió de la soca WT i per tant no veiem la disminució deguda a l'absència de GreA. Veiem una discrepància entre els resultats obtinguts per qPCR, fusions transcripcionals i estudis fenotípics, plaques de motilitat. Hem de tenir en compte que les condicions de cultiu en els diferents experiments, mentre que en els experiments fenotípics s'ha utilitzat un medi sòlid, per els experiments transcripcionals hem utilitzat un medi líquid. Observacions en el microscopi electrònic de transferència (**fig. 47**) indiquen que quan creixem MG1655 en medi líquid, la seva flagel·lació és molt baixa, fins i tot inexistent, en comparació amb el creixement en medi sòlid. Per tant, el creixement en medi líquid seria una condició no permissiva per l'expressió del flagel, fet que explicaria les discrepàncies en la observació de l'expressió de *fliC*. Tot i així, les

fusions transcripcionals ens han estat de gran utilitat per estudiar l'efecte de la competència entre DksA i GreA sobre l'expressió de *fliC*.

L'expressió dels gens del flagel està altament jerarquitzada i controlada (Chevance and Hughes, 2008). El complex FlhDC activa l'expressió dels gens que codifiquen pel cos basal del flagel i per la subunitat σ^F, FliA, que és necessària per expressar els gens responsables de formar el motor, quimioreceptors i el filament, *fliC* entre ells. Degut a aquesta jerarquia vam decidir determinar l'efecte que tenen els factors que interaccionen amb el canal secundari de l'ARNpol sobre els nivells de FliA i FliC mitjançant Western blot (**fig. 49**).

Veiem que GreA no produeix cap efecte sobre els nivells de FliA, indicant que l'efecte de GreA observat sobre l'expressió de *fliC* no es produeix a nivell d'inici de transcripció (**fig. 49A**). En canvi veiem que en absència de *dksA*, hi ha un augment (2 cops) dels nivells de FliA. Aquest augment també s'observa en el doble mutant *dksA greA*

Al determinar els nivells de FliC, veiem que en absència de DksA hi ha un augment de 57 vegades respecte a WT, que torna als nivells de la soca WT en el doble mutant *dksA greA* (**fig. 49B**). A més, en absència de GreA, els nivells de *fliC* disminueixen dramàticament (38 vegades). Atenent als resultats derivats de l'ús de les fusions distal i proximal i de les dades derivades de la immunodetecció de FliC i FliA, podem deduir que l'efecte de GreA és a nivell d'elongació de la transcripció, mentre que DksA actua a nivell d'inici de transcripció, afectant els nivells de la subunitat σ^F.

Considerant que GreA és essencial per a l'expressió de *fliC* i que l'activitat principal descrita per GreA és la de resoldre situacions de pausa o backtracking durant l'elongació de la transcripció (Laptenko *et al.*, 2003), vam decidir determinar l'efecte de l'activitat antipausa sobre l'expressió de *fliC*. Per fer-ho vam determinar si les mutacions en els residus D41 i E44 (Opalka *et al.*, 2003), necessaris per l'activitat antipausa de GreA (**fig. 51**), eren també necessàries per l'expressió de *fliC*. Utilitzant una soca que conté una mutació puntual en *greA*, produint un al·lel GreA E44K, veiem que aquesta soca no és mòtil. La

motilitat de la soca que conté GreA E44K es recupera quan afegim $GreA^{WT}$, (**fig. 51A**). A més, també vam determinar la capacitat dels al·lels GreA D41A, D41N i E44K de recuperar la motilitat d'una soca *greA* (**fig. 51B**). Veiem que cap dels mutants sense activitat antipausa és capaç de recuperar la motilitat de la soca deficient per *greA*.

Per una altra banda vam determinar tant l'expressió de *fliC* com la motilitat de soques que contenen mutacions a la subunitat β de l'ARNpol, amb la capacitat de reduir la taxa de pausa: rpoB35 i rpoB111. Amb la fusió distal del gen *fliC* (+1210), veiem que tant el mutant rpoB35 com rpoB111 augmenten l'expressió de *fliC* (**fig. 52**). Aquesta inducció és menor amb la fusió proximal, suggerint que l'expressió de *fliC* és sensible a la taxa de pausa.

Per una altra banda, quan mirem la motilitat de soques amb l'al·lel rpoB35, comparat amb el al·lel $rpoB^{WT}$, veiem que en absència de *greA* no hi ha una reducció de la motilitat amb el mutant rpoB35, a diferència de la reducció que s'observa amb l'al·lel $rpoB^{WT}$ (**fig. 53**). Aquests resultats indiquen que en absència de GreA, l'ARNpol no es capaç de passar de forma eficient per les possibles zones de pausa presents en *fliC* i per tant ni s'expressa *fliC* ni la soca és mòtil. En canvi, en un mutant rpoB35, degut a que l'ARNpol no es para a les zones de pausa, GreA ja no és necessari per la motilitat, així doncs, observem que aquesta soca és tant mòtil com la soca WT.

Per una altra banda hem vist que certs factors ambientals, com els diferents estats en què es troba el cultiu bacterià durant de creixement (**fig. 54**) o l'osmolaritat (**fig. 55**), juguen un paper important en l'expressió de *fliC*, i hem volgut determinar quin paper té GreA i DksA en aquesta regulació.

Veiem que a fase estacionària hi ha un augment de l'expressió de *fliC* (**fig. 54**). Per una banda veiem que aquesta inducció no és tant pronunciada quan utilitzem la fusió proximal, en comptes de la fusió distal. Per l'altra banda, veiem que a fase exponencial (OD_{600nm} 0.3) no s'observen diferències entre una soca WT i *dksA*, en canvi a fase estacionària si que s'observa.

Veiem que l'efecte de DksA sobre l'expressió de *fliC* depèn de l'osmolaritat (**fig. 55A**), però l'expressió de GreA no (**fig. 55C**). Aquests resultats podrien suggerir

que GreA pot patir canvis conformacionals com a resposta a elevada osmolaritat, i en conseqüència alterar l'expressió de gens que són dependents de GreA.

Efecte de la sobreexpressió de GreA sobre el creixement bacterià

Hem pogut determinar que la sobreexpressió de *greA* produeix un efecte negatiu sobre el creixement bacterià. Veiem una disminució en el creixement en cultiu en líquid (**fig. 56**), així com una disminució en la capacitat de formar colònies en cultius en sòlid (**fig. 58**). Veiem que en absència de DksA, l'efecte negatiu de la sobreexpressió de *greA* és major, presumiblement degut a que la deficiència de DksA deixa lliure el canal secundari i GreA pot interaccionar molt més eficientment amb l'ARNpol (**fig. 56** i **fig. 57**). Per una altra banda veiem que en absència de ppGpp la sobreexpressió de g*reA* produeix un efecte negatiu menor, suggerint que d'alguna manera ppGpp és necessari per la correcte unió de GreA a l'ARNpol.

També hem determinat que la sobreexpressió de *greB* produeix un efecte negatiu sobre el creixement bacterià. Tot i així, aquest efecte negatiu és molt menys dramàtic que el produït per GreA. Aquest efecte negatiu podria ser l'explicació biològica tant de l'autoregulació de GreA, com la seva regulació durant la corba de creixement.

Per estudiar més a fons l'efecte negatiu produït per a la sobreexpressió de *greA* sobre el creixement bacterià, hem determinat l'efecte que té sobre la morfologia cel·lular. Hem vist un allargament de les cèl·lules en forma de filaments (**fig. 59**). Aquesta filamentació pot ser deguda a un efecte de GreA sobre el gen *ftsN*, gen essencial per la correcte divisió cel·lular. Mutants deficients en *ftsN*, produeixen llargs filaments com els que nosaltres observem. Per una altra banda s'ha determinat, mitjançant estudis transcriptòmics (Stepanova *et al.*, 2007), que GreA pot reprimir l'expressió de *ftsN.* Aquests resultats ens permeten suggerir que la sobreexpressió de GreA podria produir una filamentació similar a la observada en absència de *ftsN,* degut a una forta repressió d'aquest gen deguda a GreA.

Estudi estructural de la proteïna GreA

Aprofitant l'efecte negatiu de la sobreexpressió de *greA* sobre el creixement bacterià, hem dut a terme una mutagènesi a l'atzar per determinar quins aminoàcids són important per a la funcionalitat de GreA, així com per a la seva unió a l'ARNpol i la competència entre factors.

Vam obtenir una llibreria de mutants puntuals en GreA mitjançant Error-prone PCR. Aquest mètode es basa en el fet que la Taq polimerasa no conté capacitat de corregir errors. De manera que es va amplificar *greA* en condicions subòbtimes amb l'objectiu que la Taq polimerasa cometi el màxim d'errors possibles. La col·lecció de mutants va ser clonada en el plàsmid pTrc99a, sota el control d'un promotor induïble per IPTG, i els plàsmids resultants es van transformar sobre una soca WT i una DksA. Finalment es van seleccionar aquells mutants que podien créixer en condicions de sobreexpressió de *greA* (**fig. 60**).

Els clons resistents van ser genotipats i seqüenciats per determinar la naturalesa de la mutació. El 27.5% dels mutants resistents a la sobreexpressió de *greA* contenen mutacions puntuals a la seqüència codificant, i com a conseqüència, produint canvis en la seqüència proteica.

Mirant la distribució dels mutants sobre la proteïna GreA veiem que es troben repartits entre els dos dominis de la proteïna, indicant així que tots dos dominis participen en l'activitat o són necessaris per l'afinitat de GreA a l'ARNpol.

Si els mutants són capaços de créixer en condicions de sobreexpressió de *greA* podria ser degut a que les diferents mutacions afectarien:

- la funcionalitat de GreA
- la unió de GreA a l'ARNpol, degut a canvis en:
    - l'afinitat pel canal secundari de l'ARNpol
    - l'habilitat per competir amb altres factors que s'uneixen al canal secundari de l'ARNpol

Per determinar l'efecte que tenen aquests mutants en la capacitat de competir amb DksA pel canal secundari de l'ARNpol, hem determinat l'efecte de la sobreexpressió d'aquests mutants en presència o absència de DksA (**taula 7**).

Per valorar el creixement de les diferents soques es va fer de la següent manera:

- es consideren positius (+) quan en presència d'IPTG trobem colònies d'un mida similar a les observades sense IPTG.
- es consideren negatius (-) quan en presència d'IPTG no es detecten colònies.
- es consideren resistents intermedis (+/-) quan en presència d'IPTG hi ha colònies però el seu creixement es veu afectat.

Aquells mutants positius tant en presència com en absència d'IPTG, com G10S, L69P, S121P, S124L i L130P, són mutants on GreA pot haver perdut la seva activitat o la seva capacitat d'unió a l'ARNpol. Per una altra banda, aquells mutants que produeixen un efecte negatiu sobre el creixement bacterià únicament en absència de DksA, com R9C, R15C, L21R, K22E, A51T, N96S, S121T, E151G i Y157H, poden tenir afectada la seva afinitat per l'ARNpol o una menor capacitat de competir amb DksA.

Per estudiar més en detall l'efecte què tenen els diferents mutants, hem estudiat dos fenotips associats a GreA: i) Efecte de l'activitat antipausa sobre l'expressió de *fliC*, ii) Capacitat de recuperar la prototròfia en soques deficients en *dksA* i ppGpp.

i) Com s'ha comentat abans, l'activitat antipausa de GreA és necessària per a l'expressió de *fliC*. Per aquest motiu hem decidit mirar quin efecte tenen els diferents mutants tenen sobre l'expressió de *fliC* i així determinar fins a quin punt la seva activitat antipausa està afectada. Així doncs, vam introduir els diferents $GreA^{Mut}$ a una soca deficient per *dksA greA*. Com ja s'ha comentat anteriorment, l'expressió de *fliC* en una soca *dksA* és molt elevada, comparada amb la soca WT. En canvi el doble mutant *dksA greA* té una expressió més reduïda, similar a la que s'observa a WT. Per aquest motiu, si en una soca *dksA greA* introduïm una proteïna GreA similar a la WT, augmentarà l'expressió de *fliC* de forma similar a la que s'observaria en un mutant *dksA*. En canvi, si introduïm una proteïna

GreA que no té activitat antipausa, l'expressió de *fliC* no variaria. Veiem, doncs que els diferents mutants tenen diferents nivells d'expressió de *fliC*, i per tant, tenen diferents activitats antipausa (**fig. 64**).

Veiem que els mutants S124L i L130P, que formen part de l'hèlix α del domini globular, no tenen pràcticament activitat antipausa. Cal destacar que els dos mutants eren capaços de créixer en condicions de sobreexpressió tant en presencia com en absència de DksA. En canvi, els mutants R9C, E151G i Y157H produeixen un efecte similar que la proteïna $GreA^{WT}$, indicant que tenen conservada l'activitat antipausa. A més aquests mutants tenien una capacitat intermedia de créixer en presencia de DksA i eren incapaços de créixer en la seva absència.

Vam dur a terme una aproximació experimental per determinar la capacitat d'unió de determinats mutants puntuals. Aquest experiment es basa en la capacitat dels $GreA^{Mut}$ de desplaçar la proteïna GreA cromosòmica. Al sobreexpressar una proteïna $GreA^{Mut}$ en una soca deficient per DksA, si el mutant és capaç d'unir a l'ARNpol, però no es funcional, la seva sobreexpressió permetria desplaçar GreA de l'ARNpol i disminuir l'expressió de *fliC*, produint un efecte similar a la doble mutació *dksA greA*. Per contra, si el $GreA^{Mut}$ no es capaç d'unir-se a l'ARNpol, la sobreexpressió d'aquesta proteïna no produirà cap efecte en l'expressió de *fliC*. Vam determinar la capacitat d'unió dels mutants C58R, S121P, S124L i L130P, així com dels mutants D41A, D41N i E44K. Tal com s'havia descrit (Opalka *et al.*, 2003), els nostres resultats (**fig. 66**) mostren que D41A, D41N i E44K, s'uneixen a l'ARNpol, però no són funcionals ja que no tenen activitat antipausa. Una cosa semblant veiem amb els mutants S124L i L130P. En canvi amb els mutants S121P i C58R, veiem que la seva sobreexpressió no produeix cap efecte sobre l'expressió de *fliC,* indicant que no són capaços d'unir-se a l'ARNpol.

ii) S'ha descrit que la soca deficient per ppGpp és auxotròfica en medi mínim M9, en canvi una soca deficient per *dksA* és braditròfica, és a dir, creix molt lentament (Vinella *et al.*, 2012). A més s'ha vist que el doble mutant *dksA greA* és auxotròfic, indicant que la capacitat de créixer del mutant *dksA* és degut a la presencia de GreA. La sobreexpressió de *greA* és capaç de recuperar la prototròfia a soques deficients per *dksA greA*, però també a la soca *dksA* ppGpp^0 (Vinella *et al.*, 2012). Cal destacar que mentre que a Vinella *et al.* (2012) s'observa que una soca deficient en *dksA* és braditròfica, nosaltres veiem que és auxotròfica (**taula 8**).

Hem determinat la capacitat dels diferents mutants de recuperar la prototròfia al ser sobreexpressats en una soca deficient en *dksA* i en una soca *dksA greA* (**taula 9**). Veiem que els mutants S124L i L130P no tenen l'habilitat de restaurar la prototròfia ni a la soca *dksA,* ni a la soca *dksA greA*. Tenint en compte que tampoc mostraven activitat antipausa, podem deduir que són mutants que han perdut completament la seva funcionalitat. Al estar els dos localitzats a la hèlix del domini globular, ens ha permès deduir que aquesta hèlix és important per la funcionalitat de GreA.

Per una altra banda els mutants R9C, E151G i Y157H amb una activitat antipausa similar a la WT, són capaços de recuperar la prototròfia a la soca *dksA greA*, però a la soca *dksA* només és capaç de fer-ho en condicions de sobreexpressió. Aquestes dades ens permeten suggerir que aquest mutants tenen afectada l'habilitat de competir amb DksA per unir-se al canal secundari de l'ARNpol.

Els mutants L21R, A51T, C58R, E59G, D98G, S121P i S121T són capaços de recuperar la prototròfia en una soca *dksA greA* només en condicions de sobreexpressió, indicant que la seva afinitat per l'ARNpol podria estar afectada.

<u>Anàlisi filogenètic de la distribució dels factors que s'uneixen al canal secundari de l'ARNpol</u>

Escherichia coli conté diferents proteïnes amb capacitat d'unir-se al canal secundari de l'ARNpol, com ara GreA, GreB, DksA i RnK (Borukhov *et al.*, 1993; Perederina *et al.*, 2004; Lamour *et al.*, 2008). Tot i així trobem altres proteïnes amb aquesta capacitat en altres organismes, com ara Gfh1 a *Thermus thermophilus* (Lamour *et al.*, 2006) o DksA2 a *Pseudomonas aeruginosa* (Blaby-Haas *et al.*, 2011; Furman *et al.*, 2013); o en elements genètics com bacteriòfags i plàsmids (Blankschien *et al.*, 2009).

Dins d'aquesta diversitat hem observat dues famílies principals. La família DksA, que conté proteïnes formades per hèlix α repartides entre un domini globular i un domini "coiled-coil", que és la part que entra dins l'ARNpol. En el domini globular acostumen a tenir un estructura de dits de Zinc tipus C4 (Perederina *et al.*, 2004).

La família GreA conté, a part d'ella mateixa, GreB, Gfh1 i RnK. Les proteïnes d'aquesta família tenen una similaritat estructural molt elevada entre elles, amb un domini N-terminal "coiled-coil" similar a DksA i amb un domini C-terminal globular format per lamina plegada β i una hèlix α.

Les dues famílies, tot i tenir una organització espacial similar, no tenen homologia a nivell de seqüència, com s'observa a la **taula 10**. A més, cap dels membre de la família GreA conté una estructura en dits de Zinc.

Estudiant més en detall la família GreA (**fig. 69**), mitjançant arbres filogenètics de Maximum Likelihood (ML), podem proposar que tant Gfh1 i GreB han aparegut per duplicació de *greA* i posterior diferenciació. Per una altra banda, veiem que RnK esta més allunyat filogenèticament de la resta de membres de la família (**taula 10**).

Si estudiem més en detall la família DksA amb arbres filogenètics de ML (**fig. 71**) observem un clade format per els membres de la família codificats en plàsmids, bacteriòfags i pseudofags. Per una altra banda veiem un segon clade que correspon a DksA, des d'on hi surt una branca corresponent a DksA2, suggerint que DksA2 va evolucionar de DksA perdent el dit de zinc. S'observa un tercer clade que engloba proteïnes similar a DksA presents a *Borrelia garinii, Hydrogenobacter thermophilus* i *Thermocrinis albus*.

Si determinem la distribució de les diferents proteïnes que interaccionen amb el canal secundari de l'ARNpol entre els diferents bacteris, veiem que tots els fílums, excepte Aquificae, Chlamydia i alguns grups de Cyanobacteria, contenen GreA (**fig. 72**), indicant que GreA podria ser la proteïna ancestral de les altres proteïnes de la seva família. A més, l'existència d'una varietat de factors es troba concentrada a Proteobacteria ja que els altres fílums només contenen GreA, excepte alguns membres de Spirochaetes i el filum Thermus.

Hem analitzat la diversitat nucleotídica a diferents parts de la proteïna GreA mitjançant comparant la quantitat de mutacions no sinònimes, mutacions que provoquen canvis en la seqüència proteica, que es detecten entre un grup amb una alta diversitat de factors que interaccionen amb el canal secundari de l'ARNpol (Enterobacteriaceae) i un grup que només conté GreA (Bacillaceae). Veiem que no hi ha diferències en el nombre de mutacions no sinònimes en el domini globular i pràcticament en tot el domini fibril·lar, però si en el linker entre els dos dominis (**fig. 73**). Veiem que en Enterobacteriaceae el linker esta més conservat que en Bacillaceae. La presència d'altres proteïnes que poden interaccionar amb el canal secundari de l'ARNpol ha fet que aquesta estructura es conservés per mantenir la seva capacitat de competir per unir-se a l'ARNpol. A més aquesta pressió podria indicar que GreA podria patir canvis conformacionals en determinades condicions.

Efecte de ppGpp i DksA en el perfil d'expressió gènica a *Salmonella enterica* serovar Typhimurium

En el nostre grup de recerca, vam determinar que GreA era important per l'expressió de factors de colonització en *E. coli*, al detectar discrepàncies observades entre el perfil d'expressió gènica de soques deficients en DksA i ppGpp. Al trobar gens regulats de forma diferencial entre ppGpp i DksA, vam hipotetitzar que això era degut a que en absència de DksA s'alterava la competència i equilibri entre els factors que interaccionen amb el canal secundari de l'ARNpol. Tenint en compte que els elements sensibles a la competència d'aquests factors en *E. coli* estaven relacionats amb la colonització, vam decidir fer un estudi similar en un bacteri patogen. El model utilitzat és *Salmonella enterica* serovar Typhimurium. Tot i que poc es coneix

sobre l'efecte de DksA a *Salmonella*, s'ha determinat que ppGpp té un important efecte sobre l'expressió de gens codificats en les illes de patogenicitat SPI1 i SPI2 (Thompson *et al.*, 2006).

Hem determinat el patró d'expressió de la soca SV5015 de *Salmonella enterica* serovar Typhimurium en cultius en LB a 37ºC crescuts fins a fase estacionària (OD_{600nm} 2.0) utilitzant un microarray de NimbleGen que conté sondes per gens cromosòmics i de diferents plàsmids que es troben a la soca SV5015, pSLT, pCol1B i pSRF1010. Considerant significativament afectats aquells gens amb un *fold-change* superior a 3 i inferior a -3, hem determinat que tant ppGpp com DksA regulen una quantitat similar de gens, un 8.3% i 10.8%, respectivament (**taula 11**). Mentre que ppGpp sembla tenir un paper més aviat activador, la proteïna DksA sembla activar un nombre similar de gens dels que reprimeix.

Per una altra banda, al determinar l'efecte de ppGpp i DksA, diferenciant entre gens que corresponen al *core* genoma i gens obtinguts per processos de HGT (**taula 12**), veiem que, sota les condicions experimentals utilitzades, ppGpp estimula l'expressió de fins a un 20% dels gens HGT. Tots els gens HGT afectats per ppGpp són estimulats per aquest, indicant que ppGpp és una molècula reguladora per a l'expressió de molts gens obtinguts per processos de HGT. DksA té un efecte similar al de ppGpp sobre els gens obtinguts per processos de transferència horitzontal, però en canvi té un paper repressor sobre els gens del *core* genoma més important que ppGpp.

Es van distribuir els gens afectats per ppGpp i DksA en diferents categories funcionals (**fig. 75**) i veiem que els dos factors, majoritàriament, estimulen gens corresponents a HGT. Per una altra banda, ppGpp estimula l'expressió de gens englobats a la categoria funcional de processos cel·lulars, i gens presents a la categoria de sense classificar, que engloba alguns factors important per la virulència de *Salmonella*. En canvi, ppGpp reprimeix l'expressió de gens presents a la categoria de destí proteic, biosíntesis d'aminoàcids i metabolisme energètic. El fet que ppGpp no estimuli, i que reprimeixi alguns gens responsables de la biosíntesi d'aminoàcids, és consistent amb el fet que els cultius es van fer créixer en medi ric i que la síntesi d'aminoàcids en aquest medi es trobarà reprimida ja que és més senzill agafar els aminoàcids del medi.

Consistent amb això, detectem que ppGpp estimula l'expressió de gens que codifiquen per transportadors d'oligopèptids i aminoàcids.

Quan estudiem els gens afectats per DksA (**fig. 75**), veiem que la majoria dels gens estimulats per DksA, pertanyen a la categoria d'embolcall cel·lular, processos cel·lulars i proteïnes sense classificar. Per una altra banda, l'expressió dels gens reprimits per DksA es troben englobats per les categories de metabolisme energètic, biosíntesis d'àcids grassos i la d'àcids nucleics.

Quan comparem les categories on trobem gens afectats per ppGpp i DksA (**fig. 75**) veiem un comportament similar en determinades categories, com biosíntesis d'aminoàcid, metabolisme cel·lular intermedi i destí de proteïnes. Tot i així hi ha gens que estan diferencialment regulats entre ppGpp i DksA, que pertanyen a les categories de metabolisme de l'ADN, metabolisme energètic i funcions regulatòries.

Diferents fenotips, presumiblement associats a gens que la seva expressió està afectada per ppGpp i DksA, van ser estudiats (**fig. 76**). Veiem que ppGpp té una supervivència al fred i a l'estrés oxidatiu més baixa que la soca WT, degut a que ppGpp estimula l'expressió de *cspB* i diferents gens necessaris per la resposta a l'estrés oxidatiu (**taula 13**). A més veiem que tant ppGpp com DksA són necessaris per la formació de biofilm i la motilitat.

Quan mirem a la distribució dels gens afectats per ppGpp i DksA corresponents a HGT, veiem que els dos factors estimulen gens presents en illes de patogenicitat, plàsmids, bacteriòfags i l'operó *pdu* (**fig. 78**).

Els dos factors estimulen gens de les mateixes illes aproximadament, afectant la majoria dels gens de les SPI 1, 2, 4 i 5 (**fig. 79**). La SPI3 és la menys afectada de les illes. Tot i així DksA estimula fortament el gen *mtgC* present a la SPI3. Aquest gen és important per la patogenicitat de *Salmonella*.

Els dos factors estimulen gens responsables de la invasió cel·lular codificats en les illes de patogenicitat. La producció de proteïnes efectores, SipBCD de la SPI1, requerides per la invasió cel·lular es pot observar determinant l'activitat hemolítica de sobrenedants lliures de cèl·lules (**fig. 79B**). En absència de

ppGpp i DksA, hi ha una disminució de l'activitat hemolítica, suggerint que ppGpp i DksA poden ser factors important per la producció dels efectors SipBDC i com a conseqüència en la invasió cel·lular.

Salmonella conté diferents bacteriòfags incorporats en el seu genoma, alguns d'ells codifiquen per factors de virulència com SopE i GtgB. Veiem que tant DksA com ppGpp estimulen aquests gens. A més, ppGpp estimula gens associats a la replicació d'aquests fags, suggerint que ppGpp podria tenir un paper en la mobilització de bacteriòfags. Per això hem determinat la producció de bacteriòfags en condicions d'inducció amb mitomicina C, o sense, en soques deficients per ppGpp o DksA. Mentre que no veiem diferències en la producció de fags en una soca deficient per DksA, veiem que ppGpp clarament estimula la producció de bacteriòfags, tant en condicions de inducció com sense (**fig. 80**). Aquestes dades suggereixen que ppGpp podria ser important pel moviment de gens per transducció natural, on ADN codificant per factors de virulència podria ser englobat dins de partícules víriques i transferides en un nou hoste (Penadés *et al.*, 2014).

Un efecte similar l'observem al plàsmid conjugatiu pSLT, sent l'únic plàsmid que conté gens afectats per ppGpp i DksA (**fig. 81A**). L'alarmona ppGpp, però no DksA, estimula l'expressió de l'operó *spvABCD* que és essencial per la reestructuració del citoesquelet d'actina de la cèl·lula hoste, i per tant en el procés d'invasió cel·lular. A més veiem que l'expressió del gen *traD*, essencial per la conjugació de pSLT (Lu *et al.*, 2008) es troba estimulat per ppGpp, indicant que ppGpp pot tenir un efecte sobre la conjugació bacteriana. Per això vam determinar la taxa de conjugació en absència de ppGpp i DksA. Mentre DksA sembla tenir cap paper en la conjugació de pSLT, ppGpp és crucial per la conjugació (**fig. 81B**).

Considerant l'efecte de ppGpp sobre la producció de fags i la conjugació, podem proposar que ppGpp és un factor important per la disseminació de gens HGT.

Finalment, si comparem l'efecte entre ppGpp i DksA, veiem que el 51% i el 62% dels gens afectats per ppGpp i DksA, respectivament, estan afectats de

forma individual. Aquest dades s'obtenen quan utilitzem un llindar de significança de 3 / -3 i per tant estan esbiaixades. Un exemple d'això el trobaríem en el gen *fruB*, on en absència de ppGpp té una expressió amb un *fold-change* de -11.58, però en absència de DksA el *fold-change* és de -2.71. Amb el llinda de significança a -3 classificaríem aquest gen com un cas de regulació independent per ppGpp, quan en realitat esta sent estimulat per els dos factors. Per això hem considerat que no hi ha cap efecte sobre l'expressió gènica amb un fold change entre -1.5 i 1.5. De manera que *fruB* estaria regulat de forma similar per ppGpp i DksA, però *fucP* ($ppGpp^0$ -3.82, *dksA* 1.27) si que només esta regulat per ppGpp.

Així doncs quan mirem als gens afectats per ppGpp i DksA (**fig. 83**), veiem que el 61% dels gens afectats estan regulats de forma similar entre ppGpp i DksA, tant estimulats com reprimits. Un 32% dels gens és afectat per un dels factors però no per l'altre, produint un efecte independent. I un 7% dels gens (47 gens) són afectats per ppGpp i DksA de forma oposada a *Salmonella.* Alguns d'aquests gens són gens de l'operó de degradació de Maltosa (*malMEFK*), així com d'altres transportadors de carbohidrats. A més també inclou algunes porines com *ompF*, la proteïna associada al nucleoide StpA o la chaperona IbpB.

Tot i així més estudis serien necessaris per determina si a *Salmonella,* el paper diferencial observat entre ppGpp i DksA pot ser produït també per la competència per el canal secundari de l'ARNpol, com s'ha vist en *Escherichia coli*.

Conclusions

En aquest projecte hem estudiat diferents aspectes de la competència entre les proteïnes que interaccionen amb el canal secundari de l'ARNpol. Canvis en l'expressió gènica d'aquests factors produirien canvis en l'equilibri entre aquestes proteïnes per unir-se al canal secundari de l'ARNpol. Per aquest motiu, hem estudiat a fons l'expressió de *greA* així com la regulació creuada entre els factors que interaccionen amb el canal secundari.

Hem determinat que la competència entre proteïnes que interaccionen amb el canal secundari pot produir un efecte sobre l'expressió de determinats gens, com ara *fliC*.

Així com hem dut a terme un estudi estructural i filogenètic de la proteïna GreA per estudiar més a fons la competència entre els diferents factors que s'uneixen dins el canal secundari, així com quins són els dominis importants per a la competència. A més hem determinat quins aminoàcids són important per a la funcionalitat de GreA.

Finalment, estudis transcripcionals a *Salmonella enterica* serovar Typhimurium s'han dut a terme per determinar l'efecte dels diferents factors que s'uneixen a l'ARNpol sobre elements mòbils i l'expressió de gens considerats HGT.

Les conclusions d'aquest treball són:

1. GreA autoreprimeix la seva expressió.
2. L'autoregulació de *greA* requereix l'activitat antipausa de GreA i la seqüència localitzada entre +3 i +101, respecte a l'inici de transcripció.
3. GraL està implicat en l'autoregulació de *greA*.
4. L'expressió de *greA* disminueix a fase estacionària. Aquest efecte requereix la presència de GreA.
5. Una alta temperatura (42ºC) estimula l'expressió de *greA*.

6. Sobreexpressió de *rpoE* o producció d'un estrés extracitoplasmatic amb proteïnes mal plegades, incrementa l'expressió de *greA*.

7. Variacions en la disponibilitat d'oxigen o magnesi, pH o osmolaritat no produeixen cap efecte sobre l'expressió de *greA* a *E.* coli.

8. El complex regulatori cAMP-CRP regula l'expressió de *greA*.

9. Existeix una regulació creuada entre GreA, GreB i DksA. GreA estimula l'expressió de *dksA*, mentre que DksA estimula l'expressió de *greB* a fase estacionària.

10. GreA i DksA afecten l'expressió de *fliC* a nivells d'elongació i iniciació de la transcripció, respectivament.

11. L'activitat antipausa de GreA és necessària per l'expressió de *fliC*.

12. Sobreexpressió de *greA* i el presumible increment de la quantitat relativa del complex ARNpol-GreA causa un efecte negatiu sobre la fisiologia cel·lular.

13. L'alarmona ppGpp podria ser necessària per la interacció de GreA amb el canal secundari de l'ARNpol.

14. L'hèlix α del domini globular de GreA és essencial per la funcionalitat de GreA.

15. Mutacions que puguin tenir un efecte sobre el linker que uneix els dos dominis de GreA, com I75V o P5S, podrien produir canvis hipotètics en la conformació de GreA.

16. Els mutants L21R, A51T, C58G, D98G, S121P i S121T poden tenir l'afinitat per l'ARNpol afectada.

17. Els mutants R9C, E151G i Y157H poden tenir afectada la capacitat de competir amb DksA per unir-se al canal secundari de l'ARNpol.

18. Estudis filogenètics ens han dut a concloure que la variabilitat de factors que s'uneixen al canal secundari de l'ARNpol ha aparegut per duplicació gènica.

19. Tot els bacteris tenen *greA,* excepte els filums *Aquificae*, *Chlamydia*, i alguns membres de *Cyanobacteria*.

20. A proteobacteries hi ha una major diversitat de factors que s'uneixen a l'ARNpol que a altres grups bacterians.

21. La presència d'altres factors que s'uneixen al canal secundari de l'ARNpol, com ara DksA o GreB, produeixen una pressió evolutiva per preservar determinades estructures de GreA.

22. L'alarmona ppGpp i DksA són reguladors globals de l'expressió gènica a *Salmonella enterica* serovar Typhimurium.

23. L'alarmona ppGpp i DksA estimulen l'expressió d'un gran nombre de gens, ppGpp estimula un 4% dels gens del *core genome* i fins a un 19.9% dels gens HGT i DksA estimula un 4% de gens del *core* i 14.4% de HGT.

24. L'alarmona ppGpp i DksA estimulen l'expressió de gens de les SPIs, sent la SPI3 la menys afectada de les illes.

25. L'activitat hemolítica associada a proteïnes efectores de la SPI1 es troba afectada en mutants deficients per ppGpp i *dksA*, suggerint que aquests factors podrien ser importants per a la invasió cel·lular.

26. L'alarmona ppGpp i DksA estimulen l'expressió de factors de virulència presents en bacteriòfags i plàsmids.

27. La mobilització de bacteriòfags i plàsmids conjugatius és estimulada per ppGpp.

28. L'alarmona ppGpp i DksA regulen de forma similar el 61% dels gens afectats.

29. El 7% dels gens afectats per ppGpp i DksA, mostra un comportament oposat entre els dos factors.

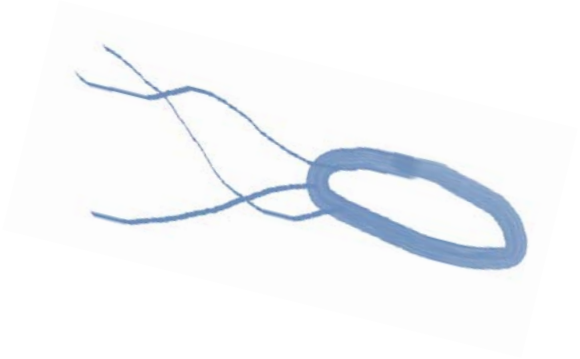

7. Bibliography

- Aberg, A., Fernández-Vázquez, J., Cabrer-Panes, J.D., Sánchez, A., and Balsalobre, C. (2009) Similar and divergent effects of ppGpp and DksA deficiencies on transcription in *Escherichia coli*. *J Bacteriol* **191**: 3226–36.
- Aberg, A., Shingler, V., and Balsalobre, C. (2006) (p)ppGpp regulates type 1 fimbriation of *Escherichia coli* by modulating the expression of the site-specific recombinase FimB. *Mol Microbiol* **60**: 1520–33.
- Aberg, A., Shingler, V., and Balsalobre, C. (2008) Regulation of the *fimB* promoter: a case of differential regulation by ppGpp and DksA in vivo. *Mol Microbiol* **67**: 1223–41.
- Adelman, K., Porta, A. La, Santangelo, T.J., Lis, J.T., Roberts, J.W., and Wang, M.D. (2002) Single molecule analysis of RNA polymerase elongation reveals uniform kinetic behavior. *Proc Natl Acad Sci U S A* **99**: 13538–43.
- Aertsen, A., and Michiels, C.W. (2008) Stress and How Bacteria Cope with Death and Survival. .
- Alba, B.M., and Gross, C.A. (2004) Regulation of the *Escherichia coli* sigma-dependent envelope stress response. *Mol Microbiol* **52**: 613–9.
- Amann, E., Ochs, B., and Abel, K.J. (1988) Tightly regulated tac promoter vectors useful for the expression of unfused and fused proteins in *Escherichia coli*. *Gene* **69**: 301–15.
- Applied Biosystems by life technologies (2011) SYBR® Green PCR Master Mix and SYBR® Green RT-PCR Reagents Kit. .
- Artsimovitch, I., and Landick, R. (2000) Pausing by bacterial RNA polymerase is mediated by mechanistically distinct classes of signals. *Proc Natl Acad Sci U S A* **97**: 7090–5.
- Artsimovitch, I., and Landick, R. (2000) Pausing by bacterial RNA polymerase is mediated by mechanistically distinct classes of signals. *Proc Natl Acad Sci* **97**: 7090–7095.
- Artsimovitch, I., Patlan, V., Sekine, S., Vassylyeva, M.N., Hosaka, T., Ochi, K., *et al.* (2004) Structural Basis for Transcription Regulation by Alarmone ppGpp. *Cell* **117**: 299–310.
- Aseev, L. V, Koledinskaya, L.S., and Boni, I. V (2014) Dissecting the Extended "-10" *Escherichia coli rpsB* Promoter Activity and Regulation in vivo. *Biochem Biokhimiia* **79**: 776–84.
- Atkinson, G.C., Tenson, T., and Hauryliuk, V. (2011) The RelA/SpoT homolog (RSH) superfamily: distribution and functional evolution of ppGpp synthetases and hydrolases across the tree of life. *PLoS One* **6**: e23479.
- Atlas, R.M., and Parks, L.C. (1993) *Handbook of microbiological media*. CRC Press, Boca Raton [Fla.] [etc.] :
- Babu, M., Díaz-Mejía, J.J., Vlasblom, J., Gagarinova, A., Phanse, S., Graham, C., *et al.* (2011) Genetic interaction maps in *Escherichia coli* reveal functional crosstalk among cell envelope biogenesis pathways. *PLoS Genet* **7**: e1002377.
- Baharoglu, Z., Lestini, R., Duigou, S., and Michel, B. (2010) RNA polymerase mutations that facilitate replication progression in the *rep uvrD recF* mutant lacking two accessory replicative helicases. *Mol Microbiol* **77**: 324–36.
- Balows, A., Trüper, H.G., Dworkin, M., Harder, W., and Schleifer, K.-H. (1992) *Escherichia coli*. In *The Prokaryotes: A handbook on the biology of bacteria: ecophysiology, isolation, identifiaction and aplications*. Springer-Verlag New York Inc., pp. 2696–2736.
- Barembruch, C., and Hengge, R. (2007) Cellular levels and activity of the flagellar sigma factor FliA of *Escherichia coli* are controlled by FlgM-modulated proteolysis. *Mol Microbiol* **65**: 76–89.
- Bar-Nahum, G., Epshtein, V., Ruckenstein, A.E., Rafikov, R., Mustaev, A., and Nudler, E. (2005) A ratchet mechanism of transcription elongation and its control. *Cell* **120**: 183–93.
- Battesti, A., and Bouveret, E. (2006) Acyl carrier protein/SpoT interaction, the switch linking SpoT-dependent stress response to fatty acid metabolism. *Mol Microbiol* **62**: 1048–63.
- Becskei, A., and Serrano, L. (2000) Engineering stability in gene networks by autoregulation. *Nature* **405**: 590–3.

- Bell, A., Gaston, K., Williams, R., Chapman, K., Kolb, A., Buc, H., *et al.* (1990) Mutations that alter the ability of the *Escherichia coli* cyclic AMP receptor protein to activate transcription. *Nucleic Acids Res* **18**: 7243–50.
- Bianchi, A.A., and Baneyx, F. (1999) Hyperosmotic shock induces the sigma32 and sigmaE stress regulons of *Escherichia coli*. *Mol Microbiol* **34**: 1029–38.
- Blaby-Haas, C.E., Furman, R., Rodionov, D. a, Artsimovitch, I., and Crécy-Lagard, V. de (2011) Role of a Zn-independent DksA in Zn homeostasis and stringent response. *Mol Microbiol* **79**: 700–15.
- Blankschien, M.D., Potrykus, K., Grace, E., Choudhary, A., Vinella, D., Cashel, M., and Herman, C. (2009) TraR, a homolog of a RNAP secondary channel interactor, modulates transcription. *PLoS Genet* **5**: e1000345.
- Bloch, S.K., Felczykowska, A., and Nejman-Faleńczyk, B. (2012) *Escherichia coli* O104:H4 outbreak--have we learnt a lesson from it? *Acta Biochim Pol* **59**: 483–8.
- Bolivar, F., Rodriguez, R.L., Greene, P.J., Betlach, M.C., Heyneker, H.L., Boyer, H.W., *et al.* (1977) Construction and characterization of new cloning vehicles. II. A multipurpose cloning system. *Gene* **2**: 95–113.
- Borisov, V.B., Gennis, R.B., Hemp, J., and Verkhovsky, M.I. (2011) The cytochrome bd respiratory oxygen reductases. *Biochim Biophys Acta* **1807**: 1398–413.
- Borukhov, S., Sagitov, V., and Goldfarb, A. (1993) Transcript cleavage factors from E. coli. *Cell* **72**: 459–466.
- Bossi, L., and Figueroa-Bossi, N. (2007) A small RNA downregulates LamB maltoporin in Salmonella. *Mol Microbiol* **65**: 799–810.
- Bougdour, A., and Gottesman, S. (2007) ppGpp regulation of RpoS degradation via anti-adaptor protein IraP. *Proc Natl Acad Sci U S A* **104**: 12896–901.
- Boyd, E.F., and Brüssow, H. (2002) Common themes among bacteriophage-encoded virulence factors and diversity among the bacteriophages involved. *Trends Microbiol* **10**: 521–9.
- Braasch, I., and Salzburger, W. (2009) In ovo omnia: diversification by duplication in fish and other vertebrates. *J Biol* **8**: 25.
- Braeken, K., Moris, M., Daniels, R., Vanderleyden, J., and Michiels, J. (2006) New horizons for (p)ppGpp in bacterial and plant physiology. *Trends Microbiol* **14**: 45–54.
- Brown, L., Gentry, D., Elliott, T., and Cashel, M. (2002) DksA affects ppGpp induction of RpoS at a translational level. *J Bacteriol* **184**: 4455–65.
- Brown, T.A. (2010) *Gene cloning and DNA analysis : an introduction*. Wiley-Blackwell, Oxford :
- Browning, D.F., and Busby, S.J. (2004) The regulation of bacterial transcription initiation. *Nat Rev Microbiol* **2**: 57–65.
- Busby, S., and Ebright, R.H. (1999) Transcription activation by catabolite activator protein (CAP). *J Mol Biol* **293**: 199–213.
- Busiek, K.K., and Margolin, W. (2014) A role for FtsA in SPOR-independent localization of the essential *Escherichia coli* cell division protein FtsN. *Mol Microbiol* **92**: 1212–26.
- Bylund, G.O., Wipemo, L.C., Lundberg, L.A., and Wikström, P.M. (1998) RimM and RbfA are essential for efficient processing of 16S rRNA in *Escherichia coli*. *J Bacteriol* **180**: 73–82.
- Byrne, R.T., Chen, S.H., Wood, E.A., Cabot, E.L., and Cox, M.M. (2014) *Escherichia coli* genes and pathways involved in surviving extreme exposure to ionizing radiation. *J Bacteriol* **196**: 3534–45.
- Camacho, E.M., and Casadesús, J. (2002) Conjugal transfer of the virulence plasmid of *Salmonella enterica* is regulated by the leucine-responsive regulatory protein and DNA adenine methylation. *Mol Microbiol* **44**: 1589–1598.
- Campanacci, V., Dubois, D.Y., Becker, H.D., Kern, D., Spinelli, S., Valencia, C., *et al.* (2004) The *Escherichia coli* YadB gene product reveals a novel aminoacyl-tRNA synthetase like activity. *J Mol Biol* **337**: 273–83.
- Campbell, E.A., Muzzin, O., Chlenov, M., Sun, J.L., Olson, C.A., Weinman, O., *et al.* (2002) Structure of the bacterial RNA polymerase promoter specificity sigma subunit. *Mol Cell* **9**: 527–39.
- Cashel, M. (1969) The control of ribonucleic acid synthesis in *Escherichia coli*. IV. Relevance of unusual phosphorylated compounds from amino acid-starved stringent strains. *J Biol Chem* **244**: 3133–41.

- Cashel, M., Gentry, D., Hernandez, V., and Vinella, D. (1996) The stringent Response. In *Escherichia coli and Salmonella: cellular and molecular biology*. ASM Press, Wastington, D.C. : pp. 1458–1489.
- Chandrangsu, P., Lemke, J.J., and Gourse, R.L. (2011) The *dksA* promoter is negatively feedback regulated by DksA and ppGpp. *Mol Microbiol* **80**: 1337–48.
- Chandrangsu, P., Wang, L., Choi, S.H., and Gourse, R.L. (2012) Suppression of a dnaKJ deletion by multicopy *dksA* results from non-feedback-regulated transcripts that originate upstream of the major *dksA* promoter. *J Bacteriol* **194**: 1437–46.
- Chevance, F.F. V, and Hughes, K.T. (2008) Coordinating assembly of a bacterial macromolecular machine. *Nat Rev Microbiol* **6**: 455–65.
- Cho, B.-K., Knight, E.M., Barrett, C.L., and Palsson, B.Ø. (2008) Genome-wide analysis of Fis binding in *Escherichia coli* indicates a causative role for A-/AT-tracts. *Genome Res* **18**: 900–10.
- Connolly, L., Pen, A.D.E.L.A.S., and Gross, C.A. (1997) E Is an Essential Sigma Factor in *Escherichia coli*. *J Bacteriol* **179**: 6862–6864.
- Costa, X.J. Da, and Artz, S.W. (1997) Mutations that render the promoter of the histidine operon of Salmonella typhimurium insensitive to nutrient-rich medium repression and amino acid downshift. *J Bacteriol* **179**: 5211–7.
- Costanzo, A., Nicoloff, H., Barchinger, S.E., Banta, A.B., Gourse, R.L., and Ades, S.E. (2008) ppGpp and DksA likely regulate the activity of the extracytoplasmic stress factor sigmaE in *Escherichia coli* by both direct and indirect mechanisms. *Mol Microbiol* **67**: 619–32.
- Croxen, M.A., Law, R.J., Scholz, R., Keeney, K.M., Wlodarska, M., and Finlay, B.B. (2013) Recent advances in understanding enteric pathogenic *Escherichia coli*. *Clin Microbiol Rev* **26**: 822–80.
- Dai, K., Xu, Y., and Lutkenhaus, J. (1993) Cloning and characterization of ftsN, an essential cell division gene in *Escherichia coli* isolated as a multicopy suppressor of ftsA12(Ts). *J Bacteriol* **175**: 3790–3797.
- Dalebroux, Z.D., Svensson, S.L., Gaynor, E.C., and Swanson, M.S. (2010) ppGpp conjures bacterial virulence. *Microbiol Mol Biol Rev* **74**: 171–99.
- Dalebroux, Z.D., and Swanson, M.S. (2012) ppGpp: magic beyond RNA polymerase. *Nat Rev Microbiol* **10**: 203–12.
- Datsenko, K.A., and Wanner, B.L. (2000) One-step inactivation of chromosomal genes in *Escherichia coli* K-12 using PCR products. *Proc Natl Acad Sci U S A* **97**: 6640–5.
- Daubin, V., and Ochman, H. (2004) Bacterial genomes as new gene homes: the genealogy of ORFans in E. coli. *Genome Res* **14**: 1036–42.
- Decker, K., Plumbridge, J., and Boos, W. (1998) Negative transcriptional regulation of a positive regulator: the expression of malT, encoding the transcriptional activator of the maltose regulon of *Escherichia coli*, is negatively controlled by Mlc. *Mol Microbiol* **27**: 381–90.
- Deutscher, J. (2008) The mechanisms of carbon catabolite repression in bacteria. *Curr Opin Microbiol* **11**: 87–93.
- Ding, L., Wang, Y., Hu, Y., Atkinson, S., Williams, P., and Chen, S. (2009) Functional characterization of FlgM in the regulation of flagellar synthesis and motility in Yersinia pseudotuberculosis. *Microbiology* **155**: 1890–900.
- Dini-Andreote, F., Andreote, F.D., Araújo, W.L., Trevors, J.T., and Elsas, J.D. van (2012) Bacterial genomes: habitat specificity and uncharted organisms. *Microb Ecol* **64**: 1–7.
- Dudin, O., Geiselmann, J., Ogasawara, H., Ishihama, A., and Lacour, S. (2014) Repression of flagellar genes in exponential phase by CsgD and CpxR, two crucial modulators of *Escherichia coli* biofilm formation. *J Bacteriol* **196**: 707–15.
- Dutta, D., Shatalin, K., Epshtein, V., Gottesman, M.E., and Nudler, E. (2011) Linking RNA polymerase backtracking to genome instability in E. coli. *Cell* **146**: 533–43.
- Ellermeier, C.D., Janakiraman, A., and Slauch, J.M. (2002) Construction of targeted single copy lac fusions using lambda Red and FLP-mediated site-specific recombination in bacteria. *Gene* **290**: 153–61.
- Erickson, D.L., Lines, J.L., Pesci, E.C., Venturi, V., and Storey, D.G. (2004) Pseudomonas aeruginosa relA contributes to virulence in Drosophila melanogaster. *Infect Immun* **72**: 5638–45.

- Fàbrega, A., and Vila, J. (2013) *Salmonella enterica* serovar Typhimurium skills to succeed in the host: virulence and regulation. *Clin Microbiol Rev* **26**: 308–41.
- Fass, E., and Groisman, E.A. (2009) Control of Salmonella pathogenicity island-2 gene expression. *Curr Opin Microbiol* **12**: 199–204.
- Felsenstein, J. (1981) Evolutionary trees from DNA sequences: a maximum likelihood approach. *J Mol Evol* **17**: 368–76.
- Feng, G.H., Lee, D.N., Wang, D., Chan, C.L., and Landick, R. (1994) GreA-induced transcript cleavage in transcription complexes containing *Escherichia coli* RNA polymerase is controlled by multiple factors, including nascent transcript location and structure. *J Biol Chem* **269**: 22282–94.
- Feng, Y., and Cronan, J.E. (2009) A new member of the *Escherichia coli* fad regulon: transcriptional regulation of fadM (ybaW). *J Bacteriol* **191**: 6320–8.
- Feng, Y., and Cronan, J.E. (2012) Crosstalk of *Escherichia coli* FadR with global regulators in expression of fatty acid transport genes. *PLoS One* **7**: e46275.
- Fengs, G., Lee, D.N., Wangs, D., Chans, C.L., and Landickall, R. (1994) GreA-induced Transcript Cleavage in Transcription *Escherichia coli* RNA Polymerase Is Complexes Containing Controlled by Multiple Factors , Including Nascent Transcript Location and Structure *. *J Biol Chem* 22282–22294.
- Field, T.R., Layton, A.N., Bispham, J., Stevens, M.P., and Galyov, E.E. (2008) Identification of novel genes and pathways affecting Salmonella type III secretion system 1 using a contact-dependent hemolysis assay. *J Bacteriol* **190**: 3393–8.
- Figueroa-Bossi, N., and Bossi, L. (1999) Inducible prophages contribute to Salmonella virulence in mice. *Mol Microbiol* **33**: 167–176.
- Figueroa-Bossi, N., Uzzau, S., Maloriol, D., and Bossi, L. (2001) Variable assortment of prophages provides a transferable repertoire of pathogenic determinants in Salmonella. *Mol Microbiol* **39**: 260–71.
- Forst, S.A., and Roberts, D.L. (1994) Signal transduction by the EnvZ-OmpR phosphotransfer system in bacteria. *Res Microbiol* **145**: 363–73.
- Friden, P., Newman, T., and Freundlich, M. (1982) Nucleotide sequence of the ilvB promoter-regulatory region: a biosynthetic operon controlled by attenuation and cyclic AMP. *Proc Natl Acad Sci U S A* **79**: 6156–60.
- Furman, R., Biswas, T., Danhart, E.M., Foster, M.P., Tsodikov, O. V, and Artsimovitch, I. (2013) DksA2, a zinc-independent structural analog of the transcription factor DksA. *FEBS Lett* **587**: 614–9.
- Furman, R., Tsodikov, O. V, Wolf, Y.I., and Artsimovitch, I. (2013) An insertion in the catalytic trigger loop gates the secondary channel of RNA polymerase. *J Mol Biol* **425**: 82–93.
- Gogarten, J.P., Doolittle, W.F., and Lawrence, J.G. (2002) Prokaryotic evolution in light of gene transfer. *Mol Biol Evol* **19**: 2226–38.
- Gopalkrishnan, S., Nicoloff, H., and Ades, S.E. (2014) Co-ordinated regulation of the extracytoplasmic stress factor, sigmaE, with other *Escherichia coli* sigma factors by (p)ppGpp and DksA may be achieved by specific regulation of individual holoenzymes. *Mol Microbiol* **93**: 479–93.
- Gordon, R.E., and Mihm, J.M. (1962) The Type Species of the Genus Nocardia. *J Gen Microbiol* **27**: 1–10.
- Gotoh, H., Okada, N., Kim, Y.G., Shiraishi, K., Hirami, N., Haneda, T., *et al.* (2003) Extracellular secretion of the virulence plasmid-encoded ADP-ribosyltransferase SpvB in Salmonella. *Microb Pathog* **34**: 227–38.
- Goudeau, D.M., Parker, C.T., Zhou, Y., Sela, S., Kroupitski, Y., and Brandl, M.T. (2013) The salmonella transcriptome in lettuce and cilantro soft rot reveals a niche overlap with the animal host intestine. *Appl Environ Microbiol* **79**: 250–62.
- Guajardo, R., and Sousa, R. (1997) A model for the mechanism of polymerase translocation. *J Mol Biol* **265**: 8–19.
- Guiney, D.G., and Fierer, J. (2011) The Role of the spv Genes in Salmonella Pathogenesis. *Front Microbiol* **2**: 129.
- Guisbert, E., Yura, T., Rhodius, V.A., and Gross, C.A. (2008) Convergence of molecular, modeling, and systems approaches for an understanding of the *Escherichia coli* heat shock response. *Microbiol Mol Biol Rev* **72**: 545–54.

- Gummesson, B., Lovmar, M., and Nyström, T. (2013) A proximal promoter element required for positive transcriptional control by guanosine tetraphosphate and DksA protein during the stringent response. *J Biol Chem* **288**: 21055–64.
- Guo, S., Alshamy, I., Hughes, K.T., and Chevance, F.F. V (2014) Analysis of factors that affect FlgM-dependent type III secretion for protein purification with *Salmonella enterica* serovar Typhimurium. *J Bacteriol* **196**: 2333–47.
- Gusarov, I., and Nudler, E. (1999) The Mechanism of Intrinsic Transcription Termination. *Mol Cell* **3**: 495–504.
- Guyer, M.S., Reed, R.R., Steitz, J.A., and Low, K.B. (1981) Identification of a sex-factor-affinity site in E. coli as gamma delta. *Cold Spring Harb Symp Quant Biol* **45 Pt 1**: 135–40.
- Hammer, B.K., and Swanson, M.S. (1999) Co-ordination of Legionella pneumophila virulence with entry into stationary phase by ppGpp. *Mol Microbiol* **33**: 721–731.
- Hanahan, D., Jessee, J., and Bloom, F.R. (1991) Plasmid transformation of *Escherichia coli* and other bacteria. *Methods Enzymol* **204**: 63–113.
- Hansen-Wester, I., and Hensel, M. (2001) Salmonella pathogenicity islands encoding type III secretion systems. *Microbes Infect* **3**: 549–59.
- Haraga, A., Ohlson, M.B., and Miller, S.I. (2008) Salmonellae interplay with host cells. *Nat Rev Microbiol* **6**: 53–66.
- Haralalka, S., Nandi, S., and Bhadra, R.K. (2003) Mutation in the relA Gene of Vibrio cholerae Affects In Vitro and In Vivo Expression of Virulence Factors. *J Bacteriol* **185**: 4672–4682.
- Harinarayanan, R., Murphy, H., and Cashel, M. (2008) Synthetic growth phenotypes of *Escherichia coli* lacking ppGpp and transketolase A (tktA) are due to ppGpp-mediated transcriptional regulation of tktB. *Mol Microbiol* **69**: 882–94.
- Haugen, S.P., Ross, W., and Gourse, R.L. (2008) Advances in bacterial promoter recognition and its control by factors that do not bind DNA. *Nat Rev Microbiol* **6**: 507–19.
- Henard, C.A., Tapscott, T., Crawford, M.A., Husain, M., Doulias, P.-T., Porwollik, S., *et al.* (2014) The 4-cysteine zinc-finger motif of the RNA polymerase regulator DksA serves as a thiol switch for sensing oxidative and nitrosative stress. *Mol Microbiol* **91**: 790–804.
- Henkin, T.M. (2000) Transcription termination control in bacteria. *Curr Opin Microbiol* **3**: 149–153.
- Hook-Barnard, I., Johnson, X.B., and Hinton, D.M. (2006) *Escherichia coli* RNA polymerase recognition of a sigma70-dependent promoter requiring a -35 DNA element and an extended -10 TGn motif. *J Bacteriol* **188**: 8352–9.
- Howarth, D.G., and Donoghue, M.J. (2006) Phylogenetic analysis of the “ECE” (CYC/TB1) clade reveals duplications predating the core eudicots. *Proc Natl Acad Sci U S A* **103**: 9101–6.
- Hurley, D., McCusker, M.P., Fanning, Sã©., and Martins, M. (2014) Salmonellaâ€“Host Interactions â€“ Modulation of the Host Innate Immune System. *Front Immunol* **5**: 481.
- Inouye, M., and Phadtare, S. (2004) Cold shock response and adaptation at near-freezing temperature in microorganisms. *Sci STKE* **2004**: pe26.
- Irizarry, R.A., Hobbs, B., Collin, F., Beazer-Barclay, Y.D., Antonellis, K.J., Scherf, U., and Speed, T.P. (2003) Exploration, normalization, and summaries of high density oligonucleotide array probe level data. *Biostatistics* **4**: 249–64.
- Ishihama, A. (2000) Functional modulation of *Escherichia coli* RNA polymerase. *Annu Rev Microbiol* **54**: 499–518.
- Ivancic, T., Jamnik, P., and Stopar, D. (2013) Cold shock CspA and CspB protein production during periodic temperature cycling in *Escherichia coli*. *BMC Res Notes* **6**: 248.
- Jacob, F., Perrin, D., Sanchez, C., and Monod, J. (1960) [Operon: a group of genes with the expression coordinated by an operator]. *C R Hebd Seances Acad Sci* **250**: 1727–9.
- Jiang, M., Datta, K., Walker, A., Strahler, J., Bagamasbad, P., Andrews, P.C., and Maddock, J.R. (2006) The *Escherichia coli* GTPase CgtAE is involved in late steps of large ribosome assembly. *J Bacteriol* **188**: 6757–70.

- Jiang, M., Sullivan, S.M., Wout, P.K., and Maddock, J.R. (2007) G-protein control of the ribosome-associated stress response protein SpoT. *J Bacteriol* **189**: 6140–7.
- Jishage, M., and Ishihama, A. (1998) A stationary phase protein in *Escherichia coli* with binding activity to the major sigma subunit of RNA polymerase. *Proc Natl Acad Sci U S A* **95**: 4953–8.
- Jishage, M., Kvint, K., Shingler, V., and Nyström, T. (2002) Regulation of sigma factor competition by the alarmone ppGpp. *Genes Dev* **16**: 1260–70.
- Jöres, L., and Wagner, R. (2003) Essential steps in the ppGpp-dependent regulation of bacterial ribosomal RNA promoters can be explained by substrate competition. *J Biol Chem* **278**: 16834–43.
- Kalia, D., Merey, G., Nakayama, S., Zheng, Y., Zhou, J., Luo, Y., *et al.* (2013) Nucleotide, c-di-GMP, c-di-AMP, cGMP, cAMP, (p)ppGpp signaling in bacteria and implications in pathogenesis. *Chem Soc Rev* **42**: 305–41.
- Kang, P.J., and Craig, E.A. (1990) Identification and characterization of a new *Escherichia coli* gene that is a dosage-dependent suppressor of a dnaK deletion mutation. *J Bacteriol* **172**: 2055–64.
- Kanjee, U., Gutsche, I., Alexopoulos, E., Zhao, B., Bakkouri, M. El, Thibault, G., *et al.* (2011) Linkage between the bacterial acid stress and stringent responses: the structure of the inducible lysine decarboxylase. *EMBO J* **30**: 931–44.
- Kearns, D.B. (2010) A field guide to bacterial swarming motility. *Nat Rev Microbiol* **8**: 634–44.
- Kishida, H., Unzai, S., Roper, D.I., Lloyd, A., Park, S.-Y., and Tame, J.R.H. (2006) Crystal structure of penicillin binding protein 4 (dacB) from *Escherichia coli*, both in the native form and covalently linked to various antibiotics. *Biochemistry* **45**: 783–92.
- Klumpp, J., and Fuchs, T.M. (2007) Identification of novel genes in genomic islands that contribute to Salmonella typhimurium replication in macrophages. *Microbiology* **153**: 1207–20.
- Korzheva, N., Mustaev, A., Kozlov, M., Malhotra, A., Nikiforov, V., Goldfarb, A., and Darst, S.A. (2000) A Structural Model of Transcription Elongation. *Science (80-)* **289**: 619–625.
- Koulich, D., Nikiforov, V., and Borukhov, S. (1998) Distinct functions of N and C-terminal domains of GreA, an *Escherichia coli* transcript cleavage factor. *J Mol Biol* **276**: 379–89.
- Koulich, D., Orlova, M., Malhotra, a., Sali, a., Darst, S. a., and Borukhov, S. (1997) Domain Organization of *Escherichia coli* Transcript Cleavage Factors GreA and GreB. *J Biol Chem* **272**: 7201–7210.
- Krebs, J.E., Goldstein, E.S., Kilpatrick, S.T., and Lewin, B. (2011) *Lewin's genes X*. Jones and Bartlett Publishers, Sudbury :
- Kulish, D., Lee, J., Lomakin, I., Nowicka, B., Das, A., Darst, S., *et al.* (2000) The functional role of basic patch, a structural element of *Escherichia coli* transcript cleavage factors GreA and GreB. *J Biol Chem* **275**: 12789–98.
- Lamour, V., Hogan, B.P., Erie, D.A., and Darst, S.A. (2006) Crystal structure of Thermus aquaticus Gfh1, a Gre-factor paralog that inhibits rather than stimulates transcript cleavage. *J Mol Biol* **356**: 179–88.
- Lamour, V., Rutherford, S.T., Kuznedelov, K., Ramagopal, U. a, Gourse, R.L., Severinov, K., and Darst, S. a (2008) Crystal structure of *Escherichia coli* Rnk, a new RNA polymerase-interacting protein. *J Mol Biol* **383**: 367–79.
- Landick, R. (2005) NTP-entry routes in multi-subunit RNA polymerases. *Trends Biochem Sci* **30**: 651–4.
- Landick, R. (2006) The regulatory roles and mechanism of transcriptional pausing. *Biochem Soc Trans* **34**: 1062–6.
- Laptenko, O., Kim, S.-S., Lee, J., Starodubtseva, M., Cava, F., Berenguer, J., *et al.* (2006) pH-dependent conformational switch activates the inhibitor of transcription elongation. *EMBO J* **25**: 2131–41.
- Laptenko, O., Lee, J., Lomakin, I., and Borukhov, S. (2003) Transcript cleavage factors GreA and GreB act as transient catalytic components of RNA polymerase. *EMBO J* **22**: 6322–34.

- Laurie, A.D., Bernardo, L.M.D., Sze, C.C., Skarfstad, E., Szalewska-Palasz, A., Nyström, T., and Shingler, V. (2003) The role of the alarmone (p)ppGpp in sigma N competition for core RNA polymerase. *J Biol Chem* **278**: 1494–503.
- Lee, S.J., Xie, A., Jiang, W., Etchegaray, J.P., Jones, P.G., and Inouye, M. (1994) Family of the major cold-shock protein, CspA (CS7.4), of *Escherichia coli*, whose members show a high sequence similarity with the eukaryotic Y-box binding proteins. *Mol Microbiol* **11**: 833–9.
- Lei, S.P., Lin, H.C., Wang, S.S., Callaway, J., and Wilcox, G. (1987) Characterization of the Erwinia carotovora pelB gene and its product pectate lyase. *J Bacteriol* **169**: 4379–83.
- Lemke, J.J., Durfee, T., and Gourse, R.L. (2009) DksA and ppGpp directly regulate transcription of the *Escherichia coli* flagellar cascade. *Mol Microbiol* **74**: 1368–79.
- Li, C., Louise, C.J., Shi, W., and Adler, J. (1993) Adverse conditions which cause lack of flagella in *Escherichia coli*. *J Bacteriol* **175**: 2229–35.
- Li, K., Jiang, T., Yu, B., Wang, L., Gao, C., Ma, C., *et al.* (2012) Transcription elongation factor GreA has functional chaperone activity. *PLoS One* **7**: e47521.
- Lu, J., Wong, J.J.W., Edwards, R.A., Manchak, J., Frost, L.S., and Glover, J.N.M. (2008) Structural basis of specific TraD-TraM recognition during F plasmid-mediated bacterial conjugation. *Mol Microbiol* **70**: 89–99.
- Maciąg-Dorszyńska, M., Szalewska-Pałasz, A., and Węgrzyn, G. (2013) Different effects of ppGpp on *Escherichia coli* DNA replication in vivo and in vitro. *FEBS Open Bio* **3**: 161–4.
- Magnusson, L.U., Farewell, A., and Nyström, T. (2005) ppGpp: a global regulator in *Escherichia coli*. *Trends Microbiol* **13**: 236–42.
- Magnusson, L.U., Gummesson, B., Joksimović, P., Farewell, A., and Nyström, T. (2007) Identical, independent, and opposing roles of ppGpp and DksA in *Escherichia coli*. *J Bacteriol* **189**: 5193–202.
- Majander, K., Anton, L., Antikainen, J., Lång, H., Brummer, M., Korhonen, T.K., and Westerlund-Wikström, B. (2005) Extracellular secretion of polypeptides using a modified *Escherichia coli* flagellar secretion apparatus. *Nat Biotechnol* **23**: 475–81.
- Malde, A., Gangaiah, D., Chandrashekhar, K., Pina-Mimbela, R., Torrelles, J.B., and Rajashekara, G. (2014) Functional characterization of exopolyphosphatase/guanosine pentaphosphate phosphohydrolase (PPX/GPPA) of Campylobacter jejuni. *Virulence* **5**: 521–33.
- Martinez-Rucobo, F.W., and Cramer, P. (2013) Structural basis of transcription elongation. *Biochim Biophys Acta* **1829**: 9–19.
- Mascher, T., Helmann, J.D., and Unden, G. (2006) Stimulus perception in bacterial signal-transducing histidine kinases. *Microbiol Mol Biol Rev* **70**: 910–38.
- McGlynn, P., and Lloyd, R.G. (2000) Modulation of RNA polymerase by (p)ppGpp reveals a RecG-dependent mechanism for replication fork progression. *Cell* **101**: 35–45.
- Mechold, U., Potrykus, K., Murphy, H., Murakami, K.S., and Cashel, M. (2013) Differential regulation by ppGpp versus pppGpp in *Escherichia coli*. *Nucleic Acids Res* **41**: 6175–89.
- Merrikh, H., Ferrazzoli, A.E., and Lovett, S.T. (2009) Growth phase and (p)ppGpp control of IraD, a regulator of RpoS stability, in *Escherichia coli*. *J Bacteriol* **191**: 7436–46.
- Miki, T., Okada, N., Shimada, Y., and Danbara, H. (2004) Characterization of Salmonella pathogenicity island 1 type III secretion-dependent hemolytic activity in *Salmonella enterica* serovar Typhimurium. *Microb Pathog* **37**: 65–72.
- Mira, A., Martín Cuadrado, A.B., D'Auria, G., and Rodríguez Valera, F. (2010) The bacterial pan-genome: a new paradigm in microbiology. *Int Microbiol Off J Spanish Soc Microbiol* **13**: 45–57.
- Mira, A., Ochman, H., and Moran, N.A. (2001) Deletional bias and the evolution of bacterial genomes. *Trends Genet* **17**: 589–96.
- Mirold, S., Rabsch, W., Rohde, M., Stender, S., Tschäpe, H., Rüssmann, H., *et al.* (1999) Isolation of a temperate bacteriophage encoding the type III effector protein SopE from an epidemic Salmonella typhimurium strain. *Proc Natl Acad Sci U S A* **96**: 9845–50.

- Mishra, S., and Imlay, J. (2012) Why do bacteria use so many enzymes to scavenge hydrogen peroxide? *Arch Biochem Biophys* **525**: 145–60.
- Mitchell, J.E., Zheng, D., Busby, S.J.W., and Minchin, S.D. (2003) Identification and analysis of "extended -10" promoters in *Escherichia coli*. *Nucleic Acids Res* **31**: 4689–95.
- Mitchell, J.G., and Kogure, K. (2006) Bacterial motility: links to the environment and a driving force for microbial physics. *FEMS Microbiol Ecol* **55**: 3–16.
- Mizuno, T., and Mizushima, S. (1990) Signal transduction and gene regulation through the phosphorylation of two regulatory components: the molecular basis for the osmotic regulation of the porin genes. *Mol Microbiol* **4**: 1077–82.
- Monod, J. (1949) The Growth of Bacterial Cultures. *Annu Rev Microbiol* **3**: 371–394.
- Montero, M., Eydallin, G., Viale, A.M., Almagro, G., Muñoz, F.J., Rahimpour, M., *et al.* (2009) *Escherichia coli* glycogen metabolism is controlled by the PhoP-PhoQ regulatory system at submillimolar environmental Mg2+ concentrations, and is highly interconnected with a wide variety of cellular processes. *Biochem J* **424**: 129–41.
- Mooney, R.A., Darst, S.A., and Landick, R. (2005) Sigma and RNA polymerase: an on-again, off-again relationship? *Mol Cell* **20**: 335–45.
- Mouslim, C., and Hughes, K.T. (2014) The effect of cell growth phase on the regulatory cross-talk between flagellar and Spi1 virulence gene expression. *PLoS Pathog* **10**: e1003987.
- Müller, C.M., Aberg, A., Straseviçiene, J., Emody, L., Uhlin, B.E., and Balsalobre, C. (2009) Type 1 fimbriae, a colonization factor of uropathogenic *Escherichia coli*, are controlled by the metabolic sensor CRP-cAMP. *PLoS Pathog* **5**: e1000303.
- Münch, R., Hiller, K., Grote, A., Scheer, M., Klein, J., Schobert, M., and Jahn, D. (2005) Virtual Footprint and PRODORIC: an integrative framework for regulon prediction in prokaryotes. *Bioinformatics* **21**: 4187–9.
- Murakami, K.S., Masuda, S., Campbell, E.A., Muzzin, O., and Darst, S.A. (2002) Structural basis of transcription initiation: an RNA polymerase holoenzyme-DNA complex. *Science* **296**: 1285–90.
- Murphy, H., and Cashel, M. (2003) Isolation of RNA polymerase suppressors of a (p)ppGpp deficiency. *Methods Enzymol* **371**: 596–601.
- My, L., Rekoske, B., Lemke, J.J., Viala, J.P., Gourse, R.L., and Bouveret, E. (2013) Transcription of the *Escherichia coli* fatty acid synthesis operon fabHDG is directly activated by FadR and inhibited by ppGpp. *J Bacteriol* **195**: 3784–95.
- Navarro, F., Robin, A., D'Ari, R., and Joseleau-Petit, D. (1998) Analysis of the effect of ppGpp on the ftsQAZ operon in *Escherichia coli*. *Mol Microbiol* **29**: 815–23.
- Naville, M., Ghuillot-Gaudeffroy, A., Marchais, A., and Gautheret, D. (2014) ARNold: A web tool for the prediction of Rho-independent transcription terminators. *RNA Biol* **8**: 11–13.
- Neidhardt, F.C. (1964) The regulation RNA synthesis in bacteria. *Prog Nucleic Acid Res Mol Biol* **3**: 145–81.
- Neidhardt, F.C., and Curtis, R. (1996) *Escherichia coli and salmonella : cellular and molecular biology*. ASM Press, Wastington, D.C. :
- Neuman, K.C., Abbondanzieri, E.A., Landick, R., Gelles, J., and Block, S.M. (2003) Ubiquitous transcriptional pausing is independent of RNA polymerase backtracking. *Cell* **115**: 437–47.
- Ng, P.C., and Henikoff, S. (2003) SIFT: Predicting amino acid changes that affect protein function. *Nucleic Acids Res* **31**: 3812–4.
- Nickels, B.E., Garrity, S.J., Mekler, V., Minakhin, L., Severinov, K., Ebright, R.H., and Hochschild, A. (2005) The interaction between sigma70 and the beta-flap of *Escherichia coli* RNA polymerase inhibits extension of nascent RNA during early elongation. *Proc Natl Acad Sci U S A* **102**: 4488–93.
- Nilsson, I., Sääf, A., Whitley, P., Gafvelin, G., Waller, C., and Heijne, G. von (1998) Proline-induced disruption of a transmembrane alpha-helix in its natural environment. *J Mol Biol* **284**: 1165–75.
- Nogales, J., Campos, R., BenAbdelkhalek, H., Olivares, J., Lluch, C., and Sanjuan, J. (2002) Rhizobium tropici genes involved in free-living salt tolerance are required for the establishment of efficient nitrogen-fixing symbiosis with Phaseolus vulgaris. *Mol Plant Microbe Interact* **15**: 225–32.

- Nudler, E. (1999) Transcription elongation: structural basis and mechanisms. *J Mol Biol* **288**: 1–12.
- Nudler, E., Mustaev, A., Lukhtanov, E., and Goldfarb, A. (1997) The RNA-DNA hybrid maintains the register of transcription by preventing backtracking of RNA polymerase. *Cell* **89**: 33–41.
- Ochman, H., Lawrence, J.G., and Groisman, E.A. (2000) Lateral gene transfer and the nature of bacterial innovation. *Nature* **405**: 299–304.
- Oh, Y.T., Park, Y., Yoon, M.Y., Bari, W., Go, J., Min, K.B., *et al.* (2014) Cholera toxin production during anaerobic trimethylamine N-oxide respiration is mediated by stringent response in *Vibrio cholerae*. *J Biol Chem* **289**: 13232–42.
- Opalka, N., Chlenov, M., Chacon, P., Rice, W.J., Wriggers, W., and Darst, S. a (2003) Structure and function of the transcription elongation factor GreB bound to bacterial RNA polymerase. *Cell* **114**: 335–45.
- Orlova, M., Newlands, J., Das, A., Goldfarb, A., and Borukhov, S. (1995) Intrinsic transcript cleavage activity of RNA polymerase. *Proc Natl Acad Sci U S A* **92**: 4596–600.
- Österberg, S., Peso-Santos, T. del, and Shingler, V. (2011) Regulation of alternative sigma factor use. *Annu Rev Microbiol* **65**: 37–55.
- Park, S.-Y., and Groisman, E.A. (2014) Signal-specific temporal response by the Salmonella PhoP/PhoQ regulatory system. *Mol Microbiol* **91**: 135–44.
- Pattery, T., Hernalsteens, J.P., and Greve, H. De (1999) Identification and molecular characterization of a novel Salmonella enteritidis pathogenicity islet encoding an ABC transporter. *Mol Microbiol* **33**: 791–805.
- Paul, B.J., Barker, M.M., Ross, W., Schneider, D.A., Webb, C., Foster, J.W., and Gourse, R.L. (2004) DksA: a critical component of the transcription initiation machinery that potentiates the regulation of rRNA promoters by ppGpp and the initiating NTP. *Cell* **118**: 311–22.
- Pearce, S.R., Mimmack, M.L., Gallagher, M.P., Gileadi, U., Hyde, S.C., and Higgins, C.F. (1992) Membrane topology of the integral membrane components, OppB and OppC, of the oligopeptide permease of Salmonella typhimurium. *Mol Microbiol* **6**: 47–57.
- Penadés, J.R., Chen, J., Quiles-Puchalt, N., Carpena, N., and Novick, R.P. (2014) Bacteriophage-mediated spread of bacterial virulence genes. *Curr Opin Microbiol* **23C**: 171–178.
- Perederina, A., Svetlov, V., Vassylyeva, M.N., Tahirov, T.H., Yokoyama, S., Artsimovitch, I., and Vassylyev, D.G. (2004) Regulation through the secondary channel--structural framework for ppGpp-DksA synergism during transcription. *Cell* **118**: 297–309.
- Persky, N.S., Ferullo, D.J., Cooper, D.L., Moore, H.R., and Lovett, S.T. (2009) The ObgE/CgtA GTPase influences the stringent response to amino acid starvation in *Escherichia coli*. *Mol Microbiol* **73**: 253–66.
- Pesavento, C., and Hengge, R. (2009) Bacterial nucleotide-based second messengers. *Curr Opin Microbiol* **12**: 170–6.
- Peters, J.M., Vangeloff, A.D., and Landick, R. (2011) Bacterial transcription terminators: the RNA 3'-end chronicles. *J Mol Biol* **412**: 793–813.
- Piper, S.E., Mitchell, J.E., Lee, D.J., and Busby, S.J.W. (2009) A global view of *Escherichia coli* Rsd protein and its interactions. *Mol Biosyst* **5**: 1943–7.
- Pizarro-Cerdá, J., and Tedin, K. (2004) The bacterial signal molecule, ppGpp, regulates Salmonella virulence gene expression. *Mol Microbiol* **52**: 1827–44.
- Plumbridge, J. (1998) Control of the expression of the manXYZ operon in *Escherichia coli*: Mlc is a negative regulator of the mannose PTS. *Mol Microbiol* **27**: 369–80.
- Popovych, N., Tzeng, S.-R., Tonelli, M., Ebright, R.H., and Kalodimos, C.G. (2009) Structural basis for cAMP-mediated allosteric control of the catabolite activator protein. *Proc Natl Acad Sci U S A* **106**: 6927–32.
- Poteete, A.R. (2011) Recombination phenotypes of *Escherichia coli greA* mutants. *BMC Mol Biol* **12**: 12.
- Potrykus, K., and Cashel, M. (2008) (p)ppGpp: still magical? *Annu Rev Microbiol* **62**: 35–51.

- Potrykus, K., Murphy, H., Chen, X., Epstein, J.A., and Cashel, M. (2010) Imprecise transcription termination within *Escherichia coli greA* leader gives rise to an array of short transcripts, GraL. *Nucleic Acids Res* **38**: 1636–51.
- Potrykus, K., Vinella, D., Murphy, H., Szalewska-Palasz, A., D'Ari, R., and Cashel, M. (2006) Antagonistic regulation of *Escherichia coli* ribosomal RNA rrnB P1 promoter activity by GreA and DksA. *J Biol Chem* **281**: 15238–48.
- Primm, T.P., Andersen, S.J., Mizrahi, V., Avarbock, D., Rubin, H., and Barry, C.E. (2000) The Stringent Response of Mycobacterium tuberculosis Is Required for Long-Term Survival. *J Bacteriol* **182**: 4889–4898.
- Pupov, D., Kuzin, I., Bass, I., and Kulbachinskiy, A. (2014) Distinct functions of the RNA polymerase σ subunit region 3.2 in RNA priming and promoter escape. *Nucleic Acids Res* **42**: 4494–504.
- Pushker, R., Mira, A., and Rodríguez-Valera, F. (2004) Comparative genomics of gene-family size in closely related bacteria. *Genome Biol* **5**: R27.
- Quinones, M., Kimsey, H.H., Ross, W., Gourse, R.L., and Waldor, M.K. (2006) LexA represses CTXphi transcription by blocking access of the alpha C-terminal domain of RNA polymerase to promoter DNA. *J Biol Chem* **281**: 39407–12.
- Ramachandran, V.K., Shearer, N., and Thompson, A. (2014) The primary transcriptome of *Salmonella enterica* Serovar Typhimurium and its dependence on ppGpp during late stationary phase. *PLoS One* **9**: e92690.
- Rambaut, A. (2006) FigTree. .
- Ranea, J.A.G., Buchan, D.W.A., Thornton, J.M., and Orengo, C.A. (2004) Evolution of protein superfamilies and bacterial genome size. *J Mol Biol* **336**: 871–87.
- Reppas, N.B., Wade, J.T., Church, G.M., and Struhl, K. (2006) The transition between transcriptional initiation and elongation in E. coli is highly variable and often rate limiting. *Mol Cell* **24**: 747–57.
- Rhodes, M.W., and Kator, H.I. (1991) Use of Salmonella typhimurium WG49 to enumerate male-specific coliphages in an estuary and watershed subject to nonpoint pollution. *Water Res* **25**: 1315–1323.
- Rhodius, V. a, Suh, W.C., Nonaka, G., West, J., and Gross, C.A. (2006) Conserved and variable functions of the sigmaE stress response in related genomes. *PLoS Biol* **4**: e2.
- Richet, E., Davidson, A.L., and Joly, N. (2012) The ABC transporter MalFGK(2) sequesters the MalT transcription factor at the membrane in the absence of cognate substrate. *Mol Microbiol* **85**: 632–47.
- Richter, D. (1980) Uncharged tRNA inhibits guanosine 3',5'-bis (diphosphate) 3'-pyrophosphohydrolase [ppGppase], the spoT gene product, from *Escherichia coli*. *Mol Gen Genet* **178**: 325–7.
- Roche, N. (2010) NimbleGen Arrays User ' s Guide. .
- Roghanian, M., Zenkin, N., and Yuzenkova, Y. (2015) Bacterial global regulators DksA/ppGpp increase fidelity of transcription. *Nucleic Acids Res* **43**: 1529–36.
- Rosenfeld, N., Elowitz, M.B., and Alon, U. (2002) Negative autoregulation speeds the response times of transcription networks. *J Mol Biol* **323**: 785–93.
- Rost, B., Yachdav, G., and Liu, J. (2004) The PredictProtein server. *Nucleic Acids Res* **32**: W321–6.
- Roth, J.R., Lawrence, J.G., and Bobik, T.A. (1996) Cobalamin (coenzyme B12): synthesis and biological significance. *Annu Rev Microbiol* **50**: 137–81.
- Rouvière, P.E., Las Peñas, A. De, Mecsas, J., Lu, C.Z., Rudd, K.E., and Gross, C.A. (1995) rpoE, the gene encoding the second heat-shock sigma factor, sigma E, in *Escherichia coli*. *EMBO J* **14**: 1032–42.
- Ruiz, N., and Silhavy, T.J. (2005) Sensing external stress: watchdogs of the *Escherichia coli* cell envelope. *Curr Opin Microbiol* **8**: 122–6.
- Rushing, M.D., and Slauch, J.M. (2011) Either periplasmic tethering or protease resistance is sufficient to allow a SodC to protect *Salmonella enterica* serovar Typhimurium from phagocytic superoxide. *Mol Microbiol* **82**: 952–63.
- Rutherford, S.T., Lemke, J.J., Vrentas, C.E., Gaal, T., Ross, W., and Gourse, R.L. (2007) Effects of DksA, GreA, and GreB on transcription initiation: insights into the mechanisms of factors that bind in the secondary channel of RNA polymerase. *J Mol Biol* **366**: 1243–57.

- Rutherford, S.T., Villers, C.L., Lee, J.-H., Ross, W., and Gourse, R.L. (2009) Allosteric control of *Escherichia coli* rRNA promoter complexes by DksA. *Genes Dev* **23**: 236–48.
- Ryals, J., Little, R., and Bremer, H. (1982) Control of rRNA and tRNA syntheses in *Escherichia coli* by guanosine tetraphosphate. *J Bacteriol* **151**: 1261–8.
- Rymer, R.U., Solorio, F.A., Tehranchi, A.K., Chu, C., Corn, J.E., Keck, J.L., *et al.* (2012) Binding mechanism of metal·NTP substrates and stringent-response alarmones to bacterial DnaG-type primases. *Structure* **20**: 1478–89.
- Sayed, A.K., Odom, C., and Foster, J.W. (2007) The *Escherichia coli* AraC-family regulators GadX and GadW activate gadE, the central activator of glutamate-dependent acid resistance. *Microbiology* **153**: 2584–92.
- Schmieger, H. (1972) Phage P22-mutants with increased or decreased transduction abilities. *Mol Gen Genet* **119**: 75–88.
- Schmittgen, T.D., and Livak, K.J. (2008) Analyzing real-time PCR data by the comparative C(T) method. *Nat Protoc* **3**: 1101–8.
- Seifart Gomes, C., Izar, B., Pazan, F., Mohamed, W., Mraheil, M.A., Mukherjee, K., *et al.* (2011) Universal stress proteins are important for oxidative and acid stress resistance and growth of Listeria monocytogenes EGD-e in vitro and in vivo. *PLoS One* **6**: e24965.
- Selander, R., Li, J., and Nelson, K. (1996) Evolutionary Genetics of *Salmonella enterica*. In *Escherichia coli and Salmonella: cellular and molecular biology*. ASM Press, Wastington, D.C. : pp. 2691–2703.
- Serra, D.O., Richter, A.M., Klauck, G., Mika, F., and Hengge, R. (2013) Microanatomy at Cellular Resolution and Spatial Order of Physiological Differentiation in a Bacterial Biofilm. **4**: 1–12.
- Shaevitz, J.W., Abbondanzieri, E.A., Landick, R., and Block, S.M. (2003) Backtracking by single RNA polymerase molecules observed at near-base-pair resolution. *Nature* **426**: 684–7.
- Shashni, R., Qayyum, M.Z., Vishalini, V., Dey, D., and Sen, R. (2014) Redundancy of primary RNA-binding functions of the bacterial transcription terminator Rho. *Nucleic Acids Res* **42**: 9677–90.
- Simm, R., Ahmad, I., Rhen, M., Guyon, S. Le, and Römling, U. (2014) Regulation of biofilm formation in *Salmonella enterica* serovar Typhimurium. .
- Simons, R.W., Houman, F., and Kleckner, N. (1987) Improved singel multicopy lac-based cloning vectors for protein and operon fusions. *Gene* **53**: 85–96.
- Singh, P., Sharma, L., Kulothungan, S.R., Adkar, B. V, Prajapati, R.S., Ali, P.S.S., *et al.* (2013) Effect of signal peptide on stability and folding of *Escherichia coli* thioredoxin. *PLoS One* **8**: e63442.
- Smyth, G.K. (2004) Linear models and empirical bayes methods for assessing differential expression in microarray experiments. *Stat Appl Genet Mol Biol* **3**: Article3.
- Song, M., Kim, H.-J., Kim, E.Y., Shin, M., Lee, H.C., Hong, Y., *et al.* (2004) ppGpp-dependent stationary phase induction of genes on Salmonella pathogenicity island 1. *J Biol Chem* **279**: 34183–90.
- Soutourina, O.A., and Bertin, P.N. (2003) Regulation cascade of flagellar expression in Gram-negative bacteria. *FEMS Microbiol Rev* **27**: 505–523.
- Sparkowski, J., and Das, A. (1990) The nucleotide sequence of *greA*, a suppressor gene that restores growth of an *Escherichia coli* RNA polymerase mutant at high temperature. *Nucleic Acids Res* **18**: 6443.
- Sparkowski, J., and Das, A. (1991) Location of a new gene, *greA*, on the *Escherichia coli* chromosome. *J Bacteriol* **173**: 5256–7.
- Stackebrandt, E., Frederiksen, W., Garrity, G.M., Grimont, P.A.D., Kämpfer, P., Maiden, M.C.J., *et al.* (2002) Report of the ad hoc committee for the re-evaluation of the species definition in bacteriology. *Int J Syst Evol Microbiol* **52**: 1043–7.
- Stamatakis, A. (2014) RAxML version 8: a tool for phylogenetic analysis and post-analysis of large phylogenies. *Bioinformatics* **30**: 1312–3.
- Stebbins, C.E., Borukhov, S., Orlova, M., Polyakov, A., Goldfarb, A., and Darst, S.A. (1995) Crystal structure of the GreA transcript cleavage factor from *Escherichia coli*. *Nature* **373**: 636–40.

- Stepanova, E., Lee, J., Ozerova, M., Semenova, E., Datsenko, K., Wanner, B.L., *et al.* (2007) Analysis of promoter targets for *Escherichia coli* transcription elongation factor GreA in vivo and in vitro. *J Bacteriol* **189**: 8772–85.
- Stepanova, E. V., Shevelev, a. B., Borukhov, S.I., and Severinov, K. V. (2010) Mechanisms of action of RNA polymerase-binding transcription factors that do not bind to DNA. *Biophysics (Oxf)* **54**: 555–568.
- Stepanovic, S., Vukovic, D., Dakic, I., Savic, B., and Svabic-Vlahovic, M. (2000) A modified microtiter-plate test for quantification of staphylococcal biofilm formation. *J Microbiol Methods* **40**: 175–9.
- Stoker, N.G., Fairweather, N.F., and Spratt, B.G. (1982) Versatile low-copy-number plasmid vectors for cloning in *Escherichia coli*. *Gene* **18**: 335–41.
- Stothard, P. (2000) The sequence manipulation suite: JavaScript programs for analyzing and formatting protein and DNA sequences. *Biotechniques* **28**: 1102, 1104.
- Susa, M., Kubori, T., and Shimamoto, N. (2006) A pathway branching in transcription initiation in *Escherichia coli*. *Mol Microbiol* **59**: 1807–17.
- Tagami, S., Sekine, S.-I., Kumarevel, T., Hino, N., Murayama, Y., Kamegamori, S., *et al.* (2010) Crystal structure of bacterial RNA polymerase bound with a transcription inhibitor protein. *Nature* **468**: 978–82.
- Takeda, K., Akimoto, C., and Kawamukai, M. (2001) Effects of the *Escherichia coli* sfsA gene on mal genes expression and a DNA binding activity of SfsA. *Biosci Biotechnol Biochem* **65**: 213–7.
- Tamura, K., Peterson, D., Peterson, N., Stecher, G., Nei, M., and Kumar, S. (2011) MEGA5: molecular evolutionary genetics analysis using maximum likelihood, evolutionary distance, and maximum parsimony methods. *Mol Biol Evol* **28**: 2731–9.
- Taylor, C.M., Beresford, M., Epton, H.A.S., Sigee, D.C., Shama, G., Andrew, P.W., and Roberts, I.S. (2002) Listeria monocytogenes relA and hpt Mutants Are Impaired in Surface-Attached Growth and Virulence. *J Bacteriol* **184**: 621–628.
- Tehranchi, A.K., Blankschien, M.D., Zhang, Y., Halliday, J. a, Srivatsan, A., Peng, J., *et al.* (2010) The transcription factor DksA prevents conflicts between DNA replication and transcription machinery. *Cell* **141**: 595–605.
- Thieffry, D., Huerta, A.M., Pérez-Rueda, E., and Collado-Vides, J. (1998) From specific gene regulation to genomic networks: a global analysis of transcriptional regulation in *Escherichia coli*. *Bioessays* **20**: 433–40.
- Thompson, A., Rolfe, M.D., Lucchini, S., Schwerk, P., Hinton, J.C.D., and Tedin, K. (2006) The bacterial signal molecule, ppGpp, mediates the environmental regulation of both the invasion and intracellular virulence gene programs of Salmonella. *J Biol Chem* **281**: 30112–21.
- Thompson, J.D., Gibson, T.J., Plewniak, F., Jeanmougin, F., and Higgins, D.G. (1997) The CLUSTAL_X windows interface: flexible strategies for multiple sequence alignment aided by quality analysis tools. *Nucleic Acids Res* **25**: 4876–82.
- Torreblanca, J., and Casadesús, J. (1996) DNA adenine methylase mutants of Salmonella typhimurium and a novel dam-regulated locus. *Genetics* **144**: 15–26.
- Torrieri, R., Oliveira, F.S., Oliveira, G., and Coimbra, R.S. (2012) Automatic assignment of prokaryotic genes to functional categories using literature profiling. *PLoS One* **7**: e47436.
- Trautinger, B.W., Jaktaji, R.P., Rusakova, E., and Lloyd, R.G. (2005) RNA polymerase modulators and DNA repair activities resolve conflicts between DNA replication and transcription. *Mol Cell* **19**: 247–58.
- Trautinger, B.W., and Lloyd, R.G. (2002) Modulation of DNA repair by mutations flanking the DNA channel through RNA polymerase. *EMBO J* **21**: 6944–53.
- Travers, A., and Muskhelishvili, G. (2005) DNA supercoiling - a global transcriptional regulator for enterobacterial growth? *Nat Rev Microbiol* **3**: 157–69.
- Traxler, M.F., Summers, S.M., Nguyen, H.-T., Zacharia, V.M., Hightower, G.A., Smith, J.T., and Conway, T. (2008) The global, ppGpp-mediated stringent response to amino acid starvation in *Escherichia coli*. *Mol Microbiol* **68**: 1128–48.
- Traxler, M.F., Zacharia, V.M., Marquardt, S., Summers, S.M., Nguyen, H.-T., Stark, S.E., and Conway, T. (2011) Discretely calibrated regulatory loops controlled by ppGpp partition gene induction across the “feast to famine” gradient in *Escherichia coli*. *Mol Microbiol* **79**: 830–45.

- Treviño-Quintanilla, L.G., Freyre-González, J.A., and Martínez-Flores, I. (2013) Anti-Sigma Factors in E. coli: Common Regulatory Mechanisms Controlling Sigma Factors Availability. *Curr Genomics* **14**: 378–87.
- Urbonavicius, J., Durand, J.M.B., and Björk, G.R. (2002) Three modifications in the D and T arms of tRNA influence translation in *Escherichia coli* and expression of virulence genes in Shigella flexneri. *J Bacteriol* **184**: 5348–57.
- Vassylyeva, M.N., Svetlov, V., Dearborn, A.D., Klyuyev, S., Artsimovitch, I., and Vassylyev, D.G. (2007) The carboxy-terminal coiled-coil of the RNA polymerase beta'-subunit is the main binding site for Gre factors. *EMBO Rep* **8**: 1038–43.
- Vinella, D., Potrykus, K., Murphy, H., and Cashel, M. (2012) Effects on growth by changes of the balance between GreA, GreB, and DksA suggest mutual competition and functional redundancy in *Escherichia coli*. *J Bacteriol* **194**: 261–73.
- Walsh, N.P., Alba, B.M., Bose, B., Gross, C.A., Sauer, R.T., and Francisco, S. (2003) OMP Peptide Signals Initiate the Envelope-Stress Response by Activating DegS Protease via Relief of Inhibition Mediated by Its PDZ Domain. *Cell* **113**: 61–71.
- Wang, S., Fleming, R.T., Westbrook, E.M., Matsumura, P., and McKay, D.B. (2006) Structure of the *Escherichia coli* FlhDC complex, a prokaryotic heteromeric regulator of transcription. *J Mol Biol* **355**: 798–808.
- Warren, W.C., Hillier, L.W., Marshall Graves, J.A., Birney, E., Ponting, C.P., Grützner, F., *et al.* (2008) Genome analysis of the platypus reveals unique signatures of evolution. *Nature* **453**: 175–83.
- Wassarman, K.M. (2007) 6S RNA: a small RNA regulator of transcription. *Curr Opin Microbiol* **10**: 164–8.
- Wayne, L.G., Brenner, D.J., Colwell, R.R., Grimont, P.A.D., Kandler, O., Krichevsky, M.I., *et al.* (1987) Report of the Ad Hoc Committee on Reconciliation of Approaches to Bacterial Systematics. *Int J Syst Bacteriol* **37**: 463–464.
- Wei, W., Jiang, J., Li, X., Wang, L., and Yang, S.S. (2004) Isolation of salt-sensitive mutants from Sinorhizobium meliloti and characterization of genes involved in salt tolerance. *Lett Appl Microbiol* **39**: 278–83.
- Wendrich, T.M., Blaha, G., Wilson, D.N., Marahiel, M.A., and Nierhaus, K.H. (2002) Dissection of the Mechanism for the Stringent Factor RelA. *Mol Cell* **10**: 779–788.
- Williams, R., Bell, A., Sims, G., and Busby, S. (1991) The role of two surface exposed loops in transcription activation by the *Escherichia coli* CRP and FNR proteins. *Nucleic Acids Res* **19**: 6705–12.
- World Health Organization (2011) Outbreaks of E. coli O104:H4 infection: update 30. .
- Wu, L.F., and Mandrand-Berthelot, M.A. (1995) A family of homologous substrate-binding proteins with a broad range of substrate specificity and dissimilar biological functions. *Biochimie* **77**: 744–50.
- Xiao, H., Kalman, M., Ikehara, K., Zemel, S., Glaser, G., and Cashel, M. (1991) Residual guanosine 3',5'-bispyrophosphate synthetic activity of relA null mutants can be eliminated by spoT null mutations. *J Biol Chem* **266**: 5980–90.
- Xiao, H., Kalman, M., Ikeharaz, K., Zemelb, S., and Glaserll, G. (1991) Residual Guanosine 3 ', 5 ' -Bispyrophosphate Synthetic Activity of reZA Null Mutants Can Be Eliminated by spoT Null Mutations *. *J Biol Chem* 5980–5990.
- Xu, J., Tozawa, Y., Lai, C., Hayashi, H., and Ochi, K. (2002) A rifampicin resistance mutation in the rpoB gene confers ppGpp-independent antibiotic production in Streptomyces coelicolor A3(2). *Mol Genet Genomics* **268**: 179–89.
- Yang, S.Y., Yang, X.Y., Healy-Louie, G., Schulz, H., and Elzinga, M. (1990) Nucleotide sequence of the fadA gene. Primary structure of 3-ketoacyl-coenzyme A thiolase from *Escherichia coli* and the structural organization of the fadAB operon. *J Biol Chem* **265**: 10424–9.
- Yang, Z. (1996) Among-site rate variation and its impact on phylogenetic analyses. *Trends Ecol Evol* **11**: 367–72.
- Yoon, S.J., Park, J.E., Yang, J.-H., and Park, J.-W. (2002) OxyR regulon controls lipid peroxidation-mediated oxidative stress in *Escherichia coli*. *J Biochem Mol Biol* **35**: 297–301.
- Zacharias, M., Göringer, H.U., and Wagner, R. (1989) Influence of the GCGC discriminator motif introduced into the ribosomal RNA P2- and tac promoter on growth-rate control and stringent sensitivity. *EMBO J* **8**: 3357–63.

- Zenkin, N., Yuzenkova, Y., and Severinov, K. (2006) Transcript-assisted transcriptional proofreading. *Science* **313**: 518–20.
- Zhang, J., Rosenberg, H.F., and Nei, M. (1998) Positive Darwinian selection after gene duplication in primate ribonuclease genes. *Proc Natl Acad Sci* **95**: 3708–3713.
- Zhang, Y., Mooney, R.A., Grass, J.A., Sivaramakrishnan, P., Herman, C., Landick, R., and Wang, J.D. (2014) DksA guards elongating RNA polymerase against ribosome-stalling-induced arrest. *Mol Cell* **53**: 766–78.
- Zhao, G., Weatherspoon, N., Kong, W., Curtiss, R., and Shi, Y. (2008) A dual-signal regulatory circuit activates transcription of a set of divergent operons in Salmonella typhimurium. *Proc Natl Acad Sci U S A* **105**: 20924–9.
- Zusman, T., Gal-Mor, O., and Segal, G. (2002) Characterization of a Legionella pneumophila relA Insertion Mutant and Roles of RelA and RpoS in Virulence Gene Expression. *J Bacteriol* **184**: 67–75.

8. Supplementary table

In light grey are indicated those genes with a fold-change lower than -3 and a p-value lower than 0.05, being stimulated by ppGpp or DksA.

In dark grey are indicated those genes with a fold-change higher than +3 and a p-value lower than 0.05, being repressed by ppGpp or DksA.

ID	gene	Description	ppGpp vs WT	dksA vs WT
		Amino acid biosynthesis		
SL0001	thrL	Hypothetical Protein SL0001	-1,28	1,19
SL0002	thrA	Bifunctional aspartokinase/homoserine dehydrogenase 1	-1,26	-1,66
SL0003	thrB	Homoserine kinase	-1,26	-1,49
SL0004	thrC	Threonine synthase	-1,26	-1,94
SL0019	-	Hypothetical	1,41	1,16
SL0065	dapB	Dihydrodipicolinate reductase	1,95	-1,86
SL0110	leuD	3-isopropylmalate dehydratase small subunit 1	-1,13	-1,16
SL0111	leuC	3-isopropylmalate dehydratase large subunit 1	-1,30	1,11
SL0112	leuB	3-isopropylmalate dehydrogenase	-1,27	-1,13
SL0113	leuA	2-isopropylmalate synthase	-1,94	-1,84
SL0114	leuL	leu operon leader peptide	-1,13	-1,09
SL0115	leuO	Probable HTH-type transcriptional regulator leuO	1,05	-2,06
SL0116	ilvI	Acetolactate synthase isozyme 3 large subunit	-1,13	-1,28
SL0117	ilvH	Acetolactate synthase isozyme 3 small subunit	1,12	-1,59
SL0214	dapD	2,3,4,5-tetrahydropyridine-2,6-dicarboxylate N-succinyltransferase	-1,19	-1,11
SL0215	glnD	[Protein-PII] uridylyltransferase	1,54	1,14
SL0317	proB	Glutamate 5-kinase	2,30	1,14
SL0318	proA	Gamma-glutamyl phosphate reductase	1,64	1,15
SL0324	leuC2	3-isopropylmalate dehydratase large subunit 2	-1,49	1,01
SL0325	leuD2	3-isopropylmalate dehydratase small subunit 2	-1,30	-1,25
SL0381	proC	Pyrroline-5-carboxylate reductase	1,05	1,05
SL0383	aroL	Shikimate kinase 2	1,32	-1,36
SL0385	aroM	Protein AroM	-1,16	1,60
SL0452	cysM	Cysteine synthase B	1,42	1,40
SL0511	gip	Hydroxypyruvate isomerase	4,14	1,80
SL0560	frlB	Fructosamine deglycase frlB	-1,00	2,15
SL0662	asnB	Asparagine synthetase B [glutamine-hydrolyzing]	-2,13	1,57
SL0737	aroG	Phospho-2-dehydro-3-deoxyheptonate aldolase, Phe-sensitive	-1,62	-1,21
SL0804	glnP	Glutamine transport system permease protein glnP	3,15	-1,35
SL0914	serC	Phosphoserine aminotransferase	-1,69	-1,66
SL0915	aroA	3-phosphoshikimate 1-carboxyvinyltransferase	-1,65	-2,16
SL0935	aspC	Aspartate aminotransferase	-1,05	-1,52
SL1040	hpaG	4-hydroxyphenylacetate degradation bifunctional isomerase/decarboxylase	1,58	2,59
SL1058	wrbA	Flavoprotein wrbA	-1,03	1,12
SL1234	gdhA	NADP-specific glutamate dehydrogenase	-1,54	-1,15
SL1238	astC	Succinylornithine transaminase	3,11	12,92
SL1281	aroH	Phospho-2-dehydro-3-deoxyheptonate aldolase, Trp-sensitive	-1,09	-1,81
SL1292	aroD	3-dehydroquinate dehydratase	-1,09	-1,22
SL1293	ydiB	Quinate/shikimate dehydrogenase	1,21	-1,04
SL1293	ydiB	Quinate/shikimate dehydrogenase	1,21	-1,04
SL1654	trpE	Anthranilate synthase component 1	1,51	-1,20
SL1656	trpC	Tryptophan biosynthesis protein trpCF	-1,18	-1,43
SL1657	trpB	Tryptophan synthase beta chain	-1,78	1,00
SL1658	trpA	Tryptophan synthase alpha chain	-1,55	-1,09
SL1723	gdhA	Glutamate dehydrogenase	5,38	6,36
SL1754	yeaB	putative NTP pyrophosphohydrolase	1,44	-1,68
SL1779	yebU	Ribosomal RNA small subunit methyltransferase F	1,12	-1,34
SL2047	yeeZ	Protein yeeZ	-1,06	1,33
SL2048	hisG	ATP phosphoribosyltransferase	-1,12	-2,01
SL2049	hisD	Histidinol dehydrogenase	-1,09	-1,50
SL2050	hisC	Histidinol-phosphate aminotransferase	1,00	-1,08
SL2053	hisA	1-(5-phosphoribosyl)-5-[(5-phosphoribosylamino)methylideneamino] imidazole-4-carboxamide isomerase	1,29	1,00
SL2054	hisF	Imidazole glycerol phosphate synthase subunit hisF	1,24	1,14
SL2055	hisI	Histidine biosynthesis bifunctional protein hisIE	1,08	1,06
SL2091	wcaB	Putative colanic acid biosynthesis acetyltransferase wcaB	2,10	1,25

SL2163	yeiT	Uncharacterized oxidoreductase yeiT	-1,96	-1,06
SL2174	serB	Phosphoserine phosphatase	1,35	1,89
SL2174	serB	Phosphoserine phosphatase	1,35	1,89
SL2300	yfbQ	Uncharacterized aminotransferase yfbQ	-1,60	-1,59
SL2315	yfcD	Uncharacterized Nudix hydrolase yfcD	1,27	1,16
SL2329	lysA	Diaminopimelate decarboxylase	2,14	-1,20
SL2338	usg	USG-1 protein	1,77	-2,22
SL2353	aroC	Chorismate synthase	1,18	1,92
SL2392	cysZ	Protein cysZ homolog	1,58	-2,07
SL2393	cysK	Cysteine synthase A	1,18	-1,38
SL2393	cysK	Cysteine synthase A	1,18	-1,38
SL2403	cysM	Cysteine synthase B	-1,00	-2,01
SL2446	dapE	Succinyl-diaminopimelate desuccinylase	1,05	1,29
SL2452	dapA	Dihydrodipicolinate synthase	1,19	-2,77
SL2517	glyA	Serine hydroxymethyltransferase 1	1,49	1,49
SL2625	pheA	P-protein	-1,22	1,40
SL2627	tyrA	T-protein	1,50	-1,23
SL2628	aroF	Phospho-2-dehydro-3-deoxyheptonate aldolase, Tyr-sensitive	1,12	-1,80
SL2970	argA	Amino-acid acetyltransferase	2,00	1,17
SL2982	rppH	RNA pyrophosphohydrolase	-1,12	-1,45
SL2991	lysA	Diaminopimelate decarboxylase	-1,01	-4,95
SL2992	lysR	Transcriptional activator protein lysR	1,21	-1,29
SL2993	ygeA	Uncharacterized protein ygeA	-1,10	-1,04
SL3038	serA	D-3-phosphoglycerate dehydrogenase	-2,34	-1,42
SL3135	metC	Cystathionine beta-lyase	-1,28	1,63
SL3165	-	Arylsulfotransferase	-1,53	1,45
SL3166	dsbA	Thiol:disulfide interchange protein dsbA	-1,55	1,18
SL3191	patA	Putrescine aminotransferase	-3,25	-2,21
SL3193	rlmG	Ribosomal RNA large subunit methyltransferase G	-1,58	2,09
SL3262	argG	Argininosuccinate synthase	1,96	-4,12
SL3303	gltD	Glutamate synthase [NADPH] small chain	1,01	1,49
SL3332	argR	Arginine repressor	1,37	1,65
SL3368	aroE	Shikimate dehydrogenase	-1,67	-1,57
SL3435	argD	Acetylornithine/succinyldiaminopimelate aminotransferase	1,01	1,18
SL3453	aroB	3-dehydroquinate synthase	1,21	-1,66
SL3454	aroK	Shikimate kinase 1	1,13	-1,19
SL3498	ilvD	Dihydroxy-acid dehydratase	-1,33	2,01
SL3498	ilvD	Dihydroxy-acid dehydratase	-1,33	2,01
SL3499	yjhH	Uncharacterized protein yjhH	-1,09	1,20
SL3506	asd	Aspartate-semialdehyde dehydrogenase	1,05	1,19
SL3558	yhiQ	UPF0341 protein yhiQ	-1,03	-1,62
SL3566	frlB	Fructosamine deglycase frlB	3,57	25,25
SL3630	avtA	Valine--pyruvate aminotransferase	1,53	1,06
SL3665	cysE	Serine acetyltransferase	1,26	-1,09
SL3761	ilvN	Acetolactate synthase isozyme 1 small subunit	3,09	2,70
SL3762	ilvB	Acetolactate synthase isozyme 1 large subunit	3,62	3,33
SL3826	ydiB	Shikimate 5-dehydrogenase-like protein HI_0607	1,25	1,66
SL3826	ydiB	Shikimate 5-dehydrogenase-like protein HI_0607	1,25	1,66
SL3844	asnA	Aspartate--ammonia ligase	-2,19	1,11
SL3861	ilvG	Acetolactate synthase isozyme 2 large subunit	-1,31	1,88
SL3862	ilvM	Acetolactate synthase isozyme 2 small subunit	-1,06	2,57
SL3863	ilvE	Branched-chain-amino-acid aminotransferase	-1,40	1,12
SL3864	ilvD	Dihydroxy-acid dehydratase	-1,21	-1,51
SL3864	ilvD	Dihydroxy-acid dehydratase	-1,21	-1,51
SL3865	ilvA	Threonine dehydratase biosynthetic	-1,12	-1,45
SL3869	ilvC	Ketol-acid reductoisomerase	-2,90	-1,30
SL3901	dapF	Diaminopimelate epimerase	1,02	-1,69
SL3918	metR	HTH-type transcriptional regulator metR	-1,19	1,31
SL3919	metE	5-methyltetrahydropteroyltriglutamate--homocysteine methyltransferase	-1,31	1,37
SL3928	tatB	Sec-independent protein translocase protein tatB homolog	1,57	1,74
SL3945	dsbA	Thiol:disulfide interchange protein dsbA	-1,51	-1,17
SL3954	glnA	Glutamine synthetase	1,22	-3,78
SL3969	yihU	Uncharacterized oxidoreductase yihU	1,56	1,52
SL4047	-	Arylsulfate Sulfotransferase	-1,04	1,64
SL4049	metB	Cystathionine gamma-synthase	1,47	-1,48
SL4050	metL	Bifunctional aspartokinase/homoserine dehydrogenase 2	1,97	-1,19

SL4055	metF	5,10-methylenetetrahydrofolate reductase	-3,04	1,08
SL4070	argE	Acetylornithine deacetylase	-2,16	-1,92
SL4071	argC	N-acetyl-gamma-glutamyl-phosphate reductase	1,30	-2,98
SL4072	argB	Acetylglutamate kinase	1,68	-1,20
SL4073	argH	Argininosuccinate lyase	1,66	-1,31
SL4078	trmA	tRNA (uracil-5-)-methyltransferase	1,50	2,16
SL4117	metA	Homoserine O-succinyltransferase	-2,06	2,19
SL4123	metH	Methionine synthase	-1,20	-1,33
SL4184	tyrB	Aromatic-amino-acid aminotransferase	-1,02	-1,32
SL4393	argR	Arginine repressor	-1,76	1,94
SL4399	argI	Ornithine carbamoyltransferase	1,76	-1,09
SL4430	yjhP	Uncharacterized protein yjhP	1,09	2,13
SL4441	ygeA	Uncharacterized protein in pnlA 3'region	-1,44	1,79
SL4471	frlB	Fructosamine deglycase frlB	1,08	1,19
SL4505	serB	Phosphoserine phosphatase	1,51	1,66
SL4505	serB	Phosphoserine phosphatase	1,51	1,66
SL4510	trpR	Trp operon repressor	1,82	1,68
		Biosynthesis of cofactors, prosthetic groups, and carriers		
SL0008	mog	Molybdopterin adenylyltransferase	1,77	1,61
SL0046	ribF	Riboflavin biosynthesis protein ribF	1,61	-1,13
SL0050	lytB	4-hydroxy-3-methylbut-2-enyl diphosphate reductase	1,90	-1,75
SL0088	folA	Dihydrofolate reductase	-1,10	2,00
SL0092	pdxA	4-hydroxythreonine-4-phosphate dehydrogenase 1	2,44	-2,15
SL0140	coaE	Dephospho-CoA kinase	1,47	1,54
SL0145	nadC	Nicotinate-nucleotide pyrophosphorylase [carboxylating]	1,58	1,06
SL0164	pdxA2	4-hydroxythreonine-4-phosphate dehydrogenase 2	1,61	1,30
SL0181	panD	Aspartate 1-decarboxylase	2,86	1,64
SL0182	panC	Pantothenate synthetase	2,51	2,67
SL0183	panB	3-methyl-2-oxobutanoate hydroxymethyltransferase	2,45	4,25
SL0184	folK	2-amino-4-hydroxy-6-hydroxymethyldihydropteridine pyrophosphokinase	-1,11	-1,01
SL0203	hemL	Glutamate-1-semialdehyde 2,1-aminomutase	1,88	1,38
SL0221	dxr	1-deoxy-D-xylulose 5-phosphate reductoisomerase	1,49	-2,79
SL0222	uppS	Undecaprenyl pyrophosphate synthase	1,19	-1,39
SL0367	hemB	Delta-aminolevulinic acid dehydratase	1,19	-1,50
SL0410	ribD	Riboflavin biosynthesis protein ribD	1,70	-1,19
SL0411	ribH	6,7-dimethyl-8-ribityllumazine synthase	1,51	1,50
SL0413	thiL	Thiamine-monophosphate kinase	1,53	1,33
SL0416	dxs	1-deoxy-D-xylulose-5-phosphate synthase	1,33	-2,15
SL0417	ispA	Geranyltranstransferase	2,05	-1,42
SL0427	thiJ	Protein thiJ	1,41	1,09
SL0428	panE	2-dehydropantoate 2-reductase	1,49	1,61
SL0433	cyoE	Protoheme IX farnesyltransferase	2,05	4,16
SL0482	hemH	Ferrochelatase	-1,97	-9,75
SL0535	folD	Bifunctional protein folD	1,46	-1,38
SL0576	entF	Enterobactin synthase component F	1,45	-1,28
SL0583	entC	Isochorismate synthase entC	1,42	1,37
SL0584	entE	Enterobactin synthase component E	1,83	1,50
SL0585	entB	Isochorismatase	1,59	2,00
SL0586	entA	2,3-dihydro-2,3-dihydroxybenzoate dehydrogenase	1,71	2,19
SL0621	lipA	Lipoyl synthase	1,12	-1,34
SL0632	cobD	Threonine-phosphate decarboxylase	3,20	3,16
SL0633	nadD	Probable nicotinate-nucleotide adenylyltransferase	1,54	-1,31
SL0733	nadA	Quinolinate synthase A	-2,81	-4,30
SL0743	oadG2	Oxaloacetate decarboxylase gamma chain	-1,01	-1,27
SL0770	bioA	Adenosylmethionine-8-amino-7-oxononanoate aminotransferase	1,91	1,20
SL0771	bioB	Biotin synthase	2,86	2,72
SL0772	bioF	8-amino-7-oxononanoate synthase	1,86	1,52
SL0773	bioC	Biotin synthesis protein BioC	1,62	1,36
SL0774	bioD	Dethiobiotin synthetase	1,60	1,39
SL0778	moaA	Molybdenum cofactor biosynthesis protein A	2,77	-1,13
SL0779	moaB	Molybdenum cofactor biosynthesis protein B	1,28	1,64
SL0780	moaC	Molybdenum cofactor biosynthesis protein C	2,00	1,60
SL0781	moaD	Molybdopterin synthase sulfur carrier subunit	2,49	1,48
SL0782	moaE	Molybdopterin synthase catalytic subunit	3,06	1,72
SL0821	moeB	Sulfur carrier protein moaD adenylyltransferase	1,36	1,15
SL0822	moeA	Molybdopterin molybdenumtransferase	1,57	1,01

SL0941	pncB	Nicotinate phosphoribosyltransferase	-1,19	-1,64
SL1102	grxB	Glutaredoxin-2	-1,70	-1,03
SL1114	flgE	Flagellar hook protein flgE	-1,32	1,36
SL1120	flgK	Flagellar hook-associated protein 1	-2,64	-1,28
SL1135	pabC	Aminodeoxychorismate lyase	1,42	-1,40
SL1158	cobB	NAD-dependent deacetylase	1,34	-1,03
SL1245	nadE	NH(3)-dependent NAD(+) synthetase	-1,25	-1,78
SL1308	sufE	Cysteine desulfuration protein sufE	-1,18	-1,54
SL1358	ribE	Riboflavin synthase alpha chain	-1,24	1,14
SL1380	pdxH	Pyridoxine/pyridoxamine 5'-phosphate oxidase	1,22	-1,71
SL1382	pdxY	Pyridoxamine kinase	1,99	-1,48
SL1528	ydcW	Gamma-aminobutyraldehyde dehydrogenase	-1,22	2,46
SL1643	ribA	GTP cyclohydrolase-2	1,68	-1,04
SL1650	btuR	Cob(I)yrinic acid a,c-diamide adenosyltransferase	2,08	4,35
SL1703	hemK	Protein methyltransferase hemK	2,91	-2,68
SL1705	hemA	Glutamyl-tRNA reductase	1,45	-1,07
SL1707	ispE	4-diphosphocytidyl-2-C-methyl-D-erythritol kinase	1,19	-1,23
SL1753	pabB	Para-aminobenzoate synthase component 1	1,35	-1,42
SL1779	yebU	Ribosomal RNA small subunit methyltransferase F	1,12	-1,34
SL1859	flhC	Flagellar transcriptional activator flhC	-3,91	-1,47
SL1864	thiJ	Protein thiJ	1,99	-1,24
SL1882	dcyD	D-cysteine desulfhydrase	-1,68	-1,47
SL2123	thiD	Hydroxymethylpyrimidine/phosphomethylpyrimidine kinase	-1,43	-1,64
SL2124	thiM	Hydroxyethylthiazole kinase	1,05	-2,07
SL2170	folE	GTP cyclohydrolase 1	-1,34	-5,82
SL2189	yeiR	Uncharacterized protein yeiR	-1,12	-1,01
SL2245	ubiG	3-demethylubiquinone-9 3-methyltransferase	-1,29	-1,55
SL2265	ais	Lipopolysaccharide core heptose(II)-phosphate phosphatase	-3,11	-1,91
SL2274	menE	2-succinylbenzoate--CoA ligase	2,57	-2,05
SL2275	menC	o-succinylbenzoate synthase	2,69	-1,83
SL2276	menB	Naphthoate synthase	3,61	-1,40
SL2278	menD	2-succinyl-5-enolpyruvyl-6-hydroxy-3-cyclohexene-1-carboxylate synthase	3,11	1,13
SL2309	dxs	Putative transketolase C-terminal section	-1,29	-1,23
SL2325	ubiX	3-octaprenyl-4-hydroxybenzoate carboxy-lyase	1,02	-1,08
SL2325	ubiX	3-octaprenyl-4-hydroxybenzoate carboxy-lyase	1,02	-1,08
SL2334	folC	Bifunctional protein folC	2,32	-1,01
SL2339	pdxB	Erythronate-4-phosphate dehydrogenase	1,58	-2,47
SL2398	pdxK	Pyridoxine kinase	1,29	-1,38
SL2414	hemF	Coproporphyrinogen-III oxidase, aerobic	1,30	1,19
SL2505	iscS	Cysteine desulfurase	1,25	-1,91
SL2517	glyA	Serine hydroxymethyltransferase 1	1,49	1,49
SL2535	panE	Putative 2-dehydropantoate 2-reductase	-1,84	-1,22
SL2540	pdxJ	Pyridoxine 5'-phosphate synthase	1,40	-1,50
SL2605	nadB	L-aspartate oxidase	-1,40	-1,35
SL2803	gshA	Glutamate--cysteine ligase	1,38	-1,45
SL2900	pad1	Probable aromatic acid decarboxylase	1,33	-1,05
SL2908	ispF	2-C-methyl-D-erythritol 2,4-cyclodiphosphate synthase	2,06	1,25
SL2909	ispD	2-C-methyl-D-erythritol 4-phosphate cytidylyltransferase	1,78	1,15
SL2928	queD	6-carboxy-5,6,7,8-tetrahydropterin synthase	-1,09	2,64
SL2965	ygdK	Uncharacterized sufE-like protein ygdK	1,58	-1,47
SL3033	ubiH	2-octaprenyl-6-methoxyphenol hydroxylase	1,39	-1,55
SL3037	ygfA	Uncharacterized protein ygfA	-1,28	1,34
SL3046	epd	D-erythrose-4-phosphate dehydrogenase	1,44	-1,22
SL3070	gshB	Glutathione synthetase	1,37	-1,17
SL3079	yggW	Oxygen-independent coproporphyrinogen-III oxidase-like protein yggW	1,93	-1,62
SL3168	ribB	3,4-dihydroxy-2-butanone 4-phosphate synthase	-1,49	-1,98
SL3179	folB	Dihydroneopterin aldolase	1,77	2,08
SL3193	rlmG	Ribosomal RNA large subunit methyltransferase G	-1,58	2,09
SL3266	folP	Dihydropteroate synthase	1,31	-1,88
SL3277	ispB	Octaprenyl-diphosphate synthase	1,49	1,51
SL3299	elbB	Enhancing lycopene biosynthesis protein 2	-1,46	1,64
SL3325	oadG2	Oxaloacetate decarboxylase gamma chain 2	-1,02	-1,21
SL3436	pabA	Para-aminobenzoate synthase glutamine amidotransferase component II	-1,01	1,28
SL3444	cysG	Siroheme synthase	3,55	1,81
SL3476	bioH	Carboxylesterase BioH	1,74	1,15

SL3517	ggt	Gamma-glutamyltranspeptidase	-1,26	-2,95
SL3558	yhiQ	UPF0341 protein yhiQ	-1,03	-1,62
SL3562	gor	Glutathione reductase	-1,02	-1,33
SL3610	bisC	Biotin sulfoxide reductase	1,29	-1,37
SL3668	grxC	Glutaredoxin-3	1,23	1,35
SL3691	coaD	Phosphopantetheine adenylyltransferase	1,88	2,22
SL3696	coaBC	Coenzyme A biosynthesis bifunctional protein coaBC	1,76	1,11
SL3875	trxA	Thioredoxin-1	-1,03	-1,05
SL3891	hemX	Putative uroporphyrinogen-III C-methyltransferase	1,27	-1,66
SL3892	hemD	Uroporphyrinogen-III synthase	1,57	-1,44
SL3893	hemC	Porphobilinogen deaminase	1,81	-1,20
SL3924	ubiE	Ubiquinone/menaquinone biosynthesis methyltransferase ubiE	1,56	1,40
SL3926	aarF	ubiquinone biosynthesis protein	1,60	-1,28
SL3940	hemG	Protoporphyrinogen oxidase	1,11	1,31
SL3941	mobB	Molybdopterin-guanine dinucleotide biosynthesis protein B	1,62	1,00
SL3942	mobA	Molybdopterin-guanine dinucleotide biosynthesis protein A	1,34	1,64
SL3951	hemN	Oxygen-independent coproporphyrinogen-III oxidase	1,33	1,27
SL3951	hemN	Oxygen-independent coproporphyrinogen-III oxidase	1,33	1,27
SL3958	hemN	Oxygen-independent coproporphyrinogen-III oxidase	-1,47	-1,53
SL3958	hemN	Oxygen-independent coproporphyrinogen-III oxidase	-1,47	-1,53
SL3969	yihU	Uncharacterized oxidoreductase yihU	1,56	1,52
SL4038	rraA	Regulator of ribonuclease activity A	2,35	-1,33
SL4039	menA	1,4-dihydroxy-2-naphthoate octaprenyltransferase	2,18	-2,05
SL4078	trmA	tRNA (uracil-5-)-methyltransferase	1,50	2,16
SL4082	birA	Bifunctional protein BirA	1,63	-1,23
SL4083	coaA	Pantothenate kinase	1,98	1,97
SL4098	thiH	Dehydroglycine synthase	-1,06	1,93
SL4099	thiG	Thiazole synthase	-1,18	2,29
SL4100	thiS	Sulfur carrier protein ThiS	1,11	2,18
SL4101	thiF	Sulfur carrier protein ThiS adenylyltransferase	1,20	2,18
SL4102	thiE	Thiamine-phosphate pyrophosphorylase	1,17	1,73
SL4103	thiC	Phosphomethylpyrimidine synthase	-1,07	1,64
SL4106	hemE	Uroporphyrinogen decarboxylase	1,09	-1,03
SL4166	malE	Maltose-binding periplasmic protein	-2,38	3,45
SL4170	ubiC	Chorismate--pyruvate lyase	-1,18	1,11
SL4171	ubiA	4-hydroxybenzoate octaprenyltransferase	1,13	1,17
SL4430	yjhP	Uncharacterized protein yjhP	1,09	2,13
		Cell envelope		
SL0012	dnaK	Chaperone protein dnaK	4,03	1,12
SL0020	yaiV	Uncharacterized protein yaiV	-1,40	-1,59
SL0020	yaiV	Uncharacterized protein yaiV	-1,40	-1,59
SL0021	bcfA	Type-1 fimbrial protein, C chain	-1,28	-2,80
SL0022	bcfB	Chaperone protein	-1,04	-2,61
SL0023	bcfC	fimbrial usher protein	1,03	-1,04
SL0024	bcfD	fimbrial subunit	1,09	1,84
SL0025	bcfE	fimbrial subunit	-1,30	1,03
SL0026	bcfF	fimbrial subunit	1,17	-1,02
SL0027	bcfG	fimbrial chaperone	1,06	-1,04
SL0035	yfeN	Uncharacterized protein yfeN	1,02	1,12
SL0064	citG1	Probable 2-(5''-triphosphoribosyl)-3'-dephosphocoenzyme-A synthase 1	1,01	2,86
SL0122	ftsI	Peptidoglycan synthase ftsI	1,37	-1,64
SL0122	ftsI	Peptidoglycan synthase ftsI	1,37	-1,64
SL0123	murE	UDP-N-acetylmuramoyl-L-alanyl-D-glutamate--2,6-diaminopimelate ligase	1,26	-1,69
SL0124	murF	UDP-N-acetylmuramoyl-tripeptide--D-alanyl-D-alanine ligase	1,10	-2,03
SL0125	mraY	Phospho-N-acetylmuramoyl-pentapeptide-transferase	1,50	-2,12
SL0126	murD	UDP-N-acetylmuramoylalanine--D-glutamate ligase	1,91	-1,48
SL0128	murG	UDP-N-acetylglucosamine--N-acetylmuramyl-(pentapeptide) pyrophosphoryl-undecaprenol N-acetylglucosamine transferase	1,82	-1,57
SL0129	murC	UDP-N-acetylmuramate--L-alanine ligase	1,35	-1,64
SL0130	ddlB	D-alanine--D-alanine ligase B	1,01	-1,45
SL0134	lpxC	UDP-3-O-[3-hydroxymyristoyl] N-acetylglucosamine deacetylase	-1,25	-1,76
SL0142	hofC	Protein transport protein hofC	1,73	1,33
SL0143	hofB	Protein transport protein hofB	1,34	2,52
SL0155	-	Hypothetical	1,14	-1,17
SL0157	yacH	Uncharacterized protein yacH	1,35	1,70

SL0158	yacH	Uncharacterized protein yacH	1,27	1,95
SL0163	ygbK	Uncharacterized protein HI_1011	1,75	1,59
SL0163	ygbK	Uncharacterized protein HI_1011	1,75	1,59
SL0177	stiB	fimbrial usher protein	-1,23	-1,53
SL0191	mrcB	Penicillin-binding protein 1B	2,60	-1,65
SL0192	fhuA	Ferrichrome-iron receptor	-1,35	-2,43
SL0196	stfA	Fimbria A protein	1,51	-1,80
SL0199	stfE	minor fimbrial subunit StfE	1,29	-1,13
SL0200	stfF	minor fimbrial subunit stfF	1,31	1,01
SL0201	stfG	putative minor fimbrial subunit	1,32	1,26
SL0207	btuF	Vitamin B12-binding protein	1,83	1,02
SL0225	yaeT	Outer membrane protein assembly factor yaeT	1,69	-1,44
SL0226	ompH	outer membrane protein OmpH	1,77	-1,09
SL0227	lpxD	UDP-3-O-[3-hydroxymyristoyl] glucosamine N-acyltransferase	1,55	-1,41
SL0229	lpxA	Acyl-[acyl-carrier-protein]--UDP-N-acetylglucosamine O-acyltransferase	1,52	-1,72
SL0230	lpxB	Lipid-A-disaccharide synthase	1,77	-2,62
SL0245	rcsF	Protein rcsF	1,41	-1,57
SL0246	yaeC	D-methionine-binding lipoprotein	-1,52	1,29
SL0275	sciN	Hypothetical	1,65	-1,60
SL0277	sciP	putative outer membrane protein, OmpA family	1,40	1,04
SL0278	sciQ	putative membrane protein, virulence associated protein	1,24	-1,28
SL0295	safA	atypical fimbria lipoprotein	-2,66	-3,63
SL0296	safB	atypical fimbria chaperone	-1,48	-1,76
SL0297	safC	atypical fimbria outer membrane usher	-1,03	1,23
SL0298	safD	fimbrial structural subunit	1,32	1,60
SL0306	gmhA	Phosphoheptose isomerase	1,38	1,04
SL0315	crl	Sigma factor-binding protein crl	1,22	1,46
SL0330	-	secreted protein	1,13	1,10
SL0331	stbE	fimbrial chaperone protein	-1,27	-1,36
SL0332	stbD	putative fimbrial protein	-1,28	-1,13
SL0333	stbC	outer membrane fimbrial usher protein	-1,30	-1,14
SL0334	stbB	fimbrial chaperone protein	-1,07	-1,11
SL0335	stbA	F17 fimbrial protein	1,12	-1,13
SL0336	-	Transmembrane Regulator	-1,45	-4,37
SL0343	-	Hypothetical	-1,61	-2,49
SL0344	yjeI	Uncharacterized protein yjeI	1,36	2,68
SL0369	yaiV	putative inner membrane protein	-2,01	-3,52
SL0369	yaiV	putative inner membrane protein	-2,01	-3,52
SL0370	ampH	Penicillin-binding protein AmpH	1,13	1,58
SL0373	yaiY	Inner membrane protein yaiY	-1,35	-2,72
SL0375	ddlA	D-alanine--D-alanine ligase A	1,27	1,04
SL0376	-	Extensin Family Protein	-1,37	1,68
SL0406	yajD	Uncharacterized protein yajD	-1,15	-1,30
SL0419	thiI	tRNA sulfurtransferase	1,52	-1,15
SL0431	ybeT	Hypothetical	1,42	-1,10
SL0432	ybeT	Hypothetical	1,22	1,53
SL0438	ampG	Protein AmpG	1,46	1,69
SL0440	bolA	Protein BolA	-1,18	1,01
SL0459	ybaY	Uncharacterized lipoprotein ybaY	-1,53	-1,05
SL0469	acrA	Acriflavine resistance protein A	1,43	-2,11
SL0501	ybbP	Uncharacterized ABC transporter permease ybbP	1,04	-2,41
SL0502	-	Outer Membrane Protein	2,97	4,41
SL0503	sfbA	D-methionine-binding lipoprotein	-3,44	-1,67
SL0506	ybbB	putative ATPase (similar to E. coli putative capsule anchoring protein)	1,97	1,54
SL0531	-	Hypothetical	1,18	-1,51
SL0532	-	Hypothetical	-1,28	-1,76
SL0536	fimA	Fimbrial subunit type 1	-4,60	-6,11
SL0538	fimC	Chaperone protein fimC	-3,07	-12,54
SL0547	-	Hypothetical	1,97	-1,35
SL0548	yfdH	Bactoprenol glucosyl transferase homolog from prophage CPS-53	1,83	-1,23
SL0549	gtrA	Bactoprenol-linked glucose translocase homolog from prophage CPS-53	1,31	-1,27
SL0560	frlB	Fructosamine deglycase frlB	-1,00	2,15
SL0625	dacA	D-alanyl-D-alanine carboxypeptidase dacA	1,93	-2,01
SL0626	rlpA	Rare lipoprotein A	1,34	-1,06

SL0628	mrdA	Penicillin-binding protein 2	1,72	1,03
SL0628	mrdA	Penicillin-binding protein 2	1,72	1,03
SL0630	ybeB	Uncharacterized protein ybeB	1,39	2,09
SL0635	rlpB	Rare lipoprotein B	1,45	-1,73
SL0644	ybeS	putative molecular chaperone, DnaJ family	-1,06	1,72
SL0647	ybeV	putative molecular chaperone, DnaJ family	1,34	1,25
SL0656	corC	Magnesium and cobalt efflux protein corC	2,01	-1,23
SL0661	-	Hypothetical	1,82	1,06
SL0700	rfbD	Probable UDP-galactopyranose mutase	1,83	1,07
SL0701	rfbD	Probable UDP-galactopyranose mutase	1,61	-1,01
SL0702	-	Glycosyltransferase	1,36	-1,00
SL0703	-	Glycosyltransferase	1,61	1,26
SL0704	rfbD	O-antigen export system permease protein rfbD	1,32	1,03
SL0705	rfbE	O-antigen export system ATP-binding protein rfbE	1,43	1,01
SL0706	glfT2	UDP-galactofuranosyl transferase GlfT2	1,37	1,01
SL0707	-	Hypothetical	1,44	1,04
SL0724	ybgT	Uncharacterized protein ybgT	-1,15	1,02
SL0725	ybgE	Uncharacterized protein ybgE	-1,32	-1,56
SL0729	tolA	Protein tolA	1,85	-2,07
SL0731	pal	Peptidoglycan-associated lipoprotein	1,58	1,47
SL0754	-	Hypothetical	1,01	-1,16
SL0757	ybhT	Uncharacterized protein ybhT	1,95	-1,31
SL0784	ybhM	Uncharacterized protein ybhM	-1,22	-1,16
SL0785	-	Inner Membrane Protein	-1,09	-1,38
SL0786	-	Inner Membrane Protein	-1,07	-1,34
SL0790	ybhQ	Inner membrane protein ybhQ	2,48	4,45
SL0798	ybiB	Uncharacterized protein ybiB	1,33	-1,05
SL0809	ybiP	Putative phosphoethanolamine transferase ybiP	1,03	2,66
SL0814	-	Hypothetical	1,11	1,24
SL0839	dacC	D-alanyl-D-alanine carboxypeptidase dacC	-1,10	2,10
SL0847	ybjM	Inner membrane protein ybjM	1,01	-1,51
SL0858	ybjO	Inner membrane protein ybjO	1,48	-1,65
SL0868	ybjP	Uncharacterized lipoprotein ybjP	-1,06	1,24
SL0877	ybjE	Uncharacterized protein ybjE	-1,10	1,00
SL0922	lpxK	Tetraacyldisaccharide 4'-kinase	1,72	-1,68
SL0924	ycaR	UPF0434 protein CKO_02153	1,90	1,31
SL0925	kdsB	3-deoxy-manno-octulosonate cytidylyltransferase	2,14	-1,15
SL0932	ycbB	Probable L,D-transpeptidase YcbB	1,22	-1,33
SL0936	ompF	Outer membrane protein F	-6,32	3,64
SL1010	ompA	Outer membrane protein A	-1,04	1,04
SL1011	sulA	Cell division inhibitor sulA	1,50	1,70
SL1019	yccV	putative inner membrane protein	1,27	2,36
SL1021	ybcL	UPF0098 protein ybcL	1,64	1,18
SL1069	yiiY	Uncharacterized protein yiiY	-2,24	1,10
SL1075	ycdZ	Inner membrane protein ycdZ	1,31	-2,34
SL1077	csgF	Curli production assembly/transport component csgF	-2,42	-3,23
SL1089	yceK	Uncharacterized protein yceK	-1,26	4,06
SL1092	htrB	Lipid A biosynthesis lauroyl acyltransferase	1,70	-1,30
SL1096	yceO	Hypothetical	1,03	-1,89
SL1108	flgN	Flagella synthesis protein flgN	-1,74	1,40
SL1109	flgM	Negative regulator of flagellin synthesis	-1,43	1,80
SL1113	flgD	Basal-body rod modification protein flgD	-1,14	1,37
SL1115	flgF	Flagellar basal-body rod protein flgF	-1,07	1,35
SL1119	flgJ	Peptidoglycan hydrolase flgJ	1,07	-1,12
SL1124	yiaF	Uncharacterized protein yiaF	2,09	6,82
SL1124	yiaF	Uncharacterized protein yiaF	2,09	6,82
SL1144	ycfM	Uncharacterized protein ycfM	1,15	-1,03
SL1149	ycfJ	Uncharacterized protein ycfJ	1,18	-2,72
SL1179	envF	Probable lipoprotein envF	-1,17	-2,52
SL1181	envE	Probable lipoprotein envE	-1,18	-4,06
SL1190	-	Outer Membrane Lipoprotein	3,27	1,45
SL1192	dppB	Putative peptide transport system permease protein BMEII0209	5,39	3,41
SL1196	ynaI	Uncharacterized mscS family protein aq_812	1,12	-1,03
SL1196	ynaI	Uncharacterized mscS family protein aq_812	1,12	-1,03
SL1263	-	Hypothetical	-44,07	-8,24
SL1264	-	DNA/RNA Non-Specific Endonuclease	-5,94	-5,85
SL1277	nlpC	Probable lipoprotein nlpC	1,15	1,09

SL1282	ydiA	Putative phosphotransferase CKO_01727	-1,41	-1,56
SL1364	ydhO	Uncharacterized protein ydhO	1,35	-1,45
SL1375	ydhI	Uncharacterized protein ydhI	1,20	1,46
SL1404	ompN	Outer membrane protein N	1,28	1,99
SL1431	ynfC	UPF0257 lipoprotein ynfC	1,02	1,02
SL1458	-	Hypothetical	-1,75	-1,85
SL1459	ompC	Outer membrane protein C	6,93	1,54
SL1459	ompC	Outer membrane protein C	6,93	1,54
SL1489	treY	Maltooligosyl trehalose synthase	-1,04	2,33
SL1490	treZ	Malto-oligosyltrehalose trehalohydrolase	-1,69	1,49
SL1491	-	Hypothetical	1,01	1,16
SL1516	ygdR	Uncharacterized lipoprotein ygdR	1,92	1,01
SL1524	srfA	putative virulence effector protein	1,09	-1,08
SL1525	srfB	Virulence Protein SrfB	1,58	1,72
SL1527	ydcX	Uncharacterized protein ydcX	1,48	1,76
SL1537	ydcL	Uncharacterized lipoprotein ydcL	-1,14	1,33
SL1562	-	Hypothetical	-1,79	-2,75
SL1567	-	Hypothetical	-1,96	-1,83
SL1579	ydbJ	Uncharacterized protein ydbJ	-1,02	1,06
SL1593	ynaJ	Uncharacterized protein ynaJ	-1,97	1,33
SL1594	ynaI	MscS family inner membrane protein ynaI	-1,07	-2,22
SL1594	ynaI	MscS family inner membrane protein ynaI	-1,07	-2,22
SL1598	-	Hypothetical	1,20	1,14
SL1603	ygdR	Outer Membrane Lipoprotein	-1,11	-1,21
SL1628	steC	Secreted effector kinase steC	-1,55	-2,01
SL1640	yciM	Uncharacterized protein yciM	1,09	-2,47
SL1641	yciS	Inner membrane protein yciS	-1,11	-2,01
SL1663	ompW	Outer membrane protein W	1,01	2,05
SL1678	-	Hypothetical	-2,02	1,26
SL1683	galU	UTP--glucose-1-phosphate uridylyltransferase	1,37	-1,10
SL1697	ychN	Protein ychN	-1,02	-1,46
SL1700	kdsA	2-dehydro-3-deoxyphosphooctonate aldolase	1,67	1,03
SL1710	ychH	Uncharacterized protein ychH	-1,07	2,43
SL1726	ycgR	Flagellar brake protein YcgR	-2,93	-2,06
SL1727	emtA	Endo-type membrane-bound lytic murein transglycosylase A	1,24	1,76
SL1730	dadX	Alanine racemase, catabolic	1,04	1,36
SL1735	dsbB	Disulfide bond formation protein B	1,37	-1,02
SL1748	yeaY	Uncharacterized lipoprotein yeaY	1,85	-1,28
SL1757	yoaE	UPF0053 inner membrane protein yoaE	1,12	1,63
SL1765	ftsI	Peptidoglycan synthase ftsI	1,45	-1,02
SL1765	ftsI	Peptidoglycan synthase ftsI	1,45	-1,02
SL1769	mgrB	Protein mgrB	-1,80	-2,85
SL1783	-	Hypothetical	-3,09	-3,53
SL1794	-	Hypothetical	-5,53	-8,02
SL1795	-	Hypothetical	-5,06	-6,18
SL1810	holE	DNA polymerase III subunit theta	1,19	4,58
SL1845	mrdA	Penicillin-binding protein 2	2,44	-1,09
SL1845	mrdA	Penicillin-binding protein 2	2,44	-1,09
SL1860	flhD	Transcriptional activator FlhD	-3,42	-1,05
SL1873	-	NLP/P60 Protein	-3,11	-2,20
SL1874	-	Hypothetical	-2,61	-2,98
SL1911	rcsA	Colanic acid capsular biosynthesis activation protein A	-1,32	-3,43
SL1915	yedQ	Cellulose synthesis regulatory protein	-1,09	1,54
SL1917	yedI	Inner membrane protein yedI	1,63	-1,51
SL1922	yedR	Inner membrane protein yedR	1,20	-6,03
SL1923	ompS1	Outer membrane protein S1	-1,54	1,14
SL2036	yeeA	Inner membrane protein yeeA	1,34	1,36
SL2038	dacD	D-alanyl-D-alanine carboxypeptidase dacD	1,29	-1,60
SL2039	phsC	Thiosulfate reductase cytochrome B subunit	-1,67	1,42
SL2056	wzzB	Chain length determinant protein	-1,22	-2,36
SL2059	rfbP	Undecaprenyl-phosphate galactose phosphotransferase	2,06	1,34
SL2061	rfbM	Mannose-1-phosphate guanylyltransferase rfbM	2,13	1,24
SL2062	rfbN	O antigen biosynthesis rhamnosyltransferase rfbN	2,11	1,18
SL2064	rfbV	O antigen biosynthesis abequosyltransferase rfbV	2,29	1,28
SL2065	rfbX	Putative O-antigen transporter	4,46	1,63
SL2066	rfbJ	CDP-abequose synthase	2,39	1,84
SL2067	rfbH	Lipopolysaccharide biosynthesis protein rfbH	1,45	1,22

SL2068	rfbG	CDP-glucose 4,6-dehydratase	1,67	1,16
SL2070	rfbI	Protein rfbI	2,76	-1,13
SL2071	rfbC	dTDP-4-dehydrorhamnose 3,5-epimerase	2,33	-1,06
SL2072	rfbA	TDP-glucose pyrophosphorylase	2,38	-1,25
SL2073	rfbD	dTDP-4-dehydrorhamnose reductase	1,92	-1,47
SL2074	rfbB	dTDP-glucose 4,6-dehydratase	2,04	-1,61
SL2076	wcaM	Colanic acid biosynthesis protein wcaM	1,17	1,14
SL2077	wcaL	Putative colanic acid biosynthesis glycosyltransferase wcaL	1,80	1,78
SL2080	wcaJ	Putative colanic biosynthesis UDP-glucose lipid carrier transferase	1,42	-1,44
SL2082	manC	Mannose-1-phosphate guanylyltransferase manC	1,46	-1,25
SL2083	wcaI	Putative colanic acid biosynthesis glycosyl transferase wcaI	2,23	-1,06
SL2084	nudD	GDP-mannose mannosyl hydrolase	2,56	-1,13
SL2085	fcl	GDP-L-fucose synthase	1,63	-1,33
SL2086	gmd	GDP-mannose 4,6-dehydratase	1,48	-1,41
SL2088	wcaE	Putative colanic acid biosynthesis glycosyl transferase wcaE	-1,41	-2,85
SL2090	wcaC	Putative colanic acid biosynthesis glycosyl transferase wcaC	1,35	1,01
SL2092	wcaA	Putative colanic acid biosynthesis glycosyl transferase wcaA	1,95	1,44
SL2095	wza	Putative polysaccharide export protein wza	1,35	-2,73
SL2097	asmA	Protein AsmA	1,25	-1,13
SL2110	-	Hypothetical	-1,12	-1,67
SL2111	-	Hypothetical	1,09	-1,28
SL2115	-	Hypothetical	-3,69	-5,31
SL2126	yehA	Uncharacterized protein yehA	-1,11	-1,42
SL2127	yehB	Uncharacterized outer membrane usher protein yehB	1,12	-1,87
SL2128	yehC	Uncharacterized fimbrial chaperone yehC	-2,61	-2,64
SL2146	pbpG	D-alanyl-D-alanine endopeptidase	1,91	-1,66
SL2161	sanA	Protein sanA	-1,04	1,05
SL2162	yeiS	Uncharacterized protein yeiS	1,56	1,28
SL2176	cirA	Colicin I receptor	-2,00	1,03
SL2185	ykgH	Hypothetical	1,33	1,18
SL2191	spr	Lipoprotein spr	1,64	-1,01
SL2202	-	Hypothetical	1,62	1,16
SL2208	yrhL	Putative peptidoglycan O-acetyltransferase yrhL	-1,32	-1,39
SL2210	-	Hypothetical	-1,37	-1,27
SL2221	-	Conserved Hypothetical Protein	-1,08	-1,97
SL2236	apbE	Thiamine biosynthesis lipoprotein ApbE	1,58	1,47
SL2237	ompC	Outer membrane protein C	1,02	1,06
SL2237	ompC	Outer membrane protein C	1,02	1,06
SL2267	arnC	Undecaprenyl-phosphate 4-deoxy-4-formamido-L-arabinose transferase	-2,24	-3,30
SL2272	arnF	Probable 4-amino-4-deoxy-L-arabinose-phosphoundecaprenol flippase subunit ArnF	-1,15	-1,77
SL2280	elaB	Protein elaB	-1,07	2,11
SL2308	yfcC	Uncharacterized protein yfcC	4,61	1,20
SL2308	yfcC	Uncharacterized protein yfcC	4,61	1,20
SL2346	-	Uncharacterized 24.3 kDa protein	3,59	1,59
SL2350	yfcM	Uncharacterized protein yfcM	2,39	1,80
SL2352	mepA	Penicillin-insensitive murein endopeptidase	1,44	1,66
SL2361	vacJ	Probable phospholipid-binding lipoprotein mlaA	-1,01	1,06
SL2369	ddg	Protein ddg	-1,91	-4,29
SL2386	yfeN	Uncharacterized protein yfeN	-1,93	-1,06
SL2386	yfeN	Uncharacterized protein yfeN	-1,93	-1,06
SL2413	amiA	Probable N-acetylmuramoyl-L-alanine amidase AmiA	1,48	-1,23
SL2415	ypfK	Uncharacterized protein ypfK	2,22	-1,02
SL2451	nlpB	Lipoprotein 34	1,21	-3,86
SL2457	yfgC	TPR repeat-containing protein yfgC	1,37	-1,46
SL2467	-	Hypothetical	-1,28	-1,21
SL2468	yfgG	Uncharacterized protein yfgG	-1,38	-1,21
SL2475	ratB	Invasin	1,41	1,01
SL2477	ratA	Invasin	-1,14	-1,33
SL2478	sinI	Outer Membrane Protein	-1,08	1,52
SL2479	sinH	Intimin	-1,23	1,08
SL2483	yfgM	UPF0070 protein yfgM	1,39	-1,61
SL2485	ispG	4-hydroxy-3-methylbut-2-en-1-yl diphosphate synthase	1,12	1,01
SL2486	rodZ	Cytoskeleton protein rodZ	1,31	-1,90
SL2493	pbpC	Penicillin-binding protein 1C	1,68	-1,15
SL2513	-	Putative nickel/cobalt efflux system HI_1248	1,21	-1,13

SL2606	yfiC	tRNA (adenine-N(6)-)-methyltransferase	1,50	1,68
SL2617	yfiM	Uncharacterized protein yfiM	1,39	1,02
SL2623	yfiO	UPF0169 lipoprotein yfiO	2,08	-1,55
SL2737	yrbE	Uncharacterized oxidoreductase yrbE	-1,68	-1,02
SL2745	-	Hypothetical	1,09	-1,23
SL2746	-	Hypothetical	1,21	1,09
SL2756	fljB	Phase 2 flagellin	-7,31	-1,25
SL2784	ygaW	Uncharacterized protein ygaW	-1,33	-2,45
SL2786	ygaM	Uncharacterized protein ygaM	-1,36	1,46
SL2801	-	Glycoporin	1,04	-1,12
SL2804	yqaA	Inner membrane protein yqaA	1,40	-1,82
SL2811	mltB	Membrane-bound lytic murein transglycosylase B	-1,00	-1,65
SL2893	rffG	Uncharacterized protein HI_1014	1,19	1,08
SL2896	ygbK	Uncharacterized protein ygbK	1,91	-1,12
SL2896	ygbK	Uncharacterized protein ygbK	1,91	-1,12
SL2904	nlpD	Lipoprotein nlpD	1,57	-1,47
SL2904	nlpD	Lipoprotein nlpD	1,57	-1,47
SL2911	ygbE	Inner membrane protein ygbE	1,40	-1,56
SL2916	ygbF	Uncharacterized protein ygbF	-1,83	-1,82
SL2961	ygdD	UPF0382 inner membrane protein ygdD	1,25	-1,63
SL2968	mltA	Membrane-bound lytic murein transglycosylase A	1,88	-1,95
SL2969	amiC	N-acetylmuramoyl-L-alanine amidase AmiC	1,30	-1,17
SL2985	ygdR	Uncharacterized lipoprotein ygdR	1,04	1,00
SL2999	-	Hypothetical	-1,22	-2,31
SL3005	-	Hypothetical	-1,72	-2,17
SL3011	-	Uncharacterized protein HI_0947	1,67	-1,65
SL3011	-	Uncharacterized protein HI_0947	1,67	-1,65
SL3013	-	Hypothetical	-1,84	-1,84
SL3014	ygeR	Uncharacterized lipoprotein ygeR	1,10	-1,00
SL3019	dsbC	Thiol:disulfide interchange protein dsbC	1,46	1,36
SL3022	ygfX	Uncharacterized protein ygfX	1,12	1,57
SL3028	-	Hypothetical	-1,39	-1,01
SL3043	mscS	Small-conductance mechanosensitive channel	-1,39	-1,24
SL3047	glmU	Bifunctional protein glmU	2,76	17,73
SL3055	yisY	AB hydrolase superfamily protein yisY	-1,80	-1,63
SL3087	mltC	Membrane-bound lytic murein transglycosylase C	1,02	-1,19
SL3090	yqgA	Uncharacterized protein yqgA	1,56	-2,59
SL3136	yghB	Inner membrane protein yghB	1,22	-1,11
SL3167	dsbB	Putative protein-disulfide oxidoreductase	-1,46	1,04
SL3171	yqiJ	Inner membrane protein yqiJ	1,20	1,52
SL3172	yqiK	Inner membrane protein yqiK	1,18	-1,12
SL3173	rfaE	ADP-heptose synthase	1,44	1,50
SL3202	yqjE	Inner membrane protein yqjE	-1,80	-1,42
SL3203	yqjK	Uncharacterized protein yqjK	-1,92	-1,61
SL3206	yhaH	Inner membrane protein yhaH	-1,12	1,17
SL3237	yraM	Uncharacterized protein yraM	1,85	-1,31
SL3239	diaA	DnaA initiator-associating protein diaA	1,41	1,10
SL3265	glmM	Phosphoglucosamine mutase	2,06	1,23
SL3272	dacB	D-alanyl-D-alanine carboxypeptidase dacB	1,46	-1,34
SL3279	murA	UDP-N-acetylglucosamine 1-carboxyvinyltransferase	1,60	-1,18
SL3289	lptC	Lipopolysaccharide export system protein lptC	1,31	-1,48
SL3298	mtgA	Monofunctional biosynthetic peptidoglycan transglycosylase	-1,28	1,32
SL3310	nanT1	Putative sialic acid transporter 1	-1,92	-1,89
SL3311	nanA	N-acetylneuraminate lyase	1,40	-1,38
SL3322	citG1	Probable 2-(5''-triphosphoribosyl)-3'-dephosphocoenzyme-A synthase 1	1,03	1,67
SL3344	mreD	Rod shape-determining protein mreD	1,88	1,82
SL3345	mreC	Rod shape-determining protein mreC	1,69	-1,82
SL3351	yedZ	Sulfoxide reductase heme-binding subunit yedZ	1,09	-1,11
SL3363	acrE	Acriflavine resistance protein E	1,40	-1,37
SL3365	yhdV	Uncharacterized protein yhdV	1,38	1,01
SL3432	yhfA	Protein yhfA	1,22	1,61
SL3447	yhfL	Uncharacterized protein yhfL	1,48	1,21
SL3455	hofQ	Protein transport protein hofQ	1,55	1,25
SL3457	yrfB	Uncharacterized protein yrfB	-1,08	1,41
SL3460	mrcA	Penicillin-binding protein 1A	1,57	-2,07
SL3466	yhgE	Uncharacterized protein yhgE	1,46	-1,33

SL3468	envZ	Osmolarity sensor protein envZ	1,91	-1,63
SL3494	ybbD	Hypothetical	-1,56	1,42
SL3506	asd	Aspartate-semialdehyde dehydrogenase	1,05	1,19
SL3515	-	Hypothetical	-11,74	-1,62
SL3539	yhhM	Uncharacterized protein yhhM	1,50	1,67
SL3540	yhhN	Uncharacterized membrane protein yhhN	-1,11	-3,96
SL3566	frlB	Fructosamine deglycase frlB	3,57	25,25
SL3569	-	Hypothetical	-2,87	2,47
SL3581	bcsC	Cellulose synthase operon protein C	1,16	-1,20
SL3584	bcsA	Cellulose synthase catalytic subunit [UDP-forming]	1,02	-1,63
SL3588	yhjT	Uncharacterized protein yhjT	-1,56	-1,30
SL3595	dppB	Dipeptide transport system permease protein dppB	-8,43	-7,97
SL3605	lpfB	Chaperone protein lpfB	1,09	-1,55
SL3611	yiaD	Inner membrane lipoprotein yiaD	1,63	-1,62
SL3613	yiaF	Uncharacterized protein yiaF	1,15	1,32
SL3613	yiaF	Uncharacterized protein yiaF	1,15	1,32
SL3624	yiaB	Hypothetical	-1,64	-1,50
SL3656	yadA	Adhesin yadA	1,08	1,65
SL3676	hldD	ADP-L-glycero-D-manno-heptose-6-epimerase	1,17	1,27
SL3677	rfaF	ADP-heptose--LPS heptosyltransferase 2	1,34	-1,24
SL3678	rfaC	Lipopolysaccharide heptosyltransferase 1	1,15	-1,52
SL3680	waaK	Lipopolysaccharide 1,2-N-acetylglucosaminetransferase	1,42	-1,61
SL3681	rfaZ	Lipopolysaccharide core biosynthesis protein rfaZ	2,29	-1,25
SL3682	rfaY	Lipopolysaccharide core heptose(II) kinase rfaY	3,15	-1,06
SL3683	rfaJ	Lipopolysaccharide 1,2-glucosyltransferase	3,80	-1,11
SL3684	rfaI	Lipopolysaccharide 1,3-galactosyltransferase	2,70	-1,09
SL3685	rfaB	Lipopolysaccharide 1,6-galactosyltransferase	2,71	-1,29
SL3686	yibR	Uncharacterized protein yibR	4,10	-1,17
SL3687	rfaP	Lipopolysaccharide core heptose(I) kinase rfaP	1,55	-1,36
SL3688	rfaG	Lipopolysaccharide core biosynthesis protein rfaG	1,30	-2,10
SL3689	rfaQ	Lipopolysaccharide core heptosyltransferase rfaQ	1,15	-2,41
SL3690	waaA	3-deoxy-D-manno-octulosonic-acid transferase	2,10	3,06
SL3752	yicN	Uncharacterized protein yicN	1,10	3,22
SL3765	-	Hypothetical	1,28	-1,04
SL3772	yidG	Inner membrane protein yidG	-1,00	1,17
SL3773	yidH	Inner membrane protein yidH	1,51	1,29
SL3777	yidQ	Uncharacterized protein yidQ	-1,08	2,30
SL3788	torA	Trimethylamine-N-oxide reductase	1,09	-1,20
SL3809	oxaA	Inner membrane protein oxaA	1,47	-1,06
SL3812	-	Inner Membrane Protein	-1,32	1,15
SL3829	glmU	Bifunctional protein glmU	1,52	1,19
SL3871	-	Inner Membrane Protein	1,52	3,48
SL3877	wecA	Undecaprenyl-phosphate alpha-N-acetylglucosaminyl 1-phosphate transferase	-1,22	-2,01
SL3878	wzzE	Lipopolysaccharide biosynthesis protein wzzE	1,05	-1,67
SL3879	wecB	UDP-N-acetylglucosamine 2-epimerase	1,32	-2,08
SL3880	wecC	UDP-N-acetyl-D-mannosamine dehydrogenase	1,45	-1,71
SL3881	rffG	dTDP-glucose 4,6-dehydratase 2	1,63	-1,54
SL3883	rffC	Lipopolysaccharide biosynthesis protein rffC	1,80	-1,54
SL3884	rffA	Lipopolysaccharide biosynthesis protein rffA	1,58	-1,19
SL3888	wecG	Probable UDP-N-acetyl-D-mannosaminuronic acid transferase	1,53	-1,48
SL3895	-	Inner Membrane Protein	1,01	-1,34
SL3896	-	Hypothetical	1,23	-1,10
SL3899	-	Hypothetical	1,01	-1,55
SL3900	yifL	Uncharacterized lipoprotein yifL	1,50	-1,44
SL3923	rmuC	DNA recombination protein rmuC	1,96	1,68
SL3957	-	Hypothetical	-1,26	-1,50
SL3969	yihU	Uncharacterized oxidoreductase yihU	1,56	1,52
SL3989	-	Hypothetical	-1,56	-3,77
SL4000	yiiY	Uncharacterized protein yiiY	1,07	1,25
SL4006	-	Hypothetical	1,97	1,90
SL4028	lsrG	Autoinducer 2-degrading protein lsrG	-2,15	-1,91
SL4032	yiiR	Uncharacterized protein yiiR	-1,21	-1,22
SL4046	-	Hypothetical	-1,04	1,24
SL4051	mscS	Small-conductance mechanosensitive channel	-1,14	-1,48
SL4052	-	Hypothetical	-1,08	-1,06
SL4075	sthA	Soluble pyridine nucleotide transhydrogenase	1,10	1,28

SL4077	yijD	Inner membrane protein yijD	1,61	1,37
SL4080	murI	Glutamate racemase	1,50	1,03
SL4081	murB	UDP-N-acetylenolpyruvoylglucosamine reductase	1,42	-1,23
SL4094	-	Inner Membrane Protein	1,76	-1,17
SL4110	yjaH	Uncharacterized protein yjaH	1,04	-1,12
SL4159	yjbF	Uncharacterized lipoprotein yjbF	-1,53	-3,86
SL4178	-	Hypothetical	1,26	1,36
SL4183	alr	Alanine racemase, biosynthetic	1,66	1,74
SL4188	-	Hypothetical	1,51	-2,63
SL4189	-	Lipoprotein	1,28	-2,55
SL4207	cidA	Holin-like protein cidA	-1,56	-9,77
SL4208	ywbG	Uncharacterized protein ywbG	-2,01	-15,23
SL4230	eptA	Phosphoethanolamine transferase eptA	-1,43	-4,20
SL4247	yjiK	Uncharacterized protein yjiK	-50,35	-15,24
SL4267	groL	60 kDa chaperonin	2,17	1,42
SL4268	yjeI	Uncharacterized protein yjeI	-1,30	1,28
SL4276	blc	Outer membrane lipoprotein blc	-1,26	1,05
SL4283	yjeO	Inner membrane protein yjeO	2,11	-1,20
SL4292	amiB	N-acetylmuramoyl-L-alanine amidase AmiB	1,44	1,29
SL4307	yjfL	UPF0719 inner membrane protein yjfL	-1,14	-2,12
SL4312	bsmA	Lipoprotein BsmA	2,05	8,24
SL4322	yjfY	Uncharacterized protein yjfY	1,28	-1,28
SL4333	ytfF	Inner membrane protein ytfF	1,09	1,39
SL4342	ytfM	Uncharacterized protein ytfM	1,43	-1,33
SL4349	mpl	UDP-N-acetylmuramate:L-alanyl-gamma-D-glutamyl-meso-diaminopimelate ligase	1,57	1,00
SL4363	yrbE	Uncharacterized oxidoreductase yrbE	-1,08	1,10
SL4373	-	Hypothetical	-1,54	1,73
SL4374	-	Hypothetical	-1,53	1,62
SL4394	yfcC	Uncharacterized protein HI_0594	-2,15	1,70
SL4394	yfcC	Uncharacterized protein HI_0594	-2,15	1,70
SL4402	ytgA	Uncharacterized protein ytgA	1,18	1,05
SL4404	yjgN	Inner membrane protein yjgN	1,55	-1,18
SL4427	-	Hypothetical	1,46	1,54
SL4433	-	Hypothetical	-1,63	-1,34
SL4435	-	Hypothetical	-2,76	-2,20
SL4445	yjiH	Uncharacterized protein yjiH	-2,10	1,37
SL4448	mdtM	Multidrug resistance protein mdtM	1,79	1,48
SL4453	-	Hypothetical	-1,14	-1,19
SL4459	-	Hypothetical	1,18	2,24
SL4471	frlB	Fructosamine deglycase frlB	1,08	1,19
SL4473	yjjA	Uncharacterized protein yjjA	1,17	-1,32
SL4476	yjjB	UPF0442 protein CKO_03436	1,35	-1,39
SL4477	yjjP	Inner membrane protein yjjP	1,67	-1,17
SL4483	yjjZ	Uncharacterized protein yjjZ	-3,01	-1,68
SL4498	-	Hypothetical	1,03	-1,13
SL4499	yhcD	Uncharacterized outer membrane usher protein yhcD	-1,39	-1,01
SL4501	yhcF	Uncharacterized protein yhcF	-1,98	-1,19
SL4502	yhcF	Uncharacterized protein yhcF	-2,18	1,13
SL4503	lplA	Lipoate-protein ligase A	1,35	1,53
SL4504	smp	Protein smp	2,02	-1,12
SL4509	slt	Soluble lytic murein transglycosylase	1,68	1,38
SL4518	sthE	Adhesin	-1,15	-1,53
SL4519	fimG	Hypothetical	-1,16	-1,47
SL4521	fimC	Chaperone protein fimC	1,21	-1,80
SL4522	ydeS	Uncharacterized fimbrial-like protein ydeS	1,56	-1,32
SL4523	yaiV	Uncharacterized protein yaiV	-1,09	-1,63
SL4523	yaiV	Uncharacterized protein yaiV	-1,09	-1,63
		Cellular processes		
SL0010	htgA	UPF0174 protein yaaW	1,44	1,14
SL0089	apaH	Bis(5'-nucleosyl)-tetraphosphatase, symmetrical	1,62	-1,43
SL0091	ksgA	dimethyladenosine transferase	1,28	-1,55
SL0094	imp	organic solvent tolerance protein	1,67	-1,57
SL0121	ftsL	Cell division protein ftsL	-1,15	-1,22
SL0127	ftsW	Cell division protein ftsW	1,89	-1,63
SL0131	ftsQ	Cell division protein ftsQ	1,20	-1,44
SL0132	ftsA	Cell division protein ftsA	1,19	-2,09

SL0133	ftsZ	Cell division protein ftsZ	-1,17	-1,20
SL0142	hofC	Protein transport protein hofC	1,73	1,33
SL0146	ampD	1,6-anhydro-N-acetylmuramyl-L-alanine amidase AmpD	1,01	-1,10
SL0169	cueO	Blue copper oxidase cueO	-1,05	1,47
SL0237	mesJ	cell cycle protein MesJ	1,42	1,12
SL0326	yisK	putative fumarylacetoacetate (faa) hydrolase	-1,15	-1,39
SL0327	dehH1	Haloacetate dehalogenase H-1	-1,51	1,03
SL0346	bepE	Efflux pump membrane transporter BepE	2,06	1,87
SL0347	mtrC	Membrane fusion protein mtrC	1,24	1,74
SL0377	mdtG	Multidrug resistance protein mdtG	1,26	-3,46
SL0397	ahpC	Probable peroxiredoxin	-2,04	-2,47
SL0406	yajD	Uncharacterized protein yajD	-1,15	-1,30
SL0475	ybaN	Inner membrane protein ybaN	-1,11	-1,42
SL0486	fsr	Fosmidomycin resistance protein	1,50	-1,41
SL0555	-	Hypothetical	-1,83	1,07
SL0596	ahpC	Alkyl hydroperoxide reductase subunit C	-1,38	-3,65
SL0597	ahpF	Alkyl hydroperoxide reductase subunit F	-1,21	-3,53
SL0617	cspE	Cold shock-like protein cspE	1,14	-3,51
SL0627	mrdB	Rod shape-determining protein rodA	1,92	1,80
SL0630	ybeB	Uncharacterized protein ybeB	1,39	2,09
SL0658	ybeZ	PhoH-like protein	2,34	-1,61
SL0702	-	Glycosyltransferase	1,36	-1,00
SL0708	-	Hypothetical	1,48	-1,09
SL0763	ybhC	Putative acyl-CoA thioester hydrolase ybhC	1,33	2,76
SL0798	ybiB	Uncharacterized protein ybiB	1,33	-1,05
SL0815	ybiV2	putative hydrolase	-1,42	-1,28
SL0838	yliJ	Uncharacterized GST-like protein yliJ	-1,69	-1,34
SL0842	mdfA	Multidrug translocase mdfA	1,44	1,32
SL0870	amiD	N-acetylmuramoyl-L-alanine amidase AmiD	1,33	-1,45
SL0882	cspD	Cold shock-like protein cspD	-1,33	1,25
SL0898	ftsK	DNA translocase ftsK	1,68	-1,12
SL0920	ycaI	Uncharacterized protein ycaI	1,40	1,16
SL0929	mukF	Chromosome partition protein mukF	1,93	1,08
SL0931	mukB	Chromosome partition protein mukB	2,63	1,51
SL1080	csgB	Minor curlin subunit	1,06	-1,03
SL1081	csgA	Major curlin subunit	-3,50	-1,69
SL1087	mdoG	Glucans biosynthesis protein G	1,41	-1,63
SL1088	mdoH	Glucans biosynthesis glucosyltransferase H	1,63	-2,05
SL1091	mdtG	Multidrug resistance protein mdtG	1,49	-1,45
SL1106	mviM	Virulence factor mviM	-1,05	1,42
SL1111	flgB	Flagellar basal-body rod protein flgB	-1,16	1,03
SL1112	flgC	Flagellar basal-body rod protein flgC	-1,15	1,04
SL1114	flgE	Flagellar hook protein flgE	-1,32	1,36
SL1116	flgG	Flagellar basal-body rod protein flgG	-1,01	1,32
SL1117	flgH	Flagellar L-ring protein	1,13	1,14
SL1118	flgI	Flagellar P-ring protein	1,00	-1,27
SL1120	flgK	Flagellar hook-associated protein 1	-2,64	-1,28
SL1121	flgL	Flagellar hook-associated protein 3	-2,92	-1,05
SL1126	yceF	Maf-like protein yceF 1	1,12	1,43
SL1146	nagZ	Beta-hexosaminidase	1,38	-1,28
SL1171	hflD	High frequency lysogenization protein hflD	1,74	-1,06
SL1184	pagC	Virulence membrane protein pagC	-16,89	-15,69
SL1199	aadA	Streptomycin 3"-adenylyltransferase	-1,94	-1,56
SL1200	-	Response Regulator	-2,08	-2,24
SL1206	yeaR	Uncharacterized protein yeaR	2,14	-1,21
SL1253	katE	Catalase HPII	-3,08	1,48
SL1363	sodB	Superoxide dismutase [Fe]	-1,84	1,26
SL1372	sodC	Superoxide dismutase [Cu-Zn] 2	-2,36	-1,18
SL1372	sodC	Superoxide dismutase [Cu-Zn] 2	-2,36	-1,18
SL1376	slyA	Transcriptional regulator slyA	-1,84	-1,30
SL1383	gst	Glutathione S-transferase	-1,62	-1,21
SL1441	ydfG	NADP-dependent L-serine/L-allo-threonine dehydrogenase ydfG	-1,24	1,01
SL1446	ydeE	Uncharacterized MFS-type transporter ydeE	-2,20	-1,51
SL1474	tetA	Tetracycline resistance protein, class G	1,40	1,45
SL1493	osmC	Peroxiredoxin osmC	-2,07	1,07
SL1538	tehB	Tellurite resistance protein tehB	1,06	-1,29
SL1549	aacA7	Aminoglycoside N(6')-acetyltransferase type 1	-1,74	-1,68

SL1552	mdoD	Glucans biosynthesis protein D	1,67	2,20
SL1553	pnbA	Para-nitrobenzyl esterase	1,81	4,58
SL1556	trg	Methyl-accepting chemotaxis protein III	-3,49	2,66
SL1578	hslJ	Heat shock protein hslJ	1,29	-3,39
SL1588	tap	Methyl-accepting chemotaxis protein IV	-3,74	-1,27
SL1597	tpx	Probable thiol peroxidase	-1,29	1,07
SL1612	tpx	Probable thiol peroxidase	1,68	1,73
SL1616	pspE	Thiosulfate sulfurtransferase PspE	-1,47	1,93
SL1617	pspD	Phage shock protein D	-5,24	-2,68
SL1618	pspC	Phage shock protein C	-6,34	-2,89
SL1619	pspB	Phage shock protein B	-7,27	-3,81
SL1621	pspF	Psp operon transcriptional activator	1,45	1,80
SL1637	osmB	Osmotically-inducible lipoprotein B	-1,54	-6,38
SL1666	ispZ	Probable intracellular septation protein	1,73	-1,76
SL1696	ychO	Uncharacterized protein ychO	-1,00	-1,48
SL1697	ychN	Protein ychN	-1,02	-1,46
SL1724	treA	Periplasmic trehalase	-1,34	2,08
SL1736	yeaR	Uncharacterized protein yeaR	1,29	1,19
SL1742	minC	Probable septum site-determining protein minC	-1,57	-1,72
SL1743	minD	Septum site-determining protein minD	-1,24	1,16
SL1744	minE	Cell division topological specificity factor	1,10	1,30
SL1766	cspC	Cold shock-like protein cspC	-1,23	-1,15
SL1772	yebQ	Uncharacterized transporter yebQ	1,49	-3,40
SL1773	htpX	Probable protease htpX homolog	1,88	1,05
SL1823	msbB	Lipid A biosynthesis (KDO)2-(lauroyl)-lipid IVA acyltransferase 1	1,16	1,02
SL1842	cutC	Copper homeostasis protein cutC	2,98	1,78
SL1848	flhA	Flagellar biosynthesis protein flhA	-1,40	-1,59
SL1849	flhB	Flagellar biosynthetic protein flhB	-1,60	-1,79
SL1851	cheY	Chemotaxis protein cheY	-2,73	-1,54
SL1852	cheB	Chemotaxis response regulator protein-glutamate methylesterase	-3,70	-1,80
SL1853	cheR	Chemotaxis protein methyltransferase	-4,57	-2,09
SL1854	tar	Methyl-accepting chemotaxis protein II	-3,28	-1,26
SL1857	motB	Motility protein B	-2,75	-1,45
SL1859	flhC	Flagellar transcriptional activator flhC	-3,91	-1,47
SL1861	uspC	Universal stress protein C	-1,42	3,43
SL1862	otsA	Alpha,alpha-trehalose-phosphate synthase [UDP-forming]	-1,13	-1,40
SL1863	otsB	Trehalose-phosphate phosphatase	-1,12	-1,35
SL1879	sdiA	Regulatory protein sdiA	-3,69	-1,66
SL1889	fliD	Flagellar hook-associated protein 2	-2,82	1,13
SL1890	fliS	Flagellar protein fliS	-3,15	1,03
SL1897	fliE	Flagellar hook-basal body complex protein fliE	-3,50	2,08
SL1898	fliF	Flagellar M-ring protein	-2,01	-1,61
SL1899	fliG	Flagellar motor switch protein FliG	-1,87	1,08
SL1900	fliH	Flagellar assembly protein fliH	-1,67	1,39
SL1901	fliI	Flagellum-specific ATP synthase	-1,25	1,11
SL1902	fliJ	Flagellar fliJ protein	-1,91	2,18
SL1903	fliK	Flagellar hook-length control protein	-2,16	1,21
SL1905	fliM	Flagellar motor switch protein FliM	-1,55	-1,18
SL1908	fliP	Flagellar biosynthetic protein fliP	-1,43	-2,07
SL1909	fliQ	Flagellar biosynthetic protein FliQ	-1,37	-2,37
SL1910	fliR	Flagellar biosynthetic protein fliR	-1,33	-2,53
SL1924	cspB	Cold shock-like protein cspB	-3,12	-1,96
SL2065	rfbX	Putative O-antigen transporter	4,46	1,63
SL2087	wcaF	Putative colanic acid biosynthesis acetyltransferase wcaF	-1,03	-3,34
SL2103	mdtA	Multidrug resistance protein mdtA	1,10	-2,86
SL2129	yehD	Uncharacterized protein yehD	-2,70	-1,96
SL2198	bcr	Bicyclomycin resistance protein	1,25	-1,81
SL2211	ycfK	Uncharacterized protein ycfK	1,03	1,26
SL2214	pifA	KAP P-Loop Domain-Containing Protein	1,48	8,00
SL2220	-	Homolog Of Virulence Protein MsgA	-1,29	-2,57
SL2265	ais	Lipopolysaccharide core heptose(II)-phosphate phosphatase	-3,11	-1,91
SL2266	arnB	UDP-4-amino-4-deoxy-L-arabinose--oxoglutarate aminotransferase	-2,25	-3,45
SL2283	cheV	Chemotaxis protein cheV	-5,49	-1,51
SL2318	yfcG	Uncharacterized GST-like protein yfcG	-1,16	-1,73
SL2319	yfcH	Epimerase family protein yfcH	-1,01	-1,12
SL2370	yfdZ	Uncharacterized aminotransferase yfdZ	-1,84	1,09

SL2391	zipA	Cell division protein zipA homolog	1,17	-1,41
SL2412	ypeA	Acetyltransferase ypeA	1,44	-1,08
SL2441	yfeW	UPF0214 protein yfeW	-1,39	-1,48
SL2458	yfgD	Uncharacterized protein yfgD	1,21	-1,01
SL2474	shdA	host colonisation factor (ShdA)	1,27	1,13
SL2495	sseA	3-mercaptopyruvate sulfurtransferase	-1,09	1,29
SL2542	era	GTP-binding protein era homolog	1,35	-2,06
SL2606	yfiC	tRNA (adenine-N(6)-)-methyltransferase	1,50	1,68
SL2652	corB	putative membrane protein	1,24	-1,42
SL2788	ydfG	Uncharacterized protein ydfG	1,25	1,74
SL2796	proX	Glycine betaine-binding periplasmic protein	-1,42	-1,51
SL2802	luxS	S-ribosylhomocysteine lyase	1,11	-1,09
SL2899	slyA	Transcriptional regulator	1,28	1,50
SL2906	surE	Multifunctional protein surE	2,52	-1,18
SL2929	-	Uncharacterized protein MJ0301	-1,33	2,67
SL2937	relA	GTP pyrophosphokinase	0,00	-2,14
SL3025	yqfA	UPF0073 inner membrane protein yqfA	-1,07	2,36
SL3032	visC	Protein visC	1,03	-2,07
SL3051	cbiO	Cobalt import ATP-binding protein CbiO	3,87	4,26
SL3074	yggR	Uncharacterized protein yggR	1,27	2,50
SL3076	yggT	Uncharacterized protein yggT	1,78	-1,16
SL3102	puuB	Gamma-glutamylputrescine oxidoreductase	-1,14	-1,01
SL3112	bdlA	Biofilm dispersion protein BdlA	-19,64	-3,42
SL3126	tse	Methyl-accepting chemotaxis serine transducer	-3,70	-1,18
SL3153	mdaB	Modulator of drug activity B	1,53	2,03
SL3178	bacA	Undecaprenyl-diphosphatase	1,18	-1,37
SL3189	cheM	methyl-accepting chemotaxis protein II	-4,93	-1,05
SL3240	yraP	Uncharacterized protein yraP	1,21	1,22
SL3254	nlpI	Lipoprotein nlpI	1,08	-1,88
SL3268	ftsH	Cell division protease ftsH	1,02	-2,69
SL3313	sspB	Stringent starvation protein B	1,24	-1,04
SL3337	aaeA	p-hydroxybenzoic acid efflux pump subunit AaeA	1,29	-1,48
SL3342	rng	Ribonuclease G	1,24	-1,25
SL3343	yceF2	Maf-like protein yceF 2	1,32	-1,58
SL3346	mreB	Rod shape-determining protein mreB	1,43	-1,42
SL3377	mscL	Large-conductance mechanosensitive channel	-1,42	1,86
SL3433	crp	Catabolite gene activator	1,47	1,06
SL3437	fic	Probable adenosine monophosphate-protein transferase fic	1,05	2,20
SL3452	damX	Protein damX	1,72	-1,17
SL3463	yrfG	Uncharacterized protein yrfG	1,16	1,39
SL3535	ftsE	Cell division ATP-binding protein ftsE	1,39	-1,47
SL3536	ftsY	Cell division protein ftsY	1,63	-1,49
SL3542	tcp	Methyl-accepting chemotaxis citrate transducer	-3,33	-1,91
SL3555	uspB	Universal stress protein B	-2,10	-1,26
SL3556	uspA	Universal stress protein A	-2,11	1,26
SL3562	gor	Glutathione reductase	-1,02	-1,33
SL3568	treF	Cytoplasmic trehalase	-1,96	-2,00
SL3615	cspA	Cold shock protein cspA	2,01	-1,04
SL3617	-	GCN5-Related N-Acetyltransferase	1,12	1,18
SL3635	-	Hypothetical	1,08	1,19
SL3649	yibF	Uncharacterized GST-like protein yibF	-1,40	1,99
SL3669	yibN	Uncharacterized protein yibN	1,34	1,50
SL3708	spoT	Guanosine-3',5'-bis(diphosphate) 3'-pyrophosphohydrolase	0,00	-1,03
SL3775	ibpB	Small heat shock protein ibpB	6,11	-2,20
SL3786	yhjA	Probable cytochrome c peroxidase	-2,21	-3,11
SL3903	xerC	Tyrosine recombinase xerC	-1,13	-2,77
SL3904	yigB	Uncharacterized protein yigB	1,02	-2,88
SL3921	ysgA	Putative carboxymethylenebutenolidase	-1,91	1,10
SL3975	yiiD	Uncharacterized protein yiiD	1,05	-1,01
SL4004	sodA	Superoxide dismutase [Mn]	1,46	2,11
SL4056	katG1	Catalase-peroxidase 1	-1,70	-2,70
SL4116	yjaB	Uncharacterized N-acetyltransferase yjaB	1,08	-1,01
SL4202	soxR	Redox-sensitive transcriptional activator soxR	1,08	-1,18
SL4203	yfcG	Glutathione S-Transferase	-2,27	-1,35
SL4248	-	Hypothetical	-26,42	-8,48
SL4254	-	GCN5-Related N-Acetyltransferase	-1,57	-1,67
SL4261	cutA	Divalent-cation tolerance protein cutA	-1,46	-1,23

SL4340	ytfL	UPF0053 inner membrane protein ytfL	1,31	-1,82
SL4368	pmbA	Protein pmbA	1,34	-1,02
SL4386	treR	HTH-type transcriptional regulator treR	1,38	-1,50
SL4403	yjgM	Uncharacterized N-acetyltransferase yjgM	-1,09	-1,11
SL4425	-	Hypothetical	1,96	1,16
SL4448	mdtM	Multidrug resistance protein mdtM	1,79	1,48
SL4464	tsr	Methyl-accepting chemotaxis protein I	-1,57	-1,30
SL4489	osmY	Osmotically-inducible protein Y	-1,07	1,09
SL4491	yjjV	Uncharacterized deoxyribonuclease yjjV	1,72	1,33
SL4517	creD	Inner membrane protein creD	1,38	1,05
		Central intermediary metabolism		
SL0033	-	Arylsulfotransferase	-2,43	-1,09
SL0036	betC	Choline-sulfatase	1,28	1,70
SL0037	aslB	Anaerobic sulfatase-maturating enzyme homolog AslB	1,43	1,17
SL0039	-	Arylsulfate Sulfotransferase	-1,21	-1,45
SL0069	caiF	Transcriptional activatory protein caiF	-1,82	-1,12
SL0070	caiE	Carnitine operon protein caiE	-1,15	-1,11
SL0072	caiC	Probable crotonobetaine/carnitine-CoA ligase	-1,22	-1,38
SL0073	caiB	Crotonobetainyl-CoA:carnitine CoA-transferase	-1,01	1,38
SL0075	caiT	L-carnitine/gamma-butyrobetaine antiporter	1,60	9,31
SL0084	yidJ	Sulfatase	-1,43	-1,58
SL0166	speD	S-adenosylmethionine decarboxylase proenzyme	1,39	-1,01
SL0167	speE	Spermidine synthase	1,23	1,17
SL0172	yadF	Carbonic anhydrase 2	1,13	-1,06
SL0208	mtnN	5'-methylthioadenosine/S-adenosylhomocysteine nucleosidase	1,81	1,41
SL0209	dgt	Deoxyguanosinetriphosphate triphosphohydrolase	-1,43	1,12
SL0250	yafB	2,5-diketo-D-gluconic acid reductase B	1,10	1,67
SL0304	yafV	UPF0012 hydrolase yafV	-1,32	-1,50
SL0305	fadE	Acyl-coenzyme A dehydrogenase	2,52	3,82
SL0379	psiF	Phosphate starvation-inducible protein psiF	-2,72	-1,84
SL0420	phnV	Putative 2-aminoethylphosphonate transport system permease protein phnV	1,33	-1,14
SL0421	phnU	Putative 2-aminoethylphosphonate transport system permease protein phnU	1,63	1,04
SL0422	phnT	Putative 2-aminoethylphosphonate import ATP-binding protein phnT	1,37	-1,70
SL0423	phnS	Putative 2-aminoethylphosphonate-binding periplasmic protein	1,41	-1,63
SL0425	phnW	2-aminoethylphosphonate--pyruvate transaminase	1,08	1,07
SL0498	ybbO	Uncharacterized oxidoreductase ybbO	1,33	-2,35
SL0510	gcl	Glyoxylate carboligase	3,30	1,60
SL0511	gip	Hydroxypyruvate isomerase	4,14	1,80
SL0561	glmS	Glucosamine--fructose-6-phosphate aminotransferase [isomerizing]	-1,25	1,28
SL0566	nfnB	Oxygen-insensitive NAD(P)H nitroreductase	1,67	1,58
SL0585	entB	Isochorismatase	1,59	2,00
SL0590	ybdH	Uncharacterized oxidoreductase ybdH	-1,64	2,30
SL0591	ybdL	Aminotransferase ybdL	-1,72	1,01
SL0595	dsbG	Thiol:disulfide interchange protein dsbG	-1,18	-1,00
SL0603	ybdR	Uncharacterized zinc-type alcohol dehydrogenase-like protein ybdR	-1,25	1,45
SL0637	-	putative hydrolase N-terminus	-9,70	-9,19
SL0658	ybeZ	PhoH-like protein	2,34	-1,61
SL0665	nagA	N-acetylglucosamine-6-phosphate deacetylase	1,02	-1,22
SL0666	nagB	Glucosamine-6-phosphate deaminase	-1,05	-1,33
SL0674	nac	Nitrogen assimilation regulatory protein nac	-1,10	-2,01
SL0683	speF	Ornithine decarboxylase, inducible	2,60	1,21
SL0743	oadG2	Oxaloacetate decarboxylase gamma chain	-1,01	-1,27
SL0798	ybiB	Uncharacterized protein ybiB	1,33	-1,05
SL0804	glnP	Glutamine transport system permease protein glnP	3,15	-1,35
SL0815	ybiV2	putative hydrolase	-1,42	-1,28
SL0837	yliI	Soluble aldose sugar dehydrogenase yliI	-1,97	-1,97
SL0838	yliJ	Uncharacterized GST-like protein yliJ	-1,69	-1,34
SL0862	yidJ	Arylsulfatase	-1,21	-1,30
SL0897	lrp	Leucine-responsive regulatory protein	-1,32	-1,21
SL0928	smtA	Protein smtA	1,52	1,17
SL0938	lrp	Uncharacterized HTH-type transcriptional regulator y4tD	-1,13	-1,23
SL1020	yccW	putative SAM-dependent methyltransferase	1,35	3,16
SL1041	hpcC	5-carboxymethyl-2-hydroxymuconate semialdehyde	1,12	2,98

		dehydrogenase		
SL1042	hpcB	3,4-dihydroxyphenylacetate 2,3-dioxygenase	-1,08	2,43
SL1048	atsA	Arylsulfatase	2,17	1,15
SL1056	agp	Glucose-1-phosphatase	1,14	3,19
SL1072	ghrA	Glyoxylate/hydroxypyruvate reductase A	1,51	1,37
SL1146	nagZ	Beta-hexosaminidase	1,38	-1,28
SL1148	ndh	NADH dehydrogenase	-1,52	-1,64
SL1223	yeaE	Uncharacterized protein yeaE	1,41	1,46
SL1231	ydjA	Putative NAD(P)H nitroreductase ydjA	-1,10	1,50
SL1257	yniC	Phosphatase yniC	1,41	-2,78
SL1368	nemA	N-ethylmaleimide reductase	-1,29	1,06
SL1383	gst	Glutathione S-transferase	-1,62	-1,21
SL1387	rnfG	Electron transport complex protein rnfG	2,57	-1,12
SL1394	ydgJ	Uncharacterized oxidoreductase ydgJ	-1,02	-1,36
SL1432	speG	Spermidine N(1)-acetyltransferase	1,41	1,05
SL1461	-	Hypothetical	-1,96	-2,19
SL1513	nhoA	N-hydroxyarylamine O-acetyltransferase	-1,61	-1,01
SL1606	ytbE	Uncharacterized oxidoreductase ytbE	-1,64	-1,87
SL1649	yciK	Uncharacterized oxidoreductase yciK	2,06	4,55
SL1779	yebU	Ribosomal RNA small subunit methyltransferase F	1,12	-1,34
SL2065	rfbX	Putative O-antigen transporter	4,46	1,63
SL2087	wcaF	Putative colanic acid biosynthesis acetyltransferase wcaF	-1,03	-3,34
SL2094	wzb	Low molecular weight protein-tyrosine-phosphatase wzb	1,79	-1,93
SL2163	yeiT	Uncharacterized oxidoreductase yeiT	-1,96	-1,06
SL2171	yeiG	S-formylglutathione hydrolase yeiG	1,02	-1,06
SL2205	yejM	Inner membrane protein yejM	1,43	-1,06
SL2251	glpQ	Glycerophosphoryl diester phosphodiesterase	-1,05	3,61
SL2291	nuoH	NADH-quinone oxidoreductase subunit H	2,35	1,07
SL2307	pta	Phosphate acetyltransferase	1,66	-2,02
SL2318	yfcG	Uncharacterized GST-like protein yfcG	-1,16	-1,73
SL2387	yfeR	Uncharacterized HTH-type transcriptional regulator yfeR	1,43	-1,19
SL2429	eutD	Ethanolamine utilization protein eutD	-1,73	1,05
SL2442	aegA	Protein AegA	3,11	2,72
SL2463	purN	Phosphoribosylglycinamide formyltransferase	1,05	-1,44
SL2464	ppk	Polyphosphate kinase	-1,01	-1,55
SL2465	ppx	Exopolyphosphatase	1,03	-1,81
SL2482	yfgL	Lipoprotein yfgL	1,71	-2,01
SL2531	yfhB	Uncharacterized protein yfhB	-1,37	-1,01
SL2537	cynR	HTH-type transcriptional regulator cynR	-1,47	1,64
SL2606	yfiC	tRNA (adenine-N(6)-)-methyltransferase	1,50	1,68
SL2775	gabD	Succinate-semialdehyde dehydrogenase [NADP+]	3,68	1,99
SL2776	gabT	4-aminobutyrate aminotransferase	2,72	1,68
SL2805	yqaB	Phosphatase yqaB	1,31	-1,42
SL2821	norW	Nitric oxide reductase FlRd-NAD(+) reductase	1,09	1,85
SL2894	ygbM	Protein ygbM	1,31	-1,33
SL2897	ygbJ	Uncharacterized oxidoreductase ygbJ	2,02	1,01
SL2910	ftsB	Cell division protein ftsB homolog	1,24	1,13
SL2912	cysC	Adenylyl-sulfate kinase	1,28	-1,13
SL2913	cysN	Sulfate adenylyltransferase subunit 1	1,28	1,02
SL2914	cysD	Sulfate adenylyltransferase subunit 2	1,14	-1,47
SL2925	cysH	Phosphoadenosine phosphosulfate reductase	-1,21	-1,73
SL2995	kduD	2-dehydro-3-deoxy-D-gluconate 5-dehydrogenase	1,38	2,11
SL3032	visC	Protein visC	1,03	-2,07
SL3054	speB	Agmatinase	-1,04	1,14
SL3062	speA	Biosynthetic arginine decarboxylase	1,10	-1,06
SL3065	metK	S-adenosylmethionine synthase	1,43	-1,26
SL3089	speC	Ornithine decarboxylase, constitutive	2,04	1,40
SL3091	-	Virulence protein STM3117	-1,85	-2,09
SL3096	atsA	Arylsulfatase	-1,20	-1,17
SL3097	atsB	Anaerobic sulfatase-maturating enzyme	-1,44	-1,48
SL3113	gsp	Bifunctional glutathionylspermidine synthetase/amidase	1,32	1,32
SL3156	yqiA	Esterase yqiA	1,46	-1,34
SL3157	icc	Protein icc	1,85	1,05
SL3193	rlmG	Ribosomal RNA large subunit methyltransferase G	-1,58	2,09
SL3205	yqjG	Uncharacterized protein yqjG	-1,14	-1,01
SL3223	garD	D-galactarate dehydratase	-1,21	1,32
SL3230	gatZ	D-tagatose-1,6-bisphosphate aldolase subunit gatZ	-2,27	-1,92

SL3245	yhbS	Uncharacterized N-acetyltransferase yhbS	1,58	1,28
SL3302	gltB	Glutamate synthase [NADPH] large chain	-1,08	1,41
SL3303	gltD	Glutamate synthase [NADPH] small chain	1,01	1,49
SL3311	nanA	N-acetylneuraminate lyase	1,40	-1,38
SL3325	oadG2	Oxaloacetate decarboxylase gamma chain 2	-1,02	-1,21
SL3366	yrdA	Protein yrdA	-1,33	1,06
SL3463	yrfG	Uncharacterized protein yrfG	1,16	1,39
SL3488	rtcR	Transcriptional regulatory protein rtcR	-1,25	-1,12
SL3496	gldA	Glycerol dehydrogenase	1,00	1,69
SL3502	glgA	Glycogen synthase	-1,21	-1,18
SL3516	php	Phosphotriesterase homology protein	-7,37	-2,10
SL3519	ugpQ	Glycerophosphoryl diester phosphodiesterase	-1,24	1,12
SL3558	yhiQ	UPF0341 protein yhiQ	-1,03	-1,62
SL3560	phoC	Major phosphate-irrepressible acid phosphatase	1,40	-1,64
SL3570	-	Conserved Hypothetical Protein	-1,71	1,12
SL3640	sgbH	3-keto-L-gulonate-6-phosphate decarboxylase sgbH	-1,13	1,08
SL3649	yibF	Uncharacterized GST-like protein yibF	-1,40	1,99
SL3771	yidF	Uncharacterized protein yidF	1,22	-1,16
SL3819	yieH	Phosphatase yieH	-1,24	1,06
SL3828	glmS	Glucosamine--fructose-6-phosphate aminotransferase [isomerizing]	1,78	1,92
SL3904	yigB	Uncharacterized protein yigB	1,02	-2,88
SL3915	pldB	Lysophospholipase L2	1,35	-1,19
SL3920	aslB	Anaerobic sulfatase-maturating enzyme homolog AslB	1,24	1,09
SL3981	fdhE	Protein fdhE homolog	1,53	-1,05
SL4033	fpr	Ferredoxin--NADP reductase	1,03	-1,58
SL4058	gldA	Glycerol dehydrogenase	1,22	1,62
SL4078	trmA	tRNA (uracil-5-)-methyltransferase	1,50	2,16
SL4184	tyrB	Aromatic-amino-acid aminotransferase	-1,02	-1,32
SL4185	aphA	Class B acid phosphatase	1,34	5,38
SL4203	yfcG	Glutathione S-Transferase	-2,27	-1,35
SL4226	phnA	Protein phnA	1,22	2,50
SL4255	phoN	Non-specific acid phosphatase	-2,15	-1,53
SL4319	ulaD	3-keto-L-gulonate-6-phosphate decarboxylase ulaD	1,20	1,74
SL4337	cysQ	3'(2'),5'-bisphosphate nucleotidase cysQ	-1,26	1,90
SL4347	ppa	Inorganic pyrophosphatase	1,46	1,77
SL4357	iolG	Inositol 2-dehydrogenase	-2,18	-1,09
SL4413	idnO	Gluconate 5-dehydrogenase	-1,54	1,86
SL4430	yjhP	Uncharacterized protein yjhP	1,09	2,13
SL4470	glmS	Glucosamine--fructose-6-phosphate aminotransferase [isomerizing]	1,51	2,82
SL4491	yjjV	Uncharacterized deoxyribonuclease yjjV	1,72	1,33
		DNA metabolism		
SL0098	polB	DNA polymerase II	1,68	-1,21
SL0160	-	Restriction Endonuclease	-1,48	-3,43
SL0190	hrpB	ATP-dependent RNA helicase hrpB	1,64	-1,04
SL0232	dnaE	DNA polymerase III subunit alpha	1,67	-1,28
SL0259	dnaQ	DNA polymerase III subunit epsilon	1,99	1,17
SL0352	mod	Type III restriction-modification system StyLTI enzyme mod	1,46	1,52
SL0353	res	Type III restriction-modification system StyLTI enzyme res	2,06	2,38
SL0390	sbcC	Nuclease sbcCD subunit C	1,95	1,76
SL0391	sbcD	Nuclease sbcCD subunit D	1,57	1,05
SL0406	yajD	Uncharacterized protein yajD	-1,15	-1,30
SL0418	xseB	Exodeoxyribonuclease 7 small subunit	2,96	1,36
SL0445	hupB	DNA-binding protein HU-beta	-1,31	1,81
SL0474	priC	Primosomal replication protein N"	1,17	1,50
SL0477	dnaX	DNA polymerase III subunit tau	1,49	-1,53
SL0479	recR	Recombination protein recR	1,52	-2,17
SL0630	ybeB	Uncharacterized protein ybeB	1,39	2,09
SL0634	holA	DNA polymerase III subunit delta	1,87	-2,06
SL0679	seqA	Protein seqA	1,82	-1,20
SL0690	phrB	Deoxyribodipyrimidine photo-lyase	-1,32	-2,30
SL0710	nei	Endonuclease 8	1,20	-1,21
SL0775	uvrB	UvrABC system protein B	1,07	1,11
SL0797	dinG	Probable ATP-dependent helicase dinG	1,94	1,12
SL0852	rimK	Ribosomal protein S6 modification protein	1,56	1,28
SL0919	ihfB	Integration host factor subunit beta	1,20	1,14

SL1015	helD	Helicase IV	1,23	-1,44
SL1138	holB	DNA polymerase III subunit delta'	2,37	-1,72
SL1140	ptsG	PTS system glucose-specific EIICB component	1,20	1,02
SL1153	mfd	Transcription-repair-coupling factor	1,90	-1,41
SL1173	nudJ	Phosphatase nudJ	1,59	1,34
SL1233	topB	DNA topoisomerase 3	1,37	-1,48
SL1237	xthA	Exodeoxyribonuclease III	-1,27	-1,57
SL1244	cho	Excinuclease cho	-1,19	-2,89
SL1273	ihfA	Integration host factor subunit alpha	-1,18	-1,29
SL1385	nth	Endonuclease III	1,98	1,17
SL1401	tus	DNA replication terminus site-binding protein	1,18	1,34
SL1467	hupB	Uptake hydrogenase large subunit	1,25	1,16
SL1571	hrpA	ATP-dependent RNA helicase hrpA	1,87	1,28
SL1580	-	Hypothetical	1,04	-1,12
SL1590	ogt	Methylated-DNA--protein-cysteine methyltransferase	-1,44	1,52
SL1646	topA	DNA topoisomerase 1	1,71	1,57
SL1682	hns	DNA-binding protein H-NS	-1,34	1,28
SL1697	ychN	Protein ychN	-1,02	-1,46
SL1750	yoaA	Probable ATP-dependent helicase yoaA	1,59	-1,34
SL1779	yebU	Ribosomal RNA small subunit methyltransferase F	1,12	-1,34
SL1802	-	Phage Membrane Protein	-1,12	-1,35
SL1810	holE	DNA polymerase III subunit theta	1,19	4,58
SL1816	yebG	Uncharacterized protein yebG	1,03	1,01
SL1828	ruvB	Holliday junction ATP-dependent DNA helicase ruvB	1,61	1,56
SL1829	ruvA	Holliday junction ATP-dependent DNA helicase ruvA	1,25	-1,23
SL1833	ruvC	Crossover junction endodeoxyribonuclease ruvC	1,52	-1,43
SL1876	uvrC	UvrABC system protein C	1,01	-1,77
SL1919	vsr	Very short patch repair protein	1,24	1,95
SL1920	dcm	DNA-cytosine methyltransferase	1,73	1,82
SL1926	umuD	Protein umuD	1,47	1,60
SL2051	hisB	Histidine biosynthesis bifunctional protein hisB	1,07	1,07
SL2101	alkA	DNA-3-methyladenine glycosylase 2	-1,19	1,06
SL2180	nfo	Probable endonuclease 4	1,82	-1,63
SL2206	umuD	Protein umuD	-1,57	1,08
SL2234	alkB	Alpha-ketoglutarate-dependent dioxygenase AlkB	-1,07	1,21
SL2241	gyrA	DNA gyrase subunit A	1,38	-1,65
SL2354	yfcB	Uncharacterized adenine-specific methylase yfcB	1,18	2,15
SL2390	ligA	DNA ligase	1,28	-1,21
SL2473	xseA	Exodeoxyribonuclease 7 large subunit	1,20	-1,62
SL2541	recO	DNA repair protein recO	1,58	-2,36
SL2611	ung	Uracil-DNA glycosylase	1,07	-1,93
SL2631	xerD	Integrase	1,36	1,41
SL2656	recN	DNA repair protein recN	1,68	1,19
SL2742	ptsG	PTS system glucose-specific EIICBA component	1,25	1,63
SL2752	-	Hypothetical	1,03	1,09
SL2783	stpA	DNA-binding protein stpA	2,01	-6,63
SL2808	recX	Regulatory protein recX	2,18	1,39
SL2809	recA	Protein recA	1,43	1,39
SL2888	mutS	DNA mismatch repair protein mutS	2,27	-1,08
SL2923	ygcB	Uncharacterized protein ygcB	-2,76	1,06
SL2952	xni	Uncharacterized exonuclease xni	1,61	2,67
SL2971	recD	Exodeoxyribonuclease V alpha chain	1,33	1,09
SL2972	recB	Exodeoxyribonuclease V beta chain	1,81	1,06
SL2974	recC	Exodeoxyribonuclease V gamma chain	2,09	1,38
SL2983	mutH	DNA mismatch repair protein mutH	1,68	-1,02
SL3018	recJ	Single-stranded-DNA-specific exonuclease recJ	2,17	-1,03
SL3020	xerD	Tyrosine recombinase xerD	1,64	1,54
SL3040	iciA	Chromosome initiation inhibitor	1,39	-1,45
SL3068	endA	Endonuclease-1	1,99	1,80
SL3085	mutY	A/G-specific adenine glycosylase	-1,04	-1,98
SL3098	moaR	Monoamine regulon transcriptional regulator	-1,31	1,17
SL3148	parC	DNA topoisomerase 4 subunit A	2,60	1,07
SL3155	parE	DNA topoisomerase 4 subunit B	-1,02	-1,61
SL3184	dnaG	DNA primase	-1,20	-1,78
SL3193	rlmG	Ribosomal RNA large subunit methyltransferase G	-1,58	2,09
SL3358	fis	DNA-binding protein fis	-1,12	-1,78
SL3359	yhdJ	Uncharacterized adenine-specific methylase yhdJ	-1,07	-1,11

SL3451	dam	DNA adenine methylase	1,82	-1,45
SL3558	yhiQ	UPF0341 protein yhiQ	-1,03	-1,62
SL3598	-	Hypothetical	1,04	1,32
SL3608	tag	DNA-3-methyladenine glycosylase 1	1,03	1,38
SL3614	yiaG	Uncharacterized HTH-type transcriptional regulator yiaG	1,06	3,52
SL3692	mutM	Formamidopyrimidine-DNA glycosylase	2,26	-1,18
SL3695	yicR	UPF0758 protein yicR	2,63	15,77
SL3705	ligB	DNA ligase B	1,79	10,68
SL3710	recG	ATP-dependent DNA helicase recG	1,17	-1,04
SL3744	yiaG	Transcriptional Regulator XRE Family	1,92	2,32
SL3802	gyrB	DNA gyrase subunit B	1,11	-1,91
SL3803	recF	DNA replication and repair protein recF	1,92	-1,58
SL3804	dnaN	DNA polymerase III subunit beta	1,37	-1,72
SL3805	dnaA	Chromosomal replication initiator protein dnaA	-1,15	-2,15
SL3813	-	RNA-directed DNA polymerase from retron EC86	-1,64	1,27
SL3872	rep	ATP-dependent DNA helicase rep	1,02	1,25
SL3905	uvrD	DNA helicase II	1,18	-1,20
SL3912	recQ	ATP-dependent DNA helicase recQ	1,12	-1,18
SL4044	priA	Primosomal protein N'	1,03	-1,04
SL4078	trmA	tRNA (uracil-5-)-methyltransferase	1,50	2,16
SL4107	nfi	Endonuclease V	1,06	-1,00
SL4109	hupA	DNA-binding protein HU-alpha	1,10	1,43
SL4127	yaiL	Uncharacterized protein yaiL	2,12	1,71
SL4174	lexA	LexA repressor	1,01	2,04
SL4175	dinF	DNA-damage-inducible protein F	1,45	1,14
SL4182	dnaB	Replicative DNA helicase	2,05	1,78
SL4190	uvrA	UvrABC system protein A	1,65	-1,56
SL4192	ssb	Single-stranded DNA-binding protein	1,44	1,20
SL4305	-	Resembles Potassium Channels	1,52	-1,40
SL4316	ulaA	Ascorbate-specific permease IIC component ulaA	1,30	3,66
SL4325	priB	Primosomal replication protein n	1,18	1,23
SL4356	iolE	Inososе dehydratase	-1,78	-1,05
SL4359	iolI	Inososе isomerase	1,18	2,16
SL4406	holC	DNA polymerase III subunit chi	2,08	1,95
SL4419	-	Restriction Endonuclease	-1,18	1,02
SL4424	-	Hypothetical	2,22	2,46
SL4430	yjhP	Uncharacterized protein yjhP	1,09	2,13
SL4455	hsdS	Type-1 restriction enzyme StySJI specificity protein	1,66	1,26
SL4456	hsdM	Type I restriction enzyme EcoKI M protein	1,28	1,46
SL4457	hsdR	Type I restriction enzyme EcoKI R protein	1,33	1,40
SL4458	mrr	Mrr restriction system protein	1,60	2,56
SL4475	dnaT	Primosomal protein 1	1,97	-1,52
SL4485	holD	DNA polymerase III subunit psi	1,92	2,57
SL4506	radA	DNA repair protein radA	1,61	1,31
		Energy metabolism		
SL0007	talB	Transaldolase 1	-1,01	-1,18
SL0018	chiA	Chitinase A	1,16	1,23
SL0051	-	putative nitrite reductase	1,47	1,47
SL0056	oadA	Oxaloacetate decarboxylase alpha chain	-1,07	1,16
SL0059	citC2	[Citrate [pro-3S]-lyase] ligase	2,45	10,46
SL0060	citD2	Citrate lyase acyl carrier protein 2	1,55	3,43
SL0061	citE	Citrate lyase subunit beta	3,64	12,65
SL0062	citF	Citrate lyase alpha chain	2,46	6,04
SL0071	caiD	Carnitinyl-CoA dehydratase	1,24	1,12
SL0076	fixA	Protein fixA	-1,55	3,23
SL0077	fixB	Protein fixB	-1,56	3,01
SL0078	fixC	Protein fixC	-1,47	2,58
SL0085	caiD	Hypothetical Protein caiD	1,27	1,05
SL0086	yabF	putative NAD(P)H oxidoreductase	1,29	-1,37
SL0101	araD	L-ribulose-5-phosphate 4-epimerase	1,47	2,94
SL0102	araA	L-arabinose isomerase	1,67	5,26
SL0103	araB	Ribulokinase	2,26	7,11
SL0152	aceE	Pyruvate dehydrogenase E1 component	1,10	1,37
SL0153	aceF	Dihydrolipoyllysine-residue acetyltransferase component of pyruvate dehydrogenase complex	2,28	2,66
SL0154	lpdA	Dihydrolipoyl dehydrogenase	2,19	1,91
SL0159	acnB	Aconitate hydratase 2	1,02	1,23

SL0170	gcd	Quinoprotein glucose dehydrogenase	-1,56	1,56
SL0188	sfsA	Sugar fermentation stimulation protein A	1,60	-1,41
SL0234	-	Chitinase	1,51	1,01
SL0235	ldcC	Lysine decarboxylase, constitutive	-1,14	-1,27
SL0255	mltD	Membrane-bound lytic murein transglycosylase D	1,20	-4,66
SL0256	gloB	Hydroxyacylglutathione hydrolase	1,11	2,79
SL0355	qtxA	cytochrome BD2 subunit I	-4,66	-1,77
SL0356	qtxB	cytochrome BD2 subunit II	-2,70	-1,51
SL0364	prpC	2-methylcitrate synthase	-5,41	-2,42
SL0389	araJ	Protein AraJ	2,04	1,59
SL0396	malZ	Maltodextrin glucosidase	-1,08	4,43
SL0434	cyoD	Cytochrome o ubiquinol oxidase protein cyoD	2,07	5,08
SL0435	cyoC	Cytochrome o ubiquinol oxidase subunit 3	2,32	4,41
SL0436	cyoB	Ubiquinol oxidase subunit 1	1,82	2,57
SL0437	cyoA	Ubiquinol oxidase subunit 2	1,68	2,05
SL0465	maa	Maltose O-acetyltransferase	1,08	1,01
SL0487	ushA	Protein ushA	1,40	5,19
SL0497	ybbN	Uncharacterized protein ybbN	2,66	-1,38
SL0509	allR	HTH-type transcriptional repressor AllR	1,04	-1,22
SL0521	allD	Ureidoglycolate dehydrogenase	1,67	3,62
SL0525	arcC	Carbamate kinase	1,47	1,07
SL0566	nfnB	Oxygen-insensitive NAD(P)H nitroreductase	1,67	1,58
SL0599	yyaE	molybdopterin-containing oxidoreductase catalytic subunit	4,06	2,19
SL0600	dmsB	Anaerobic dimethyl sulfoxide reductase chain B	2,45	1,96
SL0601	ynfH	molybdopterin-containing oxidoreductase membrane anchor subunit	1,35	1,00
SL0609	citF	Citrate lyase alpha chain	8,07	21,53
SL0610	citE	Citrate lyase subunit beta	8,23	21,38
SL0611	citD	Citrate lyase acyl carrier protein 1	9,51	22,22
SL0612	citC	[Citrate [pro-3S]-lyase] ligase	3,93	8,29
SL0673	ifcA	Fumarate reductase flavoprotein subunit	-1,04	-1,03
SL0676	fldA	Flavodoxin-1	1,34	-1,98
SL0680	pgm	Phosphoglucomutase	1,73	-1,06
SL0712	gltA	Citrate synthase	1,12	1,56
SL0714	sdhC	Succinate dehydrogenase cytochrome b556 subunit	1,22	5,16
SL0715	sdhD	Succinate dehydrogenase hydrophobic membrane anchor subunit	1,10	3,84
SL0716	sdhA	Succinate dehydrogenase flavoprotein subunit	1,34	4,37
SL0717	sdhB	Succinate dehydrogenase iron-sulfur subunit	1,64	4,79
SL0718	sucA	2-oxoglutarate dehydrogenase E1 component	1,45	1,25
SL0719	sucB	Dihydrolipoyllysine-residue succinyltransferase component of 2-oxoglutarate dehydrogenase complex	1,61	1,24
SL0720	sucC	Succinyl-CoA ligase [ADP-forming] subunit beta	1,71	1,40
SL0721	sucD	Succinyl-CoA ligase [ADP-forming] subunit alpha	1,25	1,30
SL0722	cydA	Cytochrome d ubiquinol oxidase subunit 1	-1,13	-1,11
SL0723	cydB	Cytochrome d ubiquinol oxidase subunit 2	-1,11	-1,06
SL0738	fumB	Fumarate hydratase class I, anaerobic	-1,96	-1,44
SL0739	ttdA	Putative fumarate hydratase subunit alpha	-1,81	-1,29
SL0743	oadG2	Oxaloacetate decarboxylase gamma chain	-1,01	-1,27
SL0749	gpmA	2,3-bisphosphoglycerate-dependent phosphoglycerate mutase	-1,55	1,26
SL0751	galK	Galactokinase	-1,40	-1,37
SL0752	galT	Galactose-1-phosphate uridylyltransferase	-1,13	-1,16
SL0753	galE	UDP-glucose 4-epimerase	1,10	1,14
SL0764	hutI	Imidazolonepropionase	-1,16	1,31
SL0765	hutG	Formimidoylglutamase	-1,16	1,66
SL0768	hutH	Histidine ammonia-lyase	3,27	16,86
SL0815	ybiV2	putative hydrolase	-1,42	-1,28
SL0819	ybiW	Putative formate acetyltransferase 3	2,26	1,92
SL0830	-	HpcH/HpaI Aldolase	-1,31	-2,09
SL0831	etfB	Electron transfer flavoprotein subunit beta	-1,27	-2,24
SL0832	etfA	Electron transfer flavoprotein subunit alpha	-1,02	-1,59
SL0834	ydiS	Electron transfer flavoprotein-ubiquinone oxidoreductase	-1,39	-1,53
SL0837	yliI	Soluble aldose sugar dehydrogenase yliI	-1,97	-1,97
SL0840	deoR	Deoxyribose operon repressor	1,11	-1,54
SL0848	grxA	Glutaredoxin-1	-1,77	-2,63
SL0850	mdaA	Oxygen-insensitive NADPH nitroreductase	1,79	2,17
SL0873	ltaE	Low specificity L-threonine aldolase	1,25	1,20
SL0874	poxB	Pyruvate dehydrogenase [cytochrome]	-1,49	-1,48

SL0875	hcr	NADH oxidoreductase hcr	2,78	1,77
SL0879	ybjX	Uncharacterized protein ybjX	-1,29	-3,90
SL0896	trxB	Thioredoxin reductase	1,07	-1,52
SL0902	dmsA	Anaerobic dimethyl sulfoxide reductase chain A	-1,16	-1,07
SL0903	dmsB	Anaerobic dimethyl sulfoxide reductase chain B	-1,29	-1,14
SL0904	dmsC	Anaerobic dimethyl sulfoxide reductase chain C	-1,43	-1,03
SL0907	pflA	Pyruvate formate-lyase 1-activating enzyme	1,27	-1,88
SL0910	pflB	Formate acetyltransferase 1	-1,01	-1,44
SL0939	dpaL	Diaminopropionate ammonia-lyase	1,57	2,68
SL1000	ycbX	Putative iron-sulfur protein	-1,98	-1,68
SL1016	mgsA	Methylglyoxal synthase	1,47	2,53
SL1037	hpaC	4-hydroxyphenylacetate 3-monooxygenase reductase component	-1,19	1,02
SL1038	hpaB	4-hydroxyphenylacetate 3-monooxygenase oxygenase component	1,33	1,11
SL1040	hpaG	4-hydroxyphenylacetate degradation bifunctional isomerase/decarboxylase	1,58	2,59
SL1042	hpcB	3,4-dihydroxyphenylacetate 2,3-dioxygenase	-1,08	2,43
SL1043	hpcD	5-carboxymethyl-2-hydroxymuconate Delta-isomerase	-1,08	2,36
SL1044	hpcG	2-oxo-hepta-3-ene-1,7-dioic acid hydratase	1,37	1,38
SL1045	hpcH	4-hydroxy-2-oxo-heptane-1,7-dioate aldolase	1,38	1,31
SL1062	putA	Bifunctional protein putA	6,15	14,32
SL1067	nanE1	Putative N-acetylmannosamine-6-phosphate 2-epimerase 1	1,91	2,40
SL1074	ycdY	Uncharacterized protein ycdY	1,67	1,13
SL1095	yceJ	Cytochrome b561 homolog 2	-1,60	-1,22
SL1134	fabF	3-oxoacyl-[acyl-carrier-protein] synthase 2	2,30	-1,31
SL1140	ptsG	PTS system glucose-specific EIICB component	1,20	1,02
SL1146	nagZ	Beta-hexosaminidase	1,38	-1,28
SL1148	ndh	NADH dehydrogenase	-1,52	-1,64
SL1176	icdA	Isocitrate dehydrogenase [NADP]	1,47	1,65
SL1189	yodB	Cytochrome b561 homolog 1	2,18	-1,86
SL1208	-	putative nitric oxide reductase	1,36	-1,03
SL1220	yeaG	Uncharacterized protein yeaG	-2,71	1,34
SL1225	gapA	Glyceraldehyde-3-phosphate dehydrogenase A	1,26	1,05
SL1229	ansA	L-asparaginase 1	2,38	-1,04
SL1239	astA	Arginine N-succinyltransferase	2,62	10,81
SL1240	astD	N-succinylglutamate 5-semialdehyde dehydrogenase	2,16	7,93
SL1250	celD	putative cel operon repressor	-1,50	-5,19
SL1251	celF	6-phospho-beta-glucosidase	-1,30	-2,98
SL1261	pfkB	6-phosphofructokinase isozyme 2	-1,46	1,28
SL1283	ppsA	Phosphoenolpyruvate synthase	-1,48	-1,07
SL1286	ydiS	Probable electron transfer flavoprotein-quinone oxidoreductase ydiS	-1,09	-1,70
SL1287	ydiR	Putative electron transfer flavoprotein subunit ydiR	-1,28	-2,31
SL1288	ydiQ	Putative electron transfer flavoprotein subunit ydiQ	-1,06	1,17
SL1299	ydiJ	Uncharacterized protein ydiJ	-2,10	-1,77
SL1300	ydiI	Esterase ydiI	-1,92	-1,48
SL1312	pykF	Pyruvate kinase I	1,00	-1,13
SL1316	rbsK	Ribokinase	-1,55	8,36
SL1317	ttrA	tetrathionate reductase subunit A	-1,15	-1,92
SL1319	ttrB	Tetrathionate Reductase Subunit B	1,48	-1,29
SL1367	gloA	Lactoylglutathione lyase	1,06	-1,35
SL1388	rnfD	Electron transport complex protein rnfD	2,69	-1,22
SL1389	rnfC	Electron transport complex protein rnfC	1,88	-1,79
SL1397	manA	Mannose-6-phosphate isomerase	2,27	-1,06
SL1398	fumA	Fumarate hydratase class I, aerobic	1,93	2,49
SL1400	fumC	Fumarate hydratase class II	-1,18	1,45
SL1409	pntA	NAD(P) transhydrogenase subunit alpha	-1,15	-1,31
SL1410	pntB	NAD(P) transhydrogenase subunit beta	-1,33	-1,35
SL1426	dmsC	Anaerobic dimethyl sulfoxide reductase chain C	-1,07	-1,85
SL1427	dmsB	Anaerobic dimethyl sulfoxide reductase chain B	-1,22	-1,07
SL1428	dmsA2	Probable dimethyl sulfoxide reductase chain A2	-1,13	-1,22
SL1435	rspA	Starvation-sensing protein rspA	2,46	5,16
SL1436	rspB	Starvation-sensing protein rspB	1,90	4,95
SL1438	ydfI	Uncharacterized oxidoreductase ydfI	1,11	1,24
SL1454	yneI	Aldehyde dehydrogenase-like protein yneI	-4,68	1,53
SL1455	glsA2	Glutaminase 2	-1,66	1,84
SL1461	-	Hypothetical	-1,96	-2,19

SL1462	hoxQ	Hydrogenase expression/formation protein hoxQ	-1,71	-1,89
SL1463	hyaE	Hydrogenase-1 operon protein hyaE	-2,00	-1,36
SL1465	hoxM	Hydrogenase expression/formation protein hoxM	-1,76	-1,31
SL1466	hupZ	Probable Ni/Fe-hydrogenase B-type cytochrome subunit	1,31	1,53
SL1468	hoxK	Uptake hydrogenase small subunit	1,01	1,32
SL1470	uxuR	Uxu operon transcriptional regulator	-1,31	1,11
SL1471	rspB	Uncharacterized zinc-type alcohol dehydrogenase-like protein HI_0053	-1,51	1,17
SL1485	galS	HTH-type transcriptional regulator galS	2,00	-1,38
SL1488	glgX	Glycogen operon protein glgX homolog	-1,61	1,56
SL1496	sfcA	NAD-dependent malic enzyme	1,47	1,66
SL1497	adhP	Alcohol dehydrogenase, propanol-preferring	-2,82	-1,06
SL1498	fdnI	Formate dehydrogenase, nitrate-inducible, cytochrome b556(fdn) subunit	1,51	3,85
SL1499	fdnH	Formate dehydrogenase, nitrate-inducible, iron-sulfur subunit	2,24	3,50
SL1500	fdnG	Formate dehydrogenase, nitrate-inducible, major subunit	2,17	3,60
SL1501	fdnG	Formate dehydrogenase, nitrate-inducible, major subunit	1,95	4,12
SL1508	narZ	Respiratory nitrate reductase 2 alpha chain	-1,19	3,12
SL1509	narY	Respiratory nitrate reductase 2 beta chain	-1,38	3,24
SL1510	narW	Probable nitrate reductase molybdenum cofactor assembly chaperone NarW	-1,56	3,00
SL1511	narV	Respiratory nitrate reductase 2 gamma chain	-1,44	2,99
SL1520	yncB	Putative NADP-dependent oxidoreductase yncB	-1,19	1,53
SL1547	sgcE	Protein sgcE	-1,94	-1,19
SL1550	lldD	Lactate 2-monooxygenase	1,87	1,72
SL1555	ydcI	Uncharacterized HTH-type transcriptional regulator ydcI	-2,22	1,39
SL1557	adhC	S-(hydroxymethyl)glutathione dehydrogenase	-1,02	-1,36
SL1569	cybB	Cytochrome b561	1,02	1,39
SL1573	-	Glutathione-Dependent Formaldehyde-Activating GFA	-1,38	-1,09
SL1577	ldhA	D-lactate dehydrogenase	-1,02	-1,78
SL1581	ydbK	Probable pyruvate-flavodoxin oxidoreductase	1,49	-2,06
SL1611	ycjG	L-Ala-D/L-Glu epimerase	-1,69	-2,51
SL1615	ycjX	Uncharacterized protein ycjX	1,56	1,21
SL1631	fabI	Enoyl-[acyl-carrier-protein] reductase [NADH]	1,42	-1,36
SL1640	yciM	Uncharacterized protein yciM	1,09	-2,47
SL1644	acnA	Aconitate hydratase 1	-1,25	1,65
SL1664	ykgJ	Uncharacterized protein ykgJ	1,07	1,65
SL1680	adhE	Aldehyde-alcohol dehydrogenase	-1,22	-1,25
SL1689	narI	Respiratory nitrate reductase 1 gamma chain	2,66	9,45
SL1690	narJ	Nitrate reductase molybdenum cofactor assembly chaperone NarJ	4,98	9,45
SL1691	narH	Respiratory nitrate reductase 1 beta chain	3,53	7,87
SL1692	narG	Respiratory nitrate reductase 1 alpha chain	2,72	5,16
SL1695	narL	Nitrate/nitrite response regulator protein narL	1,37	-1,09
SL1714	hyaA	Hydrogenase-1 small chain	1,10	2,88
SL1715	hyaB	Hydrogenase-1 large chain	1,39	2,40
SL1716	hyaC	Probable Ni/Fe-hydrogenase 1 B-type cytochrome subunit	1,85	2,05
SL1717	hyaD	Hydrogenase 1 maturation protease	1,69	1,82
SL1719	hyaF	Hydrogenase-1 operon protein hyaF	1,29	1,27
SL1720	appC	Cytochrome bd-II oxidase subunit 1	1,22	1,09
SL1721	appB	Cytochrome bd-II oxidase subunit 2	-1,03	1,11
SL1724	treA	Periplasmic trehalase	-1,34	2,08
SL1731	dadA	D-amino acid dehydrogenase small subunit	1,05	1,82
SL1740	ycgM	Uncharacterized protein ycgM	-1,36	-1,82
SL1755	sdaA	L-serine dehydratase 1	1,62	1,63
SL1802	-	Phage Membrane Protein	-1,12	-1,35
SL1818	eda	KHG/KDPG aldolase	1,67	-1,03
SL1819	edd	Phosphogluconate dehydratase	2,46	-2,54
SL1820	zwf	Glucose-6-phosphate 1-dehydrogenase	-1,06	-1,97
SL1822	pykA	Pyruvate kinase II	1,20	1,44
SL1872	-	Hypothetical	-2,15	-4,34
SL1888	fliC	Flagellin	-1,49	-1,03
SL1892	amyA	Cytoplasmic alpha-amylase	-1,60	1,75
SL2035	yeeX	UPF0265 protein Ent638_2575	-1,04	-1,13
SL2040	phsB	Thiosulfate reductase electron transport protein phsB	-1,48	1,75
SL2041	phsA	Thiosulfate reductase	-1,35	1,64
SL2051	hisB	Histidine biosynthesis bifunctional protein hisB	1,07	1,07
SL2058	gnd	6-phosphogluconate dehydrogenase, decarboxylating	1,57	-1,23

SL2060	rfbK	Phosphomannomutase	1,77	1,68
SL2069	rfbF	Glucose-1-phosphate cytidylyltransferase	2,74	1,21
SL2078	wcaK	Colanic acid biosynthesis protein wcaK	1,43	1,38
SL2081	cpsG	phosphomannomutase	1,19	-1,28
SL2121	yegV	Uncharacterized sugar kinase yegV	1,41	1,70
SL2145	dld	D-lactate dehydrogenase	1,22	2,02
SL2152	mhbM	3-hydroxybenzoate 6-hydroxylase	-1,12	1,82
SL2153	maiA	Probable maleylacetoacetate isomerase	1,20	1,79
SL2154	ycgM	Uncharacterized protein PYRAB13970	1,16	2,31
SL2155	gtdA	Gentisate 1 2-Dioxygenase	1,16	2,58
SL2156	pcaK	4-hydroxybenzoate transporter	1,36	1,61
SL2157	gbpR	HTH-type transcriptional regulator gbpR	-1,09	-1,14
SL2168	galS	HTH-type transcriptional regulator galS	2,04	4,52
SL2173	sdaA	L-serine dehydratase 1	1,90	-1,19
SL2181	fruA	PTS system fructose-specific EIIBC component	-1,36	-2,54
SL2182	fruK	1-phosphofructokinase	-1,29	-2,52
SL2205	yejM	Inner membrane protein yejM	1,43	-1,06
SL2215	quuD	Antitermination protein Q homolog from lambdoid prophage DLP12	1,06	-1,30
SL2222	narP	Nitrate/nitrite response regulator protein narP	1,56	1,08
SL2223	ccmH	Cytochrome c-type biogenesis protein ccmH	2,06	1,52
SL2223	ccmH	Cytochrome c-type biogenesis protein ccmH	2,06	1,52
SL2225	napC	Cytochrome c-type protein napC	6,22	6,57
SL2226	napB	Diheme cytochrome c napB	3,65	3,46
SL2227	napH	Ferredoxin-type protein napH	9,50	6,95
SL2228	napG	Ferredoxin-type protein napG	10,81	8,39
SL2229	napA	Periplasmic nitrate reductase	7,43	8,88
SL2230	napD	Protein napD	5,54	5,81
SL2231	napF	Ferredoxin-type protein napF	3,73	4,56
SL2242	dgoD	D-galactonate dehydratase	-1,41	-1,06
SL2253	glpA	Anaerobic glycerol-3-phosphate dehydrogenase subunit A	1,56	1,22
SL2254	glpB	Anaerobic glycerol-3-phosphate dehydrogenase subunit B	1,34	1,10
SL2255	glpC	Anaerobic glycerol-3-phosphate dehydrogenase subunit C	1,04	-1,05
SL2260	yfaW	L-rhamnonate dehydratase	-2,26	-1,38
SL2265	ais	Lipopolysaccharide core heptose(II)-phosphate phosphatase	-3,11	-1,91
SL2285	nuoN	NADH-quinone oxidoreductase subunit N	1,42	-1,20
SL2286	nuoM	NADH-quinone oxidoreductase subunit M	1,55	-1,19
SL2287	nuoL	NADH-quinone oxidoreductase subunit L	1,97	1,28
SL2288	nuoK	NADH-quinone oxidoreductase subunit K	2,82	1,33
SL2289	nuoJ	NADH-quinone oxidoreductase subunit J	2,23	1,16
SL2290	nuoI	NADH-quinone oxidoreductase subunit I	2,12	1,07
SL2291	nuoH	NADH-quinone oxidoreductase subunit H	2,35	1,07
SL2292	nuoG	NADH-quinone oxidoreductase subunit G	1,95	-1,14
SL2293	nuoF	NADH-quinone oxidoreductase subunit F	1,90	-1,05
SL2294	nuoE	NADH-quinone oxidoreductase subunit E	1,19	-1,24
SL2295	nuoC	NADH-quinone oxidoreductase subunit C/D	1,20	-1,71
SL2296	nuoB	NADH-quinone oxidoreductase subunit B	-1,03	-1,35
SL2297	nuoA	NADH-quinone oxidoreductase subunit A	1,02	-1,24
SL2299	lrhA	Probable HTH-type transcriptional regulator lrhA	-1,63	-4,14
SL2306	ackA	Acetate kinase	1,27	-2,28
SL2307	pta	Phosphate acetyltransferase	1,66	-2,02
SL2310	tktA	Putative transketolase N-terminal section	-2,06	-1,47
SL2314	gntR	HTH-type transcriptional regulator gntR	1,98	1,53
SL2364	pgtA	Phosphoglycerate transport system transcriptional regulatory protein pgtA	-2,57	-1,77
SL2371	glk	Glucokinase	1,07	-1,21
SL2394	ptsH	Phosphocarrier protein HPr	2,06	2,12
SL2420	eutC	Ethanolamine ammonia-lyase light chain	-1,53	1,10
SL2421	eutB	Ethanolamine ammonia-lyase heavy chain	-1,40	1,06
SL2423	eutH	Ethanolamine utilization protein eutH	-2,02	-1,21
SL2425	eutJ	Ethanolamine utilization protein eutJ	-2,00	-1,62
SL2429	eutD	Ethanolamine utilization protein eutD	-1,73	1,05
SL2435	maeB	NADP-dependent malic enzyme	2,05	2,59
SL2436	tal2	Transaldolase 2	-1,37	1,60
SL2437	tktB	Transketolase 2	-1,34	1,48
SL2490	dmsC	Anaerobic Dimethyl Sulfoxide Reductase Subunit C	2,83	-1,40
SL2491	dmsB	Anaerobic dimethyl sulfoxide reductase chain B	2,94	1,02
SL2492	dmsA	Anaerobic dimethyl sulfoxide reductase chain A	3,12	-1,06

SL2497	sseB	Protein sseB	1,25	-1,25
SL2500	fdx	2Fe-2S ferredoxin	2,21	-1,18
SL2510	asrA	Anaerobic sulfite reductase subunit A	-6,07	-1,62
SL2511	asrB	Anaerobic sulfite reductase subunit B	-6,11	-1,82
SL2512	asrC	Anaerobic sulfite reductase subunit C	-5,83	-1,82
SL2516	hcaT	Probable 3-phenylpropionic acid transporter	1,26	-1,02
SL2518	hmpA	Flavohemoprotein	2,09	2,80
SL2519	cadC	Transcriptional activator cadC	1,19	-2,23
SL2521	cadA	Lysine decarboxylase, inducible	-1,25	1,93
SL2610	grcA	Autonomous glycyl radical cofactor	-1,52	-1,70
SL2613	trxC	Thioredoxin-2	1,12	-2,94
SL2738	-	Hypothetical	-1,05	-2,33
SL2739	hxlA	3-hexulose-6-phosphate synthase	-1,38	1,06
SL2742	ptsG	PTS system glucose-specific EIICBA component	1,25	1,63
SL2764	ybjX	Uncharacterized protein ybjX	-1,03	-5,61
SL2806	csrA	Carbon storage regulator homolog	1,15	1,44
SL2815	srlD	Sorbitol-6-phosphate 2-dehydrogenase	-5,96	1,09
SL2816	gutM	Glucitol operon activator protein	-5,39	1,21
SL2817	srlR	Glucitol operon repressor	-1,03	1,59
SL2820	norV	Anaerobic nitric oxide reductase flavorubredoxin	-1,15	-1,21
SL2823	hydN	Electron transport protein hydN	-1,59	-4,73
SL2826	hycH	Formate hydrogenlyase maturation protein hycH	1,63	1,91
SL2827	hycG	Formate hydrogenlyase subunit 7	1,76	1,91
SL2828	hycF	Formate hydrogenlyase subunit 6	2,22	1,56
SL2829	hycE	Formate hydrogenlyase subunit 5	1,53	-1,50
SL2830	hycD	Formate hydrogenlyase subunit 4	-1,02	-2,29
SL2831	hycC	Formate hydrogenlyase subunit 3	-1,29	-4,84
SL2835	hypB	Hydrogenase isoenzymes nickel incorporation protein hypB	1,86	1,28
SL2838	hypE	Hydrogenase isoenzymes formation protein hypE	2,21	-1,79
SL2839	fhlA	Formate hydrogenlyase transcriptional activator	1,72	-2,09
SL2895	ygbL	Putative aldolase class 2 protein ygbL	1,81	-1,08
SL2897	ygbJ	Uncharacterized oxidoreductase ygbJ	2,02	1,01
SL2910	ftsB	Cell division protein ftsB homolog	1,24	1,13
SL2927	cysJ	Sulfite reductase [NADPH] flavoprotein alpha-component	1,01	-2,43
SL2931	eno	Enolase	-1,01	-1,08
SL2944	yqcA	Uncharacterized protein yqcA	1,21	1,09
SL2951	sdaB	L-serine dehydratase 2	2,46	8,11
SL2953	fucO	Lactaldehyde reductase	1,45	1,68
SL2954	fucA	L-fuculose phosphate aldolase	1,72	1,56
SL2956	fucI	L-fucose isomerase	1,23	-1,19
SL2957	fucK	L-fuculokinase	1,48	-1,28
SL2958	fucU	L-fucose mutarotase	1,02	1,44
SL2959	fucR	L-fucose operon activator	1,51	6,68
SL2977	ppdB	Prepilin peptidase-dependent protein B	3,21	7,11
SL2989	galR	HTH-type transcriptional regulator galR	1,29	2,07
SL3021	fldB	Flavodoxin-2	1,23	1,18
SL3027	bglA	6-phospho-beta-glucosidase BglA	1,19	-1,38
SL3029	gcvP	Glycine dehydrogenase [decarboxylating]	-6,89	-4,23
SL3030	gcvH	Glycine cleavage system H protein	-3,46	-2,33
SL3031	gcvT	Aminomethyltransferase	-2,78	-1,92
SL3032	visC	Protein visC	1,03	-2,07
SL3039	rpiA	Ribose-5-phosphate isomerase A	1,86	2,49
SL3044	fbaA	Fructose-bisphosphate aldolase class 2	1,01	-1,25
SL3045	pgk	Phosphoglycerate kinase	1,07	-1,23
SL3051	cbiO	Cobalt import ATP-binding protein CbiO	3,87	4,26
SL3052	tktA	Transketolase 1	1,85	1,74
SL3057	yjmC	Uncharacterized oxidoreductase yjmC	1,44	1,02
SL3058	yjjN	Uncharacterized zinc-type alcohol dehydrogenase-like protein yjjN	1,29	1,40
SL3059	uxuB	D-mannonate oxidoreductase	2,03	1,95
SL3060	uxuR	Uxu operon regulator	1,56	1,33
SL3081	ansB	L-asparaginase 2	2,62	4,78
SL3092	cat2	4-hydroxybutyrate coenzyme A transferase	-2,32	1,04
SL3094	citE	Citrate lyase subunit beta	-2,05	1,72
SL3103	feaB	Phenylacetaldehyde dehydrogenase	-1,11	1,18
SL3109	uxuA	Mannonate dehydratase	1,88	2,97
SL3110	uxuB	D-mannonate oxidoreductase	1,05	2,40

SL3111	uxaC	Uronate isomerase	-1,13	2,07
SL3119	hybE	Hydrogenase-2 operon protein hybE	2,72	-2,04
SL3121	hybC	Hydrogenase-2 large chain	1,33	-1,58
SL3122	hybB	Probable Ni/Fe-hydrogenase 2 b-type cytochrome subunit	1,29	-1,41
SL3123	hybA	Hydrogenase-2 operon protein hybA	1,57	-1,03
SL3124	hybO	Hydrogenase-2 small chain	1,43	1,14
SL3138	yqhD	Alcohol dehydrogenase yqhD	1,46	2,03
SL3170	glgS	Glycogen synthesis protein glgS	-1,35	-1,26
SL3190	aer	Aerotaxis receptor	-6,60	2,93
SL3212	tdcG	L-serine dehydratase tdcG	-1,48	1,61
SL3213	tdcE	Keto-acid formate acetyltransferase	-1,70	1,39
SL3214	tdcD	Propionate kinase	-2,92	1,89
SL3216	tdcB	Threonine dehydratase catabolic	-2,66	4,61
SL3223	garD	D-galactarate dehydratase	-1,21	1,32
SL3224	ydjE	Uncharacterized sugar kinase ydjE	-1,42	1,16
SL3225	glpR	Glycerol-3-phosphate regulon repressor	-1,24	-1,09
SL3226	gatY	D-tagatose-1,6-bisphosphate aldolase subunit gatY	-25,28	1,21
SL3227	fruK	1-phosphofructokinase	-15,40	-1,46
SL3228	fruA	PTS system fructose-specific EIIABC component	-14,19	-2,16
SL3230	gatZ	D-tagatose-1,6-bisphosphate aldolase subunit gatZ	-2,27	-1,92
SL3234	gatD	Galactitol-1-phosphate 5-dehydrogenase	-1,04	1,05
SL3235	gatR	Galactitol utilization operon repressor	1,11	3,15
SL3287	kdsD	Arabinose 5-phosphate isomerase	1,66	-2,31
SL3309	nanE2	Putative N-acetylmannosamine-6-phosphate 2-epimerase 2	-1,59	-1,49
SL3318	yhcM	Uncharacterized protein yhcM	1,40	1,05
SL3324	oadA	Oxaloacetate decarboxylase alpha chain	-1,09	1,11
SL3325	oadG2	Oxaloacetate decarboxylase gamma chain 2	-1,02	-1,21
SL3326	ttdB	L(+)-tartrate dehydratase subunit beta	2,03	1,98
SL3327	ttdA	L(+)-tartrate dehydratase subunit alpha	2,03	2,64
SL3331	mdh	Malate dehydrogenase	1,57	5,89
SL3349	yhdH	Putative quinone oxidoreductase yhdH	2,40	2,34
SL3350	yedY	Sulfoxide reductase catalytic subunit yedY	1,06	1,43
SL3357	dusB	tRNA-dihydrouridine synthase B	-1,34	-1,57
SL3425	kefG	Glutathione-regulated potassium-efflux system ancillary protein kefG	-1,33	-1,68
SL3431	prkB	Probable phosphoribulokinase	-1,26	-1,13
SL3441	nirB	Nitrite reductase [NAD(P)H] large subunit	4,96	4,39
SL3442	nirD	Nitrite reductase [NAD(P)H] small subunit	7,05	3,43
SL3449	gph	Phosphoglycolate phosphatase	1,75	-1,01
SL3450	rpe	Ribulose-phosphate 3-epimerase	1,63	1,22
SL3463	yrfG	Uncharacterized protein yrfG	1,16	1,39
SL3467	pckA	Phosphoenolpyruvate carboxykinase [ATP]	-1,72	1,30
SL3480	malQ	4-alpha-glucanotransferase	-2,67	-1,24
SL3481	malP	Maltodextrin phosphorylase	-3,34	1,62
SL3482	malT	HTH-type transcriptional regulator malT	1,23	5,98
SL3488	rtcR	Transcriptional regulatory protein rtcR	-1,25	-1,12
SL3489	glpR	Glycerol-3-phosphate regulon repressor	-1,30	-2,31
SL3490	glpR	Glycerol-3-phosphate regulon repressor	-1,19	-3,00
SL3491	glpG	Rhomboid protease glpG	1,51	-2,35
SL3492	glpE	Thiosulfate sulfurtransferase glpE	-1,09	-2,82
SL3493	glpD	Aerobic glycerol-3-phosphate dehydrogenase	-2,38	-1,30
SL3501	glgP	Glycogen phosphorylase	-1,31	-1,32
SL3503	glgC	Glucose-1-phosphate adenylyltransferase	-1,06	1,51
SL3504	glgX	Glycogen debranching enzyme	1,36	1,41
SL3505	glgB	1,4-alpha-glucan-branching enzyme	1,15	1,86
SL3507	gntU	Low-affinity gluconate transporter	2,69	-1,42
SL3508	gntK	Thermoresistant gluconokinase	3,26	-2,10
SL3509	gntR	HTH-type transcriptional regulator gntR	1,55	-1,21
SL3513	rbsK	Ribokinase	-4,00	1,27
SL3543	tusA	Sulfurtransferase tusA	-8,27	-6,94
SL3560	phoC	Major phosphate-irrepressible acid phosphatase	1,40	-1,64
SL3563	ansB	L-asparaginase	1,75	12,37
SL3565	frlD	Fructosamine kinase frlD	1,54	24,98
SL3568	treF	Cytoplasmic trehalase	-1,96	-2,00
SL3577	kdgK	2-dehydro-3-deoxygluconokinase	1,92	4,44
SL3590	mdeA	cystathionine gamma-synthase	-2,33	-3,58
SL3598	-	Hypothetical	1,04	1,32

SL3610	bisC	Biotin sulfoxide reductase	1,29	-1,37
SL3612	ghrB	Glyoxylate/hydroxypyruvate reductase B	1,12	1,23
SL3625	xylB	Xylulose kinase	-1,28	1,07
SL3626	xylA	Xylose isomerase	-1,88	1,70
SL3629	malS	Alpha-amylase	-2,80	1,12
SL3632	yiaJ	HTH-type transcriptional regulator yiaJ	1,17	-1,02
SL3633	dlgD	2,3-diketo-L-gulonate reductase	1,18	3,90
SL3639	lyxK	L-xylulose/3-keto-L-gulonate kinase	-1,06	1,16
SL3641	sgbU	Putative L-ribulose-5-phosphate 3-epimerase sgbU	1,25	2,13
SL3642	sgbE	L-ribulose-5-phosphate 4-epimerase sgbE	-1,60	1,78
SL3645	aldB	Aldehyde dehydrogenase B	-1,43	3,84
SL3651	mtlD	Mannitol-1-phosphate 5-dehydrogenase	1,30	1,59
SL3652	mtlR	Mannitol operon repressor	-1,04	1,25
SL3659	lldD	L-lactate dehydrogenase [cytochrome]	1,18	2,43
SL3666	gpsA	Glycerol-3-phosphate dehydrogenase [NAD(P)+]	1,65	1,59
SL3670	gpmI	2,3-bisphosphoglycerate-independent phosphoglycerate mutase	1,54	-1,28
SL3673	yibD	Uncharacterized glycosyltransferase yibD	-1,01	-1,85
SL3674	tdh	L-threonine 3-dehydrogenase	3,00	4,44
SL3675	kbl	Putative 8-amino-7-oxononanoate synthase/2-amino-3-ketobutyrate coenzyme A ligase	3,05	6,06
SL3740	gmuD	6-phospho-beta-glucosidase gmuD	1,03	3,39
SL3745	ptsH	Conserved Hypothetical Protein	-1,14	-1,07
SL3746	kbaY	D-tagatose-1,6-bisphosphate aldolase subunit kbaY	-1,09	-1,19
SL3747	glpK	Glycerol kinase	-2,12	-1,13
SL3759	rbsK	Ribokinase	-2,90	1,43
SL3760	deoR	Deoxyribose operon repressor	2,52	1,66
SL3770	dsdA	D-serine dehydratase	1,12	1,06
SL3779	ccmH	Cytochrome c-type biogenesis protein ccmH	3,11	1,51
SL3779	ccmH	Cytochrome c-type biogenesis protein ccmH	3,11	1,51
SL3781	ccmF	Cytochrome c-type biogenesis protein ccmF	4,67	1,08
SL3781	ccmF	Cytochrome c-type biogenesis protein ccmF	4,67	1,08
SL3788	torA	Trimethylamine-N-oxide reductase	1,09	-1,20
SL3789	torC	Cytochrome c-type protein torC	-1,13	-1,90
SL3792	torS	Sensor protein torS	1,53	-1,13
SL3794	dgoD1	D-galactonate dehydratase 1	-1,28	-1,03
SL3795	dgoA	2-dehydro-3-deoxy-6-phosphogalactonate aldolase	-1,15	1,89
SL3800	dgoD	D-galactonate dehydratase	-2,48	1,33
SL3825	fruA	PTS system fructose-specific EIIBC component	1,27	1,82
SL3831	atpC	ATP synthase epsilon chain	2,70	1,81
SL3832	atpD	ATP synthase subunit beta	1,72	1,42
SL3833	atpG	ATP synthase gamma chain	2,22	1,56
SL3834	atpA	ATP synthase subunit alpha	2,09	1,46
SL3835	atpH	ATP synthase subunit delta	2,64	1,75
SL3836	atpF	ATP synthase subunit b	1,74	1,47
SL3837	atpE	ATP synthase subunit c	1,41	1,16
SL3838	atpB	ATP synthase subunit a	1,44	-1,00
SL3839	atpI	ATP synthase protein I	1,06	1,55
SL3842	mioC	Protein mioC	1,25	1,37
SL3852	rbsK	Ribokinase	1,03	1,67
SL3904	yigB	Uncharacterized protein yigB	1,02	-2,88
SL3928	tatB	Sec-independent protein translocase protein tatB homolog	1,57	1,74
SL3933	ubiB	NAD(P)H-flavin reductase	1,09	-1,27
SL3946	yihG	Probable acyltransferase yihG	1,25	-1,19
SL3965	yihQ	Alpha-glucosidase yihQ	-1,67	1,40
SL3968	yihT	Uncharacterized aldolase yihT	1,87	1,89
SL3970	yihV	Uncharacterized sugar kinase yihV	1,35	3,53
SL3971	yihW	Uncharacterized HTH-type transcriptional regulator yihW	-1,03	1,15
SL3981	fdhE	Protein fdhE homolog	1,53	-1,05
SL3982	fdoI	Formate dehydrogenase, cytochrome b556(fdo) subunit	-1,02	-1,05
SL3983	fdoH	Formate dehydrogenase-O iron-sulfur subunit	-1,04	1,04
SL3984	fdoG	Formate dehydrogenase-O major subunit	-1,24	1,01
SL3985	fdoG	Formate dehydrogenase-O major subunit	-1,32	1,18
SL3986	fdhD	Protein fdhD	2,15	-1,17
SL3993	yiaY	Probable alcohol dehydrogenase	-1,23	1,05
SL3994	rhaD	Rhamnulose-1-phosphate aldolase	1,10	1,36
SL3995	rhaA	L-rhamnose isomerase	1,02	1,15
SL3996	rhaB	Rhamnulokinase	1,18	1,33

SL4011	pfkA	6-phosphofructokinase isozyme 1	-1,06	-1,05
SL4015	scrK	Fructokinase	1,30	2,56
SL4021	lsrK	Autoinducer 2 kinase lsrK	-1,48	1,54
SL4029	lsrE	Putative epimerase lsrE	-2,21	-2,31
SL4030	tpiA	Triosephosphate isomerase	1,42	-1,19
SL4035	glpK	Glycerol kinase	-1,21	1,56
SL4059	talC	Probable fructose-6-phosphate aldolase	1,54	1,04
SL4063	pflD	Formate acetyltransferase 2	-1,28	2,36
SL4064	pflC	Pyruvate formate-lyase 2-activating enzyme	1,42	1,21
SL4065	frwD	Fructose-like phosphotransferase enzyme IIB component 3	-1,03	1,59
SL4069	ppc	Phosphoenolpyruvate carboxylase	-2,24	-4,32
SL4113	zraR	Transcriptional regulatory protein zraR	1,61	1,99
SL4118	aceB	Malate synthase A	1,34	1,65
SL4119	aceA	Isocitrate lyase	-1,43	1,95
SL4120	aceK	Isocitrate dehydrogenase kinase/phosphatase	1,14	1,34
SL4122	iclR	Acetate operon repressor	1,38	1,90
SL4157	pgi	Glucose-6-phosphate isomerase	1,11	-1,24
SL4181	qorA	Quinone oxidoreductase 1	-2,35	-1,47
SL4185	aphA	Class B acid phosphatase	1,34	5,38
SL4213	nrfA	Cytochrome c-552	2,34	5,15
SL4214	nrfB	Cytochrome c-type protein nrfB	2,06	3,64
SL4215	nrfC	Protein nrfC	1,77	2,94
SL4216	nrfD	Protein nrfD	2,14	2,39
SL4218	nrfG	Formate-dependent nitrite reductase complex subunit nrfG	2,23	2,20
SL4221	fdhF	Formate dehydrogenase H	2,03	1,06
SL4222	fdhF	Formate dehydrogenase H	2,28	1,50
SL4233	adiA	Biodegradative arginine decarboxylase	-1,11	1,52
SL4234	melR	Melibiose operon regulatory protein	-1,02	5,38
SL4235	melA	Alpha-galactosidase	-4,04	1,15
SL4237	fumB	Fumarate hydratase class I, anaerobic	1,27	-1,21
SL4242	dmsA	Anaerobic dimethyl sulfoxide reductase chain A	-1,01	2,58
SL4243	dmsB	Anaerobic dimethyl sulfoxide reductase chain B	-1,16	1,94
SL4244	dmsC	Anaerobic dimethyl sulfoxide reductase chain C	-1,03	1,99
SL4263	aspA	Aspartate ammonia-lyase	1,03	1,09
SL4277	frdD	Fumarate reductase subunit D	2,16	1,18
SL4278	frdC	Fumarate reductase subunit C	1,60	-1,00
SL4279	frdB	Fumarate reductase iron-sulfur subunit	1,51	-1,12
SL4280	frdA	Fumarate reductase flavoprotein subunit	1,51	-1,25
SL4289	yjeS	Putative electron transport protein yjeS	1,26	-1,51
SL4316	ulaA	Ascorbate-specific permease IIC component ulaA	1,30	3,66
SL4320	ulaE	L-ribulose-5-phosphate 3-epimerase ulaE	1,09	1,25
SL4321	ulaF	L-ribulose-5-phosphate 4-epimerase ulaF	-1,24	1,10
SL4334	qorB	Quinone oxidoreductase 2	1,03	1,27
SL4346	-	Dihydroorotase	1,26	-1,01
SL4348	fbp	Fructose-1,6-bisphosphatase class 1	1,28	1,05
SL4350	hexR	Uncharacterized HTH-type transcriptional regulator HI_0143	1,42	-2,36
SL4354	iolA1	Methylmalonate semialdehyde dehydrogenase [acylating] 1	-1,53	1,66
SL4358	srfJ	Glucan Endo-1 6-Beta-Glucosidase	-1,04	-1,00
SL4362	iolD1	3D-(3,5/4)-trihydroxycyclohexane-1,2-dione hydrolase 1	1,45	2,17
SL4366	iolH	Protein iolH	-3,04	1,36
SL4369	cybC	Soluble cytochrome b562	-1,59	1,37
SL4384	treC	Trehalose-6-phosphate hydrolase	2,36	10,59
SL4396	arcC	Carbamate kinase	-1,99	2,87
SL4414	idnD	L-idonate 5-dehydrogenase	-1,32	2,80
SL4415	idnK	Thermosensitive gluconokinase	-1,12	2,19
SL4416	yjgB	Uncharacterized zinc-type alcohol dehydrogenase-like protein yjgB	-1,49	2,20
SL4436	yczH	Uncharacterized protein yczH	1,10	1,47
SL4437	uxuR	Uxu operon transcriptional regulator	1,35	-1,05
SL4450	ssdA	Succinate-semialdehyde dehydrogenase [NADP+]	-1,33	2,50
SL4491	yjjV	Uncharacterized deoxyribonuclease yjjV	1,72	1,33
SL4494	deoC	Deoxyribose-phosphate aldolase	1,50	-1,54
SL4512	gpmB	Probable phosphoglycerate mutase gpmB	1,70	1,68
		Fatty acid and phospholipid metabolism		
SL0074	caiA	Crotonobetainyl-CoA dehydrogenase	1,68	3,58
SL0223	cdsA	Phosphatidate cytidylyltransferase	1,29	-1,92
SL0227	lpxD	UDP-3-O-[3-hydroxymyristoyl] glucosamine N-acyltransferase	1,55	-1,41

SL0228	fabZ	(3R)-hydroxymyristoyl-[acyl-carrier-protein] dehydratase	1,42	-1,30
SL0233	accA	Acetyl-coenzyme A carboxylase carboxyl transferase subunit alpha	2,00	-1,00
SL0414	pgpA	Phosphatidylglycerophosphatase A	1,61	1,27
SL0458	tesB	Acyl-CoA thioesterase 2	1,22	1,64
SL0483	aes	Acetyl esterase	-1,39	1,02
SL0499	tesA	Acyl-CoA thioesterase I	-1,10	-1,99
SL0788	ybhO	Putative cardiolipin synthase ybhO	-2,14	-2,23
SL0815	ybiV2	putative hydrolase	-1,42	-1,28
SL0833	mmgC	Acyl-CoA dehydrogenase	-1,28	-1,48
SL0871	ybjS	putative nucleoside-diphosphate-sugar epimerase	1,28	-1,84
SL1007	fabA	3-hydroxydecanoyl-[acyl-carrier-protein] dehydratase	1,44	1,85
SL1023	yccX	Acylphosphatase	-1,14	1,31
SL1129	plsX	Phosphate acyltransferase	1,32	-1,60
SL1130	fabH	3-oxoacyl-[acyl-carrier-protein] synthase 3	1,87	-1,42
SL1131	fabD	Malonyl CoA-acyl carrier protein transacylase	2,20	-1,00
SL1132	fabG	3-oxoacyl-[acyl-carrier-protein] reductase	2,17	1,03
SL1133	acpP	Acyl carrier protein	1,52	-1,12
SL1146	nagZ	Beta-hexosaminidase	1,38	-1,28
SL1284	fadK	Short-chain-fatty-acid--CoA ligase	1,04	-1,75
SL1290	ydiO	Uncharacterized protein ydiO	-1,75	-1,45
SL1359	cfa	Cyclopropane-fatty-acyl-phospholipid synthase	-1,07	-1,49
SL1572	azoR	FMN-dependent NADH-azoreductase	1,66	-2,65
SL1605	yjgI	Uncharacterized oxidoreductase yjgI	1,53	1,04
SL1642	pgpB	Phosphatidylglycerophosphatase B	1,15	1,00
SL1670	cls	Cardiolipin synthase	1,64	1,29
SL1733	fadR	Fatty acid metabolism regulator protein	1,45	-1,10
SL1875	pgsA	CDP-diacylglycerol--glycerol-3-phosphate 3-phosphatidyltransferase	1,07	-1,00
SL2149	yohF	Uncharacterized oxidoreductase yohF	-1,55	1,63
SL2335	accD	Acetyl-coenzyme A carboxylase carboxyl transferase subunit beta	1,84	-1,18
SL2347	fabB	3-oxoacyl-[acyl-carrier-protein] synthase 1	1,99	1,38
SL2357	fadJ	Fatty acid oxidation complex subunit alpha	1,53	1,43
SL2358	fadI	3-ketoacyl-CoA thiolase	1,11	-1,08
SL2408	ucpA	Oxidoreductase ucpA	1,40	-1,10
SL2417	eutR	HTH-type transcriptional regulator eutR	-1,01	1,41
SL2422	eutA	Ethanolamine utilization protein eutA	-1,26	-1,17
SL2424	eutG	Ethanolamine utilization protein eutG	-1,25	-1,21
SL2426	eutE	Ethanolamine utilization protein eutE	-2,28	-1,31
SL2427	eutN	Ethanolamine utilization protein eutN	-1,76	-1,09
SL2428	eutM	Ethanolamine utilization protein eutM	-2,04	-1,11
SL2431	eutQ	Ethanolamine utilization protein eutQ	-1,72	2,57
SL2508	suhB	Inositol-1-monophosphatase	-1,02	-1,72
SL2539	acpS	Holo-[acyl-carrier-protein] synthase	1,12	-1,39
SL2616	pssA	CDP-diacylglycerol--serine O-phosphatidyltransferase	-1,06	-1,35
SL2988	aas	Bifunctional protein aas	-1,06	1,21
SL2997	yqeF	Probable acetyl-CoA acetyltransferase	1,16	3,16
SL3147	plsC	1-acyl-sn-glycerol-3-phosphate acyltransferase	2,54	-1,01
SL3156	yqiA	Esterase yqiA	1,46	-1,34
SL3157	icc	Protein icc	1,85	1,05
SL3192	fadH	2,4-dienoyl-CoA reductase [NADPH]	-1,14	4,94
SL3246	yhbT	Uncharacterized protein yhbT	1,93	1,56
SL3352	accB	Biotin carboxyl carrier protein of acetyl-CoA carboxylase	2,07	-1,19
SL3353	accC	Biotin carboxylase	2,22	-1,65
SL3463	yrfG	Uncharacterized protein yrfG	1,16	1,39
SL3607	yhjY	Uncharacterized protein yhjY	-1,80	-1,84
SL3904	yigB	Uncharacterized protein yigB	1,02	-2,88
SL3935	fadA	3-ketoacyl-CoA thiolase	6,71	5,63
SL3936	fadB	Fatty acid oxidation complex subunit alpha	6,83	5,93
SL3978	est	Esterase	1,36	3,79
SL4013	cdh	CDP-diacylglycerol pyrophosphatase	-1,05	1,78
SL4172	plsB	Glycerol-3-phosphate acyltransferase	1,74	-1,29
SL4173	dgkA	Diacylglycerol kinase	1,54	-1,07
SL4211	acs	Acetyl-coenzyme A synthetase	3,25	4,90
SL4285	psd	Phosphatidylserine decarboxylase proenzyme	1,31	1,10
SL4310	aidB	Protein AidB	1,89	7,60
SL4353	iolB	5-deoxy-glucuronate isomerase	-1,41	1,78

SL4472	mdoB	Phosphoglycerol transferase I	-1,21	-2,16
SL4491	yjjV	Uncharacterized deoxyribonuclease yjjV	1,72	1,33
		Hypothetical proteins		
SL0028	bcfH	putative thiol-disulfide isomerase	-1,01	-1,09
SL0034	yhcR	Endonuclease yhcR	-1,65	1,18
SL0119	mraZ	Protein mraZ	1,07	-1,24
SL0168	yacC	Uncharacterized protein yacC	1,60	-1,44
SL0290	yjiW	Hypothetical	-1,05	-1,04
SL0340	-	putative inner membrane protein	-1,31	-2,26
SL0404	-	Glyoxalase/Bleomycin Resistance Protein/Dioxygenase	1,86	1,05
SL0409	nrdR	Transcriptional repressor nrdR	1,54	1,11
SL0448	tesC	Long-chain acyl-CoA thioesterase tesC	1,79	1,52
SL0478	ybaB	UPF0133 protein KPK_4227	1,66	-1,75
SL0496	ybbM	UPF0014 inner membrane protein ybbM	1,56	-1,34
SL0629	rlmH	Ribosomal RNA large subunit methyltransferase H	1,20	1,27
SL0657	ybeY	Putative metalloprotease ybeY	1,59	-2,17
SL0692	ybgI	UPF0135 protein ybgI	-1,20	1,96
SL0693	ybgJ	Uncharacterized protein ybgJ	1,04	1,79
SL0726	ybgC	Acyl-CoA thioester hydrolase ybgC	1,93	-1,38
SL0769	ybhB	UPF0098 protein ybhB	2,48	1,56
SL0828	yliG	putative Fe-S oxidoreductases family 1	1,27	1,19
SL0883	clpS	ATP-dependent Clp protease adapter protein clpS	-1,32	-4,94
SL0999	ycbW	Uncharacterized protein ycbW	-1,97	-1,73
SL1098	bssS	Biofilm regulator BssS	-1,51	1,32
SL1136	yceG	UPF0755 protein yceG	1,70	-1,85
SL1217	yeaK	Uncharacterized protein yeaK	-1,44	-1,84
SL1227	yeaC	Uncharacterized protein yeaC	1,46	1,72
SL1415	asr	Acid shock protein	-1,03	1,18
SL1445	ydeI	Uncharacterized protein ydeI	-3,62	-2,37
SL1451	marC	UPF0056 inner membrane protein marC	-1,11	-1,97
SL1545	sgcQ	Putative sgc region protein sgcQ	-1,59	1,39
SL1602	-	Hypothetical	-5,11	-10,61
SL1671	yciU	UPF0263 protein CKO_01325	1,09	2,97
SL1679	ychE	UPF0056 membrane protein yhcE	-1,06	1,13
SL1834	yebC	UPF0082 protein CKO_01097	1,83	-1,12
SL1866	-	Hypothetical	2,44	1,02
SL2117	yegS	Probable lipid kinase yegS	1,16	-1,83
SL2159	yohK	Inner membrane protein yohK	-2,15	-13,53
SL2359	yfcZ	UPF0381 protein yfcZ	1,58	1,23
SL2440	nudK	GDP-mannose pyrophosphatase nudK	-1,24	1,09
SL2487	yfgB	putative Fe-S-cluster redox enzyme	-1,03	-1,32
SL2621	yfiH	UPF0124 protein yfiH	2,20	1,13
SL2901	vdcC	Protein vdcC	1,32	1,44
SL2907	truD	tRNA pseudouridine synthase D	2,07	-1,00
SL3069	rsmE	Ribosomal RNA small subunit methyltransferase E	1,64	-1,12
SL3071	yqgE	UPF0301 protein yqgE	1,16	-1,27
SL3072	yqgF	Putative Holliday junction resolvase	1,37	-1,56
SL3075	yggS	UPF0001 protein yggS	2,20	1,03
SL3077	yggU	UPF0235 protein CKO_04329	1,73	-1,29
SL3083	yggL	Uncharacterized protein yggL	1,48	2,23
SL3127	yqhA	UPF0114 protein yqhA	-2,13	-2,18
SL3150	ygiW	Protein ygiW	-1,86	1,43
SL3159	nudF	ADP-ribose pyrophosphatase	1,31	-1,06
SL3180	plsY	Glycerol-3-phosphate acyltransferase	1,09	1,29
SL3236	rsmI	Ribosomal RNA small subunit methyltransferase I	1,27	-1,31
SL3238	yraN	UPF0102 protein yraN	1,64	-1,46
SL3270	yhbY	RNA-binding protein yhbY	1,13	-1,70
SL3301	yhcC	Uncharacterized protein yhcC	1,71	2,46
SL3338	aaeX	Protein AaeX	2,03	1,95
SL3419	yheO	Uncharacterized protein yheO	1,41	-1,67
SL3483	yafQ	Uncharacterized protein yafQ	-1,15	1,81
SL3553	yhiN	Uncharacterized protein yhiN	1,26	1,52
SL3701	yicC	UPF0701 protein yicC	1,64	1,56
SL3808	hlyA	Putative alpha-hemolysin	1,63	-1,43
SL3845	viaA	Protein viaA	-1,18	-1,22
SL3932	ubiD	3-octaprenyl-4-hydroxybenzoate carboxy-lyase	1,28	-1,08
SL3938	yigZ	IMPACT family member yigZ	1,57	-1,41

SL4180	pspG	Phage shock protein G	-4,76	-3,56
SL4186	yjbQ	UPF0047 protein yjbQ	-1,14	1,08
SL4270	yjeK	Uncharacterized KamA family protein YjeK	1,25	-1,05
SL4291	yjeE	UPF0079 ATP-binding protein yjeE	1,37	1,59
SL4377	-	Hypothetical	1,10	1,75
SL4429	yeeN	UPF0082 protein LACR_0237	1,37	-2,05
SL4454	symE	Endoribonuclease symE	1,42	1,06
SL4511	yjjX	UPF0244 protein yjjX	1,94	1,16
		Prophages and transposons		
SL0015	-	Hypothetical	1,19	1,12
SL0286	rhsD	Putative protein rhsD	1,27	-2,21
SL0293	-	Pseudogene (putative transposase)	1,09	-1,00
SL0294	yagA	Insertion element IS407 uncharacterized 31.7 kDa protein	1,00	1,15
SL0319	insF1	Transposase insF for insertion sequence IS3A	-1,53	-1,27
SL0341	ail	Attachment invasion locus protein	-1,07	-1,27
SL0475	ybaN	Inner membrane protein ybaN	-1,11	-1,42
SL0546	nisX1	Transposase for insertion sequence element IS904 pseudogene	-1,06	1,54
SL0697	fimB	Type 1 fimbriae regulatory protein fimB	-1,74	-1,30
SL0736	ybgS	Uncharacterized protein ybgS	-2,62	-1,97
SL0808	ompX	Outer membrane protein X	-1,02	-1,37
SL0885	tnpA1	Transposase for insertion sequence element IS1541	1,56	-1,50
SL0886	insF7	Insertion element IS600 uncharacterized 31 kDa protein	-1,36	1,73
SL1181	envE	Probable lipoprotein envE	-1,18	-4,06
SL1443	ymdF	Uncharacterized protein ymdF	-3,87	-2,05
SL1560	tfpB	Protein tfpB	-2,50	-2,96
SL1568	ybcY	Putative uncharacterized protein ybcY	1,66	1,05
SL1580	-	Hypothetical	1,04	-1,12
SL1583	emrE	Multidrug transporter emrE	1,96	1,43
SL1601	-	Hypothetical Protein SL1601	-1,22	-1,20
SL1617	pspD	Phage shock protein D	-5,24	-2,68
SL1620	pspA	Phage shock protein A	-7,80	-3,48
SL1660	yciF	Protein yciF	-7,59	-1,84
SL1662	-	Probable manganese catalase	-2,93	-1,43
SL1782	pphA	Serine/threonine-protein phosphatase 1	-2,70	-2,73
SL1790	-	Transposase for insertion sequence element ISRM3	-1,34	1,66
SL1791	intE	Prophage lambda integrase	-1,16	-1,06
SL1792	-	Hypothetical	-1,58	-1,00
SL1800	ycdD	Tail fiber assembly protein homolog from lambdoid prophage Fels-1	-3,67	-2,33
SL1804	-	Hypothetical	1,41	1,20
SL1806	intE	Prophage lambda integrase	1,02	2,40
SL2043	sopA	E3 ubiquitin-protein ligase SopA	-28,13	-16,06
SL2209	yfdK	Uncharacterized protein yfdK	-1,41	1,10
SL2211	ycfK	Uncharacterized protein ycfK	1,03	1,26
SL2212	-	Prohead Protease	-1,22	-1,51
SL2214	pifA	KAP P-Loop Domain-Containing Protein	1,48	8,00
SL2343	sfsB	Sugar fermentation stimulation protein B	1,12	1,07
SL2470	insF1	Transposase insF for insertion sequence IS3A	-1,25	-1,05
SL2633	-	Putative uncharacterized protein ORFI in retron EC67	1,72	1,60
SL2634	-	Hypothetical	1,06	-1,18
SL2635	-	Putative uncharacterized protein ORFB in retron EC67	-1,18	1,09
SL2636	-	Hypothetical	1,02	-1,04
SL2637	-	Putative uncharacterized protein ORFC-like in prophage region	1,06	1,21
SL2638	-	Hypothetical	-1,82	1,08
SL2639	-	similar to TraR	-1,73	1,10
SL2640	-	Hypothetical Protein SL2640	-1,12	1,89
SL2641	-	Probable replication endonuclease from prophage-like region 1	1,16	-1,02
SL2642	gpF	P2 GpU Family Protein	1,43	1,02
SL2643	gpD	Late Control D Family Protein	-1,12	1,20
SL2644	-	Hypothetical Protein SL2644	1,02	1,56
SL2645	gpB	Prophage P2 OGR protein	1,02	1,33
SL2729	-	Hypothetical	1,16	1,85
SL2733	sfsB	Sugar fermentation stimulation protein B	-1,82	-1,39
SL2750	lcrS	Low calcium response locus protein S	1,27	1,53
SL2753	insE1	Transposase insE for insertion sequence IS3A	1,33	-1,07
SL2754	insF1	Transposase insF for insertion sequence IS3A	-1,91	-1,29
SL2756	fljB	Phase 2 flagellin	-7,31	-1,25

SL2761	iroE	Ferri-bacillibactin esterase BesA	-1,04	-2,81
SL2798	emrR	Transcriptional repressor emrR	1,58	-1,12
SL2886	pphB	Serine/threonine-protein phosphatase 2	1,43	-2,35
SL3010	-	Virulence membrane protein	1,23	1,18
SL3278	sfsB	Sugar fermentation stimulation protein B	1,12	1,15
SL3524	kil	Death On Curing Protein	1,62	1,71
SL3813	-	RNA-directed DNA polymerase from retron EC86	-1,64	1,27
SL4042	ftsN	Cell division protein ftsN	1,71	-1,91
SL4232	adiY	HTH-type transcriptional regulator AdiY	-1,88	1,78
SL4248	-	Hypothetical	-26,42	-8,48
SL4295	hfq	Protein hfq	1,19	1,17
SL4379	relB	Antitoxin RelB	1,43	2,34
SL4388	-	Conserved Hypothetical Protein	1,66	1,60
SL4417	intZ	Integrase Family Protein	-1,10	-1,07
SL4474	dnaC	DNA replication protein dnaC	1,25	-1,23
		Protein fate		
SL0012	dnaK	Chaperone protein dnaK	4,03	1,12
SL0048	lspA	Lipoprotein signal peptidase	1,92	-1,26
SL0059	citC2	[Citrate [pro-3S]-lyase] ligase	2,45	10,46
SL0082	-	secreted protein	-2,78	-2,84
SL0093	surA	Chaperone surA	2,00	-1,69
SL0136	secA	Protein translocase subunit secA	2,47	-1,17
SL0144	ppdD	Prepilin peptidase-dependent protein D	1,91	3,64
SL0197	stfC	outer membrane usher protein stfc (putative fimbrial outer membrane usher)	-1,16	-1,19
SL0198	stfD	periplasmic fimbrial chaperone stfd	1,20	-1,25
SL0210	htrA	Protease do precursor; heat shock protein HtrA	1,52	-1,16
SL0216	map	Methionine aminopeptidase	1,69	-1,01
SL0224	yaeL	Regulator of sigma E protease	1,48	-1,91
SL0266	clpB	Chaperone protein clpB	2,15	1,30
SL0312	pepD	Aminoacyl-histidine dipeptidase	1,33	1,73
SL0401	yajC	UPF0092 membrane protein yajC	2,21	1,03
SL0402	secD	Protein-export membrane protein secD	2,38	-1,71
SL0403	secF	Protein-export membrane protein secF	2,23	-1,52
SL0406	yajD	Uncharacterized protein yajD	-1,15	-1,30
SL0441	tig	Trigger factor	1,82	1,56
SL0442	clpP	ATP-dependent Clp protease proteolytic subunit	1,49	-1,09
SL0443	clpX	ATP-dependent Clp protease ATP-binding subunit clpX	1,38	-2,43
SL0444	lon	Hypothetical Protein lon	3,26	-1,03
SL0446	ppiD	Peptidyl-prolyl cis-trans isomerase D	1,23	-3,61
SL0480	htpG	Chaperone protein htpG	4,77	1,50
SL0520	allC	Allantoate amidohydrolase	1,18	2,19
SL0522	fdrA	Protein fdrA	1,22	1,84
SL0538	fimC	Chaperone protein fimC	-3,07	-12,54
SL0612	citC	[Citrate [pro-3S]-lyase] ligase	3,93	8,29
SL0620	tatE	Sec-independent protein translocase protein tatE	1,36	1,45
SL0623	lipB	Octanoyltransferase	1,42	-2,06
SL0630	ybeB	Uncharacterized protein ybeB	1,39	2,09
SL0648	hscC	Chaperone protein hscC	2,34	-1,10
SL0655	lnt	Apolipoprotein N-acyltransferase	1,66	-1,84
SL0820	ybiY	Putative pyruvate formate-lyase 3-activating enzyme	3,06	2,87
SL0879	ybjX	Uncharacterized protein ybjX	-1,29	-3,90
SL0884	clpA	ATP-dependent Clp protease ATP-binding subunit clpA	-2,55	-2,55
SL0893	aat	Leucyl/phenylalanyl-tRNA--protein transferase	1,08	1,01
SL0899	lolA	Outer-membrane lipoprotein carrier protein	1,26	-1,38
SL0997	pepN	Aminopeptidase N	-1,17	-1,71
SL1008	lonH	Putative protease	1,48	-1,21
SL1051	cbpA	Curved DNA-binding protein	-1,24	1,13
SL1084	ymdB	putative ACR protein	-1,98	1,12
SL1090	msyB	Acidic protein msyB	-1,07	5,67
SL1094	yceI	UPF0312 protein Ent638_1570	1,01	1,14
SL1140	ptsG	PTS system glucose-specific EIICB component	1,20	1,02
SL1142	hinT	HIT-like protein hinT	1,35	1,15
SL1164	pepT	Peptidase T	2,28	2,03
SL1187	ibp	Small heat shock protein ibp	1,32	-1,08
SL1230	sppA	Protease 4	2,38	-1,12
SL1314	pip	Proline iminopeptidase	-2,62	2,83

SL1376	slyA	Transcriptional regulator slyA	-1,84	-1,30
SL1442	dcp	Peptidyl-dipeptidase dcp	-1,00	-1,19
SL1460	hypA	Hydrogenase nickel incorporation protein hypA	-2,80	-1,95
SL1464	hupF	Hydrogenase expression/formation protein hupF	-1,78	-1,24
SL1524	srfA	putative virulence effector protein	1,09	-1,08
SL1525	srfB	Virulence Protein SrfB	1,58	1,72
SL1530	vanX	D-alanyl-D-alanine dipeptidase	-1,58	-1,76
SL1534	ydcP	Uncharacterized protease ydcP	-1,06	1,42
SL1542	sgcX	Putative aminopeptidase sgcX	-1,59	2,19
SL1551	yceI	UPF0312 protein VPA0850	2,31	2,13
SL1600	-	Conserved Hypothetical Protein Exported Protein	-1,12	-2,03
SL1610	mpaA	Protein mpaA	-1,04	-1,26
SL1648	sohB	Probable protease sohB	1,06	-1,30
SL1697	ychN	Protein ychN	-1,02	-1,46
SL1706	lolB	Outer-membrane lipoprotein lolB	1,55	-1,63
SL1774	prc	Tail-specific protease	1,56	-1,39
SL1802	-	Phage Membrane Protein	-1,12	-1,35
SL1813	ptrB	Protease 2	-1,41	-1,32
SL1824	yebA	Uncharacterized metalloprotease yebA	1,27	-1,40
SL1979	-	Hypothetical	-1,12	1,24
SL2051	hisB	Histidine biosynthesis bifunctional protein hisB	1,07	1,07
SL2079	wzxC	Lipopolysaccharide biosynthesis protein wzxC	1,78	-1,14
SL2144	bglX	Periplasmic beta-glucosidase	1,24	-1,58
SL2205	yejM	Inner membrane protein yejM	1,43	-1,06
SL2212	-	Prohead Protease	-1,22	-1,51
SL2224	ccmA2	Putative bifunctional cytochrome c-type biogenesis protein ccmAE	1,48	-1,22
SL2232	eco	Ecotin	2,36	1,01
SL2348	mnmC	tRNA 5-methylaminomethyl-2-thiouridine biosynthesis bifunctional protein mnmC	1,67	1,05
SL2449	ypfJ	Uncharacterized protein ypfJ	1,30	1,06
SL2495	sseA	3-mercaptopyruvate sulfurtransferase	-1,09	1,29
SL2497	sseB	Protein sseB	1,25	-1,25
SL2498	pepB	Peptidase B	1,61	1,05
SL2501	hscA	Chaperone protein hscA	1,78	-2,00
SL2502	hscB	Co-chaperone protein hscB	1,41	-2,30
SL2544	lepB	Signal peptidase I	-1,09	-1,20
SL2620	clpB	Chaperone protein clpB	3,11	1,64
SL2650	ffh	Signal recognition particle protein	1,50	-2,01
SL2654	grpE	Protein grpE	4,63	2,48
SL2662	bepC	Outer membrane efflux protein BepC	-1,17	1,67
SL2663	apxIB	Toxin RTX-I translocation ATP-binding protein	-1,77	1,64
SL2664	cyaD	Protein cyaD	-1,70	1,42
SL2742	ptsG	PTS system glucose-specific EIICBA component	1,25	1,63
SL2764	ybjX	Uncharacterized protein ybjX	-1,03	-5,61
SL2822	hypF	Carbamoyltransferase hypF	1,56	1,13
SL2825	hycI	Hydrogenase 3 maturation protease	1,79	2,71
SL2834	hypA	Protein hypA	1,79	1,09
SL2836	hypC	Hydrogenase isoenzymes formation protein hypC	1,53	1,00
SL2837	hypD	Hydrogenase isoenzymes formation protein hypD	2,33	-1,13
SL2899	slyA	Transcriptional regulator	1,28	1,50
SL2905	pcm	Protein-L-isoaspartate O-methyltransferase	2,07	-1,69
SL2973	ptrA	Protease 3	2,13	-1,23
SL2975	ppdC	Prepilin peptidase-dependent protein C	2,32	1,68
SL2978	ppdA	Prepilin peptidase-dependent protein A	1,16	3,67
SL2980	lgt	Prolipoprotein diacylglyceryl transferase	-1,08	-1,52
SL3007	stdB	putative outer membrane usher protein	1,11	-1,10
SL3034	pepP	Xaa-Pro aminopeptidase	1,38	-1,23
SL3117	hybG	Hydrogenase-2 operon protein hybG	1,28	-2,17
SL3118	hybF	Probable hydrogenase nickel incorporation protein hybF	2,02	-2,14
SL3120	hybD	Hydrogenase 2 maturation protease	1,38	-1,59
SL3166	dsbA	Thiol:disulfide interchange protein dsbA	-1,55	1,18
SL3182	gcp	Probable O-sialoglycoprotein endopeptidase	2,17	1,64
SL3247	yhbU	Uncharacterized protease yhbU	3,03	2,73
SL3264	secG	Protein-export membrane protein secG	-1,65	-1,36
SL3320	degQ	Protease degQ	1,05	-1,25
SL3321	degS	Protease degS	1,44	-1,36
SL3341	yhdP	Uncharacterized protein yhdP	1,67	-1,31

SL3373	def	Peptide deformylase	-1,32	-2,20
SL3387	secY	Preprotein translocase subunit secY	1,30	1,15
SL3409	hopD	Leader peptidase hopD	-2,98	-1,17
SL3422	slyD	FKBP-type peptidyl-prolyl cis-trans isomerase slyD	1,10	2,24
SL3439	ppiA	Peptidyl-prolyl cis-trans isomerase A	1,33	-2,27
SL3462	yrfF	Putative membrane protein igaA homolog	1,19	-1,54
SL3534	ftsX	Cell division protein ftsX	2,00	-1,37
SL3543	tusA	Sulfurtransferase tusA	-8,27	-6,94
SL3559	prlC	Oligopeptidase A	-1,31	-3,84
SL3560	phoC	Major phosphate-irrepressible acid phosphatase	1,40	-1,64
SL3592	dppF	Dipeptide transport ATP-binding protein dppF	-4,65	-3,99
SL3596	dppA	Periplasmic dipeptide transport protein	-6,01	-2,14
SL3598	-	Hypothetical	1,04	1,32
SL3605	lpfB	Chaperone protein lpfB	1,09	-1,55
SL3610	bisC	Biotin sulfoxide reductase	1,29	-1,37
SL3667	secB	Protein-export protein secB	1,50	1,83
SL3671	yibP	Uncharacterized protein yibP	1,92	-2,05
SL3776	ibpA	Small heat shock protein ibpA	5,63	-1,03
SL3780	ccmG1	Thiol:disulfide interchange protein dsbE	3,06	1,10
SL3784	ccmB	Heme exporter protein B	2,72	-1,35
SL3784	ccmB	Heme exporter protein B	2,72	-1,35
SL3785	ccmAE	Putative bifunctional cytochrome c-type biogenesis protein ccmAE	1,04	-1,29
SL3885	wzxE	Protein wzxE	1,65	-1,92
SL3937	pepQ	Xaa-Pro dipeptidase	1,43	1,21
SL3945	dsbA	Thiol:disulfide interchange protein dsbA	-1,51	-1,17
SL4040	hslU	ATP-dependent protease ATPase subunit HslU	3,39	-1,38
SL4041	hslV	ATP-dependent protease subunit HslV	2,50	-1,24
SL4086	secE	Preprotein translocase subunit secE	1,23	-1,33
SL4125	pepE	Peptidase E	1,69	1,29
SL4166	malE	Maltose-binding periplasmic protein	-2,38	3,45
SL4185	aphA	Class B acid phosphatase	1,34	5,38
SL4266	groS	10 kDa chaperonin	3,76	1,75
SL4267	groL	60 kDa chaperonin	2,17	1,42
SL4275	sugE	Quaternary ammonium compound-resistance protein sugE	-1,45	-1,05
SL4297	hflK	Protein hflK	1,50	-1,71
SL4298	hflC	Protein hflC	1,41	-1,90
SL4316	ulaA	Ascorbate-specific permease IIC component ulaA	1,30	3,66
SL4407	pepA	Probable cytosol aminopeptidase	1,55	2,24
SL4420	lon	Hypothetical	1,02	1,05
SL4443	iadA	Isoaspartyl dipeptidase	-2,04	1,32
SL4492	yjjW	Uncharacterized protein yjjW	5,75	6,32
SL4521	fimC	Chaperone protein fimC	1,21	-1,80
		Protein synthesis		
SL0038	-	Hypothetical	-1,09	1,00
SL0044	rpsT	30S ribosomal protein S20	1,17	1,12
SL0045	yaaY	Uncharacterized protein yaaY	1,84	-2,27
SL0047	ileS	Isoleucyl-tRNA synthetase	1,75	-1,24
SL0049	fkpB	FKBP-type 16 kDa peptidyl-prolyl cis-trans isomerase	1,75	-1,52
SL0091	ksgA	dimethyladenosine transferase	1,28	-1,55
SL0100	-	Hypothetical	1,29	-1,91
SL0138	yacG	UPF0243 zinc-binding protein yacG	1,81	1,91
SL0186	yadB	glutamyl-tRNA synthetase	-1,07	-45,85
SL0212	yaeH	UPF0325 protein ESA_03178	-1,03	3,85
SL0217	rpsB	30S ribosomal protein S2	1,26	1,30
SL0218	tsf	Elongation factor Ts	1,65	1,60
SL0220	frr	Ribosome-recycling factor	1,51	1,04
SL0239	yaeP	UPF0253 protein CKO_03176	-1,03	1,38
SL0243	proS	Prolyl-tRNA synthetase	1,57	-1,31
SL0260	sciA	Hypothetical	1,26	-1,50
SL0262	sciC	Hypothetical	1,73	-1,20
SL0263	sciD	Hypothetical	2,38	-1,54
SL0265	sciF	Cytoplasmic Protein	3,12	1,13
SL0268	sciI	Hypothetical	1,77	1,43
SL0270	sciJ	Cytoplasmic Protein	1,10	1,01
SL0271	sciK	Protein hcp1	1,12	-1,01
SL0272	-	Cytoplasmic Protein	1,19	-1,02

SL0274	sciK1	Protein hcp1	1,66	-1,19
SL0276	sciO	Hypothetical	1,43	-1,29
SL0281	sciT	Cytoplasmic Protein	1,38	1,21
SL0283	sciV	Hypothetical	-1,20	-2,10
SL0285	sciW	Hypothetical	1,19	1,00
SL0288	sciX	Cytoplasmic Protein	1,30	-1,23
SL0289	sciY	Phosphotriesterase	1,22	-1,36
SL0291	-	Cytoplasmic Protein	-1,18	-1,30
SL0292	-	Pseudogene	-1,15	-1,23
SL0301	-	Hypothetical	-1,60	-1,32
SL0307	yafJ	Putative glutamine amidotransferase yafJ	-1,05	1,04
SL0311	prfH	Putative peptide chain release factor homolog	1,18	-1,08
SL0322	yoaC	Uncharacterized protein yoaC	-2,02	1,93
SL0354	-	Hypothetical	-3,27	-1,16
SL0357	-	Hypothetical	-1,84	1,16
SL0378	yaiB	Anti-adapter protein	-1,42	-1,43
SL0384	yaiA	Uncharacterized protein yaiA	1,38	-1,06
SL0386	yaiE	UPF0345 protein Ent638_0862	-1,20	-1,05
SL0398	yajB	putative cytoplasmic protein	1,20	-1,23
SL0399	queA	S-adenosylmethionine:tRNA ribosyltransferase-isomerase	1,38	1,04
SL0400	tgt	Queuine tRNA-ribosyltransferase	2,50	1,32
SL0406	yajD	Uncharacterized protein yajD	-1,15	-1,30
SL0429	yajQ	UPF0234 protein CKO_02735	1,93	2,55
SL0462	rpmE2	50S ribosomal protein L31 type B	-1,81	1,73
SL0463	rpmJ	50S ribosomal protein L36	-2,04	1,26
SL0467	ybaJ	Uncharacterized protein ybaJ	-1,05	-1,40
SL0489	ybaP	Uncharacterized protein ybaP	1,28	1,33
SL0524	ylbF	Uncharacterized protein ylbF	1,09	1,04
SL0529	ppiB	Peptidyl-prolyl cis-trans isomerase B	1,17	1,58
SL0530	cysS	Cysteinyl-tRNA synthetase	1,09	-1,19
SL0624	ybeD	UPF0250 protein Ent638_1166	1,61	-1,87
SL0630	ybeB	Uncharacterized protein ybeB	1,39	2,09
SL0636	leuS	Leucyl-tRNA synthetase	1,21	-2,10
SL0641	ybeL	Uncharacterized protein ybeL	-1,52	2,12
SL0649	-	Hypothetical	1,11	2,13
SL0659	miaB	(Dimethylallyl)adenosine tRNA methylthiotransferase miaB	1,06	-1,18
SL0668	glnS	Glutaminyl-tRNA synthetase	1,81	-1,42
SL0681	-	5-Nitroimidazole Antibiotic Resistance Protein	2,07	-1,24
SL0696	-	Hypothetical	-1,47	-1,69
SL0709	-	Hypothetical	1,69	-1,49
SL0777	ybhK	UPF0052 protein ybhK	1,42	-1,02
SL0789	ybhP	Uncharacterized protein ybhP	-1,46	-2,31
SL0829	bssR	Biofilm regulator BssR	-3,01	1,27
SL0853	ybjN	Uncharacterized protein ybjN	1,78	1,29
SL0859	rumB	23S rRNA (uracil-5-)-methyltransferase rumB	1,27	-1,01
SL0887	OrfA	ISPsy11, transposase	-1,67	1,58
SL0889	yhhW	Pirin-like protein PA2418	1,12	2,03
SL0891	infA	Translation initiation factor IF-1	1,01	-1,47
SL0901	serS	Seryl-tRNA synthetase	1,45	-2,22
SL0908	-	Conserved Hypothetical Protein	1,79	-1,86
SL0918	rpsA	30S ribosomal protein S1	1,22	-1,18
SL0937	asnS	Asparaginyl-tRNA synthetase	1,64	-3,14
SL1006	rmf	Ribosome modulation factor	1,41	1,02
SL1009	ycbG	UPF0268 protein ycbG	-1,30	-1,13
SL1057	yccJ	Uncharacterized protein yccJ	1,06	1,35
SL1104	rimJ	Ribosomal-protein-alanine acetyltransferase	1,19	2,09
SL1128	rpmF	50S ribosomal protein L32	1,11	1,70
SL1145	thiK	Thiamine kinase	1,35	1,10
SL1172	trmU	tRNA-specific 2-thiouridylase mnmA	1,21	-1,23
SL1177	-	Bacteriophage Protein	-19,48	-16,74
SL1186	-	Hypothetical	-2,26	-4,93
SL1202	ymgB	Hypothetical	-3,76	1,16
SL1203	-	Hypothetical	1,08	1,00
SL1207	yoaG	Protein yoaG	2,36	1,70
SL1232	selD	Selenide, water dikinase	1,46	1,14
SL1267	thrS	Threonyl-tRNA synthetase	1,02	1,20
SL1268	infC	Translation initiation factor IF-3	-1,01	-1,14

SL1269	rpmI	50S ribosomal protein L35	-1,01	1,01
SL1270	rplT	50S ribosomal protein L20	1,34	1,23
SL1271	pheS	Phenylalanyl-tRNA synthetase alpha chain	2,56	-1,59
SL1272	pheT	Phenylalanyl-tRNA synthetase beta chain	1,99	1,00
SL1280	ydiE	Uncharacterized protein ydiE	-1,14	-2,69
SL1301	ydiH	Uncharacterized protein ydiH	-1,80	-1,37
SL1315	-	Hypothetical	-2,51	2,91
SL1322	ydhZ	Uncharacterized protein ydhZ	-1,47	-1,40
SL1381	tyrS	Tyrosyl-tRNA synthetase	1,41	-1,43
SL1393	cnu	OriC-binding nucleoid-associated protein	1,04	-1,83
SL1439	ydfZ	Putative selenoprotein ydfZ	1,31	6,74
SL1477	queA	S-adenosylmethionine:tRNA ribosyltransferase-isomerase	-2,81	-2,90
SL1479	relE	Toxin relE	1,13	-1,16
SL1480	-	Hypothetical	1,36	1,31
SL1482	-	Cytoplasmic Protein	-1,44	-1,03
SL1495	rpsV	30S ribosomal protein S22	-2,26	-1,38
SL1504	-	Glutathione-Dependent Formaldehyde-Activating GFA	1,25	2,26
SL1514	steA	Secreted effector protein steA	-1,36	-1,06
SL1523	ydcY	Uncharacterized protein ydcY	1,65	2,16
SL1630	ycjE	Uncharacterized protein ycjE	1,04	-1,37
SL1632	yciW	Uncharacterized protein yciW	1,38	-1,03
SL1638	yciH	Uncharacterized protein yciH	-1,36	1,84
SL1647	yciN	Protein yciN	1,59	1,69
SL1686	ychJ	UPF0225 protein ychJ	1,22	-1,76
SL1697	ychN	Protein ychN	-1,02	-1,46
SL1704	prfA	Peptide chain release factor 1	1,50	-2,45
SL1711	pth	Peptidyl-tRNA hydrolase	1,89	1,35
SL1713	-	Hypothetical	1,06	-1,07
SL1727	emtA	Endo-type membrane-bound lytic murein transglycosylase A	1,24	1,76
SL1732	ycgB	Uncharacterized protein ycgB	-2,14	1,63
SL1738	-	Hypothetical Protein SL1738	-2,03	1,22
SL1741	ycgL	UPF0745 protein ycgL	1,31	-1,57
SL1752	yoaH	UPF0181 protein yoaH	1,08	-1,10
SL1764	rrmA	rRNA guanine-N1-methyltransferase	-1,04	1,16
SL1779	yebU	Ribosomal RNA small subunit methyltransferase F	1,12	-1,34
SL1788	-	Hypothetical Protein SL1788	-1,08	-1,24
SL1796	pinE	DNA-invertase from lambdoid prophage e14	-1,70	-1,63
SL1830	-	Cytoplasmic Protein	-1,03	-1,05
SL1836	aspS	Aspartyl-tRNA synthetase	1,51	-1,53
SL1844	argS	Arginyl-tRNA synthetase	1,08	1,29
SL1846	yesR	Unsaturated rhamnogalacturonyl hydrolase yesR	1,15	-1,00
SL1896	-	putative 50S ribosomal protein	-5,89	-2,08
SL1916	yodC	Uncharacterized protein yodC	-1,36	1,23
SL1987	-	Hypothetical	1,57	1,57
SL2052	hisH	Imidazole glycerol phosphate synthase subunit hisH	1,35	1,00
SL2114	cesT	Tir chaperone	-1,29	-2,12
SL2132	metG	Methionyl-tRNA synthetase	1,06	-1,18
SL2188	yeiP	Elongation factor P-like protein	1,72	4,21
SL2197	yejG	Uncharacterized protein yejG	-2,52	-1,24
SL2199	rsuA	Ribosomal small subunit pseudouridine synthase A	1,19	-1,20
SL2201	rplY	50S ribosomal protein L25	1,33	2,39
SL2204	yejL	UPF0352 protein yejL	1,96	1,33
SL2216	ydfU	Uncharacterized protein ydfU	1,01	1,41
SL2256	sseL	Deubiquitinase sseL	-1,90	-2,80
SL2298	-	Hypothetical	-1,06	-1,69
SL2327	-	Amino Acid Racemase	-1,24	3,25
SL2337	truA	tRNA pseudouridine synthase A	2,45	-1,95
SL2342	-	Bacteriophage Protein	-1,06	-2,20
SL2344	-	Hypothetical	1,46	-1,28
SL2349	yfcL	Uncharacterized protein yfcL	1,54	1,20
SL2381	gltX	Glutamyl-tRNA synthetase	1,65	1,02
SL2389	ypeB	Uncharacterized protein ypeB	1,19	-1,52
SL2397	-	Hypothetical	1,20	1,00
SL2400	yfeJ	Putative glutamine amidotransferase-like protein yfeJ	1,27	1,05
SL2416	ypfL	Uncharacterized protein ypfL	-1,04	-1,47
SL2438	-	Hypothetical	-1,36	-1,66
SL2469	-	Hypothetical	1,14	1,15

SL2480	yfgJ	Uncharacterized protein yfgJ	2,83	-1,79
SL2484	hisS	Histidyl-tRNA synthetase	1,17	-1,72
SL2496	-	Hypothetical	1,83	1,52
SL2507	trmJ	tRNA (cytidine/uridine-2'-O-)-methyltransferase trmJ	1,60	-1,95
SL2619	-	Hypothetical	-1,86	4,28
SL2622	rluD	Ribosomal large subunit pseudouridine synthase D	1,35	-1,08
SL2646	rplS	50S ribosomal protein L19	1,37	1,42
SL2647	trmD	tRNA (guanine-N(1)-)-methyltransferase	1,16	1,12
SL2653	-	Hypothetical	1,11	-1,03
SL2658	rnfH	Protein rnfH	1,41	1,32
SL2660	smpB	SsrA-binding protein	1,22	-1,23
SL2726	-	Hypothetical	-1,06	-1,59
SL2727	-	Hypothetical	-1,03	1,10
SL2731	-	Hypothetical	-1,03	-2,64
SL2751	-	Hypothetical	1,28	-1,26
SL2785	ygaC	Uncharacterized protein ygaC	1,25	-2,00
SL2807	alaS	Alanyl-tRNA synthetase	1,76	1,49
SL2881	-	Hypothetical	-2,29	-1,99
SL2882	-	Cytoplasmic Protein	-1,38	-2,06
SL2889	-	Hypothetical	1,56	1,08
SL2915	iap	Alkaline phosphatase isozyme conversion protein	1,28	-2,93
SL2917	ygbT	Uncharacterized protein ygbT	-2,29	-1,86
SL2918	ygcH	Uncharacterized protein ygcH	-2,65	-1,68
SL2938	rumA	23S rRNA (uracil-5-)-methyltransferase rumA	1,25	-1,61
SL3001	rcnR	Transcriptional repressor rcnR	1,09	-1,95
SL3003	-	Hypothetical	-1,52	-1,49
SL3004	-	Hypothetical	-2,02	-2,20
SL3016	lysS	Lysyl-tRNA synthetase	1,41	1,18
SL3017	prfB	Peptide chain release factor 2	1,43	-1,34
SL3023	ygfY	UPF0350 protein ygfY	1,31	1,71
SL3036	zapA	Cell division protein zapA	-1,04	1,30
SL3099	-	Hypothetical	-2,64	-1,60
SL3101	-	Hypothetical	-1,54	-1,15
SL3105	-	Hypothetical	-1,30	-1,37
SL3125	yghW	Uncharacterized protein yghW	-2,77	-1,23
SL3129	-	Hypothetical	-2,87	-2,96
SL3130	-	Hypothetical	-4,26	-3,85
SL3154	ygiN	Probable quinol monooxygenase ygiN	1,46	1,66
SL3158	yqiB	Uncharacterized protein yqiB	1,56	1,05
SL3174	glnE	Glutamate-ammonia-ligase adenylyltransferase	1,48	-1,02
SL3183	rpsU	30S ribosomal protein S21	1,14	-1,52
SL3193	rlmG	Ribosomal RNA large subunit methyltransferase G	-1,58	2,09
SL3208	yhaK	Pirin-like protein yhaK	-1,17	1,18
SL3251	-	Conserved Hypothetical Protein	1,11	-1,04
SL3256	rpsO	30S ribosomal protein S15	1,89	1,47
SL3257	truB	tRNA pseudouridine synthase B	3,01	1,31
SL3259	infB	Translation initiation factor IF-2	1,46	1,00
SL3263	-	Hypothetical	-2,25	-1,45
SL3269	ftsJ	cell division protein	1,51	-2,96
SL3271	greA	Transcription elongation factor greA	1,31	-2,91
SL3275	rpmA	50S ribosomal protein L27	-1,05	1,01
SL3276	rplU	50S ribosomal protein L21	1,08	1,19
SL3293	yhbH	Probable sigma(54) modulation protein	-1,04	1,74
SL3315	-	Hypothetical	1,25	1,63
SL3316	rpsI	30S ribosomal protein S9	1,18	1,58
SL3317	rplM	50S ribosomal protein L13	1,10	1,68
SL3335	yhcO	Uncharacterized protein yhcO	-1,51	2,41
SL3356	prmA	Ribosomal protein L11 methyltransferase	1,64	1,59
SL3369	rimN	Putative ribosome maturation factor rimN	-1,10	-1,91
SL3374	fmt	Methionyl-tRNA formyltransferase	-1,65	-4,23
SL3375	rsmB	Ribosomal RNA small subunit methyltransferase B	-1,63	-4,63
SL3381	rplQ	50S ribosomal protein L17	2,11	1,55
SL3383	rpsD	30S ribosomal protein S4	1,10	1,07
SL3384	rpsK	30S ribosomal protein S11	1,12	1,03
SL3385	rpsM	30S ribosomal protein S13	1,47	1,21
SL3386	rpmJ1	50S ribosomal protein L36 1	1,38	1,09
SL3388	rplO	50S ribosomal protein L15	1,35	1,35

SL3389	rpmD	50S ribosomal protein L30	1,36	1,35
SL3390	rpsE	30S ribosomal protein S5	1,17	1,20
SL3391	rplR	50S ribosomal protein L18	1,33	1,35
SL3392	rplF	50S ribosomal protein L6	1,20	1,16
SL3393	rpsH	30S ribosomal protein S8	1,34	1,29
SL3394	rpsN	30S ribosomal protein S14	1,57	1,42
SL3395	rplE	50S ribosomal protein L5	1,17	1,13
SL3396	rplX	50S ribosomal protein L24	1,18	1,18
SL3397	rplN	50S ribosomal protein L14	1,21	1,17
SL3398	rpsQ	30S ribosomal protein S17	1,74	1,65
SL3399	rpmC	50S ribosomal protein L29	1,84	1,94
SL3400	rplP	50S ribosomal protein L16	1,40	1,54
SL3401	rpsC	30S ribosomal protein S3	1,54	1,65
SL3402	rplV	50S ribosomal protein L22	1,43	1,52
SL3403	rpsS	30S ribosomal protein S19	1,21	1,27
SL3404	rplB	50S ribosomal protein L2	1,26	1,35
SL3405	rplW	50S ribosomal protein L23	1,20	1,19
SL3406	rplD	50S ribosomal protein L4	1,16	1,10
SL3407	rplC	50S ribosomal protein L3	1,31	1,27
SL3408	rpsJ	30S ribosomal protein S10	1,24	1,19
SL3412	tuf	Elongation factor Tu 1	1,19	1,30
SL3413	fusA	Elongation factor G	1,28	1,14
SL3414	rpsG	30S ribosomal protein S7	1,17	1,07
SL3415	rpsL	30S ribosomal protein S12	1,45	1,25
SL3420	fkpA	FKBP-type peptidyl-prolyl cis-trans isomerase fkpA	1,51	-2,17
SL3423	yheV	Uncharacterized protein yheV	1,27	1,43
SL3428	ydhR	Putative monooxygenase ydhR	-1,29	2,42
SL3430	yheU	UPF0270 protein yheU	-1,01	-1,12
SL3438	yhfG	Uncharacterized protein yhfG	1,29	1,82
SL3448	trpS	Tryptophanyl-tRNA synthetase	1,96	1,01
SL3464	hslR	Heat shock protein 15	1,74	1,68
SL3474	feoC	Ferrous iron transport protein C	-1,51	-1,86
SL3510	yhhW	Protein yhhW	-1,19	1,07
SL3514	-	Hypothetical	-9,24	-1,47
SL3525	yhhV	Uncharacterized protein yhhV	1,18	1,68
SL3558	yhiQ	UPF0341 protein yhiQ	-1,03	-1,62
SL3587	yhjS	Uncharacterized protein yhjS	-1,59	-1,43
SL3620	glyS	Glycyl-tRNA synthetase beta subunit	1,36	-1,01
SL3621	glyQ	Glycyl-tRNA synthetase alpha subunit	1,54	-1,43
SL3647	selB	Selenocysteine-specific elongation factor	1,42	1,03
SL3648	selA	L-seryl-tRNA(Sec) selenium transferase	1,59	1,20
SL3653	yibT	Uncharacterized protein yibT	-1,74	1,96
SL3654	yibL	Uncharacterized protein yibL	1,84	-1,49
SL3660	yibK	Uncharacterized tRNA/rRNA methyltransferase yibK	2,28	3,68
SL3693	rpmG	50S ribosomal protein L33	1,06	1,11
SL3694	rpmB	50S ribosomal protein L28	1,23	1,19
SL3709	trmH	tRNA guanosine-2'-O-methyltransferase	3,81	-1,10
SL3732	-	Hypothetical	1,21	1,47
SL3733	selA	Uncharacterized protein mlr3804	-1,24	1,48
SL3757	-	Hypothetical	-3,93	1,17
SL3806	rpmH	50S ribosomal protein L34	1,24	-1,01
SL3810	mnmE	tRNA modification GTPase mnmE	2,15	1,06
SL3866	-	Hypothetical	2,09	2,84
SL3867	-	Hypothetical	1,90	1,81
SL3870	ppiC	Peptidyl-prolyl cis-trans isomerase C	-1,07	1,96
SL3897	-	Hypothetical	1,03	-1,02
SL3943	yihD	Protein yihD	-1,16	1,06
SL3950	yihI	UPF0241 protein yihI	1,01	2,32
SL3961	-	Hypothetical	1,35	1,97
SL3974	dtd	D-tyrosyl-tRNA(Tyr) deacylase	1,11	-1,13
SL3977	ygjN	Uncharacterized protein ygjN	2,17	2,42
SL4005	yiiM	Protein yiiM	-1,18	1,19
SL4019	cdh	CDP-diacylglycerol pyrophosphatase	1,28	1,23
SL4037	zapB	Cell division protein zapB	1,13	1,55
SL4045	rpmE	50S ribosomal protein L31	1,44	2,30
SL4053	-	Hypothetical	1,43	3,84
SL4078	trmA	tRNA (uracil-5-)-methyltransferase	1,50	2,16

SL4085	tuf2	Elongation factor Tu 2	1,17	1,32
SL4088	rplK	50S ribosomal protein L11	1,11	1,26
SL4089	rplA	50S ribosomal protein L1	1,22	1,41
SL4090	rplJ	50S ribosomal protein L10	1,46	1,90
SL4091	rplL	50S ribosomal protein L7/L12	1,89	2,50
SL4095	-	Hypothetical	1,67	1,09
SL4097	-	Hypothetical	-1,18	1,24
SL4121	-	Hypothetical	1,05	1,25
SL4126	-	Hypothetical Protein SL4126	1,64	-1,11
SL4176	yjbJ	UPF0337 protein yjbJ	-1,54	1,00
SL4239	-	Hypothetical	-2,01	-39,41
SL4252	-	Hypothetical	-9,05	-6,03
SL4260	dsbD	Thiol:disulfide interchange protein dsbD	-1,68	-1,93
SL4271	efp	Elongation factor P	1,45	1,04
SL4294	miaA	tRNA dimethylallyltransferase	1,27	1,26
SL4302	rlmB	23S rRNA (guanosine-2'-O-)-methyltransferase rlmB	1,78	-2,06
SL4303	yjfI	Uncharacterized protein yjfI	1,92	-1,09
SL4323	-	Hypothetical	1,03	-1,64
SL4324	rpsF	30S ribosomal protein S6	1,38	1,33
SL4326	rpsR	30S ribosomal protein S18	1,65	1,46
SL4327	rplI	50S ribosomal protein L9	1,12	1,06
SL4330	fklB	FKBP-type 22 kDa peptidyl-prolyl cis-trans isomerase	1,31	1,35
SL4339	ytfK	Uncharacterized protein ytfK	-2,61	1,30
SL4341	msrA	Peptide methionine sulfoxide reductase msrA	-1,22	1,22
SL4344	ytfP	Gamma-glutamylcyclotransferase family protein ytfP	-1,62	-1,08
SL4361	iolC	5-dehydro-2-deoxygluconokinase	1,53	2,80
SL4365	-	Xylose Isomerase Domain-Containing Protein	-2,00	1,83
SL4367	yjgA	UPF0307 protein CKO_03595	1,24	2,15
SL4370	-	Hypothetical	1,02	1,43
SL4371	-	Hypothetical	-1,35	1,87
SL4372	-	Hypothetical	-1,14	1,96
SL4376	selA	Uncharacterized protein mlr3804	1,11	1,78
SL4380	relE	Toxin relE	1,29	2,64
SL4400	yjgD	Uncharacterized protein yjgD	1,67	1,02
SL4405	valS	Valyl-tRNA synthetase	2,29	-1,46
SL4421	-	Hypothetical	1,01	-1,49
SL4422	-	Hypothetical	1,20	1,08
SL4426	-	Hypothetical	1,98	1,31
SL4430	yjhP	Uncharacterized protein yjhP	1,09	2,13
SL4432	-	Hypothetical	2,24	4,12
SL4434	-	Hypothetical	-2,74	-5,31
SL4438	trpS	Tryptophanyl-tRNA synthetase	1,18	-1,00
SL4440	-	Hypothetical	1,04	-1,09
SL4460	-	Hypothetical	-1,03	2,69
SL4486	rimI	Ribosomal-protein-alanine acetyltransferase	2,38	1,46
SL4488	prfC	Peptide chain release factor 3	2,48	1,28
SL4527	lasT	Uncharacterized tRNA/rRNA methyltransferase lasT	-1,02	-1,00
		Purines, pyrimidines, nucleosides and nucleotides		
SL0067	carA	Carbamoyl-phosphate synthase small chain	1,80	-1,29
SL0068	carB	Carbamoyl-phosphate synthase large chain	2,14	1,63
SL0137	mutT	Mutator mutT protein	1,18	1,27
SL0141	guaC	GMP reductase	1,61	-1,25
SL0171	hpt	Hypoxanthine phosphoribosyltransferase	1,49	1,08
SL0219	pyrH	Uridylate kinase	1,44	1,04
SL0313	gpt	Xanthine phosphoribosyltransferase	1,55	1,53
SL0476	apt	Adenine phosphoribosyltransferase	1,25	-1,35
SL0481	adk	Adenylate kinase	1,81	-1,36
SL0484	gsk	Inosine-guanosine kinase	1,01	-1,22
SL0521	allD	Ureidoglycolate dehydrogenase	1,67	3,62
SL0526	purK	Phosphoribosylaminoimidazole carboxylase ATPase subunit	1,35	-1,78
SL0527	purE	Phosphoribosylaminoimidazole carboxylase catalytic subunit	1,53	-1,36
SL0650	rihA	Pyrimidine-specific ribonucleoside hydrolase rihA	1,27	2,11
SL0743	oadG2	Oxaloacetate decarboxylase gamma chain	-1,01	-1,27
SL0917	cmk	Cytidylate kinase	2,18	1,17
SL0998	pyrD	Dihydroorotate dehydrogenase	1,32	-1,10
SL1100	pyrC	Dihydroorotase	1,32	-1,29
SL1137	tmk	Thymidylate kinase	1,51	-1,79

SL1170	purB	Adenylosuccinate lyase	1,48	1,16
SL1220	yeaG	Uncharacterized protein yeaG	-2,71	1,34
SL1362	purR	HTH-type transcriptional repressor purR	1,31	-1,06
SL1395	add	Adenosine deaminase	1,47	1,39
SL1455	glsA2	Glutaminase 2	-1,66	1,84
SL1639	pyrF	Orotidine 5'-phosphate decarboxylase	1,20	2,89
SL1681	tdk	Thymidine kinase	1,74	1,46
SL1687	purU	Formyltetrahydrofolate deformylase	-1,10	-1,53
SL1708	prs	Ribose-phosphate pyrophosphokinase	1,41	-1,43
SL1817	purT	Phosphoribosylglycinamide formyltransferase 2	1,69	-1,06
SL1835	ntpA	dATP pyrophosphohydrolase	1,84	-1,63
SL1986	amn	AMP nucleosidase	-1,39	1,59
SL2057	udg	UDP-glucose 6-dehydrogenase	-3,00	-8,32
SL2098	dcd	Deoxycytidine triphosphate deaminase	-1,12	-1,01
SL2099	udk	Uridine kinase	1,34	-2,47
SL2160	cdd	Cytidine deaminase	-1,69	-10,57
SL2164	yeiA	Uncharacterized protein yeiA	-2,41	-1,59
SL2246	nrdA	Ribonucleoside-diphosphate reductase 1 subunit alpha	-1,40	-2,09
SL2247	nrdB	Ribonucleoside-diphosphate reductase 1 subunit beta	-1,06	-1,06
SL2268	arnA	Bifunctional polymyxin resistance protein ArnA	-2,26	-2,78
SL2331	purF	Amidophosphoribosyltransferase	-1,01	1,11
SL2385	xapA	Xanthosine phosphorylase	-1,14	-1,87
SL2450	purC	Phosphoribosylaminoimidazole-succinocarboxamide synthase	-1,11	-1,79
SL2461	upp	Uracil phosphoribosyltransferase	1,13	1,35
SL2462	purM	Phosphoribosylformylglycinamidine cyclo-ligase	1,20	-1,23
SL2471	guaA	GMP synthase [glutamine-hydrolyzing]	1,00	-1,28
SL2472	guaB	Inosine-5'-monophosphate dehydrogenase	-1,01	-1,30
SL2488	ndk	Nucleoside diphosphate kinase	2,19	5,40
SL2517	glyA	Serine hydroxymethyltransferase 1	1,49	1,49
SL2527	purL	Phosphoribosylformylglycinamidine synthase	1,53	1,31
SL2791	nrdI	Protein nrdI	-1,25	-1,12
SL2792	nrdE	Ribonucleoside-diphosphate reductase 2 subunit alpha	1,07	-1,19
SL2793	nrdF	Ribonucleoside-diphosphate reductase 2 subunit beta	-1,50	-1,26
SL2932	pyrG	CTP synthase	1,22	-1,60
SL2949	ygdH	LOG family protein ygdH	-1,40	1,34
SL2979	thyA	Thymidylate synthase	-1,05	-2,15
SL3157	icc	Protein icc	1,85	1,05
SL3306	codA	Cytosine deaminase	1,17	3,61
SL3325	oadG2	Oxaloacetate decarboxylase gamma chain 2	-1,02	-1,21
SL3697	dut	Deoxyuridine 5'-triphosphate nucleotidohydrolase	2,50	-1,09
SL3699	pyrE	Orotate phosphoribosyltransferase	1,46	1,40
SL3706	gmk	Guanylate kinase	1,53	-1,27
SL3708	spoT	Guanosine-3',5'-bis(diphosphate) 3'-pyrophosphohydrolase	0,00	-1,03
SL3882	rffH	Glucose-1-phosphate thymidylyltransferase 2	1,85	-1,27
SL3922	udp	Uridine phosphorylase	1,20	-1,10
SL4020	-	Conserved Hypothetical Protein	-1,79	1,41
SL4054	yfkN	Trifunctional nucleotide phosphoesterase protein yfkN	1,11	3,68
SL4114	purD	Phosphoribosylamine--glycine ligase	1,19	-1,01
SL4115	purH	Bifunctional purine biosynthesis protein purH	1,14	-1,45
SL4299	purA	Adenylosuccinate synthetase	1,33	-1,35
SL4336	cpdB	2',3'-cyclic-nucleotide 2'-phosphodiesterase/3'-nucleotidase	1,00	4,02
SL4375	-	Dihydroorotase	-1,49	1,62
SL4381	nrdG	Anaerobic ribonucleoside-triphosphate reductase-activating protein	1,64	-2,38
SL4382	nrdD	Anaerobic ribonucleoside-triphosphate reductase	1,15	-2,61
SL4390	pyrI	Aspartate carbamoyltransferase regulatory chain	1,00	4,61
SL4391	pyrB	Aspartate carbamoyltransferase	-1,05	3,84
SL4494	deoC	Deoxyribose-phosphate aldolase	1,50	-1,54
SL4495	deoA	Thymidine phosphorylase	1,41	-1,41
SL4496	deoB	Phosphopentomutase	1,06	-1,86
SL4497	deoD	Purine nucleoside phosphorylase deoD-type	-1,03	-1,54
		Regulatory functions		
SL0009	yaaH	Inner membrane protein yaaH	2,64	2,69
SL0014	ybdO	Uncharacterized HTH-type transcriptional regulator ybdO	1,30	1,36
SL0030	MarT	putative transcription regulator	-1,30	-1,18
SL0031	leuO	Probable HTH-type transcriptional regulator leuO	1,03	1,08
SL0032	-	Hypothetical	1,20	1,26

SL0053	citB	Transcriptional regulatory protein CitB	-1,15	2,03
SL0066	-	putative viral protein	-1,76	-4,07
SL0118	fruR	Fructose repressor	1,45	1,57
SL0151	pdhR	Pyruvate dehydrogenase complex repressor	-1,07	-2,19
SL0165	ygbI	Uncharacterized HTH-type transcriptional regulator ygbI	1,26	1,16
SL0187	dksA	DnaK suppressor protein	-1,17	0,00
SL0188	sfsA	Sugar fermentation stimulation protein A	1,60	-1,41
SL0251	yafC	Uncharacterized HTH-type transcriptional regulator yafC	-1,14	1,06
SL0328	ttdR	putative LysR family transcriptional regulator	-1,28	-1,14
SL0339	-	Transmembrane Regulator	-1,66	-1,63
SL0342	-	Response Regulator	-1,10	-1,72
SL0349	hmrR	HTH-type transcriptional regulator hmrR	-1,59	1,82
SL0358	pchR	AraC family transcriptional regulator	-1,98	-1,35
SL0388	mak	putative sugar kinase/putative transcriptional regulator (NagC/XylR family)	1,25	2,02
SL0392	phoB	Phosphate regulon transcriptional regulatory protein phoB	1,13	-1,59
SL0393	phoR	Phosphate regulon sensor protein phoR	1,14	-2,22
SL0405	yobV	Uncharacterized HTH-type transcriptional regulator yobV	1,11	-1,46
SL0406	yajD	Uncharacterized protein yajD	-1,15	-1,30
SL0412	nusB	N utilization substance protein B homolog	1,96	1,71
SL0424	phnR	Putative transcriptional regulator of 2-aminoethylphosphonate degradation operons	1,43	-1,05
SL0453	ybaO	Uncharacterized HTH-type transcriptional regulator ybaO	1,62	-1,17
SL0456	glnK	Nitrogen regulatory protein P-II 2	6,02	-1,15
SL0492	cueR	HTH-type transcriptional regulator cueR	2,00	2,31
SL0550	cusA	Sensor kinase	-1,55	-1,79
SL0551	ykgD	Uncharacterized HTH-type transcriptional regulator ykgD	-1,02	-1,11
SL0559	levR	Transcriptional regulatory protein levR	-1,64	4,63
SL0568	-	TetR Family Transcriptional Regulator	1,76	1,35
SL0569	ramA	Transcriptional activator ramA	-1,04	-1,01
SL0588	cstA	Carbon starvation protein A	-2,62	4,30
SL0594	ybdO	Uncharacterized HTH-type transcriptional regulator ybdO	-1,66	-1,83
SL0604	rnk	Regulator of nucleoside diphosphate kinase	1,16	-2,37
SL0613	dpiB	Sensor histidine kinase DpiB	-1,01	-1,36
SL0614	dpiA	Transcriptional regulatory protein DpiA	1,24	-1,36
SL0622	ybeF	Uncharacterized HTH-type transcriptional regulator ybeF	-1,94	-1,55
SL0630	ybeB	Uncharacterized protein ybeB	1,39	2,09
SL0640	yqiR	putative sigma-54 dependent transcriptional regulato	-1,25	1,01
SL0658	ybeZ	PhoH-like protein	2,34	-1,61
SL0664	nagC	N-acetylglucosamine repressor	1,39	-1,77
SL0672	citB	Citrate utilization protein B	-1,02	1,07
SL0675	fur	Ferric uptake regulation protein	-1,18	-3,29
SL0677	ybfE	Uncharacterized protein ybfE	1,77	-1,11
SL0684	kdpE	KDP operon transcriptional regulatory protein kdpE	1,14	-1,22
SL0685	kdpD	Sensor protein kdpD	1,22	-1,76
SL0695	ybgL	UPF0271 protein ybgL	-1,29	1,10
SL0740	ywbI	Uncharacterized HTH-type transcriptional regulator ywbI	1,43	3,78
SL0741	yjiE	Uncharacterized HTH-type transcriptional regulator yjiE	1,44	-1,64
SL0742	yfbS	Uncharacterized transporter MJ0672	1,33	-1,04
SL0766	hutC	Histidine utilization repressor	-1,13	-1,05
SL0795	ybiH	Uncharacterized HTH-type transcriptional regulator ybiH	2,00	1,33
SL0806	dps	DNA protection during starvation protein	-1,33	-1,23
SL0810	mntR	iron dependent repressor family transcriptional regulator	2,39	-1,04
SL0824	gsiA	Glutathione import ATP-binding protein gsiA	1,52	-1,02
SL0835	cysL	HTH-type transcriptional regulator cysL	-1,64	-6,20
SL0845	ybjK	Uncharacterized HTH-type transcriptional regulator ybjK	-1,10	1,14
SL0879	ybjX	Uncharacterized protein ybjX	-1,29	-3,90
SL0890	yafC	Uncharacterized HTH-type transcriptional regulator HI_1364	1,25	-1,12
SL0909	sopD2	Secreted effector protein sopD2	-3,00	-5,55
SL1022	ybcM	AraC family bacterial regulatory protein	-1,01	1,27
SL1034	copS	histidine kinase	1,34	-1,48
SL1035	copR	response regulator	1,07	-1,04
SL1039	hpaR	Homoprotocatechuate degradative operon repressor	-1,03	1,50
SL1047	ydiP	Transcriptional Regulator AraC Family	1,19	-1,52
SL1060	ycdC	putative transcriptional repressor (TetR/AcrR family)	1,12	1,43
SL1065	yfeT	Uncharacterized HTH-type transcriptional regulator HI_0143	1,29	-1,26
SL1079	csgD	Probable csgAB operon transcriptional regulatory protein	-2,40	-2,72
SL1168	phoQ	Virulence sensor histidine kinase phoQ	1,08	-1,74

SL1169	phoP	Virulence transcriptional regulatory protein phoP	-1,07	-1,41
SL1201	ycgE	Uncharacterized HTH-type transcriptional regulator ycgE	1,11	-1,47
SL1215	yeaM	Uncharacterized HTH-type transcriptional regulator yeaM	1,96	1,15
SL1220	yeaG	Uncharacterized protein yeaG	-2,71	1,34
SL1246	osmE	Osmotically-inducible lipoprotein E	-2,23	-1,22
SL1289	ydiP	Uncharacterized HTH-type transcriptional regulator ydiP	-1,25	-1,47
SL1300	ydiI	Esterase ydiI	-1,92	-1,48
SL1321	ttrR	Transcriptional regulatory protein fixJ	-1,28	1,02
SL1361	ydhB	Uncharacterized HTH-type transcriptional regulator ydhB	1,66	-1,22
SL1402	rstB	Sensor protein rstB	1,18	1,04
SL1405	rstA	Transcriptional regulatory protein rstA	-1,06	-1,68
SL1417	ynfL	Uncharacterized HTH-type transcriptional regulator ynfL	1,18	-1,70
SL1418	mlc	Protein mlc	2,13	1,99
SL1422	opuCB	Glycine betaine/carnitine/choline transport system permease protein opuCB	1,28	2,33
SL1449	marA	Multiple antibiotic resistance protein marA	2,50	2,07
SL1450	marR	Multiple antibiotic resistance protein marR	2,47	1,49
SL1453	yneJ	Uncharacterized HTH-type transcriptional regulator yneJ	1,68	-1,04
SL1476	-	MarR Family Transcriptional Regulator	1,82	-1,12
SL1506	-	TetR Family Transcriptional Regulator	-1,37	-1,04
SL1524	srfA	putative virulence effector protein	1,09	-1,08
SL1525	srfB	Virulence Protein SrfB	1,58	1,72
SL1529	ydcR	Uncharacterized HTH-type transcriptional regulator ydcR	-1,19	-1,63
SL1548	sgcR	Putative sgc region transcriptional regulator	-1,81	-1,48
SL1586	dbpA	ATP-independent RNA helicase dbpA	-1,14	1,31
SL1607	yhjC	Uncharacterized HTH-type transcriptional regulator yhjC	1,24	1,38
SL1636	yciT	Uncharacterized HTH-type transcriptional regulator yciT	-1,25	-2,20
SL1645	cysB	HTH-type transcriptional regulator cysB	-1,56	-1,72
SL1694	narX	Nitrate/nitrite sensor protein narX	2,12	-1,17
SL1697	ychN	Protein ychN	-1,02	-1,46
SL1701	sirB1	Protein sirB1	2,16	-1,27
SL1754	yeaB	putative NTP pyrophosphohydrolase	1,44	-1,68
SL1771	kdgR	Pectin degradation repressor protein kdgR	1,06	1,15
SL1775	proQ	ProP effector	1,57	-1,12
SL1885	fliA	RNA polymerase sigma factor for flagellar operon	-2,59	-1,03
SL2046	yeeY	Uncharacterized HTH-type transcriptional regulator yeeY	-1,25	1,04
SL2055	hisI	Histidine biosynthesis bifunctional protein hisIE	1,08	1,06
SL2075	galF	UTP--glucose-1-phosphate uridylyltransferase	1,16	-1,45
SL2100	yegE	Probable diguanylate cyclase YegE	1,05	-1,59
SL2122	yegW	Uncharacterized HTH-type transcriptional regulator yegW	1,09	1,35
SL2138	mlrA	HTH-type transcriptional regulator mlrA	-1,44	1,41
SL2172	-	Transcriptional Regulator	1,43	-1,42
SL2178	yeiE	Uncharacterized HTH-type transcriptional regulator yeiE	-1,10	-1,00
SL2240	rcsC	Sensor protein rcsC	1,37	-1,39
SL2244	ntaR	Nta operon transcriptional regulator	1,18	1,03
SL2250	yvbU	Uncharacterized HTH-type transcriptional regulator yvbU	1,84	2,54
SL2261	yfaX	Uncharacterized HTH-type transcriptional regulator yfaX	-1,26	-1,03
SL2302	yfbS	Uncharacterized transporter yfbS	1,22	1,05
SL2330	rocR	Arginine utilization regulatory protein rocR	2,26	2,10
SL2356	sixA	Phosphohistidine phosphatase sixA	1,22	2,37
SL2365	pgtB	Phosphoglycerate transport system sensor protein pgtB	-1,94	-1,91
SL2366	pgtC	Phosphoglycerate transport regulatory protein pgtC	-1,32	1,20
SL2372	yfeO	Putative ion-transport protein yfeO	-1,78	-1,53
SL2382	xapR	HTH-type transcriptional regulator xapR	-1,51	-1,02
SL2399	ptsJ	Putative transcriptional regulatory protein ptsJ	2,34	-1,26
SL2443	narQ	Nitrate/nitrite sensor protein narQ	1,13	-2,33
SL2453	gcvR	Glycine cleavage system transcriptional repressor	-1,33	-1,78
SL2523	glnB	Nitrogen regulatory protein P-II 1	-1,03	1,68
SL2524	yfhA	Uncharacterized protein yfhA	1,24	1,08
SL2525	yfhG	Uncharacterized protein yfhG	1,15	1,05
SL2526	yfhK	Putative sensor-like histidine kinase yfhK	1,28	-1,22
SL2542	era	GTP-binding protein era homolog	1,35	-2,06
SL2601	rseC	Sigma-E factor regulatory protein rseC	1,51	-1,19
SL2602	rseB	Sigma-E factor regulatory protein rseB	1,84	-1,45
SL2603	rseA	Sigma-E factor negative regulatory protein	1,24	-1,53
SL2608	yfiE	Uncharacterized HTH-type transcriptional regulator yfiE	-1,23	-1,58
SL2728	-	Cytoplasmic Protein	1,19	3,68

SL2732	-	Transcriptional Regulator XRE Family	-1,14	-1,01
SL2764	ybjX	Uncharacterized protein ybjX	-1,03	-5,61
SL2765	mig-14	putative transcriptional regulator	-1,26	-6,91
SL2778	ygaE	Uncharacterized HTH-type transcriptional regulator ygaE	-1,84	-1,60
SL2787	mocR	Probable rhizopine catabolism regulatory protein mocR	1,26	1,58
SL2806	csrA	Carbon storage regulator homolog	1,15	1,44
SL2819	norR	Anaerobic nitric oxide reductase transcription regulator norR	1,53	-1,07
SL2833	hycA	Formate hydrogenlyase regulatory protein hycA	1,39	-2,89
SL2891	ptxR	HTH-type transcriptional regulator ptxR	1,23	1,34
SL2898	ygbI	Uncharacterized HTH-type transcriptional regulator ygbI	2,02	1,56
SL2939	barA	Signal transduction histidine-protein kinase BarA	1,92	-1,45
SL2949	ygdH	LOG family protein ygdH	-1,40	1,34
SL2962	gcvA	Glycine cleavage system transcriptional activator	1,25	-3,31
SL2982	rppH	RNA pyrophosphohydrolase	-1,12	-1,45
SL2990	ascG	HTH-type transcriptional regulator AscG	1,08	1,40
SL2998	allS	HTH-type transcriptional activator AllS	1,41	-1,25
SL3073	-	global regulatory protein	-1,01	1,44
SL3095	budR	HTH-type transcriptional regulator BudR	2,76	1,82
SL3137	yqhC	Uncharacterized HTH-type transcriptional regulator yqhC	1,53	1,11
SL3149	ygiV	Probable transcriptional regulator ygiV	-1,35	-1,02
SL3151	qseB	Transcriptional regulatory protein qseB	1,91	1,46
SL3152	qseC	Sensor protein qseC	1,88	1,10
SL3185	rpoD	RNA polymerase sigma factor rpoD	1,52	-1,54
SL3207	yhaJ	Uncharacterized HTH-type transcriptional regulator yhaJ	1,10	1,23
SL3217	tdcA	HTH-type transcriptional regulator tdcA	-1,35	32,27
SL3300	arcB	Aerobic respiration control sensor protein ArcB	2,05	1,77
SL3312	nanR	Transcriptional regulator nanR	1,05	-1,21
SL3314	sspA	Stringent starvation protein A	1,12	-1,19
SL3328	yfbS	Uncharacterized transporter MJ0672	1,48	2,26
SL3330	pdhR	GntR Family Transcriptional Regulator	2,07	1,35
SL3332	argR	Arginine repressor	1,37	1,65
SL3339	aaeR	HTH-type transcriptional activator AaeR	1,25	1,45
SL3340	tldD	Protein tldD	1,62	-1,64
SL3379	zntR	HTH-type transcriptional regulator zntR	1,15	1,50
SL3469	ompR	Transcriptional regulatory protein ompR	1,14	1,11
SL3500	yfaX	Uncharacterized HTH-type transcriptional regulator yfaX	1,77	1,06
SL3567	yvoA	HTH-type transcriptional repressor yvoA	2,22	1,62
SL3571	yhjB	Putative HTH-type transcriptional regulator yhjB	-3,15	-4,61
SL3572	yhjC	Uncharacterized HTH-type transcriptional regulator yhjC	1,56	1,62
SL3599	celR	HTH-type transcriptional regulator celR	1,11	1,12
SL3610	bisC	Biotin sulfoxide reductase	1,29	-1,37
SL3627	xylR	Xylose operon regulatory protein	-1,25	1,04
SL3643	yisR	Uncharacterized HTH-type transcriptional regulator yisR	-1,14	2,76
SL3646	yajF	Uncharacterized protein CPE0188	-1,45	-2,40
SL3658	lldR	Putative L-lactate dehydrogenase operon regulatory protein	1,16	2,01
SL3661	idnR	HTH-type transcriptional regulator idnR	1,45	1,45
SL3698	slmA	HTH-type protein slmA	1,79	1,06
SL3702	ybeF	LysR Family Transcriptional Regulator	1,49	-1,14
SL3708	spoT	Guanosine-3',5'-bis(diphosphate) 3'-pyrophosphohydrolase	0,00	-1,03
SL3738	levR	Transcriptional regulatory protein levR	1,86	2,42
SL3751	mngR	Mannosyl-D-glycerate transport/metabolism system repressor mngR	1,51	5,24
SL3768	dsdC	HTH-type transcriptional regulator dsdC	2,09	3,74
SL3790	torR	TorCAD operon transcriptional regulatory protein torR	1,22	2,32
SL3791	torT	Periplasmic protein torT	-1,00	-1,23
SL3797	dgoR	Galactonate operon transcriptional repressor	1,12	1,20
SL3801	ybhD	Uncharacterized HTH-type transcriptional regulator ybhD	1,52	2,82
SL3815	yidZ	HTH-type transcriptional regulator yidZ	1,03	-1,08
SL3820	phoU	Phosphate transport system protein phoU	1,06	1,09
SL3843	asnC	Regulatory protein AsnC	1,42	1,26
SL3846	ravA	ATPase ravA	1,08	1,69
SL3853	rbsR	Ribose operon repressor	-1,12	1,19
SL3858	hdfR	HTH-type transcriptional regulator hdfR	-1,07	-1,60
SL3868	ilvY	HTH-type transcriptional regulator ilvY	-1,18	1,71
SL3873	gppA	Guanosine-5'-triphosphate,3'-diphosphate pyrophosphatase	1,11	-1,70
SL3894	cyaA	Adenylate cyclase	-1,85	-3,10
SL3918	metR	HTH-type transcriptional regulator metR	-1,19	1,31

SL3931	rfaH	Transcriptional activator rfaH	1,65	1,40
SL3952	glnG	Nitrogen regulation protein NR(I)	1,89	-1,32
SL3953	glnL	Nitrogen regulation protein NR(II)	1,84	-2,53
SL3980	-	Transcriptional Regulator XRE Family	1,24	2,38
SL3997	rhaS	HTH-type transcriptional activator rhaS	1,02	5,18
SL3998	rhaR	HTH-type transcriptional activator rhaR	1,77	5,45
SL4007	cpxA	Sensor protein cpxA	1,76	1,19
SL4008	cpxR	Transcriptional regulatory protein cpxR	1,29	1,77
SL4017	mngR	Mannosyl-D-glycerate transport/metabolism system repressor mngR	1,08	1,37
SL4043	cytR	HTH-type transcriptional repressor cytR	1,47	-1,04
SL4048	metJ	Met repressor	1,75	1,96
SL4066	yijO	Uncharacterized HTH-type transcriptional regulator yijO	-1,18	1,61
SL4074	oxyR	Hydrogen peroxide-inducible genes activator	1,06	1,13
SL4104	rsd	Regulator of sigma D	-1,21	2,95
SL4112	zraS	Sensor protein zraS	1,79	2,94
SL4166	malE	Maltose-binding periplasmic protein	-2,38	3,45
SL4174	lexA	LexA repressor	1,01	2,04
SL4177	zur	Zinc uptake regulation protein	-1,30	1,33
SL4202	soxR	Redox-sensitive transcriptional activator soxR	1,08	-1,18
SL4206	ywbI	Uncharacterized HTH-type transcriptional regulator ywbI	1,54	-1,23
SL4224	phnO	Protein phnO	-1,02	-1,23
SL4228	basS	Sensor protein BasS	-1,64	-1,57
SL4229	basR	Transcriptional regulatory protein BasR	-1,16	-1,38
SL4240	dcuR	Transcriptional regulatory protein dcuR	1,35	-1,23
SL4241	dcuS	Sensor protein dcuS	2,28	-1,84
SL4250	rtsB	GerE Family Regulatory Protein	-62,07	-9,42
SL4258	ybbI	Transcriptional Regulator MerR Family	1,12	1,29
SL4259	yjdC	HTH-type transcriptional regulator yjdC	-1,50	-1,25
SL4274	ecnR	Transcriptional regulatory protein entR	-1,50	-1,08
SL4296	hflX	GTP-binding protein hflX	1,40	-1,11
SL4300	nsrR	HTH-type transcriptional repressor nsrR	1,35	-1,24
SL4304	yjfJ	Uncharacterized protein YjfJ	1,65	-1,08
SL4314	ulaR	HTH-type transcriptional regulator ulaR	1,85	2,20
SL4355	ydiP	Uncharacterized HTH-type transcriptional regulator ydiP	1,22	4,58
SL4393	argR	Arginine repressor	-1,76	1,94
SL4395	arcB	Ornithine carbamoyltransferase, catabolic	-2,08	2,30
SL4397	arcA	Arginine deiminase	-1,86	3,40
SL4411	idnR	HTH-type transcriptional regulator idnR	-1,66	-1,15
SL4442	yjiE	Uncharacterized HTH-type transcriptional regulator yjiE	-1,88	1,59
SL4463	yjiY	Inner membrane protein yjiY	-1,46	-3,30
SL4465	levR	Transcriptional regulatory protein levR	-1,99	-1,08
SL4478	yjjQ	Uncharacterized protein yjjQ	1,25	1,52
SL4479	bglJ	Transcriptional activator protein BglJ	1,33	2,06
SL4480	ywhH	Uncharacterized protein ywhH	1,13	1,61
SL4510	trpR	Trp operon repressor	1,82	1,68
SL4513	rob	Right origin-binding protein	1,35	-1,20
SL4515	creB	Transcriptional regulatory protein creB	2,42	1,12
SL4516	creC	Sensor protein creC	2,76	-1,13
SL4525	arcA	Aerobic respiration control protein ArcA	1,41	1,15
		Transcription		
SL0053	citB	Transcriptional regulatory protein CitB	-1,15	2,03
SL0097	hepA	ATP-dependent helicase HepA	1,23	-1,39
SL0185	pcnB	Poly(A) polymerase	1,20	-1,44
SL0231	rnhB	Ribonuclease HII	2,34	-2,44
SL0258	rnhA	Ribonuclease H	1,77	1,48
SL0605	rna	Ribonuclease I	1,45	-1,99
SL0672	citB	Citrate utilization protein B	-1,02	1,07
SL0695	ybgL	UPF0271 protein ybgL	-1,29	1,10
SL0796	rhlE	ATP-dependent RNA helicase rhlE	1,88	-1,21
SL0900	rarA	Replication-associated recombination protein A	1,49	-1,73
SL1122	rne	Ribonuclease E	1,87	-1,25
SL1366	rnt	Ribonuclease T	1,25	-1,86
SL1633	rnb	Exoribonuclease 2	1,51	-1,02
SL1745	rnd	Ribonuclease D	1,68	-2,92
SL1810	holE	DNA polymerase III subunit theta	1,19	4,58
SL2107	baeS	Signal transduction histidine-protein kinase BaeS	-1,25	-2,41

SL2108	baeR	Transcriptional regulatory protein BaeR	-1,21	-1,68
SL2200	yejH	Uncharacterized protein yejH	1,28	-1,26
SL2543	rnc	Ribonuclease 3	1,19	-2,16
SL2604	rpoE	RNA polymerase sigma-E factor	1,73	-1,85
SL2607	srmB	ATP-dependent RNA helicase srmB	1,47	2,07
SL2624	raiA	Ribosome-associated inhibitor A	-2,75	1,85
SL2756	fljB	Phase 2 flagellin	-7,31	-1,25
SL2768	tctE	Sensor protein tctE	1,31	3,07
SL2769	tctD	Transcriptional regulatory protein tctD	1,65	3,86
SL2903	rpoS	RNA polymerase sigma factor rpoS	-1,21	-1,28
SL3177	cca	Multifunctional CCA protein	1,33	-2,17
SL3185	rpoD	RNA polymerase sigma factor rpoD	1,52	-1,54
SL3253	deaD	Cold-shock DEAD box protein A	1,01	-7,63
SL3255	pnp	Polyribonucleotide nucleotidyltransferase	-1,02	-1,57
SL3258	rbfA	Ribosome-binding factor A	3,05	1,32
SL3260	nusA	Transcription elongation protein nusA	1,26	-1,16
SL3292	rpoN	RNA polymerase sigma-54 factor	1,30	-1,34
SL3382	rpoA	DNA-directed RNA polymerase subunit alpha	1,25	1,15
SL3470	greB	Transcription elongation factor greB	1,58	-2,08
SL3485	rtcA	Probable RNA 3'-terminal phosphate cyclase	-1,95	-2,07
SL3533	rpoH	RNA polymerase sigma-32 factor	1,22	-1,39
SL3573	yhjD	Inner membrane protein yhjD	1,20	-1,07
SL3700	rph	Ribonuclease PH	1,61	1,16
SL3707	rpoZ	DNA-directed RNA polymerase subunit omega	1,34	1,42
SL3738	levR	Transcriptional regulatory protein levR	1,86	2,42
SL3807	rnpA	Ribonuclease P protein component	1,57	-1,46
SL3874	rhlB	ATP-dependent RNA helicase rhlB	1,37	-1,64
SL3876	rho	Transcription termination factor rho	-1,48	-2,45
SL3973	rbn	UPF0761 membrane protein CKO_03126	-1,14	1,36
SL4087	nusG	Transcription antitermination protein nusG	1,98	-1,44
SL4092	rpoB	DNA-directed RNA polymerase subunit beta	1,48	-1,13
SL4093	rpoC	DNA-directed RNA polymerase subunit beta'	1,49	1,34
SL4228	basS	Sensor protein BasS	-1,64	-1,57
SL4301	rnr	Ribonuclease R	1,13	1,04
SL4389	yjgF	UPF0076 protein yjgF	1,24	1,68
		Transport and binding proteins		
SL1247	celA	N,N'-diacetylchitobiose-specific phosphotransferase enzyme IIB component	1,04	-1,41
SL1248	celB	N,N'-diacetylchitobiose permease IIC component	1,58	-1,52
SL1546	sgcA	Putative phosphotransferase IIA component sgcA	-2,17	-1,02
SL2137	yehU	Inner membrane protein yehU	2,49	10,40
SL2181	fruA	PTS system fructose-specific EIIBC component	-1,36	-2,54
SL2311	ulaA	Ascorbate-specific permease IIC component ulaA	-2,08	-1,15
SL2312	ulaB	putative sugar phosphotransferase component IIB	-1,30	1,16
SL2313	ulaC	Ascorbate-specific phosphotransferase enzyme IIA component	1,88	2,57
SL2532	ybbF	Putative PTS system EIIBC component ybbF	1,08	2,21
SL3228	fruA	PTS system fructose-specific EIIABC component	-14,19	-2,16
SL3231	gatA	Galactitol-specific phosphotransferase enzyme IIA component	-1,64	-1,18
SL3233	gatC	Galactitol permease IIC component	-1,71	1,61
SL3294	ptsN	Nitrogen regulatory protein	1,38	1,74
SL3643	yisR	Uncharacterized HTH-type transcriptional regulator yisR	-1,14	2,76
SL3735	agaC	N-acetylgalactosamine permease IIC component 1	-1,63	1,68
SL3736	levE	Fructose-specific phosphotransferase enzyme IIB component	-1,32	2,33
SL4468	agaC	N-acetylgalactosamine permease IIC component 1	-1,16	3,49
SL0006	yaaJ	Uncharacterized transporter yaaJ	2,57	1,05
SL0040	nhaA	Na(+)/H(+) antiporter nhaA	1,38	-1,78
SL0041	nhaR	Transcriptional activator protein nhaR	1,24	-1,85
SL0043	xylP	putative sodium galactoside symporter	1,13	5,23
SL0054	citA	Sensor histidine kinase CitA	-1,02	1,55
SL0055	oadB1	Oxaloacetate decarboxylase beta chain 1	1,11	1,66
SL0056	oadA	Oxaloacetate decarboxylase alpha chain	-1,07	1,16
SL0057	oadG1	Probable oxaloacetate decarboxylase gamma chain 1	2,26	8,83
SL0058	citC	Citrate-sodium symporter	1,31	9,18
SL0087	kefC	Glutathione-regulated potassium-efflux system protein kefC	1,54	-1,64
SL0106	yabJ	Thiamine import ATP-binding protein ThiQ	1,45	1,04
SL0107	yabK	Thiamine transport system permease protein thiP	2,06	-1,24
SL0108	tbpA	thiamine-binding periplasmic protein	1,03	1,05

SL0109	yabN	putative ABC transporter periplasmic solute binding protein	1,77	-1,04
SL0147	ampE	Protein AmpE	-1,09	-1,26
SL0148	uidB	glycosyl hydrolase	1,35	1,49
SL0149	yicJ	Inner membrane symporter yicJ	1,11	2,14
SL0150	aroP	Aromatic amino acid transport protein AroP	-1,36	1,74
SL0156	-	secreted protein	1,83	2,65
SL0162	kdgT	2-keto-3-deoxygluconate permease 1	1,31	1,66
SL0173	yadG	Uncharacterized ABC transporter ATP-binding protein yadG	1,28	-1,21
SL0174	yadH	Inner membrane transport permease yadH	1,44	-1,19
SL0179	yadI	Putative phosphotransferase enzyme IIA component yadI	1,14	1,35
SL0193	fhuC	Iron(3+)-hydroxamate import ATP-binding protein fhuC	-1,03	-1,19
SL0194	fhuD	Iron(3+)-hydroxamate-binding protein fhuD	1,02	-1,12
SL0204	yadQ	putative ClC family chlorine transport protein	1,69	-1,12
SL0207	btuF	Vitamin B12-binding protein	1,83	1,02
SL0213	shiA	Shikimate transporter	-1,15	-2,58
SL0247	yaeE	D-methionine transport system permease protein	1,04	-1,08
SL0248	metN1	Methionine import ATP-binding protein MetN 1	1,31	-1,22
SL0252	ytbD	Uncharacterized MFS-type transporter ytbD	1,36	1,81
SL0273	-	Hypothetical	1,64	-1,09
SL0282	sciU	secreted protein	1,43	-1,03
SL0323	ynfM	Inner membrane transport protein ynfM	-1,40	1,10
SL0337	-	Periplasmic Protein	1,12	-2,46
SL0348	actP	Copper-transporting P-type ATPase	-1,04	1,67
SL0350	-	putative copper chaperone	1,34	1,61
SL0351	yjhB	Putative metabolite transport protein yjhB	2,13	1,58
SL0359	foxA	Ferrioxamine B receptor	1,07	1,14
SL0360	yahN	Uncharacterized membrane protein yahN	1,48	5,41
SL0371	sbmA	Protein sbmA	1,36	-3,76
SL0394	brnQ	Branched-chain amino acid transport system 2 carrier protein	1,49	1,06
SL0395	proY	Proline-specific permease proY	1,62	-2,21
SL0407	tsx	Nucleoside-specific channel-forming protein tsx	2,44	3,41
SL0415	yajO	Uncharacterized oxidoreductase yajO	-3,14	-1,02
SL0430	yajR	Inner membrane transport protein yajR	1,51	-1,42
SL0454	mdlA	Multidrug resistance-like ATP-binding protein mdlA	1,92	-1,43
SL0455	mdlB	Multidrug resistance-like ATP-binding protein mdlB	1,75	-1,26
SL0457	amtB	Ammonia channel	2,71	1,97
SL0468	acrB	Acriflavine resistance protein B	1,70	-2,14
SL0470	acrR	HTH-type transcriptional regulator AcrR	1,31	-1,34
SL0485	ybaL	Inner membrane protein ybaL	-1,62	-3,63
SL0490	-	secreted protein	-1,77	-1,19
SL0491	copA	Copper-exporting P-type ATPase A	1,09	1,12
SL0495	ybbL	Uncharacterized ABC transporter ATP-binding protein ybbL	1,95	-1,17
SL0500	ybbA	Uncharacterized ABC transporter ATP-binding protein ybbA	-1,21	-2,38
SL0504	sfbB	Methionine import ATP-binding protein	-3,94	-2,65
SL0505	sfbC	Probable D-methionine transport system permease protein	-3,31	-2,41
SL0513	yybO	metabolite transport protein	-1,04	1,01
SL0515	ybbW	Putative allantoin permease	-1,04	1,49
SL0517	ybbY	Putative purine permease ybbY	-1,48	-1,02
SL0557	ybdG	Uncharacterized protein ybdG	-1,03	-1,40
SL0562	manZ	Mannose permease IID component	1,26	2,31
SL0563	manY	Mannose permease IIC component	1,12	1,81
SL0564	manX	PTS system mannose-specific EIIAB component	1,01	1,21
SL0565	manX	PTS System Fructocific IIA Component	1,14	1,14
SL0572	entD	4'-phosphopantetheinyl transferase entD	-1,01	-1,32
SL0573	fepA	Ferrienterobactin receptor	1,26	1,32
SL0574	fes	Enterochelin esterase	1,05	-1,47
SL0577	fepE	Ferric enterobactin transport protein fepE	1,29	1,38
SL0578	fepC	Ferric enterobactin transport ATP-binding protein fepC	1,22	-1,38
SL0579	fepG	Ferric enterobactin transport system permease protein fepG	1,78	1,02
SL0580	fepD	Ferric enterobactin transport system permease protein fepD	1,57	1,06
SL0581	ybdA	membrane protein p43	1,23	-1,06
SL0585	entB	Isochorismatase	1,59	2,00
SL0615	dcuC	Anaerobic C4-dicarboxylate transporter dcuC	2,36	-1,19
SL0639	kdgT2	2-keto-3-deoxygluconate permease 2	-1,65	-3,33
SL0651	gltL	Glutamate/aspartate transport ATP-binding protein gltL	4,20	3,26
SL0652	gltK	Glutamate/aspartate transport system permease protein gltK	2,67	2,42
SL0653	gltJ	Glutamate/aspartate transport system permease protein gltJ	1,55	1,58

SL0654	gltI	Glutamate/aspartate periplasmic-binding protein	2,61	1,58
SL0667	nagE	PTS system N-acetylglucosamine-specific EIICBA component	-1,53	1,39
SL0671	citA	Citrate-proton symporter	-1,37	1,56
SL0682	potE	Putrescine-ornithine antiporter	2,35	-1,11
SL0686	kdpC	Potassium-transporting ATPase C chain	1,45	1,32
SL0688	kdpA	Potassium-transporting ATPase A chain	1,61	-1,03
SL0689	ybfA	Uncharacterized protein ybfA	-1,93	-1,87
SL0691	dtpD	Dipeptide permease D	3,04	-4,97
SL0728	tolR	Protein tolR	1,38	-1,97
SL0730	tolB	Protein tolB	1,49	1,13
SL0734	pnuC	Nicotinamide riboside transporter pnuC	-1,72	1,31
SL0735	zitB	Zinc transporter zitB	-2,06	1,09
SL0745	oadB2	Oxaloacetate decarboxylase beta chain	1,30	1,69
SL0747	fecD	Putative ABC transporter permease protein MJ0087	2,46	1,24
SL0748	fhuC	Iron(3+)-hydroxamate import ATP-binding protein fhuC	1,75	1,18
SL0755	modF	Putative molybdenum transport ATP-binding protein modF	-1,15	-1,22
SL0756	modE	Transcriptional regulator modE	1,45	-1,13
SL0758	modA	Molybdate-binding periplasmic protein	-1,24	-1,02
SL0759	modB	Molybdenum transport system permease protein modB	-1,51	-1,52
SL0760	modC	Molybdenum import ATP-binding protein ModC	-2,18	-1,47
SL0793	ybhF	Uncharacterized ABC transporter ATP-binding protein ybhF	1,03	-2,64
SL0794	ybhG	UPF0194 membrane protein CKO_02332	-1,01	-2,11
SL0802	ybiO	Uncharacterized mscS family protein ybiO	1,36	-1,40
SL0803	glnQ	Glutamine transport ATP-binding protein glnQ	3,21	-1,17
SL0805	glnH	Glutamine-binding periplasmic protein	3,04	1,24
SL0813	ybiT	Uncharacterized ABC transporter ATP-binding protein ybiT	1,41	-3,51
SL0816	ybiT	Hypothetical Protein ybiT	1,11	-1,50
SL0825	gsiB	Glutathione-binding protein gsiB	1,07	1,50
SL0826	gsiC	Glutathione transport system permease protein gsiC	1,05	1,28
SL0827	gsiD	Glutathione transport system permease protein gsiD	1,10	1,19
SL0844	ybjJ	Inner membrane protein ybjJ	1,53	-1,33
SL0846	ybjL	Putative transport protein ybjL	1,25	-3,92
SL0854	potF	Putrescine-binding periplasmic protein	-1,01	-1,24
SL0856	potH	Putrescine transport system permease protein potH	1,37	1,11
SL0857	potI	Putrescine transport system permease protein potI	-1,03	-1,34
SL0861	sgaB	Phosphotransferase II B Component	-1,29	-1,16
SL0863	artJ	ABC transporter arginine-binding protein 1	1,60	-1,57
SL0864	artM	Arginine ABC transporter permease protein ArtM	1,90	-1,51
SL0865	artQ	Arginine ABC transporter permease protein ArtQ	1,53	-1,48
SL0866	artI	Putative ABC transporter arginine-binding protein 2	1,33	1,07
SL0867	artP	Arginine transport ATP-binding protein ArtP	1,48	-1,48
SL0881	macB	Macrolide export ATP-binding/permease protein macB	-1,32	-3,32
SL0894	cydC	ATP-binding/permease protein cydC	1,04	-1,12
SL0895	cydD	ATP-binding/permease protein cydD	-1,09	-2,15
SL0905	ycaD	Uncharacterized MFS-type transporter ycaD	-3,14	-2,48
SL0906	ycaM	Inner membrane transporter ycaM	-1,22	2,46
SL0911	focA	Probable formate transporter 1	-1,13	-3,08
SL0921	msbA	Lipid A export ATP-binding/permease protein msbA	1,56	-1,41
SL0940	yflA	putative transcriptional regulator, Lrp family	1,44	1,65
SL1002	uup	ABC transporter ATP-binding protein uup	2,58	1,36
SL1017	yccT	UPF0319 protein yccT	-1,39	1,22
SL1046	hpaX	putative 4-hydroxyphenylacetate permease	1,15	1,35
SL1061	-	Uncharacterized protein R02472	1,58	3,52
SL1063	putP	Sodium/proline symporter	1,44	3,39
SL1064	phoH	Protein phoH	-43,63	-2,38
SL1066	sglT	Sodium/glucose cotransporter	-1,89	-1,01
SL1076	csgG	Curli production assembly/transport component csgG	-1,23	-2,40
SL1078	csgE	Curli production assembly/transport component csgE	-2,05	-2,07
SL1141	fhuE	FhuE receptor	1,03	-1,36
SL1154	lolC	Lipoprotein-releasing system transmembrane protein lolC	2,06	-1,78
SL1155	lolD	Lipoprotein-releasing system ATP-binding protein LolD	1,88	-1,69
SL1156	lolE	Lipoprotein-releasing system transmembrane protein lolE	1,92	-1,72
SL1159	potD	Spermidine/putrescine-binding periplasmic protein	1,41	-1,01
SL1160	potC	Spermidine/putrescine transport system permease protein potC	1,54	-1,11
SL1162	potB	Spermidine/putrescine transport system permease protein potB	1,47	1,10
SL1163	potA	Spermidine/putrescine import ATP-binding protein PotA	1,79	1,49
SL1174	-	Hypothetical	1,90	1,60

SL1185	-	Lysozyme Inhibitor	-1,17	-1,77
SL1191	xp55	Protein XP55	4,46	4,29
SL1192	dppB	Putative peptide transport system permease protein BMEII0209	5,39	3,41
SL1193	nikC	Putative peptide transport system permease protein BruAb2_1032	3,80	1,93
SL1195	potA	Spermidine/putrescine import ATP-binding protein PotA	2,18	2,07
SL1198	yodA	Metal-binding protein yodA	-1,14	2,10
SL1205	leuE	Leucine efflux protein	-1,15	-1,15
SL1212	-	Hypothetical	-1,19	-1,52
SL1214	yeaN	Inner membrane transport protein yeaN	1,59	-1,22
SL1248	celB	N,N'-diacetylchitobiose permease IIC component	1,58	-1,52
SL1249	celC	N,N'-diacetylchitobiose-specific phosphotransferase enzyme IIA component	-1,00	-1,96
SL1255	ydjN	Uncharacterized symporter ydjN	1,50	1,84
SL1274	btuC	Vitamin B12 import system permease protein BtuC	1,75	1,16
SL1275	btuE	Vitamin B12 transport periplasmic protein BtuE	1,39	1,68
SL1276	btuD	Vitamin B12 import ATP-binding protein BtuD	-1,08	1,42
SL1294	ydiN	Inner membrane transport protein ydiN	-1,96	-1,80
SL1295	ydiN	Inner membrane transport protein ydiN	-1,02	1,02
SL1296	ydiM	Inner membrane transport protein ydiM	-1,88	-1,30
SL1302	ydjN	Uncharacterized symporter ydjN	1,78	8,97
SL1305	sufC	Probable ATP-dependent transporter sufC	-1,67	-1,86
SL1313	puuP	Putrescine importer	-2,18	2,88
SL1357	mdtK	Multidrug resistance protein mdtK	-1,46	-2,08
SL1360	ydhC	Inner membrane transport protein ydhC	1,21	-8,66
SL1374	ydhJ	Uncharacterized protein ydhJ	1,84	-1,33
SL1384	dtpA	Dipeptide and tripeptide permease A	-1,11	-1,35
SL1403	aepA	Exoenzymes regulatory protein AepA	-1,85	-1,60
SL1407	ydgI	Putative arginine/ornithine antiporter	1,22	1,44
SL1412	mdtJ	Spermidine export protein mdtJ	1,38	2,91
SL1413	mdtI	Spermidine export protein mdtI	1,14	2,62
SL1416	ynfM	Inner membrane transport protein ynfM	1,25	-1,07
SL1420	clcB	Voltage-gated ClC-type chloride channel clcB	2,09	1,29
SL1421	opuBA	Choline transport ATP-binding protein opuBA	1,21	2,34
SL1423	opuCC	Glycine betaine/carnitine/choline-binding protein	1,51	2,35
SL1424	opuCB	Glycine betaine/carnitine/choline transport system permease protein opuCB	1,13	2,03
SL1437	ydfJ	Putative inner membrane metabolite transport protein ydfJ	1,15	1,70
SL1446	ydeE	Uncharacterized MFS-type transporter ydeE	-2,20	-1,51
SL1448	marB	Multiple antibiotic resistance protein marB	1,55	1,52
SL1452	sotB	Probable sugar efflux transporter	-1,53	-7,72
SL1472	exuT	Hexuronate transporter	-1,64	1,38
SL1474	tetA	Tetracycline resistance protein, class G	1,40	1,45
SL1486	-	Uncharacterized Na(+)/H(+) antiporter HI_1107	1,10	2,78
SL1503	ompD	Outer membrane porin protein ompD	1,04	1,26
SL1507	narU	Nitrite extrusion protein 2	-1,39	1,61
SL1515	ansP	L-asparagine permease	1,62	2,67
SL1517	yncE	Uncharacterized protein YncE	-1,57	-1,70
SL1518	yncD	Probable tonB-dependent receptor yncD	-2,51	1,20
SL1521	yncA	Uncharacterized N-acetyltransferase yncA	-1,67	-1,23
SL1533	yncJ	Uncharacterized protein yncJ	-2,31	-2,27
SL1536	ydcO	Inner membrane protein ydcO	1,62	1,56
SL1539	tehA	Tellurite resistance protein tehA	1,74	-1,43
SL1543	sgcB	Putative phosphotransferase enzyme IIB component sgcB	-2,05	2,16
SL1544	sgcC	Putative permease IIC component	-2,56	1,92
SL1546	sgcA	Putative phosphotransferase IIA component sgcA	-2,17	-1,02
SL1563	fliY	Cystine-binding periplasmic protein	-1,55	1,14
SL1564	yecS	Inner membrane amino-acid ABC transporter permease protein yecS	-1,14	1,01
SL1565	glnQ	Glutamine transport ATP-binding protein glnQ	1,08	1,16
SL1566	yecS	Inner membrane amino-acid ABC transporter permease protein yecS	-1,36	1,02
SL1587	zntB	Zinc transport protein zntB	-1,03	-1,09
SL1609	mppA	Periplasmic murein peptide-binding protein	1,81	-1,22
SL1613	tyrR	Transcriptional regulatory protein tyrR	1,16	-1,56
SL1615	ycjX	Uncharacterized protein ycjX	1,56	1,21
SL1622	sapA	Peptide transport periplasmic protein sapA	2,23	-1,17
SL1623	sapB	Peptide transport system permease protein sapB	2,82	-1,35

SL1624	sapC	Peptide transport system permease protein sapC	2,97	-1,03
SL1625	sapD	Peptide transport system ATP-binding protein sapD	1,83	-1,06
SL1626	sapF	Peptide transport system ATP-binding protein sapF	1,79	1,13
SL1674	oppD	Oligopeptide transport ATP-binding protein oppD	-2,23	-1,15
SL1675	oppC	Oligopeptide transport system permease protein oppC	-2,56	-1,45
SL1676	oppB	Oligopeptide transport system permease protein oppB	-2,74	-1,34
SL1693	narK	Nitrite extrusion protein 1	7,78	32,48
SL1698	chaB	Cation transport regulator chaB	-2,32	1,09
SL1699	chaA	Calcium/proton antiporter	1,63	-1,93
SL1709	ychM	Putative sulfate transporter ychM	1,59	-1,97
SL1729	cvrA	Cell volume regulation protein A	-3,15	-3,26
SL1734	nhaB	Na(+)/H(+) antiporter nhaB	-1,07	-1,70
SL1759	manX	PTS system mannose-specific EIIAB component	-1,71	1,08
SL1760	manY	Mannose permease IIC component	-1,31	-1,07
SL1761	manZ	Mannose permease IID component	-2,23	-1,23
SL1768	yebO	Uncharacterized protein yebO	-1,89	-2,49
SL1772	yebQ	Uncharacterized transporter yebQ	1,49	-3,40
SL1808	yebZ	Inner membrane protein yebZ	-1,12	1,11
SL1865	ftnB	Ferritin-like protein 2	-1,11	2,31
SL1868	ftnA	Ferritin-1	1,09	2,47
SL1870	tyrP	Tyrosine-specific transport protein	1,87	1,03
SL1880	yecC	Uncharacterized amino-acid ABC transporter ATP-binding protein yecC	-1,24	-1,41
SL1881	yecS	Inner membrane amino-acid ABC transporter permease protein yecS	-1,42	-1,75
SL1883	fliY	Cystine-binding periplasmic protein	-2,60	-1,21
SL1981	-	Hypothetical	1,07	1,84
SL1983	-	Hypothetical	-1,67	1,06
SL2045	yeeF	Inner membrane transport protein yeeF	-1,06	-2,44
SL2106	mdtD	Putative multidrug resistance protein mdtD	1,75	-1,40
SL2119	yegT	Putative nucleoside transporter yegT	1,83	2,44
SL2141	yehX	Putative osmoprotectant uptake system ATP-binding protein yehX	-1,22	1,17
SL2143	osmF	Putative osmoprotectant uptake system substrate-binding protein osmF	-1,08	1,90
SL2150	mdtQ	Multidrug resistance outer membrane protein mdtQ	1,99	1,16
SL2165	mglC	Galactoside transport system permease protein mglC	-1,87	2,33
SL2166	mglA	Galactose/methyl galactoside import ATP-binding protein MglA	-1,88	2,14
SL2167	mglB	D-galactose-binding periplasmic protein	-1,24	3,67
SL2177	lysP	Lysine-specific permease	1,13	-2,05
SL2183	fruB	Multiphosphoryl transfer protein	1,01	-2,11
SL2184	setB	Sugar efflux transporter B	1,79	-1,31
SL2194	yejB	Inner membrane ABC transporter permease protein yejB	1,10	-1,95
SL2195	yejE	Inner membrane ABC transporter permease protein yejE	1,07	-1,70
SL2196	yejF	Uncharacterized ABC transporter ATP-binding protein yejF	-1,45	-1,53
SL2198	bcr	Bicyclomycin resistance protein	1,25	-1,81
SL2224	ccmA2	Putative bifunctional cytochrome c-type biogenesis protein ccmAE	1,48	-1,22
SL2233	yojI	ABC transporter ATP-binding protein yojI	-1,33	-1,68
SL2243	ttuB	Putative tartrate transporter	-1,08	1,01
SL2249	ywoG	Uncharacterized MFS-type transporter ywoG	-1,28	1,22
SL2252	glpT	Glycerol-3-phosphate transporter	1,04	1,72
SL2259	yfaV	Inner membrane transport protein yfaV	-1,88	-1,64
SL2320	hisP	Histidine transport ATP-binding protein hisP	1,55	-1,82
SL2322	hisQ	Histidine transport system permease protein hisQ	1,90	-2,24
SL2323	hisJ	Histidine-binding periplasmic protein	2,06	-1,11
SL2326	rocC	Amino-acid permease rocC	1,18	1,42
SL2328	xasA	Uncharacterized transporter lpg1691	-1,18	1,91
SL2341	yfcJ	UPF0226 membrane protein SARI_00527	1,12	1,04
SL2345	-	Hypothetical	1,31	-1,23
SL2351	yfcA	UPF0721 transmembrane protein yfcA	1,79	1,49
SL2360	fadL	Long-chain fatty acid transport protein	2,35	7,03
SL2362	yfdC	Inner membrane protein yfdC	-1,79	-3,14
SL2367	pgtP	Phosphoglycerate transporter protein	-1,52	1,38
SL2372	yfeO	Putative ion-transport protein yfeO	-1,78	-1,53
SL2374	yghZ	Uncharacterized protein yghZ	-1,11	-1,14
SL2376	mntH	Manganese transport protein mntH	-1,17	-1,67
SL2377	nupC	Nucleoside permease nupC	2,60	2,08

SL2384	xapB	Xanthosine permease	-1,93	-1,69
SL2388	yfeH	Uncharacterized protein yfeH	1,37	-1,12
SL2392	cysZ	Protein cysZ homolog	1,58	-2,07
SL2395	ptsI	Phosphoenolpyruvate-protein phosphotransferase	1,38	1,32
SL2396	crr	Glucose-specific phosphotransferase enzyme IIA component	1,23	1,26
SL2401	yfeK	Uncharacterized protein yfeK	2,24	-1,27
SL2404	cysA	Sulfate/thiosulfate import ATP-binding protein cysA	1,29	-1,07
SL2405	cysW	Sulfate transport system permease protein cysW	1,29	-1,26
SL2406	cysU	Sulfate transport system permease protein cysT	1,36	-1,10
SL2407	cysP	Thiosulfate-binding protein	1,05	1,12
SL2444	acrD	Probable aminoglycoside efflux pump	1,45	-1,64
SL2456	perM	Putative permease perM	1,28	1,48
SL2460	uraA	Uracil permease	2,67	1,40
SL2514	-	Uncharacterized protein HI_1249	1,47	1,39
SL2520	cadB	Probable cadaverine/lysine antiporter	-1,12	1,15
SL2522	yjdL	Probable dipeptide and tripeptide permease YjdL	-1,02	2,24
SL2529	yfhD	Membrane-bound lytic murein transglycosylase F	1,96	1,16
SL2536	yhjX	Inner membrane protein yhjX	-1,07	-1,36
SL2609	eamB	Cysteine/O-acetylserine efflux protein	-1,36	-4,44
SL2618	kgtP	Alpha-ketoglutarate permease	1,22	1,46
SL2629	yfiR	Uncharacterized protein yfiR	1,23	-1,66
SL2725	-	Hypothetical Protein SL2725	-1,64	2,45
SL2734	srlA	Glucitol/sorbitol permease IIC component	-1,98	-1,30
SL2735	srlB	Glucitol/sorbitol-specific phosphotransferase enzyme IIA component	-1,65	1,37
SL2736	srlE	Glucitol/sorbitol-specific phosphotransferase enzyme IIB component	-2,06	-1,00
SL2737	yrbE	Uncharacterized oxidoreductase yrbE	-1,68	-1,02
SL2759	iroC	Putative multidrug export ATP-binding/permease protein	-1,70	-1,51
SL2760	iroD	Enterochelin esterase	-1,32	-2,69
SL2762	iroN	TonB-dependent outer membrane siderophore receptor protein	-2,34	-1,04
SL2767	hoxN	High-affinity nickel transport protein	-2,12	-2,78
SL2777	gabP	GABA permease	1,13	1,51
SL2780	yqaE	UPF0057 membrane protein yqaE	-2,21	1,26
SL2794	proV	Glycine betaine/L-proline transport ATP-binding protein proV	-1,46	-3,01
SL2795	proW	Glycine betaine/L-proline transport system permease protein proW	-1,45	-2,21
SL2797	ygaY	Uncharacterized transporter ygaY	1,47	-1,79
SL2799	emrA	Multidrug resistance protein A	2,07	-1,46
SL2800	emrB	Multidrug resistance protein B	2,58	-2,20
SL2812	srlA	Glucitol/sorbitol permease IIC component	-5,89	1,61
SL2813	srlE	Glucitol/sorbitol-specific phosphotransferase enzyme IIB component	-6,24	1,53
SL2814	srlB	Glucitol/sorbitol-specific phosphotransferase enzyme IIA component	-7,11	1,32
SL2824	-	Conserved Hypothetical Protein	2,16	2,60
SL2890	yhcA	Uncharacterized MFS-type transporter yhcA	-1,07	1,38
SL2892	ygbN	Uncharacterized permease HI_1015	-1,02	-1,02
SL2943	gudP	Probable glucarate transporter	2,74	6,47
SL2950	sdaC	Serine transporter	2,67	6,74
SL2976	ygdB	Uncharacterized protein ygdB	2,23	1,70
SL2981	ptsP	Phosphoenolpyruvate-protein phosphotransferase ptsP	-1,44	-1,84
SL2984	ygdQ	UPF0053 inner membrane protein ygdQ	-1,47	-3,45
SL2987	lplT	Lysophospholipid transporter lplT	1,04	1,00
SL2994	araE	Arabinose-proton symporter	-1,10	2,27
SL3000	yqeG	Inner membrane transport protein yqeG	1,90	-1,92
SL3009	yfdX	Protein yfdX	-1,20	-1,01
SL3041	yggE	Uncharacterized protein yggE	1,40	-1,89
SL3042	argO	Arginine exporter protein ArgO	1,54	3,40
SL3050	cbiO1	Cobalt import ATP-binding protein CbiO 1	3,90	4,71
SL3066	galP	Galactose-proton symporter	-1,63	1,88
SL3080	yggM	Uncharacterized protein yggM	5,96	9,61
SL3088	nupG	Nucleoside permease nupG	1,29	2,51
SL3100	steT	Serine/threonine exchanger steT	-2,23	-1,25
SL3108	exuT	Hexuronate transporter	-1,13	5,32
SL3115	-	Uncharacterized protein PM1146	1,88	-1,15
SL3116	-	Uncharacterized protein HI_1472	4,30	-1,24
SL3132	exbD	Biopolymer transport protein exbD	1,31	-1,85

SL3140	yflS	Putative malate transporter yflS	1,53	1,09
SL3143	yiiZ	Uncharacterized protein yiiZ	1,61	3,36
SL3144	-	C4-Dicarboxylate Transport System Permease Small Protein	1,26	2,47
SL3187	yqjH	Uncharacterized protein yqjH	-1,34	1,02
SL3197	alx	Inner membrane protein alx	-1,64	-1,87
SL3198	sstT	Serine/threonine transporter sstT	-1,72	2,18
SL3211	yhaO	Inner membrane transport protein yhaO	1,03	3,93
SL3215	tdcC	Threonine/serine transporter tdcC	-2,91	1,90
SL3229	fruB	Multiphosphoryl transfer protein	-11,58	-2,71
SL3232	gatB	Galactitol-specific phosphotransferase enzyme IIB component	-1,25	1,37
SL3233	gatC	Galactitol permease IIC component	-1,71	1,61
SL3252	mtr	Tryptophan-specific transport protein	1,77	-1,56
SL3283	mlaD	Probable phospholipid ABC transporter-binding protein mlaD	1,57	-1,20
SL3284	mlaE	Probable phospholipid ABC transporter permease protein mlaE	2,23	-1,66
SL3285	mlaF	Probable phospholipid import ATP-binding protein mlaF	1,47	-1,36
SL3291	lptB	Lipopolysaccharide export system ATP-binding protein lptB	1,62	-1,41
SL3296	ptsO	Phosphocarrier protein NPr	1,93	1,21
SL3318	yhcM	Uncharacterized protein yhcM	1,40	1,05
SL3319	yhcB	Putative cytochrome d ubiquinol oxidase subunit 3	-1,00	-1,11
SL3323	oadB1	Oxaloacetate decarboxylase beta chain 1	1,23	1,54
SL3324	oadA	Oxaloacetate decarboxylase alpha chain	-1,09	1,11
SL3355	panF	Sodium/pantothenate symporter	1,75	1,42
SL3360	yhdU	Uncharacterized protein yhdU	1,37	2,98
SL3362	envR	Probable acrEF/envCD operon repressor	1,01	1,05
SL3364	acrF	Acriflavine resistance protein F	1,12	1,13
SL3367	yrdB	Uncharacterized protein yrdB	-1,22	-1,45
SL3376	trkA	Trk system potassium uptake protein trkA	-1,17	-3,78
SL3410	bfr	Bacterioferritin	-2,43	1,39
SL3424	kefB	Glutathione-regulated potassium-efflux system protein kefB	1,31	-1,24
SL3426	yheS	Uncharacterized ABC transporter ATP-binding protein yheS	1,64	1,02
SL3433	crp	Catabolite gene activator	1,47	1,06
SL3440	tsgA	Protein tsgA	1,51	-3,97
SL3472	feoA	Ferrous iron transport protein A	1,37	-1,31
SL3473	feoB	Ferrous iron transport protein B	-1,74	-1,62
SL3479	gntT	High-affinity gluconate transporter	2,71	2,48
SL3520	ugpC	sn-glycerol-3-phosphate import ATP-binding protein UgpC	1,09	1,88
SL3521	ugpE	sn-glycerol-3-phosphate transport system permease protein ugpE	-1,45	1,31
SL3522	ugpA	sn-glycerol-3-phosphate transport system permease protein ugpA	-1,02	1,19
SL3523	ugpB	sn-glycerol-3-phosphate-binding periplasmic protein ugpB	-1,12	3,38
SL3526	livF	High-affinity branched-chain amino acid transport ATP-binding protein livF	-1,59	1,02
SL3527	livG	High-affinity branched-chain amino acid transport ATP-binding protein livG	-1,88	-1,07
SL3528	livM	High-affinity branched-chain amino acid transport system permease protein livM	-1,73	-1,01
SL3529	livH	High-affinity branched-chain amino acid transport system permease protein livH	-1,43	1,35
SL3532	livJ	Leu/Ile/Val-binding protein	1,13	1,76
SL3541	zntA	Lead, cadmium, zinc and mercury-transporting ATPase	1,04	-1,05
SL3546	yhhS	UPF0226 membrane protein SEN3404	-1,11	-1,01
SL3550	yhhJ	Inner membrane transport permease yhhJ	-2,43	-1,11
SL3551	yhiH	Uncharacterized ABC transporter ATP-binding protein yhiH	-2,51	-1,32
SL3552	yhiI	Uncharacterized protein yhiI	-1,45	1,15
SL3554	pitA	Low-affinity inorganic phosphate transporter 1	1,52	-1,17
SL3557	dtpB	Dipeptide and tripeptide permease B	-1,10	2,86
SL3564	dcuB	Anaerobic C4-dicarboxylate transporter dcuB	2,03	25,68
SL3574	yhjE	Inner membrane metabolite transport protein yhjE	-1,32	-1,07
SL3579	dctA	C4-dicarboxylate transport protein	2,15	8,22
SL3591	yhjV	Inner membrane transport protein yhjV	1,42	1,39
SL3593	dppD	Dipeptide transport ATP-binding protein dppD	-6,29	-4,77
SL3594	dppC	Dipeptide transport system permease protein dppC	-7,27	-6,99
SL3595	dppB	Dipeptide transport system permease protein dppB	-8,43	-7,97
SL3597	pucK	Uric acid permease pucK	1,10	1,70
SL3616	-	Hypothetical	-1,53	-1,99
SL3636	yiaM	2,3-diketo-L-gulonate TRAP transporter small permease protein yiaM	-1,04	1,14
SL3638	yiaO	2,3-diketo-L-gulonate-binding periplasmic protein yiaO	-1,22	1,64

SL3650	mtlA	PTS system mannitol-specific EIICBA component	1,08	2,62
SL3657	lldP	L-lactate permease	1,13	1,21
SL3662	mdlA	Mandelate racemase	1,59	2,01
SL3663	gudP	Probable glucarate transporter	-1,06	2,07
SL3672	yibQ	Uncharacterized protein yibQ	1,31	-1,80
SL3712	gltS	Sodium/glutamate symport carrier protein	1,88	3,17
SL3713	xanP	Xanthine permease XanP	1,26	3,94
SL3716	yicJ	Inner membrane symporter yicJ	1,29	1,46
SL3734	manZ	Mannose permease IID component	-1,35	1,73
SL3737	manX	PTS System Fructose Subfamily IIA Component	-1,55	2,74
SL3748	gatC	Galactitol permease IIC component	-2,47	1,09
SL3749	gatB	Galactitol-specific phosphotransferase enzyme IIB component	-1,90	1,48
SL3750	gatA	PTS IIA-Like Nitrogen-Regulatory Protein PtsN	-1,44	2,98
SL3753	uhpT	Hexose phosphate transport protein	1,10	3,98
SL3755	uhpB	Sensor protein uhpB	2,11	1,43
SL3756	uhpA	Transcriptional regulatory protein uhpA	1,70	1,70
SL3758	fucP	L-fucose-proton symporter	-3,82	1,27
SL3766	emrD	Multidrug resistance protein D	1,38	2,07
SL3767	-	Hypothetical	1,02	2,56
SL3769	dsdX	DsdX permease	-1,20	1,29
SL3774	yidE	Putative transport protein CKO_00031	1,83	3,18
SL3782	ccmE1	Cytochrome c-type biogenesis protein ccmE 1	3,70	1,04
SL3783	ccmC	Heme exporter protein C	3,00	-1,09
SL3783	ccmC	Heme exporter protein C	3,00	-1,09
SL3784	ccmB	Heme exporter protein B	2,72	-1,35
SL3784	ccmB	Heme exporter protein B	2,72	-1,35
SL3785	ccmAE	Putative bifunctional cytochrome c-type biogenesis protein ccmAE	1,04	-1,29
SL3793	dgoT	D-galactonate transporter	1,32	1,12
SL3799	gudP	Probable glucarate transporter	-1,29	1,54
SL3814	mdtL	Multidrug resistance protein mdtL	-1,16	-1,22
SL3821	pstB	Phosphate import ATP-binding protein pstB	1,41	1,29
SL3822	pstA	Phosphate transport system permease protein pstA	1,26	-1,98
SL3823	pstC	Phosphate transport system permease protein pstC	-1,12	-2,12
SL3824	pstS	Phosphate-binding protein pstS	-1,81	-2,30
SL3825	fruA	PTS system fructose-specific EIIBC component	1,27	1,82
SL3827	sgrR	HTH-type transcriptional regulator sgrR	1,65	1,37
SL3830	-	Hypothetical	1,41	-1,08
SL3847	kup	Low affinity potassium transport system protein kup	1,51	-1,57
SL3848	rbsD	D-ribose pyranase	-1,13	-4,44
SL3849	rbsA1	Ribose import ATP-binding protein RbsA 1	1,12	-4,19
SL3850	rbsC	Ribose transport system permease protein rbsC	1,02	-2,24
SL3851	rbsB	D-ribose-binding periplasmic protein	-1,18	1,19
SL3889	yifK	Probable transport protein yifK	-1,05	3,81
SL3906	corA	Magnesium transport protein corA	-1,11	-1,38
SL3917	yigM	Uncharacterized membrane protein yigM	1,60	-1,33
SL3928	tatB	Sec-independent protein translocase protein tatB homolog	1,57	1,74
SL3939	trkH	Trk system potassium uptake protein trkH	1,65	-1,01
SL3960	-	Hypothetical	-1,58	-1,45
SL3963	yihO	Uncharacterized symporter yihO	-1,48	1,24
SL3964	yihP	Inner membrane symporter yihP	-1,18	1,15
SL3999	rhaT	L-rhamnose-proton symporter	1,09	1,59
SL4002	yiaM	Tripartite ATP-Independent Periplasmic Transporter DctQ	1,54	1,63
SL4003	yiiZ	Uncharacterized protein yiiZ	-1,40	1,13
SL4010	fieF	Cation-efflux pump fieF	1,49	-1,18
SL4012	sbp	Sulfate-binding protein	1,02	1,01
SL4014	yagG	Uncharacterized symporter yagG	1,28	2,24
SL4018	-	Hypothetical	1,33	-1,09
SL4022	lsrR	Transcriptional regulator lsrR	2,77	3,64
SL4023	lsrA	Autoinducer 2 import ATP-binding protein lsrA	2,75	22,29
SL4024	lsrC	Autoinducer 2 import system permease protein lsrC	-1,40	5,57
SL4025	lsrD	Autoinducer 2 import system permease protein lsrD	-1,87	2,42
SL4026	lsrB	Autoinducer 2-binding protein lsrB	-3,11	-1,79
SL4036	glpF	Glycerol uptake facilitator protein	-1,98	1,96
SL4060	ptsA	Multiphosphoryl transfer protein 2	1,34	1,37
SL4061	frwC	Fructose-like permease IIC component 2	1,86	17,80
SL4062	frwB	Fructose-like phosphotransferase enzyme IIB component 2	1,28	7,78

SL4079	btuB	Vitamin B12 transporter BtuB	2,32	1,18
SL4124	yjbB	Uncharacterized protein yjbB	2,05	-1,05
SL4163	malG	Maltose transport system permease protein malG	-4,46	1,84
SL4164	malF	Maltose transport system permease protein malF	-3,99	4,45
SL4167	malK	Maltose/maltodextrin import ATP-binding protein MalK	-3,69	12,13
SL4168	lamB	Maltoporin	-1,47	2,16
SL4205	yjcE	Uncharacterized Na(+)/H(+) exchanger yjcE	-1,60	-2,73
SL4209	actP	Cation/acetate symporter ActP	1,88	2,48
SL4219	gltP	Proton glutamate symport protein	1,88	1,02
SL4227	proP	Proline/betaine transporter	1,22	-1,61
SL4231	adiC	Arginine/agmatine antiporter	-1,10	1,36
SL4236	melB	Melibiose carrier protein	-9,49	1,17
SL4238	dcuB	Anaerobic C4-dicarboxylate transporter dcuB	-2,43	-9,28
SL4246	-	putative periplasmic or exported protein	-1,41	-1,12
SL4262	dcuA	Anaerobic C4-dicarboxylate transporter dcuA	-1,14	1,00
SL4265	yjeH	Inner membrane protein yjeH	-1,11	-1,36
SL4282	yjeM	Inner membrane transporter yjeM	2,32	-2,23
SL4284	yjeP	Uncharacterized mscS family protein yjeP	1,62	-1,02
SL4288	artJ	ABC transporter arginine-binding protein 1	-1,45	-1,25
SL4317	ulaB	Ascorbate-specific phosphotransferase enzyme IIB component	1,77	2,92
SL4318	ulaC	Ascorbate-specific phosphotransferase enzyme IIA component	1,60	2,55
SL4331	cycA	D-serine/D-alanine/glycine transporter	-1,37	-1,04
SL4345	dgoT	D-galactonate transporter	1,20	1,50
SL4351	xylE	D-xylose-proton symporter	-2,11	1,22
SL4352	xylE	D-xylose-proton symporter	-1,61	1,08
SL4360	yfcJ	UPF0226 protein STM4428	1,07	1,39
SL4363	yrbE	Uncharacterized oxidoreductase yrbE	-1,08	1,10
SL4364	csbX	Alpha-ketoglutarate permease	-1,17	1,07
SL4387	mgtA	Magnesium-transporting ATPase, P-type 1	1,52	-2,79
SL4409	lptF	Lipopolysaccharide export system permease protein lptF	1,64	-2,03
SL4412	idnT	Gnt-II system L-idonate transporter	-1,32	1,46
SL4444	yjiG	Inner membrane protein yjiG	-2,57	1,71
SL4446	yjiJ	Uncharacterized protein yjiJ	1,05	-1,80
SL4466	manX	PTS System Fructocific IIA Component	-1,58	5,24
SL4467	manX	Probable phosphotransferase enzyme IIB component M6_Spy0801	-1,29	4,12
SL4469	manZ	Mannose permease IID component	-1,23	2,92
		Unclassified		
SL0013	dnaJ	Chaperone protein dnaJ	4,05	-1,56
SL0016	-	Hypothetical	1,36	1,39
SL0017	yqeI	Hypothetical	1,22	1,08
SL0090	apaG	Protein ApaG	1,56	-1,34
SL0104	araC	Arabinose operon regulatory protein	1,73	9,28
SL0175	lpfD	Protein lpfD	1,26	-1,25
SL0176	lpfC	Outer membrane usher protein lpfC	1,15	-1,04
SL0178	fimF	Fimbrial subunit type 1	1,02	2,50
SL0195	fhuB	Iron(3+)-hydroxamate import system permease protein fhuB	1,09	-1,13
SL0205	erpA	Iron-sulfur cluster insertion protein erpA	-1,04	-1,06
SL0254	yafE	Uncharacterized protein yafE	-1,12	-1,17
SL0279	sciR	putative shiga-like toxin A subunit	1,46	-1,10
SL0280	sciS	IcmF-related integral membrane ATP-binding protein, virulence associated protein	1,19	-1,03
SL0287	rhsE	Putative protein rhsE	-1,24	-1,94
SL0300	sinR	Probable HTH-type transcriptional regulator sinR	-4,83	-2,72
SL0303	sciZ	secreted protein (homology to Shigella VirG protein)	1,18	-1,44
SL0308	yafK	Putative L,D-transpeptidase YafK	-1,16	1,12
SL0316	phoE	Outer membrane pore protein E	-1,07	1,59
SL0345	oprM	putative outer membrane efflux lipoprotein	1,42	1,42
SL0362	prpR	Propionate catabolism operon regulatory protein	-1,42	1,11
SL0363	prpB	Methylisocitrate lyase	-3,23	-3,95
SL0368	yaiU	autotransporter/virulence factor	-1,57	-1,26
SL0426	phnX	Phosphonoacetaldehyde hydrolase	-1,13	-1,25
SL0461	ylaB	Uncharacterized protein ylaB	1,18	-1,28
SL0466	hha	Hemolysin expression-modulating protein	1,02	-1,05
SL0512	glxR	2-hydroxy-3-oxopropionate reductase	2,04	1,44
SL0528	lpxH	UDP-2,3-diacylglucosamine hydrolase	1,60	-1,43
SL0537	fimI	Putative fimbrin-like protein fimI	-3,86	-9,92

SL0539	fimD	Outer membrane usher protein fimD	-2,30	-4,82
SL0540	fimH	Protein fimH	-1,76	-3,62
SL0541	fimF	Fimbrial-like protein fimF	-1,41	-1,87
SL0542	fimZ	Fimbriae Z protein	-1,35	-1,90
SL0543	fimY	Fimbriae Y protein	-2,31	-2,74
SL0545	fimW	Fimbriae W protein	-2,20	-1,91
SL0556	pheP	Phenylalanine-specific permease	1,02	3,17
SL0558	apeE	outer membrane N-acetyl phenylalanine beta-naphthyl ester-cleaving esterase	-2,02	1,13
SL0582	fepB	Ferrienterobactin-binding periplasmic protein	1,30	-1,24
SL0598	ynfI	Cytoplasmic Chaperone rD Family Protein	1,42	-2,26
SL0607	citG2	Probable 2-(5''-triphosphoribosyl)-3'-dephosphocoenzyme-A synthase 2	3,38	5,25
SL0631	cobC	Alpha-ribazole phosphatase	1,67	1,14
SL0638	uxaA	putative hydrolase C-terminus	-9,54	-8,11
SL0687	kdpB	Potassium-transporting ATPase B chain	1,59	1,20
SL0727	tolQ	Protein tolQ	1,75	-1,65
SL0746	citG	2-(5''-triphosphoribosyl)-3'-dephosphocoenzyme-A synthase	1,93	1,56
SL0750	galM	Aldose 1-epimerase	-1,23	-1,82
SL0762	ybhE	putative 3-carboxymuconate cyclase	-1,55	1,84
SL0807	ybiF	Inner membrane transporter rhtA	1,16	-1,47
SL0836	yxjC	Uncharacterized transporter yxjC	-1,99	-3,76
SL0855	potG	Putrescine transport ATP-binding protein potG	1,22	-1,13
SL0869	ybjQ	UPF0145 protein Ent638_1382	1,11	-1,13
SL0872	ybjT	Uncharacterized protein ybjT	1,02	1,01
SL0926	mukF	killing factor KicB	1,04	-1,84
SL0927	ycbC	Uncharacterized protein ycbC	1,62	-2,35
SL1001	ycbY	N6-adenine-specific DNA methylase	1,56	1,07
SL1025	yccA	Inner membrane protein yccA	-1,06	-1,02
SL1052	scsA	membrane protein, suppressor for copper-sensitivity A	-1,07	1,40
SL1053	scsB	membrane protein, suppressor for copper-sensitivity B	1,76	1,96
SL1054	scsC	secreted protein, suppressor for copper-sensitivity C	1,71	1,79
SL1055	scsD	secreted protein, suppressor for copper-sensitivity D	1,54	1,20
SL1070	yjhB	Putative metabolite transport protein yjhB	-1,82	-1,87
SL1082	csgC	Curli assembly protein csgC	-1,27	-1,24
SL1097	solA	N-methyl-L-tryptophan oxidase	-1,07	-1,62
SL1107	mviN	Virulence factor mviN	2,06	-1,50
SL1110	flgA	Flagella basal body P-ring formation protein flgA	1,65	4,05
SL1127	yceD	Uncharacterized protein yceD	-1,08	-1,06
SL1161	sifA	Secreted effector protein sifA	-1,44	-2,70
SL1180	msgA	Virulence protein msgA	-1,63	-2,62
SL1182	cspH	Cold shock-like protein cspH	-1,58	-1,12
SL1183	pagD	Virulence protein pagD	-6,34	-10,07
SL1188	-	Hypothetical	-1,79	-2,04
SL1194	nikD	Nickel import ATP-binding protein NikD	3,11	2,54
SL1221	mipA	MltA-interacting protein	-1,28	-1,27
SL1254	cedA	Cell division activator cedA	1,61	-1,05
SL1265	nucA	Nuclease	-12,33	-14,89
SL1266	rfc	O-antigen polymerase	1,20	-2,08
SL1291	ydiF	Uncharacterized protein ydiF	1,75	1,13
SL1318	ttrC	Tetrathionate Reductase Subunit C	1,30	-1,45
SL1320	ttrS	Sensor protein	1,23	1,75
SL1373	ydhK	Uncharacterized transporter ydhK	1,71	-1,29
SL1377	slyB	Outer membrane lipoprotein slyB	1,00	-1,06
SL1425	dmsD	Twin-arginine leader-binding protein dmsD	-1,01	-2,31
SL1429	dmsA1	Putative dimethyl sulfoxide reductase chain A1	1,81	1,76
SL1473	pqaA	PhoPQ-activated protein	-3,78	-1,35
SL1484	-	Coiled-Coil Protein	1,12	1,01
SL1505	smvA	Methyl viologen resistance protein smvA	-1,52	-3,14
SL1512	yddE	Uncharacterized isomerase yddE	-1,20	1,22
SL1526	srfC	Virulence Factor	1,20	1,53
SL1531	ugtL	D-Alanyl-D-Alanine Dipeptidase	-7,52	-9,15
SL1532	sifB	Secreted effector protein sifB	-3,43	-3,52
SL1558	yaiN	Uncharacterized protein in bioA 5'region	1,61	-1,66
SL1561	sseJ	Secreted effector protein sseJ	-3,13	-4,11
SL1591	fnr	Fumarate and nitrate reduction regulatory protein	1,03	-1,33
SL1596	-	Hypothetical	1,13	5,27
SL1599	yeeJ	Invasin	1,13	1,11

SL1608	-	NmrA Family Protein	-1,06	-1,04
SL1614	ycjF	UPF0283 membrane protein ycjF	1,37	-1,21
SL1629	-	Hypothetical A	1,27	1,14
SL1653	trpH	Protein trpH	1,73	-1,33
SL1655	trpD	Anthranilate synthase component II	1,24	1,07
SL1668	tonB	Protein tonB	-1,10	-1,89
SL1672	-	Putative potassium channel protein RPA4233	-1,26	1,94
SL1673	oppF	Oligopeptide transport ATP-binding protein oppF	-1,74	1,06
SL1677	oppA	Periplasmic oligopeptide-binding protein	-3,30	1,43
SL1684	hnr	Protein hnr	1,37	1,16
SL1718	hyaE	hydrogenase-1 operon protein HyaE	1,77	1,82
SL1747	fadD	Long-chain-fatty-acid--CoA ligase	1,91	-1,27
SL1784	sopE2	Guanine nucleotide exchange factor sopE2	-52,09	-5,12
SL1793	pagO	Protein pagO	-3,30	-4,98
SL1799	pagK	bacteriophage encoded pagK (phoPQ-activated protein)	-5,49	-4,51
SL1805	recE	Exodeoxyribonuclease 8	1,15	1,12
SL1825	znuA	High-affinity zinc uptake system protein znuA	-1,11	1,64
SL1826	znuC	Zinc import ATP-binding protein ZnuC	1,95	-1,07
SL1847	flhE	Flagellar protein flhE	-1,81	-1,45
SL1850	cheZ	Chemotaxis protein cheZ	-3,23	-1,73
SL1855	cheW	Chemotaxis protein cheW	-3,07	-1,17
SL1856	cheA	Chemotaxis protein cheA	-2,45	-1,53
SL1858	motA	Motility protein A	-2,44	-1,72
SL1877	uvrY	Response regulator uvrY	-1,12	-1,44
SL1887	fliB	Lysine-N-methylase	-4,79	-1,84
SL1891	fliT	Flagellar protein fliT	-3,04	1,06
SL1893	yedD	Uncharacterized lipoprotein yedD	1,09	1,78
SL1894	yedE	UPF0394 inner membrane protein yedE	2,21	17,08
SL1895	yedF	UPF0033 protein yedF	2,43	17,78
SL1904	fliL	Flagellar protein FliL	-1,61	1,04
SL1906	fliN	Flagellar motor switch protein FliN	-1,77	-1,13
SL1907	fliO	Flagellar protein fliO	-1,49	-1,68
SL1914	yedP	Putative mannosyl-3-phosphoglycerate phosphatase	1,38	-1,42
SL1925	umuC	Protein umuC	1,22	1,49
SL1991	erfK	Probable L,D-transpeptidase ErfK/SrfK	-2,09	-1,17
SL2044	sbcB	Exodeoxyribonuclease I	1,26	-2,02
SL2063	rfbU	Protein rfbU	2,23	1,26
SL2070	rfbI	Protein rfbI	2,76	-1,13
SL2102	yegD	Uncharacterized chaperone protein yegD	1,05	1,63
SL2109	-	Hypothetical	-1,95	-2,43
SL2140	yehW	Putative osmoprotectant uptake system permease protein yehW	-1,70	-1,07
SL2142	yehY	Putative osmoprotectant uptake system permease protein yehY	-1,29	1,22
SL2175	uhpC	Regulatory protein uhpC	1,28	1,79
SL2207	msgA	Virulence protein msgA	-1,29	1,12
SL2213	-	Hypothetical	-1,20	-1,48
SL2218	-	Bacteriophage Tail Fiber Assembly Protein	-1,49	-1,43
SL2219	stfR	Side Tail Fiber Protein	-1,99	-1,99
SL2235	ada	Regulatory protein ada	1,19	1,47
SL2238	yojN	Hypothetical Protein yojN	1,34	-1,40
SL2239	rcsB	Capsular synthesis regulator component B	1,41	-1,61
SL2273	pmrD	Signal transduction protein pmrD	1,18	-1,29
SL2279	menF	Menaquinone-specific isochorismate synthase	1,10	-1,19
SL2284	yfbK	Uncharacterized protein yfbK	1,31	-1,34
SL2321	hisM	Histidine transport system permease protein hisM	1,98	-2,16
SL2324	argT	Lysine-arginine-ornithine-binding periplasmic protein	5,77	2,23
SL2333	dedD	Protein dedD	1,01	-1,15
SL2340	flk	Flagellar regulator flk	1,69	1,03
SL2363	pgtE	Outer membrane protease E	-4,08	-3,07
SL2402	yfeL	Uncharacterized protein yfeL	1,89	-1,37
SL2499	iscX	Protein iscX	2,22	1,01
SL2648	rimM	Ribosome maturation factor rimM	1,29	1,24
SL2649	rpsP	30S ribosomal protein S16	1,18	1,10
SL2655	ppnK	Probable inorganic polyphosphate/ATP-NAD kinase	-1,31	-1,19
SL2659	yfjG	UPF0083 protein yfjG	1,90	1,31
SL2730	-	ATPase	1,61	-2,06
SL2741	-	Glucose-6-Phosphate Isomerase	-1,27	1,49
SL2743	sgrR	HTH-type transcriptional regulator sgrR	1,16	4,48

SL2744	-	Hypothetical	1,04	1,55
SL2755	fljA	Repressor of phase 1 flagellin gene	-37,56	-1,47
SL2757	hin	DNA-invertase hin	-3,06	3,30
SL2758	iroB	putative glycosyltransferase	-6,14	-1,34
SL2770	yflP	UPF0065 protein yflP	1,38	34,16
SL2771	-	Hypothetical	1,39	42,49
SL2772	-	Uncharacterized 52.8 kDa protein in TAR-I ttuC' 3'region	1,85	6,58
SL2790	nrdH	Glutaredoxin-like protein nrdH	-1,39	-1,10
SL2832	hycB	Formate hydrogenlyase subunit 2	-1,07	-4,99
SL2924	sopD	Secreted effector protein sopD	-80,68	-16,87
SL2926	cysI	Sulfite reductase [NADPH] hemoprotein beta-component	1,08	-2,06
SL2941	gudD	Glucarate dehydratase	3,16	4,39
SL2942	gudX	Glucarate dehydratase-related protein	3,04	6,36
SL2947	syd	Protein syd	2,13	1,32
SL2996	kduI	4-deoxy-L-threo-5-hexosulose-uronate ketol-isomerase	2,36	2,72
SL3006	stdC	putative fimbrial chaparone protein	-1,13	-1,08
SL3008	stdA	Uncharacterized fimbrial-like protein ybgD	-1,68	-2,25
SL3015	idi	Isopentenyl-diphosphate Delta-isomerase	1,08	-1,13
SL3026	yqfB	UPF0267 protein yqfB	-1,02	2,02
SL3106	-	Polysaccharide Deacetylase	-20,62	-2,34
SL3128	-	Hypothetical	-3,42	-1,49
SL3133	exbB	Biopolymer transport protein exbB	1,36	-1,59
SL3145	ygiK	Uncharacterized protein ygiK	1,14	1,15
SL3146	sufI	Protein sufI	1,30	-1,12
SL3160	tolC	Outer membrane protein tolC	1,14	1,02
SL3162	ygiC	Uncharacterized protein ygiC	1,11	-1,30
SL3221	garR	2-hydroxy-3-oxopropionate reductase	1,87	1,64
SL3241	yraR	Uncharacterized protein yraR	1,03	1,16
SL3250	yafK	Putative L,D-transpeptidase YafK	1,09	-1,12
SL3261	rimP	Ribosome maturation factor rimP	1,02	-1,46
SL3288	kdsC	3-deoxy-D-manno-octulosonate 8-phosphate phosphatase	1,93	-1,96
SL3290	lptA	Lipopolysaccharide export system protein lptA	1,73	-1,50
SL3295	yhbJ	UPF0042 nucleotide-binding protein PC1_0271	1,22	1,19
SL3305	codB	Cytosine permease	1,09	3,48
SL3443	nirC	Probable nitrite transporter	7,52	2,27
SL3478	nfuA	Fe/S biogenesis protein nfuA	3,11	-2,21
SL3487	rsr	60 kDa SS-A/Ro ribonucleoprotein homolog	-7,28	-2,62
SL3530	livK	Leucine-specific-binding protein	-1,50	1,53
SL3549	nikR	Nickel-responsive regulator	1,21	1,07
SL3581	bcsC	Cellulose synthase operon protein C	1,16	-1,20
SL3582	bcsZ	Endoglucanase	1,24	-1,79
SL3601	lpfE	Protein lpfE	-1,04	1,15
SL3602	lpfD	Protein lpfD	1,04	-1,97
SL3603	lpfD	Protein lpfD	-1,28	-1,05
SL3604	lpfC	Outer membrane usher protein lpfC	1,02	1,27
SL3606	lpfA	Long polar fimbria protein A	-1,09	-1,40
SL3679	rfaL	O-antigen ligase	1,13	-2,63
SL3754	uhpC	Regulatory protein uhpC	2,59	1,86
SL3796	dgoK	2-dehydro-3-deoxygalactonokinase	1,51	1,98
SL3886	wecF	4-alpha-L-fucosyltransferase	1,58	-1,96
SL3887	rffT	Putative ECA polymerase	1,58	-1,46
SL3898	cyaY	Protein cyaY	1,44	1,40
SL3907	yigF	Uncharacterized protein yigF	-2,14	-2,15
SL3911	pldA	Phospholipase A1	1,26	-2,69
SL3934	-	Arylsulfotransferase	1,34	1,33
SL3948	engB	Probable GTP-binding protein engB	1,59	2,04
SL3959	-	Hypothetical	-1,20	-1,72
SL3966	yihR	Uncharacterized protein yihR	-1,16	1,31
SL4001	ygiK	Uncharacterized protein ygiK	1,14	1,24
SL4169	malM	Maltose operon periplasmic protein	-3,00	2,47
SL4201	soxS	Regulatory protein soxS	-2,40	-2,53
SL4217	nrfE	Cytochrome c-type biogenesis protein nrfE	2,25	1,60
SL4223	lpxO	putative dioxygenase for synthesis of lipid	1,03	1,94
SL4245	dmsD	Twin-arginine leader-binding protein dmsD	-1,05	1,92
SL4272	ecnA	Entericidin A	1,73	-1,49
SL4293	mutL	DNA mismatch repair protein mutL	1,31	1,43
SL4309	yjfC	Uncharacterized protein yjfC	1,50	1,35

SL4338	ytfJ	Uncharacterized protein ytfJ	-1,08	2,14
SL4378	licR	Probable licABCH operon regulator	1,17	1,88
SL4401	miaE	tRNA-(ms[2]io[6]A)-hydroxylase	1,92	1,00
SL4418	yjhR	Putative uncharacterized protein yjhR	-1,07	1,16
SL4423	-	ABC-Type Transporter	1,09	1,07
SL4484	rsmC	Ribosomal RNA small subunit methyltransferase C	1,75	-1,07
SL4490	yjjU	Uncharacterized protein yjjU	-1,18	-1,08
SL4500	yhcA	Uncharacterized fimbrial chaperone yhcA	-2,05	-2,10
SL4507	nadR	Transcriptional regulator nadR	1,41	1,27
SL4508	yjjK	Uncharacterized ABC transporter ATP-binding protein yjjK	1,70	1,24
SL4520	lpfC	Outer membrane usher protein lpfC	-1,10	-1,25
		Unknown function		
SL0005	yaaA	UPF0246 protein yaaA	-1,40	-1,82
SL0011	yaaI	UPF0412 protein yaaI	2,29	-1,26
SL0029	-	Hypothetical	1,14	-1,15
SL0042	yicI	Uncharacterized family 31 glucosidase ORF2	-2,08	2,29
SL0052	rihC	Non-specific ribonucleoside hydrolase rihC	1,01	1,74
SL0063	citX	Apo-citrate lyase phosphoribosyl-dephospho-CoA transferase	1,59	4,27
SL0079	fixX	Ferredoxin-like protein fixX	-1,46	2,02
SL0080	yaaU	Putative metabolite transport protein yaaU	-1,42	1,18
SL0081	ygdI	Uncharacterized lipoprotein ygdI	-2,43	-1,45
SL0083	yhcN	Hypothetical	-3,01	-1,85
SL0095	djlA	DnaJ-like protein djlA	1,61	-1,06
SL0096	rluA	Ribosomal large subunit pseudouridine synthase A	1,78	1,04
SL0099	ygjQ	Hypothetical	1,20	-2,19
SL0105	yabI	Inner membrane protein yabI	-1,32	1,42
SL0120	mraW	Ribosomal RNA small subunit methyltransferase H	1,21	-1,45
SL0135	secM	Secretion monitor	1,70	1,01
SL0139	yacF	UPF0289 protein CKO_03274	1,67	1,32
SL0161	yacL	UPF0231 protein yacL	1,34	1,76
SL0180	yadE	Uncharacterized protein yadE	1,52	-1,18
SL0189	ligT	2'-5'-RNA ligase	1,54	-1,20
SL0202	yadU	putative outer membrane protein	-1,03	1,07
SL0206	yadS	UPF0126 inner membrane protein yadS	-1,26	-1,24
SL0211	cdaR	Carbohydrate diacid regulator	2,32	5,18
SL0236	yaeR	Uncharacterized protein yaeR	1,08	1,23
SL0238	rof	Protein rof	-1,36	1,26
SL0240	yaeQ	Uncharacterized protein yaeQ	2,92	1,04
SL0241	yaeJ	Uncharacterized protein yaeJ	3,10	-1,03
SL0242	cutF	copper homeostasis protein CutF precursor (lipoprotein nlpE)	1,46	-1,73
SL0244	yaeB	UPF0066 protein yaeB	1,89	-3,80
SL0249	gmhB	D,D-heptose 1,7-bisphosphate phosphatase	1,05	-1,17
SL0253	yafD	UPF0294 protein Ent638_0743	-1,00	1,35
SL0257	yafS	Uncharacterized protein yafS	1,01	-1,10
SL0261	sciB	Hypothetical	2,06	1,04
SL0264	sciE	Virulence Protein SciE Type	2,32	1,13
SL0267	sciH	Hypothetical	2,11	1,66
SL0284	vrgS	Type VI secretion protein	-1,10	-1,05
SL0299	ybeJ	putative xylanase/chitin deacetylase	-1,69	1,29
SL0302	pagN	outer membrane adhesin	-1,80	-1,23
SL0309	dinP	DNA polymerase IV	-1,38	1,21
SL0310	ykfJ	Uncharacterized protein ykfJ (pseudo)	-1,44	-1,07
SL0314	frsA	putative hydrolase of the alpha/beta superfamily	1,24	-1,07
SL0320	dhaF	pseudogene	-1,16	1,02
SL0329	-	Hypothetical	-2,10	-1,78
SL0338	rtn	Protein rtn	-2,17	-2,10
SL0361	yahO	Uncharacterized protein yahO	-4,11	-1,10
SL0365	prpD	2-methylcitrate dehydratase	-2,37	-1,50
SL0366	prpE	Propionate--CoA ligase	-1,86	-1,92
SL0372	yaiW	Uncharacterized protein yaiW	1,01	-2,75
SL0374	yaiZ	Uncharacterized protein yaiZ	1,37	2,88
SL0380	adrA	putative diguanylate cyclase/phosphodiesterase domain 1	-1,95	-1,85
SL0382	yaiI	UPF0178 protein yaiI	1,40	-1,88
SL0387	rdgC	Recombination-associated protein rdgC	1,97	1,13
SL0406	yajD	Uncharacterized protein yajD	-1,15	-1,30
SL0408	yajI	Uncharacterized lipoprotein yajI	1,72	-1,93
SL0439	yajG	Uncharacterized lipoprotein yajG	1,63	2,34

SL0447	ybaV	Uncharacterized protein ybaV	1,29	1,55
SL0449	queC	7-cyano-7-deazaguanine synthase (putative aluminum resistance protein)	1,32	-1,72
SL0450	ybaE	Uncharacterized protein ybaE	1,42	3,86
SL0451	cof	HMP-PP phosphatase	2,64	1,53
SL0460	ybaZ	Uncharacterized protein ybaZ	-1,20	-2,58
SL0464	ylaC	Inner membrane protein ylaC	-1,72	-1,64
SL0471	aefA	Potassium efflux system KefA	1,49	-2,15
SL0472	yhgA	putative transposase	1,38	1,68
SL0473	ybaM	Uncharacterized protein ybaM	1,17	1,48
SL0488	ybaK	Cys-tRNA(Pro)/Cys-tRNA(Cys) deacylase ybaK	1,70	1,13
SL0493	ybbJ	Inner membrane protein ybbJ	1,46	1,51
SL0494	ybbK	putative inner membrane protein	-1,05	1,36
SL0507	allS	lysR family transcriptional regulator	1,42	1,77
SL0508	allA	Ureidoglycolate hydrolase	1,24	2,02
SL0516	allB	Allantoinase	1,03	1,50
SL0518	glxK	Glycerate kinase 1	-1,31	1,47
SL0519	ylbA	Uncharacterized protein ylbA	1,22	1,46
SL0523	ylbE	Uncharacterized protein ylbE	1,27	1,51
SL0533	ybcI	Inner membrane protein ybcI	-1,18	-2,14
SL0534	ybcJ	Uncharacterized protein ybcJ	1,69	-1,02
SL0544	-	putative diguanylate cyclase/phosphodiesterase	-2,80	-3,69
SL0552	ykgC	Probable pyridine nucleotide-disulfide oxidoreductase ykgC	-1,27	1,55
SL0553	ykgI	Uncharacterized protein ykgI	-1,19	-1,08
SL0554	ykgB	Inner membrane protein ykgB	-1,30	1,00
SL0567	ybdF	Uncharacterized protein ybdF	1,61	1,08
SL0570	ybdJ	Uncharacterized protein ybdJ	1,11	-1,66
SL0571	ybdK	Carboxylate-amine ligase ybdK	-1,29	1,43
SL0575	ybdZ	Uncharacterized protein ybdZ	1,38	1,02
SL0587	ybdB	Esterase ybdB	1,49	1,97
SL0589	ybdD	Uncharacterized protein ybdD	-1,61	2,74
SL0592	ybdM	Uncharacterized protein ybdM	-1,88	1,06
SL0593	ybdN	Uncharacterized protein ybdN	-1,72	-2,98
SL0602	uspG	Universal stress protein G	-1,24	2,00
SL0606	citT	Citrate carrier	2,39	4,10
SL0608	citX	Apo-citrate lyase phosphoribosyl-dephospho-CoA transferase	7,00	18,14
SL0616	pagP	antimicrobial peptide resistance and lipid A acylation protein	1,78	-4,69
SL0618	crcB	Protein crcB homolog	-1,18	-2,74
SL0619	ybeM	UPF0012 hydrolase ybeM	-1,77	1,56
SL0630	ybeB	Uncharacterized protein ybeB	1,39	2,09
SL0642	ybeQ	Uncharacterized protein ybeQ	-1,26	1,18
SL0643	ybeR	Uncharacterized protein ybeR	-1,43	-1,23
SL0645	ybeU	Uncharacterized protein ybeU	1,30	1,40
SL0646	ybeU	Uncharacterized protein ybeU	1,21	1,34
SL0660	ubiF	2-octaprenyl-3-methyl-6-methoxy-1,4-benzoquinol hydroxylase	1,47	1,54
SL0663	nagD	Protein nagD	1,73	1,06
SL0669	ybfM	Uncharacterized protein ybfM	1,00	3,25
SL0670	ybfN	Uncharacterized lipoprotein ybfN	1,16	3,37
SL0678	ybfF	Esterase ybfF	1,49	-2,15
SL0694	ybgK	Uncharacterized protein ybgK	-1,16	1,52
SL0698	-	Hypothetical	1,31	1,02
SL0699	-	Hypothetical	1,27	-1,07
SL0711	abrB	Protein AbrB	-1,25	1,22
SL0713	-	Hypothetical	-1,22	2,02
SL0732	ybgF	Uncharacterized protein YbgF	1,83	1,10
SL0761	ybhA	Phosphatase ybhA	1,91	2,20
SL0767	hutU	Urocanate hydratase	3,68	23,77
SL0776	slrP	E3 ubiquitin-protein ligase slrP	-6,09	-5,25
SL0783	ybhL	Inner membrane protein ybhL	1,19	1,75
SL0787	ybhN	Inner membrane protein ybhN	-1,70	-2,06
SL0791	ybhR	Inner membrane transport permease ybhR	1,36	-1,80
SL0792	ybhS	Inner membrane transport permease ybhS	1,16	-2,46
SL0799	ybiJ	Uncharacterized protein ybiJ	-1,42	-5,03
SL0800	ybiI	Uncharacterized protein ybiI	-1,00	-1,37
SL0801	ybiN	putative SAM-dependent methyltransferase	1,09	2,03
SL0811	ybiR	Inner membrane protein ybiR	1,16	-2,07
SL0812	ybiS	Probable L,D-transpeptidase YbiS	1,27	-1,99

SL0817	ybiU	Uncharacterized protein ybiU	1,41	1,47
SL0818	ybiV1	putative hydrolase	1,48	-1,06
SL0823	ybiK	Isoaspartyl peptidase	1,45	-1,36
SL0841	ybjG	Putative undecaprenyl-diphosphatase ybjG	-1,14	-3,26
SL0843	ybjI	Phosphatase ybjI	1,14	1,11
SL0849	ybjC	Uncharacterized protein ybjC	1,83	2,07
SL0860	ulaA	Ascorbate-specific permease IIC component ulaA	1,00	-1,31
SL0876	hcp	Hydroxylamine reductase	4,19	2,53
SL0878	ybjD	Uncharacterized protein ybjD	1,70	1,74
SL0879	ybjX	Uncharacterized protein ybjX	-1,29	-3,90
SL0880	macA	Macrolide-specific efflux protein macA	-1,21	-4,80
SL0888	ycaC	Uncharacterized protein ycaC	1,06	2,05
SL0892	-	Inner Membrane Protein	1,44	-2,09
SL0912	ycaO	UPF0142 protein ycaO	1,62	-1,88
SL0913	ycaP	UPF0702 transmembrane protein ycaP	-1,29	-1,11
SL0916	ycaL	Uncharacterized metalloprotease ycaL	-1,13	-1,47
SL0923	ycaQ	Uncharacterized protein ycaQ	1,62	-1,13
SL0930	mukE	Chromosome partition protein mukE	1,91	-1,11
SL0933	ycbK	Uncharacterized protein ycbK	1,18	1,29
SL0934	ycbL	Uncharacterized protein ycbL	1,06	-1,36
SL1003	pqiA	Paraquat-inducible protein A	2,63	1,57
SL1004	pqiB	Paraquat-inducible protein B	2,44	1,51
SL1005	ymbA	Uncharacterized lipoprotein ymbA	1,86	2,08
SL1012	yccR	putative DNA transformation protein	2,30	4,04
SL1013	yccS	Inner membrane protein yccS	2,04	-1,40
SL1014	yccF	Inner membrane protein yccF	2,24	-1,10
SL1018	yccU	Uncharacterized protein yccU	1,04	1,49
SL1024	tusE	Sulfurtransferase tusE	-1,01	1,10
SL1036	yedX	putative periplasmic or exported protein	-1,33	-1,00
SL1049	iraM	Anti-adapter protein iraM	-2,20	-1,50
SL1050	cbpM	Chaperone modulatory protein cbpM	-1,11	1,28
SL1059	ymdF	Uncharacterized protein ymdF	-1,28	1,18
SL1068	nanM	N-acetylneuraminate epimerase	1,01	1,16
SL1071	yjhC	Uncharacterized oxidoreductase yjhC	-2,01	1,14
SL1073	ycdX	Putative hydrolase ycdX	1,51	1,24
SL1083	ymdA	Uncharacterized protein ymdA	-2,48	1,64
SL1085	ymdC	Uncharacterized protein ymdC	-1,47	-1,22
SL1086	mdoC	Glucans biosynthesis protein C	1,45	-1,99
SL1093	yceA	UPF0176 protein yceA	1,22	1,17
SL1099	dinI	DNA-damage-inducible protein I	1,33	-1,08
SL1101	yceB	Uncharacterized lipoprotein yceB	1,20	-2,08
SL1103	mdtH	Multidrug resistance protein mdtH	-1,40	-2,23
SL1105	yceH	UPF0502 protein yceH	1,39	2,06
SL1123	rluC	Ribosomal large subunit pseudouridine synthase C	2,06	1,28
SL1125	-	Hypothetical	1,12	2,83
SL1139	ycfH	Uncharacterized deoxyribonuclease ycfH	1,83	-1,23
SL1143	ycfL	Uncharacterized protein ycfL	1,25	1,04
SL1147	ycfP	UPF0227 protein KPN78578_10770	1,02	1,21
SL1150	ycfQ	Uncharacterized HTH-type transcriptional regulator ycfQ	1,46	1,35
SL1151	bhsA	Multiple stress resistance protein BhsA	-1,08	-3,31
SL1152	ycfS	Probable L,D-transpeptidase YcfS	2,06	-1,44
SL1157	nagK	N-acetyl-D-glucosamine kinase	1,62	-1,12
SL1165	-	Hypothetical Protein SL1165	3,46	1,23
SL1167	ycfD	Uncharacterized protein ycfD	1,10	1,07
SL1175	rluB	Ribosomal large subunit pseudouridine synthase B	2,54	1,54
SL1197	yhjQ	Uncharacterized cysteine-rich protein yhjQ	-1,35	2,97
SL1204	aroQ	Monofunctional chorismate mutase	-3,40	-1,13
SL1209	-	Hypothetical	1,51	-1,12
SL1210	yeaQ	UPF0410 protein yeaQ	-1,96	1,57
SL1211	yaoF	putative hemolysin	-1,38	-1,52
SL1213	yeaO	Uncharacterized protein yeaO	1,03	1,02
SL1216	yeaL	UPF0756 membrane protein yeaL	-1,11	-1,56
SL1218	yeaJ	Putative diguanylate cylase YeaJ	-1,01	-2,57
SL1219	yeaH	UPF0229 protein yeaH	-3,21	1,15
SL1222	chuR	Anaerobic sulfatase-maturating enzyme	-1,47	-1,90
SL1224	yeaD	Putative glucose-6-phosphate 1-epimerase	1,56	-1,31
SL1226	msrB	Peptide methionine sulfoxide reductase msrB	1,36	1,38

SL1228	pncA	Pyrazinamidase/nicotinamidase	2,20	1,23
SL1235	ynjH	Uncharacterized protein ynjH	-3,19	1,31
SL1236	nudG	CTP pyrophosphohydrolase	-2,30	1,12
SL1241	astB	N-succinylarginine dihydrolase	2,30	4,94
SL1242	astE	Succinylglutamate desuccinylase	1,74	3,04
SL1243	spy	Spheroplast protein Y	-1,51	1,17
SL1252	celG	putative glucosidase	-1,30	-1,83
SL1256	ydjM	Inner membrane protein ydjM	1,09	-1,59
SL1258	yniB	Uncharacterized protein yniB	-1,03	1,10
SL1259	yniA	Uncharacterized protein yniA	-2,45	2,01
SL1260	ydiZ	Uncharacterized protein ydiZ	-2,09	1,08
SL1262	ydiY	Uncharacterized protein ydiY	-2,02	-1,20
SL1278	cdgR	Cyclic di-GMP regulator cdgR	-1,31	-5,00
SL1279	ydiU	UPF0061 protein ydiU	-1,06	-1,26
SL1285	ydiT	Ferredoxin-like protein ydiT	1,16	-1,74
SL1297	ydiL	Uncharacterized protein ydiL	-2,58	-2,47
SL1298	ydiK	UPF0118 inner membrane protein ydiK	1,15	-1,54
SL1303	sufA	Protein sufA	1,08	1,12
SL1304	sufB	FeS cluster assembly protein sufB	-1,33	-1,21
SL1306	sufD	FeS cluster assembly protein sufD	-1,38	-1,80
SL1307	sufS	Cysteine desulfurase	-1,42	-1,66
SL1309	ynhG	Probable L,D-transpeptidase YnhG	-1,32	2,05
SL1310	lppB	Major outer membrane lipoprotein 2	2,49	-1,06
SL1311	lppA	Major outer membrane lipoprotein 1	1,01	1,41
SL1365	grxD	Glutaredoxin-4	1,60	1,44
SL1369	nemR	HTH-type transcriptional repressor nemR	2,17	1,11
SL1370	ydhL	Uncharacterized protein ydhL	-1,10	-1,02
SL1371	ydhF	Oxidoreductase ydhF	1,73	3,41
SL1378	anmK	Anhydro-N-acetylmuramic acid kinase	1,54	1,22
SL1379	mliC	Membrane-bound lysozyme inhibitor of C-type lysozyme	1,20	-2,39
SL1386	rnfE	Electron transport complex protein rnfE	2,55	1,22
SL1390	rnfB	Electron transport complex protein rnfB	2,09	-1,58
SL1391	rnfA	Electron transport complex protein rnfA	1,30	-1,67
SL1392	ydgK	Inner membrane protein ydgK	-1,04	-1,48
SL1396	ydgA	Protein ydgA	-1,04	-1,36
SL1406	ydgC	Inner membrane protein ydgC	1,03	1,23
SL1408	ydgH	Protein ydgH	1,73	1,40
SL1411	tqsA	AI-2 transport protein tqsA	-1,40	-1,42
SL1414	ydgD	Uncharacterized serine protease ydgD	-1,43	1,05
SL1419	ynfK	Putative dethiobiotin synthetase	1,70	1,12
SL1430	ynfD	Uncharacterized protein ynfD	-1,43	1,68
SL1433	ynfB	UPF0482 protein CKO_01577	1,37	1,05
SL1434	ynfA	UPF0060 membrane protein ynfA	-1,20	3,16
SL1440	ydfH	Uncharacterized HTH-type transcriptional regulator ydfH	1,10	-1,63
SL1444	ydeJ	Protein ydeJ	-2,52	-3,51
SL1447	eamA	Probable amino-acid metabolite efflux pump	-1,38	1,39
SL1456	yneG	Uncharacterized protein yneG	-1,37	1,76
SL1457	yneE	UPF0187 protein yneE	-1,57	-2,84
SL1469	cbh	Choloylglycine hydrolase	-1,41	-1,35
SL1475	yhjG	Uncharacterized aromatic compound monooxygenase yhjG	1,73	2,79
SL1478	yjgH	UPF0076 protein yjgH	-1,54	-1,36
SL1481	-	Hypothetical	-1,39	-1,07
SL1483	-	Putative transposase y4bF (pseudogene)	-1,04	1,01
SL1487	patB	Cystathionine beta-lyase patB	1,26	1,70
SL1492	hdeB	Protein hdeB	1,25	3,96
SL1494	bdm	Protein bdm homolog	-1,58	-4,75
SL1502	yddG	Inner membrane protein yddG	-1,07	1,37
SL1516	ygdR	Uncharacterized lipoprotein ygdR	1,92	1,01
SL1519	mcbR	HTH-type transcriptional regulator mcbR	-1,81	1,69
SL1522	ydcZ	Inner membrane protein ydcZ	1,19	-1,06
SL1535	ydcN	Uncharacterized HTH-type transcriptional regulator ydcN	1,80	-1,15
SL1540	ydcK	Uncharacterized acetyltransferase ydcK	-1,17	-1,04
SL1541	rimL	Ribosomal-protein-serine acetyltransferase	-1,06	1,80
SL1554	ydcJ	Uncharacterized protein ydcJ	2,20	15,31
SL1559	steB	Secreted effector protein steB	-13,37	-30,72
SL1570	ydcF	Protein ydcF	1,49	1,50
SL1574	ydbL	Uncharacterized protein ydbL	1,86	-1,73

SL1575	ynbE	Uncharacterized protein ynbE	1,75	-1,60
SL1576	ydbH	Uncharacterized protein ydbH	1,65	-2,76
SL1582	uspF	Universal stress protein F	-1,35	2,05
SL1584	intR	Putative lambdoid prophage Rac integrase	1,58	2,47
SL1585	ttcA	tRNA 2-thiocytidine biosynthesis protein TtcA	1,38	2,24
SL1589	ydaL	Uncharacterized protein ydaL	-1,85	1,49
SL1592	uspE	Universal stress protein E	-1,31	1,55
SL1595	ydcN	XRE Family Transcriptional Regulator	1,24	1,21
SL1601	-	Hypothetical Protein SL1601	-1,22	-1,20
SL1603	ygdR	Outer Membrane Lipoprotein	-1,11	-1,21
SL1604	yjgJ	Uncharacterized HTH-type transcriptional regulator yjgJ	1,58	1,81
SL1627	ydiV	Uncharacterized protein ydiV	1,75	3,11
SL1634	yciR	putative PAS/PAC domain protein	1,13	1,39
SL1635	yciZ	UPF0509 protein yciZ	1,32	-1,59
SL1651	rluB	Ribosomal large subunit pseudouridine synthase B	1,20	1,87
SL1652	yciO	Uncharacterized protein yciO	1,59	-1,29
SL1659	ymdF	Uncharacterized protein ymdF	-8,50	-1,52
SL1661	yciE	Protein yciE	-6,89	-1,98
SL1665	yciC	UPF0259 membrane protein CKO_01332	1,81	-1,34
SL1667	yciA	Acyl-CoA thioester hydrolase yciA	1,61	1,45
SL1669	yciI	Protein yciI	1,16	1,18
SL1685	rssA	NTE family protein rssA	1,09	1,79
SL1688	ybeQ	Uncharacterized protein ybeQ	1,33	1,32
SL1697	ychN	Protein ychN	-1,02	-1,46
SL1702	sirB2	Protein sirB2	3,29	-2,38
SL1712	engD	GTP-dependent nucleic acid-binding protein engD	1,80	-1,77
SL1722	yccB	Hypothetical Protein yccB	-1,73	-1,15
SL1725	ymgE	UPF0410 protein ymge	-2,80	1,45
SL1728	ldcA	Murein tetrapeptide carboxypeptidase	1,15	-1,15
SL1737	gns	Protein gns	-1,03	3,14
SL1739	ycgN	UPF0260 protein CKO_01185	1,17	3,15
SL1749	yeaZ	M22 peptidase homolog yeaZ	2,22	-1,46
SL1751	yoaB	UPF0076 protein yoaB	1,41	-1,16
SL1756	yoaD	Hypothetical Protein yoaD	1,58	1,72
SL1762	yobD	UPF0266 membrane protein yobD	-3,86	-1,41
SL1763	yebN	UPF0059 membrane protein CKO_01156	1,54	1,59
SL1767	yobF	Uncharacterized protein yobF	-1,44	-1,18
SL1770	yobH	Uncharacterized protein yobH	-2,08	-3,58
SL1776	yebR	Protein yebR	2,75	1,14
SL1777	yebS	Inner membrane protein yebS	1,75	-1,32
SL1778	yebT	Uncharacterized protein yebT	-1,09	-1,87
SL1780	yebV	Uncharacterized protein yebV	-3,48	-5,37
SL1781	yebW	Uncharacterized protein yebW	-1,85	-1,64
SL1785	ycgX	Uncharacterized protein ycgX	1,81	-4,00
SL1786	-	Hypothetical	-1,21	-2,77
SL1787	bls	Blasticidin-S acetyltransferase	-1,45	1,91
SL1789	-	Hypothetical	-2,05	1,19
SL1797	pagM	virulence factor	-3,45	-1,76
SL1798	insF1	Hypothetical Protein insF1	-1,94	-3,08
SL1801	-	Hypothetical	1,06	-1,30
SL1803	rzpQ	Uncharacterized protein rzpQ	-1,34	-1,08
SL1807	yebY	Uncharacterized protein yebY	-1,03	-1,07
SL1809	yobA	Protein yobA	-1,09	1,68
SL1811	yobB	Uncharacterized protein yobB	-1,02	1,46
SL1812	exoX	Exodeoxyribonuclease 10	-1,12	1,38
SL1814	yebE	Inner membrane protein yebE	-1,20	-1,66
SL1815	yebF	Protein yebF	1,08	1,47
SL1816	yebG	Uncharacterized protein yebG	1,03	1,01
SL1821	hexR	HTH-type transcriptional regulator hexR	1,45	2,52
SL1827	znuB	High-affinity zinc uptake system membrane protein znuB	1,23	-1,64
SL1832	yebB	Uncharacterized protein yebB	1,61	-1,24
SL1837	yecD	Uncharacterized isochorismatase family protein yecD	1,57	1,05
SL1838	yecE	UPF0759 protein yecE	2,13	1,36
SL1839	yecN	Inner membrane protein yecN	1,51	-1,68
SL1840	cmoA	tRNA (cmo5U34)-methyltransferase	1,42	-1,47
SL1841	cmoB	tRNA (mo5U34)-methyltransferase	1,71	-1,62
SL1843	yecM	Protein yecM	2,74	2,18

SL1867	yecR	Uncharacterized protein yecR	1,37	1,31
SL1869	yecH	Uncharacterized protein yecH	1,31	2,41
SL1871	yecA	Uncharacterized protein yecA	-1,11	1,46
SL1878	yecF	Uncharacterized protein yecF	-4,32	-3,51
SL1884	fliZ	Protein fliZ	-3,07	-1,08
SL1912	dsrB	Protein dsrB	-1,33	1,22
SL1913	yodD	Uncharacterized protein yodD	-1,01	1,16
SL1918	yedA	Uncharacterized inner membrane transporter yedA	1,16	-1,24
SL1921	yedJ	Uncharacterized protein yedJ	-1,04	2,57
SL1977	mtfA	Protein mtfA	1,06	1,87
SL1978	intB	Putative prophage P4 integrase	-1,96	-1,10
SL1980	-	Hypothetical	1,02	-1,06
SL1982	ybeQ	Uncharacterized protein ybeQ	1,04	1,09
SL1985	-	Hypothetical	-1,36	1,03
SL1988	-	Hypothetical Protein SL1988	1,31	1,40
SL1989	-	Hypothetical	-1,56	1,34
SL1990	yeeO	Uncharacterized transporter yeeO	-1,25	-2,38
SL2037	gyrI	DNA gyrase inhibitory protein homolog	1,73	2,61
SL2042	ybjQ	Cytoplasmic Protein	1,22	-1,11
SL2089	wcaD	Putative colanic acid polymerase	1,08	-1,04
SL2093	wzc	Tyrosine-protein kinase wzc	2,06	-1,13
SL2096	yegH	UPF0053 protein yegH	1,16	-2,62
SL2104	mdtB	Multidrug resistance protein mdtB	1,99	-1,74
SL2105	mdtC	Multidrug resistance protein mdtC	1,68	-1,44
SL2112	yegQ	Uncharacterized protease yegQ	1,09	1,41
SL2113	-	Hypothetical	-1,32	-1,23
SL2116	-	Hypothetical	-1,04	-1,23
SL2118	fbaB	Fructose-bisphosphate aldolase class 1	-2,06	1,31
SL2120	yegU	Uncharacterized protein yegU	1,45	2,02
SL2125	yohN	Uncharacterized protein yohN	1,73	-1,98
SL2130	yehE	Uncharacterized protein yehE	-3,43	-31,09
SL2131	mrp	Protein mrp	1,66	-1,19
SL2133	yehR	Uncharacterized lipoprotein yehR	-1,86	-1,26
SL2134	yehR	Uncharacterized lipoprotein Lmo0207	1,03	-1,12
SL2135	yehS	Uncharacterized protein yehS	1,38	-1,26
SL2136	yehT	Uncharacterized response regulatory protein yehT	1,95	21,86
SL2139	yohO	UPF0387 membrane protein yohO	-1,36	-1,25
SL2147	yohC	Inner membrane protein yohC	-1,39	1,30
SL2148	yohD	Inner membrane protein yohD	-1,06	1,53
SL2151	dusC	tRNA-dihydrouridine synthase C	1,11	1,09
SL2158	yohJ	UPF0299 membrane protein CKO_00648	-1,52	-9,78
SL2169	yeiB	Uncharacterized protein yeiB	-1,15	-6,56
SL2179	yeiH	UPF0324 inner membrane protein yeiH	-1,01	1,03
SL2186	-	Hypothetical	1,35	1,29
SL2187	yeiW	UPF0153 protein yeiW	-1,88	1,30
SL2190	yeiU	Inner membrane protein yeiU	1,26	-1,04
SL2192	rtn	Protein rtn	1,23	-1,32
SL2193	yejA	Uncharacterized protein yejA	-1,18	-2,55
SL2203	ndpA	Nucleoid-associated protein ndpA	1,59	1,28
SL2217	sspH2	E3 ubiquitin-protein ligase sspH2	1,31	-1,70
SL2248	yfaE	Uncharacterized ferredoxin-like protein yfaE	-1,25	-1,51
SL2257	cinA	CinA-like protein	-1,15	-1,26
SL2258	yfaU	2-keto-3-deoxy-L-rhamnonate aldolase	-1,53	-1,15
SL2262	cinA	CinA-like protein	1,54	1,02
SL2263	yfaZ	Uncharacterized protein yfaZ	1,27	-1,01
SL2264	nudI	Nucleoside triphosphatase nudI	-1,46	1,33
SL2265	ais	Lipopolysaccharide core heptose(II)-phosphate phosphatase	-3,11	-1,91
SL2269	arnD	Probable 4-deoxy-4-formamido-L-arabinose-phosphoundecaprenol deformylase ArnD	-1,92	-2,87
SL2270	arnT	Undecaprenyl phosphate-alpha-4-amino-4-deoxy-L-arabinose arabinosyl transferase	-1,85	-2,29
SL2271	arnE	Probable 4-amino-4-deoxy-L-arabinose-phosphoundecaprenol flippase subunit ArnE	-1,61	-1,73
SL2277	menH	2-succinyl-6-hydroxy-2,4-cyclohexadiene-1-carboxylate synthase	4,44	-1,47
SL2281	elaA	Protein elaA	1,19	2,35
SL2282	rnz	Ribonuclease Z	1,36	-1,48
SL2301	yfbR	UPF0207 protein KPK_1466	1,24	-1,76
SL2303	yfbT	Phosphatase yfbT	-1,88	-1,56

SL2304	yfbU	UPF0304 protein yfbU	-1,46	-1,11
SL2305	yfbV	UPF0208 membrane protein yfbV	1,08	-1,44
SL2316	yfcE	Phosphodiesterase yfcE	1,23	1,10
SL2317	yfcF	Uncharacterized GST-like protein yfcF	-1,74	-1,41
SL2332	cvpA	Colicin V production protein	1,06	1,15
SL2336	dedA	Protein dedA	1,70	-2,73
SL2355	yfcN	UPF0115 protein KPK_1418	1,39	1,13
SL2368	yfdY	Uncharacterized protein yfdY	-1,64	1,51
SL2373	ipdC	Indole-3-pyruvate decarboxylase	-1,10	2,04
SL2375	ypeC	Uncharacterized protein ypeC	-1,49	-2,24
SL2378	yfeA	Uncharacterized protein yfeA	1,06	-1,26
SL2379	yfeC	Uncharacterized protein yfeC	2,78	5,24
SL2380	yfeD	Uncharacterized protein yfeD	4,21	3,64
SL2383	-	Hypothetical N	1,04	1,12
SL2409	yfeX	putative iron-dependent peroxidase	1,93	1,21
SL2410	yfeY	putative outer membrane lipoprotein	2,12	-1,72
SL2411	yfeZ	Inner membrane protein yfeZ	1,35	-1,29
SL2418	eutK	Ethanolamine utilization protein eutK	-1,21	1,41
SL2419	eutL	Ethanolamine utilization protein eutL	-1,46	1,04
SL2430	eutT	Ethanolamine utilization cobalamin adenosyltransferase	-1,79	2,01
SL2432	eutP	Ethanolamine utilization protein eutP	-1,17	4,93
SL2433	eutS	Ethanolamine utilization protein eutS	1,02	4,42
SL2439	ypfG	Uncharacterized protein ypfG	1,63	-2,45
SL2445	yffB	Protein yffB	1,33	1,72
SL2447	-	UPF0370 protein YpsIP31758_1253	-1,19	1,54
SL2448	ypfI	Uncharacterized protein ypfI	1,40	1,15
SL2454	bcp	Putative peroxiredoxin bcp	1,28	1,07
SL2455	garK	Glycerate Kinase	1,46	-1,02
SL2459	hda	DnaA-homolog protein hda	1,19	1,35
SL2466	yfgF	putative diguanylate cyclase	1,88	-1,54
SL2481	engA	GTP-binding protein engA	1,43	-3,03
SL2489	ysaA	Polyferredoxin	2,68	-2,74
SL2494	yfhM	Uncharacterized lipoprotein yfhM	1,72	1,23
SL2503	iscA	Iron-binding protein iscA	1,26	-1,71
SL2504	nifU	NifU-like protein	1,15	-1,72
SL2506	iscR	HTH-type transcriptional regulator iscR	1,21	-2,77
SL2509	yfhR	Uncharacterized protein yfhR	1,19	1,39
SL2515	csiE	Stationary phase-inducible protein csiE	1,52	6,04
SL2530	tadA	tRNA-specific adenosine deaminase	-1,34	1,01
SL2533	murQ	N-acetylmuramic acid 6-phosphate etherase	1,33	2,27
SL2534	yfhH	Uncharacterized HTH-type transcriptional regulator yfhH	1,45	1,44
SL2538	yfhL	Uncharacterized ferredoxin-like protein yfhL	-2,37	1,02
SL2545	lepA	GTP-binding protein lepA	1,41	-1,42
SL2612	yfiF	Uncharacterized tRNA/rRNA methyltransferase yfiF	1,13	2,18
SL2614	yfiP	DTW domain-containing protein yfiP	1,54	-1,36
SL2615	yfiQ	Uncharacterized protein yfiQ	-1,06	1,38
SL2626	yvrE	Uncharacterized protein yvrE	-1,09	1,55
SL2630	yfiN	Probable diguanylate cyclase YfiN	1,02	-2,41
SL2632	yebY	Hypothetical Protein yebY	1,27	1,49
SL2651	corE	putative cytochrome c-type biogenesis protein	1,41	-1,04
SL2657	smpA	Small protein A	1,61	1,20
SL2661	-	Hypothetical	-6,11	2,18
SL2710	yopC	SPBc2 prophage-derived uncharacterized protein yopC	1,86	2,67
SL2740	hxlB	3-hexulose-6-phosphate isomerase	-1,22	1,65
SL2747	intA	Prophage CP4-57 integrase	-2,24	-1,04
SL2763	pipB2	Secreted effector protein pipB2	-3,15	-3,40
SL2764	ybjX	Uncharacterized protein ybjX	-1,03	-5,61
SL2773	csiD	Protein csiD	1,15	1,04
SL2774	ygaF	Uncharacterized protein ygaF	1,38	-1,02
SL2779	ygaU	Uncharacterized protein ygaU	-4,86	-1,14
SL2781	ygaV	Probable HTH-type transcriptional regulator ygaV	1,28	-1,24
SL2782	ygaP	Inner membrane protein ygaP	-1,21	-1,43
SL2789	-	Hypothetical	-1,06	1,52
SL2810	ygaD	Protein ygaD	1,65	2,46
SL2818	gutQ	Protein gutQ	1,28	1,76
SL2840	ygbA	Uncharacterized protein ygbA	2,12	1,11
SL2880	-	Hypothetical	-3,24	-1,46

SL2883	-	Hypothetical Protein SL2883	-1,22	1,07
SL2884	-	Hypothetical	1,60	1,87
SL2885	-	GCN5-Related N-Acetyltransferase	1,13	1,67
SL2887	-	Phage Integrase Family Protein	1,41	-1,31
SL2902	bsdD	Phenolic acid decarboxylase subunit D	-1,42	-1,32
SL2919	ygcI	Uncharacterized protein ygcI	-2,86	-1,88
SL2920	ygcJ	Uncharacterized protein ygcJ	-3,70	-1,59
SL2921	-	Hypothetical	-4,26	-1,59
SL2922	ygcL	Uncharacterized protein ygcL	-4,47	-1,98
SL2930	ygcF	7-carboxy-7-deazaguanine synthase homolog	1,23	-1,09
SL2933	mazG	Protein mazG	1,71	-2,13
SL2934	-	putative major fimbrial subunit	1,55	-1,56
SL2935	-	Plasmid Stabilization System	1,82	-1,82
SL2936	-	Hypothetical	1,25	-2,30
SL2940	garK	Glycerate kinase 2	1,77	3,66
SL2945	truC	tRNA pseudouridine synthase C	1,67	-1,32
SL2946	yqcC	Uncharacterized protein yqcC	1,17	-2,78
SL2948	queF	NADPH-dependent 7-cyano-7-deazaguanine reductase	1,80	-1,05
SL2955	fucP	L-fucose-proton symporter	1,14	1,44
SL2960	rlmM	Ribosomal RNA large subunit methyltransferase M	-1,04	-1,39
SL2963	ygdI	Uncharacterized lipoprotein ygdI	-1,97	-1,69
SL2964	csdA	Cysteine sulfinate desulfinase	1,21	-1,66
SL2966	rarD	Protein rarD	3,20	-1,55
SL2967	ygdL	Uncharacterized protein ygdL	1,25	-1,83
SL2985	ygdR	Uncharacterized lipoprotein ygdR	1,04	1,00
SL2986	tas	Protein tas	1,01	1,47
SL3002	rcnA	Nickel/cobalt efflux system rcnA	1,00	-1,37
SL3012	-	Uncharacterized protein CP0246	1,05	1,28
SL3024	ygfZ	tRNA-modifying protein ygfZ	-1,08	1,66
SL3035	ygfB	UPF0149 protein ygfB	1,52	-1,21
SL3048	-	Hypothetical	3,49	11,28
SL3049	-	Permease Protein Of ABC-Type Cobalt Transporter	4,41	6,30
SL3053	yggG	Uncharacterized metalloprotease yggG	1,39	-3,11
SL3056	yjgK	Uncharacterized protein yjgK	1,23	1,19
SL3061	-	Hypothetical	1,04	-1,22
SL3063	yqgB	Hypothetical	-1,24	-1,15
SL3064	yqgD	Uncharacterized protein yqgD	1,10	-1,56
SL3067	sprT	Protein sprT	1,14	1,96
SL3078	rdgB	Nucleoside-triphosphatase rdgB	2,01	-1,39
SL3082	yggN	Uncharacterized protein yggN	1,53	2,13
SL3084	trmB	tRNA (guanine-N(7)-)-methyltransferase	1,46	1,82
SL3086	yggX	Probable Fe(2+)-trafficking protein	-1,00	-1,24
SL3093	maoC	MaoC Domain Protein Dehydratase	-2,42	1,52
SL3104	iraD	Anti-adapter protein iraD	-1,43	-1,31
SL3107	yhcX	UPF0012 hydrolase yhcX	-14,18	-1,87
SL3114	yghU	Uncharacterized GST-like protein yghU	-1,62	1,96
SL3131	yghA	Uncharacterized oxidoreductase yghA	-1,37	-1,97
SL3134	-	Hypothetical	2,72	4,98
SL3139	dkgA	2,5-diketo-D-gluconic acid reductase A	1,00	2,62
SL3141	-	Uncharacterized HIT-like protein MJ0866	-1,39	-1,64
SL3142	ygiQ	UPF0313 protein ygiQ	1,32	1,18
SL3161	ygiB	UPF0441 protein ygiB	1,11	1,08
SL3163	ygiD	Uncharacterized protein ygiD	-10,82	-6,71
SL3164	zupT	Zinc transporter zupT	1,21	2,57
SL3169	yqiC	Uncharacterized protein yqiC	1,38	2,04
SL3175	ygiF	Uncharacterized protein ygiF	1,53	-1,18
SL3176	ygiM	Uncharacterized protein ygiM	1,92	-1,46
SL3186	mug	G/U mismatch-specific DNA glycosylase	-1,13	1,11
SL3188	yqjI	Uncharacterized protein yqjI	-1,20	1,11
SL3194	ygjP	Uncharacterized protein ygjP	2,04	-1,33
SL3195	ygjQ	Uncharacterized protein ygjQ	1,55	-1,54
SL3196	ygjR	Uncharacterized oxidoreductase ygjR	-1,12	1,60
SL3199	yqjA	Inner membrane protein yqjA	-1,03	-1,51
SL3200	yqjB	Uncharacterized protein yqjB	1,02	-1,66
SL3201	yqjC	Protein yqjC	-1,14	-1,11
SL3204	yqjF	Inner membrane protein yqjF	-1,12	-1,39
SL3209	yhaL	Hypothetical Protein yhaL	-1,12	5,71

SL3210	yhaM	UPF0597 protein yhaM	-1,36	1,39
SL3220	garK	Glycerate kinase 2	1,70	2,12
SL3222	garL	5-keto-4-deoxy-D-glucarate aldolase	2,26	2,03
SL3242	yhbO	Protein yhbO	-1,67	1,17
SL3243	yhbP	UPF0306 protein yhbP	1,98	1,18
SL3244	yhbQ	UPF0213 protein yhbQ	1,67	1,22
SL3248	yhbV	Uncharacterized protein yhbV	3,86	2,68
SL3249	yhbW	Uncharacterized protein yhbW	1,36	1,16
SL3273	yhbZ	GTPase obg	1,10	-1,43
SL3274	yhbE	Uncharacterized inner membrane transporter yhbE	1,25	-1,31
SL3280	yrbA	Uncharacterized protein yrbA	1,88	-1,53
SL3281	mlaB	Probable phospholipid ABC transporter-binding protein mlaB	1,88	-2,04
SL3282	mlaC	Probable phospholipid-binding protein mlaC	1,34	-1,31
SL3286	yrbG	Inner membrane protein yrbG	1,46	1,01
SL3297	yrbL	Uncharacterized protein yrbL	-1,05	1,17
SL3304	yhcG	Uncharacterized protein yhcG	1,24	6,91
SL3307	yhcH	Uncharacterized protein yhcH	-1,40	-1,04
SL3308	nanK	N-acetylmannosamine kinase	-1,29	-1,33
SL3329	ydfH	GntR Family Transcriptional Regulator	1,28	1,43
SL3333	yhcN	Uncharacterized protein yhcN	1,41	-2,17
SL3334	yhcN	Uncharacterized protein yhcN	1,27	-1,04
SL3336	aaeB	p-hydroxybenzoic acid efflux pump subunit AaeB	1,33	-1,19
SL3348	yhdA	Hypothetical Protein yhdA	-1,51	1,08
SL3354	yhdT	Uncharacterized protein yhdT	2,05	1,99
SL3361	yciR	Uncharacterized signaling protein PA1727	-1,07	1,54
SL3370	yrdD	Uncharacterized protein yrdD	-1,19	-1,47
SL3371	smg	Protein smg	-1,68	1,04
SL3372	smf	Protein smf	1,16	3,26
SL3378	yhdL	Uncharacterized protein yhdL	-1,02	1,65
SL3380	yhdN	Uncharacterized protein yhdN	1,70	-1,07
SL3411	bfd	Bacterioferritin-associated ferredoxin	-2,24	-4,61
SL3416	tusB	Protein tusB	2,23	-1,80
SL3417	tusC	Protein tusC	2,33	-1,64
SL3418	tusD	Sulfurtransferase tusD	2,23	-1,91
SL3421	slyX	Protein slyX	-1,08	-1,16
SL3427	-	ABC Transporter ATPase	-1,05	2,10
SL3429	yheT	Putative esterase yheT	-1,12	1,12
SL3434	yhfK	Uncharacterized protein yhfK	2,57	-1,24
SL3445	bigA	Putative surface-exposed virulence protein BigA	1,90	1,88
SL3456	yrfA	Uncharacterized protein yrfA	1,73	1,97
SL3458	yrfC	Uncharacterized protein yrfC	1,08	1,95
SL3459	yrfD	Uncharacterized protein yrfD	1,10	1,72
SL3461	nudE	ADP compounds hydrolase nudE	1,40	-2,04
SL3465	hslO	33 kDa chaperonin	2,31	1,55
SL3471	yhgF	Protein yhgF	1,15	-1,28
SL3475	yfcI	Uncharacterized protein yfcI	1,40	2,08
SL3477	gntX	Protein gntX	1,75	2,48
SL3484	dinJ	DNA-damage-inducible protein J	-1,45	-1,60
SL3486	rtcB	Protein rtcB	-3,34	-2,14
SL3495	pstS1	Phosphate-binding protein pstS 1	1,28	2,05
SL3497	ttuB	Putative tartrate transporter	-1,22	1,90
SL3511	yhhX	Uncharacterized oxidoreductase yhhX	-1,13	-1,53
SL3512	yhhY	Uncharacterized N-acetyltransferase yhhY	-1,20	-1,40
SL3518	yhhA	Uncharacterized protein yhhA	-1,89	1,17
SL3531	yhhK	Uncharacterized protein yhhK	1,46	-1,41
SL3537	rsmD	Ribosomal RNA small subunit methyltransferase D	2,66	-1,08
SL3538	yhhL	Uncharacterized protein yhhL	1,79	1,13
SL3544	yhhQ	Inner membrane protein yhhQ	-2,28	-1,17
SL3545	dcrB	Protein dcrB	1,15	-1,54
SL3547	yhhT	UPF0118 inner membrane protein yhhT	-1,64	-1,46
SL3548	acpT	4'-phosphopantetheinyl transferase AcpT	1,30	1,16
SL3561	yhiR	Uncharacterized protein yhiR	1,91	-1,77
SL3575	yhjG	Uncharacterized protein yhjG	-1,44	-1,21
SL3576	yhjH	Cyclic di-GMP phosphodiesterase YhjH	-3,77	1,16
SL3578	yhjJ	Protein yhjJ	1,42	-1,44
SL3580	yhjK	Protein YhjK	1,60	-1,10
SL3583	bcsB	Cyclic di-GMP-binding protein	-1,15	-1,64

SL3585	yhjQ	Uncharacterized protein yhjQ	-1,08	1,00
SL3586	yhjR	Uncharacterized protein yhjR	-1,08	1,25
SL3589	yhjU	Uncharacterized protein yhjU	-1,32	-1,51
SL3600	eptB	Phosphoethanolamine transferase eptB	1,57	-1,54
SL3609	yiaC	Uncharacterized N-acetyltransferase yiaC	1,04	1,60
SL3618	-	Hypothetical	1,33	1,23
SL3619	yafP	Uncharacterized N-acetyltransferase yafP	-1,41	-1,22
SL3622	ysaB	Uncharacterized lipoprotein ysaB	1,06	-1,62
SL3623	yiaH	Inner membrane protein yiaH	-1,31	-1,28
SL3628	bax	Protein bax	1,07	-2,16
SL3631	ysaA	Putative electron transport protein ysaA	1,21	2,22
SL3634	yiaL	Protein yiaL	1,11	1,41
SL3637	yiaN	2,3-diketo-L-gulonate TRAP transporter large permease protein yiaN	-1,51	-1,12
SL3644	-	Hypothetical	1,20	2,01
SL3655	-	Hypothetical	1,18	1,13
SL3664	-	MFS Transporter ACS Family Glucarate Transporter	1,04	1,03
SL3703	ycbL	Metallo-beta-lactamase L1	1,42	2,81
SL3704	yicG	UPF0126 inner membrane protein yicG	3,17	-1,74
SL3711	-	Cytoplasmic Protein	2,23	1,98
SL3714	yicH	Uncharacterized protein yicH	1,38	1,18
SL3715	yicI	Alpha-xylosidase	1,10	1,22
SL3731	yfcI	Uncharacterized protein yfcI	1,11	2,34
SL3739	yicS	Uncharacterized protein yicS	1,29	1,25
SL3741	nepI	Purine ribonucleoside efflux pump nepI	1,29	1,21
SL3743	-	Hypothetical	2,23	2,38
SL3752	yicN	Uncharacterized protein yicN	1,10	3,22
SL3763	ivbL	ilvBN operon attenuator peptide	1,01	-1,03
SL3778	yidR	Uncharacterized protein yidR	1,35	1,11
SL3787	torD	Chaperone protein torD	-1,25	-1,53
SL3798	yidA	Phosphatase yidA	1,08	-1,50
SL3811	intA	Prophage CP4-57 integrase	-1,47	1,15
SL3816	yieE	Uncharacterized protein yieE	1,01	-1,02
SL3817	yieF	Uncharacterized protein yieF	-1,54	1,25
SL3818	purP	Probable adenine permease PurP	-1,50	-1,75
SL3840	gidB	glucose inhibited division protein	1,66	1,59
SL3841	gidA	glucose inhibited division protein	1,16	-1,02
SL3854	-	Pseudogene	1,70	1,36
SL3857	yieP	Uncharacterized HTH-type transcriptional regulator yieP	2,01	1,29
SL3859	yifE	UPF0438 protein yifE	-1,78	7,01
SL3860	yifB	Uncharacterized protein yifB	-1,33	2,92
SL3890	hemY	Protein hemY	1,25	-2,03
SL3902	yigA	Uncharacterized protein yigA	-1,12	-1,99
SL3908	yigG	Inner membrane protein yigG	1,47	-1,41
SL3909	rarD	Protein rarD	1,14	-1,95
SL3910	yigI	Uncharacterized protein yigI	-1,05	1,18
SL3913	rhtC	Threonine efflux protein	1,19	-1,35
SL3914	rhtB	Homoserine/homoserine lactone efflux protein	1,15	2,42
SL3916	yigL	Uncharacterized protein yigL	1,41	-1,29
SL3925	yigP	Uncharacterized protein yigP	1,37	1,21
SL3927	tatA	Sec-independent protein translocase protein tatA	1,68	2,05
SL3929	tatC	Sec-independent protein translocase protein tatC	2,77	-1,13
SL3930	tatD	Deoxyribonuclease tatD	1,56	2,36
SL3944	rdoA	Protein rdoA	1,16	-1,49
SL3947	polA	DNA polymerase I	1,01	1,24
SL3955	typA	GTP-binding protein TypA/BipA	1,07	-2,38
SL3956	ybhA	Phosphatase ybhA	-1,11	-1,18
SL3962	ompL	Porin ompL	1,42	2,21
SL3967	yihS	Uncharacterized sugar isomerase yihS	1,16	1,59
SL3972	yihX	Phosphatase yihX	-1,16	1,48
SL3976	ygjM	Uncharacterized HTH-type transcriptional regulator ygjM	1,30	1,23
SL3979	higB-2	Toxin higB-2	1,43	2,12
SL3987	yiiG	Uncharacterized protein yiiG	-1,34	-2,36
SL3988	yiiG	Uncharacterized protein yiiG	1,07	1,13
SL3990	azlC	Branched-chain amino acid transport protein AzlC	-1,19	-2,88
SL3991	ydcN	Uncharacterized HTH-type transcriptional regulator ydcN	1,51	1,11
SL3992	rhaM	L-rhamnose mutarotase	1,20	-1,11

SL4009	cpxP	Periplasmic protein cpxP	-2,14	-2,98
SL4016	yegU	Uncharacterized protein yegU	1,07	1,69
SL4027	lsrF	Uncharacterized aldolase lsrF	-2,68	-2,26
SL4031	yiiQ	Uncharacterized protein yiiQ	1,96	1,32
SL4034	glpX	Fructose-1,6-bisphosphatase class 2	2,36	2,36
SL4042	ftsN	Cell division protein ftsN	1,71	-1,91
SL4057	yijF	Uncharacterized protein yijF	-3,56	-5,09
SL4068	cptA	Phosphoethanolamine transferase cptA	-1,05	-1,13
SL4076	fabR	HTH-type transcriptional repressor fabR	1,13	1,20
SL4084	-	Hypothetical	1,11	-1,40
SL4096	-	Cytoplasmic Protein	-1,12	-1,15
SL4105	nudC	NADH pyrophosphatase	-1,30	-1,06
SL4108	yjaG	Uncharacterized protein yjaG	1,53	1,45
SL4111	zraP	Zinc resistance-associated protein	-1,20	-2,38
SL4128	rluF	Ribosomal large subunit pseudouridine synthase F	1,19	1,26
SL4129	yjbD	Uncharacterized protein yjbD	1,10	-1,36
SL4158	yjbE	Hypothetical Protein yjbE	-1,29	-2,54
SL4160	yjbG	Uncharacterized protein yjbG	-1,28	-3,95
SL4161	yjbH	Uncharacterized lipoprotein yjbH	1,38	-1,36
SL4162	psiE	Protein psiE	-3,02	-4,25
SL4179	dusA	tRNA-dihydrouridine synthase A	-1,07	1,03
SL4187	yjbR	Uncharacterized protein yjbR	1,13	-1,11
SL4191	-	Cytoplasmic Protein	1,53	-1,90
SL4199	yjcB	Uncharacterized protein yjcB	-1,14	-20,52
SL4200	yjcC	Uncharacterized protein yjcC	-7,52	-6,40
SL4204	yjcD	Putative permease yjcD	-1,32	1,10
SL4210	yjcH	Inner membrane protein yjcH	4,19	5,66
SL4212	-	Hypothetical	1,33	2,23
SL4220	yjcO	Uncharacterized protein yjcO	1,93	-1,31
SL4225	phnB	Protein phnB	-1,41	2,80
SL4249	-	Cytoplasmic Protein	-49,04	-9,33
SL4251	rtsA	Transcriptional regulator sirC	-67,10	-8,74
SL4253	-	Hypothetical	-2,09	-3,33
SL4256	-	Ail And OmpX Homolog	1,13	1,00
SL4257	-	Hypothetical	1,09	2,24
SL4264	fxsA	UPF0716 protein fxsA	3,79	1,57
SL4269	yjeJ	Uncharacterized protein yjeJ	-1,19	-2,01
SL4273	ecnB	Entericidin B	-1,51	1,03
SL4281	yjeA	Uncharacterized protein YjeA	2,18	1,35
SL4286	rsgA	Putative ribosome biogenesis GTPase RsgA	1,31	1,06
SL4287	orn	Oligoribonuclease	1,05	1,42
SL4290	yjeF	Uncharacterized protein yjeF	1,01	2,49
SL4306	yjfK	Uncharacterized protein yjfK	1,45	-1,05
SL4308	yjfM	Uncharacterized protein yjfM	-1,03	-1,88
SL4311	yjfN	Uncharacterized protein yjfN	2,38	9,48
SL4313	yjfP	Esterase yjfP	-1,64	1,58
SL4315	ulaG	Probable L-ascorbate-6-phosphate lactonase ulaG	1,15	-1,09
SL4328	ydeD	Hypothetical	1,16	-1,17
SL4329	ytfB	Uncharacterized protein ytfB	-1,16	1,73
SL4332	ytfE	Regulator of cell morphogenesis and NO signaling	1,19	1,19
SL4335	ytfH	Uncharacterized HTH-type transcriptional regulator ytfH	1,29	1,30
SL4343	ytfN	Uncharacterized protein ytfN	1,04	-1,31
SL4379	relB	Antitoxin RelB	1,43	2,34
SL4383	-	Hypothetical	1,78	5,18
SL4385	treB	PTS system trehalose-specific EIIBC component	4,85	37,70
SL4392	pyrL	PyrBI operon leader peptide	1,13	3,07
SL4398	yjgK	Uncharacterized protein yjgK	1,67	2,60
SL4408	-	Cytoplasmic Protein	1,50	1,44
SL4410	lptG	Lipopolysaccharide export system permease protein lptG	1,70	-1,96
SL4431	-	UPF0386 protein KPN78578_02510	2,02	5,45
SL4439	-	Hypothetical	1,36	1,06
SL4447	yjiN	Uncharacterized protein yjiN	1,75	1,18
SL4449	yfcI	Uncharacterized protein yfcI	1,88	2,14
SL4451	-	Hypothetical	1,06	1,62
SL4452	yjiS	Hypothetical	1,02	1,17
SL4461	yjiA	Uncharacterized GTP-binding protein yjiA	-1,04	1,07
SL4462	yjiX	Uncharacterized protein yjiX	-1,19	-1,52

SL4481	fhuF	Ferric iron reductase protein fhuF	-1,56	-1,31
SL4482	ycdT	Inner membrane protein ycdT	1,01	-1,46
SL4487	yjjG	5'-nucleotidase yjjG	1,94	-1,03
SL4493	yjjI	Uncharacterized protein yjjI	4,39	6,45
SL4514	creA	Protein creA	2,82	1,36
SL4526	yjjY	Uncharacterized protein yjjY	1,17	1,11
		Pathogenicity island		
SL1026	pipA	Hypothetical	-3,71	-2,23
SL1027	pipB	Secreted effector protein pipB	-26,14	-6,51
SL1028	-	Inner Membrane Protein	-77,61	-12,86
SL1029	pipC	cell invasion protein	-47,87	-6,14
SL1030	sopB	Inositol phosphate phosphatase sopB	-83,07	-7,58
SL1031	orfX	Hypothetical	1,25	9,42
SL1032	-	Hypothetical	1,04	7,87
SL1033	pipD	Probable dipeptidase	-2,67	1,93
SL1323	ybgA	Uncharacterized protein ybgA	-1,61	1,48
SL1324	mlrA	HTH-type transcriptional regulator mlrA	1,10	-2,05
SL1325	ssrB	putative two-component response regulator	-8,84	-3,72
SL1326	spiR	Sensor kinase protein	-6,92	-5,34
SL1327	spiC	Salmonella pathogenicity island protein C	-9,87	-9,52
SL1328	spiA	Yop proteins translocation protein C	-6,97	-7,91
SL1329	ssaD	Type-III Secretion Protein	-9,89	-8,23
SL1330	-	Secretion System Protein	-6,20	-7,09
SL1331	sseA	Type III secretion system chaperone sseA	-7,19	-4,87
SL1332	sseB	Secreted effector protein sseB	-6,64	-3,85
SL1333	sscA	Type III Secretion Low Calcium Response Chaperone LcrH/SycD	-5,80	-3,32
SL1334	sseC	Secreted effector protein sseC	-5,26	-2,58
SL1335	sseD	Secreted effector protein sseD	-4,24	-2,53
SL1336	sseE	Secreted Effector Protein	-4,41	-2,25
SL1337	sscB	Type III Secretion Chaperone	-3,57	-3,87
SL1338	sseF	Hypothetical	-2,24	-2,27
SL1339	sseG	Hypothetical	-1,71	-1,96
SL1340	ssaG	Secretion System Apparatus SsaG	-1,59	-1,81
SL1341	ssaH	Hypothetical	-18,51	-14,03
SL1342	ssaI	Type III Secretion System Apparatus Protein	-21,94	-15,77
SL1343	ssaJ	Secretion system apparatus lipoprotein ssaJ	-17,06	-15,33
SL1344	-	Type III Secretion Apparatus	-16,22	-11,84
SL1345	ssaK	Secretion system apparatus protein ssaK	-10,15	-9,59
SL1346	ssaL	Secretion system apparatus protein ssaL	-7,78	-8,72
SL1347	ssaM	Secretion system apparatus protein ssaM	-8,90	-12,72
SL1348	ssaV	Secretion system apparatus protein ssaV	-3,55	-3,70
SL1349	ssaN	Probable secretion system apparatus ATP synthase ssaN	-2,97	-1,73
SL1350	ssaO	Secretion system apparatus protein ssaO	-2,05	1,10
SL1351	ssaP	Secretion system apparatus protein ssaP	-2,25	-1,04
SL1352	ssaQ	Secretion system apparatus protein SsaQ	-2,22	-1,38
SL1353	yscR	Virulence protein yscR	-6,45	-3,66
SL1354	ssaS	Secretion system apparatus protein SsaS	-5,53	-6,29
SL1355	ssaT	Secretion system apparatus protein ssaT	-3,78	-4,26
SL1356	ssaU	Secretion system apparatus protein ssaU	-2,02	-2,09
SL2841	znuA	Uncharacterized periplasmic iron-binding protein HI_0362	-1,87	-1,50
SL2842	sitB	Chelated iron transport system membrane protein	-1,47	-1,16
SL2843	sitC	Chelated iron transport system membrane protein yfeC	-1,86	-1,28
SL2844	sitD	Probable iron transport system membrane protein HI_0359	-5,89	-2,82
SL2845	yopJ	Effector protein yopJ	-13,68	-5,19
SL2846	sprB	AraC family transcriptional regulator	-32,26	-8,00
SL2847	sirC	Transcriptional regulator sirC	-18,16	-5,01
SL2848	-	Hypothetical	-10,65	-10,57
SL2849	orgB	Oxygen-regulated invasion protein orgB	-3,84	-4,16
SL2850	orgA	Oxygen-regulated invasion protein orgA	-30,38	-8,93
SL2851	prgK	Lipoprotein prgK	-21,47	-4,18
SL2852	prgJ	Protein prgJ	-23,03	-3,95
SL2853	prgI	Protein prgI	-12,75	-2,47
SL2854	prgH	Protein prgH	-20,65	-6,16
SL2855	hilD	Transcriptional regulator hilD	-22,40	-3,33
SL2856	hilA	Transcriptional regulator hilA	-51,51	-8,69
SL2857	iagB	Invasion protein iagB	-30,75	-6,81
SL2858	sptP	Secreted effector protein sptP	-13,51	-5,70

SL2859	sicP	Chaperone protein sicP	-16,25	-6,65
SL2860	iacP	Probable acyl carrier protein iacP	-65,17	-10,41
SL2861	sipA	Cell invasion protein sipA	-62,47	-8,69
SL2862	sipD	Cell invasion protein sipD	-74,89	-10,28
SL2863	sipC	Cell invasion protein sipC	-21,31	-3,67
SL2864	sipB	Cell invasion protein sipB	-28,47	-4,20
SL2865	sicA	Chaperone protein sicA	-44,81	-5,55
SL2866	spaS	Surface presentation of antigens protein spaS	-44,80	-21,32
SL2867	spaR	Surface presentation of antigens protein spaR	-45,60	-23,99
SL2868	spaQ	Surface presentation of antigens protein SpaQ	-59,09	-33,25
SL2869	spaP	Surface presentation of antigens protein spaP	-59,37	-31,82
SL2870	spaO	Surface presentation of antigens protein SpaO	-56,65	-14,20
SL2871	spaN	Surface presentation of antigens protein spaN	-55,06	-10,53
SL2872	spaM	Surface presentation of antigens protein spaM	-30,45	-8,84
SL2873	spaL	Probable ATP synthase spaL	-34,06	-10,05
SL2874	spaK	Surface presentation of antigens protein spaK	-29,33	-5,56
SL2875	invA	Invasion protein invA	-29,45	-12,19
SL2876	invE	Invasion protein invE	-37,53	-18,50
SL2877	invG	Protein invG	-15,56	-6,34
SL2878	invF	Invasion protein invF	-16,66	-5,21
SL2879	invH	Invasion lipoprotein invH	-23,62	-5,38
SL3717	-	Hypothetical	-1,07	1,23
SL3718	sugR	Hypothetical	-1,05	1,28
SL3720	rhuM	putative DNA-binding protein	-1,23	1,12
SL3722	yqeH	Uncharacterized protein yqeH	1,08	1,04
SL3723	misL	putative autotransported protein	1,15	1,72
SL3724	fidL	putative inner membrane protein	1,01	1,08
SL3725	marT	putative transcriptional regulatory protein	-1,19	-1,81
SL3726	slsA	Hypothetical protein	1,27	1,64
SL3727	cigR	putative inner membrane protein	-2,09	-1,52
SL3728	mgtB	Magnesium-transporting ATPase, P-type 1	-1,40	-7,14
SL3729	mgtC	Protein mgtC	-5,15	-44,71
SL3730	yicL	Uncharacterized inner membrane transporter yicL	1,24	-1,17
SL4193	siiA	Hypothetical	-58,21	-8,63
SL4194	siiB	Integral Membrane Protein	-58,89	-8,57
SL4195	siiC	Outer membrane protein tolC	-67,18	-7,84
SL4196	siiD	Proteases secretion protein prtE	-84,22	-7,15
SL4197	siiiE	Hypothetical	-42,14	-8,49
SL4198	siiF	Leukotoxin translocation ATP-binding protein lktB	-46,86	-17,32
		Bacteriophages		
SL0942	intQ	Putative lambdoid prophage Qin defective integrase	-1,12	-1,01
SL0943	xisW	Excisionase	-1,92	1,25
SL0944	-	Hypothetical, regulador	-2,85	1,33
SL0944	-	Hypothetical, regulador	-2,85	1,33
SL0945	-	Hypothetical	-3,24	1,33
SL0946	recE	Exodeoxyribonuclease 8	-3,79	-1,15
SL0947	-	Hypothetical	-4,49	1,14
SL0948	ydaE	Hypothetical	-3,19	1,35
SL0949	-	Hypothetical	-2,66	1,03
SL0950	dicA	Regulatory Protein	-1,20	-1,61
SL0951	C1	Gifsy-2 Prophage CI Protein	-2,85	1,10
SL0952	ydaU	Gifsy-2 replication Protein O	-2,40	1,43
SL0953	ydaV	DNA Replication Protein	-1,78	1,72
SL0954	-	Hypothetical	-2,18	1,62
SL0954	-	Hypothetical	-2,18	1,62
SL0955	-	Hypothetical	-2,23	1,43
SL0955	-	Hypothetical	-2,23	1,43
SL0956	-	Hypothetical	-1,19	1,01
SL0956	-	Hypothetical	-1,19	1,01
SL0957	dinI	DNA-damage-inducible protein I	-1,07	1,36
SL0958	-	Hypothetical	-2,02	-1,14
SL0959	ninG	Hypothetical	-1,64	1,32
SL0960	-	Hypothetical	-2,57	1,68
SL0961	quuQ	Antitermination protein Q homolog from lambdoid prophage Qin	-1,33	1,91
SL0962	-	Hypothetical	-2,44	1,28
SL0963	-	Bacteriophage Protein	-2,01	1,61
SL0964	-	Hypothetical	-1,74	2,25

SL0964	-	Hypothetical	-1,74	2,25
SL0965	gtgA	putative bacteriophage encoded virulence protein	-2,24	-1,12
SL0966	nucD	Probable lysozyme from lambdoid prophage DLP12	-1,62	1,02
SL0967	rzpD	Putative Rz endopeptidase from lambdoid prophage DLP12	-1,26	-1,16
SL0968	-	Hypothetical	-1,12	-1,48
SL0969	-	Phage Terminase Large Subunit	-1,35	-1,03
SL0970	-	Hypothetical	-1,65	1,02
SL0971	-	Phage Portal Protein Lambda Family	-1,30	1,07
SL0972	clpP1	ATP-dependent Clp protease proteolytic subunit 1	-1,93	1,36
SL0973	-	putative RecA/RadA recombinase	-2,00	-1,03
SL0973	-	putative RecA/RadA recombinase	-2,00	-1,03
SL0974	-	ATP-binding sugartransporter-like protein	-2,25	-1,05
SL0975	-	Minor Tail Protein Z-Like	-2,47	-1,10
SL0976	-	Minor Tail Protein U	-2,33	-1,01
SL0977	-	Tail Protein V	-1,75	-1,04
SL0978	-	Minor Tail Component Of Putative Prophage	-1,22	-1,07
SL0979	-	Minor Tail Protein	-1,44	-1,26
SL0980	-	Hypothetical	-1,53	-1,55
SL0981	-	Minor Tail Protein	-1,66	-1,29
SL0982	ail	Attachment invasion locus protein	-1,89	1,17
SL0983	sodC1	Superoxide dismutase [Cu-Zn] 1	-2,38	-1,21
SL0984	-	Phage Minor Tail Protein L	-1,09	-1,03
SL0985	-	NLP/P60 Protein	-1,29	-1,22
SL0986	-	Phage Tail Assembly Protein	-1,63	-1,13
SL0987	-	Hocificity Protein J	-1,11	-1,26
SL0988	stfQ	Side tail fiber protein homolog from lambdoid prophage Qin	-1,72	-1,49
SL0989	ycdD	Tail fiber assembly protein homolog from lambdoid prophage Fels-1	-1,55	-1,34
SL0990	-	Hypothetical (pseudo)	-1,44	-1,53
SL0991	sseI	Secreted effector protein sseI (gtgB / srfH)	1,05	-1,31
SL0992	-	Hypothetical (pseudo)	1,00	-1,41
SL0993	yedK	Uncharacterized protein yedK (gtgD)	-1,38	-1,39
SL0994	-	Hypothetical	-2,08	-2,56
SL0995	gtgE	Prophage Encoded Virulence Factor	-3,13	-3,35
SL0995	gtgE	Prophage Encoded Virulence Factor	-3,13	-3,35
SL0996	msgA	Virulence protein msgA (gtgF)	-2,69	-2,83
SL1927	-	Hypothetical	-1,36	-1,97
SL1928	-	Cytoplasmic Protein	-2,01	-3,87
SL1929	ycdD	Tail fiber assembly protein homolog from lambdoid prophage Fels-1	1,31	1,13
SL1930	ycfK	Uncharacterized protein ycfK	1,34	1,29
SL1931	ymfQ	Uncharacterized protein ymfQ in lambdoid prophage e14 region	1,32	1,24
SL1932	ymfP	Putative protein ymfP	1,29	1,15
SL1933	ymfP	Putative protein ymfP	1,52	1,03
SL1934	-	Hypothetical	1,96	-1,07
SL1935	-	Mu-like prophage FluMu protein gp45	1,42	-1,05
SL1936	-	Tail Protein	1,29	-1,02
SL1937	-	Mu-like prophage FluMu DNA circulation protein	1,50	-1,07
SL1938	-	Phage Tail Tape Measure Protein	1,49	1,18
SL1939	-	Hypothetical	1,72	1,77
SL1940	-	Hypothetical	1,57	1,70
SL1941	-	Mu-like prophage FluMu tail sheath protein	1,31	1,43
SL1942	-	Hypothetical	1,70	1,07
SL1943	-	Hypothetical	1,85	-1,04
SL1944	-	Hypothetical	1,98	-1,04
SL1945	-	Hypothetical	2,50	1,24
SL1946	-	Hypothetical	1,77	1,07
SL1947	-	Phage Capsid Protein	1,47	1,39
SL1948	-	Phage Prohead Protease	2,30	1,45
SL1949	ymfO	Putative uncharacterized protein ymfO	1,84	-1,14
SL1950	ymfN	Uncharacterized protein ymfN	1,73	1,02
SL1951	-	P27 Family Phage Terminase Small Subunit	1,54	1,03
SL1952	-	Hypothetical	1,96	1,25
SL1953	-	Hypothetical Protein SL1953	1,94	1,23
SL1954	-	Hypothetical	1,19	1,17
SL1955	rzpD	Putative Rz endopeptidase from lambdoid prophage DLP12	1,31	1,03
SL1956	-	Uncharacterized protein HI_1415	1,76	1,24
SL1957	-	Phage Holin Lambda Family	1,58	1,15

SL1958	-	Hypothetical Protein SL1958	1,45	1,02
SL1959	-	Hypothetical	1,18	1,49
SL1960	ydfU	Uncharacterized protein ydfU	-1,02	1,40
SL1961	-	Hypothetical	-1,17	1,85
SL1962	yfdM	Putative uncharacterized protein yfdM	-1,18	1,69
SL1963	yfdN	Uncharacterized protein yfdN	-1,04	1,62
SL1964	yfdO	Hypothetical	1,19	1,60
SL1965	-	Hypothetical	-1,18	1,48
SL1966	ymfL	Uncharacterized protein ymfL	-1,21	1,82
SL1967	-	Phage Repressor	1,33	1,07
SL1968	yfdP	Uncharacterized protein yfdP	-1,59	1,90
SL1969	yfdQ	Uncharacterized protein yfdQ	-1,18	1,90
SL1970	yfdR	Uncharacterized protein yfdR	-1,61	2,68
SL1971	-	Hypothetical	-1,52	2,10
SL1972	-	Hypothetical	-1,68	2,08
SL1973	-	Hypothetical	-1,53	2,55
SL1974	-	Endodeoxyribonuclease	-1,14	1,89
SL1975	-	Phage Protein	-1,01	1,73
SL1976	intE	Phage Integrase Family Protein	-1,34	1,22
SL2546	gogB	Hypothetical	-1,22	-2,04
SL2547	-	Gifsy-1 Prophage Protein	-4,37	-1,70
SL2548	-	Hypothetical Protein SL2548	-1,90	-2,00
SL2549	-	PagK-Like Protein	-5,61	-4,06
SL2550	ycdD	Tail fiber assembly protein homolog from lambdoid prophage Fels-1	-3,34	-1,49
SL2551	-	Appr-1-P Processing Domain-Containing Protein	-4,04	-1,52
SL2552	stfQ	Side tail fiber protein homolog from lambdoid prophage Qin	-2,87	-1,38
SL2553	-	Hocificity Protein J	-3,07	-1,84
SL2554	-	Phage Tail Assembly Protein	-1,43	-1,78
SL2555	-	NLP/P60 Protein	-1,73	-1,38
SL2556	-	Phage Minor Tail Protein L	-1,82	-1,11
SL2557	-	Minor Tail Protein	-1,36	-1,15
SL2558	-	Hypothetical	-1,48	-1,17
SL2559	-	Minor Tail Protein	-2,52	-1,70
SL2560	-	Minor Tail Component Of Putative Prophage	-2,60	-1,50
SL2561	-	Tail Protein V	-2,48	-1,27
SL2562	-	Minor Tail Protein U	-2,14	-1,37
SL2563	gipA	Putative transposase in snaA-snaB intergenic region	-1,26	-1,31
SL2564	-	Phage Tail Component	-2,57	-1,14
SL2565	-	Tail Attachment Protein	-2,99	-1,20
SL2566	-	DNA Packaging-Like Protein	-3,19	-1,25
SL2567	-	P21 prophage-derived major head protein	-4,38	-1,34
SL2568	-	Head Decoration Protein	-4,37	-1,25
SL2569	sppA	Putative signal peptide peptidase sppA	-4,78	-1,10
SL2570	-	Lambda Family Phage Portal Protein	-3,24	1,01
SL2571	-	Lambda prophage-derived head-to-tail joining protein W	-1,69	1,45
SL2572	tfaD	Putative tail fiber assembly protein homolog from lambdoid prophage DLP12	-2,31	1,39
SL2573	nohA	P21 prophage-derived terminase small subunit	-2,91	-1,00
SL2574	ycgK	Uncharacterized protein ycgK	-1,71	1,92
SL2575	rzpD	Putative Rz endopeptidase from lambdoid prophage DLP12	-2,54	-1,01
SL2576	arrD	Probable lysozyme from lambdoid prophage DLP12	-1,64	1,01
SL2576	arrD	Probable lysozyme from lambdoid prophage DLP12	-1,64	1,01
SL2577	-	Hypothetical	-2,34	-1,13
SL2578	-	Hypothetical	-1,42	1,52
SL2579	-	Phage Antitermination Protein Q	-1,89	1,09
SL2580	ylcG	Hypothetical	-2,26	1,14
SL2581	-	Hypothetical	-1,64	1,33
SL2582	-	Hypothetical	-2,19	-1,13
SL2583	-	Hypothetical	-1,25	1,73
SL2585	-	Hypothetical Protein SL2585	-1,57	-1,04
SL2586	-	Hypothetical	-1,88	-1,06
SL2587	-	Hypothetical	-1,17	1,27
SL2588	-	Methyltransferase	-2,11	1,51
SL2589	-	Hypothetical	-1,86	1,52
SL2590	gpP	Hypothetical	-2,36	1,44
SL2591	gpO	Uncharacterized protein	-2,15	1,36
SL2592	-	Gifsy-1 Prophage CI Protein	-2,61	-1,05

SL2593	-	Hypothetical	1,12	-1,13
SL2594	-	ATPase Domain-Containing Protein	-1,30	-1,60
SL2595	-	Hypothetical	-1,97	-3,18
SL2596	-	Hypothetical	-2,66	-1,08
SL2597	recE	Exodeoxyribonuclease 8	-4,45	-1,49
SL2598	-	Hypothetical	-2,90	1,32
SL2599	-	Excisionase-Like Protein	-2,86	1,05
SL2600	intB	Putative prophage P4 integrase	1,43	-1,03
SL2665	ogrK	Prophage P2 OGR protein	-1,26	-2,05
SL2666	b2083	Late Control D Family Protein	1,08	-1,01
SL2667	gpU	P2 GpU Family Protein	1,31	1,37
SL2668	-	Hypothetical	1,16	-1,04
SL2669	gpE'	Hypothetical	1,45	1,01
SL2670	gpE	Phage Tail Protein	1,77	1,21
SL2671	-	Phage Tail Tube Protein	1,27	1,12
SL2672	-	Phage Tail Sheath Protein	1,43	1,02
SL2673	pinE	DNA-invertase from lambdoid prophage e14	-3,97	-3,29
SL2674	sopE	Guanine nucleotide exchange factor sopE	-47,15	-4,85
SL2675	ycdD	Tail fiber assembly protein homolog from lambdoid prophage Fels-1	-2,94	-1,27
SL2676	-	Hypothetical	-1,17	1,15
SL2677	gpI	Phage Tail Protein I	1,30	1,11
SL2678	gpJ	Baseplate J Family Protein	1,58	1,30
SL2679	gpW	GPW/Gp25 Family Protein	1,51	1,16
SL2680	-	Phage Baseplate Assembly Protein V	1,16	1,09
SL2681	-	Phage Virion Morphogenesis Protein	1,51	1,17
SL2682	-	P2 Phage Tail Completion R Family Protein	2,01	1,79
SL2683	-	Fels-2 Prophage Protein	1,92	1,93
SL2684	-	Hypothetical	1,28	1,71
SL2685	-	Hypothetical	1,32	2,39
SL2686	nucD2	Probable lysozyme from lambdoid prophage DLP12	1,35	1,38
SL2687	nucE2	Secretion Protein	1,25	-1,01
SL2688	-	Tail X Family Protein	-1,08	-1,07
SL2689	-	Head Completion Protein	1,16	1,22
SL2690	-	Phage Small Terminase Subunit	1,62	1,15
SL2691	-	P2 Family Phage Capsid Protein	1,56	1,36
SL2692	-	Phage Capsid Scaffolding Protein	1,46	1,31
SL2693	-	Hypothetical	1,10	1,23
SL2694	-	Putative uncharacterized protein ORF5 in retron EC67	-1,21	-1,32
SL2695	smf	Protein smf	-1,30	1,17
SL2696	-	Hypothetical	1,01	1,92
SL2697	-	Hypothetical	1,40	-1,51
SL2698	-	Hypothetical	2,03	1,71
SL2699	-	DinI-like protein in retron EC67	2,09	1,87
SL2700	-	Hypothetical	2,00	1,80
SL2701	-	Probable replication endonuclease from prophage-like region	1,16	1,21
SL2702	dam	Retron EC67 DNA adenine methylase	-1,69	-1,05
SL2703	ybil	Hypothetical (similar a P2p38)	-1,35	1,39
SL2704	-	Putative uncharacterized protein ORFC-like in prophage region	-1,30	1,29
SL2705	-	Hypothetical	1,10	1,38
SL2706	CII	Putative uncharacterized protein ORFB in retron EC67	-1,09	-1,32
SL2707	apl	Phage Regulatory Protein	-1,12	1,02
SL2708	CI	Putative uncharacterized protein ORFI in retron EC67	1,51	1,32
SL2709	xerD	Tyrosine recombinase xerD	1,40	1,42
SL2712	intA	Prophage CP4-57 integrase	2,32	1,36
SL2713	-	Hypothetical	1,02	1,25
SL2714	-	Hypothetical Protein SL2714	1,26	1,71
SL2715	-	Hypothetical Protein SL2715	1,49	2,11
SL2716	-	Phage Polarity Suppression Protein	1,10	-1,10
SL2717	ogrK	Prophage P2 OGR protein	-1,08	-1,16
SL2718	-	Hypothetical	1,39	1,05
SL2719	-	Hypothetical	1,38	3,48
SL2720	-	Hypothetical	1,27	3,25
SL2721	-	P4 prophage-derived uncharacterized protein t2655	-1,03	2,62
SL2722	traC	DNA primase traC	1,01	2,56
SL2723	intA	Prophage CP4-57 integrase	1,13	5,32
SL2724	intA	Integrase	-1,01	2,89

SL4130	yocS	Uncharacterized sodium-dependent transporter yocS	-2,00	-2,23
SL4131	-	Hypothetical	1,60	-1,33
SL4132	-	Inner Membrane Protein	1,45	1,15
SL4133	-	Hypothetical	-1,40	1,23
SL4134	-	Cytoplasmic Protein	-1,28	1,66
SL4135	stfR	Tail Fiber Protein	-1,23	1,29
SL4136	-	Phage Tail Protein	-1,04	-1,14
SL4137	-	Baseplate J Family Protein	1,10	-1,20
SL4138	-	Phage Baseplate Protein	1,08	1,02
SL4139	-	Hypothetical	1,68	-1,78
SL4140	gtrB	SfII prophage-derived bactoprenol glucosyl transferase	1,34	-2,02
SL4141	gtrA	Bactoprenol-linked glucose translocase homolog from prophage CPS-53	1,14	-1,07
SL4142	-	Phage Baseplate Assembly Protein V	1,26	2,41
SL4143	-	Late Control D Family Protein	1,68	1,50
SL4144	-	Bacteriophage Tail Fibre Protein	1,55	1,38
SL4145	-	Hypothetical	1,27	1,35
SL4146	-	Phage Tail Protein	1,75	1,66
SL4147	-	Hypothetical	-1,09	1,81
SL4148	-	Phage Tail Tube Protein	-1,11	1,36
SL4149	-	Phage Tail Sheath Protein	-1,28	1,66
SL4150	-	Cytoplasmic Protein	-1,42	1,62
SL4151	-	Hypothetical	1,13	1,08
SL4152	-	Hypothetical	-1,31	-1,39
SL4153	-	Lytic Transglycosylase Catalytic	-1,27	-1,08
SL4154	-	Phage-Related Membrane Protein	-1,06	1,33
SL4155	rdgB	DNA-binding protein rdgB	-1,94	-1,09
SL4156	lysC	Lysine-sensitive aspartokinase 3	-1,28	-1,04
		cob/pdu operon		
SL1992	cobT	Nicotinate-nucleotide--dimethylbenzimidazole phosphoribosyltransferase	-2,04	-2,32
SL1993	cobS	Cobalamin synthase	-1,40	-2,58
SL1994	cobU	Bifunctional adenosylcobalamin biosynthesis protein cobU	-1,39	-2,83
SL1995	cbiP	Cobyric acid synthase	-1,40	-2,17
SL1996	cbiO	Cobalt import ATP-binding protein CbiO	-1,31	-2,14
SL1997	cbiQ	Cobalt transport protein cbiQ	-1,46	-2,17
SL1998	cbiN	Cobalt transport protein cbiN	-1,47	-2,00
SL1999	cbiM	Protein cbiM	-1,51	-1,98
SL2000	cbiL	Cobalt-precorrin-2 C(20)-methyltransferase	-1,30	-2,33
SL2001	cbiK	Sirohydrochlorin cobaltochelatase	-1,27	-2,04
SL2002	cbiJ	Cobalt-precorrin-6A reductase	-1,23	-1,88
SL2003	cbiH	Cobalt-precorrin-3B C(17)-methyltransferase	-1,18	-1,86
SL2004	cbiG	Protein cbiG	-1,42	-1,63
SL2005	cbiF	Cobalt-precorrin-4 C(11)-methyltransferase	-1,39	-1,61
SL2006	cbiT	Probable cobalt-precorrin-6Y C(15)-methyltransferase [decarboxylating]	-1,15	-1,98
SL2007	cbiE	Probable cobalt-precorrin-6Y C(5)-methyltransferase	-1,16	-1,97
SL2008	cbiD	Putative cobalt-precorrin-6A synthase [deacetylating]	-1,31	-1,55
SL2009	cbiC	Cobalt-precorrin-8X methylmutase	-1,47	-1,14
SL2010	cbiB	Cobalamin biosynthesis protein cbiB	-1,37	-1,69
SL2011	cbiA	Cobyrinic acid A,C-diamide synthase	-1,08	1,18
SL2012	pocR	Regulatory protein pocR	-2,48	2,87
SL2013	pduF	Propanediol diffusion facilitator	-5,80	-1,60
SL2014	pduA	Propanediol utilization protein pduA	-46,70	-1,26
SL2015	pduB	Propanediol utilization protein pduB	-63,82	-1,93
SL2017	pduD	Propanediol dehydratase medium subunit	-61,45	-4,45
SL2018	pduE	Propanediol dehydratase small subunit	-100,77	-6,69
SL2019	pduG	propanediol utilization protein	-66,07	-8,05
SL2020	pduH	propanediol utilization protein	-66,77	-12,58
SL2021	pduJ	propanediol utilization protein	-27,09	-11,89
SL2022	pduK	propanediol utilization protein	-28,47	-12,06
SL2023	pduL	propanediol utilization protein	-25,01	-14,23
SL2024	pduM	propanediol utilization protein	-21,47	-13,88
SL2025	pduN	propanediol utilization protein	-18,79	-11,06
SL2026	pduO	propanediol utilization protein	-20,45	-10,59
SL2027	pduP	putative CoA-dependent proprionaldehyde dehydrogenase	-13,64	-4,51
SL2028	pduQ	putative propanol dehydrogenase	-14,08	-4,82

SL2029	pduS	propanediol utilization ferredoxin	-6,39	-2,90
SL2030	pduT	putative propanediol utilization protein	-5,08	-2,19
SL2031	pduU	putative propanediol utilization protein PduU	-6,92	-2,04
SL2032	pduV	putative propanediol utilization protein PduV	-4,77	-2,07
SL2033	pduW	Acetokinase	-4,63	-1,80
SL2034	pduX	putative propanediol utilization protein	1,24	1,39
		Plasmids		
SLP1_0001	finO	Fertility inhibition protein	1,13	-1,13
SLP1_0002	traX	Protein traX	1,52	-1,28
SLP1_0003	traI	Protein traI	1,33	-1,13
SLP1_0004	trbH	Protein trbH	1,21	-1,88
SLP1_0005	-	Uncharacterized protein CP0246	1,41	1,21
SLP1_0006	-	Uncharacterized protein HI_0947	-1,05	-1,00
SLP1_0007	traD	Protein traD	-2,15	-2,34
SLP1_0008	traT	TraT complement resistance protein	-1,61	-1,18
SLP1_0009	-	Surface Exclusion Inner Membrane Protein TraS	-1,56	1,25
SLP1_0010	traG	Protein traG	-1,25	1,20
SLP1_0011	traH	Protein traH	1,03	-1,21
SLP1_0012	trbB	Protein trbB	-1,31	-1,14
SLP1_0013	traQ	Protein traQ	-1,04	-1,08
SLP1_0014	traF	Protein traF	1,05	1,17
SLP1_0015	trbE	Conjugative Transfer Protein	1,07	1,20
SLP1_0016	traN	Protein traN	1,21	1,06
SLP1_0017	trbC	Periplasmic protein trbC	1,21	-1,10
SLP1_0018	-	Conjugative Transfer Protein	1,19	-1,01
SLP1_0019	traU	Protein traU	1,31	1,40
SLP1_0020	traW	Protein traW	1,24	1,33
SLP1_0021	trbI	Protein trbI	1,29	1,58
SLP1_0022	traC	Protein traC	1,28	1,08
SLP1_0023	-	Conjugative Transfer	1,15	-1,03
SLP1_0024	traR	Protein TraR	-1,14	-1,09
SLP1_0025	traV	Protein TraV	-1,75	1,02
SLP1_0026	trbD	Conjugal Transfer Protein TrbD	-1,23	1,26
SLP1_0027	traP	Protein traP	-1,19	-1,16
SLP1_0028	traB	Protein traB	-1,04	-1,18
SLP1_0029	traK	TraK lipoprotein	-1,30	-1,42
SLP1_0030	traE	Protein traE	-1,28	-3,15
SLP1_0031	traL	Protein traL	-1,29	-3,38
SLP1_0032	traA	Pilin	-1,65	-1,93
SLP1_0033	traY	Protein traY	-1,60	-2,05
SLP1_0034	traJ	Protein traJ	1,05	1,03
SLP1_0035	traM	Protein traM	-1,61	1,71
SLP1_0036	X	X polypeptide	-2,36	1,90
SLP1_0037	psiA	Protein psiA	1,72	1,74
SLP1_0038	psiB	Protein psiB	1,64	2,29
SLP1_0039	yubM	Uncharacterized protein yubM	1,29	1,68
SLP1_0040	yubL	UPF0401 protein yubL	-1,11	-1,26
SLP1_0041	ssb2	Single-stranded DNA-binding protein 2	1,22	1,02
SLP1_0042	holE	DNA polymerase III subunit theta	-1,03	1,33
SLP1_0043	-	Hypothetical	-1,26	1,46
SLP1_0044	yubI	Putative antirestriction protein YubI	-1,18	1,14
SLP1_0045	-	Uncharacterized protein yubG	-1,22	1,70
SLP1_0047	-	Hypothetical	1,00	2,33
SLP1_0048	yubE	Uncharacterized protein YubE	1,28	2,02
SLP1_0049	yubD	Putative methylase yubD	1,06	1,58
SLP1_0050	-	Cytoplasmic Protein	1,14	1,45
SLP1_0051	-	Hypothetical	1,14	1,00
SLP1_0052	samA	Protein samA	1,28	2,03
SLP1_0053	samB	Protein samB	1,12	2,04
SLP1_0054	parB	Plasmid Partition par B protein	1,19	3,01
SLP1_0055	parA	Plasmid partition protein A	1,73	3,75
SLP1_0056	yfcI	Uncharacterized protein pSLT051	1,18	-1,02
SLP1_0057	-	Cytoplasmic Protein	1,20	1,45
SLP1_0058	-	Uncharacterized protein pSLT049	1,22	1,47
SLP1_0059	-	Myosin Heavy Chain Gizzard Smooth	1,54	1,21
SLP1_0060	-	Hypothetical	1,20	1,68
SLP1_0061	yadF	Carbonic anhydrase	-1,06	-1,87

SLP1_0062	pinE	Integrase-like protein y4lS	1,12	-1,22
SLP1_0063	-	Transposase	1,63	1,02
SLP1_0064	-	AAA ATPase	1,02	1,23
SLP1_0065	-	Insertion element IS630 uncharacterized 39 kDa protein	-1,23	-2,13
SLP1_0066	vsdA	Virulence genes transcriptional activator	-1,29	2,00
SLP1_0067	spvA	28.1 kDa virulence protein	-17,29	1,16
SLP1_0068	vsdC	65 kDa virulence protein	-20,52	1,35
SLP1_0069	spvC	27.5 kDa virulence protein	-31,40	-1,61
SLP1_0070	vsdE	Virulence protein vsdE	-11,61	-2,05
SLP1_0071	-	Transposase	1,16	-2,23
SLP1_0072	vsdF	Virulence protein vsdF	1,12	1,01
SLP1_0073	yeeJ	Uncharacterized protein yeeJ	1,29	-1,58
SLP1_0074	-	Hypothetical	1,07	-1,27
SLP1_0075	yahA	Cyclic di-GMP phosphodiesterase yahA	1,35	1,40
SLP1_0076	resD	Resolvase	1,31	1,69
SLP1_0077	-	Cytoplasmic Protein	1,44	1,97
SLP1_0078	-	Hypothetical	1,20	1,82
SLP1_0079	ccdB	Cytotoxic protein CcdB	1,31	2,24
SLP1_0080	ccdA	Protein CcdA	1,64	2,99
SLP1_0081	-	Hypothetical	-1,29	-1,31
SLP1_0082	-	Cytoplasmic Protein	-1,99	-2,19
SLP1_0083	-	Replication Protein	-1,17	-1,30
SLP1_0084	repA	RepFIB replication protein A	-1,17	-1,38
SLP1_0085	ygiW	Protein ygiW	-1,46	1,31
SLP1_0086	papB	Major pilu subunit operon regulatory protein papB	-1,57	-1,14
SLP1_0087	fedA	F107 fimbrial protein	1,08	2,07
SLP1_0088	pefC	Outer membrane usher protein pefC	1,30	1,68
SLP1_0089	fanE	Chaperone protein fanE	1,24	1,90
SLP1_0090	-	Outer Membrane Protein	-1,29	1,93
SLP1_0091	-	Hypothetical	-1,33	1,15
SLP1_0092	-	Regulatory Protein	1,05	-1,24
SLP1_0093	rcsB	GerE Family Regulatory Protein	1,24	-1,19
SLP1_0094	dsbA	Thiol:disulfide interchange protein DsbA	1,82	-1,17
SLP1_0095	yjiK	Uncharacterized protein yjiK	2,15	1,15
SLP1_0096	pagC	Virulence membrane protein pagC	1,27	2,33
SLP1_0097	gadX	HTH-type transcriptional regulator gadX	1,24	1,84
SLP1_0098	yjiK	Outer Membrane Protein	1,25	1,16
SLP1_0099	repA	Replication initiation protein	-1,22	-1,29
SLP1_0100	-	Hypothetical Protein SLP1_0100	1,09	-1,07
SLP1_0101	-	DNA Replication Protein	1,32	1,09
SLP1_0102	repA2	Replication regulatory protein repA2	2,25	1,36
SLP1_0103	-	Endonuclease	-1,17	-1,35
SLP1_0104	-	DSBA Oxidoreductase	1,27	-1,03
SLP2_0001	-	Hypothetical Protein SLP2_0001	-1,24	1,46
SLP2_0002	repA	Replication initiation protein	-1,42	1,15
SLP2_0003	-	Hypothetical	1,50	3,16
SLP2_0004	-	Addiction Module Antitoxin	1,14	2,74
SLP2_0005	dnaQ	Uncharacterized protein pSLT049	1,28	5,21
SLP2_0006	-	Hypothetical	-1,21	1,48
SLP2_0007	-	Hypothetical Protein SLP2_0007	-2,74	1,71
SLP2_0008	-	Hypothetical	-3,04	2,42
SLP2_0009	-	Hypothetical	-3,10	2,78
SLP2_0010	-	Hypothetical	-4,02	2,36
SLP2_0011	-	Uncharacterized protein in cib 5'region	-3,00	1,88
SLP2_0012	cib	Colicin-Ib	-3,13	1,63
SLP2_0013	-	Colicin-Ib immunity protein	-1,25	-1,22
SLP2_0014	-	Hypothetical	-1,73	-1,19
SLP2_0015	-	Hypothetical	-1,28	1,71
SLP2_0016	-	Hypothetical	-1,19	2,48
SLP2_0017	resD	Resolvase	-1,06	2,08
SLP2_0018	-	Hypothetical Protein SLP2_0018	1,42	1,25
SLP2_0019	-	Hypothetical	1,16	1,11
SLP2_0020	-	Hypothetical	1,03	1,43
SLP2_0021	parM	Plasmid segregation protein parM	1,20	1,44
SLP2_0022	-	Plasmid Stability Protein	-1,05	1,40
SLP2_0023	impC	Protein impC	1,16	1,21
SLP2_0024	yuaZ	Uncharacterized protein yuaZ	1,30	1,22

SLP2_0025	yubA	Uncharacterized protein YubA	1,06	1,50
SLP2_0026	yubC	Uncharacterized protein yubC	1,12	1,30
SLP2_0027	yubD	Putative methylase yubD	1,15	1,52
SLP2_0028	yubE	Uncharacterized protein YubE	1,56	1,94
SLP2_0029	yubF	Uncharacterized protein yubF	1,27	2,26
SLP2_0030	-	Uncharacterized protein yubG	-1,33	2,50
SLP2_0031	yubH	Uncharacterized protein yubH	1,53	2,45
SLP2_0032	yubI	Putative antirestriction protein YubI	2,42	3,23
SLP2_0033	yubJ	Uncharacterized protein yubJ	1,81	2,54
SLP2_0034	-	Hypothetical	-1,23	1,06
SLP2_0035	ssb	Plasmid-derived single-stranded DNA-binding protein	1,11	1,76
SLP2_0036	yubM	Uncharacterized protein yubM	-1,05	1,98
SLP2_0037	psiB	Protein psiB	1,20	2,79
SLP2_0038	psiA	Protein psiA	1,23	3,67
SLP2_0039	-	Hypothetical	1,22	3,30
SLP2_0040	yubH	Uncharacterized protein yubH	-1,01	1,14
SLP2_0041	-	Antirestriction Protein	-1,11	-1,05
SLP2_0042	-	Hypothetical	-1,45	-1,69
SLP2_0043	-	Hypothetical	1,34	1,55
SLP2_0044	yfcI	Uncharacterized protein pSLT051	1,42	2,26
SLP2_0045	-	Hypothetical	-1,31	-1,02
SLP2_0047	-	Hypothetical	-1,13	-1,09
SLP2_0048	-	Hypothetical	1,60	-1,20
SLP2_0049	traI	Protein traI	1,05	1,03
SLP2_0050	-	Hypothetical	-1,02	1,06
SLP2_0051	-	Hypothetical	1,16	1,16
SLP2_0052	-	Hypothetical	-1,11	1,31
SLP2_0053	-	Plasmid Stability Protein	-1,94	-1,55
SLP2_0054	pndA	Protein pndA	-1,88	-1,37
SLP2_0055	exc	Exclusion-determining protein	-2,03	1,40
SLP2_0056	-	Hypothetical	-1,00	1,54
SLP2_0057	-	TraX-Like Protein	-1,28	1,32
SLP2_0058	-	Hypothetical	1,01	2,44
SLP2_0059	-	Conjugal Transfer Protein	1,07	2,25
SLP2_0060	-	Hypothetical	1,35	1,70
SLP2_0061	-	Hypothetical	-1,08	1,43
SLP2_0062	-	Hypothetical	1,01	1,58
SLP2_0063	-	Hypothetical	-1,07	1,36
SLP2_0064	-	TraQ Protein	-1,07	1,38
SLP2_0065	-	TraP Protein	-1,04	1,44
SLP2_0066	-	Hypothetical	1,17	1,20
SLP2_0067	-	Hypothetical	1,14	1,49
SLP2_0068	-	Hypothetical	1,21	1,95
SLP2_0069	-	TraL Protein	1,23	2,07
SLP2_0070	-	DNA Primase	-1,00	1,93
SLP2_0072	pld	Phospholipase D	1,71	2,55
SLP2_0073	-	Hypothetical	1,60	2,28
SLP2_0074	yggR	Uncharacterized protein yggR	1,23	2,07
SLP2_0075	-	Hypothetical	1,42	1,63
SLP2_0076	-	TraH Protein	1,80	1,35
SLP2_0077	ais	Lipopolysaccharide core heptose(II)-phosphate phosphatase	1,64	-1,26
SLP2_0078	-	Hypothetical	-1,37	1,11
SLP2_0079	-	Hypothetical	1,85	1,63
SLP2_0080	rci	Shufflon-specific DNA recombinase	1,16	2,05
SLP2_0081	-	Shufflon protein B'	-1,07	-1,15
SLP2_0082	-	Shufflon protein B	-1,09	-1,19
SLP2_0083	-	Shufflon protein A	1,05	1,11
SLP2_0085	-	Shufflon protein A'	1,09	1,07
SLP2_0086	-	Prepilin Peptidase	1,51	1,25
SLP2_0087	pbl	Peptidoglycan-binding-like protein	1,45	1,41
SLP2_0088	-	Type IV Prepilin	1,19	1,79
SLP2_0089	-	Type II Secretion System Protein	1,34	1,65
SLP2_0090	tcpT	Toxin coregulated pilus biosynthesis protein T	1,18	1,80
SLP2_0091	-	Pilus Assembly Protein	1,17	1,67
SLP2_0092	-	Hypothetical	-1,03	1,37
SLP2_0093	bfpB	Outer membrane lipoprotein BfpB	1,01	1,55
SLP2_0094	-	PilM Protein	1,07	1,81

SLP2_0095	-	Hypothetical	-1,06	1,85
SLP2_0096	-	Hypothetical	1,36	2,44
SLP2_0097	-	Hypothetical	1,20	2,81
SLP2_0098	-	Hypothetical	1,04	1,66
SLP2_0100	-	Hypothetical	1,51	1,83
SLP2_0101	-	Conjugal Transfer Protein	-1,58	1,51
SLP2_0102	-	Transcription Antitermination Factor	-1,65	-1,12
SLP2_0103	-	Hypothetical Protein SLP2_0103	-2,42	-2,07
SLP3_0001	sulII	Dihydropteroate synthase type-2	1,13	1,04
SLP3_0002	-	Hypothetical	-1,16	1,45
SLP3_0003	-	Replication C Family Protein	-1,04	1,25
SLP3_0004	repA	Regulatory protein repA	-1,10	1,92
SLP3_0005	-	Hypothetical Protein SLP3_0005	-1,07	1,84
SLP3_0006	-	Hypothetical Protein SLP3_0006	-1,15	1,87
SLP3_0007	mobA	Mobilization protein A	1,15	1,54
SLP3_0008	mobA	Mobilization protein A	1,18	1,07
SLP3_0009	mobB	Mobilization protein B	1,13	1,40
SLP3_0010	-	Uncharacterized mobilization operon protein F	-1,02	1,02
SLP3_0011	mobC	Mobilization protein C	1,05	1,44
SLP3_0012	-	Transposase	1,28	1,21
SLP3_0013	str	Streptomycin 3''-kinase	1,23	1,03
SLP3_0014	aphE	Streptomycin 3''-kinase	-1,02	-1,00
Not found				
SL0269	-	Hypothetical Protein SL0269	1,96	-1,11
SL0321	-		1,23	-1,20
SL0514	ybbV		1,24	1,06
SL0851	-		2,00	2,08
SL1178	-	Hypothetical Protein SL1178	-8,51	-6,61
SL1399	-	Hypothetical Protein SL1399	1,34	2,13
SL1758	-	Cytoplasmic Protein	1,56	1,26
SL1831	-	Hypothetical	1,45	1,17
SL1984	-	Hypothetical	-1,07	1,02
SL2476	-	Invasin	1,34	1,03
SL2528	-	Periplasmic Protein	2,74	1,53
SL2711	-	Hypothetical Protein SL2711	-1,02	1,12
SL2748	-	Hypothetical Protein SL2748	-1,69	-1,23
SL2749	-	Hypothetical Protein SL2749	-1,06	1,31
SL2766	-	Hypothetical	-1,77	-3,68
SL3181	-	Hypothetical	1,12	-1,03
SL3218	-	Hypothetical	1,12	1,11
SL3219	-	Hypothetical	-2,39	-1,46
SL3347	-	Conserved Hypothetical Protein	1,78	-1,19
SL3719	-	Hypothetical	1,42	-1,23
SL3721	-	Hypothetical Protein SL3721	1,07	-1,21
SL3742	-		1,40	-3,40
SL3764	-	Hypothetical Protein SL3764	1,66	1,27
SL3855	-		1,45	-1,31
SL3856	-		1,90	-1,08
SL3949	-	Hypothetical	-2,37	-1,40
SL4067	-	Hypothetical Protein SL4067	1,50	1,72
SL4165	-	Hypothetical Protein SL4165	-3,64	11,67
SL4428	-	Molybdopterin-Guanine Dinucleotide Biosynthesis Protein A	-1,45	-1,62
SL4524	-	Hypothetical	2,21	-1,07